THE FUNGAL CELL WALL

EDITED BY: Fausto Almeida, Joshua D. Nosanchuk and Gustavo Alexis Niño-Vega
PUBLISHED IN: Frontiers in Microbiology

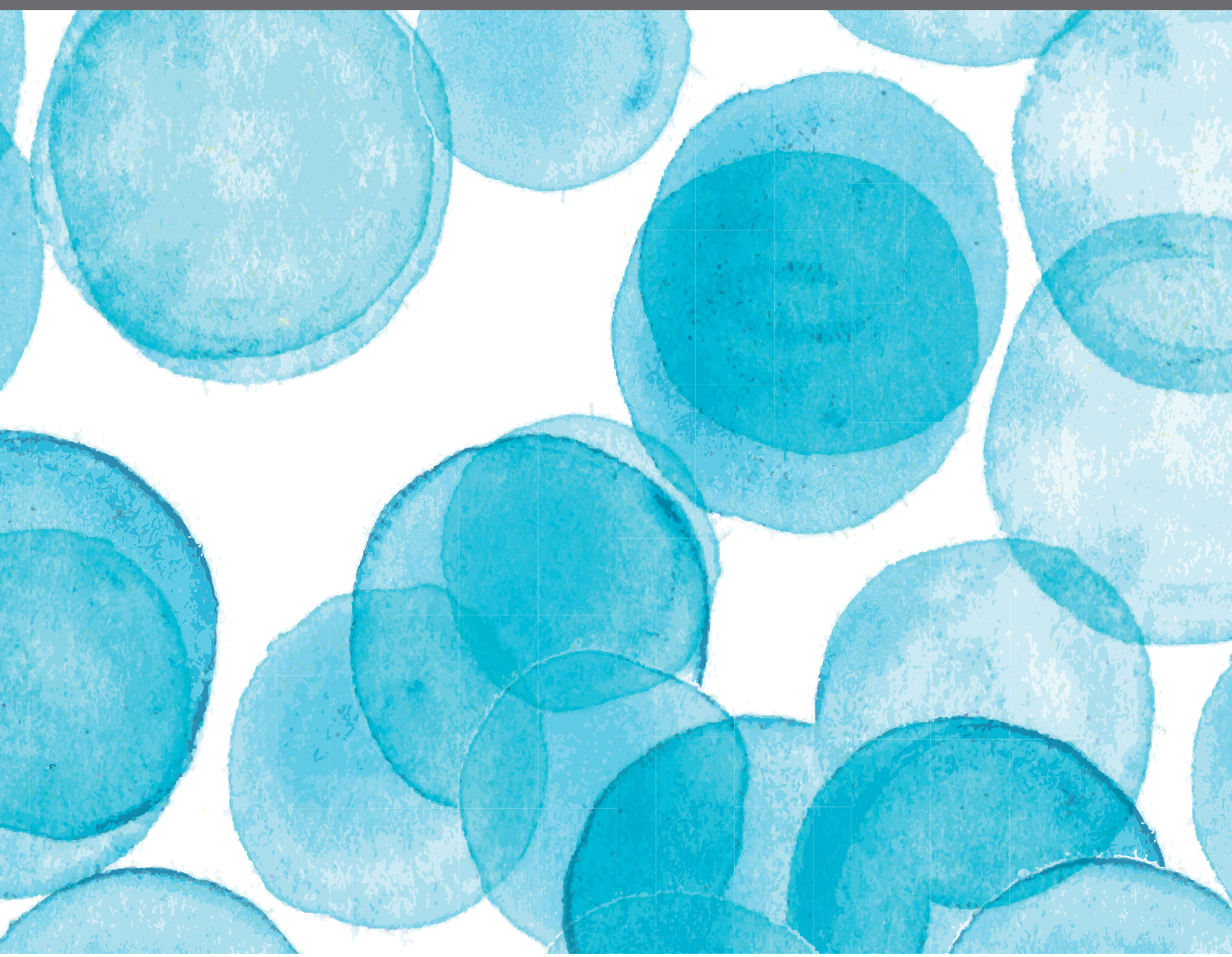

frontiers Research Topics

frontiers

ISSN 1664-8714
ISBN 978-2-88966-132-9
DOI 110.3389/978-2-88966-132-9

About Frontiers

Frontiers is more than just an open-access publisher of scholarly articles: it is a pioneering approach to the world of academia, radically improving the way scholarly research is managed. The grand vision of Frontiers is a world where all people have an equal opportunity to seek, share and generate knowledge. Frontiers provides immediate and permanent online open access to all its publications, but this alone is not enough to realize our grand goals.

Frontiers Journal Series

The Frontiers Journal Series is a multi-tier and interdisciplinary set of open-access, online journals, promising a paradigm shift from the current review, selection and dissemination processes in academic publishing. All Frontiers journals are driven by researchers for researchers; therefore, they constitute a service to the scholarly community. At the same time, the Frontiers Journal Series operates on a revolutionary invention, the tiered publishing system, initially addressing specific communities of scholars, and gradually climbing up to broader public understanding, thus serving the interests of the lay society, too.

Dedication to Quality

Each Frontiers article is a landmark of the highest quality, thanks to genuinely collaborative interactions between authors and review editors, who include some of the world's best academicians. Research must be certified by peers before entering a stream of knowledge that may eventually reach the public - and shape society; therefore, Frontiers only applies the most rigorous and unbiased reviews.
Frontiers revolutionizes research publishing by freely delivering the most outstanding research, evaluated with no bias from both the academic and social point of view. By applying the most advanced information technologies, Frontiers is catapulting scholarly publishing into a new generation.

What are Frontiers Research Topics?

Frontiers Research Topics are very popular trademarks of the Frontiers Journals Series: they are collections of at least ten articles, all centered on a particular subject. With their unique mix of varied contributions from Original Research to Review Articles, Frontiers Research Topics unify the most influential researchers, the latest key findings and historical advances in a hot research area! Find out more on how to host your own Frontiers Research Topic or contribute to one as an author by contacting the Frontiers Editorial Office: researchtopics@frontiersin.org

THE FUNGAL CELL WALL

Topic Editors:
Fausto Almeida, University of São Paulo, Brazil
Joshua D. Nosanchuk, Albert Einstein College of Medicine, United States
Gustavo Alexis Niño-Vega, University of Guanajuato, Mexico

Citation: Almeida, F., Nosanchuk, J. D., Niño-Vega, G. A., eds. (2020). The Fungal Cell Wall. Lausanne: Frontiers Media SA. doi: 10.3389/978-2-88966-132-9

Table of Contents

frontiers in Microbiology

EDITORIAL
published: 09 September 2020
doi: 10.3389/fmicb.2020.01682

Editorial: The Fungal Cell Wall

Fausto Almeida[1]*, *Joshua D. Nosanchuk*[2,3]* and *Gustavo Alexis Niño-Vega*[4]*

[1] Department of Biochemistry and Immunology, Ribeirão Preto Medical School, University of São Paulo, São Paulo, Brazil, [2] Division of Infectious Diseases, Department of Medicine, Albert Einstein College of Medicine, New York, NY, United States, [3] Department of Microbiology, Albert Einstein College of Medicine, New York, NY, United States, [4] Division de Ciencias Naturales y Exactas, Departamento de Biologia, Universidad de Guanajuato, Guanajuato, Mexico

Keywords: cell wall, fungi, pathogenic fungi, pathogenic fungal disease, non-pathogenic fungi, fungal structure, fungal metabolism

Editorial on the Research Topic

The Fungal Cell Wall

A robust understanding of the complexity and functionality of the fungal cell wall is crucial to the development of new therapeutic and prophylactic strategies. The cell wall plays several key functions in fungal pathobiology as diverse factors, such as cell shape, encapsulation, and rigidity, influence events during interaction with the host (Gow et al., 2017). These interactions may be proinflammatory or may subvert host responses. The fungal cell wall has a flexible structure that is highly complex and intricately organized of α- and β- linked glucans, chitin, glycoproteins, and pigments (Gow et al., 2017).

The researchers who contributed to this Research Topic presented 13 themed articles that highlighted the latest advances in our understanding of the biological importance of the fungal cell wall. For example, Garcia-Rubio et al. summarized recent findings on the characteristics and influence of cell wall components on fungi-host interaction with a specific focus on three fungal species, *Aspergillus fumigatus*, *Candida albicans*, and *Cryptococcus neoformans*. Lima et al. discussed the wealth of information available regarding antifungal therapy and the development of antimicrobial resistance subsequent to cell wall modifications by several important human pathogenic fungi. Patel and Free addressed the genetics and biochemistry that lead to the formation of the complex *Neurospora crassa* cell wall, comparing this species' cell wall with that of other fungal species.

Two reports focused on the dermatophyte *Trichophyton rubrum*. Martins et al. evaluated RNA-seq results under stress conditions, using undecanoic acid and acriflavine as well as the influence of the carbon source, on the modulation of genes regulating *T. rubrum* cell wall metabolism. These investigators described that keratin mimics the host environment and undecanoic acid and acriflavine present non-specific antifungal activity against *T. rubrum*. Thus, the authors identified genes putatively encoding *T. rubrum* virulence factors. Celestrino et al. verified that Toll-like receptor 2 (TLR2) is required for efficient phagocytosis of *T. rubrum* conidia by adherent monocytes, and the absence of TLR2 signaling in human monocytes impairs the expected inflammatory responses.

In the work by Sun et al., we learnt that the farnesyltranferase β subunit Ram1 regulates pathogenicity, mating, and cell wall integrity, and it also plays an important role as a virulence factor in the sugarcane smut fungus *Sporisorium scitamineum*. Miyazawa et al. described that both α-1,3-glucan and galactosaminogalactan are adhesive molecules and these glucans contribute to aggregation on the hyphal surface of *Aspergillus oryzae*. In *P. brasiliensis*, Souza et al. verified that cell wall α-glucan induced differentiation of dendritic cells, which could contribute to pathogen persistence since this process potentially affects Th1 polarization. de Oliveira et al. demonstrated that thioredoxin reductase 1 is a highly immunogenic surface antigen in the cell walls of

OPEN ACCESS

Edited by:
Gustavo Henrique Goldman, University of São Paulo, Brazil

Reviewed by:
Carol Munro, University of Aberdeen, United Kingdom
Iran Malavazi, Federal University of São Carlos, Brazil

***Correspondence:**
Fausto Almeida
fbralmeida@usp.br
Joshua D. Nosanchuk
josh.nosanchuk@einsteinmed.org
Gustavo Alexis Niño-Vega
gustavo.nino@ugto.mx

Specialty section:
This article was submitted to Fungi and Their Interactions, a section of the journal Frontiers in Microbiology

Received: *18 May 2020*
Accepted: *26 June 2020*
Published: *09 September 2020*

Citation:
Almeida F, Nosanchuk JD and Niño-Vega GA (2020) Editorial: The Fungal Cell Wall. Front. Microbiol. 11:1682. doi: 10.3389/fmicb.2020.01682

Candida albicans, *Paracoccidioides* spp., and *Cryptococcus neoformans*, and that the enzyme has conserved epitopes in fungi, but there are no homologs in humans. In *Candida parapsilosis*, Oh et al. verified the nature of the agglutinin-like sequence gene family, which encodes cell-surface glycoproteins involved in the adhesion of fungal cells to host and abiotic surfaces. The authors also demonstrated allelic variability and expression patterns. The Zheng et al. verified that the deletion of a gene responsible for coding a calcineurin homolog from *Talaromyces marneffei* affects germination, cell wall integrity, morphogenesis, and resistance to external stresses. Orner et al. demonstrated that the cell-wall-associated antiphagocytic protein 1 and laccase enzymes (named Lac1 and Lac2) play important roles in increasing resistance to amphotericin B and host-mediated killing during infection as well as enhancing the subsequent accumulation of old *C. neoformans* cells (10 generations old), which melanized to a greater extent than younger *C. neoformans* cells (0–2 generations old). Helal et al., which includes one of us, presented the first description that pan-antigens displayed on the cell surface of pathogenic fungi can effectively be targeted with radioimmunotherapy. The authors described the ability of a radiolabeled anti-(1-3)-β-D-glucan antibody to specifically target *Blastomyces dermatitidis in vitro* and *in vivo*. Furthermore, this specific radioimmunotherapy selectively killed *B. dermatitidis* under both *in vitro* and *in vivo* conditions.

In conclusion, this themed collection enhances our knowledge of the diverse functions of the fungal cell wall in host-pathogen interactions, and the papers particularly highlighted potential targets and methods for antifungal development, reinforcing the relevance of studies focused on elucidating the biology of the fungal cell wall.

AUTHOR CONTRIBUTIONS

FA drafted the Editorial while JN and GN-V contributed to editing. All authors conceived and designed the work and provided final approval of the version to be published.

REFERENCES

Gow, N., Latge, J., and Munro, C. (2017). "The fungal cell wall: structure, biosynthesis, and function," in *The Fungal Kingdom*, eds J. Heitman, B. Howlett, P. Crous, E. Stukenbrock, T. James, and N. Gow (Washington, DC: ASM Press), 267–292. doi: 10.1128/microbiolspec.FUNK-0035-2016

Conflict of Interest: The authors declare that the research was conducted in the absence of any commercial or financial relationships that could be construed as a potential conflict of interest.

The handling editor declared a shared affiliation with one of the authors, FA, at time of review.

frontiers in Microbiology

ORIGINAL RESEARCH
published: 26 April 2019
doi: 10.3389/fmicb.2019.00781

Agglutinin-Like Sequence (*ALS*) Genes in the *Candida parapsilosis* Species Complex: Blurring the Boundaries Between Gene Families That Encode Cell-Wall Proteins

*Soon-Hwan Oh[1], Brooke Smith[2], Andrew N. Miller[3], Bart Staker[4], Christopher Fields[5], Alvaro Hernandez[5] and Lois L. Hoyer[1]**

[1] Department of Pathobiology, University of Illinois at Urbana-Champaign, Urbana, IL, United States, [2] Department of Biology, Millikin University, Decatur, IL, United States, [3] Illinois Natural History Survey, Urbana, IL, United States, [4] Seattle Structural Genomics Center for Infectious Disease, Seattle Children's Hospital, Seattle, WA, United States, [5] Roy J. Carver Biotechnology Center, University of Illinois at Urbana-Champaign, Urbana, IL, United States

OPEN ACCESS

Edited by:
Joshua D. Nosanchuk, Albert Einstein College of Medicine, United States

Reviewed by:
Maria Rapala-Kozik, Jagiellonian University, Poland
Renata Toth, University of Szeged, Hungary

***Correspondence:**
Lois L. Hoyer
lhoyer@illinois.edu

Specialty section:
This article was submitted to Fungi and Their Interactions, a section of the journal Frontiers in Microbiology

Received: 07 February 2019
Accepted: 27 March 2019
Published: 26 April 2019

Citation:
Oh S-H, Smith B, Miller AN, Staker B, Fields C, Hernandez A and Hoyer LL (2019) Agglutinin-Like Sequence (ALS) Genes in the Candida parapsilosis Species Complex: Blurring the Boundaries Between Gene Families That Encode Cell-Wall Proteins. Front. Microbiol. 10:781. doi: 10.3389/fmicb.2019.00781

The agglutinin-like sequence (Als) proteins are best-characterized in *Candida albicans* and known for their role in adhesion of the fungal cell to host and abiotic surfaces. *ALS* sequences are often misassembled in whole-genome sequence data because each species has multiple *ALS* loci that contain similar sequences, most notably tandem copies of highly conserved repeated sequences. The *Candida parapsilosis* species complex includes *Candida parapsilosis*, *Candida orthopsilosis*, and *Candida metapsilosis*, three distinct but closely related species. Using publicly available genome resources, *de novo* genome assemblies, and laboratory experimentation including Sanger sequencing, five *ALS* genes were characterized in *C. parapsilosis* strain CDC317, three in *C. orthopsilosis* strain 90–125, and four in *C. metapsilosis* strain ATCC 96143. The newly characterized *ALS* genes shared similar features with the well-known *C. albicans ALS* family, but also displayed unique attributes such as novel short, imperfect repeat sequences that were found in other genes encoding fungal cell-wall proteins. Evidence of recombination between *ALS* sequences and other genes was most obvious in *CmALS2265*, which had the 5′ end of an *ALS* gene and the repeated sequences and 3′ end from the *IFF/HYR* family. Together, these results blur the boundaries between the fungal cell-wall families that were defined in *C. albicans*. TaqMan assays were used to quantify relative expression for each *ALS* gene. Some measurements were complicated by the assay location within the *ALS* gene. Considerable variation was noted in relative gene expression for isolates of the same species. Overall, however, there was a trend toward higher relative gene expression in saturated cultures rather than younger cultures. This work provides a complete description of the *ALS* genes in the *C. parapsilosis* species complex and a toolkit that promotes further investigations into the role of the Als proteins in host-fungal interactions.

Keywords: agglutinin-like sequence genes, *ALS* family, *Candida* species, adhesion, cell-wall proteins, fungi

INTRODUCTION

The study of adhesive mechanisms is pivotal in pathogenic microbiology because adhesion promotes host colonization, which is a foothold in the process of causing disease. The agglutinin-like sequence (*ALS*) gene family encodes cell-surface glycoproteins that are involved in adhesion of fungal cells to host and abiotic surfaces (Hoyer and Cota, 2016). *ALS* genes and their encoded proteins are best characterized in *C. albicans*. A binding cavity located within the N-terminal Als domain is responsible for adhesion to peptide ligands (Lin et al., 2014). Another hallmark of *C. albicans* Als proteins is an often-extensive central domain of tandemly repeated sequences that are rich in serine, threonine, and sometimes proline.

The rapid pace at which draft genome sequences are developed is a benefit to the research community. At this time, however, most available draft genomes were assembled from short-read DNA sequences of no more than a few hundred nucleotides (e.g., Riccombeni et al., 2012; Pryszcz et al., 2015). Considering that the repeated DNA unit in *ALS* genes is 108 bp and that the tandemly repeated copies of highly similar sequences may extend for several kilobases, it is no surprise that many genome assemblies fail within the *ALS* coding regions. In some published fungal genomes, *ALS* genes may be assembled accurately, while in others, it is not possible to calculate basic information such as the number of loci present in the gene family. Long-read DNA sequence technology provides the opportunity to create a larger template upon which the more-accurate short-read sequences can be assembled (Madoui et al., 2015), providing a new approach to characterizing the *ALS* genes in pathogenic fungi.

The focus of this work is the *Candida parapsilosis* species complex: *Candida parapsilosis*, *Candida orthopsilosis*, and *Candida metapsilosis*. The three species are closely related; recognition as separate species is a relatively recent event (Tavanti et al., 2005). The species are gaining importance as pathogens, with adhesion and colonization mechanisms playing a central role in the disease process (Bliss, 2015). As such, it is important to understand the nature of the *ALS* family, its variability across alleles within and among various strains, and the relative gene expression patterns that may reveal which of the genes could play the largest role in the adhesion process.

Using a combination of published sequence data and *de novo* approaches, we establish the nature of the *ALS* genes in the *C. parapsilosis* species complex, their allelic variability, and expression patterns. The resulting data reveal novel sequences and recombination between genes that demonstrate the blurring of gene family definitions that were developed in *C. albicans*. The work provides a toolkit that can be used to further knowledge of the *ALS* genes, as well as highlights mechanisms for maintaining the diversity of cell-surface adhesins in the pathogenic fungi.

MATERIALS AND METHODS

Microbial Strains

Table 1 shows the microbial strains used in this study. Fungal identifications were validated using RAPD methodology (Tavanti et al., 2005). Products were separated on 1% agarose/Tris-Acetate-EDTA gels and visualized by ethidium bromide staining. Routine PCR analyses were conducted as described previously (Green et al., 2004).

TABLE 1 | *C. parapsilosis*, *C. orthopsilosis*, and *C. metapsilosis* strains and sources.

Species	Strain	Source
Candida parapsilosis	CDC317 (ATCC MYA-4646)	Geraldine Butler (UC Dublin)
	949 (44)	Patricia Kammeyer (Loyola)
	950 (X36406)	Patricia Kammeyer (Loyola)
	1125 (ATCC 22019)	American Type Culture Collection
Candida orthopsilosis	90–125	Arianna Tavanti (Pisa)
Candida metapsilosis	ATCC 96143	Arianna Tavanti (Pisa)
	61	Arianna Tavanti (Pisa)
	88	Arianna Tavanti (Pisa)
	397	Arianna Tavanti (Pisa)
	482	Arianna Tavanti (Pisa)

Publicly Available Genome Sequences

Previously published genome sequences were used for this study. These included *C. parapsilosis* strains CDC317 (Butler et al., 2009; GenBank accession number ASM18276v2; GCA_000182765.2), CBS6318 (GCA_0000982555.2), and GA1 (GCA_0000982675.1). Strain CDC317 was used as the representative genome sequence. A genome sequence was available for *C. orthopsilosis* strain 90-125 (GCA_000315875.1). A new 90–125 sequence was derived from short-read and long-read sequence data as described previously (Lombardi et al., 2019; PQBP00000000). Sequences for strains MCO456 (GCA_900002835.2) and AY2 (GCA_000304155.1) were also examined. The *C. metapsilosis* genome sequence under accession number CBZN0200000000 was included in the analysis although it was compiled from more than one isolate (Pryszcz et al., 2015). A new *C. metapsilosis* genome sequence was generated from short-read and long-read sequence data as described below.

Genome Sequence Data Collection, Assembly, and Validation

A new genome sequence was generated for *C. metapsilosis* strain ATCC 96143. Genomic DNA initially was extracted from cells that were grown to saturation (16 h) at 37°C in YPD medium (per liter: 10 g yeast extract, 20 g peptone, 20 g glucose) with 200 rpm shaking. The genome assembly from this preparation was of lower quality than desired, so the method was repeated, this time with a culture that was grown to mid-log phase. Mid-log-phase cells appeared to lack an extracellular polysaccharide that was present in the saturated culture, presumably leading to a cleaner DNA preparation that did not clog the pores of the MinION sequencer (see below). The mid-log phase sequence data replaced those from the saturated culture prep in the GenBank deposit (PQNC00000000) and were used in the analysis presented here.

DNA was extracted using the method of Sherman et al. (1986). Briefly, cells were treated with zymolyase (MP Biomedicals) to form spheroplasts that were lysed with sodium dodecyl sulfate. Gentle mixing by inversion was used to handle the spheroplasts, and during subsequent phenol extraction and isopropyl alcohol precipitation of the DNA. Verification of the quality of the high-molecular-weight DNA was assessed using agarose gel electrophoresis.

C. metapsilosis DNA libraries were constructed and sequenced at the Roy J. Carver Biotechnology Center, University of Illinois at Urbana-Champaign. Data were derived using Illumina (short-read) and Oxford Nanopore (long-read) methods. MiSeq shotgun genomic libraries were prepared with the Hyper Library construction kit (Kapa Biosystems). The library was quantitated by qPCR and sequenced on one MiSeq flowcell for 151 cycles from each end of the fragment using a MiSeq 300-cycle sequencing kit (version 2). FASTQ files were generated and demultiplexed with the bcl2fastq Conversion Software (Illumina, version 2.17.1.14). MiSeq reads were quality trimmed using Trimmomatic (Bolger et al., 2014) with the parameters "LEADING:30 TRAILING:30" prior to assembly.

For Oxford Nanopore long-read sequencing, 1 μg of genomic DNA was sheared in a gTube (Covaris, Woburn, MA, United States) for 1 min at 6,000 rpm in a MiniSpin plus microcentrifuge (Eppendorf, Hauppauge, NY, United States). The sheared DNA was converted into a shotgun library with the LSK-108 kit from Oxford Nanopore, following their manual. The library was sequenced on a SpotON R9.4 RevC flowcell for 48 h using a MinION MK 1B sequencer.

Basecalling was performed with the software Albacore version 2.3.1 from Oxford Nanopore. Sixty nucleotides were removed from both ends of each Oxford Nanopore read, followed by additional trimming using a Github checkout (commit 92c0b65f) of Porechop (Wick et al., 2017a) to remove reads with potential internal barcodes which were likely chimeric. Only reads longer than 800 nt were used in the final assembly. Canu v1.7 (Koren et al., 2017) was used for assembly with the following parameters: 'canu -p asm -d C_meta_default genomeSize = 14m useGrid = false -nanopore-raw c_metapsilosis.qualtrim.clean.fastq.gz.'

Oxford Nanopore reads were then aligned against the assembly using minimap v2.8 (Li, 2018), and the alignment was then used to polish the assembly using nanopolish v 0.9.0 (Senol Cali et al., 2018). Quality-trimmed MiSeq data were used to iteratively polish the assembly using a Python script based on the iterative polishing method utilized during assembly with the hydrid assembler Unicycler (Wick et al., 2017b) using Pilon v1.22 for error correction (Walker et al., 2014). Haplomerger2 (release 20180603; Huang et al., 2017) was then used to both locate and resolve potential haplotypes, generating a haploid reference genome with a separate assembly with alternate haplotypes.

Ambiguities in the genome sequence data were corrected by PCR amplification of the region and Sanger sequencing of the product. **Supplementary Table S1** lists PCR primer sequences. **Supplementary File S1** includes details regarding the computational analyses and characteristics of the resulting *C. metapsilosis* genome sequence.

Tools for Identification of *ALS* Genes and Features of Predicted Als Proteins

BLAST[1] was used to identify potential *ALS* genes and Als proteins in the various genome sequences. *C. albicans* sequences used as queries included *CaALS1* (L25902), *CaALS2* (AH006927), *CaALS3* (AY223552), *CaALS4* (AH006929), *CaALS5* (AY227440), *CaALS6* (AY225310), *CaALS7* (AF201684), *CaALS9-1* (AY269423), and *CaALS9-2* (AY269422). As additional *ALS* genes were located, those sequences were also used as BLAST queries until no additional new sequences were detected.

Secretory signal peptides were detected in putative Als proteins using the SignalP 4.1 Server[2] (Nielsen, 2017). Putative GPI anchor addition sites were identified using the big-PI Predictor[3] (Eisenhaber et al., 1999). Nucleotide sequence translation, multiple sequence alignments, and other general bioinformatic processes used the European Bioinformatics Institute (EMBL-EBI) tools and data resources[4] (Cook et al., 2017).

Phylogenetics Analysis

Nucleotide sequences from 21 concatenated genes from the *ALS* family were analyzed using maximum likelihood (ML) and Bayesian methods. Alignment of genes was conducted in SeaView v4.6.1 (Gouy et al., 2010) using Muscle v3.8 (Edgar, 2004). Ambiguous regions were removed using Gblocks v0.91b (Castresana, 2000), allowing for less strict flanking regions, gap positions within the final blocks, and smaller final blocks. Maximum likelihood analysis was conducted using PhyML (Guindon and Gascuel, 2003) under the GTR substitution model with four rate classes and optimized invariable sites based on the results from jModelTest 2.0 (Posada, 2008). The best nearest neighbor interchange and subtree pruning and regrafting tree improvement was implemented on the unrooted BioNJ starting tree and branch support was determined with 1,000 non-parametric bootstrap replicates. Bayesian analysis was conducted using MrBayes 3.2.2 on XSEDE (3.2.6) through the CIPRES Science Gateway (Miller et al., 2010). Bayesian analysis was conducted using the GTR + I + G model with four rate classes and four independent chains and ran for 10 million generations sampling every 1,000 trees with the first 25% of trees discarded as burn-in. A consensus tree with the remaining 7,500 trees was produced using PAUP 4.0a (Swofford, 2002). Nodes with ≥70% bootstrap support and ≥95% Bayesian posterior probability were considered significantly supported (Alfaro et al., 2003).

Structural Analysis

Structural homology models were calculated using Phyre2 (Kelly et al., 2015). Sequence alignments were created to identify structurally conserved residues and models were built using the Threading option to maintain the integrity of the peptide-binding

[1]https://blast.ncbi.nlm.nih.gov/Blast.cgi

[2]http://www.cbs.dtu.dk/services/SignalP

[3]http://mendel.imp.ac.at/sat/gpi/gpi_server.html

[4]https://www.ebi.ac.uk/services

cavity (PBC) and allow for comparison of side-chain residue changes between sequence variants. Structures were compared and analyzed using Coot (Emsley et al., 2010) and Maestro (Schrodinger LLC, Portland, OR, United States).

Growth Conditions for Gene Expression Analysis

All fungal isolates were stored as pure cultures in 30% glycerol at −80°C. Isolates were streaked to YPD agar as needed. YPD plates were stored at 4°C for no more than 1 week prior to use. Some growth conditions were used for assessing *ALS* gene expression because they mimicked conditions used in another publication. Other selected conditions were intended to detect large trends in differential gene expression that are characteristic of the *C. albicans ALS* family (e.g., assessing gene expression at early or late time points in different growth media; Hoyer et al., 2008). In each experiment, cells were collected from the specified growth condition, pelleted by centrifugation, and the pellet flash frozen in a dry ice-ethanol bath. Frozen pellets were stored at −80°C until RNA was extracted.

C. orthopsilosis strain 90-125 was grown to mimic the conditions described by Lombardi et al. (2019). A single colony from a YPD plate was inoculated into 10 ml YPD liquid medium and incubated for 24 h at 30°C and 200 rpm shaking. 0.5 ml of the culture was inoculated into 20 ml fresh YPD medium and incubated for either 1 h or 24 h under the same temperature and agitation conditions. Cells were harvested by centrifugation, flash frozen in dry ice/ethanol, and stored at −80°C. Duplicate cultures were grown on three separate occasions.

A similar approach was used for gene expression analysis of the *C. parapsilosis* genome isolate (CDC317) and the type strain (ATCC 22019). A single colony from a YPD plate was inoculated into 10 ml YPD medium and grown for 24 h at 30°C and 200 rpm shaking. *C. parapsilosis* cells were also grown using the liquid filament induction conditions of Lackey et al. (2013). In preliminary experiments, growth of strain ATCC 22019 for 24 h produced slightly elongated cells while strain CDC317 appeared as a typical budding yeast. One colony was inoculated into 20 ml YPD at 30°C and 200 rpm shaking for 24 h. Cells were pelleted by centrifugation and washed twice in sterile water. A culture of SC medium [6.7 g/liter yeast nitrogen base without amino acids, supplemented 2% glucose and 2 g of complete amino acid mixture as defined by Lackey et al. (2013)] containing 20% fetal bovine serum (Gibco; 26140-079) was inoculated at an OD_{600} of 0.6. The culture was incubated for 2 h at 37°C and 200 rpm shaking. Duplicate cultures were grown on three separate occasions.

For *C. metapsilosis*, genome strain (ATCC 96143) and strains 61, 397, and 482 were studied. A single colony from the YPD plate was inoculated into 10 ml YPD liquid medium and incubated for 24 h at 37°C and 200 rpm shaking. Cells were harvested from the 24-h culture, replicate 2.5-ml aliquots were removed from the culture; cells were collected, frozen, and stored as described above. The remaining 5 ml of culture was washed in Dulbecco's Phosphate Buffered Saline (BioWhittaker; 17-512Q), diluted, and counted using a hemocytometer. The total cell number was resuspended in RPMI 1640 tissue culture medium (Gibco; 11875-135) at a density of 5×10^7 cells/ml. The culture was incubated for 1 h at 37°C and 200 rpm shaking. Cells were collected by filtration across a 0.45-micron membrane (GVS Life Sciences; 1213776). The filter was placed into a 50-ml conical centrifuge tube, flash frozen, and stored at −80°C.

Design and Validation of TaqMan Assays to Quantify Relative *ALS* Gene Expression Levels

All steps for developing, validating, and running the TaqMan assays followed the Guide to Performing Relative Quantitation of Gene Expression Using Real-Time Quantitative PCR (Applied Biosystems Inc., 2008). TaqMan primers and probes were designed using PrimerQuest (Integrated DNA Technologies). Primers had an optimal T_m of 61°C, GC content of 40% and 25-nt length. Probes had an optimal T_m of 70°C, GC content of 40% and 28-nt length. To identify divergent sequences that could be exploited for TaqMan assay design, Clustal Omega[5] was used to align the nucleotide sequences from the 5′ end of each *ALS* gene. An amplicon size of 140 bp was sought; some products were larger or smaller, depending on the availability of unique sequences among the genes. PCR efficiencies were measured for each TaqMan assay; each was between 90 and 110% (**Supplementary Table S2**).

Because some genes were so similar within a given species, specificity of the TaqMan assays was demonstrated experimentally (**Supplementary Table S3**). Fragments were PCR amplified and cloned into the pJet1.2/blunt vector and transformed into *E. coli* INVαF' (Thermo Fisher). The accuracy of cloned fragments was verified using Sanger sequencing (Roy J. Carver Biotechnology Center, Urbana, IL, United States). Dilutions of purified, quantified plasmid DNA were used as templates to demonstrate specificity of TaqMan assays (see section "Results").

Control TaqMan assays featured the *ACT1* and *TEF1* genes from each species. Primers (**Supplementary Table S1**) were used to amplify the genes from each species and validate its sequence using the Sanger method. Some TaqMan control assays were designed to recognize a single species (**Supplementary Table S2**). Control assays that recognize multiple species were also designed with an eye on cost savings, as use of a common control would eliminate the need to order one control assay per species.

Real-Time PCR Analysis of Gene Expression

RNA was extracted using the hot acidic phenol method of Collart and Oliviero (1993) with the addition of approximately 100 μl volume of 0.5 mm sterile, baked, acid-washed glass beads to each tube. Nucleic acid concentration was measured using a NanoDrop spectrophotometer (Thermo Scientific). The presence

[5]https://www.ebi.ac.uk/Tools/msa/clustalo

of contaminating genomic DNA in RNA preparations was detected by PCR using ITS4 and ITS5 primers[6] (White et al., 1990). The reaction template was 25 ng of RNA in a 25 μl reaction containing PCR buffer with 2.5 mM of $MgCl_2$, 1 μM of each primer, 0.5 mM of dNTP, and Taq polymerase (Invitrogen; 10342-020). PCR conditions were 93°C for 5 min followed by 40 cycles of 93°C for 30 s, 53°C for 30 s, 72°C for 1 min with a 7-min final extension at 72°C. DNase (Invitrogen; AM2224) was used according to manufacturer's instructions to digest contaminating genomic DNA. Often, multiple rounds of DNase digestion were required to eliminate DNA below the detection limit of the PCR assay. Each RNA sample was cleaned using an RNeasy Mini spin column (Qiagen; 74104). RNA preparations were quantified and their quality assessed using Qubit (Invitrogen; Q10210) and/or the 2100 Bioanalyzer (Agilent Technologies). Aliquots were stored at −80°C until used for real-time gene expression assays.

The Superscript III cDNA synthesis kit (Invitrogen; 18080-051) was used to make cDNA according to manufacturer's instructions. The amount of RNA added to the cDNA synthesis reaction was titrated by adding RNA dilutions to the cDNA synthesis reaction, then using the reaction products as the basis for real-time PCR quantification of a control gene. The C_t value for 0.2 μg RNA was in the linear portion of the graph of RNA amount vs. C_t, so 0.2 μg RNA was used for all cDNA synthesis reactions.

The TaqMan assay reaction mixture was 15 μl in PrimeTime Gene Expression Master Mix (Integrated DNA Technologies) with 500 nM of each primer and 250 nM of probe. Synthesized cDNA was diluted 1:5 and 5 μl added to each reaction. PCR amplification used an ABI 7500 Real-Time PCR System (Applied Biosystems) with 95°C for 3 min followed by 40 cycles of 95°C for 15 s and 60°C for 1 min. Triplicate reactions were run for the *C. metapsilosis* RNA samples while duplicate reactions were run for the other species to fit as many reactions from the same species onto a single PCR plate.

Combining data across plates relied on an identical set of controls that were present on each: CmACT1 and CmTEF1 for *C. metapsilosis* RNA, and CmCoCpACT1 and CmCoCpTEF1 for *C. parapsilosis* and *C. orthopsilosis* samples. TaqMan analyses for comparison to SYBR Green data used only the CmCoCpACT1 control since the published SYBR Green assay relied only on *ACT1* as a control (Lombardi et al., 2019). The default threshold for each primer was applied and ΔC_t calculated using Expression Suite software v1.1 (Thermo Fisher Scientific).

A control sample of RNA without reverse transcriptase was analyzed using the CmCoCpACT1 TaqMan assay to monitor background amplification caused by residual genomic DNA. In all reactions but one (*C. metapsilosis* 1-Y-61; C_t = 38.7), no detectable product was generated during 40 amplification cycles.

Simple calculation of means and standard errors of the mean used Prism7 software (GraphPad). The statistical significance of results was assessed using a mixed-model analysis of variance (PROC MIXED in SAS 9.4; SAS Institute Inc., Cary, NC, United States). Separation of means used the LSMEANS option.

[6]https://sites.duke.edu/vilgalyslab/rdna_primers_for_fungi

RESULTS

Number and Nature of *ALS* Genes in Each Species of the *C. parapsilosis* Complex

Three *C. parapsilosis* genome sequences (strains CDC317, CBS6318, GA1) were found in the National Center for Biotechnology Information (NCBI) database[7]. The annotated CDC317 sequence was also located in the *Candida* Genome Database[8]. BLAST using *C. albicans ALS* gene sequences as queries revealed five *ALS* genes in strain CDC317 (**Figure 1**). Four of the *ALS* genes were located on contig 006372 and transcribed in the same direction; the fifth gene was located on contig 006139 (**Figure 1**). The same five *ALS* genes were detected in strain CBS6318 and their arrangement appeared similar to strain CDC317. Only two *ALS* genes were apparent in the GA1 genome sequence: one was most similar to *CpALS4800* while the other most closely resembled *CpALS660*.

ALS genes in *C. orthopsilosis* were noted originally in the sequence of strain 90-125 that was available on the *Candida* Gene Order Browser (Maguire et al., 2013) and in the NCBI database. Because these sequences were incomplete due primarily to misassembled repeated sequence regions, we generated a new genome sequence using both Oxford Nanopore (long-read) and Illumina data (Lombardi et al., 2019). In collaboration with the laboratory of Arianna Tavanti (Pisa, Italy), we deduced the *ALS* genes and validated their sequence and variability. Strain 90-125 encoded three *C. orthopsilosis* genes (**Figure 1**). Two were contiguous on chromosome 3 and transcribed in the same direction while the third gene was on chromosome 2, reminiscent of the *ALS* gene arrangement in *C. parapsilosis*. Flanking regions of the genome were orthologous in each species. Genome sequences for two more *C. orthopsilosis* strains were available on the NCBI database: MCO456 and AY2. BLAST searches with *C. albicans* and *C. parapsilosis ALS* queries revealed multiple "hits," however, the sequences were not assembled completely enough to determine an accurate number of *ALS* loci.

A genome sequence for *C. metapsilosis* was available in the NCBI database (accession CBZN0200000000) and was reported to encode a single *ALS* gene (Pryszcz et al., 2015). We generated a novel genome assembly for strain ATCC 96143 using the long-read and Illumina technologies. The Oxford Nanopore flowcell produced over 4.3 Gb of sequence from 670,717 reads. The minimum read length was 1,000 bp while the maximum was 89,846 bp. The mean read length was 6,476 bp. The majority of reads were 6–30 kb in length, with the longest at 89 kb. The genome assembly separated into diploid chromosomes and was deposited in GenBank as assembly PQNC00000000. A summary of computational analyses and characteristics of the resulting genome sequences was provided in **Supplementary File S1**.

BLAST using previously identified *ALS* genes (including those from *C. albicans*, *C. parapsilosis*, and *C. orthopsilosis*) revealed four *ALS* genes in *C. metapsilosis* (**Figure 1**). Three

[7]www.ncbi.nlm.nih.gov

[8]www.candidagenome.org

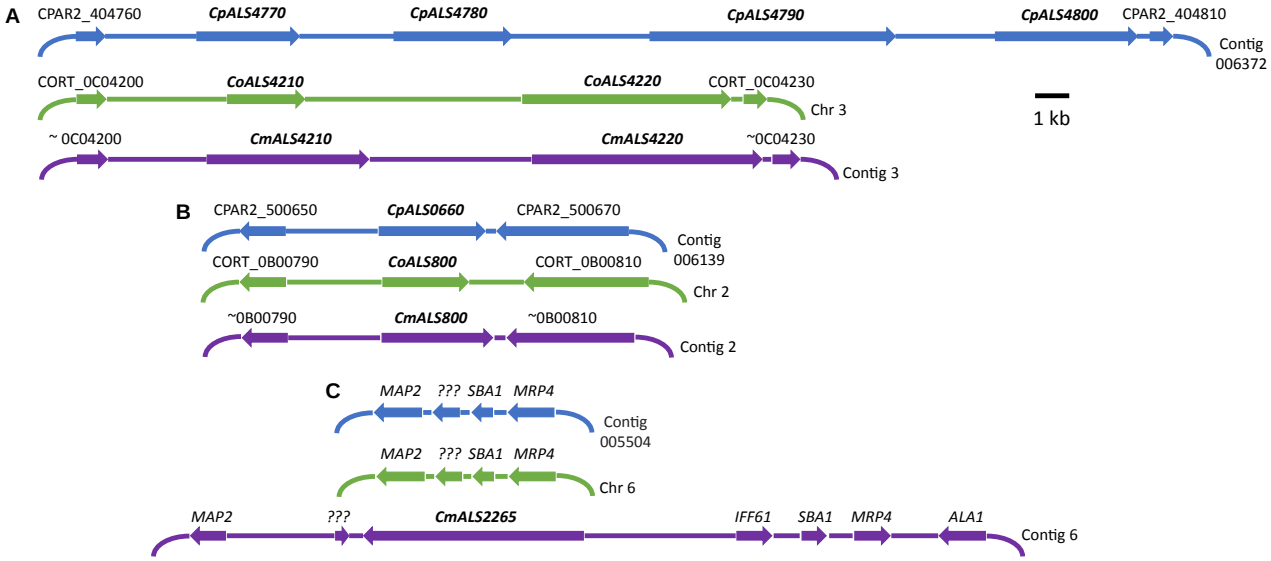

FIGURE 1 | Schematic of chromosomal locations of *ALS* genes in *C. parapsilosis*, *C. orthopsilosis*, and *C. metapsilosis*, drawn to scale. **(A)** Location of contiguous *ALS* genes on *C. parapsilosis* contig 006372, *C. orthopsilosis* chromosome 3, and contig 3 from the *C. metapsilosis* genome assembly PQNC00000000. *ALS* gene names are in bold italics type. Arrows show the direction of transcription for each gene. Flanking sequences were identified to indicate gene order conservation among the three species. Names of the flanking ORFs were taken from the *Candida* Genome Database (www.candidagenome.org) and/or GenBank. **(B)** Location of genes *CpALS0660* (*C. parapsilosis* contig 006139), *CoALS800* (*C. orthopsilosis* chromosome 2), and *CmALS800* (*C. metapsilosis* contig 2). Features were drawn similarly to **(A)**. **(C)** Location of the fourth *C. metapsilosis ALS* gene (*CmALS2265*) on contig 6. This region was orthologous to *C. parapsilosis* contig 005504 and *C. orthopsilosis* chromosome 6 but contained approximately 16 kb of extra sequence. The region contained the reading frame for *CmIff61* (GenBank accession number MK205443) that encoded a 341-amino acid protein not present in the other species. Gene names were shown above other coding regions. *???* encoded a hypothetical protein (*CPAR2_601270*; *CORT_0F02270*) that was conserved in all three species, but shorter in *C. metapsilosis*. *MAP2* = *CPAR2_601280*, *CORT_0F02280*; *SBA1* = *CPAR2_601260*, *CORT_0F02260*; *MRP4* = *CPAR2_601250*, *CORT_0F02250*. Some genes in this region (*ALA1*, *MRP4*, *SBA1*) were reminiscent of those that are located near *CaALS5*, *CaALS1*, and *CaALS9* on *C. albicans* chromosome 6 (Zhao et al., 2003).

were orthologs of the *C. orthopsilosis ALS* genes, reflecting the close relationship between the species (Tavanti et al., 2005). The fourth *C. metapsilosis ALS* gene did not have an ortholog in either *C. parapsilosis* or *C. orthopsilosis*. **Figure 1** shows the corresponding genome region where the fourth *C. metapsilosis ALS* gene was located and insertion of a 16-kb DNA fragment that was not present in either *C. parapsilosis* or *C. orthopsilosis*. BLAST of the published *C. metapsilosis* genome assembly (CBZN0200000000) showed the same four genes as detected in the new ATCC 96143 assembly.

The 20 diploid contigs for the new *C. metapsilosis* ATCC 96143 genome assembly were arranged in descending order by size; similar data were examined for the *C. orthopsilosis* and *C. parapsilosis* genomes (**Table 2**). Color coding indicated the location of *ALS* genes from **Figure 1A** (red), **Figure 1B** (blue), and **Figure 1C** (purple). Variable chromosomal localizations for the *ALS* genes suggested the potential for large karyotypic differences between these three closely related species. For example, the *ALS* gene cluster was located on chromosome 3 in *C. orthopsilosis*, and on the fourth-largest contig in *C. parapsilosis*. Although *CpALS0660* and *CoALS800* appear to be orthologs, one is found on the sixth-largest contig in *C. parapsilosis* and on the second-largest in *C. orthopsilosis*. Karyotypes for these species were not apparent in the literature, nor were tools such as a physical map that was essential for guiding assembly of the *C. albicans* genome (Chu et al., 1993).

Identification of new *ALS* genes raised the question of how they should be named. *ALS* genes in *C. albicans* are numbered starting with "1" and include *ALS1* through *ALS7*, and *ALS9* (Hoyer et al., 2008). Because the new genes presented here were different from the *C. albicans ALS* genes, we developed a new naming scheme based on **Figure 1**. The gene names (**Table 3**) reflected the close relationships between *ALS* genes in the *C. parapsilosis* species complex. The names accurately reflected the arrangement of genes on the various contigs, and the annotation available in the first genome assembly deposited in the NCBI database. For example, the names *CpALS4770* and *CpALS4780* suggested that the ORFs were *ALS* genes from *C. parapsilosis*. The consecutive numbers (4770 and 4780) were taken directly from the genome annotation and indicated that the genes were contiguous. Literature precedent for these ideas was already present (**Table 3**).

Annotation of the *C. orthopsilosis* assembly proceeded somewhat differently than for *C. parapsilosis* (Riccombeni et al., 2012), leading to a different numbering scheme (**Figure 1**). We preserved the genome annotation tags in the names of the *ALS* genes (e.g., *CoALS800* came from *CORT_0B00800*). This scheme was carried forward to the gene names for the relatively unannotated *C. metapsilosis* genome assembly. Because the *C. orthopsilosis* and *C. metapsilosis* species were more closely related to each other than either was to *C. parapsilosis* (Tavanti et al., 2005), *C. metapsilosis ALS* gene names were

TABLE 2 | Chromosomes and contigs for the *C. parapsilosis*, *C. orthopsilosis*, and *C. metapsilosis* genome sequences.

C. orthopsilosis			*C. parapsilosis*			*C. metapsilosis*	
Chr.	**Size (Mb)**	**Accession number**	**Contig**	**(Mb)**	**Accession number**	**Contig**	**Size (Mb)**
1	2.94	HE681719.1	005809	3.02	HE605206.1	0	3.75, 3.68
2	**2.43**	**HE681720.1**	005569	2.24	HE605203.1	1	2.11, 2.06
3	**1.64**	**HE681721.1**	005807	2.09	HE605205.1	**2**	**1.70, 1.69**
4	1.59	HE681722.1	**006372**	**1.79**	**HE605208.1**	**3**	**1.37, 1.34**
5	1.47	HE681723.1	005806	1.04	HE605204.1	4	1.08, 1.07
6	**1.03**	**HE681724.1**	**006139**	**0.96**	**HE605207.1**	5	0.90, 0.89
7	0.94	HE681725.1	006110	0.96	HE605209.1	**6**	**0.70, 0.70**
8	0.61	HE681726.1	**005504**	**0.90**	**HE605202.1**	7	0.68, 0.64
						8	0.33, 0.33
						9	0.32, 0.31
						10	0.23, 0.22
						130	0.11, 0.11
						11	0.10, 0.09
						12	0.073, 0.064
						13	0.050, 0.050
						14	0.039, 0.039
						15	0.037, 0.036
						16	0.034, 0.034

Information was recorded for C. orthopsilosis 90-125 genome assembly ASM31587v1, C. parapsilosis CDC 317 genome assembly ASM18276v2, and the C. metapsilosis ATCC 96143 assembly PQNC00000000. Chromosome and contig sequences were ordered from largest to smallest within each species. C. orthopsilosis and C. parapsilosis were reported as haploid assemblies; diploid contigs were available for C. metapsilosis. Color coding indicated the location of the ALS gene cluster shown in ***Figure 1A*** *(red), the single ALS gene shown in* ***Figure 1B*** *(blue), and the region encoding the unique CmALS2265 gene in* ***Figure 1C*** *(purple). Two C. metapsilosis contigs that encode mitochondrial genome sequences were not included in the table.*

matched to the *C. orthopsilosis* names. The name of the new gene, *CmALS2265*, reflected its location in the *C. metapsilosis* genome, while paying homage to the *C. orthopsilosis* assembly (i.e., it occupied the orthologous physical location between *CORT_0F02260* and *CORT_0F02270*).

TABLE 3 | *ALS* genes from the *Candida parapsilosis* species complex and their GenBank accession numbers.

Gene	**Size (bp)**	**GenBank Accession**	**Other References**
***C. parapsilosis* strain CDC317**			
CpALS4770	3003	MH753532	*ALS1*[a], *404770*[b]
CpALS4780	3450	MH753533	*ALS5*[a], *404780*[b]
CpALS4790	7179	BK010629	*ALS3*[a], *404790*[b]
CpALS4800	4152	BK010630	*ALS4*[a], *CpALS7*[b], *CPAR2_404800*[c]
CpALS660	3072	MH753534	*ALS2*[a], *500660*[b]
***C. orthopsilosis* strain 90-125**			
CoALS4210	2457	MG799558	
CoALS4220	6078	MG799559	
C0ALS800	2499	MG799557	
***C. metapsilosis* strain ATCC 96143**			
CmALS4210-1	4722	MH753528	
CmALS4210-2	3267	MH753529	
CmALS4220-1	6714	MH753512	
CmALS4220-2	6837	MH753527	
CmALS800	3234	MH753530	
CmALS2265	6489	MH765692	

Other references to the ALS genes were from [a]Pryszcz et al., 2013; [b]Neale et al., 2018; [c]Bertini et al., 2016.

Als Protein Structure Encoded by the *C. parapsilosis* Species Complex *ALS* Genes

ALS gene sequences were translated to amino acids, then used to draw a schematic of Als protein features (**Figure 2**). Color coding indicated similarities between the proteins. Visualization of the protein sequences provided additional insight into the gene arrangement displayed in **Figure 1**. For example, *CpALS4790* and *CpALS4800* each encoded proteins with a central tandem repeat domain, while proteins predicted by *CpALS4770* and *CpALS4780* were very similar to each other. These observations suggested that *CpALS4780* and *CpALS4800* arose by duplication of genes *CpALS4770* and *CpALS4790*, respectively. *CoALS4210* and *CmALS4210* were orthologs of *CpALS4770* while a similar relationship was evident for *CoALS4220*, *CmALS4220*, and *CpALS4790*. Proteins predicted from genes *CpALS0660*, *CoALS800*, and *CmALS800* were all very similar, consistent with the conserved genomic context for these ORFs.

Each predicted protein from the *C. parapsilosis* species complex (**Figure 2**) fulfilled various criteria for inclusion in the Als family. The proteins had a secretory signal peptide and a site for GPI anchor addition, consistent with a final localization in the fungal cell wall, linked to β-1,6-glucan (Lu et al., 1994). The high percentage of Ser and Thr in each protein, particularly in repeated sequences and toward the C-terminal end, also was consistent

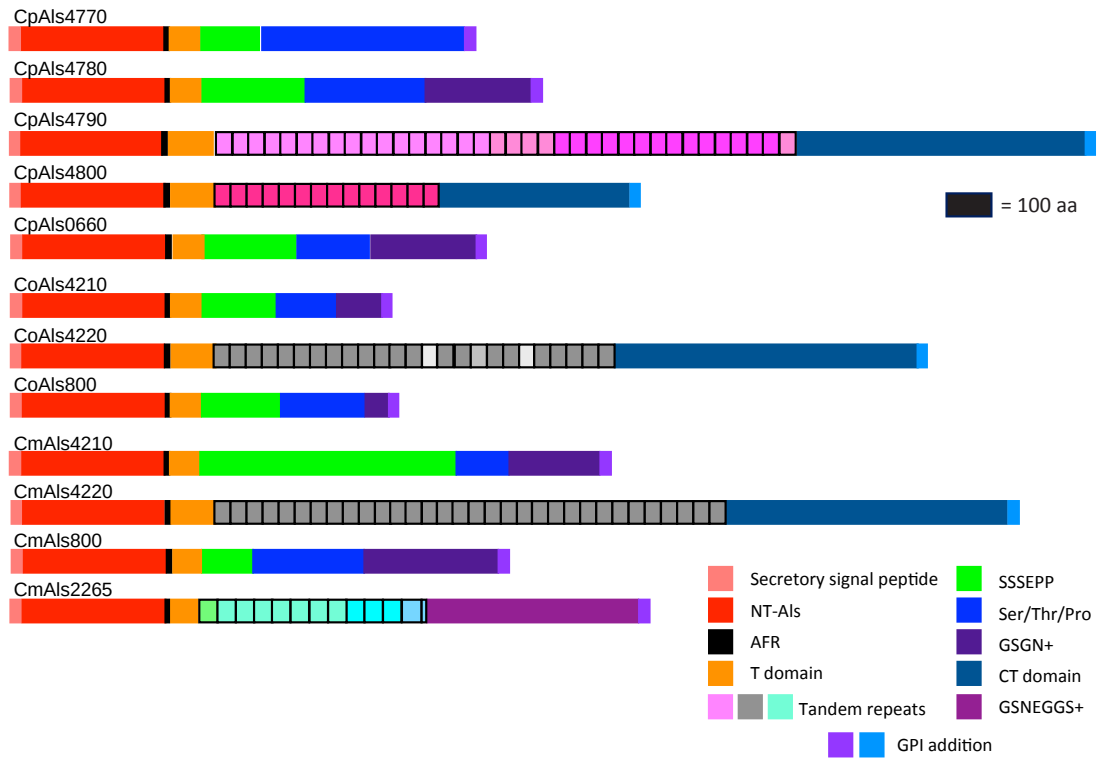

FIGURE 2 | Schematic of proteins predicted from the *ALS* genes of the *C. parapsilosis* species complex. Each predicted protein had a secretory signal peptide, a classical NT-Als domain with eight conserved Cys residues to direct folding, an amyloid-forming region (AFR; Garcia et al., 2011), a Thr-rich sequence (T domain), a C-terminal domain rich in Ser/Thr, and a signal for addition of a GPI anchor that directs the mature protein to a final localization linked to β-1,6-glucan in the fungal cell wall (Lu et al., 1994). Only 5 of the 12 proteins included a central domain of tandemly repeated sequences like those found in *C. albicans* Als proteins (Hoyer et al., 2008). Different colors of the repeated units indicated differences in consensus sequence; shading within the same protein indicated repeat units that varied in the number of amino acids. The other proteins had regions of short, imperfect repeated sequences such as Ser-Ser-Ser-Glu-Pro-Pro (SSSEPP) and/or Gly-Ser-Gly-Asn (GSGN). CmAls2265 had the NT-Als domain attached to tandemly repeated sequences from the Iff/Hyr family (Bates et al., 2007; Boisramé et al., 2011) and a C-terminal region more-characteristic of Iff/Hyr proteins than *C. albicans* Als proteins.

with composition of *C. albicans* Als proteins (Hoyer et al., 2008). Most importantly, each protein had an N-terminal domain that was similar to *C. albicans* NT-Als3 where adhesive function resides (Lin et al., 2014). NT-Als folding is driven by eight conserved Cys residues (Salgado et al., 2011), that were found in each predicted protein from the *C. parapsilosis* species complex.

NT-Als adhesive function is due to a PBC that can accommodate up to six C-terminal amino acids from peptide ligands in an extended conformation (reviewed in Hoyer and Cota, 2016). Als proteins recognize diverse peptide ligands with different Als proteins demonstrating higher-affinity interactions for specific sequences. Nucleotide sequences encoding NT-Als from the newly characterized genes were included in a phylogenetic analysis with the corresponding regions from the *C. albicans ALS* genes (**Figure 3**). *C. albicans* sequences grouped together in a manner that reflected known protein function (reviewed in Hoyer and Cota, 2016).

Based on positions of the genes in the phylogenetic tree, a few examples were selected for further examination of variation within the predicted PBC. Models of CpAls4790, CoAls4210, and CmAls2265 were created based on the structure of *C. albicans* Als9-2 (CaAls9-2) bound to the C-terminal residues of human fibrinogen gamma peptide (Protein Data Bank ID 2y7n; Salgado et al., 2011). For CaAls9-2, peptide binding is anchored by a salt bridge with an invariant Lys59 and further stabilized by main chain hydrogen bonding interactions residues S170, T293, and W295. The peptide has an extended conformation with side chains oriented alternatively on opposite sides of the peptide backbone similar to residues in a β strand. The amino acid side chains are inserted into conserved pockets of the protein. Amino acids lining the cavity are variable among known Als protein sequences, presumably modulating binding specificities among proteins in the Als family (Lin et al., 2014).

Peptide-binding cavities for the new Als proteins were analyzed by sequence and structural comparisons (**Figure 4A**). Differences in size and electrostatic potential were assessed to compare peptide-binding capacities among the NT-Als proteins. The PBC was considered as multiple pockets (called C1 through C5) to facilitate this analysis. The sixth amino acid was not included in the analysis since the position was highly solvent-exposed in the CaAls9-2 structure.

There were large differences in PBC shape and charge among the proteins consistent with accommodation of peptides of various sequences. For example, the pocket surrounding the first

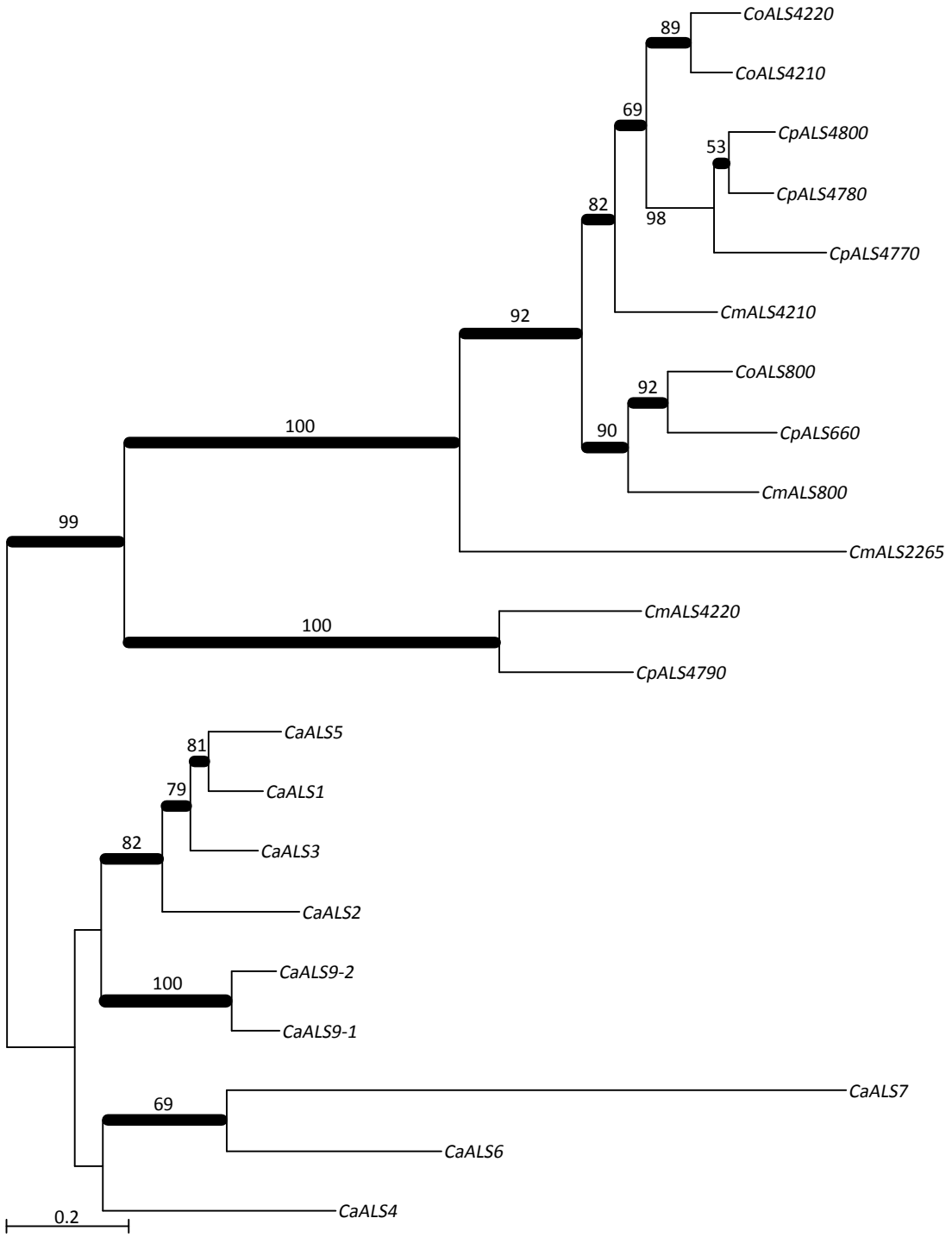

FIGURE 3 | Phylogenetic tree of *ALS* sequences from *C. albicans* and the *C. parapsilosis* species complex. The tree was drawn using a ML analysis after removing ambiguous regions using Gblocks. Thickened branches indicated Bayesian posterior probabilities >95% while the numbers above the branches were bootstrap values >50%. The tree showed strong support for many branches.

C-terminal residue (proximal to the invariant Lys) in CaAls9-2 was formed by hydrophobic and hydrophilic residues suggesting the likelihood to accommodate a variety of amino acids. However, in CpAls4790, the pocket was much more constrained by substitution of CaAls9-2 Val22 with Arg in CpAls4790. The Arg residue filled a large part of the pocket and presented a positive charge directly adjacent to the C1 amino acid of the bound peptide. The substitution of Val22Arg in CpAls4790 suggested

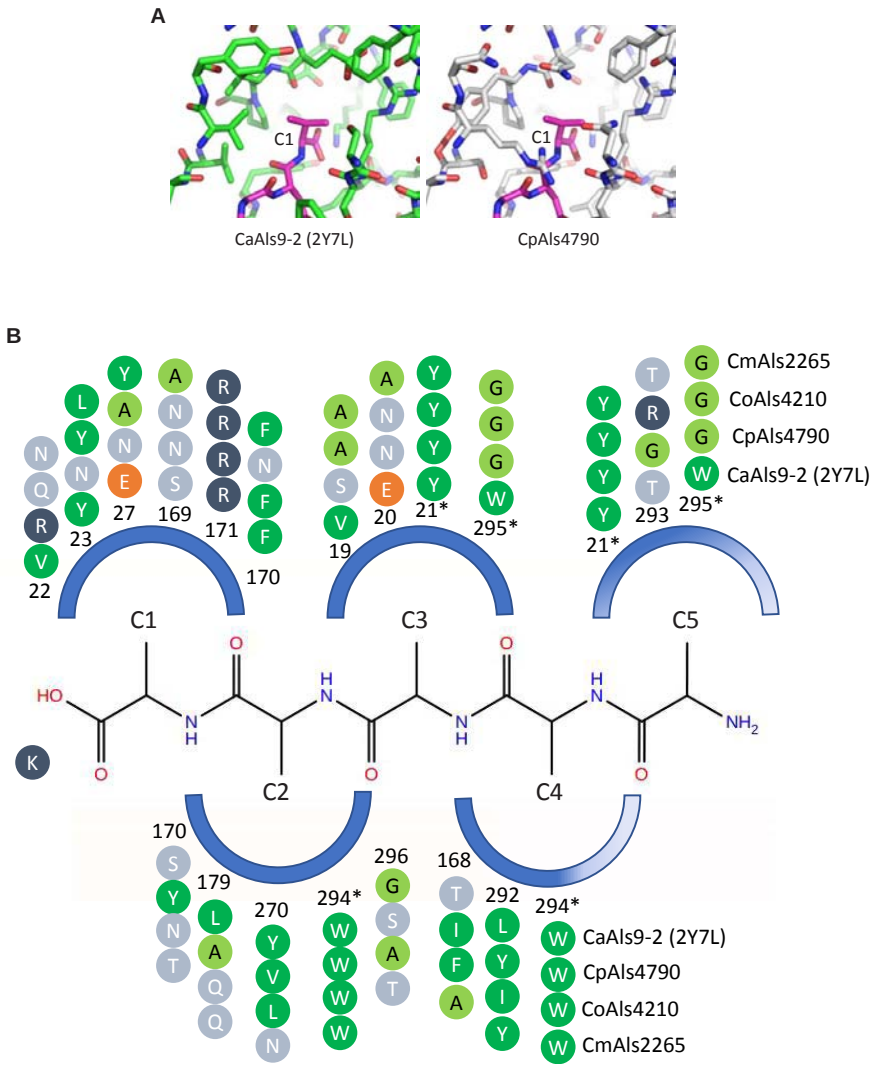

FIGURE 4 | Structural comparison among peptide-binding cavities (PBCs) of a model Als protein and selected proteins from the *C. parapsilosis* species complex. **(A)** Side-by-side comparison of the C1 binding pocket of CaAls9-2 (left, green carbons; Protein Data Bank ID 2Y7N; Salgado et al., 2011) and a structural model of CpAls4790 (right, gray carbons) bound to fibrinogen gamma peptide (magenta carbons). The pocket was more constrained in CpAls4790 by the Val22Arg substitution, suggesting a more-selective binding activity than present in CaAls9-2. **(B)** Schematic of the NT-Als PBC showing the pockets surrounding amino acids of the bound peptide ligand (C1 through C5, with C1 proximal to the invariant Lys at the bottom of the PBC). Only residues which form the binding pocket were shown. Example proteins (CpAls4790, CoAls4210, CmAls2265) were selected from diverse parts of the phylogenetic tree in **Figure 3**. Side chain residues were indicated as circles and color-coded green (medium to large hydrophobic), light green (small hydrophobic), dark blue (positively charged), orange (negatively charged), or light blue (hydrophilic), and numbered to indicate their position within each protein. Residues with an asterisk were part of two pockets and the sequence was repeated for each pocket. The schematic highlights conserved positions (e.g., Y21, R171, W294) and illustrates variability found throughout the PBC.

a more-selective ability to accommodate amino acids in the C1 position of the peptide sequence compared to CaAls9-2.

Further analysis of the first five C-terminal amino acids of the bound peptide identified the nearest residues within 8 Å of the β carbon of each amino acid in the peptide (or hypothetical β carbon in the case of glycine residues) which form the surface of the amino acid binding pocket. The sequence patterns of the C1 through C5 pockets showed variations in ability to accommodate peptide residues by both size and electrostatics (**Figure 4B**). Pocket C3 was highly constrained by close packing of neighboring residues allowing for accommodation of only very small or small residues like Gly, Ala, or Ser. Pockets C4 and C5 were partially solvent-exposed suggesting the likelihood of higher size promiscuity in accepting hydrophilic residues in these positions. Overall, the analysis was consistent with the conclusion that the *C. parapsilosis* species complex Als proteins possessed peptide-ligand binding activity similar to the highly characterized examples in *C. albicans* and, like the CaAls proteins, the newly identified proteins will demonstrate differences in selectivity for peptide binding.

Another common feature of *C. albicans* Als proteins is a central domain of multiple tandem copies of a 36-amino acid

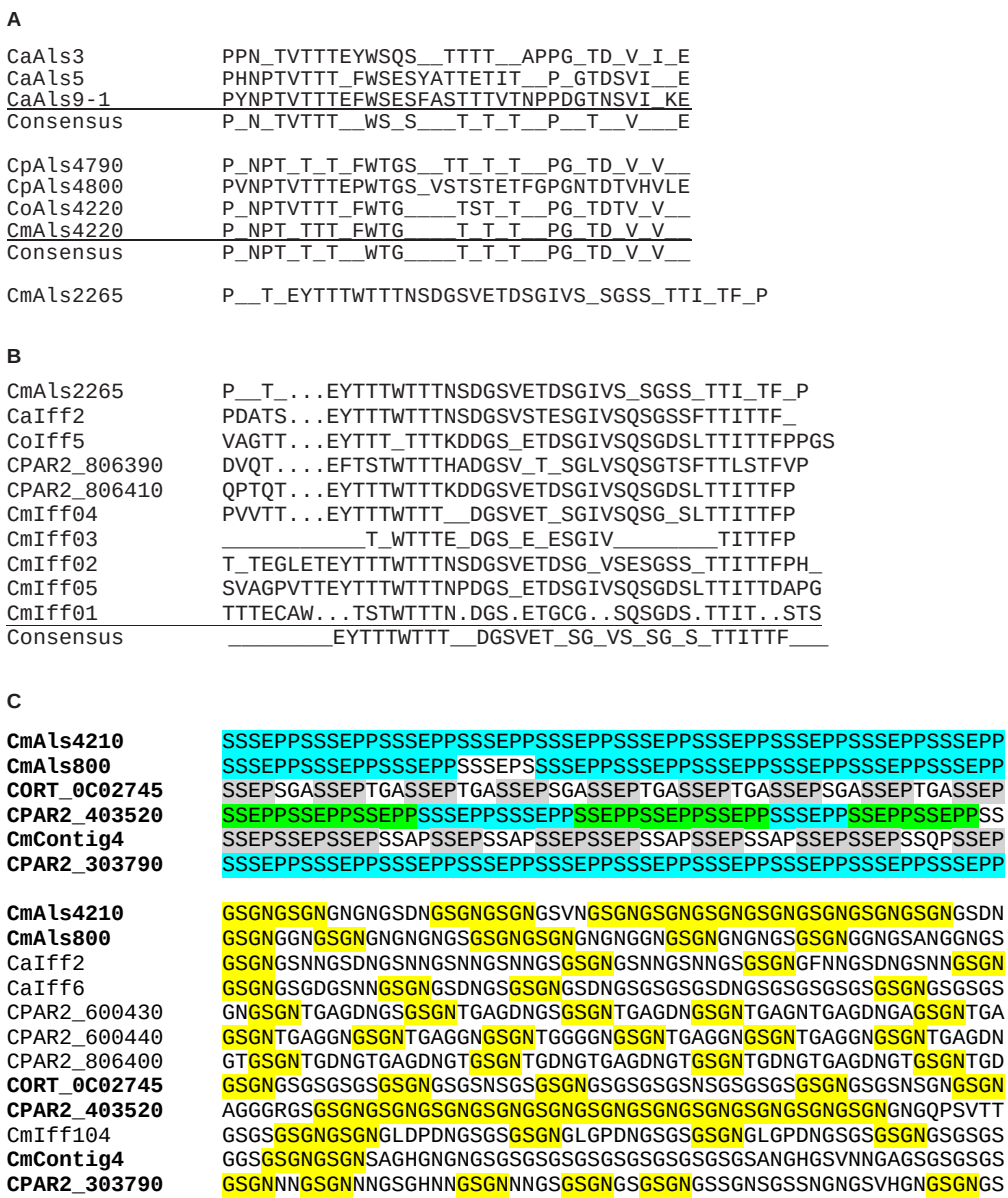

FIGURE 5 | Conservation of tandemly repeated sequence units and short, imperfect repeats in various *C. albicans* and *C. parapsilosis* species complex proteins. **(A)** Consensus tandem repeat sequences were derived for *C. albicans* Als3 (CaAls3; GenBank accession number AY223552), CaAls5 (AY227440), and CaAls9-1 (AY269423). In *C. albicans*, each tandemly repeated unit was a perfect 36-aa length. Consensus sequences required that 80% or more of the amino acids were identical at each position. A similar approach was taken to aligning the consensus tandem repeat units from proteins from *C. parapsilosis*, *C. orthopsilosis*, and *C. metapsilosis*. GenBank accession numbers were shown in **Table 3**. In these proteins, the 36-amino acid repeat unit length was not necessarily conserved in each copy as color coded in **Figure 2**. The consensus repeat unit from CmAls2265 was 42 amino acids and different from the other Als proteins. **(B)** Alignment of consensus tandemly repeated sequence units from CmAls2265 and proteins from the Iff family. Repeat unit length was not necessarily conserved among the proteins, but a consensus sequence emerged from comparison among multiple proteins. GenBank accession numbers for the proteins were shown in **Supplementary Table S4**. **(C)** Top panel: *C. parapsilosis* species complex proteins that encode the short, imperfect SSSEPP (blue)/SSEPP (green)/SSEP (gray) repeated motif. Lower panel: Proteins that encode the GSGN (yellow) repeated motif. Protein identifiers were noted at the left of each sequence. The sequence labeled CmContig4 (GenBank accession number MK215077) most closely matched CORT_0E05950, which was annotated as Cdc24 GDP-GTP exchange factor, an unlikely identification of its function. Other proteins were labeled with identifiers from GenBank sequences or from the proteins listed in **Supplementary Table S4**. Names for proteins that had both SSEP/SSSEPP and GSGN short, imperfect repeats were listed in bold type in the top and lower panels.

Ser/Thr-rich sequence. Previous thought had considered the *C. albicans* tandem repeats as grouping into three consensus sequences, represented by CaAls3, CaAls5, and CaAls9-2 (Hoyer et al., 2008). Although the absolute sequences are notably variable among different *C. albicans* Als proteins, a consensus sequence can be derived (**Figure 5A**). This consensus sequence

was also found among proteins in the *C. parapsilosis* species complex tandemly repeated sequence units in the center of the protein (**Figure 2**). However, the repeated unit in CmAls2265 was clearly different in length and sequence from the other proteins. A BLAST search using the CmAls2265 repeat sequence as a query revealed the sequence in the *C. albicans* Iff family (**Figure 5B**) (Bates et al., 2007; Boisramé et al., 2011). This protein family was initially defined during annotation of the *C. albicans* genome sequence with "Iff" denoting Ipf family F, a group of proteins with similar sequence. The *C. albicans* Iff family also includes Hyr1 (Bailey et al., 1996). Subsequent investigations demonstrated various roles for these proteins, with a common feature being exposure on the cell surface (Boisramé et al., 2011). **Supplementary Table S4** lists the currently recognized Iff proteins in *C. albicans*, as well as those revealed by BLAST searches of the *C. parapsilosis*, *C. orthopsilosis*, and *C. metapsilosis* genomes.

Analysis of the Iff family revealed its own consensus repeat sequence (**Figure 5B**) although the repeat was not found in each protein, and protein length varied considerably (**Supplementary Table S4**). A thorough description of the Iff family in *C. parapsilosis* and *C. orthopsilosis*, and comparison to the *C. albicans* Iff family was presented by Riccombeni et al. (2012) so will not be expanded upon here. Of highest importance to the current discussion was the idea that CmAls2265 was a hybrid protein, comprised of an NT-Als adhesive domain placed upon the "foundation" of an Iff protein. CmAls2265 was evidence of a recombination event between genes from two different cell wall-protein-encoding families as defined in *C. albicans*. The recombination event appeared specific to *C. metapsilosis*, as a similar gene was not found in either *C. parapsilosis* or *C. orthopsilosis*, highlighting another difference between the closely related species.

Some of the predicted Als proteins (**Figure 2**) had short, imperfect repeated sequences instead of the longer tandemly repeated units. Predominant sequence motifs in these proteins included SSSEPP, which tended to immediately follow the classical Als T domain, and GSGN, which was located more-proximal to the C-terminal end of the protein. These sequences were present in other cell-wall proteins from *C. albicans* and the *C. parapsilosis* species complex (**Figure 5C**). The GSGN motif was common among the Iff proteins including CaIff2, CaIff6, CPAR2_600430, CPAR2_600440, CPAR2_806400, and CmIff104. The SSSEPP motif was found in other proteins, such as CPAR2_303790, a hypothetical protein that also included the GSGN motif. The SSSEPP sequence sometimes was truncated (SSEPP or SSEP) and found in proteins that also included the GSGN sequences. One example was CORT_0C02745 (an Iff protein) and another was CPAR2_403520, which was annotated as a hypothetical protein with similarity to *C. albicans* Hwp1 (Staab et al., 1999). Sequence alignments between CPAR2_403520 and *C. albicans* Hwp1 did not produce convincing evidence of sequence conservation that suggested CPAR2_403520 had similar function to CaHwp1 (data not shown). The final protein that had both GSGN and SSEP was located on contig 4 of the new *C. metapsilosis* assembly and deposited in GenBank under accession number MK215077. The best match to this sequence was CORT_0E05950, currently annotated as Cdc24 GDP-GTP exchange factor. The presence of several sequences with the potential for such diverse function suggested more widespread domain swapping among proteins than indicated for CmALS2265. These observations also suggested the need for more-careful annotation of the sequences of the pathogenic fungi with respect to genes that encode cell-wall proteins with potential to interact with the host, other microbes, and the external environment.

Allelic Variability Among the *C. parapsilosis* Complex *ALS* Genes

Allelic variability can be considered at multiple levels: the number of *ALS* genes in a specific fungal isolate is perhaps the most general. PCR was used to monitor *ALS* gene presence in additional strains of each species (**Table 1**). Primers were detailed in **Supplementary Table S1**. *C. parapsilosis* strains 949, 950, and 1125 each had the five known *ALS* genes, suggesting at least five *ALS* genes in each strain. Similar results were obtained for *C. orthopsilosis* and reported by Lombardi et al. (2019) where four different clinical isolates each encoded the three known *C. orthopsilosis ALS* genes. Analysis of *C. metapsilosis* isolates 61, 88, 397, and 482 indicated that, like the genome isolate ATCC 96143, each encoded four *ALS* genes.

C. parapsilosis, *C. orthopsilosis*, and *C. metapsilosis* are diploid, suggesting the potential for sequence and gene-length polymorphisms within each isolate. Current genome sequences for *C. parapsilosis* (CDC317; GenBank accession ASM18276v2) and *C. orthopsilosis* (90-125; ASM31587v1) are presented as haploid assemblies. These sequences were used as the basis for design of PCR primers to assess sequence and length polymorphisms among the *ALS* genes. Sequence polymorphisms were detected by Sanger sequencing of the PCR product. Length polymorphisms were visualized on agarose gels. This approach was effective at general validation of the published genome sequences although limitations must be recognized. For example, Sanger sequence reads were approximately 800-nt long, indicating the largest DNA fragment that could be assembled accurately was around 1.5 kb. PCR products larger than this size, or those that provided diploid allelic fragments of considerably different size were not amenable to this analysis. Accurate assignment of sequence polymorphisms to a specific allele would require construction of a heterozygous deletion mutant for each gene.

Overall, however, these methods validated the high degree of accuracy of the CDC317 genome assembly. Because PCR products represented both alleles of the diploid species, sequence ambiguities were present in the Sanger data where there was variation in the allelic sequences. In general, sequence variation was greater toward the 3′ end of the gene, perhaps due to conservation of the sequence that encodes the NT-Als binding domain. Polymorphic nucleotides were less than 1% of the total sequence reads among the fragments meeting the criteria described above. In one instance, the CDC317 sequence diverged from our Sanger validation (**Figure 6A**), but only by 12 nucleotides in a region of short, imperfect repeats. Repeated

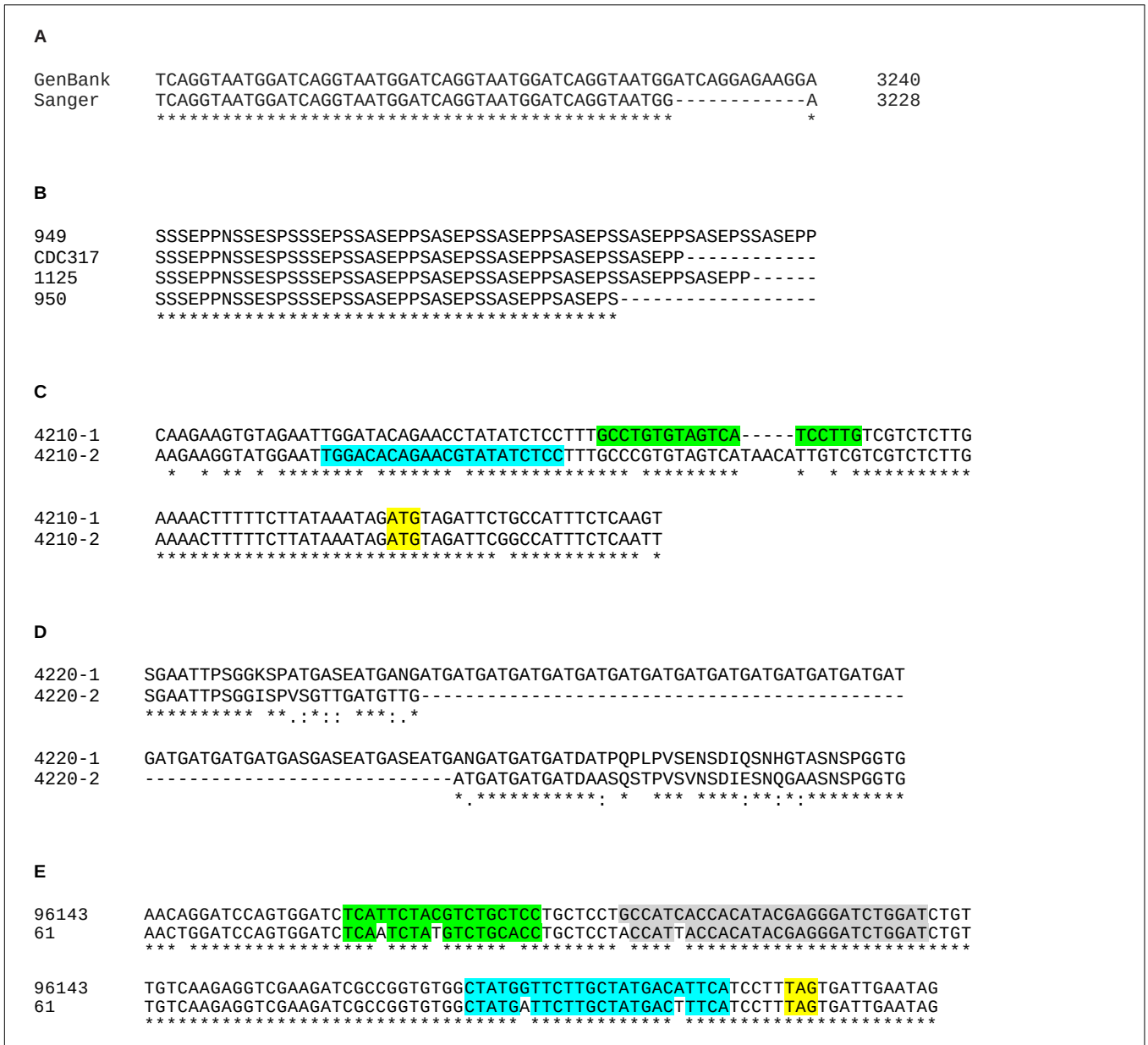

FIGURE 6 | Examples of allelic sequence variation among *ALS* genes in the *C. parapsilosis* species complex. **(A)** The representative genome sequence for *C. parapsilosis* CDC317 (GenBank accession ASM18276v2) presented *ALS* genes in a highly accurate manner. Sanger sequencing in the current study revealed many sequence polymorphisms in the diploid *C. parapsilosis ALS* genes that were not reflected in the haploid GenBank assembly. However, there was only one notable example where Sanger sequence varied from the GenBank genome: *CpALS4780* had 12 fewer nucleotides in the region of the gene that encodes the GSGN short, imperfect repeat. **(B)** Regions of repeated sequences were often variable in length as shown in this example of *CpALS4770* alleles from various *C. parapsilosis* isolates (949, CDC317, 1125, 950). Manual alignment of the amino acid sequences underscored the different length of *CpALS4770* alleles in this region, leading to differing numbers of copies of the SSSEPP short, imperfect repeat. **(C)** The new *C. metapsilosis* genome assembly resolved into alleles and revealed previously unrecognized allelic variation that affected data interpretation. Primers to amplify *C. metapsilosis ALS* genes initially were designed from the representative genome sequence in GenBank (CBZN0200000000). The original forward primer to amplify *CmALS4210* (highlighted in green) amplified only allele 1 due to mismatches and extra nucleotides in the sequence for allele 2. Re-design of the primer (highlighted in blue) led to successful amplification of the *CmALS4210-2* allele, distinguishing it from *CmALS4210-1*. The *CmALS4210* start codon was highlighted in yellow. **(D)** Alignment between amino acid sequences predicted from the *CmALS4220* alleles. Considerable sequence variation between the alleles was observed including an expanded repeated sequence (Gly-Ala-Thr; GAT) in *CmAls4220-1*. These differences were predicted by the new *C. metapsilosis* genome sequence and verified by Sanger sequencing. **(E)** Allelic variation between strains of *C. metapsilosis* that affected interpretation of TaqMan assay data (see below). TaqMan assays were designed from the sequence of *C. metapsilosis* strain ATCC 96143. Nucleotide polymorphisms at the 3′ end of *CmALS2265* in strain 61 resulted in reduced detection by the TaqMan assay. The stop codon for *CmALS2265* was highlighted in yellow. The mismatches between the sequences for the forward primer (green), reverse primer (blue), and probe (gray) were sufficient to severely under-estimate relative gene expression for *CmALS2265* in strain 61, suggesting that the gene was barely transcribed.

DNA was the largest source of length variation between alleles in the same strain and between different strains. Allelic variation in the "classic" *ALS* repeat units was the most notable, with the potential to vary by as much as a few kb between alleles. **Figure 6B** shows an example of length variation within a region of short, imperfect repeats of CpALS4770 in five different *C. parapsilosis* isolates. Length polymorphisms between alleles in the same and different *C. orthopsilosis* isolates were documented clearly by Lombardi et al. (2019).

Advances in genome assembly software provide the tempting possibility to resolve allelic variation without the tedious and self-limiting validation steps described above. The newly derived *C. metapsilosis* ATCC 96143 genome assembly separated into allelic sequences. *CmALS800* was a complete, accurate sequence in both alleles, without any differences between the allelic nucleotide sequences. *CmALS800* was deposited in GenBank as a single allele (**Table 3**). In contrast, *CmALS4210* and *CmALS4220* each produced distinct allelic sequences in the new genome assembly that were deposited separately into GenBank (**Table 3**). Sequence polymorphisms were present throughout the coding region. In fact, sequence polymorphisms prevented *CmALS4210-2* from amplification with PCR primers designed against the published genome sequence (**Figure 6C**). Sequence differences within the region encoding NT-Als produced conservative changes unlikely to affect protein function. Length polymorphisms were most evident in regions of repeated sequences, with size estimates confirmed by agarose gel analysis of PCR products. The 3′ end of *CmALS4220-1* encoded expansion of a novel repeated sequence (**Figure 6D**).

CmALS2265 was essentially identical in the genome assembly allelic sequences, although neither produced a complete open reading frame that encoded a full-length protein. The *CmALS2265* sequence had to be corrected by the PCR amplification and Sanger sequencing steps described above. To the extent possible using PCR amplification and Sanger data, the allelic sequences were validated as accurate in length and sequence. In one instance, nucleotide differences between *C. metapsilosis* strains affected use of a TaqMan assay designed to measure relative gene expression (**Figure 6E**; see below). Overall, these data provided evidence that the combination of short- and long-read sequence data and use of emerging genome assembly methodologies promise to more-accurately assemble genes that contain repeated sequences and resolve allelic variation in diploid species.

Relative Expression Levels of *ALS* Genes in the *C. parapsilosis* Species Complex

One major goal of this work was to design and validate real-time PCR assays that can be used for quantification of relative *ALS* expression. Assay design was complicated by the high degree of similarity between *ALS* loci in the same species. TaqMan assays were used to exploit their ability to specifically differentiate between highly similar sequences. Initial assay design attempted to standardize the location of the assay in each gene by using the region approximately 800 to 1,000 nt after the start codon. Primer and probe sequences for each assay were shown in **Supplementary Table S2**. Initial work focused on *C. orthopsilosis* since it encoded only three *ALS* genes.

CoALS4210, *CoALS4220*, and *CoALS800* were >75% identical in the targeted region (**Figure 7A**), providing the opportunity to demonstrate the ability of TaqMan assays to generate highly specific results. Dilutions of cloned target sequences were tested with the various assays and showed specific amplification only for matches between a given TaqMan assay and its intended target. Mismatched assay and targets were generally undetectable, even when adding large quantities of cloned plasmid to the reaction (**Figure 7B**).

Validated *CoALS* TaqMan results were compared to results from a previously reported SYBR Green-based assay (Lombardi et al., 2019). *C. orthopsilosis* strain 90-125 was grown in YPD Medium for 1 h and gene expression assessed using the SYBR Green and TaqMan assays. For SYBR Green, *CoALS4220* showed the highest relative expression, followed by *CoALS4210* (**Figure 8A**). The expression level for *CoALS800* was considerably lower than the other two genes. Results from the TaqMan assays showed the highest expression for *CoALS4220*, with *CoALS4210* and *CoALS800* at a similarly low expression level (**Figure 8A**).

One set of the SYBR Green assay primers (*CoALS800*) was located within the region to which the TaqMan assays were targeted while the others were located at the 3′ end of each gene (Lombardi et al., 2019). We used the gene with the highest expression level, *CoALS4220*, to test the effect of TaqMan assay location (5′ end vs. 3′ end of the gene), and method for priming cDNA synthesis (random hexamers vs. oligo dT). Since *CoALS4220* was 6078 bp long, we expected a low estimate of gene expression for the combination of the 5′ end assay and oligo dT priming of cDNA synthesis (**Figure 8B**). The relative gene expression from the combination of random hexamer priming and the 3′ end TaqMan assay was significantly higher than the other combinations ($P < 0.0001$). For each cDNA priming method, the 3′ end TaqMan assay gave a significantly higher gene expression estimate than the 5′ end assay ($P = 0.002$ for random hexamers; $P < 0.0001$ for oligo dT). Subsequent assays used random hexamer priming to make cDNA and both the 5′ and 3′ assays. The trend of lower gene expression (higher C_t) estimates from the 5′ end assay continued in cells grown for 24 h in YPD medium (**Figure 8C**). *CoALS4220* was expressed more highly than the other genes in the two growth conditions studied ($P < 0.0001$).

Because of these results, both 5′ and 3′ end assays were developed for each of the 5 *ALS* genes in *C. parapsilosis* (**Figure 8D**). Two different strains were studied (genome strain CDC317, and ATCC 22019, the *C. parapsilosis* type strain). Cells were grown under two different conditions to dissect potential effects of strain, growth stage, and growth medium. One growth condition was suggested by the work of Lackey et al. (2013) who indicated that it promoted *C. parapsilosis* morphological change. *CpALS4790* was the most highly expressed gene in each growth condition, with similar estimates produced by the 5′ and 3′ end TaqMan assays. In many instances, the gene expression estimates from the 5′ end and 3′ end TaqMan assays were similar. Color coding in the image highlighted exceptions where the 3′ end assay provided as much as five cycles higher gene expression estimate

A

```
CoALS800    TCCTACTGGTCAAAGTTTACAAACATCTTATACTAACACATACTTGTGTGCTGGAGATTCGTTTCCTAACGATGGATCAAGATCTGTTACT
CoAls4210   TCCGGCTGGTCAACAATTACGCACAAGTTATACTAATACGTATCAATGTGCAGGGCAGTTATTTCCGCGCGACAATTCGAGACTGATAAGA
CoAls4220   TCCAAATGGTCAGAGATTGAAAGCAAGTTACACAAACAGATACCAATGCGCTGATGAAGTTGGTAGTCACGACAACTCCAAATCAATTACA
            ***   ******    **      **  *** ** ** *  **    ** ** *   *      *     ***    ** * *    * *

CoALS800    TGGTCACCATACAACAATAACGATGCTGGTGCCAACGGTAATGAAGTCGTTGTCACTACTTCTACATACTATGGATCAACTACATCAGTAA
CoAls4210   TGGGGAGCTTACAACAACAATGAGGCAGGTGCTAATGGTAATGAAGTCGTCGTCACCACATCCACATGGCTTGGATCAACTACTGCGGTAA
CoAls4220   TGGTCACCTTACAGCAATAACGTGGCAGGAGCCAATGGTAATGAAGTCGTTGTTACAACATCTACATACCTAGGATCAACTACTGCGGTAA
            ***  * * **** *** ** *  ** ** ** ** ************** ** ** ** ** ****      ***********  * ****
```

B

TaqMan Assay	DNA (ng)	Template Plasmid *CoALS4210* (3575)		*CoALS4220* (3576)		*CoALS800* (3577)	
CoALS4210	50	8.3	8.4	U/D	U/D	U/D	35.3
	5	11.3	11.3	U/D	U/D	U/D	36.1
	0.5	13.2	13.1	U/D	U/D	U/D	37.2
	0.05	15.3	14.9	U/D	U/D	U/D	U/D
CoALS4220	50	37.3	38.6	8.2	8.1	35.2	35.0
	5	U/D	U/D	11.2	11.2	U/D	32.9
	0.5	U/D	U/D	13.1	12.9	U/D	34.8
	0.05	U/D	U/D	14.9	14.9	U/D	36.7
CoALS800	50	35.0	36.1	U/D	U/D	4.9	5.0
	5	37.5	36.7	U/D	U/D	7.8	7.8
	0.5	U/D	38.4	U/D	U/D	9.8	9.7
	0.05	U/D	U/D	U/D	U/D	12.0	11.9

FIGURE 7 | Demonstration of TaqMan assay specificity. TaqMan assays were selected for quantification of relative gene expression because of their exquisite specificity, which was needed to distinguish between highly similar loci in the same species. The most-extreme example was from *C. orthopsilosis* where sequences in the 5′ end of the gene were >75% identical. **(A)** Nucleotide sequences that were the most dissimilar in the 5′ end of *CoALS4210*, *CoALS4220*, and *CoALS800*. Yellow highlighting marked positions where at least two of the three sequences were identical. Asterisks marked the positions that were identical in all three sequences. In each sequence, the forward TaqMan primer sequence was underlined and shown in bold type. The TaqMan probe sequence was double underlined; each was in the sense orientation. The TaqMan reverse primer was underlined in bold, red type. **(B)** C_t values from TaqMan assays using cloned plasmid DNA as the reaction template. Dilutions of plasmid DNA were added to replicate TaqMan assays where the assay and template matched or were mismatched to gauge assay specificity. C_t values were recorded in the table and demonstrated recognition of the plasmid only when matched with the correct assay. For example, 5 ng of the cloned 5′ end of *CoALS4210* gave a C_t value of 11.3 when assayed with the *CoALS4210* TaqMan primers and probe. Undetectable signal (U/D) or a signal that was nearly undetectable (cycle 36.1) were recorded when the same amount of plasmid DNA was tested with the *CoALS4220* or *CoALS800* TaqMan assays. The data clearly demonstrated specificity of the TaqMan assays for their intended targets, even among genes as similar as the *ALS* genes of *C. orthopsilosis*.

than for the 5′ end assay. *CpALS4780* and *CpALS660* were more highly expressed at 24 h compared to 2 h, which could indicate a growth-stage or growth-medium effect on gene expression.

The same approach was used to assess relative *ALS* gene expression levels in 4 isolates of *C. metapsilosis* (**Figure 8E**) where gene expression differences between strains were more apparent than for the smaller sample of *C. parapsilosis* isolates. For example, *CmALS4210* expression was much higher in strain 397 than the others. The trend of higher gene expression estimates for the 3′ end assay was generally observed. One notable exception was *CmALS2265* in strain 61, for which the 3′ end assay produced considerably lower gene expression estimates than the 5′ end assay. PCR amplification of the assay site indicated that the 3′ end assay reverse primer sequence was not present in strain 61 due to sequence polymorphisms in that portion of the coding region (**Figure 6E**). Overall, these results demonstrated the complications with assay design to estimate relative gene expression and highlighted the need for sequence verification prior to studying gene expression in a variety of isolates.

DISCUSSION

The increasingly common availability of draft genome sequences for microbial pathogens is a tremendous benefit to the scientific community. Insight into genome composition promotes development of testable hypotheses regarding host-pathogen interaction. Genes in the *ALS* family have proven difficult to assemble because each fungal species encodes multiple, highly similar loci, and the loci tend to have extensive tracts of repeated DNA sequences (Hoyer et al., 2008); these repeated sequence units are similar in size to the read lengths from second-generation DNA sequencers posing a difficult assembly problem. Therefore, it is not surprising that genome assemblies frequently break within *ALS* coding regions or genes are misassembled with the 5′ end from one locus computationally attached to the 3′ end of a gene from a different physical location. The goal of this work was to develop an accurate description of the *ALS* family in each species within the *C. parapsilosis* species complex.

ALS gene sequences were well-assembled in the *C. parapsilosis* representative genome (CDC317) that was generated from whole-genome shotgun sequencing and available in GenBank. PCR amplification and Sanger DNA sequencing of *C. parapsilosis ALS* genes revealed numerous instances of nucleotide polymorphisms that are not specified in the public, haploid genome assembly, but only identified one instance where the genome assembly sequence diverged from the Sanger verification (**Figure 6**). In contrast, *ALS* genes were not completely assembled in the *C. orthopsilosis* representative genome (Co90-125), with gaps located in the repeated sequences. This observation prompted generation of a new Co90-125 sequence derived from a combination of long- and short-read sequence data

A

			4210	4220	800
90-125	Y 1h	TaqMan 5' End	13.1 ± 0.2	4.6 ± 0.3	10.0 ± 0.2
		SYBR	6.9 ± 0.1	4.8 ± 0.1	11.9 ± 0.1

B

			CoALS4220	Random Hexamers	Oligo dT
90-125	Y 1h	5' End		6.3 ± 0.3	11.8 ± 0.5
		3' End		5.0 ± 0.1	6.3 ± 0.1

C

			4210	4220	800
90-125	Y 1h	5'	14.9 ± 0.1	6.4 ± 0.2	11.7 ± 0.1
		3'	10.1 ± 0.1	5.1 ± 0.1	6.6 ± 0.1
	Y 24h	5'	14.7 ± 0.4	12.6 ± 0.5	10.7 ± 0.6
		3'	8.6 ± 0.5	2.1 ± 0.4	6.1 ± 0.1

D

			4770	4780	4790	4800	660
CDC 317	Y	5'	7.6 ± 0.5	11.3 ± 0.3	3.6 ± 0.1	11.9 ± 0.4	12.1 ± 0.2
	24h	3'	8.2 ± 0.7	5.9 ± 0.5	3.6 ± 0.1	6.9 ± 0.5	6.7 ± 0.5
	SC	5'	11.8 ± 0.1	13.6 ± 0.3	4.1 ± 0.1	11.1 ± 0.04	13.9 ± 0.1
	2h	3'	9.8 ± 0.1	9.5 ± 0.1	4.3 ± 0.1	9.4 ± 0.1	10.4 ± 0.1
ATCC 22019	Y	5'	9.4 ± 0.3	11.0 ± 0.3	4.5 ± 0.1	9.7 ± 0.2	9.3 ± 0.1
	24h	3'	8.6 ± 0.2	5.7 ± 0.1	5.4 ± 0.1	6.6 ± 0.1	5.5 ± 0.1
	SC	5'	11.9 ± 0.1	11.2 ± 0.3	3.2 ± 0.1	6.7 ± 0.4	11.7 ± 0.3
	2h	3'	10.2 ± 0.1	8.8 ± 0.1	4.3 ± 0.1	7.9 ± 0.1	9.9 ± 0.1

E

			4210	4220	800	2265
96143	Y	5'	4.9 ± 0.7	4.6 ± 0.6	9.9 ± 1.1	9.5 ± 0.2
	24h	3'	5.4 ± 0.3	4.1 ± 0.7	8.5 ± 0.8	3.7 ± 0.3
	R	5'	9.5 ± 1.2	8.8 ± 0.2	14.6 ± 0.5	13.0 ± 0.2
	1h	3'	8.6 ± 0.7	8.3 ± 0.2	11.8 ± 0.3	7.0 ± 0.2
61	Y	5'	5.9 ± 0.3	4.2 ± 0.4	8.1 ± 0.3	9.1 ± 0.2
	24h	3'	6.3 ± 0.3	3.9 ± 0.3	8.2 ± 0.1	16.4 ± 0.5
	R	5'	10.1 ± 0.4	8.4 ± 0.2	14.8 ± 0.2	11.9 ± 0.2
	1h	3'	9.1 ± 0.03	7.3 ± 0.3	10.3 ± 0.3	16.8 ± 0.3
397	Y	5'	2.1 ± 0.3	5.5 ± 0.3	5.4 ± 0.6	10.5 ± 0.1
	24h	3'	2.8 ± 0.3	5.3 ± 0.2	5.4 ± 0.7	3.1 ± 0.2
	R	5'	1.7 ± 0.2	7.1 ± 0.1	7.1 ± 0.3	12.3 ± 0.2
	1h	3'	2.9 ± 0.2	7.4 ± 0.4	8.2 ± 0.3	5.0 ± 0.2
482	Y	5'	11.0 ± 0.03	5.1 ± 0.5	13.6 ± 1.7	9.6 ± 0.3
	24h	3'	7.9 ± 0.3	5.6 ± 0.5	10.5 ± 0.3	2.7 ± 0.3
	R	5'	11.1 ± 0.6	8.6 ± 0.2	16.3 ± 0.7	11.5 ± 0.2
	1h	3'	9.8 ± 0.2	8.8 ± 0.5	12.5 ± 0.4	4.8 ± 0.2

FIGURE 8 | Relative gene expression measured by TaqMan assays. **(A)** *C. orthopsilosis* strain 90-125 was grown in YPD for 1 h. RNA preparations from these cells were assayed by TaqMan or the SYBR Green method of Lombardi et al. (2019). Mean (± standard error of the mean) C_t values were reported. Results were shaded to indicate the intensity of relative gene expression. The color key at the bottom of the diagram was shaded from red (high relative gene expression) to purple (low relative gene expression) to facilitate comparison between results. *CoALS4220* was expressed more highly than either of the other genes in the growth conditions tested. The SYBR Green method suggested a higher relative expression level for *CoALS4210* than did the TaqMan assay. **(B)** *CoALS4220* was used as a model gene to test the effect of cDNA synthesis priming method and TaqMan assay location on estimates of relative gene expression. Placement of the TaqMan assay at the 3′ end of the gene produced higher expression estimates than placement at the 5′ end of the gene. Priming with random hexamers produced a higher gene expression estimate than oligo dT priming. **(C)** Themes illustrated in **(A,B)** carried forward to a more-extensive analysis of *C. orthopsilosis ALS* gene expression. Strain 90-125 was grown for 1 h and 24 h in YPD medium. *CoALS4220* was more-highly expressed than the other genes. Estimates of relative gene expression were higher for TaqMan assays at the 3′ end of the gene than at the 5′ end of the gene. **(D)** Relative expression of *C. parapsilosis ALS* genes in two strains (CDC317, ATCC 22019) grown in two different conditions (YPD for 24 h; SC with fetal bovine serum for 2 h). *CpALS4790* was more-highly expressed than the other genes, even *CpALS4800* which was proposed to arise from duplication of *CpALS4790*. **(E)** Relative expression of *C. metapsilosis ALS* genes in four strains (ATCC 96143, 61, 397, 482) in two different growth conditions (YPD for 24 h; RPMI 1640 for 1 h). Considerable strain variation was observed with genes that were relatively quiet in one isolate (e.g., *CmALS4210* in strain 482) but extremely highly expressed in another (strain 397). In many instances, gene expression estimates from the 5′ end and 3′ end TaqMan assays provided similar results, although several notable exceptions were present. The apparent lack of *CmALS2265* expression in strain 61 (as measured with the 3′ end assay) prompted examination of the gene sequence at the site of the TaqMan assay (**Figure 6E**). Sequence variation between the TaqMan assay and gene sequence in this region explained the falsely low estimate.

(Lombardi et al., 2019). The effort aided completion of the three *ALS* gene sequences in this *C. orthopsilosis* isolate. The *C. metapsilosis* representative genome sequence was assembled from primarily short-read data from more than one strain (Pryszcz et al., 2015). Despite the published claim of one *ALS* gene in this species, four *ALS* genes were detected in both the representative genome and a new sequence generated from long- and short-read data from strain ATCC 96143. Overall, availability of long-read sequence data facilitated accurate *ALS* gene assembly although Sanger sequencing of PCR products was still needed in some instances to correct premature stop codons and produce a complete open reading frame.

C. albicans ALS genes were named by numbering them in the order in which they were characterized (*ALS1* to *ALS7*, *ALS9*; Hoyer et al., 2008). This traditional approach to naming genes was initiated before *C. albicans* genome data were available. These *C. albicans* names set a precedent and provide ample potential for confusion if applied to *ALS* genes in other fungal species. Orthology could be used as a criterion for naming genes among the fungal species considered here (Maguire et al., 2013); genes

sharing a common physical location in different species could be given the same name with the expectation of similar function. These ideas become complicated for the *ALS* family because most species have a different number of *ALS* genes, gene order is not conserved well among the fungal species of interest, and there is a tendency toward tandem duplications of *ALS* loci (**Figure 1**). Als proteins are adhesins, yet function promiscuously, so looking toward shared function as the means for assigning names is also not an effective method. Some authors have referred to *ALS* genes using the label assigned in the annotation of the representative genome assembly (Bertini et al., 2016; Neale et al., 2018; Zoppo et al., 2018). This appealing approach provides a unique name for each gene and, like a street address, communicates physical location information. For example, it is obvious that *CPAR2_404770*, *CPAR2_404780*, *CPAR2_404790*, and *CPAR2_404800* are contiguous in the *C. parapsilosis* genome. The final gene names proposed here (*CpALS4770*, *CpALS4780*, *CpALS4790*, and *CpALS4800*) included physical location information from the genome annotation labels, an abbreviation to indicate species of origin, and "*ALS*" to signal inclusion in the gene family. A similar method was used to name the genes in *C. orthopsilosis* and *C. metapsilosis*.

Hoyer and Cota (2016) used "NT/T/TR/CT" to describe the standard composition of Als proteins in *C. albicans* where NT is the NT-Als domain that contains the PBC, T is the Thr-rich region, TR denotes the tandem repeats of the consensus 36-amino-acid sequence (**Figure 2**), and CT is the Ser/Thr-rich C-terminal domain. *C. albicans ALS* genes were used as BLAST queries to pull sequences from the *C. parapsilosis* species complex genomes. However, only four of the resulting Als protein sequences fit the ideal *C. albicans* definition. Seven of the predicted proteins lacked the TR domain and in the last protein, the TR domain was from a different family as defined in *C. albicans*. Other predicted proteins that lacked the TR domain instead encoded regions with short, imperfect repeats. Finding these short, imperfect repeats in other cell-surface proteins suggests additional recombination between *ALS* sequences and others. To incorporate the new *C. parapsilosis* species complex proteins into the Als family, the definition must shift away from NT/T/TR/CT. Instead, the Als family appears to include proteins that have an Als adhesive domain presented on a structure that promotes cell-surface display. This alternative Als family definition encompasses all proteins identified in this study and designates CmAls2265 as an Als protein, rather than an Iff/Hyr protein. Indeed, several of the genes discussed here have been tested for their contributions to cell adhesion. Bertini et al. (2016) showed that deletion of *CpALS4800* resulted in a *C. parapsilosis* strain with reduced adhesion to human buccal epithelial cells. Neale et al. (2018) documented a role for CpAls4800 in adhesion of *C. parapsilosis* to extracellular matrix proteins in a microfluidics assay using physiological fluid shear conditions. Zoppo et al. (2018) deleted *CoALS4210* and showed decreased adhesion to human buccal epithelial cells for the resulting *C. orthopsilosis* mutant strain. Overall, data presented here suggest that definitions of gene families established in *C. albicans* will need to be modified to accommodate data from other fungi.

Extensive analyses of *C. albicans ALS* gene expression revealed differential expression regulated by morphological form, growth medium, and stage of culture growth (reviewed in Hoyer et al., 2008). This information provided the foundation to assess Als protein function *in vitro*. TaqMan assays specific for individual *ALS* genes were developed to collect similar data for *ALS* genes in the *C. parapsilosis* species complex. Since *ALS* genes are large, assays were placed at a similar position within each coding region to avoid effects of assay location on gene expression estimates. Initial assays were placed within the region that encodes the NT-Als domain; a second set of assays was designed at the 3′ end of each gene. Surprisingly, results from the 5′ end and 3′ end assays frequently varied by several C_t units with the tendency toward higher expression estimates from the 3′ end assays. Since the TaqMan assays quantify cDNA as a reflection of RNA abundance, results showed that cDNA from the 3′ end of the genes is more abundant than cDNA from the 5′ region of the gene. Several factors can be invoked to explain this imbalance between cDNA abundance including the 3′ end of the transcript being more accessible to reverse transcription than the 5′ end, selective degradation of the 5′ end of the transcript, or the presence of another promoter that overlaps with the 3′ end of the transcript and boosts its relative abundance. Examination of the genome sequence did not provide obvious evidence for the presence of an overlapping ORF that could result in greater abundance of 3′ end transcripts. Use of the TaqMan assays to compare gene expression across several isolates of the same species revealed sequence heterogeneity that interfered with assay function in certain strains. Lack of target recognition could also partially explain the relative gene expression estimate disparities discussed above. For example, sequence variation between alleles within the same strain could reduce relative estimates of gene expression if the assay recognizes only one of the alleles in the diploid species. Regardless of the issues, TaqMan data pointed to certain genes as being the most-highly expressed and indicated considerable strain variation in gene expression. The TaqMan assays are useful for gene expression analyses but must be validated with the specific strains to be tested. Using more than one assay per locus is also recommended to avoid potential misinterpretations as described above.

The literature contains a few reports regarding relative expression of *ALS* genes in the *C. parapsilosis* species complex. Comparisons of *C. orthopsilosis* TaqMan data to gene expression studies conducted in the laboratory of Dr. Arianna Tavanti (University of Pisa) were presented in the "Results" section. Results were not directly comparable, leading to questions of whether gene expression is influenced by local factors. One potential factor that is noted in the *Candida* literature is water quality, which despite modern purification systems, may vary widely and influence biological function of fungal cells (Nickerson et al., 2012). Neale et al. (2018) measured expression of the five *C. parapsilosis ALS* genes using a SYBR Green-based method. Differential expression of *CpALS4800* and *CpALS4780* was noted when cells were transferred from saturated YPD cultures to tissue culture medium for 3 h. Like the TaqMan data presented here, expression of *CpALS4790* was highest in the saturated YPD culture, with *CpALS4780* next-most abundant

and others at a lower level. Collectively, the data highlight and prioritize research questions to pursue. *CpALS4790* may be at the top of this list because of its high relative expression that predicts an abundance of CpAls4790 on the cell surface. However, structural predictions suggest that ligand binding may be more selective than for some of the other Als proteins (**Figure 4**). Perhaps CpAls4790 serves a more-focused adhesive role than deduced for the *C. albicans* Als proteins for which function was studied in detail (reviewed in Hoyer and Cota, 2016).

Future studies should also pursue greater insights into *ALS* gene expression patterns within the *C. parapsilosis* species complex. The current study was intended to assess whether *ALS* gene expression displayed the same differential patterns as observed in *C. albicans* and to identify genes that may produce proteins most abundantly on the fungal cell surface. In *C. albicans*, *ALS* genes that always showed a low expression level produced protein at a level undetectable by immunolabeling with specific monoclonal antibodies (Zhao et al., 2011). Genes expressed at a high level produced Als protein that could be long-lived on the cell surface (Coleman et al., 2010). It is also important to consider that gene expression and protein production can vary between *in vitro* and *in vivo* environments, suggesting the need for *in vivo* work to best understand the contributions of Als protein function in the host (Coleman et al., 2012).

Data presented here also set up intriguing experiments to pursue in *C. metapsilosis*. For example, the previous report that claimed only one *ALS* gene in the species was perhaps accepted without question because *C. metapsilosis* does not readily display phenotypes *in vitro* that are associated with pathogenic species. *C. metapsilosis* is less adherent to human buccal epithelial cells than either *C. parapsilosis* or *C. orthopsilosis* and shows a lower fungal burden at early stages of a murine vaginal infection model (Bertini et al., 2013). However, *C. metapsilosis* has four *ALS* genes, some are expressed at high levels, and the predicted proteins have an NT-Als domain like those in *C. albicans*. This new information must be reconciled with the relative lack of an adhesive phenotype for *C. metapsilosis* when assayed *in vitro*. Overall, data presented here highlight key questions that remain to be answered regarding the Als proteins and demonstrate the hypothesis-generating power of accurate genome assemblies.

AUTHOR CONTRIBUTIONS

CF, AH, and LH designed the experiments. S-HO, BSm, BSt, AM, CF, AH, and LH conducted the experiments. All authors analyzed the data, and wrote and approved the manuscript.

FUNDING

This work was funded by grant number R15 DE026401 from the National Institute of Dental and Craniofacial Research, National Institutes of Health.

ACKNOWLEDGMENTS

We thank Jessie Kirk, Erica Forbes, Allyson Isenhower, Quinn Nguyen, Anton Bershanskiy, Mariah McNamer, and Kaia Ball for assistance with DNA sequence analysis. Drs. Travis Wilcoxen and Laura Zimmerman, Millikin University Department of Biology, coordinated student participation and supervised research credit for students in the Undergraduate Program in Fungal Genomics.

SUPPLEMENTARY MATERIAL

The Supplementary Material for this article can be found online at: https://www.frontiersin.org/articles/10.3389/fmicb.2019.00781/full#supplementary-material

REFERENCES

Alfaro, M. E., Zoller, S., and Lutzoni, F. (2003). Bayes or bootstrap? A simulation study comparing the performance of Bayesian Markov chain Monte Carlo sampling and bootstrapping in assessing phylogenetic confidence. *Mol. Biol. Evol.* 20, 255–266. doi: 10.1093/molbev/msg028

Applied Biosystems Inc. (2008). *Guide to Performing Relative Quantitation of Gene Expression using Real-Time Quantitative PCR*. Available at: https://www.thermofisher.com/document-connect/document-connect.html?url=https://assets.thermofisher.com/TFS-Assets/LSG/manuals/cms-042380.pdf&title=Guide%20to%20Performing%20Relative%20Quantitation%20of%20Gene%20Expression%20Using%20Real-Time%20Quantitative%20PCR (accessed December 20, 2017).

Bailey, D. A., Feldmann, P. J. F., Bovey, M., Gow, N. A. R., and Brown, A. J. P. (1996). The *Candida albicans HYR1* gene, which is activated in response to hyphal development, belongs to a gene family encoding yeast cell wall proteins. *J. Bacteriol.* 178, 5353–5360.

Bates, S., de la Rosa, J. M., MacCallum, D. M., Brown, A. J. P., Gow, N. A. R., and Odds, F. C. (2007). *Candida albicans* Iff1, a secreted protein required for cell wall structure and virulence. *Infect. Immun.* 75, 2922–2928. doi: 10.1128/IAI.00102-07

Bertini, A., De Bernardis, F., Hensgens, L. A. M., Sandini, S., Senesi, S., and Tavanti, A. (2013). Comparison of *Candida parapsilosis*, *Candida orthopsilosis*, and *Candida metapsilosis* adhesive properties and pathogenicity. *Int. J. Med. Microbiol.* 303, 98–103. doi: 10.1016/j.ijmm.2012.12.006

Bertini, A., Zoppo, M., Lombardi, L., Rizzato, C., De Carolis, E., Vella, A., et al. (2016). Targeted gene disruption in *Candida parapsilosis* demonstrates a role for *CPAR2_404800* in adhesion to a biotic surface and in a murine model of ascending urinary tract infection. *Virulence* 7, 85–97. doi: 10.1080/21505594.2015.1112491

Bliss, J. M. (2015). *Candida parapsilosis*: an emerging pathogen developing its own identity. *Virulence* 6, 109–111. doi: 10.1080/21505594.2015.1008897

Boisramé, A., Cornu, A., Da Costa, G., and Richard, M. L. (2011). Unexpected role for a serine/threonine-rich domain in the *Candida albicans* Iff protein family. *Eukaryot. Cell* 10, 1317–1330. doi: 10.1128/EC.05044-11

Bolger, A. M., Lohse, M., and Usadel, B. (2014). Trimmomatic: a flexible trimmer for Illumina sequence data. *Bioinformatics* 30, 2114–2120. doi: 10.1093/bioinformatics/btu170

Butler, G., Rasmussen, M. D., Lin, M. F., Santos, M. A., Sakthikumar, S., Munro, C. A., et al. (2009). Evolution of pathogenicity and sexual reproduction in eight *Candida* genomes. *Nature* 459, 657–662. doi: 10.1038/nature08064

Castresana, J. (2000). Selection of conserved blocks from multiple alignments for their use in phylogenetic analysis. *Mol. Biol. Evol.* 17, 540–552.

Chu, W. S., Magee, B. B., and Magee, P. T. (1993). Construction of an *Sfi*I macrorestriction map of the *Candida albicans* genome. *J. Bacteriol.* 175, 6637–6651. doi: 10.1128/jb.175.20.6637-6651.1993

Coleman, D. A., Oh, S.-H., Manfra-Maretta, S. L., and Hoyer, L. L. (2012). A monoclonal antibody specific for *Candida albicans* Als4 demonstrates overlapping localization of Als family proteins on the fungal cell surface and highlights differences between Als localization in vitro and in vivo. *FEMS Immunol. Med. Micobiol.* 64, 321–333. doi: 10.1111/j.1574-695X.2011.00914.x

Coleman, D. A., Oh, S.-H., Zhao, X., and Hoyer, L. L. (2010). Heterogeneous distribution of *Candida albicans* cell-surface antigens demonstrated with an Als1-specific monoclonal antibody. *Microbiology* 156, 3645–3659. doi: 10.1099/mic.0.043851-0

Collart, M. A., and Oliviero, S. (1993). "Preparation of yeast RNA," in *Current Protocols in Molecular Biology*, Vol. 2, ed. F. M. Ausubel (New York: Wiley). doi: 10.1099/mic.0.043851-0

Cook, C. E., Bergman, M. T., Cochrane, G., Apweiler, R., and Birney, E. (2017). The European Bioinformatics Institute in 2017: data coordination and integration. *Nucleic Acids Res.* 46, D21–D29. doi: 10.1093/nar/gkx1154

Edgar, R. C. (2004). MUSCLE: multiple sequence alignment with high accuracy and high throughput. *Nucleic Acids Res.* 32, 1792–1797. doi: 10.1093/nar/gkh340

Eisenhaber, B., Bork, P., and Eisenhaber, F. (1999). Prediction of potential GPI-modification sites in proprotein sequences. *Mol. Cell Biol.* 292, 741–758. doi: 10.1006/jmbi.1999.3069

Emsley, P., Lohkamp, B., Scott, W. G., and Cowtan, K. (2010). Features and development of Coot. *Acta Crystallogr. D Biol. Crystallogr.* 66, 486–501. doi: 10.1107/S0907444910007493

Garcia, M. C., Lee, J. T., Ramsook, C. B., Alsteens, D., Dufrene, Y., and Lipke, P. N. (2011). A role for amyloid in cell aggregation and biofilm formation. *PLoS One* 6:e17632. doi: 10.1371/journal.pone.0017632

Gouy, M., Guindon, S., and Gascuel, O. (2010). SeaView version 4: a multiplatform graphical user interface for sequence alignment and phylogenetic tree building. *Mol. Biol. Evol.* 27, 221–224. doi: 10.1093/molbev/msp259

Green, C. B., Cheng, G., Chandra, J., Mukherjee, P., Ghannoum, M. A., and Hoyer, L. L. (2004). RT-PCR detection of *Candida albicans* ALS gene expression in the reconstituted human epithelium (RHE) model of oral candidiasis and in model biofilms. *Microbiology* 150, 267–275. doi: 10.1099/mic.0.26699-0

Guindon, S., and Gascuel, O. (2003). A simple, fast, and accurate algorithm to estimate large phylogenies by maximum likelihood. *Syst. Biol.* 52, 696–704. doi: 10.1080/10635150390235520

Hoyer, L. L., and Cota, E. (2016). *Candida albicans* agglutinin-like sequence (Als) family vignettes: a review of Als protein structure and function. *Front. Microbiol.* 7:280. doi: 10.3389/fmicb.2016.00280

Hoyer, L. L., Green, C. B., Oh, S.-H., and Zhao, X. (2008). Discovering the secrets of the *Candida albicans* agglutinin-like sequence (ALS) gene family—a sticky pursuit. *Med. Mycol.* 46, 1–15. doi: 10.1080/13693780701435317

Huang, S., Kang, M., and Xu, A. (2017). HaploMerger2: rebuilding both haploid sub-assemblies from high-heterozygosity diploid genome assembly. *Bioinformatics* 33, 2577–2579. doi: 10.1093/bioinformatics/btx220

Kelly, L. A., Mezulis, S., Yates, C. M., Wass, M. N., and Sternberg, M. J. E. (2015). The Phyre2 web portal for protein modeling, prediction and analysis. *Nat. Protoc.* 10, 845–858. doi: 10.1038/nprot.2015.053

Koren, S., Walenz, B. P., Berlin, K., Miller, J. R., Bergman, N. H., and Phillippy, A. M. (2017). Canu: scalable and accurate long-read assembly via adaptive k-mer weighting and repeat separation. *Genome Res.* 27, 722–736. doi: 10.1101/gr.215087.116

Lackey, E., Vipulananadan, G., Childers, D. S., and Kadosh, D. (2013). Comparative evolution of morphological regulatory functions in *Candida* species. *Eukaryot. Cell* 12, 1356–1368. doi: 10.1128/EC.00164-13

Li, H. (2018). Minimap2: pairwise alignment for nucleotide sequences. *Bioinformatics* 34, 3094–3100. doi: 10.1093/bioinformatics/bty191

Lin, J., Oh, S.-H., Jones, R., Garnett, J. A., Salgado, P. S., Rushnakova, S., et al. (2014). The peptide-binding cavity is essential for Als3-mediated adhesion of *Candida albicans* to human cells. *J. Biol. Chem.* 289, 18401–18412. doi: 10.1074/jbc.M114.547877

Lombardi, L., Zoppo, M., Rizzato, C., Bottai, D., Hernandez, A., Hoyer, L. L., et al. (2019). Characterization of the *Candida orthopsilosis* agglutinin-like sequence (ALS) genes. *PLoS One* (in press).

Lu, C. F., Kurjan, J., and Lipke, P. N. (1994). A pathway for cell wall anchorage of *Saccharomyces cerevisiae* alpha-agglutinin. *Mol. Cell. Biol.* 14, 4825–4833. doi: 10.1128/MCB.14.7.4825

Madoui, M. A., Engelen, S., Cruaud, C., Belser, C., Bertrand, L., Alberti, A., et al. (2015). Genome assembly using nanopore-guided long and error-free DNA reads. *BMC Genom.* 16:327. doi: 10.1186/s12864-015-1519-z

Maguire, S. L., OhEigeartaigh, S. S., Byrne, K. P., Schroder, M. S., O'Gaora, P., Wolfe, K. H., et al. (2013). Comparative genome analysis and gene finding in *Candida* species using CGOB. *Mol. Biol. Evol.* 30, 1281–1291. doi: 10.1093/molbev/mst042

Miller, M. A., Pfeiffer, W., and Schwartz, T. (2010). "Creating the CIPRES science gateway for inference of large phylogenetic trees," in *Proceedings of the Gateway Computing Environments Workshop (GCE)*, (New Orleans, LA). doi: 10.1109/GCE.2010.5676129

Neale, M. N., Glass, K. A., Longley, S. J., Kim, D. J., Laforce-Nesbitt, S. S., Wortzel, J. D., et al. (2018). Role of the inducible adhesin, CpAls7, in binding of *Candida parapsilosis* to extracellular matrix under fluid shear. *Infect. Immun.* 86, e00892–e00917. doi: 10.1128/IAI.00892-17

Nickerson, K. W., Atkin, A. L., Hargarten, J. C., Pathirana, R. U., and Hasim, S. (2012). "Thoughts on quorum sensing and fungal dimorphism," in *Biocommunication of Fungi*, ed. G. Witzany (Dordrecht: Springer), 189–204.

Nielsen, H. (2017). "Predicting secretory proteins with SignalP," in *Protein Function Prediction, Methods in Molecular Biology*, ed. D. Kihara 59–73. doi: 10.1007/978-1-4939-7015-5_6

Posada, D. (2008). jModelTest: phylogenetic model averaging. *Mol. Biol. Evol.* 25, 1253–1256. doi: 10.1093/molbev/msn083

Pryszcz, L. P., Nemeth, T., Gacser, A., and Gabaldon, T. (2013). Unexpected genomic variability in clinical and environmental strains of the pathogenic yeast *Candida parapsilosis*. *Genome Biol. Evol.* 5, 2382–2392. doi: 10.1093/gbe/evt185

Pryszcz, L. P., Nemeth, T., Saus, E., Ksiezopolska, E., Hegedusova, E., Nosek, J., et al. (2015). The genomic aftermath of hybridization in the opportunistic pathogen *Candida metapsilosis*. *PLoS Genet.* 11:e1005626. doi: 10.1371/journal.pgen.1005626

Riccombeni, A., Vidanes, G., Proux-Wera, E., Wolfe, K. H., and Butler, G. (2012). Sequence and analysis of the genome of the pathogenic yeast *Candida orthopsilosis*. *PLoS One* 7:e35750. doi: 10.1371/journal.pone.0035750

Salgado, P. S., Yan, R., Taylor, J. D., Burcehll, L., Jones, R., Hoyer, L. L., et al. (2011). Structural basis for the broad specificity to host-cell ligands by the pathogenic fungus *Candida albicans*. *Proc. Natl. Acad. Sci. U.S.A.* 108, 15775–15779. doi: 10.1073/pnas.1103496108

Senol Cali, D., Kim, J. S., Ghose, S., Alkan, C., and Mutlu, O. (2018). Nanopore sequencing technology and tools for genome assembly: computational analysis of the current state, bottlenecks and future directions. *Brief. Bioinform.* doi: 10.1093/bib/bby017 [Epub ahead of print].

Sherman, F., Fink, G. R., and Hicks, J. B. (1986). *Laboratory Course Manual for Methods in Yeast Genetics*. Cold Spring Harbor, NY: Cold Spring Harbor Press.

Staab, J. F., Bradway, S. D., Fidel, P. L., and Sundstrom, P. (1999). Adhesive and mammalian transglutaminase substrate properties of *Candida albicans* Hwp1. *Science* 283, 1535–1538.

Swofford, D. L. (2002). PAUP*. Phylogenetic Analysis Using Parsimony (*and Other Methods). Version 4. Sunderland, MA: Sinauer Associates.

Tavanti, A., Davidson, A. D., Gow, N. A., Maiden, M. C., and Odds, F. C. (2005). *Candida orthopsilosis* and *Candida metapsilosis* spp. nov. replace *Candida parapsilosis* groups II and III. *J. Clin. Microbiol.* 43, 284–292. doi: 10.1128/JCM.43.1.284-292.2005

Walker, B. J., Abeel, T., Shea, T., Priest, M., Abouelliel, A., Sakthikumar, S., et al. (2014). Pilon: an integrated tool for comprehensive microbial variant detection and genome assembly improvement. *PLoS One* 9:e112963. doi: 10.1371/journal.pone.0112963

White, T. J., Bruns, T., Lee, S., and Taylor, J. W. (1990). "Amplification and direct sequencing of fungal ribosomal RNA genes for phylogenetics," in *PCR Protocols: A Guide to Methods and Applications*, eds M. A. D. Innis, D. H. Gelfand, J. J. Sninsky, and T. J. White (New York: Academic Press, Inc.), 315–322.

Wick, R. R., Judd, L. M., Gorrie, C. L., and Holt, K. E. (2017a). Completing bacterial genome assemblies with multiplex MinION sequencing. *Microb. Genom.* 3:e000132. doi: 10.1099/mgen.0.000132

Wick, R. R., Judd, L. M., Gorrie, C. L., and Holt, K. E. (2017b). Unicycler: resolving bacterial genome assemblies from short and long sequencing reads. *PLoS Comput. Biol.* 13:e1005595. doi: 10.1371/journal.pcbi.1005595

Zhao, X., Oh, S.-H., Coleman, D. A., and Hoyer, L. L. (2011). *ALS51*, a newly discovered gene in the *Candida albicans* ALS family, created by intergenic recombination: analysis of the gene and protein, and implications for evolution of microbial gene families. *FEMS Immunol. Med. Microbiol.* 61, 245–257. doi: 10.1111/j.1574-695X.2010.00769.x

Zhao, X., Pujol, C., Soll, D. R., and Hoyer, L. L. (2003). Allelic variation in the contiguous loci encoding *Candida albicans ALS5*, *ALS1* and *ALS9*. *Microbiology* 149, 2947–2960. doi: 10.1099/mic.0.26495-0

Zoppo, M., Lombardi, L., Rizzato, C., Lupetti, A., Bottai, D., Papp, C., et al. (2018). *CORT0C04210* is required for *Candida orthopsilosis* adhesion to human buccal cells. *Fungal Genet. Biol.* 120, 19–29. doi: 10.1016/j.fgb.2018.09.001

Conflict of Interest Statement: The authors declare that the research was conducted in the absence of any commercial or financial relationships that could be construed as a potential conflict of interest.

frontiers in Microbiology

ORIGINAL RESEARCH
published: 08 May 2019
doi: 10.3389/fmicb.2019.00976

The Farnesyltransferase β-Subunit Ram1 Regulates *Sporisorium scitamineum* Mating, Pathogenicity and Cell Wall Integrity

Shuquan Sun[1], Yizhen Deng[1], Enping Cai[1], Meixin Yan[2], Lingyu Li[1], Baoshan Chen[3], Changqing Chang[1] and Zide Jiang[1]**

[1] Guangdong Province Key Laboratory of Microbial Signals and Disease Control, College of Agriculture, South China Agricultural University, Guangzhou, China, [2] Sugarcane Research Institute, Guangxi Academy of Agricultural Sciences, Nanning, China, [3] State Key Laboratory of Conservation and Utilization of Subtropical Agro-Bioresources, Guangxi University, Nanning, China

OPEN ACCESS

Edited by:
Fausto Almeida,
University of São Paulo, Brazil

Reviewed by:
Andrei Steindorff,
Joint Genome Institute and Lawrence Berkeley National Laboratory, United States
Jarrod R. Fortwendel,
The University of Tennessee Health Science Center, United States

***Correspondence:**
Changqing Chang
changcq@scau.edu.cn
Zide Jiang
zdjiang@scau.edu.cn

Specialty section:
This article was submitted to Fungi and Their Interactions, a section of the journal Frontiers in Microbiology

Received: 13 March 2019
Accepted: 18 April 2019
Published: 08 May 2019

Citation:
Sun S, Deng Y, Cai E, Yan M, Li L, Chen B, Chang C and Jiang Z (2019) The Farnesyltransferase β-Subunit Ram1 Regulates Sporisorium scitamineum Mating, Pathogenicity and Cell Wall Integrity. Front. Microbiol. 10:976. doi: 10.3389/fmicb.2019.00976

The basidiomycetous fungus *Sporisorium scitamineum* causes a serious sugarcane smut disease in major sugarcane growing areas. Sexual mating is essential for infection to the host; however, its underlying molecular mechanism has not been fully studied. In this study, we identified a conserved farnesyltransferase (FTase) β subunit Ram1 in *S. scitamineum*. The *ram1*Δ mutant displayed significantly reduced mating/filamentation, thus of weak pathogenicity to the host cane. The *ram1*Δ mutant sporidia showed more tolerant toward cell wall stressor Congo red compared to that of the wild-type. Transcriptional profiling showed that Congo red treatment resulted in notable up-regulation of the core genes involving in cell wall integrity pathway in *ram1*Δ sporidia compared with that of WT, indicating that Ram1 may be involved in cell wall integrity regulation. In yeast the heterodimeric FTase is responsible for post-translational modification of Ras (small G protein) and a-factor (pheromone). We also identified and characterized two conserved Ras proteins, Ras1 and Ras2, respectively, and a *MAT-1* pheromone precursor Mfa1. The *ras1*Δ, *ras2*Δ and *mfa1*Δ mutants all displayed reduced mating/filamentation similar as the *ram1*Δ mutant. However, both *ras1*Δ and *ras2*Δ mutants were hypersensitive to Congo red while the *mfa1*Δ mutant was the same as wild-type. Overall our study displayed that *RAM1* plays an essential role in *S. scitamineum* mating/filamentation, pathogenicity, and cell wall stability.

Keywords: cell wall integrity, mating, *RAM1*, Ras, *Sporisorium scitamineum*

INTRODUCTION

Sugarcane smut disease caused by the basidiomycetous fungus *Sporisorium scitamineum* is one of the most severe diseases in world-wide sugarcane growing areas. The three-stage morphological transitions are most prominent during the smut fungus life cycle: the haploid sporidia switch to dikaryotic hyphal growth to infect the plant cane; in the later growth period, diploid teliospores form within the host stem; and after teliospore germination, haploid sporidia are generated

by successive budding (Taniguti et al., 2015). Therefore switching from non-pathogenic yeast-like sporidia to pathogenic hypha through sexual mating between two compatible sporidia is a prerequisite for infection. In the phytopathogenic basidiomycete model fungus, *Ustilago maydis*, biallelic a locus and multiallelic b locus comprise the tetrapolar mating system. The a locus encodes pheromone precursor *MFA1/2* and receptor *PRA1/2*, controlling sporidial recognition and fusion during the sexual mating process. The b locus encodes bE and bW proteins forming a heterodimeric transcription factor, activating the filamentation (Hartmann et al., 1996; Kahmann and Kamper, 2004). In *S. scitamineum* mfa2 knock-out mutants in *MAT-2* background were mating-deficient (Lu et al., 2017), and b locus deletion mutants were defective in filamentous growth (Yan et al., 2016a), suggesting common molecular characters between *S. scitamineum* and *U. maydis*. However, the molecular mechanisms of *S. scitamineum* mating/filamentation and/or pathogenicity remain largely unclear.

The biogenesis of mature pheromones has been well elaborated in *Saccharomyces cerevisiae* for its pheromone a-factor (Michaelis and Barrowman, 2012), during which the a-factor precursor undergoes a sequential processing by three separate modules, namely the C-terminal processing (prenylation by farnesyltransferase Ram1/Ram2, proteolysis by endoproteases Ste24 or Rce1, and Carboxymethylation by methyltransferase Ste14), the N-terminal proteolytic cleavage by endoproteases Ste24 and Axl1, and non-classical export by the ATP binding cassette (ABC) transporter Ste6 (Young et al., 2005; Paumi et al., 2009). The prenylation of the secreted a-factor-like pheromones is a common feature of ascomycetes and basidiomycetes (Brown and Casselton, 2001; Whiteway, 2011), including *U. maydis* (Spellig et al., 1994; Koppitz et al., 1996), *Ustilago hordei* (Kosted et al., 2000), *Cryptococcus neoformans* (Shen et al., 2002), *Schizophyllum commune* (Fowler et al., 1999), and *Sporisorium reilianum* (Schirawski et al., 2005).

Prenylation is a post-translational modification in which hydrophobic groups are added to the C-terminus of the protein (Michaelis and Barrowman, 2012). Modification of proteins at C-terminal cysteine residue(s) by the isoprenoids farnesyl (C15) and geranylgeranyl (C20) as lipid donors is essential for the biological function of a number of eukaryotic proteins (Leach and Brown, 2012). Three highly conserved prenyltransferases have been described in eukaryotic cells, and are responsible for these protein modifications: protein farnesyltransferase (FTase) and protein geranyltransferase (GGTase) types I and II. β subunit Ram1 (Ras and a-factor maturation) and α subunit Ram2 comprising the heterodimeric FTase (Omer and Gibbs, 1994). Ultimately, yeast and mammalian Ras proteins, yeast a-factor, and the mammalian nuclear scaffold protein lamin B, share a common motif CAAX ("C" is cysteine, "A" is often an aliphatic amino acid, and "X" is any residue except Phe or Leu) at their C-terminus, which are farnesylated by Ram1/Ram2 (Leung et al., 2006). The biological functions of FTase have been investigated by characterizing *RAM1*-deletion mutants in *S. cerevisiae* (He et al., 1991), *C. neoformans* (Vallim et al., 2004; Esher et al., 2016), *Candida albicans* (Song and White, 2003) and *Aspergillus fumigatus* (Qiao et al., 2017), while the *RAM2* gene seems to be essential. However, the *RAM1* function has not been reported in *S. scitamineum*.

In this study, we identified and characterized conserved *RAM1*, *RAS1*, *RAS2,* and *MFA1* genes in *S. scitamineum*. The *ram1*Δ, *ras1*Δ, *ras2*Δ, and *mfa1*Δ mutants all displayed reduced mating/filamentation compared with wild-type, which could be differentially restored by exogenous addition of Synthetic (farnesylated) Mfa1 peptide or cAMP. The *ram1*Δ mutant displayed enhanced tolerance, while the *ras1*Δ and *ras2*Δ mutants were hypersensitive toward cell wall stressor Congo red. However, and the *mfa1*Δ mutant was comparable with WT in stress tolerance to Congo red. In summary, we here report that the FTase β subunit Ram1 as a critical virulence factor in sugarcane smut fungus *S. scitamineum*. Ram1 and Ras proteins are both involved in cell wall integrity pathway of *S. scitamineum* but maybe of different signaling pathway.

MATERIALS AND METHODS

Multiple Sequence Alignment and Phylogenetic Analysis

Amino acid sequences were aligned by ClustalX 2.0 (Thompson et al., 1994) with the following parameters: pairwise alignment parameters (gap opening = 10, gap extension = 0.1) and multiple alignment parameters (gap opening = 10, gap extension = 0.2, transition weight = 0.5, delay divergent sequences = 25%). The alignment was phylogenetically analyzed with maximum likelihood by MEGA 6.0 (Kenaley et al., 2018), using a Le-Gasquel amino acid replacement matrix with 1,000 bootstrap replications. The tree graph was viewed in Tree-View1.1. The alignment of amino acid sequence was adjusted in BioEdit software.

Strains and Growth Conditions

Two *S. scitamineum* wild-type haploid *MAT-1* (a1b1) and *MAT-2* (a2b2) isolates were obtained from teliospores on sugarcane in Guangdong providence, China (Yan et al., 2016c), and stored locally. The culture medium used in this study included YePSA medium (yeast extract 1%, peptone 2%, sucrose 2%, and agar 2%) and YePSL medium (yeast extraction 1%, peptone 2%, sucrose 2%). For mating and stress tolerance assays, *S. scitamineum* strains were grown in shake culture in YePSL at 28°C for 12 h. The sporidia were harvested via centrifugation and washed twice in distilled water, and concentrations adjusted to obtain OD600 = 1.0 for serial 10-fold dilutions in distilled water (Krombach et al., 2018). The diluted sporidial suspensions of compatible mating type were mixed together in equal volume and plated on YePSA, incubated in dark at 28°C for 48 h before assessment, and photographed. For stress tolerance assessment, the sporidial culture at OD600 = 1.0 and its serial 10-fold dilutions were spotted on MM medium (Chakraborty et al., 1991) in the absence or presence of stress inducers, including 20 μg/mL Congo red (GENVIEW, DC241), 25 μg/mL calcofluor white (Sigma, 18909), 20 μg/mL SDS (GENVIEW, GS286), 1 M Sorbitol (TGI, S0065), 0.5 mM H_2O_2 (Damao, 7722841), and incubated in dark at 28°C for 48 h before assessment and

photographing. For testing the effects of exogenous cyclic AMP (cAMP; Sigma, A9501) was added to MM plates to reach final concentrations of 2.5 or 5 mM. For testing the effect of *MAT-1* pheromone, exogenous synthetic Mfa1 (Sigma, with or without farnesylation at C-terminal CAAX motif) was added to MM to reach a final concentration of 1 or 10 μg/mL. For colony counting, the *S. scitamineum* strains were shake cultured in YePSL at 28°C for 12 h, before harvesting. Sporidia were washed twice and diluted in distilled water to OD600 = 1.0, from which serial 10-fold dilutions were generated in distilled water to an OD600 of 10^{-5}. An aliquot of 150 μL of this diluted sporidial suspension was incubated on solid medium at 28°C, and the colony forming unit (CFU) was counted after 48 h. At least three independent biological replicates of colony counting were performed each time.

Strains for Gene Deletion and Complementation

Deletion of targeted genes (listed in **Supplementary Table S1**) follows the same strategy previously described (Li et al., 2014). For generation of deletion mutants, the 1–1.5 kb left and 1–1.5 kb right borders of each targeted gene were PCR-amplified from *S. scitamineum* wild-type genomic DNA separately, and two overlapping *HPT* fragments (for hygromycin resistance) were amplified from pDAN (HYG^R). These PCR products were used as templates in fusion PCR to generate two PCR fragments separately containing the left or right border of targeted genes with the truncated, partial-overlapped *HPT* fragments. These two fusion-PCR products were transformed into *S. scitamineum* wild-type *MAT-1* protoplasts via polyethylene glycol (PEG)-mediated transformation (Deng et al., 2018).

For *RAM1*, *RAS1*, *RAS2,* and *MFA1* complementation, a fragment containing the 1–1.5 kb 5′ flanking sequence, whole coding sequence and 1 kb 3′ flanking sequence of the respective gene was PCR amplified with wild-type genomic DNA as template, using the primers pair listed in **Supplementary Table S2**. This fragment was inserted into the engineered pEX2 ($Zeocin^R$) derived plasmid (Williams and Birnbaum, 1988) through homologous recombination by using ClonExpress II One Step Cloning Kit (Vazyme, C112-01), to form the complementary plasmid pEX2-RAM1, pEX2-RAS1, or pEX2-RAS2, respectively. The complementary plasmid was, respectively, transformed into the corresponding deletion mutant via PEG-mediated transformation and screened by Zeocin resistance, and confirmed by PCR and Southern blot analysis.

For construction of *eGFP-RAM1* plasmid, coding sequence of eGFP was PCR amplified using pEX1 (Sun et al., 2014) as template, and 1818 bp of *RAM1* coding sequence was PCR amplified using genomic DNA of wild-type strain as template. These two PCR amplified fragments were then fused by PCR amplification and cloned into the engineered pEX2 ($Zeocin^R$) derived plasmid, driven by a constitutive (*G3PD*) promoter. The two fusion homologous fragments were PCR amplified as one fragment containing HPT-LB fused with complete *G3PD-eGFP-RAM1* sequence and partially overlapped fragments of the zeocin gene, and the other containing partially overlapped fragments of the zeocin gene and HPT-RB. This construct was used to replace the hygromycin gene (*HPT*) in the *ram1*Δ mutant, with complementary *eGFP-RAM1* coding sequence and zeocin resistance gene. Primers used in this study are listed in **Supplementary Table S2**.

Nucleic Acid Manipulation

Fungal genomic DNA was extracted using a modified SDS method (Yan et al., 2016b). PCR amplification was performed using KOD High-Fidelity DNA Polymerase FX (TOYOBO, KEX-101). Purification of DNA fragments was done using a Gel Extraction Kit (Omega, D2500-02) or a Cycle Pure Kit (Omega, D6492-02). Homologous recombination for fragment ligation with the plasmid was performed using Exnase Multis (Vazyme, C113-01). Total RNA was extracted with Trizol (Invitrogen), and the PrimeScript RT Master Mix (TAKARA, RR036A) was used for cDNA synthesis. NANODROP ONE (Thermo scientific) was used for measuring concentrations and purity testing. In Southern blot assay, restriction enzymes (*HindIII*, *Xba*I, and *Spe*I) used for genomic DNA digestion were from New England Biolabs (United States). For probe preparation, the PCR amplified fragment was purified using Cycle Pure Kit (Omega, D6492-02), and labeled with digoxin using DIG-High Prime DNA Labeling and Detection Starter Kit I (Roche, 11745832910). Probe hybridization was performed using a DIG Probe Synthesis Kit (Roche, 11636090910) and detected by DIG Nucleic Acid Detection Kit (Roche, 11175 041910).

Plant Infection and Fungal Biomass Assessment

Strains were grown in YePSL medium under shake culture conditions at 28°C for 12 h. The sporidia were harvested via centrifugation and resuspended in distilled water to a final OD600 of 1.0. Sporidial suspension (1 mL) was syringe-injected into the 3-week-old seedlings of the highly susceptible sugarcane cultivar ROC22 (Guangxi Province, China). Mock inoculations were carried out by injecting distilled water. The sugarcane stem tissue used for *S. scitamineum* biomass evaluation was collected at 3 days post inoculation (dpi), and quantification of relative fungal biomass in infected sugarcane stem tissue was performed using the fungal *ACTIN* gene as reference (Brefort et al., 2014). The sugarcane glyceraldehyde dehydrogenase (*GAPDH*) gene served as reference for normalization (Su et al., 2016). The black whip symptoms were evaluated for disease rating (Chang et al., 2018). Three biological repeats, each containing three technical replicas for each sample, were performed.

Quantitative Real-Time PCR

Quantitative reverse transcription polymerase chain reaction (qRT-PCR) was performed on a $qTOWER^3G$ (Analytik Jena) using the TB Green Premix Ex Tag (TAKARA, RR820A). The qRT-PCR was run with the following settings: 95°C/3 min – (95°C/10 s – 60°C/30 s –72°C/30 s) × 40 cycles and 72°C 10 s. Relative expression values were calculated with the $2^{-\Delta\Delta Ct}$ method (Livak and Schmittgen, 2001), using *ACTIN* as internal control. Three biological repeats, each containing three technical

replicas for each sample, were performed. Primers used in this study are listed in **Supplementary Table S3**.

Protoplast Production Assay

For protoplast generation assay the cultured *S. scitamineum* sporidia (OD600 ≈ 0.6) were harvested, and incubated with the lyzing solution (the lyzing enzyme, Sigma L1412, was dissolved in SCS solution comprised of 20 mM trisodium citrate and 1M D-sorbitol, at pH 5.8, to reach a concentration of 15 mg/mL) and incubated for 20 min (Chang et al., 2018). The lysis was stopped by placing the reaction tube on ice. The protoplasts production were examined by microscopy (OLYMPUS, CX21) and counted using a hemacytometer (Jeon et al., 2008). Three biological repeats, each containing three technical replicas for each sample, were performed.

Malondialdehyde (MDA) Content Measurement

Sporisorium scitamineum sporidia (OD600 ≈ 0.1) were harvested, and 150 μL of sporidial suspension was used for culturing on MM plates with or without 25 μg/mL SDS treatment for 48 h at 28°C before determination of MDA content. The sporidia samples were gently scraped from the plates and homogenized in an ice bath with 2.0 mL of 5% trichloroacetic acid solution (m/v), and then centrifuged at 10,000 rpm for 15 min at 4°C. Approximately 2.0 mL of the resulting supernatant was mixed with 1.0 mL of 5% trichloroacetic acid containing 0.67% thiobarbituric acid solution (m/v), and the container heated in boiling water for 5 min. The mixture was rapidly transferred to an ice bath, and measured for its absorbance at 532 nm using a spectrophotometer (METASH, UV5100B). Non-specific turbidity of the sample was corrected by subtracting its absorbance at 600 nm. The MDA concentration was calculated and expressed as μmol/g FW (Lanubile et al., 2015).

Sporidial Staining and Microscopy

Sporisorium scitamineum sporidia (OD600 ≈ 1.0) were harvested via centrifugation and washed twice, before further processing and staining. The sporidial suspension with or without SDS in full 200 μg/mL SDS treatment for 10 min was harvested and washed twice in distilled water, and subjected to staining with propidium iodide PI (Sigma, 25535-16-4), by incubating with 60 μg/mL PI solution (in DPBS, Dulbecco's Phosphate-Buffered Saline: 2.67 mM KCl, 1.47 mM KH_2PO_4, 138.00 mM NaCl, and 8.10 mM Na_2HPO_4) for 15 min in the dark (Silva et al., 2005). The stained sporidia were washed twice and placed on a slide for examination under an epifluorescent microscope (OLYMPUS, BX53) using a DAPI filter. For Concanavalin A (ConA) staining, 100 μL of sporidial suspension was collected and stained in 100 μg/mL ConA type VI conjugated to FITC (Sigma, C7642) for 45 min as described (Li et al., 2014). The stained sporidia were washed twice and observed by epifluorescent microscopy using a GFP filter. For staining with the fluorescent brightener calcofluor white (CFW), 100 μL of sporidial suspension were collected and stained in 10 μg/mL fluorescent brightener (calcofluor white; Sigma, 18909) as described (Krombach et al., 2018), and examined by epifluorescent microscopy using a DAPI filter. Microscopic images were taken with a digital camera (OLYMPUS, DP80) equipped with the microscope.

Intercellular cAMP Extraction and Detection

Intracellular cAMP of *S. scitamineum* sporidia were extracted and detected by cAMP Enzyme Immunoassay Kit (Sigma, CA201), using the procedure previous reported (Chang et al., 2018).

RESULTS

Identification of a Conserved Farnesyltransferase β Subunit Encoding Gene *RAM1*

A tBLASTx search with *Neurospora crassa* Ram1 protein (XM_953714.2:176-1807) as the query revealed the presence of one putative *RAM1* gene in *S. scitamineum*. A phylogenetic analysis of the putative *S. scitamineum* Ram1 protein and previously characterized Ram1 proteins from other fungi, including smut fungi and ascomycetous fungi, indicated the presence of two distinct phylogenetic clades (**Figure 1**). *S. scitamineum* Ram1 was 87% identical to putative *Sporisorium reilianum* Ram1, 78% to *U. maydis* Ram1, 34% to *C. neoformans* Ram1, and 34% to *A. fumigatus* Ram1, respectively. *RAM1* is predicted to encode a peptide of 606 amino acids, with two prenyltransferase domains and one squalene oxidase repeat (PF00432.16) at positions of 139–180 and 207–250 amino acid in *S. scitamineum*. The domain and amino acid sequences of Ram1 proteins were highly conserved among all smut fungi analyzed (**Supplementary Figure S1A**).

RAM1 Is Required for *S. scitamineum* Mating/Filamentation

To evaluate the impact of *RAM1* on mating and growth, a *ram1*Δ mutant and its complementation strain *RAM1c* were generated. The number of insertion copy was verified by Southern blotting using *HPT* fragment as probe (**Supplementary Figure S1B**), and the replacement of *RAM1* gene was also confirmed by Southern blotting using locus-specific probe (**Supplementary Figure S1C**). The re-introduction of *RAM1* gene was verified by PCR amplification (**Supplementary Figure S1D**). For haploid vegetative growth, the *ram1*Δ colony surface appeared drier than that of the wild-type *MAT-1* or *RAM1c* strain when grown on YePSA (**Figure 2A**: left panel), but the growth speed of sporidia was indistinguishable among these three strains when cultured in YePS liquid medium (**Figure 2B**). The mating of *ram1*Δ sporidia with compatible wild-type *MAT-2* was obviously reduced, compared to that of wild-type or *RAM1c* strains (**Figure 2A**: right panel). Furthermore, we found that mixing of two *ram1*Δ of compatible mating types displayed a complete blockage of mating and filamentous growth/filamentation (**Supplementary Figure S2A**). qRT-PCR analysis was performed for assessing expression of genes related to fungal mating and filamentation in mutants and wild-type.

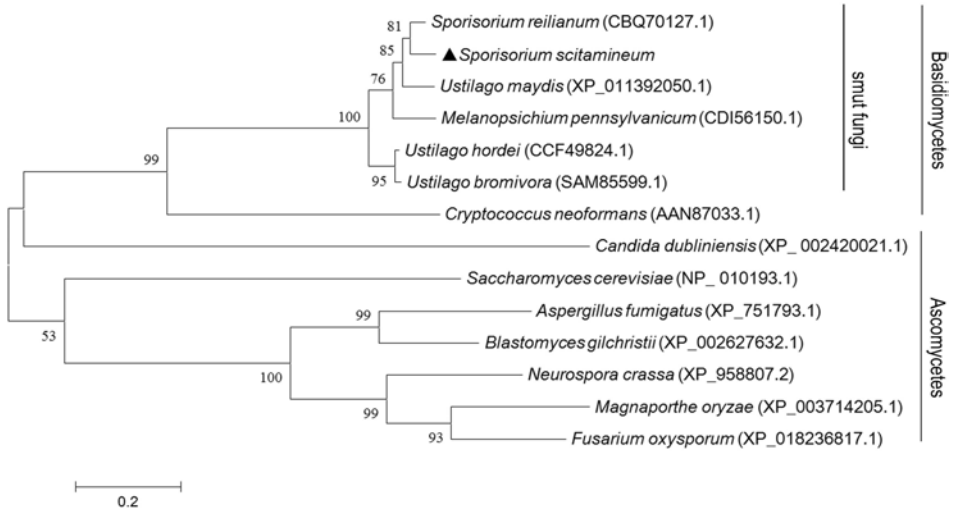

FIGURE 1 | Phylogenetic analysis and amino acid sequences arrangement with *Sporisorium scitamineum Ram1* protein and its orthologs. Phylogenetic analysis of fungal orthologous Ram1 proteins. Amino acid sequences were aligned with ClustalX 2.0 (Thompson et al., 1994) with the following parameters: pairwise alignment parameters (gap opening = 10, gap extension = 0.1) and multiple alignment parameters (gap opening = 10, gap extension = 0.2, transition weight = 0.5, delay divergent sequences = 25%). The alignment was phylogenetically analyzed with maximum likelihood by MEGA 6.0 (Kenaley et al., 2018), by using a Le-Gasquel amino acid replacement matrix with 1,000 bootstrap replications. *S. scitamineum* Ram1 was denoted by a solid triangle.

The results showed that in *ram1*Δ sporidia, the a locus genes *MFA1* and *PRA1*, and the b locus genes *bE1* and *bW1* were all comparable to that in the complementary or wild-type strains, while *PRF1*, the master transcriptional regulator for mating and filamentation, was significantly down-regulated (**Supplementary Figure S2B**). Overall these results showed that *Ram1* is required for *S. scitamineum* mating and filamentation.

Expression of *RAM1* During Development of Sporidia to Hyphal in *S. scitamineum*

To determine the potential function of *RAM1* at the haploid sporidia switch to dikaryotic hyphal growth, we assessed transcriptional profile of *RAM1* gene every 12 h over a period of 72 h in haploid or mating condition using qRT-PCR. In wild-type sporidia, the expression of *RAM1* was elevated with cultural time. The maximal expression level occurred at around 60 h, of more than 10-fold compared to that at 12 h. Then we examined the expression of *RAM1* gene from 12 to 72 h in dikaryotic hyphal stage. The results showed that the expression of *RAM1* was obviously reduced compared to that in sporidia stage (**Figure 3A**). We also found the pattern of pheromone precursor gene *MFA1* was similar to that of *RAM1* (**Figure 3B**), but the elevated expression initially started at 48 h and reached the maximum at around 60 h (**Figures 3A,B**).

To observe the subcellular localization of Ram1 protein, a copy of *eGFP-RAM1* fusion fragment was transferred into the *ram1*Δ mutant. The mating ability was restored in the resulting *ram1*Δ/eGFP-Ram1 strain, indicating that the eGFP-Ram1 fusion protein is functional. By epifluorescent microscopy, we observed that the eGFP-Ram1 signal localized in the cytosol of sporidial cells (**Figure 3C**), with occasional punctate structure in the cytoplasm (**Figure 3C**, arrows). These data imply that *RAM1* plays an important role in development of sporidia.

Mfa1 Farnesylation Could Partially Restore *ram1*Δ Mating/Filamentation Defect

The *S. cerevisiae* and *U. maydis* pheromone precursor Mfa1 undergoes C-terminal farnesylation before its maturation and functioning as a hormone in compatible sporidial recognition and induction of sexual mating (Ashby and Rine, 1995; Koppitz et al., 1996). Therefore we intended to investigate whether the mating/filamentation defect of the *ram1*Δ was due to failure of the Mfa1 precursor in farnesylation (Spellig et al., 1994; Ashby and Rine, 1995). In *S. scitamineum*, the *MFA1* gene codes a 41-amino-acid pheromone precursor in *MAT-1* (CAI59747.1), which contains a predicted farnesylation motif CTIA at its C-terminal. We generated *mfa1*Δ mutants and its complementation strains *MFA1c* with wild-type *MAT-1* background. The mutants and complementation strains were verified by PCR and Southern blotting (**Supplementary Figure S3**). As expected the mating of the *mfa1*Δ mutant with compatible mating type *MAT-2* was completely blocked when cultured on YePSA media, and significant reduced on MM plates, compared to that of wild-type or *MFA1c* strains (**Figure 4A**). To confirm that such mating/filamentation defect was caused by loss of functional (farnesylated) a-pheromone encoded by *MFA1*, we generated and supplied the synthetic Mfa1 peptide with or without C-terminal farnesylation to MM plates to reach a final concentration of 1 or 10 μg/mL, and tested its effect on restoring mating/filamentation of the *mfa1*Δ or *ram1*Δ mutant. We found that the farnesylated Mfa1 peptide could effectively restore mating/filamentation in the *mfa1*Δ mutant at

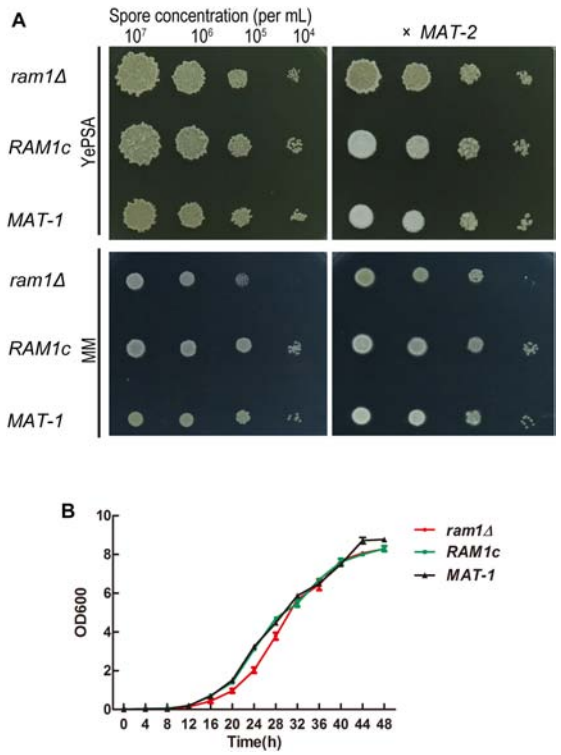

FIGURE 2 | *RAM1* is required for *S. scitamineum* sexual mating. **(A)** Haploid (left) and mating (right, x MAT-2) colony of *ram1*Δ, wild-type *MAT-1* and the complementation strain *RAM1c*. A sporidial suspension (1 μL) of OD600 = 1.0, and the serial 10-fold dilutions of indicated strains, were spotted on YePSL or MM plates and incubated at 28°C for 24 h, before examination. **(B)** Saprophytic growth curve of *ram1*Δ, wild-type *MAT-1* and the complementation strain *RAM1c*. For the growth curve, strains were cultured in YePSL over a period of 48 h. Three biological replicates, each containing three technical replicates for each sample, were performed.

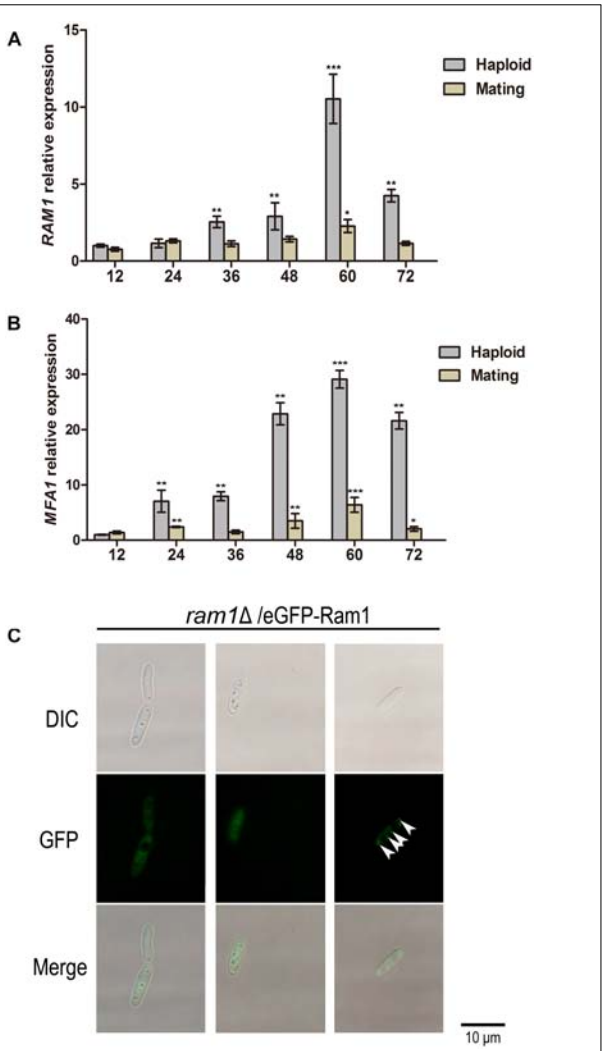

FIGURE 3 | Transcriptional profile of *RAM*1 gene and *MFA1* gene and subcellular localization of Ram1 protein in *S. scitamineum*. **(A)** qRT-PCR analysis of *RAM1* expression in wild-type strain under sporidial growth or mating condition on YePSA plate. *RAM1* expression in 12 h was set as 1 and the relative gene expression fold change in a period of 72 h was calculated with $2^{-\Delta\Delta Ct}$ method (Livak and Schmittgen, 2001), using *ACTIN* as internal control. Statistical significance of the expression data was determined at $^{***}p < 0.005$, $^{**}p < 0.01$, and $^{*}p < 0.05$ using Student's *t*-test, and error bars represent ± standard deviation values. **(B)** qRT-PCR analysis of *MFA1* expression in wild-type strain under sporidial growth or mating condition on YePSA plate. *MFA1* expression in 12 h was set as 1 and the relative gene expression fold change in a period of 72 h was calculated with $2^{-\Delta\Delta Ct}$ method (Livak and Schmittgen, 2001), using *ACTIN* as internal control. Statistical significance of the expression data was determined at $^{***}p < 0.005$, $^{**}p < 0.01$, and $^{*}p < 0.05$ using Student's *t*-test, and error bars represent ± standard deviation values. **(C)** Localization of eGFP-Ram1 fusion proteins in the *ram1*Δ sporidia. Sporidial suspension of OD600 = 1.0 were spotted on YePSA plates and incubated at 28°C for 24 h, before epifluorescent microscopic observation and imaging. Arrows denote punctate structure visualized by eGFP-Ram1. Scale bar = 10 μm.

the concentration of 10 μg/mL, and only partially restored that of the *ram1*Δ mutant (**Figure 4B**). In contrast, addition of the Mfa1 peptide without farnesylation failed to rescue the defective mating/filamentation in *ram1*Δ or *mfa1*Δ mutant (**Figure 4B**). Putting together, these results suggested that Ram1 is likely required for farnesylation of pheromone precursor Mfa1, which is essential for *S. scitamineum* mating/filamentation.

RAM1 Is Required for Full Pathogenicity of *S. scitamineum*

To test whether the *RAM1* is required for *S. scitamineum* pathogenicity, we inoculated the mixture of *ram1*Δ × *MAT-2* sporidia by injection, into a susceptible sugarcane seedling, and evaluated the disease symptoms. Inoculation with the wild-type *MAT-1* × *MAT-2* or the *RAM1c* × *MAT-2* combination served as positive control, and sterile water as mock. The *ram1*Δ × *MAT-2* combination displayed significantly reduced pathogenicity, with only around 10% of the infected seedlings showing black whip symptoms at 200 dpi. In contrast, the wild-type *MAT-1* and *MAT-2* mixture lead to 70% of the infected seedlings with black whip symptoms, while that in the *RAM1c* and wild-type *MAT-2* mixture was approximately 50% (**Figure 5A**). Consistently, relative fungal biomass was significantly lower at 3 dpi in seedling stems inoculated with *ram1*Δ × *MAT-2*, compared

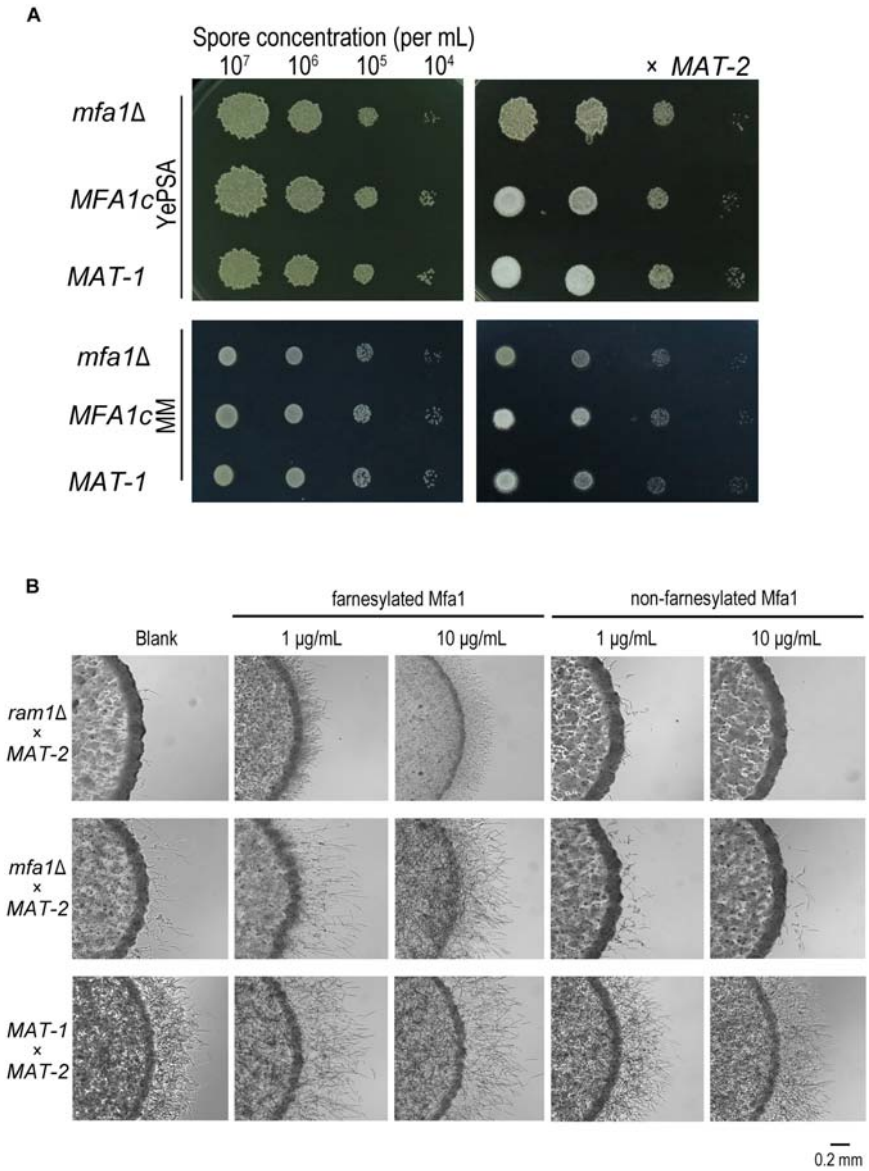

FIGURE 4 | Mfa1 farnesylation could partially restore *ram1*Δ mating/filamentation defect in *S. scitamineum*. **(A)** Haploid (left) and mating (right, x *MAT-2*) colony of *m1*Δ and wild-type *MAT-1*. 1 μL sporidia suspension of OD600 = 1.0, and the serial 10-fold dilutions of indicated strains, were spotted on YePSA or MM plates and incubated at 28°C for 24 h. **(B)** Mating/filamentation assay with synthetic (farnesylated or non-farnesylated) Mfa1 exogenously supplied to MM plates to reach a final concentration of 1 μg/mL or 10 μg/mL. 1 μL sporidial suspension (of the mutants *ram1*Δ, *mfa1*Δ or wild-type strain) of OD600 = 1.0 were, respectively, mixed with compatible mating partner and cultured on MM plates at 28°C for 24 h.

to that inoculated with the wild-type or complementary strain combinations (**Figure 5B**). These data suggest that *Ram1* is also essential for full pathogenicity of *S. scitamineum*.

RAS Genes Are Required for *S. scitamineum* Mating and Filamentation

It has been reported that Ram1/Ram2 FTase complex controls fungal differentiation and/or pathogenicity via post-translational modifications of Ras proteins, the small G proteins playing an important role in cell signaling (Omer and Gibbs, 1994). Therefore we wondered whether defects mating and filamentation defects in the *ram1*Δ were related to Ras protein modification and the Ras-mediated signaling pathway. A BLASTP search with *U. maydis* Ras1 protein (XP_011386972.1) as the query revealed the presence of one putative *RAS1* gene in *S. scitamineum*, which is predicted to encode a protein of 215 amino acids, with one RAS superfamily domain (PF00071) from amino acids 11–172. A BLASTP search with *U. maydis* Ras2 (XP_011387629.1) as the query revealed the presence of one putative *RAS2* gene in *S. scitamineum*, encoding a protein

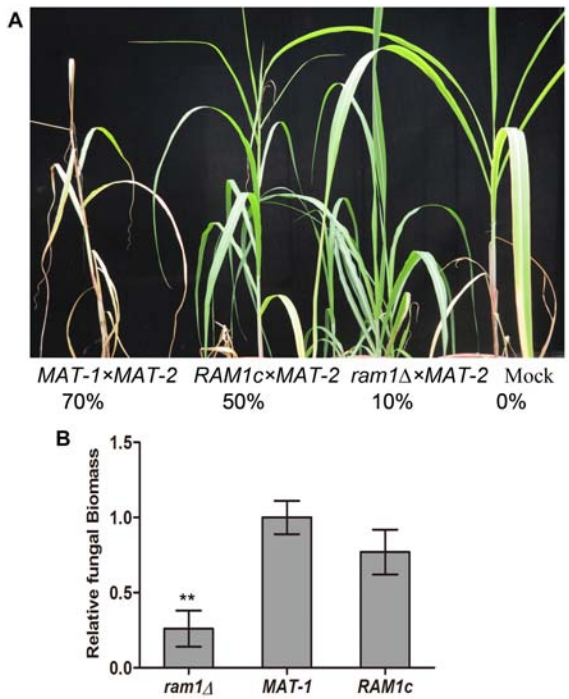

FIGURE 5 | *RAM1* is required for *S. scitamineum* pathogenicity. **(A)** The susceptible sugarcane cultivar ROC22 was inoculated with mixed sporidia (1:1) of the indicated wild-type or mutant combination through injection at the 5–6-leaf seedling stage, and the symptoms of 'black whip' were assessed and documented at 200 days post inoculation (dpi). The infection assays were performed with at least 20 seedlings. Percentage of plants with 'black whip' symptoms is illustrated. **(B)** Colonization of the plant tissue by *ram1*Δ, wild-type *MAT-1*, or the complementation strain *RAM1c*. Relative fungal biomass was determined by qRT-PCR with *S. scitamineum* genomic DNA isolated from infected sugarcane stems at 3 dpi. The fungal *ACTIN* gene was used for estimation of relative fungal biomass through $2^{-\Delta\Delta Ct}$ method (Livak and Schmittgen, 2001), normalized to the plant *GADPH* gene. Barchart depicts the average ± standard error (SE) derived from three biological replicates. Significance of differences between wild-type *MAT-1* and *ram1*Δ was calculated using Student's *t*-test, $^{**}p < 0.01$.

of 192 amino acids, with one RAS superfamily (PF00071) from amino acids 5–173. *S. scitamineum* Ras1 and Ras2 shared 58% identity from Ras1 amino acids 10–171 covering the entire RAS domain, which indicated the conservation of Ras proteins at the amino acid sequence level. However, this indicated the other portions outside of the RAS domain of the Ras1 and Ras2 proteins probably serve other functions. A phylogenetic analysis of *S. scitamineum* Ras1 and Ras2 proteins with predicted or characterized Ras proteins from other basidiomycetous or ascomycetous fungi indicates that Ras1 and Ras2 proteins are divergent with each other, but is respective well conserved within its own group (**Supplementary Figure S4**).

To further investigate the function of *S. scitamineum RAS* genes, we generated *ras1*Δ and *ras2*Δ mutants, and their complementation strains *RAS1c*, *RAS2c*, both with wild-type *MAT-1* background, and verified by Southern blotting and PCR (**Supplementary Figures S5, S6**). The *ras1*Δ haploid colonies were obviously smaller and wetter than that of the wild-type *MAT-1* strain (**Figure 6A**, left panel). The compatibility of *ras1*Δ with *MAT-2* sporidia was obviously reduced compared to that of wild-type *MAT-1* and the *RAS1* complementation strain, which displayed normal filament formation after mating (**Figures 6A** right panel, **6B**). The *ras2*Δ haploid colonies were also obviously smaller and wetter than that of the wild-type *MAT-1* strain (**Figure 6A**, left panel). However, the mating of *ras2*Δ with *MAT-2* sporidia was only mildly reduced, and the mating of complementation strains was normal (**Figures 6A** right panel, 6B). Exogenous applications of cAMP (concentrations from 2.5 to 5 mM) could enhance (but not fully restore) sexual mating of mutants of *ras1*Δ or *ras2*Δ but not the one of *ram1*Δ and *mfa1*Δ (**Figure 6C**). This result indicates that cAMP signaling may be at downstream of Ras proteins, but not sufficient for fully restore Ram1 or Mfa1 function. Exogenous applications of synthetic (farnesylated) Mfa1 (concentrations 1 or 10 μg/mL) only or together with 5 mM cAMP couldn't restore sexual mating of mutants of *ram1*Δ, *ras1*Δ, or *ras2*Δ except for *mfa1*Δ, synthetic (non-farnesylated) Mfa1 couldn't restore mating/filamentation in these four mutants (**Figure 6C**). The phenotype of mating defect in *ras1*Δ or *ras2*Δ mutants were slighter than that in *ram1*Δ imply function of Ras1/Ras2 proteins are probably redundant in regulating mating/filamentation in *S. scitamineum*.

Ram1 and Ras Signaling Are Involved in *S. scitamineum* Cell Wall Integrity

Next we evaluated the stress tolerance of the *ram1*Δ, *ras1*Δ, *ras2*Δ, and *mfa1*Δ mutants, toward 20 μg/mL Congo red (cell wall stress), 20 μg/mL SDS (membrane stress), 25 μg/mL CFW (cell wall stress), 1 M Sorbitol (osmotic stress) and 0.5 mM H_2O_2 (oxidative stress). The mutants *ram1*Δ, *ras1*Δ, and *ras2*Δ displayed greater growth inhibition by treatment with SDS (20 μg/mL) or H_2O_2 (0.5 mM) than the wild-type *MAT-1* strain, and the tolerance abilities were restored in the complementation strains (**Supplementary Figures S7–S9**). Both *ras1*Δ and *ras2*Δ mutants were hypersensitive to CR (20 μg/mL) while *ram1*Δ mutant was not hypersensitive (**Supplementary Figure S7**). With respect to osmotic stress sensitivity against sorbitol (1 M), all the mutant strains were indistinguishable from the wild-type strain (**Supplementary Figure S7**). On the other hand, the *mfa1*Δ mutant displayed no obvious difference in tolerance toward all these testing stressors, compared to that of WT (**Supplementary Figure S7**).

Given that the *ram1*Δ mutant was hypersensitive toward SDS, we intended to measure malondialdehyde (MDA) content of *S. scitamineum* sporidia, which indicates the degree of cell membrane damage (Li et al., 1998). The results showed that the *ram1*Δ sporidia contained notably higher MDA content than that of the wild-type *MAT-1* or the complementation strain after SDS treatment (**Figure 7A**), which may account for reduced tolerance to SDS in the *ram1*Δ. It has been reported that SDS strongly increases solubilization of membrane lipid, leading to lipid peroxidation and cell membrane damage (He et al., 2005). MDA is the final product, and also an important indicator, of lipid oxidation (Lanubile et al., 2015), hence it

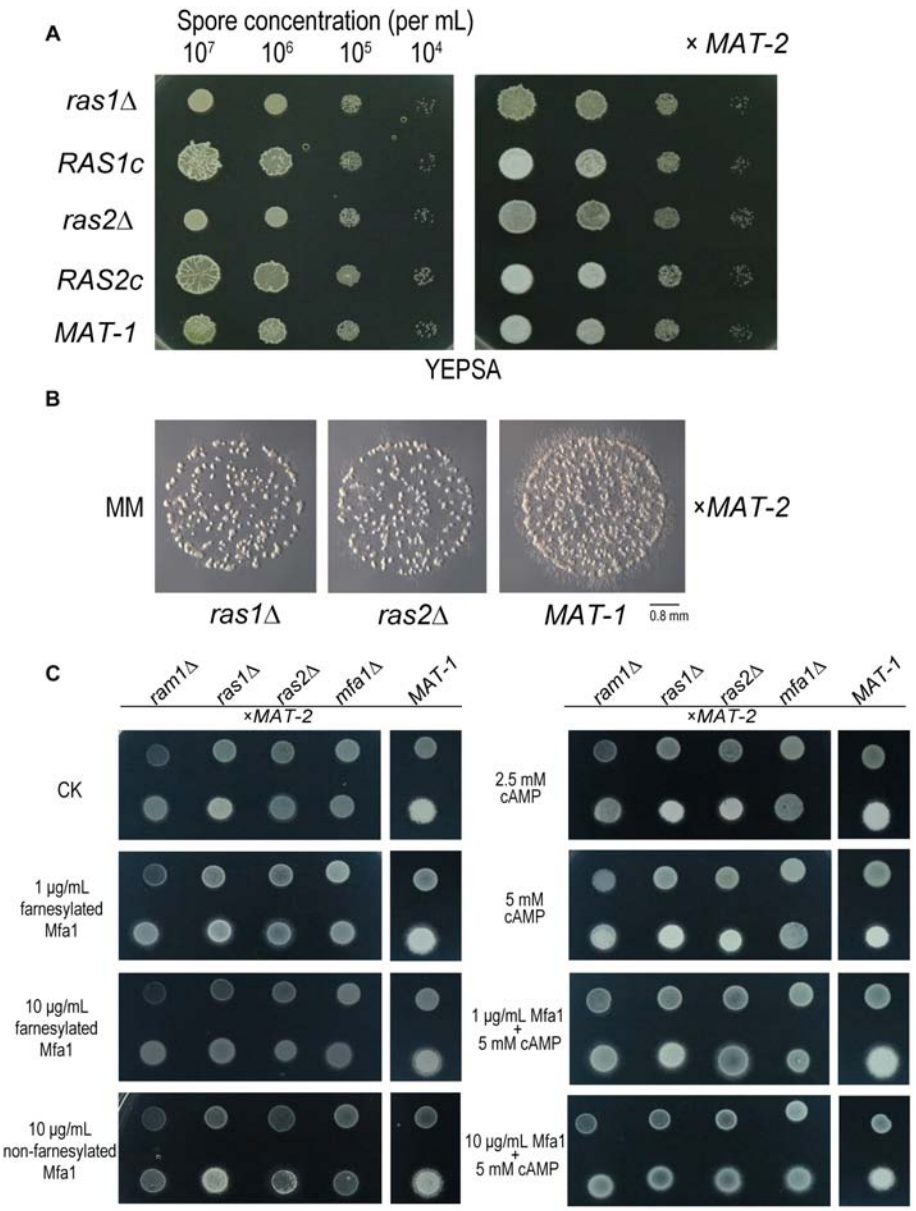

FIGURE 6 | *RAS1* and *RAS2* are required for *S. scitamineum* mating/filamentation. **(A)** Haploid (left) or mating (right, x *MAT-2*) colonies of *ras1*Δ, *RAS1c*, *ras2*Δ, *RAS2c*, and wild-type *MAT-1*. One microliter sporidial suspension of OD600 = 1.0, and serial 10-fold dilutions, of indicated strains, were spotted on YePSA plates and incubated at 28°C for 24 h. **(B)** Microscopic observation of mating colonies of *ras1*Δ, *ras2*Δ, and wild-type *MAT-1* on MM plates with 1 μL sporidial suspension (OD600 = 0.1) and incubated for 12 h at 28°C. Scale bar = 0.8 mm. **(C)** Haploid (upper) and mating (lower, x *MAT-2*) colony of *ras1*Δ, *ras2*Δ, *ram1*Δ, and *mfa1*Δor wild-type *MAT-1* on MM plates with 1 μL OD600 = 1.0 sporidia suspension with exogenous cAMP of 0, 2.5, or 5 mM, synthetic (farnesylated) Mfa1 exogenously supplied to MM plates to reach a final concentration of 1 or 10 μg/mL, synthetic (non-farnesylated) Mfa1 exogenously supplied to MM plates to reach a final concentration of 10 μg/mL at 28°C for 24 h.

is expected that the increased MDA content indicates cell membrane damage caused by SDS treatment. Correspondingly, the *ram1*Δ sporidia displayed notable propidium iodide (PI) positive staining compared to that of the wild-type or the complementation strains, after treatment with 200 μg/mL SDS for 10 min (**Figure 7B**), suggesting that the cell membrane of *ram1*Δ sporidia was weaker than that of the wild-type or the complementation strains.

On MM media supplemented with 20 μg/mL Congo red (CR), the *ram1*Δ mutant displayed no obvious difference in growth compared to the wild-type strain (**Supplementary Figure S7**). We further verified the inhibition effect of CR by colony counting from the sporidial suspension on the MM plates with or without 50 μg/mL CR. Growth inhibition of *ram1*Δ mutant on CR-supplemented MM plate was 71.94% while that of wild-type or the complementation strain was 98%, of that

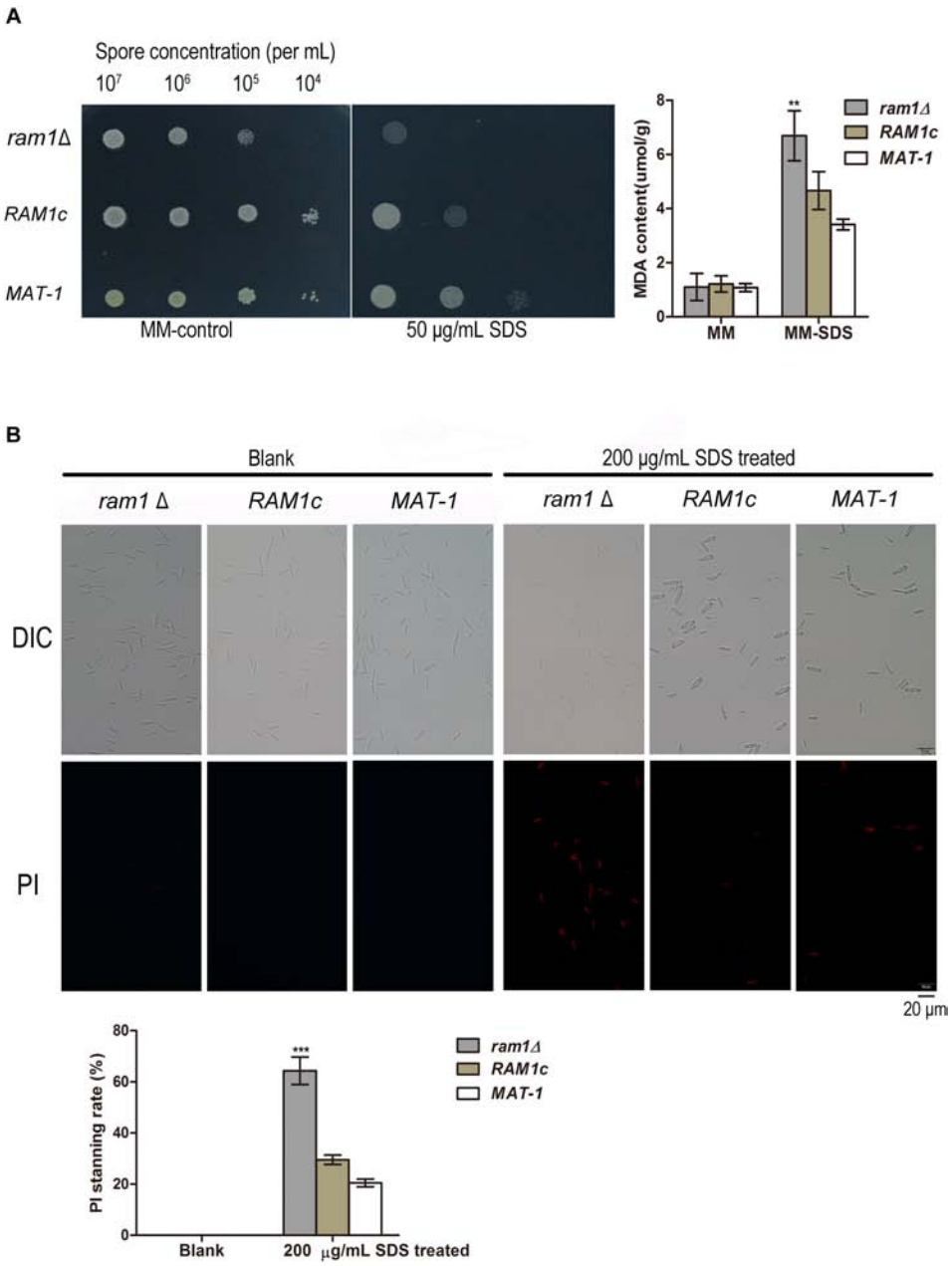

FIGURE 7 | *RAM1* is required for membrane stability of *S. scitamineum* sporidia. **(A)** Malondialdehyde (MDA) content of *ram1* Δ, wild-type *MAT-1* and the complementation strain *RAM1c* with or without treatment of 50 μg/mL SDS. Barchart on the right panel depicts the average ± standard error (SE) derived from three independent biological replicates. Significance of differences between wild-type *MAT-1* and ram1 was calculated by Student's *t*-test, $^{**}p < 0.01$. **(B)** Microscopic examination (upper panel) of *ram1* Δ, wild-type *MAT-1* and the complementation strain *RAM1c* with Propidium iodide (PI) staining after 200 μg/mL SDS treatment for 10 min. PI staining was assessed after 15 min of staining. Scale bar = 20 mm. Barchart on the lower panel depicts the average ± standard error (SE) derived from three independent replicates. Significance of differences between wild-type *MAT-1* and *ram1* Δ was calculated using a Student's *t*-test, $^{***}p < 0.005$.

on the MM plate without CR (**Figure 8A**). This indicates that the *ram1*Δ mutant was more tolerant toward CR compared to the wild-type or the complementation strains. To test cell wall integrity, an equal amount of sporidia from the *ram1*Δ mutant, the *RAM1c* and wild-type *MAT-1* strains were treated with 15 mg/mL cell wall lyzing enzyme at 28°C for 20 min. The percentage of protoplasts generated was viewed as an indicator of cell wall integrity. The result showed that the *RAM1c* and wild-type *MAT-1* sporidia were hypersensitive to the enzyme treatment, producing more protoplasts than the *ram1*Δ mutant (**Figure 8B**). This also suggested that the cell wall integrity was enhanced in the *ram1*Δ mutant, and thus it was more tolerant to CR. Furthermore, we assessed the expression of the genes involved in the cell wall integrity (CWI) pathway by

qRT-PCR, in the *ram1*Δ mutant in comparison of the wild-type *MAT-1*, with or without treatment of 25 μg/mL CR. Our results showed that *MID2* and *WSC1* (membrane proteins as main sensors) (Philip and Levin, 2001), *ROM2* (GEF which sensors interacted with) (Ozaki et al., 1996), *RHO1* (small GTPase) (Schmelzle et al., 2002), *PKC1* (protein kinase c) (Paravicini and Friedli, 1996), *BCK1* (MAPKKK) (Lee and Levin, 1992), *MKK1* (MAPKK) (Kim et al., 2008), *SLT2* (MAPK) (Rui and Hahn, 2007), *RLM1* (downstream transcription factors) (Jung et al., 2002), *FKS3* and *SMI1* (glycan synthase) (Lesage and Bussey, 2006) were all significantly up-regulated in the *ram1*Δ mutant treated with CR, compared to wild-type *MAT-1* sporidia (**Figure 8C**). This result indicated that the *RAM1* gene may regulate CWI via transcriptional regulation of the genes involved in this signaling pathway.

On the other hand, the *ras1*Δ and *ras2*Δ mutants displayed hypersensitivity to cell wall stressors CR, CFW, and SDS, and the tolerance abilities were restored in the complementation strains (**Supplementary Figures S7, S9**). We further investigated whether *Ras1* and/or *Ras2* affect the cell wall integrity by conA and CFW staining. ConA is lectin specifically binding to internal and non-reducing terminal α-D-mannosyl groups and thus is routinely used to assay the presence of mannan moieties in fungal cell walls (Maddi et al., 2012). Our results showed that the *ras1*Δ mutant exhibited weaker fluorescence staining by conA, indicating reduced conA binding sites, while the *ras2*Δ mutant displayed indistinguishable conA staining compared to that of the wild-type (**Figure 9A**). For CFW staining, the *ras1*Δ mutant exhibited a significantly brighter staining pattern than the wild-type, and the *ras2*Δ mutant was slightly brighter than wild-type *MAT-1* (**Figure 9A**). This result implied that the cell wall permeability toward CFW dye was enhanced in the *ras1*Δ and the *ras2*Δ mutants, but not in wild-type.

In *U. maydis*, both Ras1 and Ras2 regulate intercellular cAMP level (Nadal et al., 2008; Zhu et al., 2009). In *C. neoformans*, intercellular cAMP level regulates the cell wall integrity pathway (Donlin et al., 2014). To furthermore evaluate the role of cAMP in cell wall integrity we measured the intercellular cAMP concentration in the *ras1*Δ and *ras2*Δ mutants in comparison with wild-type. The results showed no obvious differences in the intercellular cAMP concentrations between the *ras1*Δ and the *ras2*Δ mutants and the wild-type strain (**Figure 9B**). We proposed that *Ras1*/*Ras2*-regulating CWI pathway is likely independent of cAMP/PKA signaling pathway.

Overall, in this section we found that Ram1 may negatively, and Ras proteins positively, regulate CWI pathway in *S. scitamineu*m. The a-factor Mfa1 may not be involved in *S. scitamineum* CWI regulation.

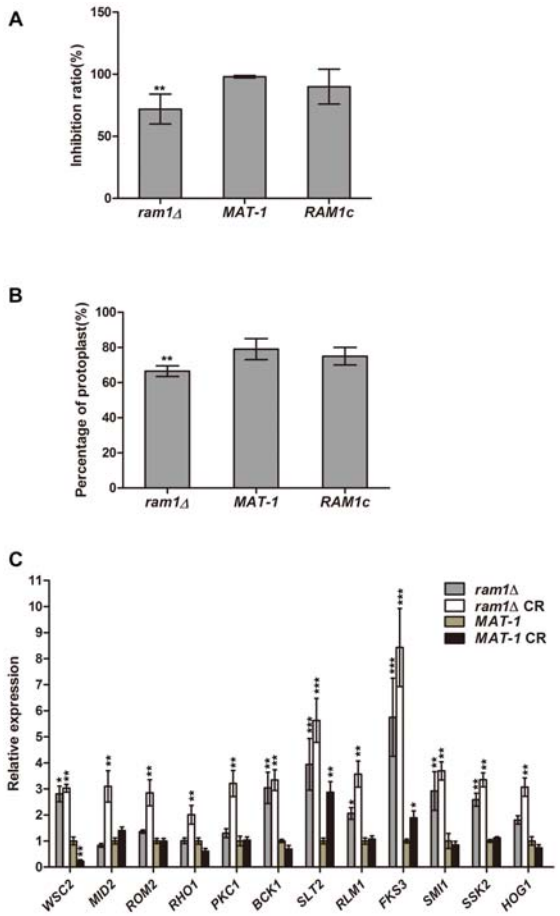

FIGURE 8 | *RAM1* regulates *S. scitamineum* cell wall integrity. **(A)** Growth inhibition calculated by number of colonies formed following streaking of *ram1*Δ, wild-type *MAT-1* and the complementation strain *RAM1c* sporidial suspension (OD = 10^{-5}; 150 mL), on MM plates with or without 50 μg/mL Congo red (CR). Statistical significance of the inhibition was determined at $^{**}p < 0.01$ using Student's *t*-test, and mean ± standard deviation was derived from three independent biological replicates. **(B)** Enzymatic digestion and protoplast production assay with *ram1*Δ, wild-type *MAT-1* and the complementation strain *RAM1c*. Protoplast production was counted at 20 min post lyzing enzyme incubation. Statistical significance of the protoplast production was determined at $^{**}p < 0.01$ using Student's *t*-test, and mean ± standard deviation was derived from three independent biological replicates. **(C)** qRT-PCR analysis with genes involved in cell wall integrity pathway in *ram1*Δ and wild-type *MAT-1*, with or without treatment of 25 μg/mL CR. Gene expression in the wild-type *MAT-1* strain (untreated) was set as 1 and the relative gene expression fold change in other strains/conditions was calculated with $2^{-\Delta\Delta Ct}$ method (Livak and Schmittgen, 2001), using *ACTIN* as internal control. Barchart depicts the average ± standard error (SE) derived from three independent biological replicates. Statistical significance of the expression data was determined at $^{***}p < 0.005$, $^{**}p < 0.01$, $^{*}p < 0.05$ using Student's *t*-test, and error bars represent ± standard deviation values.

DISCUSSION

The predominant function of FTase composed of Ram1 and Ram2 is conserved among eukaryotes (Omer and Gibbs, 1994). In our study, the *ram1*Δ mutant is viable, whereas the *ram2*Δ mutants could not be generated although repeated attempts were made, which is consistent with what has been reported in *S. cerevisiae, C. neoformans,* and *C. albicans* that the *RAM2* gene is essential while *RAM1* is not (Alspaugh et al., 2000; Song and White, 2003; He et al., 2005). It remains a possibility that some suppressors can directly or indirectly enhance cross-prenylation of certain CAAX substrates

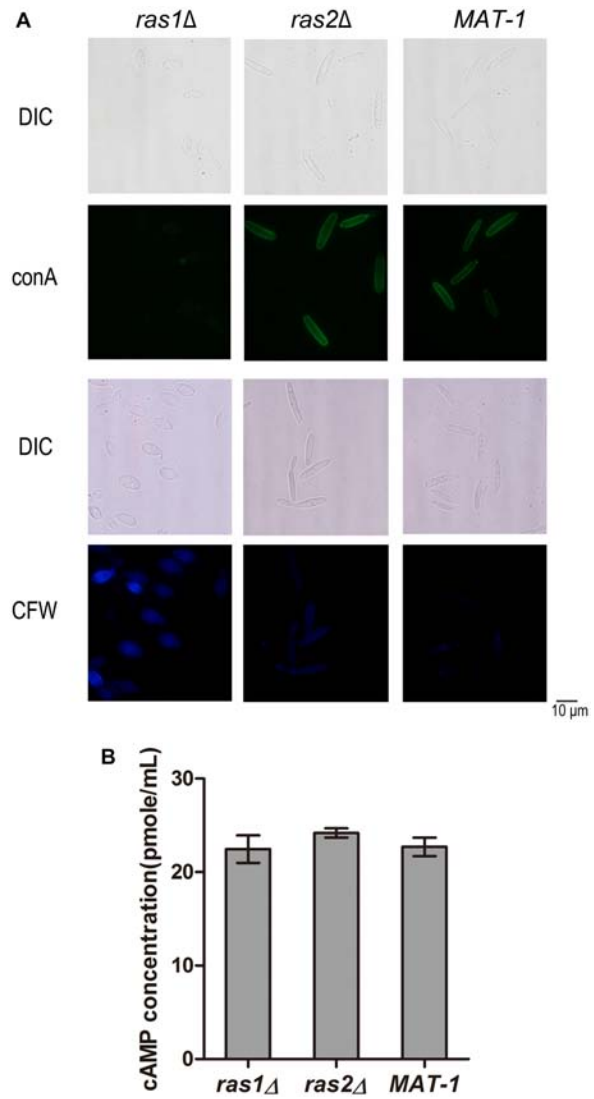

FIGURE 9 | *RAS1* and *RAS2* regulates *S. scitamineum* cell wall integrity. **(A)** Microscopic examination of *ras1*Δ, *ras2*Δ, and wild-type *MAT-1* stained with 100 μg/mL Concanavalin A (conA, type VI conjugated to FITC), or with 10 μg/mL fluorescent brightener calcofluor white (CFW). Scale bar = 10 mm. **(B)** Measurement of intracellular cAMP in 2-day-old sporidia of strains *ras1*Δ, *ras2*Δ and wild-type *MAT-1*, cultured on YePSA plates at 28°C for 24 h. The cAMP concentration was calculated and expressed as pmol/mL. Barchart depicts the average ± standard error (SE) derived from three independent replicates. Statistical analysis was performed by Student's *t*-test.

to replace the function of Ram1 but not Ram2. *S. cerevisiae* Ram1 is associated to sexual mating and survival in stressful conditions including high temperature, but is not essential for haploid growth (Michaelis and Barrowman, 2012). However, *C. neoformans* Ram1 is involved in diploid growth (Nadal et al., 2008). In *A. fumigatus*, *ramA*Δ mutants resulted in growth abnormalities including impaired hyphal branching, delayed conidial germination, reduced conidial viability, and aberrant distribution of nuclei in growing hyphae (Fortwendel et al., 2004). In this study, we found that the virulence of the *S. scitamineum ram1*Δ mutant (mixed with compatible wild-type sporidia) was significantly reduced compared to the wild-type strain, possibly resulting from reduced mating/filamentation and/or weakening stress resistance. For the Ram1 subcellular localization, we generated an eGFP-Ram1 strain and found it localized in the cytosol of sporidial cells. We made attempts to use the native promoter fused with eGFP-Ram1, but we found such ectopic expression of *RAM1* was less than 20% compared to wild-type. Relative expression of *RAM1* driven by G3PD promoter in *ram1*Δ/eGFP-Ram1 strain was about 70% compared to that of wild-type and the mating ability was restored (data not shown). Therefore, we believe in the localization of Ram1 protein was original not GFP-artifactual. *S. scitamineum ram1*Δ mutant showed notably down-regulation of the *PRF1* gene, encoding a master transcription factor governing mating and filamentation, which may account for its defect in mating/filamentation. However, we did not find down-regulation of the a or b locus genes, which were shown to be transcriptionally induced by Prf1 in *U. maydi*s mating/filamentation (Hartmann et al., 1999). We infer that *S. scitamineum* may possess redundant (un-identified) regulator of the a or b locus genes' transcription, which may not depend on Ram1 function.

In *S. cerevisiae*, a-factor precursor (with CVIA C-terminal motif), Ras1 (with CIIC C-terminal motif), Ras2 (with CIIS C-terminal motif), G protein gamma subunit Ste18 (with CTLM C-terminal motif) are farnesylated by the FTase composed of Ram1 and Ram2 (Omer and Gibbs, 1994; Flom et al., 2008; Michaelis and Barrowman, 2012). Currently, fungal Ras1 and Ras2 are known to be involved in regulating not only growth, development and conidiation, but also virulence and tolerance to oxidation, cell wall disturbance, or heat sensitivity in either independent or interactive manners (Mosch et al., 1996; Lee and Kronstad, 2002; Bluhm et al., 2007; Xie et al., 2013). Disruption of fungal Ras2 has been previously reported in several fungi and also in this study, but deletion of *RAS1* gene was only reported in haploid pathogenic fungus *A. fumigatus* (Fortwendel et al., 2004; Boyce et al., 2005). It was reported that in *U. maydis* or *C. albicans*, both Ras1 and Ras2 regulate intracellular cAMP level, with Ras1 as cAMP-dependent, and Ras2 as MAPK-dependent (Nadal et al., 2008; Zhu et al., 2009). In this study, we successfully deleted *RAS1* gene in *S. scitamineum*. Both *S. scitamineum ras1*Δ and *ras2*Δ mutants showed defective sexual mating which could enhance but not restore obviously by exogenous cAMP. To evaluate whether the concentration of intercellular cAMP of *ras1*Δ and *ras2*Δ mutants changed, ELISA method was conducted and the results showed no obvious differences in the intercellular cAMP concentrations between the *ras1*Δ and the *ras2*Δ mutants and the wild-type strain. Similarly, in *S. pombe* and *Schizophyllum commune*, deletion of *RAS1* couldn't reduce the cAMP; in *Fusarium graminearum*, the intercellular cAMP level was not affected by deletion of *RAS2* (Hughes et al., 1993; Yamagishi et al., 2004; Bluhm et al., 2007). On the other hand, we found that exogenous addition of synthetic (farnesylated) Mfa1 peptide could effectively restore mating/filamentation in the *S. scitamineum mfa1*Δ mutant, and partially restore that in the *ram1*Δ *ras1*Δ and *ras2*Δ mutants; synthetic (non-farnesylated) Mfa1 couldn't

restore mating/filamentation in these four mutants. We infer that both Mfa1 farnesylation and Ras-mediated signaling pathway are critical for *S. scitamineum* mating/filamentation, and may both depend on Ram1 function. It would be worth generating and assessing mislocalization of Ras and Mfa1 proteins by comparing their phenotype with the *ram1*Δ mutant in the future.

Fungal cell wall allows exchange of the compounds and signals between environment and fungal cells, or to build parasitical structures. Cell wall integrity (CWI) signal pathway is highly conserved in eukaryotic organisms, and is involved in stress tolerance and fungal pathogenicity (Hamel et al., 2012). We found that the *ram1*Δ sporidia were more tolerant to cell wall disrupting agent Congo red (CR), and CR treatment could induce a significantly higher up-regulation of several conserved CWI genes, especially Slt2 (MAPK) and Fks3 (glucan synthase), compared to that of wild-type sporidia. These results together demonstrate that Ram1 likely regulates the cell wall integrity in *S. scitamineum*.

In *S. scitamineum*, both *ras1*Δ and *ras2*Δ mutants were hypersensitive toward cell wall disrupt agents and cell membrane disrupt agents. In *C. neoformans*, intracellular cAMP level regulates the cell wall integrity pathway (Donlin et al., 2014), however, we found no obvious difference in terms of intracellular cAMP concentration of *S. scitamineum ras1*Δ or *ras2*Δ mutant compared to that of the wild-type strain. Sensitivity toward cell wall stressor Congo red was opposite in the *ras1*Δ or *ras2*Δ sporidia (hypersensitive) compared to that of *ram1*Δ mutant (tolerant). Both *ras1*Δ and *ras2*Δ were hypersensitive toward cell wall stressors, which supported the Ras involved in cell wall integrity pathway. But CFW dye on *ras2*Δ has almost no intensity but *ras1*Δ has strong intensity. From our unpublished data, three kinase genes involving in cell wall integrity pathway deletion mutants had slightly intensity by CFW dye, as the *ras2*Δ showed. We speculate the Ras1 and Ras2 involve in CWI pathway but have different compensation mechanism for cell wall composition. Overall, these results suggested that Ras may regulate *S. scitamineum* cell wall integrity through a signaling pathway independent or parallel of the cAMP/PKA pathway.

In summary, our study revealed a possible regulatory function of Ram1 by farnesylation of a-factor and/or Ras proteins, which are both critical for *S. scitamineum* mating/filamentation and/or stress tolerance.

DATA AVAILABILITY

All datasets generated for this study are included in the manuscript and/or the **Supplementary Files**.

AUTHOR CONTRIBUTIONS

YD, BC, CC, and ZJ conceived and designed the experiments. SS, CC, EC, MY, and LL performed the experiments. YD, SS, CC, and ZJ analyzed the data and wrote the manuscript.

FUNDING

This research was supported by the National 973 Program of China (2015CB150600) and National Natural Science Foundation of China (31672091).

ACKNOWLEDGMENTS

We are grateful for the critical reading and helpful comments on our manuscript by Prof. Tom Hsiang (University of Guelph).

SUPPLEMENTARY MATERIAL

The Supplementary Material for this article can be found online at: https://www.frontiersin.org/articles/10.3389/fmicb.2019.00976/full#supplementary-material

REFERENCES

Alspaugh, J. A., Cavallo, L. M., Perfect, J. R., and Heitman, J. (2000). RAS1 regulates filamentation, mating and growth at high temperature of *Cryptococcus neoformans*. *Mol. Microbiol.* 36, 352–365. doi: 10.1046/j.1365-2958.2000.01852.x

Ashby, M. N., and Rine, J. (1995). Ras and a-factor converting enzyme. *Methods Enzymol.* 250, 235–251. doi: 10.1016/0076-6879(95)50076-50076

Bluhm, B. H., Zhao, X., Flaherty, J. E., Xu, J. R., and Dunkle, L. D. (2007). RAS2 regulates growth and pathogenesis in *Fusarium graminearum*. *Mol. Plant-Microbe Interact.* 20, 627–636. doi: 10.1094/MPMI-20-6-0627

Boyce, K. J., Hynes, M. J., and Andrianopoulos, A. (2005). The Ras and Rho GTPases genetically interact to co-ordinately regulate cell polarity during development in *Penicillium marneffei*. *Mol. Microbiol.* 55, 1487–1501. doi: 10.1111/j.1365-2958.2005.04485.x

Brefort, T., Tanaka, S., Neidig, N., Doehlemann, G., Vincon, V., and Kahmann, R. (2014). Characterization of the largest effector gene cluster of *Ustilago maydis*. *PLoS Pathog.* 10:e1003866. doi: 10.1371/journal.ppat.1003866

Brown, A. J., and Casselton, L. A. (2001). Mating in mushrooms: increasing the chances but prolonging the affair. *Trends Genet.* 17, 393–400. doi: 10.1016/S0168-9525(01)02343-2345

Chakraborty, B. N., Patterson, N. A., and Kapoor, M. (1991). An electroporation-based system for high-efficiency transformation of germinated conidia of filamentous fungi. *Can. J. Microbiol.* 37, 858–863. doi: 10.1139/m91-147

Chang, C., Cai, E., Deng, Y. Z., Mei, D., Qiu, S., Chen, B., et al. (2018). cAMP/PKA signaling pathway regulates redox homeostasis essential for *Sporisorium scitamineum* mating/filamentation and virulence. *Environ. Microbiol.* 21, 959–971. doi: 10.1111/1462-2920.14496

Deng, Y. Z., Zhang, B., Chang, C., Wang, Y., Lu, S., Sun, S., et al. (2018). The MAP kinase SsKpp2 is required for mating/filamentation in *Sporisorium scitamineum*. *Front. Microbiol.* 9:2555. doi: 10.3389/fmicb.2018.02555

Donlin, M. J., Upadhya, R., Gerik, K. J., Lam, W., VanArendonk, L. G., Specht, C. A., et al. (2014). Cross talk between the cell wall integrity and cyclic AMP/protein kinase A pathways in *Cryptococcus neoformans*. *Mbio* 5:e01573-14. doi: 10.1128/mBio.01573-1514

Esher, S. K., Ost, K. S., Kozubowski, L., Yang, D. H., Kim, M. S., Bahn, Y. S., et al. (2016). Relative contributions of prenylation and postprenylation processing

in *Cryptococcus neoformans* pathogenesis. *mSphere* 1:e00084-15. doi: 10.1128/mSphere.00084-15

Flom, G. A., Lemieszek, M., Fortunato, E. A., and Johnson, J. L. (2008). Farnesylation of ydj1 is required for in vivo interaction with Hsp90 client proteins. *Mol. Biol. Cell* 19, 5249–5258. doi: 10.1091/mbc.E08-04-0435

Fortwendel, J. R., Panepinto, J. C., Seitz, A. E., Askew, D. S., and Rhodes, J. C. (2004). *Aspergillus fumigatus* rasA and rasB regulate the timing and morphology of asexual development. *Fungal Genet. Biol.* 41, 129–139. doi: 10.1016/j.fgb.2003.10.004

Fowler, T. J., DeSimone, S. M., Mitton, M. F., Kurjan, J., and Raper, C. A. (1999). Multiple sex pheromones and receptors of a mushroom-producing fungus elicit mating in yeast. *Mol. Biol. Cell* 10, 2559–2572. doi: 10.1091/mbc.10.8.2559

Hamel, L. P., Nicole, M. C., Duplessis, S., and Ellis, B. E. (2012). Mitogen-activated protein kinase signaling in plant-interacting fungi: distinct messages from conserved messengers. *Plant Cell* 24, 1327–1351. doi: 10.1105/tpc.112.096156

Hartmann, H. A., Kahmann, R., and Bolker, M. (1996). The pheromone response factor coordinates filamentous growth and pathogenicity in *Ustilago maydis*. *EMBO J.* 15, 1632–1641. doi: 10.1002/j.1460-2075.1996.tb00508.x

Hartmann, H. A., Krüge, J., Lottspeich, F., and Kahmann, R. (1999). Environmental signals controlling sexual development of the corn Smut fungus Ustilago maydis through the transcriptional regulator Prf1. *Plant Cell.* 11, 1293–1305. doi: 10.2307/3870750

He, B., Chen, P., Chen, S. Y., Vancura, K. L., Michaelis, S., and Powers, S. (1991). RAM2, an essential gene of yeast, and RAM1 encode the two polypeptide components of the farnesyltransferase that prenylates a-factor and Ras proteins. *Proc. Natl. Acad. Sci. U.S.A.* 88, 11373–11377. doi: 10.1073/pnas.88.24.11373

He, Y. L., Liu, X. Z., and Huang, B. R. (2005). Changes in protein content, protease activity, and amino acid content associated with heat injury in creeping bentgrass. *J. Am. Soc. Hortic. Sci.* 130, 842–847. doi: 10.21273/JASHS.130.6.842

Hughes, D. A., Ashworth, A., and Marshall, C. J. (1993). Complementation of byr1 in fission yeast by mammalian MAP kinase kinase requires coexpression of Raf kinase. *Nature* 364, 349–352. doi: 10.1038/364349a0

Jeon, J., Goh, J., Yoo, S., Chi, M. H., Choi, J., Rho, H. S., et al. (2008). A putative MAP kinase kinase kinase, MCK1, is required for cell wall integrity and pathogenicity of the rice blast fungus, *Magnaporthe oryzae*. *Mol. Plant Microbe Interact.* 21, 525–534. doi: 10.1094/MPMI-21-5-0525

Jung, U. S., Sobering, A. K., Romeo, M. J., and Levin, D. E. (2002). Regulation of the yeast Rlm1 transcription factor by the Mpk1 cell wall integrity MAP kinase. *Mol. Microbiol.* 46, 781–789. doi: 10.1046/j.1365-2958.2002.03198.x

Kahmann, R., and Kamper, J. (2004). *Ustilago maydis*: how its biology relates to pathogenic development. *New Phytol.* 164, 31–42. doi: 10.1111/j.1469-8137.2004.01156.x

Kenaley, S. C., Quan, M., Aime, M. C., and Bergstrom, G. C. (2018). New insight into the species diversity and life cycles of rust fungi (*Pucciniales*) affecting bioenergy switchgrass (*Panicum virgatum*) in the Eastern and Central United States. *Mycol. Prog.* 17, 1251–1267.

Kim, K. Y., Truman, A. W., and Levin, D. E. (2008). Yeast mpk1 mitogen-activated protein kinase activates transcription through Swi4/Swi6 by a noncatalytic mechanism that requires upstream signal. *Mol. Cell. Biol.* 28, 2579–2589. doi: 10.1128/MCB.01795-1797

Koppitz, M., Spellig, T., Kahmann, R., and Kessler, H. (1996). Lipoconjugates: structure-activity studies for pheromone analogues of *Ustilago maydis* with varied lipophilicity. *Int. J. Pept. Protein Res.* 48, 377–390. doi: 10.1111/j.1399-3011.1996.tb00855.x

Kosted, P. J., Gerhardt, S. A., Anderson, C. M., Stierle, A., and Sherwood, J. E. (2000). Structural requirements for activity of the pheromones of *Ustilago hordei*. *Fungal Genet. Biol.* 29, 107–117. doi: 10.1006/fgbi.2000.1191

Krombach, S., Reissmann, S., Kreibich, S., Bochen, F., and Kahmann, R. (2018). Virulence function of the *Ustilago maydis* sterol carrier protein 2. *New Phytol.* 220, 553–566. doi: 10.1111/nph.15268

Lanubile, A., Maschietto, V., De Leonardis, S., Battilani, P., Paciolla, C., and Marocco, A. (2015). Defense responses to mycotoxin-producing fungi *Fusarium proliferatum*, F. subglutinans, and *Aspergillus flavus* in kernels of susceptible and resistant maize genotypes. *Mol. Plant Microbe Interact.* 28, 546–557. doi: 10.1094/MPMI-09-14-0269-R

Leach, M. D., and Brown, A. J. (2012). Posttranslational modifications of proteins in the pathobiology of medically relevant fungi. *Eukaryot. Cell* 11, 98–108. doi: 10.1128/EC.05238-5211

Lee, K. S., and Levin, D. E. (1992). Dominant mutations in a gene encoding a putative protein kinase (BCK1) bypass the requirement for a *Saccharomyces cerevisiae* protein kinase C homolog. *Mol. Cell. Biol.* 12, 172–182. doi: 10.1128/mcb.12.1.172

Lee, N., and Kronstad, J. W. (2002). ras2 controls morphogenesis, pheromone response, and pathogenicity in the fungal pathogen *Ustilago maydis*. *Eukaryot. Cell* 1, 954–966. doi: 10.1128/EC.1.6.954-966.2002

Lesage, G., and Bussey, H. (2006). Cell wall assembly in *Saccharomyces cerevisiae*. *Microbiol. Mol. Biol. Rev.* 70, 317–343. doi: 10.1128/MMBR.00038-35

Leung, K. F., Baron, R., and Seabra, M. C. (2006). Thematic review series: lipid posttranslational modifications. geranylgeranylation of Rab GTPases. *J. Lipid Res.* 47, 467–475. doi: 10.1194/jlr.R500017-JLR200

Li, D., Yang, B., and Mehta, J. L. (1998). Ox-LDL induces apoptosis in human coronary artery endothelial cells: role of PKC, PTK, bcl-2, and Fas. *Am. J. Physiol.* 275(Pt 2), H568–H576. doi: 10.1016/S0002-9149(98)00337-333

Li, M. H., Xie, X. L., Lin, X. F., Shi, J. X., Ding, Z. J., Ling, J. F., et al. (2014). Functional characterization of the gene FoOCH1 encoding a putative alpha-1,6-mannosyltransferase in *Fusarium oxysporum* f. sp. cubense. *Fungal Genet. Biol.* 65, 1–13. doi: 10.1016/j.fgb.2014.01.005

Livak, K. J., and Schmittgen, T. D. (2001). Analysis of relative gene expression data using real-time quantitative PCR and the 2(-Delta Delta C(T) Method. *Methods* 25, 402–408. doi: 10.1006/meth.2001.1262

Lu, S., Shen, X., and Chen, B. (2017). Development of an efficient vector system for gene knock-out and near in-cis gene complementation in the sugarcane smut fungus. *Sci. Rep.* 7:3113. doi: 10.1038/s41598-017-03233-3237

Maddi, A., Fu, C., and Free, S. J. (2012). The *Neurospora crassa* dfg5 and dcw1 genes encode alpha-1,6-mannanases that function in the incorporation of glycoproteins into the cell wall. *PLoS One* 7:e38872. doi: 10.1371/journal.pone.0038872

Michaelis, S., and Barrowman, J. (2012). Biogenesis of the *Saccharomyces cerevisiae* pheromone a-factor, from yeast mating to human disease. *Microbiol. Mol. Biol. Rev.* 76, 626–651. doi: 10.1128/MMBR.00010-12

Mosch, H. U., Roberts, R. L., and Fink, G. R. (1996). Ras2 signals via the Cdc42/Ste20/mitogen-activated protein kinase module to induce filamentous growth in *Saccharomyces cerevisiae*. *Proc. Natl. Acad. Sci. U.S.A.* 93, 5352–5356. doi: 10.2307/39435

Nadal, M., Garcia-Pedrajas, M. D., and Gold, S. E. (2008). Dimorphism in fungal plant pathogens. *FEMS Microbiol. Lett.* 284, 127–134. doi: 10.1111/j.1574-6968.2008.01173.x

Omer, C. A., and Gibbs, J. B. (1994). Protein prenylation in eukaryotic microorganisms: genetics, biology and biochemistry. *Mol. Microbiol.* 11, 219–225. doi: 10.1111/j.1365-2958.1994.tb00302.x

Ozaki, K., Tanaka, K., Imamura, H., Hihara, T., Kameyama, T., Nonaka, H., et al. (1996). Rom1p and Rom2p are GDP/GTP exchange proteins (GEPs) for the Rho1p small GTP binding protein in *Saccharomyces cerevisiae*. *EMBO J.* 15, 2196–2207. doi: 10.1002/j.1460-2075.1996.tb00573.x

Paravicini, G., and Friedli, L. (1996). Protein-protein interactions in the yeast PKC1 pathway: Pkc1p interacts with a component of the MAP kinase cascade. *Mol. Gen. Genet.* 251, 682–691. doi: 10.1007/BF02174117

Paumi, C. M., Chuk, M., Snider, J., Stagljar, I., and Michaelis, S. (2009). ABC transporters in *Saccharomyces cerevisiae* and their interactors: new technology advances the biology of the ABCC (MRP) subfamily. *Microbiol. Mol. Biol. Rev.* 73, 577–593. doi: 10.1128/mmbr.00020-29

Philip, B., and Levin, D. E. (2001). Wsc1 and Mid2 are cell surface sensors for cell wall integrity signaling that act through Rom2, a guanine nucleotide exchange factor for Rho1. *Mol. Cell. Biol.* 21, 271–280. doi: 10.1128/MCB.21.1.271-280.2001

Qiao, J., Song, Y., Ling, Z., Liu, X., and Fang, H. (2017). ram1 gene, encoding a subunit of farnesyltransferase, contributes to growth, antifungal susceptibility to amphotericin B of *Aspergillus fumigatus*. *Med. Mycol.* 55, 883–889. doi: 10.1093/mmy/myx002

Rui, O., and Hahn, M. (2007). The Slt2-type MAP kinase Bmp3 of botrytis cinerea is required for normal saprotrophic growth, conidiation, plant surface sensing

and host tissue colonization. *Mol. Plant Pathol.* 8, 173–184. doi: 10.1111/j.1364-3703.2007.00383.x

Schirawski, J., Heinze, B., Wagenknecht, M., and Kahmann, R. (2005). Mating type loci of *Sporisorium reilianum*: novel pattern with three a and multiple b specificities. *Eukaryot. Cell* 4, 1317–1327. doi: 10.1128/EC.4.8.1317-1327.2005

Schmelzle, T., Helliwell, S. B., and Hall, M. N. (2002). Yeast protein kinases and the RHO1 exchange factor TUS1 are novel components of the cell integrity pathway in yeast. *Mol. Cell. Biol.* 22, 1329–1339. doi: 10.1128/MCB.22.5.1329-1339.2002

Shen, W. C., Davidson, R. C., Cox, G. M., and Heitman, J. (2002). Pheromones stimulate mating and differentiation via paracrine and autocrine signaling in *Cryptococcus neoformans*. *Eukaryot. Cell* 1, 366–377. doi: 10.1128/EC.1.3.366-377.2002

Silva, R. D., Sotoca, R., Johansson, B., Ludovico, P., Sansonetty, F., Silva, M. T., et al. (2005). Hyperosmotic stress induces metacaspase- and mitochondria-dependent apoptosis in *Saccharomyces cerevisiae*. *Mol. Microbiol.* 58, 824–834. doi: 10.1111/j.1365-2958.2005.04868.x

Song, J. L., and White, T. C. (2003). RAM2: an essential gene in the prenylation pathway of *Candida albicans*. *Microbiology* 149(Pt 1), 249–259. doi: 10.1099/mic.0.25887-25880

Spellig, T., Bolker, M., Lottspeich, F., Frank, R. W., and Kahmann, R. (1994). Pheromones trigger filamentous growth in *Ustilago maydis*. *EMBO J.* 13, 1620–1627. doi: 10.1002/j.1460-2075.1994.tb06425.x

Su, Y., Xu, L., Wang, Z., Peng, Q., Yang, Y., Chen, Y., et al. (2016). Comparative proteomics reveals that central metabolism changes are associated with resistance against *Sporisorium scitamineum* in sugarcane. *BMC Genomics* 17:800. doi: 10.1186/s12864-016-3146-3148

Sun, L., Yan, M., Ding, Z., Liu, Y., Du, M., Xi, P., et al. (2014). Improved dominant selection markers and co-culturing conditions for efficient *Agrobacterium tumefaciens*-mediated transformation of *Ustilago scitaminea*. *Biotechnol. Lett.* 36, 1309–1314. doi: 10.1007/s10529-014-1486-1485

Taniguti, L. M., Schaker, P. D., Benevenuto, J., Peters, L. P., Carvalho, G., Palhares, A., et al. (2015). Complete genome sequence of *Sporisorium scitamineum* and biotrophic interaction transcriptome with sugarcane. *PLoS One* 10:e0129318. doi: 10.1371/journal.pone.0129318

Thompson, J. D., Higgins, D. G., and Gibson, T. J. (1994). CLUSTAL W: improving the sensitivity of progressive multiple sequence alignment through sequence weighting, position-specific gap penalties and weight matrix choice. *Nucleic Acids Res.* 22, 4673–4680. doi: 10.1007/978-1-4020-6754-9_3188

Vallim, M. A., Fernandes, L., and Alspaugh, J. A. (2004). The RAM1 gene encoding a protein-farnesyltransferase beta-subunit homologue is essential in *Cryptococcus neoformans*. *Microbiology* 150(Pt 6), 1925–1935. doi: 10.1099/mic.0.27030-27030

Whiteway, M. (2011). Yeast mating: trying out new pickup lines. *Curr. Biol.* 21, R626–R628.

Williams, S. A., and Birnbaum, M. J. (1988). The rat facilitated glucose transporter gene. transformation and serum-stimulated transcription initiate from identical sites. *J. Biol. Chem.* 263, 19513–19518.

Xie, X. Q., Guan, Y., Ying, S. H., and Feng, M. G. (2013). Differentiated functions of Ras1 and Ras2 proteins in regulating the germination, growth, conidiation, multi-stress tolerance and virulence of *Beauveria bassiana*. *Environ. Microbiol.* 15, 447–462. doi: 10.1111/j.1462-2920.2012.02871.x

Yamagishi, K., Kimura, T., Suzuki, M., Shinmoto, H., and Yamaki, K. J. (2004). Elevation of intracellular cAMP levels by dominant active heterotrimeric G protein alpha subunits ScGP-A and ScGP-C in homobasidiomycete, *Schizophyllum commune*. *Biosci. Biotechnol. Biochem.* 68, 1017–1026. doi: 10.1271/bbb.68.1017

Yan, M., Zhu, G., Lin, S., Xian, X., Chang, C., Xi, P., et al. (2016a). The mating-type locus b of the sugarcane smut *Sporisorium scitamineum* is essential for mating, filamentous growth and pathogenicity. *Fungal Genet. Biol.* 86, 1–8. doi: 10.1016/j.fgb.2015.11.005

Yan, M. X., Cai, E. P., Zhou, J. N., Chang, C. Q., Xi, P. G., Shen, W. K., et al. (2016b). A dual-color imaging system for sugarcane smut fungus *Sporisorium scitamineum*. *Plant Dis.* 100, 2357–2362. doi: 10.1094/PDIS-02-16-0257-SR

Yan, M. X., Dai, W. J., Cai, E. P., Deng, Y. Z., Chang, C. Q., Jiang, Z. D., et al. (2016c). Transcriptome analysis of *Sporisorium scitamineum* reveals critical environmental signals for fungal sexual mating and filamentous growth. *BMC Genomics* 17:354. doi: 10.1186/s12864-016-2691-2695

Young, S. G., Fong, L. G., and Michaelis, S. (2005). Prelamin A, Zmpste24, misshapen cell nuclei, and progeria–new evidence suggesting that protein farnesylation could be important for disease pathogenesis. *J. Lipid Res.* 46, 2531–2558. doi: 10.1194/jlr.R500011-JLR200

Zhu, Y., Fang, H. M., Wang, Y. M., Zeng, G. S., Zheng, X. D., and Wang, Y. (2009). Ras1 and Ras2 play antagonistic roles in regulating cellular cAMP level, stationary-phase entry and stress response in *Candida albicans*. *Mol. Microbiol.* 74, 862–875. doi: 10.1111/j.1365-2958.2009.06898.x

Conflict of Interest Statement: The authors declare that the research was conducted in the absence of any commercial or financial relationships that could be construed as a potential conflict of interest.

frontiers in Microbiology

ORIGINAL RESEARCH
published: 13 September 2019
doi: 10.3389/fmicb.2019.02090

Both Galactosaminogalactan and α-1,3-Glucan Contribute to Aggregation of *Aspergillus oryzae* Hyphae in Liquid Culture

*Ken Miyazawa[1], Akira Yoshimi[2], Motoaki Sano[3], Fuka Tabata[1], Asumi Sugahara[1], Shin Kasahara[4], Ami Koizumi[1], Shigekazu Yano[5], Tasuku Nakajima[2] and Keietsu Abe[1,2,6]**

[1]*Laboratory of Applied Microbiology, Department of Microbial Biotechnology, Graduate School of Agricultural Science, Tohoku University, Sendai, Japan,* [2]*ABE-Project, New Industry Creation Hatchery Center, Tohoku University, Sendai, Japan,* [3]*Genome Biotechnology Laboratory, Kanazawa Institute of Technology, Hakusan, Japan,* [4]*Department of Environmental Sciences, School of Food, Agricultural and Environmental Sciences, Miyagi University, Taiwa, Japan,* [5]*Department of Biochemical Engineering, Graduate School of Engineering, Yamagata University, Yonezawa, Japan,* [6]*Laboratory of Microbial Resources, Department of Microbial Biotechnology, Graduate School of Agricultural Science, Tohoku University, Sendai, Japan*

Filamentous fungi generally form aggregated hyphal pellets in liquid culture. We previously reported that α-1,3-glucan-deficient mutants of *Aspergillus nidulans* did not form hyphal pellets and their hyphae were fully dispersed, and we suggested that α-1,3-glucan functions in hyphal aggregation. However, *Aspergillus oryzae* α-1,3-glucan-deficient (AGΔ) mutants still form small pellets; therefore, we hypothesized that another factor responsible for forming hyphal pellets remains in these mutants. Here, we identified an extracellular matrix polysaccharide galactosaminogalactan (GAG) as such a factor. To produce a double mutant of *A. oryzae* (AG-GAGΔ), we disrupted the genes required for GAG biosynthesis in an AGΔ mutant. Hyphae of the double mutant were fully dispersed in liquid culture, suggesting that GAG is involved in hyphal aggregation in *A. oryzae*. Addition of partially purified GAG fraction to the hyphae of the AG-GAGΔ strain resulted in formation of mycelial pellets. Acetylation of the amino group in galactosamine of GAG weakened GAG aggregation, suggesting that hydrogen bond formation by this group is important for aggregation. Genome sequences suggest that α-1,3-glucan, GAG, or both are present in many filamentous fungi and thus may function in hyphal aggregation in these fungi. We also demonstrated that production of a recombinant polyesterase, CutL1, was higher in the AG-GAGΔ strain than in the wild-type and AGΔ strains. Thus, controlling hyphal aggregation factors of filamentous fungi may increase productivity in the fermentation industry.

Keywords: α-1,3-glucan, *Aspergillus oryzae*, cell wall, galactosaminogalactan, hyphal aggregation, recombinant-protein production

OPEN ACCESS

Edited by:
Gustavo Alexis Niño-Vega, University of Guanajuato, Mexico

Reviewed by:
Thierry Fontaine, Institut Pasteur, France
Gerardo Díaz-Godínez, Autonomous University of Tlaxcala, Mexico

***Correspondence:**
Keietsu Abe
keietsu.abe.b5@tohoku.ac.jp

Specialty section:
This article was submitted to Fungi and Their Interactions, a section of the journal Frontiers in Microbiology

Received: *03 April 2019*
Accepted: *26 August 2019*
Published: *13 September 2019*

Citation:
Miyazawa K, Yoshimi A, Sano M, Tabata F, Sugahara A, Kasahara S, Koizumi A, Yano S, Nakajima T and Abe K (2019) Both Galactosaminogalactan and α-1,3-Glucan Contribute to Aggregation of Aspergillus oryzae Hyphae in Liquid Culture. Front. Microbiol. 10:2090. doi: 10.3389/fmicb.2019.02090

INTRODUCTION

The hyphae of filamentous fungi generally form aggregated pellets in liquid culture. Although filamentous fungi have been used for industrial production of enzymes and secondary metabolites for a long time (Abe et al., 2006; Kobayashi et al., 2007), hyphal pellet formation decreases productivity in liquid culture (Driouch et al., 2010; Karahalil et al., 2017). Formation of hyphal pellets might be related to a property of the cell surface (Beauvais et al., 2014), and elucidation

of the relationship between hyphal aggregation and cell surface components, especially polysaccharides, is needed.

The fungal cell wall is essential for survival because it maintains the cell's shape, prevents cell lysis, and protects cells from environmental stresses (Yoshimi et al., 2016). Fungal cell walls are composed mainly of polysaccharides. In *Aspergillus* species, the cell wall is composed of α-glucan (mainly α-1,3-glucan), β-1,3/1,6-glucan, galactomannan, and chitin (Latgé, 2010; Yoshimi et al., 2016, 2017). Cell walls of some filamentous fungi are covered with extracellular matrix, which is composed mainly of polysaccharides, including α-glucan (α-1,3-glucan with a small amount of α-1,4-linkage), galactomannan, or galactosaminogalactan (GAG) (Lee and Sheppard, 2016; Sheppard and Howell, 2016).

We reported that the Δ*agsB* and Δ*agsA*Δ*agsB* strains of *Aspergillus nidulans* have no α-1,3-glucan in the cell wall (Yoshimi et al., 2013) and their hyphae are fully dispersed in liquid culture, whereas the wild-type strain forms aggregated pellets. In *Aspergillus fumigatus*, addition of α-1,3-glucanase prevents aggregation of germinating conidia (Fontaine et al., 2010). These findings strongly suggest that α-1,3-glucan is an adhesive factor. We disrupted the three α-1,3-glucan synthase genes in the industrial fungus *Aspergillus oryzae* (Δ*agsA*Δ*agsB*Δ*agsC*; AGΔ) and confirmed the loss of α-1,3-glucan in the cell wall of the AGΔ strain, but the strain still formed small hyphal pellets in liquid culture (Miyazawa et al., 2016). Although the AGΔ hyphae were not fully dispersed, the strain produced more recombinant polyesterase (cutinase) CutL1 than did a wild-type strain (WT-cutL1) because of the smaller pellets of the AGΔ strain (Miyazawa et al., 2016). We predicted that another cell wall or cell surface component is responsible for hyphal aggregation in the AGΔ strain. Identification of this factor, distinct from α-1,3-glucan, is important, because full dispersion of *A. oryzae* hyphae would enable higher cell density and increase production of commercially valuable products in liquid culture.

GAG is a hetero-polysaccharide composed of linear α-1,4-linked galactose (Gal), *N*-acetylgalactosamine (GalNAc), and galactosamine (GalN). GAG is an important pathogenetic factor in the human pathogen *A. fumigatus* (Fontaine et al., 2011; Lee et al., 2015); it is involved in adherence to host cells, biofilm formation, and avoidance of immune response by masking β-1,3-glucan and chitin (Gravelat et al., 2013; Sheppard and Howell, 2016). Disruption of genes encoding the transcription factors StuA and MedA significantly decreases GAG content and has led to identification of the *uge3* (UDP-glucose 4-epimerase) gene (Gravelat et al., 2013). Four genes (*sph3*, *gtb3*, *ega3*, and *agd3*) located near *uge3* have been identified (Lee et al., 2016). In *stuA* and *medA* gene disruptants, these five genes are downregulated, suggesting that they are co-regulated by StuA and MedA (Lee et al., 2016). GAG biosynthesis by the five encoded proteins is predicted in *A. fumigatus* (Bamford et al., 2015; Sheppard and Howell, 2016). First, the epimerase Uge3 produces UDP-galactopyranose (Gal*p*) from UDP-glucose and UDP-*N*-GalNAc from UDP-*N*-acetylglucosamine (GlcNAc) (Gravelat et al., 2013; Lee et al., 2014). Second, glycosyltransferase Gtb3 seems to polymerize UDP-Gal*p* and UDP-GalNAc and export the polymer from the cytoplasm (Speth et al., 2019), although Gtb3 has not yet been characterized. Third, deacetylase Agd3 deacetylates the synthesized GAG polymer (Lee et al., 2016). The predicted glycoside hydrolase Ega3 has yet to be characterized. Sph3 belongs to a novel glycoside hydrolase family, GH135, and is essential for GAG production (Bamford et al., 2015), but its role in GAG synthesis remains unknown.

Here, we confirmed that *A. oryzae* has the GAG biosynthetic gene cluster. We disrupted *sphZ* (ortholog of *A. fumigatus sph3*) and *ugeZ* (ortholog of *uge3*) in the wild-type and AGΔ strains to produce Δ*sphZ*Δ*ugeZ* (GAGΔ) and Δ*agsA*Δ*agsB*Δ*agsC*Δ*sphZ*Δ*ugeZ* (AG-GAGΔ), respectively. In liquid culture, the hyphae of the AG-GAGΔ strain were fully dispersed, suggesting that GAG plays a role in hyphal adhesion in *A. oryzae*, along with α-1,3-glucan. Using the wild-type, AGΔ, GAGΔ, and AG-GAGΔ strains of *A. oryzae*, we characterized hyphal aggregation and discuss its mechanism in *A. oryzae*. Our findings may have wide implications, because the genomes of many filamentous fungi encode enzymes required for α-1,3-glucan or GAG biosynthesis, or both (Lee et al., 2016; Yoshimi et al., 2017).

MATERIALS AND METHODS

Strains and Growth Media

Strains used are listed in **Table 1**. *Aspergillus oryzae* NS4 (*sC*$^-$, *niaD*$^-$) with Δ*ligD* (Δ*ligD*::*sC*, Δ*adeA*::*ptrA*) was used for all genetic manipulations (Mizutani et al., 2008). All *A. oryzae* strains were cultured in standard Czapek-Dox (CD) medium as described previously (Yoshimi et al., 2013; Miyazawa et al., 2016). The *niaD*$^-$ strains were cultured in CDE medium (CD

TABLE 1 | Strains used in this study.

Strain	Genotype	Reference
Wild type	Δ*ligD*::*sC*, Δ*adeA*::*ptrA*, *niaD*$^-$, *adeA*$^+$	Mizutani et al., (2008)
Δ*agsA*Δ*agsB*Δ*agsC* (AGΔ)	Δ*ligD*::*sC*, Δ*adeA*::*ptrA*, *niaD*$^-$, *adeA*$^+$, *agsA*::*loxP*, *agsB*::*loxP*, *agsC*:: *loxP*	Miyazawa et al., (2016)
Δ*sphZ*Δ*ugeZ* (GAGΔ)	Δ*ligD*::*sC*, Δ*adeA*::*ptrA*, *niaD*$^-$, *sphZugeZ*::*adeA*	This study
Δ*agsA*Δ*agsB*Δ*agsC*Δ*sphZ*Δ*ugeZ* (AG-GAGΔ)	Δ*ligD*::*sC*, Δ*adeA*::*ptrA*, *niaD*$^-$, *agsA*::*loxP*, *agsB*::*loxP*, *agsC*::*loxP*, *sphZugeZ*::*adeA*	This study
WT-cutL1	Δ*ligD*::*sC*, Δ*adeA*::*ptrA*, *niaD*$^-$, *adeA*$^+$, P*glaA142-cutL1*::*niaD*	Miyazawa et al., (2016)
AGΔ-cutL1	Δ*ligD*::*sC*, Δ*adeA*::*ptrA*, *niaD*$^-$, *adeA*$^+$, *agsA*::*loxP*, *agsB*::*loxP*, *agsC*:: *loxP*, P*glaA142-cutL1*::*niaD*	Miyazawa et al., (2016)
AG-GAGΔ-cutL1	Δ*ligD*::*sC*, Δ*adeA*::*ptrA*, *niaD*$^-$, *agsA*::*loxP*, *agsB*::*loxP*, *agsC*::*loxP*, *sphZugeZ*::*adeA*, P*glaA142-cutL1*::*niaD*	This study

medium containing 70 mM sodium hydrogen L(+)-glutamate monohydrate as the nitrogen source instead of sodium nitrate).

Conidia of *A. oryzae* used to inoculate flask cultures were isolated from cultures grown on malt medium, as described previously (Miyazawa et al., 2016). YPD medium containing 2% peptone (Becton Dickinson and Company, Sparks, Nevada, USA), 1% yeast extract (Becton Dickinson and Company), and 2% glucose was used for flask culture to analyze growth characteristics. YPM medium containing 2% peptone, 1% yeast extract, and 2% maltose was used for flask culture to evaluate production of recombinant cutL1.

Construction of Dual *sphZ ugeZ* Gene Disruptant in *Aspergillus oryzae*

The sequences of all primers are listed in **Table 2**. Fragments containing the 3′ non-coding regions of *ugeZ* (amplicon 1) and *sphZ* (amplicon 2) derived from *A. oryzae* genomic DNA, and the *adeA* gene (amplicon 3) from the TOPO-2.1-adeA plasmid (Miyazawa et al., 2016), were amplified by PCR. Amplicon 1 was amplified with the primers sphZ+ugeZ-LU and sphZ+ugeZ-LL+ade, amplicon 2 with the primers sphZ+ugeZ-RU+ade and sphZ+ugeZ-RL, and amplicon 3 with the primers sphZ+ugeZ-AU and sphZ+ugeZ-AL. The primers sphZ+ugeZ-LL+ade, sphZ+ugeZ-AU, and sphZ+ugeZ-AL were chimeric; each contained a reverse-complement sequence for PCR fusion. The PCR products were gel-purified and used as substrates for the second round of PCR with the primers sphZ+ugeZ-LU and sphZ+ugeZ-RL to fuse the three fragments (**Supplementary Figure S1A**). The resulting major PCR product was gel-purified and used to transform *A. oryzae* wild-type and AGΔ strains (**Supplementary Figure S1B**). Disruption of the *sphZ* and *ugeZ* genes was confirmed by Southern blot analysis (**Supplementary Figure S1C**).

Analysis of Growth Characteristics of *Aspergillus oryzae* in Liquid Culture

Conidia (final concentration, 1×10^5/ml) of the wild-type, AGΔ, GAGΔ, and AG-GAGΔ strains were inoculated into 50-ml of YPD medium in 200-mL Erlenmeyer flasks and rotated at 120 rpm at 30°C for 24 h. The mean diameter of the hyphal pellets was determined as described previously (Miyazawa et al., 2016).

Scanning Electron Microscopy

Conidia (final concentration, 1×10^5/ml) of the wild-type, AGΔ, GAGΔ, and AG-GAGΔ *A. oryzae* strains were inoculated and grown as above. The culture broths were filtered through Miracloth (Merck Millipore, Darmstadt, Germany). The mycelia were washed with water twice, dehydrated with tert-butanol, lyophilized, and coated with platinum-vanadium. Mycelia were observed under a Hitachi SU8000 scanning electron microscope (Hitachi, Tokyo, Japan) at an accelerating voltage of 3 kV.

Visualization of Biofilms

Biofilms were visualized by using the method of Gravelat et al. (2010), with some modifications. Conidia (final concentration, 1×10^5/ml) of the wild-type, AGΔ, GAGΔ, and AG-GAGΔ *A. oryzae* strains were inoculated in 10 ml of CDE medium on a polystyrene plate (internal diameter 60 mm) and incubated for 24 h at 30°C. Spent culture medium was removed from the plate, and the plate was then washed three times with PBS. Then 5 ml of 0.5% (w/v) crystal violet solution was added to the plate, which was incubated at room temperature for 5 min. Excess stain was removed, and the plate was washed twice with water. The visualized biofilm was imaged by using a flatbed scanner (GT-X820; Seiko Epson Corp., Nagano, Japan).

Assay for Cell Wall Susceptibility to Lysing Enzymes

Susceptibility of the fungal cell wall to Lysing Enzymes (LE), a commercial preparation containing β-1,3-glucanase and chitinase (Sigma, St. Louis, MO, USA), was assayed as described previously (Yoshimi et al., 2013). Washed 1-day-old mycelia of the wild-type, AGΔ, GAGΔ, and AG-GAGΔ strains (30 mg fresh weight) grown in CDE medium at 30°C were suspended in 1 ml of 0.8 M NaCl in sodium phosphate buffer (10 mM, pH 6.0) containing 10 mg/ml LE and incubated for 1, 2, or 4 h at 30°C. The number of protoplasts generated from the mycelia was counted with a hemocytometer (A106, SLGC, Tokyo, Japan).

TABLE 2 | PCR primers used in this study.

Purpose	Primer name	Sequence (5′ to 3′)
sphZ, *ugeZ* disruption		
	sphZ+ugeZ-LU	TCTCCATAGTGTTCACCA
	sphZ+ugeZ-LL + Ade	ATATACCGTGACTTTTTAGCACAACATTGGAGCTACT
	sphZ+ugeZ-RU + Ade	AGTTTCGTCGAGATACTGCGCGTTGTCATATTTGCAAG
	sphZ+ugeZ-RL	AGGGCTCAGAATACGTATC
	sphZ+ugeZ-AU	AGTAGCTCCAATGTTGTGCTAAAAAGTCACGGTATATCATGAC
	sphZ+ugeZ-AL	TTGCAAATATGACAACGCGCAGTATCTCGACGAAACTACCTAA
Quantitative PCR		
	agsA-RT-F	CAAACCTGGAGAGACGCGAT
	agsA-RT-R	CGAGGGTATTCGCAAGTGTTG
	agsB-RT-F	GAACTTTGTCGCGGTCATCCTTCAG
	agsB-RT-R	CCAAGGGAGGTAGTAGCCAATG
	agsC-RT-F	TTGGAGACGGACCATCACTG
	agsC-RT-R	GTTGCAGGTCTCGTTGTACTC

Assay for Growth Inhibition by Congo Red

Sensitivity of the wild-type, AGΔ, GAGΔ, and AG-GAGΔ strains to Congo Red was evaluated by using our previously described method (Yoshimi et al., 2013), with a minor modification. Briefly, conidial suspensions of each strain (1.0×10^4 cells) were spotted on the centers of CDE plates containing Congo Red (10, 20, 40, 80, or 120 μg/ml) and incubated at 30°C for 3 days. The dose response was determined by plotting the mean diameters of the colonies on media with Congo Red as a percentage of those on control medium. Each experiment was performed in quadruplicate.

Fractionation of Cell Wall Components and Quantification of Carbohydrate Composition

Conidia (final concentration, 1.0×10^5/ml) of the wild-type, AGΔ, GAGΔ, and AG-GAGΔ strains were inoculated into 200 ml of YPD medium in 500-ml Erlenmeyer flasks and rotated at 120 rpm at 30°C. Mycelia were collected by filtration through Miracloth, washed twice with 20 ml of water, and lyophilized. Mycelia were pulverized with a MM400 bench-top mixer mill (Retsch, Haan, Germany), and the resulting powder (1 g) was suspended in 40 ml of 0.1 M sodium phosphate buffer (pH 7.0). Cell wall components were fractionated by hot-water and alkali treatment (Miyazawa et al., 2016); the fractionation resulted in hot-water-soluble (HW), alkali-soluble (AS), and alkali-insoluble (AI) fractions. The AS fraction was further separated into a fraction soluble in water at neutral pH (AS1) and an insoluble fraction (AS2). The carbohydrate composition of the fractions was quantified as described previously (Yoshimi et al., 2013). Briefly, 10 mg of each cell wall fraction was hydrolyzed with sulfuric acid and then neutralized with barium sulfate. The carbohydrate composition of the hydrolysate was determined by using high-performance anion-exchange chromatography (HPAEC). For GalN quantification, the carbohydrate composition of sulfuric acid-hydrolyzed HW fractions (50 mg each) was quantified.

Purification of Galactosaminogalactan From Culture Supernatant of the α-1,3-Glucan-Deficient Strain by Fractional Precipitation With Ethanol

Conidia (final concentration, 1.0×10^6/ml) of the AGΔ or AG-GAGΔ strain (negative control) were inoculated into three flasks, each containing 1 L of modified Brian medium (Fontaine et al., 2011), and rotated at 160 rpm at 30°C for 72 h. The mycelia were removed by filtration through Miracloth. The supernatants were combined and concentrated to 1 L by evaporation, dialyzed against water at 4°C, and concentrated again to 1 L; then, 20 g of NaOH was added (final concentration, 0.5 M) at 4°C with stirring. The mixture was centrifuged at 3000 ×*g* at 4°C for 10 min and a pellet was obtained (referred to hereafter as the 0 vol). EtOH (0.5 L) was added to the supernatant and the mixture was incubated for 5 h at 4°C with stirring, then centrifuged at 3000 ×*g* at 4°C for 10 min, and a pellet (0.5-vol. EtOH fraction) was obtained. These procedures were repeated to obtain 1-, 1.5-, 2-, and 2.5-vol. EtOH fractions. Each fraction was neutralized with 3 M HCl, dialyzed against water, and freeze-dried. The carbohydrate composition of each fraction was determined as above. For mycelial aggregation assay, each freeze-dried EtOH fraction from the AGΔ strain (2 mg) and the 1.5-vol. EtOH fraction from the AG-GAGΔ strain were dissolved in 1 ml of 0.1 M HCl and vortexed for 10 min.

Conidial and Mycelial Aggregation Assay

A modified method of Fontaine et al. (2010) was used. Conidia (5×10^5) were inoculated into 500 μl of CDE liquid medium containing 0.05% Tween 20 in a 48-well plate and agitated at 1,200 rpm with a microplate mixer (NS-P; As One, Osaka, Japan) at 30°C for 3, 6, or 9 h. Conidial aggregates were then examined under a stereomicroscope (M125; Leica Microsystems, Wetzlar, Germany). Mycelial aggregation in the presence of GAG was evaluated as follows. Conidia (final concentration, 1.0×10^7/ml) of the AG-GAGΔ strain were inoculated into 50 ml of YPD medium and rotated at 120 rpm at 30°C for 9 h. The mycelia were collected by filtration through Miracloth and washed twice with water. The mycelia (wet weight, 500 mg) were resuspended in 10 ml of PBS, and the suspension (25 μl) was added into a mixture of 400 μl of water, 50 μl of 1 M sodium phosphate buffer (pH 7.0), and 25 μl of the EtOH fraction (from AGΔ) or the mock fraction (from AG-GAGΔ). Aggregates were examined under a stereomicroscope after 1 h.

An aggregation assay in the presence of the AS2 fraction was performed by using the following method. The AS2 fraction (10 mg) was dissolved in 1 M NaOH (100 μl). Then, an aliquot of water (900 μl) was mixed into the solution (AS2 fraction concentration, 10 mg/ml). Mycelial suspension (25 μl) was added to a mixture of 400 μl of water, 50 μl of 1 M sodium phosphate buffer (pH 7.0), and 25 μl of the solution containing the AS2 fraction. Aggregates were examined under a stereomicroscope after 1 h.

To quantify the conidial aggregation, the total number of conidia was counted by observing microscopic images (× 1,000). Then the aggregated conidia were counted in the same images. Aggregated conidia were defined as aggregates in which more than five conidia were gathered. The aggregation percentage was determined by observing at least 100 conidia.

To evaluate the effect of pH on mycelial aggregation by GAG, mycelial suspension (25 μl) was added to a mixture of 450 μl of buffer (final concentration, 100 mM) and 25 μl of the 1.5-vol. EtOH fraction. The following buffers were used: pH 4.0–5.0, sodium acetate; pH 6.0–7.0, sodium phosphate; pH 8.0, Tricine-NaOH. Aggregates were examined after 1 h.

To examine the effect of inhibiting hydrogen bond formation, mycelial suspension (25 μl) was added to a mixture of 450 μl of 100 mM sodium phosphate buffer (pH 7.0) and 0, 1, 2, 4, or 8 M urea, and 25 μl of the 1.5-vol. EtOH fraction.

Visualization of α-1,3-Glucan and Galactosaminogalactan in the Cell Wall

Germinating conidia cultured in a 48-well plate were dropped onto a glass slide, washed twice with PBS, and fixed with

4% (w/v) paraformaldehyde for 10 min. Samples were washed twice with 50 mM potassium phosphate buffer (pH 6.5) and stained at room temperature for 2 h with Alexa Fluor 647-conjugated soybean agglutinin (SBA; 100 μg/ml) (Invitrogen) and α-1,3-glucanase-α-1,3-glucan-binding domain fused with GFP (AGBD-GFP; 100 μg/ml) (Suyotha et al., 2013) in 50 mM phosphate buffer (pH 6.5). After being washed with the same buffer, the samples were imaged under a FluoView FV1000 confocal laser-scanning microscope (Olympus, Tokyo, Japan). Cells were then washed three times with PBS, and a drop of PBS containing secondary antibody (anti-rabbit IgG antibody-Alexa Fluor 568 conjugate; Invitrogen) was added. The sample was incubated at room temperature for 1 h, washed as above, and imaged under a confocal laser-scanning microscope.

Acetylation of the Amino Group of Galactosaminogalactan

The 1.5-vol. EtOH fraction from the AGΔ (5 mg) was dissolved in ice cold 0.5 M NaOH (800 μl), neutralized with ice cold 2 M HCl, and then added to 4 ml of 50 mM sodium acetate. Then, methanol (4 ml) and acetic anhydrate (10 mg) were added and the mixture was stirred at room temperature for 24 h. The sample was then evaporated, washed three times with methanol, dialyzed against water, and freeze-dried. The procedure was then repeated.

Determination of Degree of Deacetylation of Galactosaminogalactan by Colloidal Titration

The degree of deacetylation (DD) of GAG was determined by colloidal titration in accordance with the method used to determine the DD of chitosan (Terayama, 1951; Senju, 1969; Hattori et al., 2009). Freeze-dried GAG (5 mg) was dissolved in 0.1 M HCl, and the solution was then made up to 1 g with 0.1 M HCl. Water (30 ml) was added to the GAG solution, and the mixture was stirred thoroughly. A few drops of 0.1% (w/v) toluidine blue solution as an indicator were added to the mixture. The GAG solution was titrated with N/400 potassium polyvinylsulfate (PVSK). The endpoint of the titration was determined by the color change of the indicator from blue to red. The DD of GalNAc in the 1.5-vol. EtOH fraction from AGΔ was determined by using the following equations:

$$\mathrm{DD}(\%) = \frac{\frac{X}{161}}{\frac{X}{161} + \frac{Y}{203}} \times 100$$

$$X = \frac{1}{400} \times \frac{1}{1000} \times f \times 161 \times v$$

$$Y = a \times b - X$$

where:

a, sample (g); *b*, ratio of total hexosamine in 1.5-vol. EtOH fraction from AGΔ; *v*, titer of N/400 PVSK solution (ml); *f*, factor of N/400 PVSK solution.

The DD of GalNAc residues of the sample was determined by these equations. The ratio of total hexosamine in the 1.5-vol. EtOH fraction was determined with *p*-(dimethylamino)-benzaldehyde reagent after 4 h of 8 N HCl hydrolysis at 100°C using galactosamine as a standard (Johnson, 1971; Fontaine et al., 2011). For considering non-GAG components in the sample, the titer background (1.5-vol. EtOH fraction from AG-GAGΔ titrated with N/400 PVSK) was subtracted from the titer of each sample.

Quantification of CutL1 Production

A *cutL1*-overexpressing strain (AG-GAGΔ-cutL1) was constructed as described previously (Miyazawa et al., 2016) with the pNGA-gla-Cut plasmid (Maeda et al., 2005). Integration of a single copy of the *cutL1*-overexpression construct at the *niaD* locus was confirmed by Southern blot analysis (**Supplementary Figure S2**). Enzyme production in the mutants was evaluated as described previously (Miyazawa et al., 2016), with some modifications. Briefly, conidia (final concentration, 1×10^4/ml) of the WT-cutL1, AGΔ-cutL1, and AG-GAGΔ-cutL1 strains were inoculated into 50 ml of YPM medium and rotated at 100 rpm at 30°C for 24 h. The culture broth was filtered through Miracloth. Mycelial cells were dried at 70°C for 24 h and weighed. Proteins were precipitated from an aliquot of the filtrate (400 μl) with 100% (w/v) trichloroacetic acid (200 μl), separated by SDS-PAGE, and stained with Coomassie Brilliant Blue. ImageJ software was used to quantify the CutL1 in the broth; purified CutL1 was used for calibration.

^{13}C NMR Analysis of Cell Wall Fractions

^{13}C NMR analysis was performed as described previously (Miyazawa et al., 2018). The AS2 fractions from the wild-type and GAGΔ strains were dissolved in 1 M NaOH/D_2O. Me_2SO-d_6 (deuterated dimethyl sulfoxide; 5 μl) was added to each sample. ^{13}C NMR spectra were obtained by using a JNM-ECX400P spectrometer (JEOL, Tokyo, Japan) at 400 MHz, 35°C (72,000 scans).

RNA Purification, Reverse Transcription, and Quantitative Polymerase Chain Reaction

Total RNA was extracted by using Sepasol-RNA I Super according to the manufacturer's instructions (Nacalai Tesque, Kyoto, Japan). Total RNA (2 μg) was reverse transcribed and cDNA was amplified by using a High-Capacity cDNA Reverse Transcription Kit according to the manufacturer's instructions (Thermo Fisher Scientific, Waltham, MA, USA). Quantitative PCR was performed with the primers AoagsA-RT-F and AoagsA-RT-R, AoagsB-RT-F and AoagsB-RT-R, and AoagsC and AoagsC-RT-R (**Table 2**), in sequence, using KOD SYBR qPCR Mix (Toyobo Co., Ltd., Osaka, Japan).

Statistical Analysis

Student's *t*-test was used for the comparison of paired samples, and Tukey's test was used to compare multiple samples.

RESULTS

Aspergillus oryzae Has a Galactosaminogalactan Biosynthetic Gene Cluster

In *A. fumigatus*, GAG biosynthesis is regulated by a cluster of five genes, and this cluster is conserved in a wide range of filamentous fungi (Lee et al., 2016). To check whether *A. oryzae* possesses the GAG gene cluster, we used a BLAST search[1]. We found that all five GAG biosynthetic genes, orthologous to *A. fumigatus uge3*, *sph3*, *ega3*, *agd3*, and *gtb3* (**Figure 1A**), are conserved in *A. oryzae*: *ugeZ*, *sphZ*, *egaZ*, *agdZ*, and *gtbZ* (**Figure 1B**). *Aspergillus oryzae* UgeZ had motifs conserved among group 2 epimerases (Lee et al., 2014), SphZ contained a spherulin 4 conserved region (Bamford et al., 2015), and AgdZ had the conserved motifs of the carbohydrate esterase family 4 (Lee et al., 2016). These findings indicated that *A. oryzae*, similar to *A. fumigatus*, can produce GAG.

Hyphae of the AG-GAGΔ Strain Are Completely Dispersed in Liquid Culture

Because disruption of the *sph3* and *uge3* genes leads to a loss of GAG in *A. fumigatus* (Lee et al., 2014; Bamford et al., 2015), we disrupted *sphZ* and *ugeZ* in *A. oryzae* in the genetic background of the wild-type and AGΔ strains, and we obtained the GAGΔ and AG-GAGΔ strains, respectively. The wild-type, AGΔ, AG-GAGΔ, and GAGΔ strains showed almost the same mycelial growth and conidiation on CD agar plates after 5 days at 30°C (**Supplementary Figure S3**). When grown in YPD liquid medium at 30°C for 24 h, the wild-type strain formed significantly larger hyphal pellets (3.7 ± 0.2 mm in diameter) than did the AGΔ strain (2.7 ± 0.3 mm; **Figures 2A,B**), in good agreement with our previous results (Miyazawa et al., 2016). The hyphae of the AG-GAGΔ strain were completely dispersed, and the GAGΔ strain formed significantly larger hyphal pellets (6.2 ± 0.0 mm) than did the wild-type strain (**Figures 2A,B**). These results strongly suggest that, in addition to α-1,3-glucan, GAG has a role in hyphal adhesion in *A. oryzae* and that the defect in both α-1,3-glucan and GAG biosynthetic genes is required for full dispersion of *A. oryzae* hyphae.

Scanning electron microscopy revealed that the surface of *A. fumigatus* hyphae has GAG-dependent decorations in liquid culture; these are lost in the *sph3*, *uge3*, and *agd3* gene disruptants (Lee et al., 2014, 2016; Bamford et al., 2015). We investigated whether the hyphae of *A. oryzae* GAGΔ and AG-GAGΔ strains lack such decorations. As expected, we observed fibrous decorations on the hyphal cells of the wild-type and AGΔ *A. oryzae* strains (**Figure 2C**), but the hyphae of the GAGΔ and AG-GAGΔ strains had smooth surfaces (**Figure 2C**). These results suggest that the fibrous decorations on the cell surface are attributable to the presence of the GAG biosynthetic gene cluster in *A. oryzae*. A defect in GAG led to a loss of formation of adherent biofilm on solid surfaces (**Figure 2D**).

Gravelat et al. (2013) quantified the GAG content as the amount of GalN after complete hydrolysis of ethanol-precipitated supernatant from *A. fumigatus* culture. To apply this approach to *A. oryzae*, we analyzed the hydrolyzed HW fractions of each strain by HPAEC. The HW fractions from both the wild-type and AGΔ strains contained 0.2–0.3 mg/g biomass GalN (**Figure 2E**), whereas GalN was hardly detectable in the HW fractions from the GAGΔ and AG-GAGΔ strains (**Figure 2E**). These results show that *ugeZ* or *sphZ*, or both, are essential for GAG production in *A. oryzae*.

We used three approaches to analyze why the GAGΔ strain formed larger hyphal pellets in liquid culture: (1) HPAEC-pulsed amperometric detection analysis of cell wall components in alkali-soluble fractions showed no significant difference in the amount of glucose in the AS2 fractions between the wild-type and GAGΔ strains (**Supplementary Figure S4A**). The other cell wall components were similar among the four strains, except for the amount of glucose in the AS2 fractions (**Supplementary Figure S4A**). (2) Expression of the *agsB* gene, which encodes the main α-1,3-glucan synthase of *A. oryzae* (Zhang et al., 2017), was slightly lower in the GAGΔ strain than in the wild-type strain at 6 h of culture, but it was slightly higher at 24 h (**Supplementary Figure S4B**). The *agsA* and *agsC* genes, which encode minor α-1,3-glucan synthases, were scarcely expressed at 6 h (**Supplementary Figure S4B**).

[1]https://blast.ncbi.nlm.nih.gov/Blast.cgi

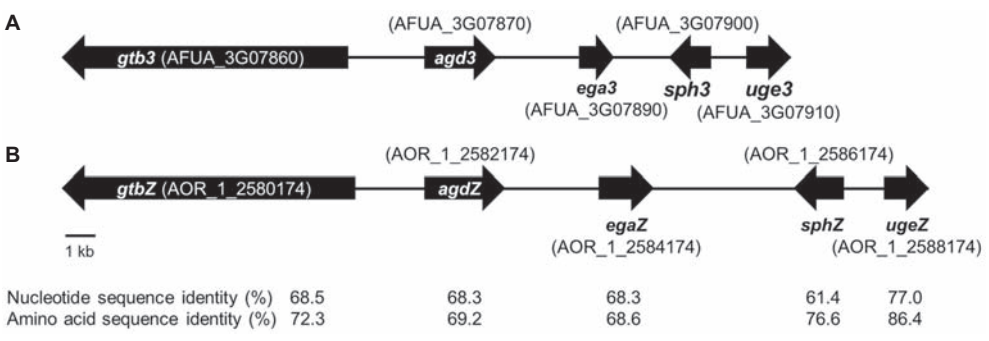

FIGURE 1 | GAG biosynthetic cluster in **(A)** *Aspergillus fumigatus* and **(B)** *Aspergillus oryzae.* The cluster of *A. oryzae* was predicted from the sequence of the cluster of *A. fumigatus* by using a BLAST search.

(3) ^{13}C NMR analysis of the AS2 fraction showed that the main component was α-1,3-glucan in both strains (**Supplementary Figure S4C**). (4) The AS2 fraction from the wild-type or GAGΔ strain was added to the hyphae of the AG-GAGΔ strain, resulting in the formation of similar hyphal aggregates in both samples; no aggregate formation was observed in the presence of the AS2 fraction from the AGΔ or the AG-GAGΔ strain (**Supplementary Figure S4D**). The reason why the GAGΔ strain formed larger aggregated pellets remains unclear from the results of our experiments.

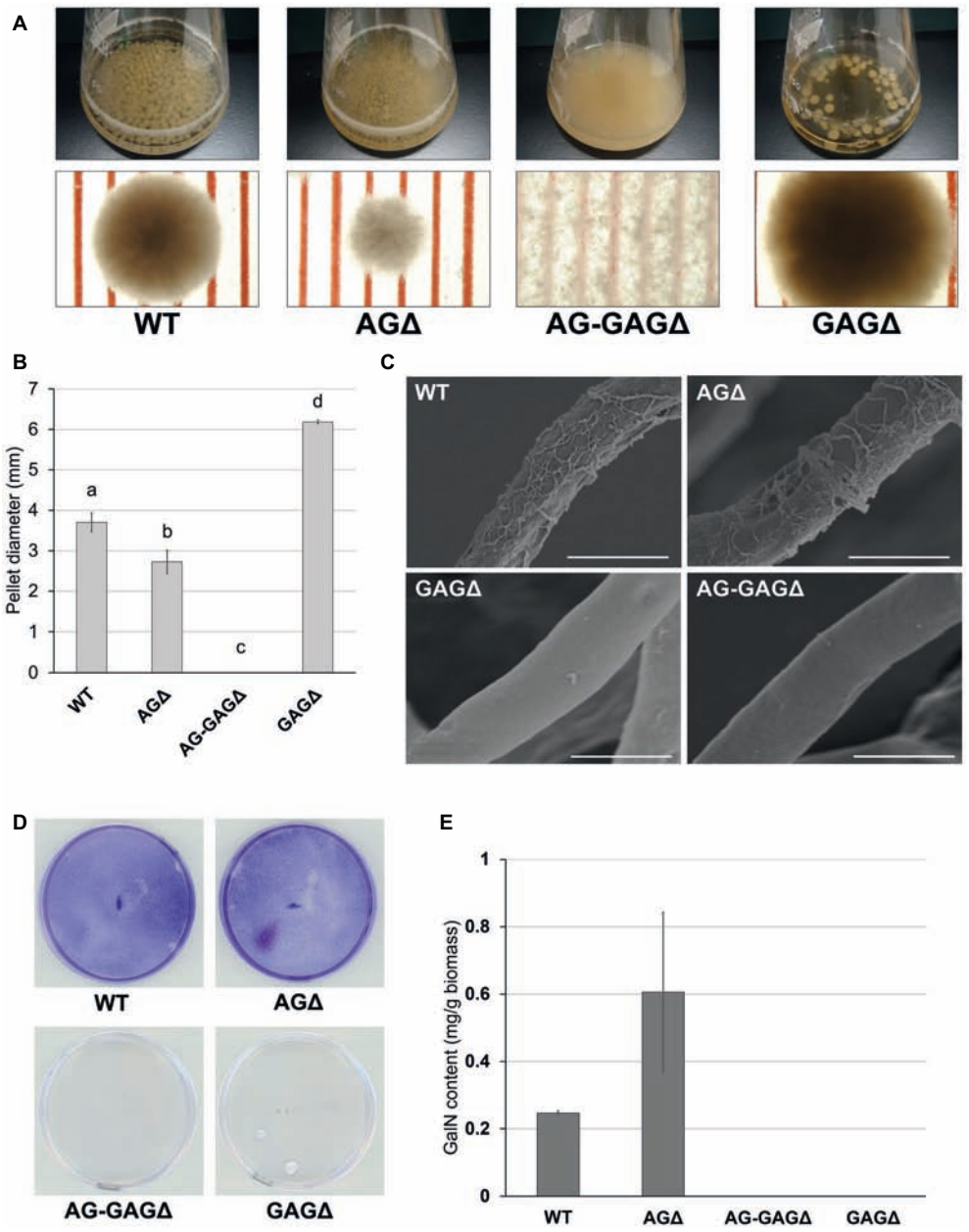

FIGURE 2 | Phenotypes of *Aspergillus oryzae* Δ*agsA*Δ*agsB*Δ*agsC*Δ*sphZ*Δ*ugeZ* (AG-GAGΔ) and Δ*sphZ*Δ*ugeZ* (GAGΔ) strains in liquid culture. **(A)** The wild-type (WT), Δ*agsA*Δ*agsB*Δ*agsC* (AGΔ), AG-GAGΔ, and GAGΔ strains were cultured in Erlenmeyer flasks (upper row), and images of hyphal pellets were taken under a stereomicroscope (bottom row; scale, 1 mm) at 24 h of culture. **(B)** The mean diameter of hyphal pellets was determined by measuring 10 randomly selected pellets per replicate under a stereomicroscope. Error bars represent standard deviations calculated from three replicates. Different letters indicate significant differences within each condition by Tukey's test ($p < 0.05$). **(C)** Morphology of each strain was examined under a scanning electron microscope. Scale bars, 5 μm. **(D)** Biofilm formation on polystyrene plates. Each strain was cultured for 24 h on a polystyrene plate (internal diameter 6 cm), after which the biofilms were washed and stained with crystal violet. **(E)** Galactosamine (GalN) content in the hot water-soluble fraction of the cell wall from the WT, AGΔ, AG-GAGΔ, and GAGΔ strains. Error bars represent standard error of the mean calculated from three replicates.

Disruptants of AG and Galactosaminogalactan Biosynthetic Genes Are Sensitive to Lysing Enzymes and Congo Red

To investigate the consequences of cell wall alteration caused by the loss of GAG, we assessed the susceptibility of the wild-type, AGΔ, AG-GAGΔ, and GAGΔ strains to LE and CR. The concentrations of protoplasts formed from hyphae tended to be higher for the AGΔ strain than for the wild-type strain after 2 and 4 h of treatment with LE ($0.05 < p < 0.1$; **Figure 3A**). In contrast, the protoplast concentration was significantly higher for the AG-GAGΔ strain than for the wild-type and AGΔ strains at each time point (**Figure 3A**). The protoplast concentration was also significantly higher for the GAGΔ strain than for the wild-type and AGΔ strains after 1 and 4 h (**Figure 3A**), but it was significantly lower than for the AG-GAGΔ strain after 4 h (**Figure 3A**). All three mutant strains were significantly more sensitive to CR than the wild type: the AG-GAGΔ strain was most sensitive, and the AGΔ and GAGΔ strains showed similar sensitivity (**Figure 3B**). These data revealed that α-1,3-glucan and GAG additively contribute to cell wall protection from cell wall-degrading enzymes and environmental chemicals.

Temporally and Spatially Different Contributions of α-1,3-Glucan and Galactosaminogalactan to Hyphal Aggregation in Liquid Culture

The complete dispersion of the AG-GAGΔ hyphae demonstrated that both α-1,3-glucan and GAG function as adhesive factors for hyphal aggregation in *A. oryzae*, and consequently the hyphae expressing both polysaccharides form pellets (**Figure 2**). To analyze the temporal and spatial contribution of the two polysaccharides, wild-type, AGΔ, GAGΔ, and AG-GAGΔ conidia were cultured in 48-well plates, and formation of hyphal pellets was examined (**Figure 4A**). The presence of α-1,3-glucan and GAG on the surfaces of conidia and germinating hyphae in liquid culture was analyzed by fluorescence microscopy with AGBD-GFP, which binds specifically to α-1,3-glucan, and lectin SBA, which binds specifically to GalNAc (**Figure 5**). At the initiation of culture (0 h), conidia of all strains formed scarce aggregates (**Figures 4A,B**). Fluorescence of AGBD-GFP was observed on wild-type and GAGΔ conidia, but not on AGΔ or AG-GAGΔ conidia (**Figure 5A**). SBA fluorescence was undetectable on conidia of any strains (**Figure 5A**). At 3 h after inoculation, 63 and 76%, respectively, of swollen conidia of the wild-type and GAGΔ strains had aggregated and formed small pellets, but aggregates of AGΔ and AG-GAGΔ swollen conidia were scarce (**Figures 4A,B**). At 3 h, AGBD-GFP fluorescence was detectable on wild-type and GAGΔ germinated conidia, but none of the strains was stained with SBA (**Figure 5B**). At 6 h, the wild-type, AGΔ, and GAGΔ formed hyphal pellets, but aggregates of AG-GAGΔ were scarce (**Figure 4A**). Aggregation reached nearly 95% in the wild-type and GAGΔ, 80% in AGΔ, and 0% in AG-GAGΔ (**Figure 4B**). AGBD-GFP fluorescence was observed on hyphae of the wild-type and GAGΔ, and that of SBA was observed in the wild-type and AGΔ strains (**Figure 5C**). At 9 h, the wild-type, GAGΔ, and AGΔ strains formed hyphal pellets (**Figure 4A**) similar to those formed after 24 h of culture in YPD medium. Aggregation of germinating conidia reached about 90%, except in AG-GAGΔ (**Figure 4B**). The fluorescence profiles of AGBD-GFP and SBA for each strain were similar to those observed at 6 h (**Figure 5D**). The AG-GAGΔ strain hardly formed any hyphal pellets at any time point (**Figures 4, 5**). Neither conidia nor hyphae of AG-GAGΔ were stained by AGBD-GFP or SBA (**Figure 5**). These results indicate that hyphal aggregation

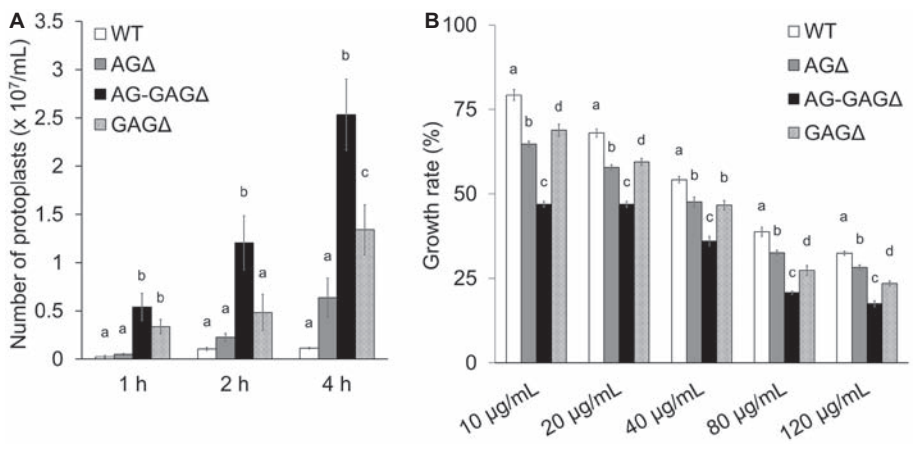

FIGURE 3 | Sensitivity to Congo Red and Lysing Enzymes. **(A)** Mycelia cultured for 1 day were suspended in sodium phosphate buffer (10 mM, pH 6.0) containing 0.8 M NaCl and 10 mg/ml Lysing Enzymes. After 1, 2, and 4 h, protoplasts were counted under a microscope. Error bars represent the standard deviation calculated from three replicates. **(B)** Growth rates after 3 days on CDE medium at the indicated concentrations of Congo Red. Diameter of the colonies grown on CDE medium without Congo Red was considered as 100%. Error bars represent standard deviations calculated from three replicates. In both panels, different letters indicate significant differences within each condition by Tukey's test ($p < 0.05$).

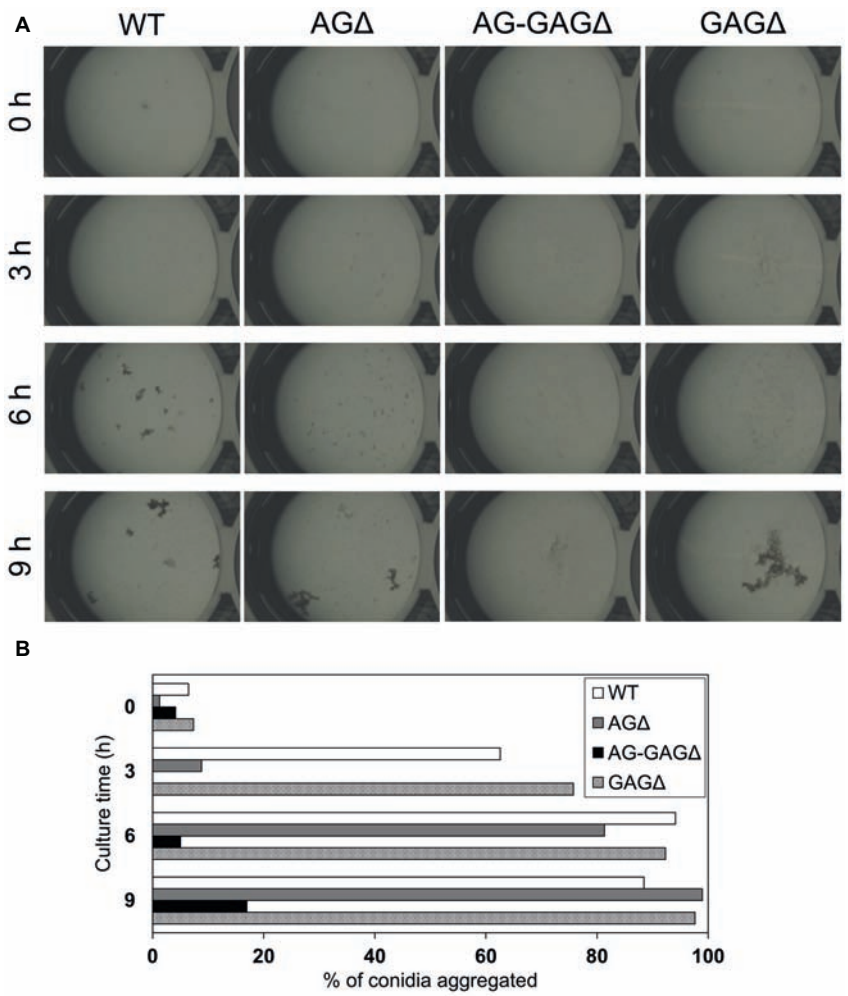

FIGURE 4 | Conidial aggregation assay. **(A)** Conidia (5×10^5) of the wild-type (WT), Δ*agsA*Δ*agsB*Δ*agsC* (AGΔ), Δ*agsA*Δ*agsB*Δ*agsC*Δ*sphZ*Δ*ugeZ* (AG-GAGΔ), and Δ*sphZ*Δ*ugeZ* (GAGΔ) strains were inoculated into 500 μl of CDE liquid medium and incubated at 30°C with shaking (1,200 rpm). Photographs were taken at the indicated time points under a stereomicroscope (magnification, ×8). **(B)** Percentage conidial aggregation at indicated culture times.

caused by α-1,3-glucan was initiated just after inoculation, whereas GAG-dependent hyphal aggregation started 3–6 h after inoculation.

Galactosaminogalactan-Dependent Aggregation of Hyphae *in vitro* and Its pH Dependence

According to the previously described GAG purification method (Fontaine et al., 2011), we obtained the ethanol precipitates from the AGΔ strain and washed them with 150 mM sodium chloride. However, the precipitates were fully solubilized in 150 mM sodium chloride. Therefore, we developed an EtOH fractional precipitation method to isolate GAG from culture supernatants, and we obtained six fractions. The 0-, 0.5-, 1-, 2-, and 2.5-vol. fractions from the AGΔ strain contained approximately 8% of Gal and 5% of mannose, with a small amount of GalN (**Figure 6A**). The 1.5-vol. fraction from the AGΔ strain contained 16% of GalN, 17% of Gal, and 4% of mannose (**Figure 6A**); thus, this fraction but not the other fractions appeared to contain mainly GAG and galactomannan. The 1.5-vol. fraction from the AG-GAGΔ strain contained no GalN but contained 8% of Gal and 5% of mannose (**Figure 6A**). As calculated from the composition of the 1.5-vol. fraction from the AG-GAGΔ strain, the 1.5-vol. fraction from AGΔ appeared to contain approximately 25% of GAG. To evaluate whether the aggregation of hyphae could be reproduced *in vitro*, the fractions were added to the mycelia of the AG-GAGΔ strain and mycelial aggregation was examined. Only the 1.5-vol. fraction from the AGΔ strain induced aggregation (**Figure 6B**). The aggregates were stained with an SBA-Alexa Fluor 647 conjugate (**Figure 6C**). The 1.5-vol. fraction from AGΔ did not form aggregates without mycelia (**Figure 6D**). The DD of GalNAc residues of GAG in the 1.5-vol. fraction, as determined by colloidal titration, was 48.9 ± 4.6% (**Table 3**).

In *A. fumigatus*, GalNAc moieties in GAG are partly deacetylated and consequently positively charged (Fontaine et al., 2011), and

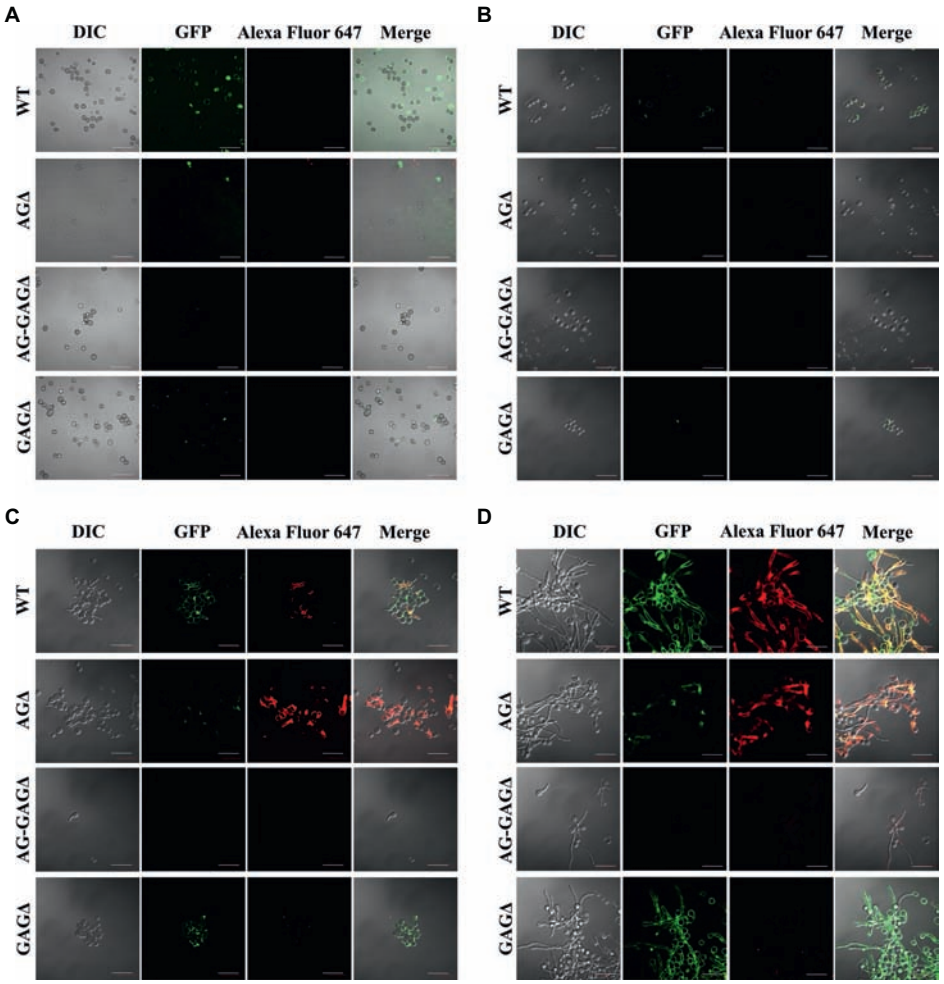

FIGURE 5 | Visualization of AG and GAG in the cell wall by staining with AGBD-GFP and lectin (soybean agglutinin). Conidia (5.0×10^5) of the wild-type (WT), *ΔagsAΔagsBΔagsC* (AGΔ), *ΔagsAΔagsBΔagsCΔsphZΔugeZ* (AG-GAGΔ), and *ΔsphZΔugeZ* (GAGΔ) strains were inoculated into 500 µl of CDE liquid medium and incubated at 30°C for **(A)** 0, **(B)** 3, **(C)** 6, and **(D)** 9 h with shaking (1,200 rpm). At each time point, the cells were dropped on a glass slide, fixed with 4% (w/v) paraformaldehyde, stained with AGBD-GFP and soybean agglutinin-Alexa Fluor 647 conjugate (100 µg/ml each), and observed under a confocal laser-scanning microscope (×1,000). Scale bars, 20 µm.

we wondered whether GAG-dependent aggregation depends on pH. Addition of GAG to mycelia of the AG-GAGΔ strain led to aggregation at pH 6, 7; aggregates were scarce at pH 4, 5, and 8 (**Figure 7A**). The conidia remained dispersed upon the addition of the mock fraction at pH 4, 6, 7, and 8 (**Figure 7B**). At pH 5, slight aggregates were formed when the mock fraction was added (**Figure 7B**). In addition, although the degree of aggregation was very low compared with that in the presence of GAG at neutral pH, the AG-GAGΔ hyphae formed slight, or very small, aggregates at pH 4 and 5 in the absence of GAG or the mock fraction (**Figure 7B**). There might therefore still be some unknown aggregation factor working at low pH in AG-GAGΔ hyphae. These results suggest that the increased positive charge in GAG at acidic pH leads to electric repulsion among GAG chains and consequently prevents GAG-dependent mycelial aggregation. Around the neutral pH, the positive charge might be lower and consequently GAG might contribute to hyphal adhesion *via* non-electrostatic interactions. The reason for the absence of aggregate formation at pH 8 is unknown.

Galactosaminogalactan-Dependent Aggregation Is Caused by Hydrogen Bonding Between Polysaccharides

We hypothesized that GAG-dependent aggregation was caused by hydrogen bonding *via* the amino groups of GalN. To test this hypothesis, we treated the 1.5-vol. EtOH fraction with (acetylation) or without acetic anhydrate and then evaluated the aggregation. In the presence of non-*N*-acetylated GAG, the AG-GAGΔ mycelia aggregated, similar to the results in **Figure 6A**, whereas GAG *N*-acetylation weakened mycelial aggregation (**Figure 8A**). The DD of the *N*-acetylated 1.5-vol. fraction was 2.0 ± 0.5%, which was significantly smaller than that of the non-*N*-acetylated 1.5-vol. fraction (43.6 ± 5.2%; $p < 0.01$) (**Table 3**). These

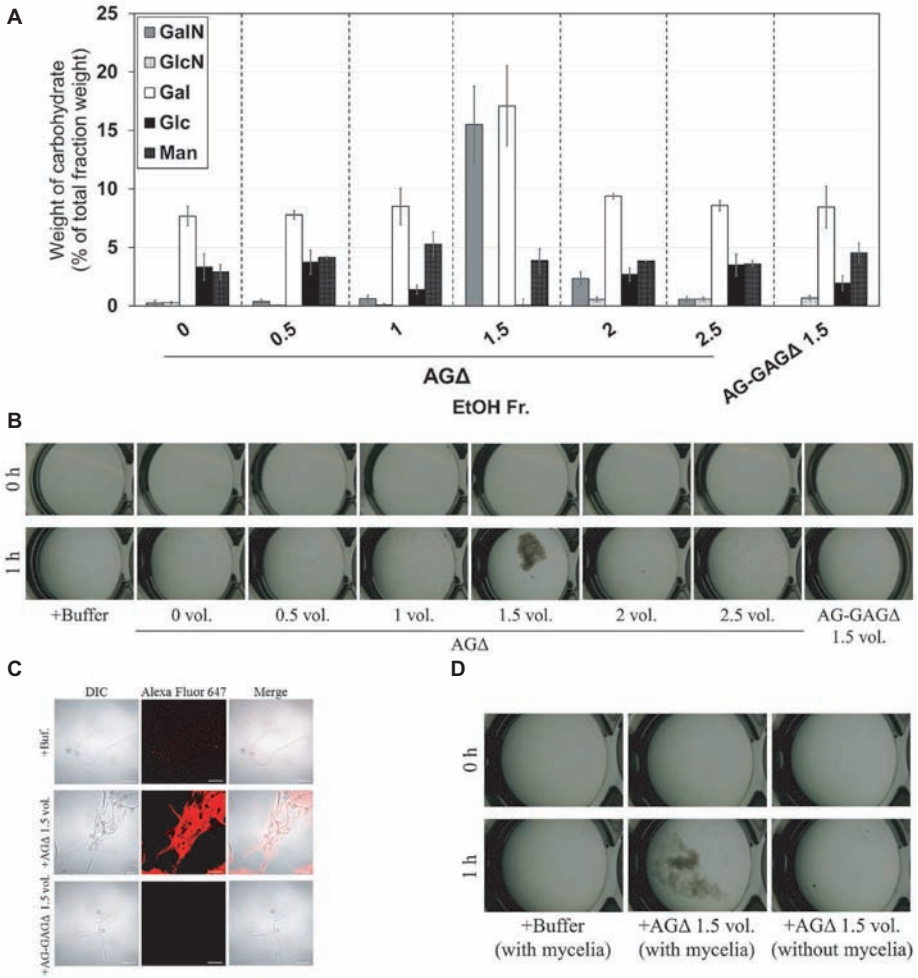

FIGURE 6 | Aggregation of mycelia of the AG-GAGΔ strain induced by ethanol-precipitated GAG. **(A)** Monosaccharide composition of the fractions obtained from culture supernatant by ethanol precipitation. **(B)** Mycelial suspension of the AG-GAGΔ strain (25 μl) was added into a mixture of 400 μl of water, 50 μl of 1 M sodium phosphate buffer (pH 7.0), and 25 μl of 2 mg/ml of the fractions prepared from the AGΔ or AG-GAGΔ strains, as indicated. Samples were incubated at 30°C for 1 h with shaking and examined under a stereomicroscope (magnification, ×8). **(C)** Mycelia incubated for 1 h in the presence of EtOH-precipitated GAG were stained with soybean agglutinin-Alexa Flour 647 conjugates and observed under a confocal laser-scanning microscope (×1,000). Scale bars, 20 μm. **(D)** Aggregation assay with the 1.5-vol. fraction from AGΔ was performed as in **(A)**, with or without mycelial suspension of AG-GAGΔ.

TABLE 3 | Degrees of deacetylation of *N*-acetylgalactosamine residues of galactosaminogalactan.

Sample	Degree of deacetylation (%)
AGΔ 1.5-vol. EtOH Fr.	48.9 ± 4.6
AGΔ 1.5-vol. EtOH Fr. (acetylated)	2.0 ± 0.5*
AGΔ 1.5-vol. EtOH Fr. (non-acetylated)	43.6 ± 5.2

Values represent the mean ± standard error of the three replicates. Asterisk indicates significant difference ($p < 0.01$) with the AGΔ 1.5-vol. EtOH Fr. (non-acetylated).

results suggest that the amino groups of GalN are involved in GAG-dependent aggregation.

To confirm that GAG-dependent aggregation relies on hydrogen bonds, we performed mycelial aggregation assay in the presence of urea, which breaks hydrogen bonds. Mycelia aggregated without urea, but aggregation was weakened by increasing urea concentrations (**Figure 8B**). Taken together, these results strongly suggest that hydrogen bond formation *via* the amino groups of GalN is important for GAG-dependent aggregation.

Production of a Recombinant Enzyme Is Increased in the AG-GAGΔ-cutL1 Strain

We investigated whether hyphal dispersion would increase biomass and enzyme production in *A. oryzae*. As expected, hyphae of the AG-GAGΔ-cutL1 strain cultured in YPM medium were fully dispersed and those of the AGΔ-cutL1 strain formed smaller pellets than those of the WT-cutL1 strain (**Figure 9A**). After 24 h of culture, the culture supernatant of each strain was subjected to SDS-PAGE, resulting in greater secreted protein profiles in AG-GAGΔ-cutL1 than in the WT-cutL1 and AGΔ-cutL1 strains (**Figure 9B**). Both biomass and cutinase production was higher in the AG-GAGΔ-cutL1 strain (approximately 10 times) and in the AGΔ-cutL1 strain (4 times) than in the wild-type (**Figures 9C,D**). This result suggests that hyphal dispersion caused

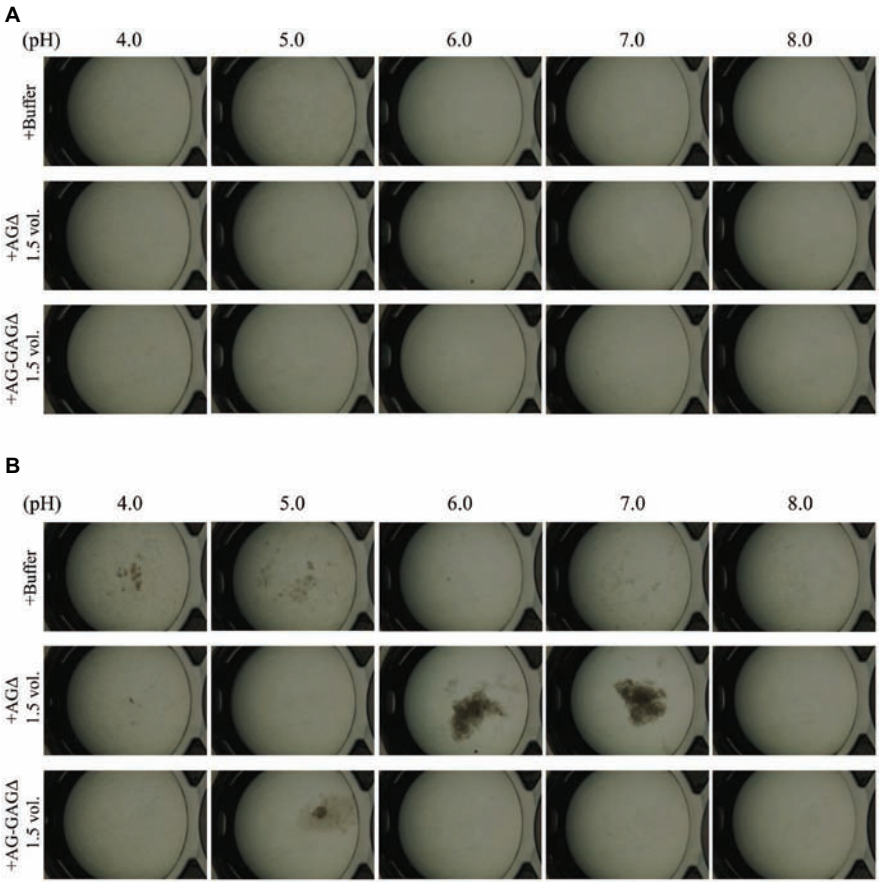

FIGURE 7 | pH-dependence of GAG aggregation. Mycelial suspension of the AG-GAGΔ strain (25 μl) was added to 450 μl of buffers with different pH and 25 μl of the 1.5-vol. EtOH fraction prepared from the AGΔ or AG-GAGΔ strain as indicated. Samples were incubated at 30°C for **(A)** 0 h and **(B)** 1 h with shaking and examined under a stereomicroscope (magnification, ×8).

by a loss of the hyphal aggregation factors α-1,3-glucan and GAG can increase biomass and recombinant enzyme production in filamentous fungi that have α-1,3-glucan or GAG or both.

DISCUSSION

Hyphae of filamentous fungi generally form large aggregated pellets in liquid culture, thus limiting the fermentative production of commercially valuable enzymes and metabolites (Driouch et al., 2010, 2012). Aggregation of hyphae seems to be related to their cell surface properties (Fontaine et al., 2010; Priegnitz et al., 2012; Yoshimi et al., 2017), but the mechanism of hyphal aggregation is not well understood. We previously demonstrated that α-1,3-glucan in the cell wall has a role in hyphal adhesion in *A. nidulans* (Yoshimi et al., 2013; Miyazawa et al., 2018), and that the hyphae of α-1,3-glucan-deficient mutants of *A. oryzae* form smaller pellets than those of the wild-type but are not dispersed (Miyazawa et al., 2016). We concluded that α-1,3-glucan is an adhesive factor for *A. oryzae* hyphae, but another factor involved in hyphal adhesion remains in the AGΔ strain. Here, we focused on GAG, a component of the extracellular matrix, as a candidate adhesive factor. Lee et al. (Lee et al., 2016) revealed that GAG biosynthesis is controlled by five clustered genes (*gtb3*, *agd3*, *ega3*, *sph3*, and *uge3*) in *A. fumigatus*, and that similar gene clusters are conserved in various fungi, such as *A. niger* and *A. nidulans*. We found that the gene cluster is also conserved in the genome of *A. oryzae*.

α-1,3-Glucan contributes to hyphal and mycelial adhesion in *A. nidulans*, *A. oryzae*, and *A. fumigatus* (Fontaine et al., 2010; Yoshimi et al., 2013; Miyazawa et al., 2016). GAG mediates hyphal adhesion to plastic, fibronectin, and epithetical cells, and its function is related to pathogenesis in *A. fumigatus* (Gravelat et al., 2013). GAG also mediates biofilm formation in plate cultures (Gravelat et al., 2013). However, neither the relationship between GAG and hyphal aggregation nor the phenotype of an AG-GAG double mutant (AG-GAGΔ) has been reported. Here, we constructed AG-GAGΔ and a single mutant (GAGΔ) in *A. oryzae* and analyzed their growth in liquid culture. The AG-GAGΔ hyphae were completely dispersed, but the GAGΔ hyphae formed pellets larger than those of the wild-type strain (**Figure 2**). These results suggest that not only α-1,3-glucan but also GAG contributes to hyphal aggregation in *A. oryzae*.

We investigated whether α-1,3-glucan and GAG showed temporal and spatial differences in their effects on hyphal aggregation during germination and hyphal growth. Because

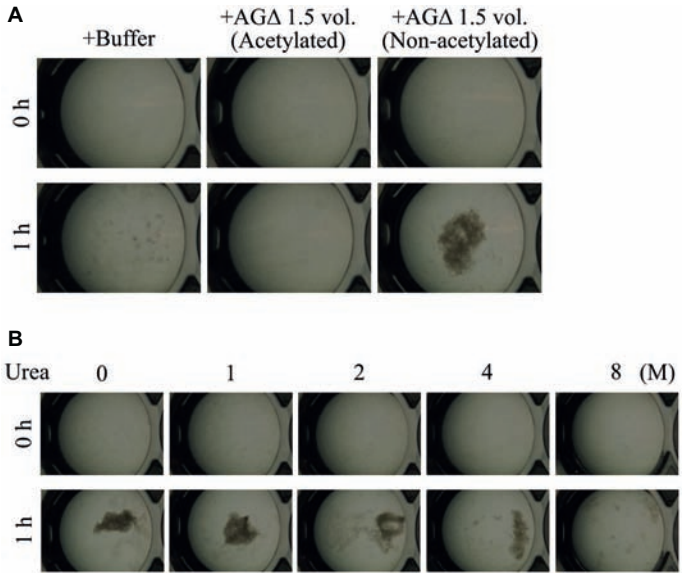

FIGURE 8 | Mycelial aggregation in the presence of **(A)** acetylated GAG or **(B)** urea. **(A)** The amino groups of ethanol-precipitated GAG were acetylated with acetic anhydrate. Mycelial suspension of the AG-GAGΔ strain (25 μl) was added to a mixture of 450 μl of 100 mM sodium phosphate buffer (pH 7.0) and 25 μl of the 1.5-vol. EtOH fraction prepared from AGΔ (acetylated or not). **(B)** Mycelial suspension of the AG-GAGΔ strain (25 μl) was added to a mixture of 450 μl of 100 mM sodium phosphate buffer (pH 7.0) containing 0, 1, 2, 4, or 8 M urea, and 25 μl of the 1.5-vol. EtOH fraction prepared from the AGΔ strain. Samples were incubated at 30°C for 1 h with shaking and examined under a stereomicroscope (magnification, ×8).

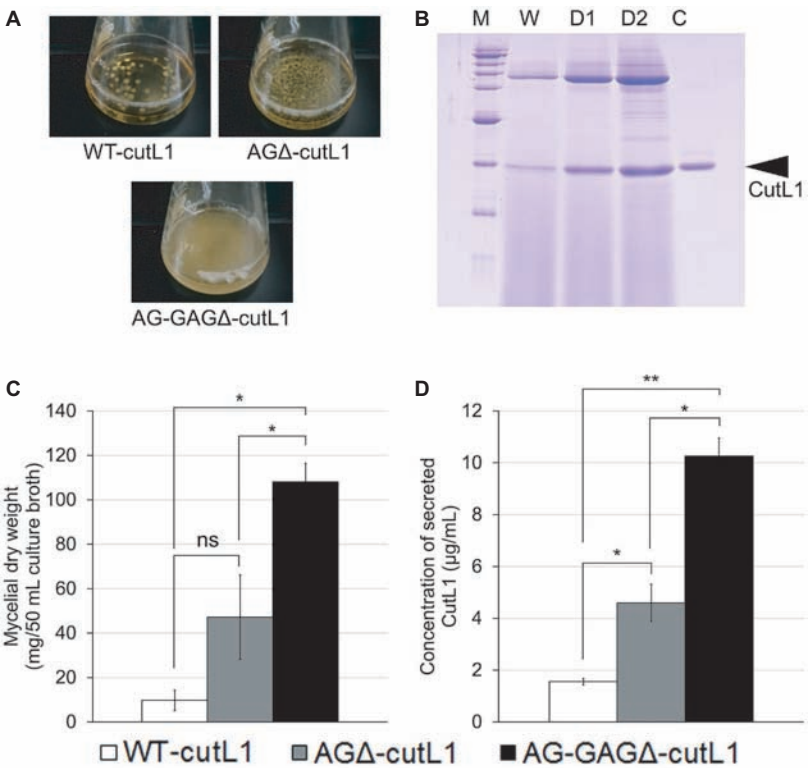

FIGURE 9 | Recombinant CutL1 production by the WT-cutL1, AGΔ-cutL1, and AG-GAGΔ-cutL1 strains in liquid culture. **(A)** Phenotypes of the WT-cutL1, AGΔ-cutL1, and AG-GAGΔ-cutL1 strains under liquid culture conditions. Conidia (final concentration, 1×10^4/ml) of each strain were inoculated into YPM medium and rotated at 100 rpm at 30°C for 24 h. **(B)** Secreted protein profiles of each strain. Lanes W, D1, D2: proteins precipitated from culture supernatants (250 μl) of the WT-cutL1, AGΔ-cutL1, and AG-GAGΔ-cutL1 strains, respectively; lane C: 1 μg of purified CutL1. **(C)** Mycelial dry weight of each strain. Mycelia grown for 24 h were collected by filtration through Miracloth, dried at 70°C and weighed. **(D)** Concentration of secreted CutL1 in culture supernatants. In **(C)** and **(D)**, error bars represent the standard error of the mean calculated from three replicates (*$p < 0.05$; **$p < 0.01$). ns, not significant.

the germ tubes of the wild-type and GAGΔ strains aggregated at 3 h after inoculation of their conidia, whereas those of AGΔ did so at 6 h, we conclude that α-1,3-glucan is present on the surface of most hyphae just after germination and acts as an adhesive factor, whereas GAG, which is secreted and presented around the hyphal tips, contributed to hyphal aggregation at 6 h after inoculation (**Figures 4, 5**). We succeeded in *in vitro* aggregation of AG-GAGΔ hyphae by adding GAG partially purified from AGΔ strains (**Figure 6**). In the presence of GAG, AG-GAGΔ mycelia aggregated at pH 6 and 7, but aggregation was reduced at acidic pH (**Figure 7B**).

In the GAG biosynthetic gene cluster, *agd3* encodes *N*-acetylgalactosamine deacetylase, and GalNAc molecules in GAG chains from *A. fumigatus* are partly deacetylated (Fontaine et al., 2011). Disruption of *agd3* in *A. fumigatus* abolishes GAG deacetylation and results in a loss of cell wall-associated GAG (Lee et al., 2016). Positively charged amino groups in deacetylated GalNAc in GAG are thought to be required for the attachment of hyphae to negatively charged surfaces (Lee et al., 2016) and likely prevent hyphal aggregation at acidic pH because of electric repulsion; these groups would be unprotonated at pH close to neutral, in particular at the putative isoelectric point of GAG. Therefore, attachment of GAG in this pH range might be attributable to hydrogen bonding between the amino groups of GalN and the OH groups of the sugar moieties in the glucan of the hyphal cell wall or GAG chains pre-attached to the cell wall. The DD of GAG derived from AGΔ was about 50% (**Table 3**). Addition of GAG with amino groups acetylated by acetic anhydrate barely induced mycelial aggregation (**Figure 8A**), and the DD of acetylated GAG of AGΔ was significantly decreased by the acetylation (**Table 3**). These results strongly suggest that deacetylation of GalNAc residues in the GAG molecule is important for GAG-dependent aggregation. In addition, GAG-induced mycelial aggregation was inhibited in the presence of 8 M urea (**Figure 8B**). These observations indicate that amino group acetylation abolishes hydrogen bonding between GAG and hyphal glucans or GAG pre-attached to hyphae. Hydrogen bonds might be a major force in GAG-dependent hyphal aggregation at pH close to neutral. When hyphae aggregated by addition of GAG at neutral pH were subsequently transferred to acidic buffer (pH 4), they remained aggregated (data not shown), suggesting that, once formed, the adhesion among GAG chains is resistant to acidic conditions.

Formation of hyphal pellets limits productivity in the fermentation industry that uses filamentous fungi, including *Aspergillus* species, because the inner part of the pellet is inactive (Driouch et al., 2010). In *A. niger*, titanate particles are used as a scaffold for hyphal pellets to minimize their size (Driouch et al., 2012). Although physical approaches are efficient, they limit the range of culture media. The AG-GAGΔ strain produced significantly larger amounts of biomass and cutinase than did the AGΔ and wild-type strains; it did not require any scaffold particles, suggesting that controlling the hyphal aggregation factors of hyphae is an innovative approach for the fermentation industry.

We demonstrated that both α-1,3-glucan and GAG on the hyphal surface contribute to the formation of hyphal pellets and are adhesive molecules. The physicochemical properties of the two polysaccharides differ. α-1,3-Glucan is a water-insoluble major cell wall polysaccharide, whereas GAG is secreted and is a water-soluble component of the extracellular matrix. Further studies are necessary to understand the molecular mechanism underlying the interactions among α-1,3-glucan and GAG chains.

DATA AVAILABILITY

The datasets generated for this study are available on request to the corresponding author.

AUTHOR CONTRIBUTIONS

KM, AY, and KA conceived and designed the experiments. AY determined the sensitivity to LE and CR. KM and MS constructed fungal mutants. FT performed the assay of CutL1 production. KM and AS performed the Southern blot analysis. SK performed the ^{13}C NMR analysis. AK and SY produced AGBD-GFP. KM and TN performed fractional precipitation of GAG. KM performed most experiments and analyzed the data.

FUNDING

This work was supported by a Grant-in-Aid for Scientific Research (B) (26292037) and (C) (18K05384) from the Japan Society for the Promotion of Science (JSPS) and a Grant-in-Aid for JSPS Fellows (18J11870). It was also supported by the Institute for Fermentation, Osaka, Japan (Grant No. L-2018-2-014).

ACKNOWLEDGMENTS

We are grateful to Associate Professor Toshikazu Komoda (Miyagi University) for operating the NMR spectrometer. We are also grateful to Dr. Makoto Ogata (National Institute of Technology, Fukushima College) for advice on the method of acetylation of polysaccharides. We thank Yuki Terauchi (Tohoku University) for calculating the degree of deacetylation of GAG. The manuscript was edited by ELSS, Inc. (http://www.elss.co.jp/en/).

SUPPLEMENTARY MATERIAL

The Supplementary Material for this article can be found online at: https://www.frontiersin.org/articles/10.3389/fmicb.2019.02090/full#supplementary-material

REFERENCES

Abe, K., Gomi, K., Hasegawa, F., and Machida, M. (2006). Impact of *Aspergillus oryzae* genomics on industrial production of metabolites. *Mycopathologia* 162, 143–153. doi: 10.1007/s11046-006-0049-2

Bamford, N. C., Snarr, B. D., Gravelat, F. N., Little, D. J., Lee, M. J., Zacharias, C. A., et al. (2015). Sph3 is a glycoside hydrolase required for the biosynthesis of galactosaminogalactan in *Aspergillus fumigatus*. *J. Biol. Chem.* 290, 27438–27450. doi: 10.1074/jbc.M115.679050

Beauvais, A., Fontaine, T., Aimanianda, V., and Latgé, J. P. (2014). *Aspergillus* cell wall and biofilm. *Mycopathologia* 178, 371–377. doi: 10.1007/s11046-014-9766-0

Driouch, H., Hänsch, R., Wucherpfennig, T., Krull, R., and Wittmann, C. (2012). Improved enzyme production by bio-pellets of *Aspergillus niger*: targeted morphology engineering using titanate microparticles. *Biotechnol. Bioeng.* 109, 462–471. doi: 10.1002/bit.23313

Driouch, H., Sommer, B., and Wittmann, C. (2010). Morphology engineering of *Aspergillus niger* for improved enzyme production. *Biotechnol. Bioeng.* 105, 1058–1068. doi: 10.1002/bit.22614

Fontaine, T., Beauvais, A., Loussert, C., Thevenard, B., Fulgsang, C. C., Ohno, N., et al. (2010). Cell wall α1-3glucans induce the aggregation of germinating conidia of *Aspergillus fumigatus*. *Fungal Genet. Biol.* 47, 707–712. doi: 10.1016/j.fgb.2010.04.006

Fontaine, T., Delangle, A., Simenel, C., Coddeville, B., van Vliet, S. J., van Kooyk, Y., et al. (2011). Galactosaminogalactan, a new immunosuppressive polysaccharide of *Aspergillus fumigatus*. *PLoS Pathog.* 7:e1002372. doi: 10.1371/journal.ppat.1002372

Gravelat, F. N., Beauvais, A., Liu, H., Lee, M. J., Snarr, B. D., Chen, D., et al. (2013). *Aspergillus* galactosaminogalactan mediates adherence to host constituents and conceals hyphal β-glucan from the immune system. *PLoS Pathog.* 9:e1003575. doi: 10.1371/journal.ppat.1003575

Gravelat, F. N., Ejzykowicz, D. E., Chiang, L. Y., Chabot, J. C., Urb, M., Macdonald, K. D., et al. (2010). *Aspergillus fumigatus* MedA governs adherence, host cell interactions and virulence. *Cell. Microbiol.* 12, 473–488. doi: 10.1111/j.1462-5822.2009.01408.x

Hattori, M., Munezane, S., Kato, R., and Kawauchi, T. (2009). Evaluation of colloidal titration with potasium poly (vinylsulfate) to determine the degree of chitosan deacetylation. *Chitin and Chitosan Res.* 15, 13–19.

Johnson, A. R. (1971). Improved method of hexosamine determination. *Anal. Biochem.* 44, 628–635. doi: 10.1016/0003-2697(71)90252-1

Karahalil, E., Demirel, F., Evcan, E., and Germec, M. (2017). Microparticle-enhanced polygalacturonase production by wild type *Aspergillus sojae*. *BioTechniques* 7:361. doi: 10.1007/s13205-017-1004-2.

Kobayashi, T., Abe, K., Asai, K., Gomi, K., Juvvadi, P. R., Kato, M., et al. (2007). Genomics of *Aspergillus oryzae*. *Biosci. Biotechnol. Biochem.* 71, 646–670. doi: 10.1271/bbb.60550

Latgé, J.-P. (2010). Tasting the fungal cell wall. *Cell. Microbiol.* 12, 863–872. doi: 10.1111/j.1462-5822.2010.01474.x

Lee, M. J., Geller, A. M., Bamford, N. C., Liu, H., Gravelat, F. N., Snarr, B. D., et al. (2016). Deacetylation of fungal exopolysaccharide mediates adhesion and biofilm formation. *mBio* 7, 1–14. doi: 10.1128/mBio.00252-16

Lee, M. J., Gravelat, F. N., Cerone, R. P., Baptista, S. D., Campoli, P. V., Choe, S. I., et al. (2014). Overlapping and distinct roles of *Aspergillus fumigatus* UDP-glucose 4-epimerases in galactose metabolism and the synthesis of galactose-containing cell wall polysaccharides. *J. Biol. Chem.* 289, 1243–1256. doi: 10.1074/jbc.M113.522516

Lee, M. J., Liu, H., Barker, B. M., Snarr, B. D., Gravelat, F. N., Al Abdallah, Q., et al. (2015). The fungal exopolysaccharide galactosaminogalactan mediates virulence by enhancing resistance to neutrophil extracellular traps. *PLoS Pathog.* 11:e1005187. doi: 10.1371/journal.ppat.1005187

Lee, M. J., and Sheppard, D. C. (2016). Recent advances in the understanding of the *Aspergillus fumigatus* cell wall. *J. Microbiol.* 54, 232–242. doi: 10.1007/s12275-016-6045-4

Maeda, H., Yamagata, Y., Abe, K., Hasegawa, F., Machida, M., Ishioka, R., et al. (2005). Purification and characterization of a biodegradable plastic-degrading enzyme from *Aspergillus oryzae*. *Appl. Microbiol. Biotechnol.* 67, 778–788. doi: 10.1007/s00253-004-1853-6

Miyazawa, K., Yoshimi, A., Kasahara, S., Sugahara, A., Koizumi, A., Yano, S., et al. (2018). Molecular mass and localization of α-1,3-glucan in cell wall control the degree of hyphal aggregation in liquid culture of *Aspergillus nidulans*. *Front. Microbiol.* 9:2623. doi: 10.3389/fmicb.2018.02623

Miyazawa, K., Yoshimi, A., Zhang, S., Sano, M., Nakayama, M., Gomi, K., et al. (2016). Increased enzyme production under liquid culture conditions in the industrial fungus *Aspergillus oryzae* by disruption of the genes encoding cell wall α-1,3-glucan synthase. *Biosci. Biotechnol. Biochem.* 80, 1853–1863. doi: 10.1080/09168451.2016.1209968

Mizutani, O., Kudo, Y., Saito, A., Matsuura, T., Inoue, H., Abe, K., et al. (2008). A defect of LigD (human Lig4 homolog) for nonhomologous end joining significantly improves efficiency of gene-targeting in *Aspergillus oryzae*. *Fungal Genet. Biol.* 45, 878–889. doi: 10.1016/j.fgb.2007.12.010

Priegnitz, B. E., Wargenau, A., Brandt, U., Rohde, M., Dietrich, S., Kwade, A., et al. (2012). The role of initial spore adhesion in pellet and biofilm formation in *Aspergillus niger*. *Fungal Genet. Biol.* 49, 30–38. doi: 10.1016/j.fgb.2011.12.002

Senju, R. (ed.) (1969). "'Koroido tekiteiki no tyousei to hyoutei' (Preparation and standardization of colloid titrant)" in *"Koroido tekitei-ho" (Colloidal titration)*. Tokyo: Nanko-do, 39–41.

Sheppard, D. C., and Howell, P. L. (2016). Biofilm exopolysaccharides of pathogenic fungi: lessons from bacteria. *J. Biol. Chem.* 291, 12529–12537. doi: 10.1074/jbc.R116.720995

Speth, C., Rambach, G., Lass-flörl, C., Howell, P. L., Sheppard, D. C., Speth, C., et al. (2019). Galactosaminogalactan (GAG) and its multiple roles in Aspergillus pathogenesis. *Virulence*, 1–8. doi: 10.1080/21505594.2019.1568174 [Epub ahead of print].

Suyotha, W., Yano, S., Takagi, K., Rattanakit-Chandet, N., Tachiki, T., and Wakayama, M. (2013). Domain structure and function of α-1,3-glucanase from *Bacillus circulans* KA-304, an enzyme essential for degrading basidiomycete cell walls. *Biosci. Biotechnol. Biochem.* 77, 639–647. doi: 10.1271/bbb.120900

Terayama, H. (1951). Method of colloid titration (a new titration between polymer ions). *J. Polym. Sci.* 8, 243–253.

Yoshimi, A., Miyazawa, K., and Abe, K. (2016). Cell wall structure and biogenesis in *Aspergillus* species. *Biosci. Biotechnol. Biochem.* 80, 1700–1711. doi: 10.1080/09168451.2016.1177446

Yoshimi, A., Miyazawa, K., and Abe, K. (2017). Function and biosynthesis of cell wall α-1,3-glucan in fungi. *J. Fungi* 3:E63. doi: 10.3390/jof3040063

Yoshimi, A., Sano, M., Inaba, A., Kokubun, Y., Fujioka, T., Mizutani, O., et al. (2013). Functional analysis of the α-1,3-glucan synthase genes *agsA* and *agsB* in *Aspergillus nidulans*: AgsB is the major α-1,3-glucan synthase in this fungus. *PLoS One* 8:e54893. doi: 10.1371/journal.pone.0054893

Zhang, S., Sato, H., Ichinose, S., Tanaka, M., Miyazawa, K., Yoshimi, A., et al. (2017). Cell wall α-1,3-glucan prevents α-amylase adsorption onto fungal cell in submerged culture of *Aspergillus oryzae*. *J. Biosci. Bioeng.* 124, 47–53. doi: 10.1016/j.jbiosc.2017.02.013

Conflict of Interest Statement: The authors declare that the research was conducted in the absence of any commercial or financial relationships that could be construed as a potential conflict of interest.

frontiers in Microbiology

ORIGINAL RESEARCH
published: 19 September 2019
doi: 10.3389/fmicb.2019.02168

Global Analysis of Cell Wall Genes Revealed Putative Virulence Factors in the Dermatophyte *Trichophyton rubrum*

*Maíra P. Martins†, Larissa G. Silva†, Antonio Rossi, Pablo R. Sanches, Larissa D. R. Souza and Nilce M. Martinez-Rossi**

Department of Genetics, Ribeirão Preto Medical School, University of São Paulo, Ribeirão Preto, Brazil

OPEN ACCESS

Edited by:
Joshua D. Nosanchuk, Albert Einstein College of Medicine, United States

Reviewed by:
Ludmila Baltazar, Federal University of Minas Gerais, Brazil
Caroline Barcelos Costa-Orlandi, São Paulo State University, Brazil

***Correspondence:**
Nilce M. Martinez-Rossi
nmmrossi@usp.br

† These authors have contributed equally to this work

Specialty section:
This article was submitted to Fungi and Their Interactions, a section of the journal Frontiers in Microbiology

Received: *22 July 2019*
Accepted: *04 September 2019*
Published: *19 September 2019*

Citation:
Martins MP, Silva LG, Rossi A, Sanches PR, Souza LDR and Martinez-Rossi NM (2019) Global Analysis of Cell Wall Genes Revealed Putative Virulence Factors in the Dermatophyte Trichophyton rubrum. Front. Microbiol. 10:2168. doi: 10.3389/fmicb.2019.02168

The fungal cell wall is a structure in constant contact with the external environment. It confers shape to the cell and protects it from external threats. During host adaptation, the cell wall structure of fungal pathogens is continuously reshaped by the orchestrated action of numerous genes. These genes respond to environmental stresses and challenging growth conditions, influencing the infective potential of the fungus. Here, we aimed to identify cell wall biosynthesis-related genes that putatively encode virulence factors in *Trichophyton rubrum*. We used RNA-seq to examine the impact of two drugs, namely undecanoic acid, and acriflavine as well as the effects of the carbon source switching from glucose to keratin on *T. rubrum* cell wall metabolism. By using functional annotation based on Gene Ontology terms, we identified significantly differentially expressed cell wall-related genes in all stress conditions. We also exposed *T. rubrum* to osmotic and other cell wall stressors and evaluated the susceptibility and gene modulation in response to stress. The changes in the ambient environment caused continuous cell wall remodeling, forcing the fungus to undergo modulatory restructuring. The influence of the external challenges indicated a highly complex response pattern. The genes that were modulated simultaneously in the three stress conditions highlight potential targets for antifungal development.

Keywords: ambient stress, dermatophyte, drug targets, host-pathogen interactions, RNA-seq

INTRODUCTION

The fungal cell wall directly interacts with the external environment and is vital to the survival of the organism. Its structural integrity is actively modulated in response to external and internal stresses. The cell wall supports fungal growth and development and enables the organism to endure hostile ambient conditions (Perlin, 2015; Valiante et al., 2015).

Pathogenic fungi use their cell walls to sense the host milieu and detect nutrients there. By modulating their cell wall components, fungal pathogens escape host immunity and invade the organism (Muszewska et al., 2017; Beauvais and Latge, 2018). Dermatophytes are fungal pathogens

that infect keratinized tissues and dead epidermis in humans and animals. They produce several cell wall components that prevent them from being recognized by the host and function as virulence factors. Genome sequencing revealed that LysM binding domains are abundant in dermatophytes and probably mask pathogen cell wall components to confound the host immune response (Martinez et al., 2012; Kar et al., 2019). Also, the enrichment of several chitinase-encoding gene domains produces proteins supporting pathogen growth on a wide variety of substrates including soil and human skin. Thus, they enhance fungal infectiveness (Martinez et al., 2012). Differential protease secretion intensifies the inflammatory response induced by dermatophyte infection (Vermout et al., 2008). Moreover, through the production of extracellular vesicles the host innate immunity can be modulated (Bitencourt et al., 2018).

The constituents of the cell wall of the dermatophyte *Trichophyton rubrum* determine pathogen virulence. Mannans are associated with lymphocyte inhibition (Blake et al., 1991), a subtilisin homolog induces both immediate and delayed host immune responses (Woodfolk et al., 2000), and LysM proteins hide chitin and glucans from the host immune system (Kar et al., 2019). However, little is known about the relationships among dermatophyte pathogenesis, cell wall biosynthesis, and cell wall morphology.

Fungal virulence is determined by the coordinated expression of various genes mediating host-fungus interactions. Identification of the specific gene products or pathways crucial for fungal survival and infectiveness may potentially direct the development of new antifungal therapeutics (Bok et al., 2005; Martinez-Rossi et al., 2017). Changes in the ambient environment and external stressors continuously remodel the cell wall. Therefore, elucidation of the cell wall-related genes modulated in response to external challenges may disclose potential targets for antifungal drug development.

The cell wall is highly pertinent to antifungal drug discovery as it has a unique polysaccharide composition. For example, echinocandins inhibit β-(1,3)-*D*-glucan synthase biosynthesis in fungal cell walls. Thus, it is important to broaden our knowledge of fungal cell wall structure and the pathways regulating its formation (Grover, 2010; Perlin, 2015; Beauvais and Latge, 2018). Cell wall modulation in response to stressors may reveal putative targets for antifungal drug development (Martinez-Rossi et al., 2018).

The present study aimed to establish the modulation profile of cell wall genes in response to ambient challenges in the dermatophyte *T. rubrum*. We evaluated RNA-seq results under stress conditions wherein the pathogen was exposed to two drugs, or forced to switch its carbon source from glucose to keratin. Keratin mimics the host environment, and the drugs chosen, acriflavine and undecanoic acid, present a non-specific antifungal activity against *T. rubrum*. We identified a wide range of genes putatively encoding the virulence factors of *T. rubrum*. Those genes whose expression levels were altered under all stress conditions were considered as possible targets for antifungal drug development. We also challenged *T. rubrum* with various osmotic and cell wall stressor agents and evaluated their effects on the modulation of different genes controlling cell wall morphology.

MATERIALS AND METHODS

T. rubrum Strain and Culture Conditions for RNA-seq

T. rubrum strain CBS118892 (*Centraalbureau voor Schimmelcultures*, Netherlands) was maintained on malt extract agar (MEA; 2% (w/v) glucose, 2% (w/v) malt extract, 0.1% (w/v) peptone, pH 5.7) for 17 d at 28°C. Approximately 10^6 conidia mL^{-1}, obtained as previously described (Fachin et al., 1996; Jacob et al., 2012), were inoculated into 100 mL Sabouraud dextrose broth (SDB; 2% (w/v) glucose, 1% (w/v) peptone) and incubated at 28°C for 96 h under agitation; one flask was used for each time point of each tested condition (keratin or glucose). The mycelia in each flask were aseptically filtered and transferred into a new flask containing 100 mL minimal medium (MM) at pH 5.0 (Cove, 1966) supplemented with 70 mM nitrate (Sigma Aldrich Corp., St. Louis, MO, United States) and either 50 mM glucose (Sigma Aldrich Corp., St. Louis, MO, United States) (control) or 0.5% (w/v) bovine keratin (treatment) as the carbon source. All experiments were performed in three biological replicates. The cultures were incubated under agitation at 28°C for 24 h, 48 h, or 96 h. Mycelia were collected and the RNA was extracted from them. Drug-related library data are available in the GEO database under accession nos. GSE102872 and GSE40425; these results were obtained through the exposure of 96 h-grown SDB mycelia to 1.75 μg mL^{-1} acriflavine (ACF; Sigma Aldrich Corp., St. Louis, MO, United States) (Persinoti et al., 2014) or 17.5 μg mL^{-1} undecanoic acid (UDA; Sigma Aldrich Corp., St. Louis, MO, United States) (Mendes et al., 2018) in RPMI 1640 medium (Thermo Fisher Scientific, Waltham, MA, United States). *T. rubrum* susceptibility, as previously described, was determined by assessing MIC using the microdilution approach (M38-A) proposed by the Clinical and Laboratory Standards Institute (CLSI) (Persinoti et al., 2014; Mendes et al., 2018).

Stress Conditions

Susceptibility of *T. rubrum* to stressors was evaluated using plates containing SDB medium (1.5% (w/v) agar) supplemented with KCl (0.5 M), NaCl (0.5 M), SDS (0.01% (w/v)), sorbitol (1.2 M), Congo Red (CR; 200 μg mL^{-1}), or Calcofluor White (CFW; 200 μg mL^{-1}). Radial growth was measured using the diameter of propagated mycelia in centimeters on the 6th day of development. Data correspond to the means of three measurements. For qRT-PCR, mycelia grown for 96 h in flasks containing SDB were filtered, transferred, and incubated for 1 or 3 h in SDB containing the afore mentioned stressor agents. After incubation, mycelia from each experiment were frozen in liquid nitrogen, stored at −80°C, and used for RNA extraction.

RNA Isolation, Sequencing, and Data Analysis

Total RNA was isolated from ∼100 mg mycelia using an Illustra RNAspin mini isolation kit (GE Healthcare, Chicago, IL, United States). The RNA concentrations were determined

using a NanoDrop ND-1000 spectrophotometer (Thermo Fisher Scientific, Waltham, MA, United States). RNA quality was validated with an Agilent 2100 bioanalyzer (Agilent Technologies, Santa Clara, CA, United States). Equal amounts of RNA from three independent biological replicates of *T. rubrum* keratin/glucose cultures at 24, 48, or 96 h were used for the synthesis of cDNA with the TruSeq RNA library Kit (Illumina, San Diego, CA, United States), and sequenced with a Hiseq 2000 sequencer (Illumina, San Diego, CA, United States) according to the manufacturer's instructions. Paired-end reads 150 bp in size were generated. Raw read data obtained via RNA-seq were filtered for quality control by FastQC tool and trimmed with Trimmomatic (Bolger et al., 2014) to remove adapters and Illumina-specific sequences. Trimmed paired-end reads from each sample were aligned to the *T. rubrum* reference genome[1] with STAR aligner (Dobin et al., 2013). Gene-level read counts were quantified with STAR's '-quantModeGeneCounts' parameter. Differential expression was analyzed with the DESeq2 Bioconductor package (Love et al., 2014). A Benjamini-Hochberg correction (Benjamini and Hochberg, 1995) adjusted the *P* threshold and was applied to reveal statistically significant changes in gene expression levels. It was set to 0.05, with a $\log_2$ fold change $\pm$ 1.5 and postulated as a significantly modulated transcript abundance level. Genes surpassing these thresholds are hereinafter referred to as differentially expressed genes (DEG). They were functionally categorized with the Gene Ontology (GO) terms assigned by the Blast2GO algorithm (Robinson et al., 2011; Thorvaldsdottir et al., 2012). Highly represented categories were determined by enrichment analysis with the BayGO algorithm (Vencio et al., 2006). After functional annotation analysis, the cell wall-related genes in *T. rubrum* RNA-seq were identified with the R script mapping modulated Genes and Gene Ontology terms. A customized R script detected the descendant terms of the GO cellular component 'cell wall' with the Bioconductor GO.db package (Carlson, 2018). The genes are listed in **Supplementary Table S1**. Nine of these genes were arbitrarily selected to validate the results obtained through RNA-seq.

cDNA Synthesis, and qRT-PCR Analysis

Total RNA was treated with DNase I (Sigma Aldrich Corp., St. Louis, MO, United States) to remove residual genomic DNA. The complementary DNA (cDNA) was generated with a high-capacity cDNA reverse transcription kit (Applied Biosystems, Foster City, CA, United States). The qRT-PCR was performed with a StepOnePlus Real-Time PCR system (Applied Biosystems, Foster City, CA, United States). Gene expression was analyzed to confirm keratin RNA-seq and evaluate transcriptional responses to osmotic- and cell wall stressors. Reactions were run in a total volume of 12.5 μL with Power SYBR Green PCR Master Mix (Applied Biosystems, Foster City, CA, United States) and 50 ng template cDNA. Primer sequences, concentrations, and reaction efficiencies are listed in **Supplementary Table S2**. Glyceraldehyde-3-phosphate dehydrogenase (*gapdh*) and DNA-dependent RNA polymerase II (*rpb 2*) were used as internal controls (Jacob et al., 2012). Data were derived from three independent replicates. The $2^{-\Delta\Delta ct}$ relative expression quantification method was used to calculate gene responsiveness (Livak and Schmittgen, 2001). Data were statistically analyzed with Student's *t*-test (RNA-seq validation) or one-way ANOVA followed by Tukey's *post hoc* test. The statistical software was GraphPad Prism v. 5.1 (GraphPad Software, La Jolla, CA, United States).

[1] ftp://ftp.broadinstitute.org/pub/annotation/fungi

RESULTS

Global DEG Identification in Response to Keratin

For comprehensive analysis of the *T. rubrum* genes expressed in response to keratin, we performed high-throughput sequencing (RNA-seq) using glucose as the control. Approximately 192 million high-quality reads generated ∼167 million mapped paired-end sequences (**Supplementary Table S3**). The dataset comprised 2,797 genes that were modulated in response to keratin relative to glucose. The upregulated and downregulated transcripts were defined using a 1.5-fold change cutoff ($\geq$ 2.8-fold difference and a stringent statistical significance threshold of $P < 0.05$). We used the Blast2Go tool (Gotz et al., 2008) to depict the functional distribution of the modulated genes. This information elucidated the functionality of the DEGs in response to changing growth conditions.

Identification of the Genes Associated With Cell Wall Synthesis in the RNA-seq Libraries

We used functional annotation based on GO terms to identify cell wall-related genes among the DEGs for the keratin, acriflavine, and undecanoic acid RNA-seq (**Figure 1** and **Supplementary Table S1**). The R script found cell wall-related genes by detecting direct child terms of the cellular component 'cell wall' in GO.

We identified genes common to all three libraries and those that were common to two of them. We also determined those unique to each library. We obtained 20 downregulated and 47 upregulated genes in response to keratin culture. Acriflavine treatment induced five genes and repressed 12 others. There were 19 downregulated and nine upregulated genes in response after undecanoic acid exposure. Five of the genes modulated in response to acriflavine were common to all three libraries. Four were altered after acriflavine undecanoic acid treatment. Two others changed after exposure to acriflavine keratin (**Supplementary Table S1**).

Genes Modulated in Response to Acriflavine

Acriflavine treatment repressed acetyltransferases of the GNAT (Gcn5-related *N*-acetyltransferase) family (TERG_02517, TERG_05545, and TERG_07408) and induced genes essential for cell wall resistance such as catalases (TERG_01252, TERG_06053) and the hydrophobin (TERG_04234)

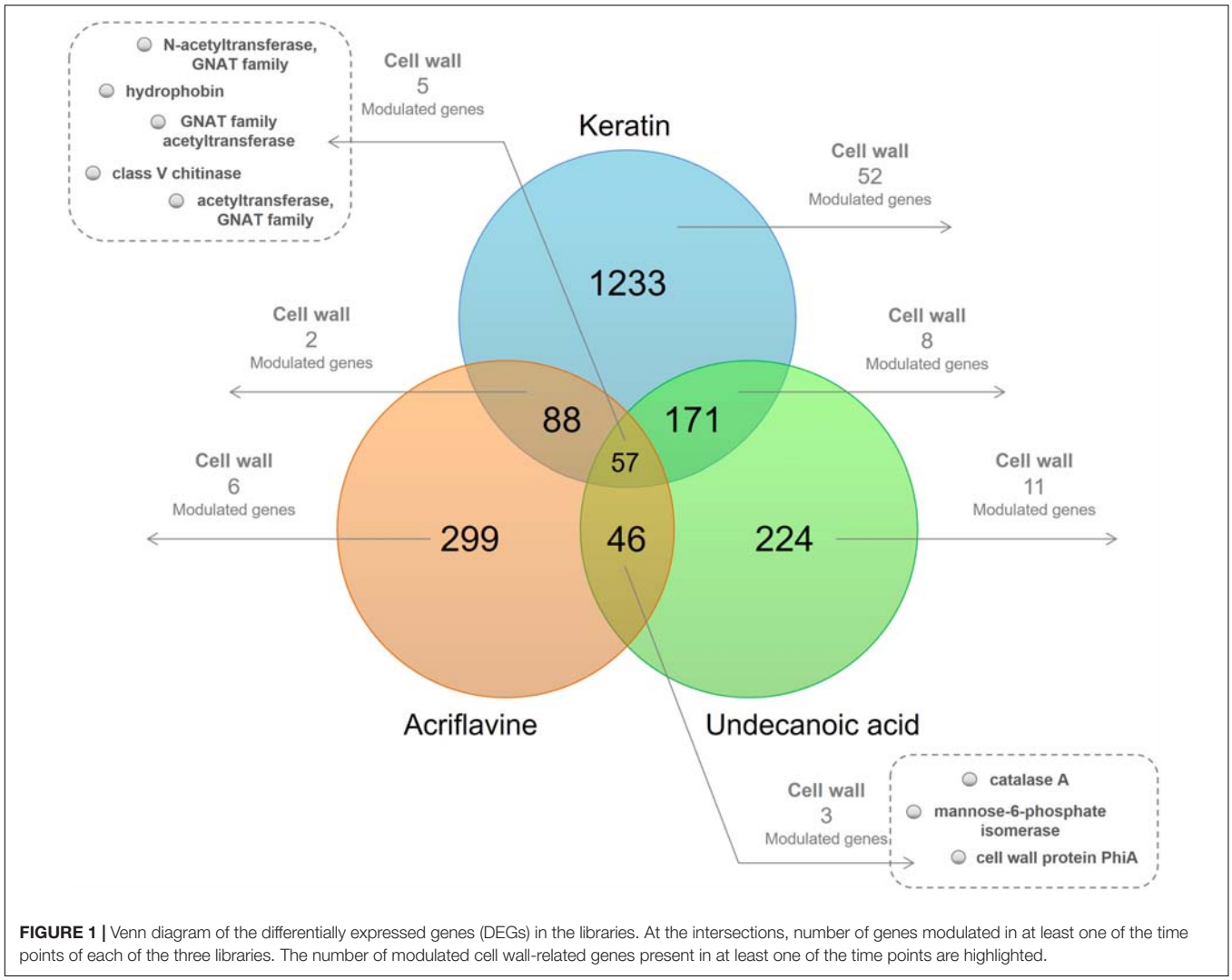

FIGURE 1 | Venn diagram of the differentially expressed genes (DEGs) in the libraries. At the intersections, number of genes modulated in at least one of the time points of each of the three libraries. The number of modulated cell wall-related genes present in at least one of the time points are highlighted.

(**Supplementary Table S1** and results extracted from Persinoti et al., 2014).

Genes Modulated in Response to Undecanoic Acid

Undecanoic acid treatment upregulated genes encoding glycosyl hydrolases (TERG_12281, TERG_12282, TERG_06016), a cytosolic Cu/Zn superoxide dismutase (TERG_08969), and catalase A (TERG_01252). The latter two were also induced by acriflavine exposure.

Undecanoic acid also downregulated the cell wall glucanase *scw11* (TERG_05576), genes encoding chitinases (TERG_05626, TERG_05625, and TERG_02350), and other cell wall-associated genes (TERG_03624, TERG_06144, and TERG_07456). Both undecanoic acid and acriflavine downregulated genes encoding three GNAT family *N*-acetyltransferases (TERG_02517, TERG_05545, and TERG_07408). Whereas undecanoic acid downregulated the gene encoding hydrophobin (TERG_04234), acriflavine upregulated it (**Supplementary Table S1** and results extracted from Mendes et al., 2018).

Genes Modulated in Response to Keratin

The shift from culture media containing glucose to those with keratin induced significantly more genes than it repressed. Media with keratin downregulated certain genes encoding GNAT family acetyltransferases (TERG_05545, TERG_07987, TERG_08211, and TERG_07408), and the Wiskott-Aldrich syndrome protein family member 2 (TERG_00693).

Genes encoding glycosyl hydrolases (TERG_05530, TERG_01837, TERG_02742, and others), glucanases (TERG_04887 and TERG_07817), chitinases (TERG_05626 and TERG_06925), and an alpha-1,2-mannosyltransferase (TERG_06397) were upregulated in response to keratin. Hydrophobin (TERG_04234) overexpression was observed as it was for the acriflavine treatment.

Osmotic and Cell Wall Stressors Influence *T. rubrum* Development

We evaluated the relative sensitivities of *T. rubrum* grown on SDB medium with or without KCl, NaCl, SDS, sorbitol, CR, and CFW. **Figure 2** shows radial colony growth inhibition

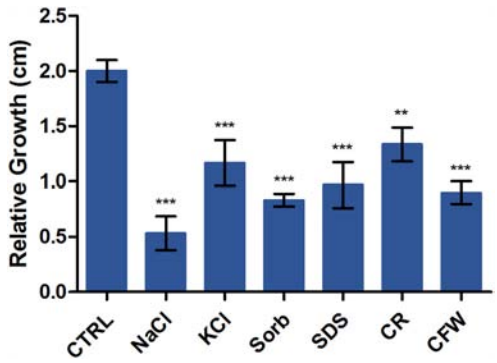

FIGURE 2 | Susceptibility of *T. rubrum* to various stressors. Strains were inoculated on Sabouraud dextrose broth with or without the stressors NaCl, KCl, sorbitol (Sorb), SDS, Congo Red (CR), and Calcofluor White (CFW) at 28°C for 6 d. The graph represents the relative colony diameters (in centimeters) of each strain in the presence of the stressors relative to the control (CTRL), without the stressors. Data are means of three biological replicates. The error bar indicates the standard deviation (SD). Asterisks indicate statistical significance determined by ANOVA followed by Tukey's *ad hoc* test (**$P < 0.01$; ***$P < 0.001$).

induced by each stressor. A qRT-PCR analysis evaluated the effects of these stressors on the transcription profiles of STE/STE20/YSK protein kinase *kic1* (TERG_01721), cell morphogenesis protein *sog2* (TERG_07599), conidiophore development protein *hym1* (TERG_00759), AGC/NDR/NDR protein kinase *cbk1* (TERG_03379), kinase activator protein *mob2* (TERG_02863), cell morphogenesis protein *tao3* (TERG_01788), 1,3-β-glucan synthase component *fks* (TERG_01127), chitin synthase 2 *chs* (TERG_12319), class III chitinase *cts* (TERG_02705), and cell wall glucanase *scw11* (TERG_05576).

RNA-Seq Validation by qRT-PCR

The DEGs selected and assayed through qRT-PCR validated the RNA-seq results. The expression patterns were observed in the samples, examined in triplicate, and confirmed the reliability of the RNA-seq results (Pearson's correlation, $r > 0.82$; $P < 0.001$) (**Figure 3**).

DISCUSSION

The Cell Wall Is a Virulence Factor Modulated in Response to Environmental Conditions

The fungal cell wall is the most promising virulence factor target for drug discovery because of its location, mediation of fungal-host interactions, uniqueness of composition, and absolute necessity for the survival of the pathogen. The roles of the cell wall in adhesion, colonization, signaling, and immune recognition make it vital for pathogen infection (Arana et al., 2009; Hasim and Coleman, 2019). As cell wall of fungi enables them to interact dynamically with the ambient environment, evaluation of the genes responsive to environmental stresses may lead to a better comprehension of the role of the cell wall in *T. rubrum*.

Only a Few Cell Wall-Related Genes Were Modulated in Response to Acriflavine

T. rubrum was subjected to sublethal doses of acriflavine which has antiseptic and anticancer properties but whose use is limited by its toxicity (Persinoti et al., 2014). RNA sequencing analysis revealed modulation of only a few cell wall-related genes. Thus, acriflavine had minimal influence on *T. rubrum* cell growth, shape, or protection.

Two catalase genes were upregulated in response to acriflavine. Acriflavine resistance was observed in *Dictyostelium*, as a result of catalase A gene (*catA*) disruption. This gene has peroxidase activity that modifies acriflavine into its cytotoxic form (Garcia et al., 2002). Catalases protect cells against peroxide-induced damage. They are also essential for pathogen virulence and cell wall integrity during host invasion (Skamnioti et al., 2007). The observed upregulation of two catalases in *T. rubrum* suggests that the pathogen metabolized the drug and induced catalase during cell wall formation and/or maintenance in the attempt to increases its virulence.

Hydrophobin is a small cysteine-rich protein secreted only by filamentous fungi. It regulates cell wall integrity (Wosten, 2001; Mankel et al., 2002) and is upregulated in response to acriflavine exposure. Acriflavine increases hydrophobicity, decreases hydrophilicity, induces impermeability, and alters cell wall thickness (Glynn and Priest, 1970; Kawai et al., 2009). Hydrophobins are amphiphilic and lower the surface tension of water (Linder et al., 2005). The hydrophobin induction detected in *T. rubrum* in response to acriflavine exposure suggests that the fungus was attempting to counterbalance the increase in cell wall hydrophobicity caused by the drug.

Only a few genes are repressed in response to acriflavine including three members of the GNAT family of acetyltransferases. They are involved in post-translational modification by transferring acetyl groups from acetyl-CoA to their cognate substrates (Favrot et al., 2016). GNATs regulate transcriptional responses to various environmental stressors such as heat, cold, oxidative stress, and low nutrient availability (Huisinga and Pugh, 2004; O'Meara et al., 2010). The GNAT repression observed in our results suggests increasing stress-mediated activation and drug susceptibility in *T. rubrum*.

Undecanoic Acid Mainly Represses *T. rubrum* Cell Wall-Associated Genes

Undecanoic acid exposure, especially for 3 h, downregulated several genes associated with cell wall morphogenesis, including *scw11*, which encodes the cell wall-based endo-1,3-β-glucanase (Millet et al., 2018), the SUN domain protein Uth1-like, encoding a β-(1,3)-glucan-hydrolyzing enzyme (Gastebois et al., 2013), a cell wall serine-threonine-rich galactomannoprotein Mp1 (Gautam et al., 2011), and a cell wall structural protein PhiA. Repression of genes related to cell wall maintenance was reported for *Aspergillus fumigatus* exposed to the antimalarial

A

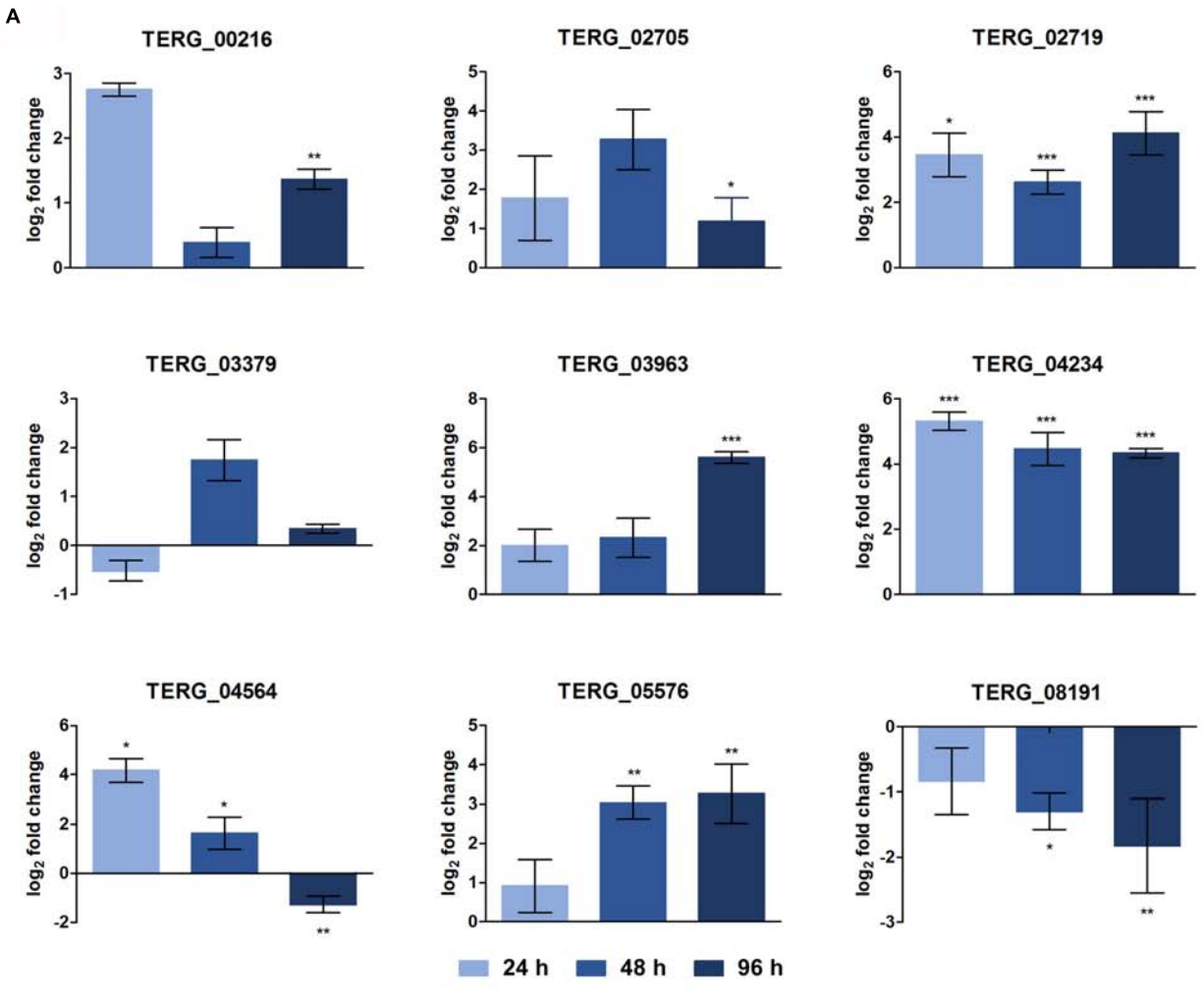

B

ID	Gene Product Name	24 hours		48 hours		96 hours	
		RNA-seq	qPCR	RNA-seq	qPCR	RNA-seq	qPCR
TERG_00216	Endochitinase (*T. equinum*)	1.90	2.66	-	0.39	-	1.33
TERG_02705	Class III chitinase (*T. tonsurans*)	2.77	1.61	3.69	3.12	2.74	1.57
TERG_02719	Glycosyl hydrolase (*T. equinum*)	3.41	3.19	3.27	2.60	4.52	4.12
TERG_03379	AGC/NDR/NDR protein kinase	-	-0.55	1.53	1.13	-	0.16
TERG_03963	Mannosyl phosphorylinositol ceramide synthase SUR1 (*T. equinum*)	1.53	1.52	2.14	1.86	2.24	5.32
TERG_04234	Hydrophobin, putative *(T. verrucosum)*	4.10	5.67	3.49	4.47	3.30	4.27
TERG_04564	Mixed-linked glucanase (*T. equinum*)	1.91	3.85	1.78	1.60	-	-1.13
TERG_05576	Cell wall glucanase (Scw11), putative (*A. benhamiae*)	-	0.91	1.76	2.84	2.60	3.34
TERG_08191	Glucooligosaccharide oxidase *(T. equinum)*	-	-0.41	-1.58	-1.14	-1.67	-1.82

FIGURE 3 | Validation of DEGs under keratin cultivation by qRT-PCR. **(A)** Gene expression levels are represented as $\log_2$-fold changes relative to each control condition (24 h keratin × 24 h glucose; 48 h keratin × 48 h glucose; 96 h keratin × 96 h glucose). Asterisks indicate statistical significance determined by Student's *t*-tests comparing treatment and control conditions at each time point (*$P < 0.05$; **$P < 0.01$; ***$P < 0.001$). **(B)** Comparison of gene expression levels determined by RNA-seq with those evaluated by qRT-PCR (Pearson's correlation, $r > 0.82$; $P < 0.001$).

drug artemisinin, which is known to have antifungal activity (Gautam et al., 2011). This same effect was also reported in *T. rubrum* subjected to ketoconazole and amphotericin B (Yu et al., 2007). It was shown that the antifungal agent undecanoic acid effectively impairs *T. rubrum* cell wall formation (Mendes et al., 2018).

Undecanoic acid represses GNAT family *N*-acetyltransferase genes, similarly to what was observed for acriflavine. The gene encoding a hydrophobin, upregulated by acriflavine was downregulated in response to undecanoic acid exposure. Undecanoic acid damages the cell wall of *T. rubrum* by reducing its ergosterol content and altering its fatty acid metabolism (Mendes et al., 2018). Ergosterol controls water penetration and regulates enzymes involved in protein transport and chitin synthesis. Excessive intracellular water uptake may occur when ergosterol metabolism is deregulated. The hydrophobin gene appears to be involved in the water flux across the fungal cell wall (Abe et al., 2009; Zuza-Alves et al., 2017) and is associated with fungal pathogenesis, mediating the attachment of fungal infective structures to their targets (Wosten, 2001). Undecanoic acid exposure in *T. rubrum* may have negatively impacted its pathogenicity by downregulating hydrophobins.

The gene encoding a class V chitinase (glycoside hydrolase family 18 protein-GH18) and another encoding an endochitinase were repressed by undecanoic acid. As chitin is absent in mammalian cells and essential for fungal cell wall integrity, it is a promising target for antifungal drug development (Ruiz-Herrera and San-Blas, 2003). The observed repressive effect against chitinases emphasize the promising use of undecanoic acid in fungal treatment. Acriflavine also repressed the GH18; therefore, both drugs may disrupt important biochemical events involved in the establishment and maintenance of fungal infection in the host (Persinoti et al., 2014). In *T. rubrum*, this chitinase presents LysM domains and may be involved in keratin degradation (Lopes et al., 2019).

Three glycosyl hydrolase genes were upregulated in response to undecanoic acid. The TERG_06016, identified as a PHO system negative regulator, responsible for the hydrolysis of O-glycosyl compounds, and two cell wall acid trehalases, that shelter fungi against several physiological and environmental stressors (Arguelles, 2000). These inductions were detected 3 h after undecanoic acid treatment. Thus, *T. rubrum* immediately responded to this exposure and attempted to offset the damage caused by the stress in the cell walls. We also observed that the genes improving fungal stress tolerance were upregulated after 12 h incubation. These included the cytosolic Cu/Zn superoxide dismutase and catalase A. Moreover, cell wall formation was repressed.

The Cell Wall Is Actively Synthesized When *T. rubrum* Is Cultured With Keratin

We supplied *T. rubrum* with keratin to mimic the initial host infection stages. Mycelia harvested after 96 h incubation in glucose-rich media were shifted to keratin or glucose (test and control, respectively) and forced to adapt to a stress-inducing environment.

After 96 h culture in keratin, *T. rubrum* had upregulated more cell wall-related genes than it had downregulated. The highest number of DEGs was observed at 96 h. Thus, *T. rubrum* endeavored to grow, develop, establish, and maintain cell wall integrity in the keratin-containing medium.

Among the genes repressed in keratin only two were also repressed in both the acriflavine and undecanoic acid treatments. They belonged to the stress-responsive GNAT acetyltransferase family. A gene encoding Wiskott-Aldrich syndrome protein family member 2 was also downregulated. It encodes a β-1,6-glucan putatively belonging to the KRE family. β-1,6-glucan integrates into the fungal cell wall, acts as the central core of the protein-carbohydrate network, interconnecting chitin and β-1,3-glucan, and associating mannoproteins there (Shahinian and Bussey, 2000). As this gene was repressed only after 96 h of fungal adaptation to keratin, the pathogen avoided excessive remodeling by restraining cell wall formation.

We observed the up-modulation of the hydrophobin gene, also modulated in response to acriflavine and undecanoic acid, attesting its role in the stress response of *T. rubrum*. Thus, the hydrophobin plays a role in the stress response of *T. rubrum*. The upregulation of hydrophobins in *T. rubrum* at all measurement time points of keratin incubation indicates that the pathogen tries to increase its cell wall hydrophobicity and, by extension, its virulence, during the early stages of host infection.

Genes encoding glycosyl hydrolase, glucanase, and chitinase were induced in response to keratin. These are the most commonly occurring hydrolases in the fungal cell wall. They are associated with cell wall polymer branching and cross-linking and the maintenance of cell wall plasticity during morphogenesis (Adams, 2004). They also influence fungal virulence as they participate in non-self cell wall degradation and enable the pathogen to penetrate and invade the host (Gruber and Seidl-Seiboth, 2012).

Keratin incubation also upregulated α-1,2-mannosyltransferase. In the human pathogenic mold *A. fumigatus*, deletion of an orthologous gene resulted in attenuated virulence. This gene is a potential target for novel antifungal therapies as it is unique in fungi (Wagener et al., 2008). The observed induction of α-1,2-mannosyltransferase in *T. rubrum* grown with keratin indicates that the fungus was trying to maintain its virulence and sustain its development under these conditions.

Genes Involved in Hyphal Extension and Cell Growth Are Induced in *T. rubrum* Challenged With Cell Wall Stressors

Various stressors (CFW, CR, SDS, NaCl, KCl, and sorbitol) were added to the culture medium to determine their effects on radial colony growth (**Figure 2**). The fungal cell walls were sensitive to osmotic and cell wall stresses, and mycelial growth and development were inhibited. We then used qRT-PCR to evaluate the expression of genes involved in polarized growth, cell wall remodeling, and hyphal growth after exposure to the abovementioned cell wall stressors. The genes selected for evaluation are either regulated by the Ace2 transcription

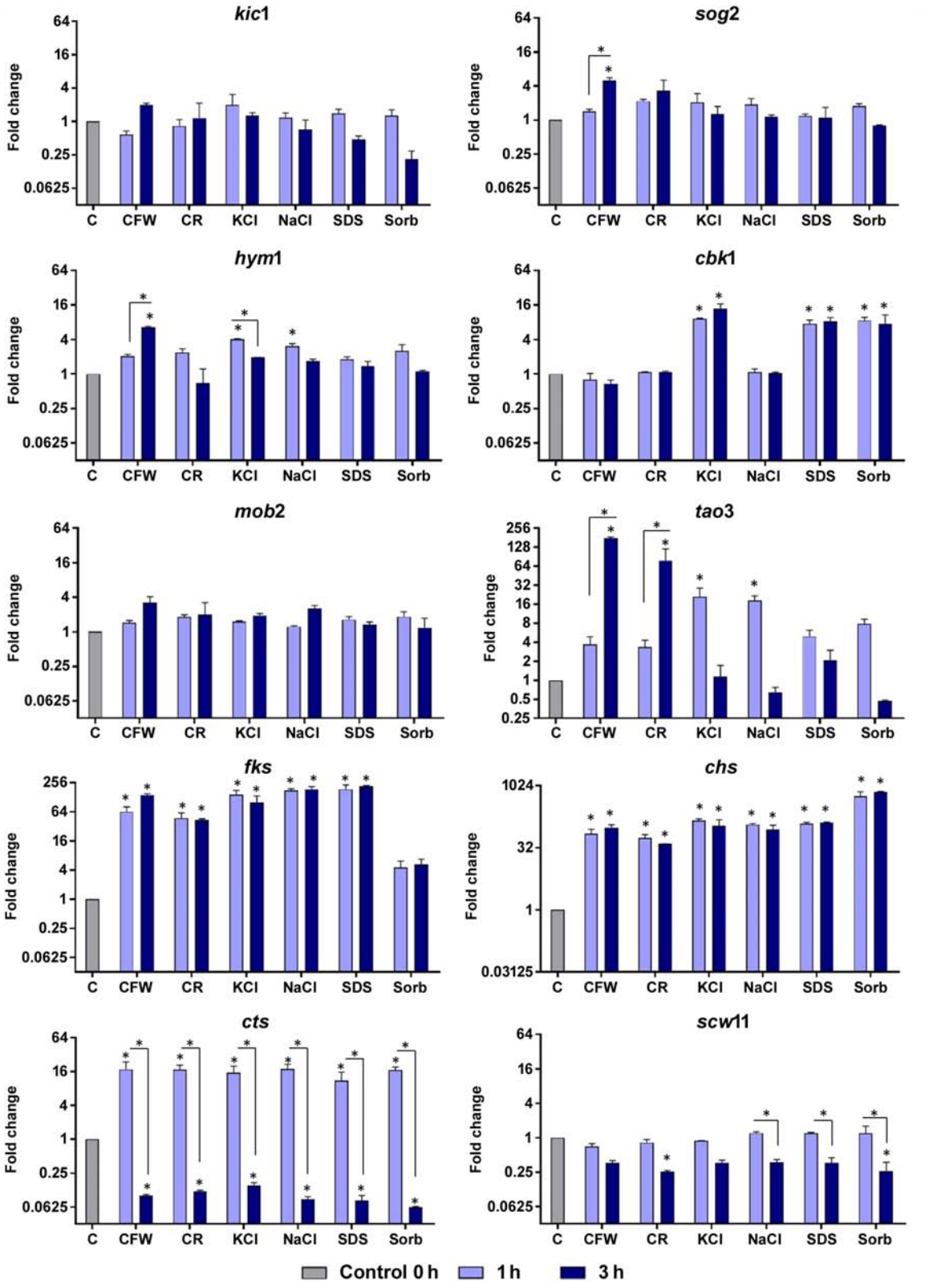

FIGURE 4 | Relative expression levels of genes encoding components of the RAM network or putatively regulated by Ace2 after exposure of *T. rubrum* to Calcofluor White (CFW), Congo Red (CR), KCl, NaCl, SDS, and sorbitol (Sorb), for 1 or 3 h. Control (C) is the growth of *T. rubrum* for 96 h before addition of the stressors. Data are means and SD of three independent experiments. Asterisks indicate statistical significance determined by ANOVA followed by Tukey's *ad hoc* test ($P < 0.05$).

factor or belong to the RAM (regulation of Ace2 activity and cellular morphogenesis) signaling pathway. The RAM network is a protein kinase-signaling pathway associated to the maintenance of the cell wall integrity. RAM regulates the zinc finger transcriptional factor Ace2 which governs *fks*, *chs*, *cts*, and *scw11* genes, encoding 1,3-β-glucan synthase, chitin synthase, chitinase, and β-glucanase, respectively. These play vital roles in cell wall morphogenesis (Sbia et al., 2008; Saputo et al., 2012).

Figure 4 shows that osmotic stressors did not affect the expression levels of the *mob2* and *kic1* genes. The leucine-rich repeat-containing *sog2* was induced only in response to CFW and *scw11* was repressed upon challenge with CR and sorbitol; both genes responded at the latest time of exposure. Saline stress induced an immediate response by the *hym1* gene and CFW exposure resulted in its induction after 3 h of. At both time points, *cbk1* responded to KCl, SDS, and sorbitol. The protein kinase *tao3* is strongly induced upon challenge with the cell wall stressors CFW and CR and is upmodulated in response to saline stress after 3h. The unique transcriptional pattern observed suggests that, although all these genes are directly related to cell wall integrity, as part of the RAM signaling network, their activation is time- and stress-responsive.

Fungal cell walls increase their chitin content in reaction to stress conditions (Walker et al., 2008; Fortwendel et al., 2009). This response is mediated by the upregulation of chitin synthases and/or the downregulation of chitinases (Heilmann et al., 2013). In the present study, we observed that *T. rubrum* induced *chs* and *fks1* and repressed *cts* following exposure to osmotic stressors (**Figure 4**). Cell wall restoration and selective modulatory activation of the RAM pathway genes are indicative of the efforts of *T. rubrum* to restore and maintain homeostasis in response to external stressors.

Cell Wall, Virulence, and Antifungal Drug Development

Increasing global transcriptome data favors more robust studies on fungal gene modulation that may elucidate fungal metabolism, pathogenesis, and drug resistance. The results obtained herein may also afford strategies for the identification of novel drug development targets.

Here, five genes were modulated in *T. rubrum* in response to the various stressors. Three belonged to the GNAT family, one was a class V chitinase, and the fifth was a hydrophobin. The observed stress-mediated response of the hydrophobin gene suggests its possible use as a therapeutic antifungal drug target. Antifungal targets must be essential proteins, have a high degree of sequential similarity across pathogenic fungal species, and be absent in the human genome (Liu et al., 2006). Hydrophobins present with low overall sequence conservation. Nevertheless, they have a broad range of functions including the regulation of cell wall integrity. They can also change the hydrophilic/hydrophobic properties of cell surfaces and are unique to filamentous fungi (Wosten, 2001; Linder et al., 2005; Bayry et al., 2012).

The GNAT superfamily is ubiquitous across many taxa, including humans and fungi. However, a few of its members are potential antifungal drug targets. Identification of the structural differences between human and fungal GNAT members may facilitate selective antifungal drug design (Masubuchi et al., 2003; Hurtado-Guerrero et al., 2008).

A class V chitinase was repressed in response to acriflavine and undecanoic acid exposure but induced in the presence of keratin. Thus, it plays a vital role in substrate adaptation. It was reported that in *T. rubrum* this gene participates in keratin degradation (Lopes et al., 2019). Fungal cell walls contain high levels of chitin and they are cleaved by chitinases during cell wall remodeling. Thus, disruption of this process is expected to affect fungal virulence and survival and points to chitinases as antifungal drug targets (Rush et al., 2010).

CONCLUSION

Environmental changes and external stresses induce continuous remodeling of fungal cell walls, and the transcriptional responses of *T. rubrum* to those observed in this study are essential for its resistance and pathogenicity. We have generated a robust dataset, which underscores the relevance of the cell wall in pathogen-host interactions, advancing our knowledge on the cell wall regulatory mechanisms of dermatophyte fungi. Our results indicate that stress conditions forced *T. rubrum* to restructure its cell wall by modifying the cell wall composition; thus, affecting fungal virulence. The modulation of genes controlling the fungal cell-wall structure has great potential in the identification of putative targets for the development of novel antifungal drug therapies.

DATA AVAILABILITY STATEMENT

The RNA-seq data is available at the GEO database under the accession number GSE134406.

AUTHOR CONTRIBUTIONS

MM and LGS drafted the manuscript. MM, LGS, and LDS performed the experiments. PS performed the computational analyses. AR and NM-R supervised the study and prepared the manuscript. NM-R designed the project. All authors participated in the data analysis and critical revision of the manuscript, and approved the final version.

FUNDING

This study was supported by grants from the following Brazilian funding agencies: Research Support Foundation of São Paulo State - FAPESP (Grant No. 2014/03847-7, Postdoctoral Fellowship No. 2018/11319-1 to MM, and Doctoral Fellowship No. 2010/15017-8 to LGS), National Council for Scientific and Technological Development - CNPq (Grant Nos. 305252/2013-5 and 304222/2013-5), Coordination for the Improvement of Higher Education Personnel - CAPES (Finance Code 001), and Foundation for Support to Teaching, Research and Assistance - FAEPA of the HCFMRP-USP.

ACKNOWLEDGMENTS

The authors thank V. M. Oliveira and M. Mazucato for technical assistance and M. D. Martins for laboratory services.

SUPPLEMENTARY MATERIAL

The Supplementary Material for this article can be found online at: https://www.frontiersin.org/articles/10.3389/fmicb.2019.02168/full#supplementary-material

REFERENCES

Abe, F., Usui, K., and Hiraki, T. (2009). Fluconazole modulates membrane rigidity, heterogeneity, and water penetration into the plasma membrane in *Saccharomyces cerevisiae*. *Biochemistry* 48, 8494–8504. doi: 10.1021/bi900578y

Adams, D. J. (2004). Fungal cell wall chitinases and glucanases. *Microbiology* 150, 2029–2035. doi: 10.1099/mic.0.26980-0

Arana, D. M., Prieto, D., Roman, E., Nombela, C., Alonso-Monge, R., and Pla, J. (2009). The role of the cell wall in fungal pathogenesis. *Microb. Biotechnol.* 2, 308–320. doi: 10.1111/j.1751-7915.2008.00070.x

Arguelles, J. C. (2000). Physiological roles of trehalose in bacteria and yeasts: a comparative analysis. *Arch. Microbiol.* 174, 217–224. doi: 10.1007/s002030000192

Bayry, J., Aimanianda, V., Guijarro, J. I., Sunde, M., and Latge, J. P. (2012). Hydrophobins-unique fungal proteins. *PLoS Pathog.* 8:e1002700. doi: 10.1371/journal.ppat.1002700

Beauvais, A., and Latge, J. P. (2018). Special issue: fungal cell wall. *J. Fungi* 4:91. doi: 10.3390/jof4030091

Benjamini, Y., and Hochberg, Y. (1995). Controlling the false discovery rate: a practical and powerful approach to multiple testing. *J. R. Stat. Soc. Ser. B* 57, 289–300. doi: 10.1111/j.2517-6161.1995.tb02031.x

Bitencourt, T. A., Rezende, C. P., Quaresemin, N. R., Moreno, P., Hatanaka, O., Rossi, A., et al. (2018). Extracellular vesicles from the dermatophyte *Trichophyton interdigitale* modulate macrophage and keratinocyte functions. *Front. Immunol.* 9:2343. doi: 10.3389/fimmu.2018.02343

Blake, J. S., Dahl, M. V., Herron, M. J., and Nelson, R. D. (1991). An immunoinhibitory cell wall glycoprotein (mannan) from *Trichophyton rubrum*. *J. Invest. Dermatol.* 96, 657–661.

Bok, J. W., Balajee, S. A., Marr, K. A., Andes, D., Nielsen, K. F., Frisvad, J. C., et al. (2005). LaeA, a regulator of morphogenetic fungal virulence factors. *Eukaryot. Cell* 4, 1574–1582. doi: 10.1128/ec.4.9.1574-1582.2005

Bolger, A. M., Lohse, M., and Usadel, B. (2014). Trimmomatic: a flexible trimmer for Illumina sequence data. *Bioinformatics* 30, 2114–2120. doi: 10.1093/bioinformatics/btu170

Carlson, M. (2018). *GO.db: A Set of Annotation Maps Describing the Entire Gene Ontology, in: R Package Version* 3.7.0.

Cove, D. J. (1966). The induction and repression of nitrate reductase in the fungus *Aspergillus nidulans*. *Biochim. Biophys. Acta* 113, 51–56. doi: 10.1016/s0926-6593(66)80120-0

Dobin, A., Davis, C. A., Schlesinger, F., Drenkow, J., Zaleski, C., Jha, S., et al. (2013). STAR: ultrafast universal RNA-seq aligner. *Bioinformatics* 29, 15–21. doi: 10.1093/bioinformatics/bts635

Fachin, A. L., Maffei, C. M., and Martinez-Rossi, N. M. (1996). *In vitro* susceptibility of *Trichophyton rubrum* isolates to griseofulvin and tioconazole. Induction and isolation of a resistant mutant to both antimycotic drugs. Mutant of *Trichophyton rubrum* resistant to griseofulvin and tioconazole. *Mycopathologia* 135, 141–143. doi: 10.1007/bf00632334

Favrot, L., Blanchard, J. S., and Vergnolle, O. (2016). Bacterial GCN5-Related N-Acetyltransferases: from resistance to regulation. *Biochemistry* 55, 989–1002. doi: 10.1021/acs.biochem.5b01269

Fortwendel, J. R., Juvvadi, P. R., Pinchai, N., Perfect, B. Z., Alspaugh, J. A., Perfect, J. R., et al. (2009). Differential effects of inhibiting chitin and 1,3-β D-glucan synthesis in ras and calcineurin mutants of *Aspergillus fumigatus*. *Antimicrob. Agents Chemother.* 53, 476–482. doi: 10.1128/aac.01154-08

Garcia, M. X., Roberts, C., Alexander, H., Stewart, A. M., Harwood, A., Alexander, S., et al. (2002). Methanol and acriflavine resistance in *Dictyostelium* are caused by loss of catalase. *Microbiology* 148, 333–340. doi: 10.1099/00221287-148-1-333

Gastebois, A., Aimanianda, V., Bachellier-Bassi, S., Nesseir, A., Firon, A., Beauvais, A., et al. (2013). SUN proteins belong to a novel family of beta-(1,3)-glucan-modifying enzymes involved in fungal morphogenesis. *J. Biol. Chem.* 288, 13387–13396. doi: 10.1074/jbc.M112.440172

Gautam, P., Upadhyay, S. K., Hassan, W., Madan, T., Sirdeshmukh, R., Sundaram, C. S., et al. (2011). Transcriptomic and proteomic profile of *Aspergillus fumigatus* on exposure to artemisinin. *Mycopathologia* 172, 331–346. doi: 10.1007/s11046-011-9445-3

Glynn, A. A., and Priest, C. M. (1970). The effect of acriflavine on complement sensitive and resistant strains of *Escherichia coli* and on complement resistant mutants. *Immunology* 18, 19–22.

Gotz, S., Garcia-Gomez, J. M., Terol, J., Williams, T. D., Nagaraj, S. H., Nueda, M. J., et al. (2008). High-throughput functional annotation and data mining with the Blast2GO suite. *Nucleic Acids Res.* 36, 3420–3435. doi: 10.1093/nar/gkn176

Grover, N. D. (2010). Echinocandins: a ray of hope in antifungal drug therapy. *Indian J. Pharmacol.* 42, 9–11.

Gruber, S., and Seidl-Seiboth, V. (2012). Self versus non-self: fungal cell wall degradation in Trichoderma. *Microbiology* 158, 26–34. doi: 10.1099/mic.0.052613-0

Hasim, S., and Coleman, J. J. (2019). Targeting the fungal cell wall: current therapies and implications for development of alternative antifungal agents. *Future Med. Chem.* 11, 869–883. doi: 10.4155/fmc-2018-0465

Heilmann, C. J., Sorgo, A. G., Mohammadi, S., Sosinska, G. J., De Koster, C. G., Brul, S., et al. (2013). Surface stress induces a conserved cell wall stress response in the pathogenic fungus *Candida albicans*. *Eukaryot. Cell* 12, 254–264. doi: 10.1128/EC.00278-12

Huisinga, K. L., and Pugh, B. F. (2004). A genome-wide housekeeping role for TFIID and a highly regulated stress-related role for SAGA in *Saccharomyces cerevisiae*. *Mol. Cell.* 13, 573–585. doi: 10.1016/s1097-2765(04)00087-5

Hurtado-Guerrero, R., Raimi, O. G., Min, J., Zeng, H., Vallius, L., Shepherd, S., et al. (2008). Structural and kinetic differences between human and *Aspergillus fumigatus* D-glucosamine-6-phosphate N-acetyltransferase. *Biochem. J.* 415, 217–223. doi: 10.1042/BJ20081000

Jacob, T. R., Peres, N. T., Persinoti, G. F., Silva, L. G., Mazucato, M., Rossi, A., et al. (2012). rpb2 is a reliable reference gene for quantitative gene expression analysis in the dermatophyte *Trichophyton rubrum*. *Med. Mycol.* 50, 368–377. doi: 10.3109/13693786.2011.616230

Kar, B., Patel, P., and Free, S. J. (2019). *Trichophyton rubrum* LysM proteins bind to fungal cell wall chitin and to the N-linked oligosaccharides present on human skin glycoproteins. *PLoS One* 14:e0215034. doi: 10.1371/journal.pone.0215034

Kawai, M., Yamada, S., Ishidoshiro, A., Oyamada, Y., Ito, H., and Yamagishi, J. (2009). Cell-wall thickness: possible mechanism of acriflavine resistance in meticillin-resistant *Staphylococcus aureus*. *J. Med. Microbiol.* 58, 331–336. doi: 10.1099/jmm.0.004184-0

Linder, M. B., Szilvay, G. R., Nakari-Setala, T., and Penttila, M. E. (2005). Hydrophobins: the protein-amphiphiles of filamentous fungi. *FEMS Microbiol. Rev.* 29, 877–896. doi: 10.1016/j.femsre.2005.01.004

Liu, M., Healy, M. D., Dougherty, B. A., Esposito, K. M., Maurice, T. C., Mazzucco, C. E., et al. (2006). Conserved fungal genes as potential targets for broad-spectrum antifungal drug discovery. *Eukaryot. Cell* 5, 638–649. doi: 10.1128/ec.5.4.638-649.2006

Livak, K. J., and Schmittgen, T. D. (2001). Analysis of relative gene expression data using real-time quantitative PCR and the 2-ΔΔCT Method. *Methods* 25, 402–408. doi: 10.1006/meth.2001.1262

Lopes, L., Bitencourt, T. A., Lang, E. A. S., Sanches, P. R., Peres, N. T. A., Rossi, A., et al. (2019). Genes coding for LysM domains in the dermatophyte *Trichophyton rubrum*: a transcription analysis. *Med. Mycol* doi: 10.1093/mmy/myz068 [Epub ahead of print].

Love, M. I., Huber, W., and Anders, S. (2014). Moderated estimation of fold change and dispersion for RNA-seq data with DESeq2. *Genome Biol.* 15:550.

Mankel, A., Krause, K., and Kothe, E. (2002). Identification of a hydrophobin gene that is developmentally regulated in the ectomycorrhizal fungus *Tricholoma terreum*. *Appl. Environ. Microbiol.* 68, 1408–1413. doi: 10.1128/aem.68.3.1408-1413.2002

Martinez, D. A., Oliver, B. G., Graser, Y., Goldberg, J. M., Li, W., Martinez-Rossi, N. M., et al. (2012). Comparative genome analysis of *Trichophyton rubrum* and related dermatophytes reveals candidate genes involved in infection. *mBio* 3, e259–12. doi: 10.1128/mBio.00259-12

Martinez-Rossi, N. M., Bitencourt, T. A., Peres, N. T. A., Lang, E. A. S., Gomes, E. V., Quaresemin, N. R., et al. (2018). Dermatophyte resistance to antifungal drugs: mechanisms and prospectus. *Front. Microbiol.* 9:1108. doi: 10.3389/fmicb.2018.01108

Martinez-Rossi, N. M., Peres, N. T., and Rossi, A. (2017). Pathogenesis of dermatophytosis: sensing the host tissue. *Mycopathologia* 182, 215–227. doi: 10.1007/s11046-016-0057-9

Masubuchi, M., Ebiike, H., Kawasaki, K., Sogabe, S., Morikami, K., Shiratori, Y., et al. (2003). Synthesis and biological activities of benzofuran antifungal agents targeting fungal N-myristoyltransferase. *Bioorg. Med. Chem.* 11, 4463–4478. doi: 10.1016/s0968-0896(03)00429-2

Mendes, N. S., Bitencourt, T. A., Sanches, P. R., Silva-Rocha, R., Martinez-Rossi, N. M., and Rossi, A. (2018). Transcriptome-wide survey of gene expression changes and alternative splicing in Trichophyton rubrum in response to undecanoic acid. *Sci. Rep.* 8:2520. doi: 10.1038/s41598-018-20738-x

Millet, N., Latge, J. P., and Mouyna, I. (2018). Members of glycosyl-hydrolase family 17 of *A. fumigatus* differentially affect morphogenesis. *J. Fungi* 4:E18. doi: 10.3390/jof4010018

Muszewska, A., Pilsyk, S., Perlinska-Lenart, U., and Kruszewska, J. S. (2017). Diversity of cell wall related proteins in human pathogenic fungi. *J. Fungi* 4:E6.

O'Meara, T. R., Hay, C., Price, M. S., Giles, S., and Alspaugh, J. A. (2010). Cryptococcus neoformans histone acetyltransferase Gcn5 regulates fungal adaptation to the host. *Eukaryot. Cell* 9, 1193–1202. doi: 10.1128/EC.00098-10

Perlin, D. S. (2015). Mechanisms of echinocandin antifungal drug resistance. *Ann. N. Y. Acad. Sci.* 1354, 1–11. doi: 10.1111/nyas.12831

Persinoti, G., De Aguiar Peres, N., Jacob, T., Rossi, A., Vencio, R., and Martinez-Rossi, N. (2014). RNA-sequencing analysis of *Trichophyton rubrum* transcriptome in response to sublethal doses of acriflavine. *BMC Genomics* 15:S1. doi: 10.1186/1471-2164-15-S7-S1

Robinson, J. T., Thorvaldsdottir, H., Winckler, W., Guttman, M., Lander, E. S., Getz, G., et al. (2011). Integrative genomics viewer. *Nat. Biotechnol.* 29, 24–26. doi: 10.1038/nbt.1754

Ruiz-Herrera, J., and San-Blas, G. (2003). Chitin synthesis as target for antifungal drugs. *Curr. Drug Targets. Infect. Disord.* 3, 77–91. doi: 10.2174/1568005033342064

Rush, C. L., Schuttelkopf, A. W., Hurtado-Guerrero, R., Blair, D. E., Ibrahim, A. F., Desvergnes, S., et al. (2010). Natural product-guided discovery of a fungal chitinase inhibitor. *Chem. Biol.* 17, 1275–1281. doi: 10.1016/j.chembiol.2010.07.018

Saputo, S., Chabrier-Rosello, Y., Luca, F. C., Kumar, A., and Krysan, D. J. (2012). The RAM network in pathogenic fungi. *Eukaryot. Cell* 11, 708–717. doi: 10.1128/EC.00044-12

Sbia, M., Parnell, E. J., Yu, Y., Olsen, A. E., Kretschmann, K. L., Voth, W. P., et al. (2008). Regulation of the yeast Ace2 transcription factor during the cell cycle. *J. Biol. Chem.* 283, 11135–11145. doi: 10.1074/jbc.M800196200

Shahinian, S., and Bussey, H. (2000). β-1,6-Glucan synthesis in *Saccharomyces cerevisiae*. *Mol. Microbiol.* 35, 477–489. doi: 10.1046/j.1365-2958.2000.01713.x

Skamnioti, P., Henderson, C., Zhang, Z., Robinson, Z., and Gurr, S. J. (2007). A novel role for catalase B in the maintenance of fungal cell-wall integrity during host invasion in the rice blast fungus *Magnaporthe grisea*. *Mol. Plant Microbe Interact.* 20, 568–580. doi: 10.1094/mpmi-20-5-0568

Thorvaldsdottir, H., Robinson, J. T., and Mesirov, J. P. (2012). Integrative genomics viewer (IGV): high-performance genomics data visualization and exploration. *Brief. Bioinform.* 14, 178–192. doi: 10.1093/bib/bbs017

Valiante, V., Macheleidt, J., Foge, M., and Brakhage, A. A. (2015). The *Aspergillus fumigatus* cell wall integrity signaling pathway: drug target, compensatory pathways, and virulence. *Front. Microbiol.* 6:325. doi: 10.3389/fmicb.2015.00325

Vencio, R. Z., Koide, T., Gomes, S. L., and Pereira, C. A. (2006). BayGO: bayesian analysis of ontology term enrichment in microarray data. *BMC Bioinformatics* 7:86.

Vermout, S., Tabart, J., Baldo, A., Mathy, A., Losson, B., and Mignon, B. (2008). Pathogenesis of dermatophytosis. *Mycopathologia* 166, 267–275. doi: 10.1007/s11046-008-9104-5

Wagener, J., Echtenacher, B., Rohde, M., Kotz, A., Krappmann, S., Heesemann, J., et al. (2008). The putative alpha-1,2-mannosyltransferase AfMnt1 of the opportunistic fungal pathogen *Aspergillus fumigatus* is required for cell wall stability and full virulence. *Eukaryot. Cell* 7, 1661–1673. doi: 10.1128/EC.00221-08

Walker, L. A., Munro, C. A., De Bruijn, I., Lenardon, M. D., Mckinnon, A., and Gow, N. A. (2008). Stimulation of chitin synthesis rescues *Candida albicans* from echinocandins. *PLoS Pathog.* 4:e1000040. doi: 10.1371/journal.ppat.1000040

Woodfolk, J. A., Sung, S. S., Benjamin, D. C., Lee, J. K., and Platts-Mills, T. A. (2000). Distinct human T cell repertoires mediate immediate and delayed-type hypersensitivity to the *Trichophyton* antigen, Tri r 2. *J. Immunol.* 165, 4379–4387. doi: 10.4049/jimmunol.165.8.4379

Wosten, H. A. (2001). Hydrophobins: multipurpose proteins. *Annu. Rev. Microbiol.* 55, 625–646. doi: 10.1146/annurev.micro.55.1.625

Yu, L., Zhang, W., Wang, L., Yang, J., Liu, T., Peng, J., et al. (2007). Transcriptional profiles of the response to ketoconazole and amphotericin B in *Trichophyton rubrum*. *Antimicrob. Agents Chemother.* 51, 144–53. doi: 10.1128/AAC.00755-06

Zuza-Alves, D. L., Silva-Rocha, W. P., and Chaves, G. M. (2017). An update on *Candida tropicalis* based on basic and clinical approaches. *Front. Microbiol.* 8:1927. doi: 10.3389/fmicb.2017.01927

Conflict of Interest: The authors declare that the research was conducted in the absence of any commercial or financial relationships that could be construed as a potential conflict of interest.

frontiers in Microbiology

REVIEW
published: 10 October 2019
doi: 10.3389/fmicb.2019.02294

The Genetics and Biochemistry of Cell Wall Structure and Synthesis in *Neurospora crassa*, a Model Filamentous Fungus

*Pavan K. Patel and Stephen J. Free**

Department of Biological Sciences, SUNY University at Buffalo, Buffalo, NY, United States

OPEN ACCESS

Edited by:
Fausto Almeida,
University of São Paulo, Brazil

Reviewed by:
Akira Yoshimi,
Tohoku University, Japan
Meritxell Riquelme,
Ensenada Center for Scientific Research and Higher Education (CICESE), Mexico
Vishukumar Aimanianda,
Institut Pasteur, France

****Correspondence:***
Stephen J. Free
free@buffalo.edu

Specialty section:
This article was submitted to Fungi and Their Interactions, a section of the journal Frontiers in Microbiology

Received: *25 July 2019*
Accepted: *20 September 2019*
Published: *10 October 2019*

Citation:
Patel PK and Free SJ (2019) The Genetics and Biochemistry of Cell Wall Structure and Synthesis in Neurospora crassa, a Model Filamentous Fungus. Front. Microbiol. 10:2294. doi: 10.3389/fmicb.2019.02294

This review discusses the wealth of information available for the *N. crassa* cell wall. The basic organization and structure of the cell wall is presented and how the wall changes during the *N. crassa* life cycle is discussed. Over forty cell wall glycoproteins have been identified by proteomic analyses. Genetic and biochemical studies have identified many of the key enzymes needed for cell wall biogenesis, and the roles these enzymes play in cell wall biogenesis are discussed. The review includes a discussion of how the major cell wall components (chitin, β-1,3-glucan, mixed β-1,3-/β-1,4- glucans, glycoproteins, and melanin) are synthesized and incorporated into the cell wall. We present a four-step model for how cell wall glycoproteins are covalently incorporated into the cell wall. In *N. crassa*, the covalent incorporation of cell wall glycoproteins into the wall occurs through a glycosidic linkage between lichenin (a mixed β-1,3-/β-1,4- glucan) and a "processed" galactomannan that has been attached to the glycoprotein N-linked oligosaccharides. The first step is the addition of the galactomannan to the N-linked oligosaccharide. Mutants affected in galactomannan formation are unable to incorporate glycoproteins into their cell walls. The second step is carried out by the enzymes from the GH76 family of α-1,6-mannanases, which cleave the galactomannan to generate a processed galactomannan. The model suggests that the third and fourth steps are carried out by members of the GH72 family of glucanosyltransferases. In the third step the glucanosyltransferases cleave lichenin and generate enzyme/substrate intermediates in which the lichenin is covalently attached to the active site of the glucanosyltransferases. In the final step, the glucanosyltransferases attach the lichenin onto the processed galactomannans, which creates new glycosidic bonds and effectively incorporates the glycoproteins into the cross-linked cell wall glucan/chitin matrix.

Keywords: cell wall, filamentous fungi, Neurospora, glucan, galactomannan, mannanase, glucanosyltransferase, melanin

INTRODUCTION

The cell wall is a vital structure for virtually all fungal cells. The wall provides protection from environmental stresses such as UV light, desiccation, freezing, and attack from enzymes that might otherwise cause cell lysis. It provides the tensile strength required to protect the cell against cell lysis from osmotic pressure. It facilitates adhesion to the substratum. Receptors in the cell wall allow the fungus to assess a large variety of environmental conditions and to activate cell signaling pathways. The cell wall is also the major determinant of fungal cell morphology. Mutations affecting cell wall synthesis affect the growth rate, morphology, and viability of fungal cells.

The major cell wall components include glucans, glycoproteins, and chitin (Klis et al., 2006; Latge, 2007; Chaffin, 2008; Free, 2013; Gow et al., 2017). Almost all fungal cell walls contain β-1,3-glucan (laminarin), chitin, and a variety of glycoproteins that function in cell wall biogenesis, adhesion, environmental sensing, and as cell wall structural elements. In addition to these general components, fungal cell walls often contain additional polysaccharides such as α-1,3-glucan, β-1,6-glucan, mixed β-1,3-/β-1,4-glucans, galactomannans, xylogalactomannans, and other less well-characterized glucans. Many fungi incorporate melanin into their cell walls. While we will address each of these various components individually, it is important to recognize that they are all cross-linked together and function as an assemblage.

Fungal cell walls are dynamic structures. Their composition is responsive to environmental changes. The well-characterized cell wall integrity signal transduction pathway is a signaling pathway for modifying the cell wall under stress conditions. When activated, the cell wall integrity pathway directs the synthesis of addition cell wall glycoproteins and an increase in cell wall chitin and glucans. The filamentous fungi have life cycles that include a variety of different cell types. It is clear that the cell wall can be dramatically changed as different types of cell are generated during fungal life cycles and cell type-specific cell wall proteins and glucans are expressed.

While a great deal of information is available on the cell walls from a number of fungi, this review is focused on the cell walls from the model filamentous fungus *Neurospora crassa*. Pertinent information is available about *N. crassa* cell walls from vegetative hyphae, from conidia (asexual spores), from cells in the perithecium (female mating structure), and from the developing ascospores (sexual spores) (Bowman et al., 2006; Maddi et al., 2009; Ao et al., 2016). The fungus therefore presents a broad overview of cell wall structures and serves as an excellent model for the characterization of cell wall structure and biosynthesis. Neurospora is particularly well suited for the study of the fungal cell wall. *N. crassa* is a haploid fungus, which greatly facilitates the isolation and characterization of mutants affected in the generation of the cell wall. *N. crassa* is currently the only filamentous fungus with a nearly complete single gene knockout library, and mutants lacking almost any gene of interest are readily available from the Fungal Genetics Stock Center (Colot et al., 2006). The knockout library has proven to be a valuable resource for the characterization of *N. crassa* cell walls. The library allows an investigator to rapidly determine if a putative cell wall protein or a polysaccharide synthase plays an important role in generating the cell wall for all of the different cell types in the *N. crassa* life cycle. The tools for the genetic manipulation of *N. crassa* are well developed and have been immensely valuable in the characterization of cell wall glycoproteins. With all these advantages, *N. crassa* cell walls are among the best-characterized cell walls among the filamentous fungi. While this review concentrates on the genetics and biochemistry of *N. crassa* cell walls, some comparisons and contrasts with the cell walls of other fungi are included to illustrate elements that are in common among all cell walls and to point out features that may be unique to *N. crassa* and closely related fungal species.

In addition to the genetics and biochemistry of *N. crassa* cell wall biogenesis described in this article, a great deal is known about how chitin synthase, glucan synthase, and cell wall enzymes are being targeted to the hyphal tip, the locale where the cell wall is produced. The polysaccharide synthases and cell wall glycoproteins are trafficked through the Spitzenkorper, a densely packed region of intracellular vesicles that acts as a vesicle supply center to provide secretory vesicle to the hyphal tip. The Spitzenkorper has been shown to contain an inner area of chitin synthase-containing small microvesicles (chitosomes) at its core and a ring of larger macrovesicles surrounding the chitosome core. These macrovesicles have been shown to contain glucan synthase and cell wall enzymes. Both microvesicles and macrovesicles are targeted for fusion at the hyphal tip where cell wall formation occurs. An excellent review article detailing these aspects of *N. crassa* cell wall biogenesis has recently been published (Verdin et al., 2019). The reader is referred to that review article for more detailed information on vesicle trafficking of polysaccharide synthases to the plasma membrane and secretion of cell wall glycoproteins to the cell wall space.

THE STRUCTURES, SYNTHESIS AND FUNCTIONS OF *N. crassa* CELL WALL COMPONENTS

The *N. crassa* cell wall has been shown the contain β-1,3-glucan, mixed β-1,3-/β-1,4- glucans, α-1,3-glucan, chitin, melanin, and over forty different glycoproteins. We will discuss the structure and location of these *N. crassa* cell wall components within the cell wall structure. We also discuss how these components are made and incorporated into the cell wall. A representation of the *N. crassa* vegetative hyphal cell wall is shown in **Figure 1**.

CHITIN

Chitin is an important cell wall polysaccharide and is found in almost all fungal cell walls with the exception of the cell walls from *Schizosaccharomyces pombe* and *Pneumocystis* species (Magnelli et al., 2005; de Groot et al., 2007; Klis et al., 2010; Lenardon et al., 2010; Ma et al., 2016). Chitin is a long polysaccharide of repeating β-1,4-*N*-acetylglucosamine residues. Chitin makes up approximately 4% of the vegetative *N. crassa*

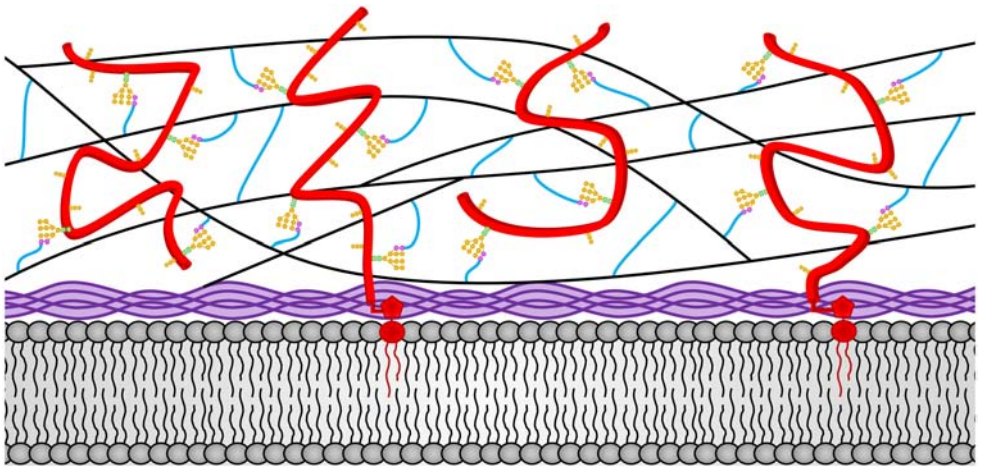

FIGURE 1 | The *N. crassa* vegetative hyphae cell wall. The locations of the various cell wall components and how they are cross-linked together in the vegetative cell wall are depicted. Chitin is shown in purple and is located adjacent to the plasma membrane at the bottom of the diagram. The β-1,3-glucan is shown in black and located in the middle of the cell wall. Cell wall glycoproteins are shown in red. GPI anchors are shown in red and extent into the plasma membrane. N-linked oligosaccharides are shown with *N*-acetylglucosamine residues in green squares, mannoses from the N-linked oligosaccharide shown in orange circles, and processed galactomannans shown in magenta circles. O-linked oligosaccharides are also shown in orange. Lichenin is shown in blue and is attached to the processed galactomannan and to β-1,3-glucans. Note that the β-1,3-glucan, lichenin, and glycoproteins form a cross-linked cell wall matrix.

cell wall mass (Aranda-Martinez et al., 2016). It is thought to be the major polysaccharide found in the *N. crassa* septae (Hunsley and Gooday, 1974). Multiple chitin polymers form interchain hydrogen bonds with each other and self-assemble into microfibrils, in which the individual chitin molecules are arranged in an antiparallel manner to create "crystalline" chitin (Ruiz-Herrera et al., 2006). The chitin is vital for the strength and integrity of the cell walls. It is localized in the membrane proximal portion of the cell wall and is incorporated into the wall matrix by being cross-linked to the glucans (**Figure 1**).

Fungi generally contain several genes encoding chitin synthases and vegetative hyphae express multiple chitin synthase genes. In the filamentous fungi, these chitin synthase genes are organized into seven different groups or classes, with the fungi having one or more genes from each of these seven classes (Choquer et al., 2004). It is thought that these chitin synthases may be producing chitin polymers of different lengths, at different cellular locations, and at different points in time across the fungal life cycles. Some chitin synthases have been shown to deposit chitin in the cell wall at the growing hyphal tip while other function to deposit chitin into the growing septum cell wall during septum formation (Roncero, 2002; Lee et al., 2004; Fukuda et al., 2009; Fajardo-Somera et al., 2015). All of the chitin synthases are thought to extrude chitin monomers into the cell wall space through a pore formed by their multiple transmembrane domains, and the formation of chitin fibrils occurs *in situ* in the cell wall space.

The *N. crassa* genome contains 7 chitin synthase genes, *chs-1/ncu03611*, *chs-2/ncu05239*, *chs-3/ncu04251*, *chs-4/ncu09324*, *chs-5/ncu04352*, *chs-6/ncu05268*, and *chs-7/ncu04350*, one from each of the seven groups commonly found in filamentous fungi (Fajardo-Somera et al., 2015). CHS-1, CHS-3, and CHS-4 were identified as being involved in cell wall synthesis by more classical genetic studies (Yarden and Yanofsky, 1991; Din and Yarden, 1994; Din et al., 1996). CHS-1, a class III chitin synthase, was found to be required for cell wall formation (Yarden and Yanofsky, 1991) and CHS-3, a class I chitin synthase, played an important role during vegetative growth. More recently, the cellular locations for all of these chitin synthases have been characterized and deletion mutants lacking each of these chitin synthases have been analyzed (Sanchez-Leon et al., 2011; Fajardo-Somera et al., 2015). Two of these chitin synthases, CHS-5 and CHS-7, contain a myosin-motor domain (MMD) and play important roles in apical growth, conidia development, and perithecia formation. All of the chitin synthases were shown to be localized in small vesicles, termed chitosomes, found in the Spitzenkorper, a region of vesicles just behind the growing hyphal tip that supplies vesicle for fusion at the hyphal tip. Slight differences in their locations suggests that they be located in different subpopulations of chitosomes. The chitin synthases were also found in association with developing septa, where cell wall is also being deposited. The septa are particularly well stained with Calcoflour white, a chitin staining reagent. The chitin synthases are also localized at the cross-walls between developing conidia, indicating a role in asexual development (Fajardo-Somera et al., 2015). Analysis of the chitin synthase deletion mutants showed that some of the chitin synthases were required for sexual development and loss of some of the chitin synthases affected vegetative growth and/or the production of conidia.

Many fungi contain chitin deacetylase enzymes which deacetylate chitin to form chitosan, which is much more soluble than chitin. Chitin deacetylases have been shown to generate chitosan during sporulation in *S. cerevisiae* (Christodoulidou et al., 1996). Chitosan formation has also been shown to be necessary for pathogenicity in *C. neoformans* (Baker et al., 2011). *N. crassa* has two chitin deacetylase genes, *ncu09508*

and *ncu09582*, which may be more highly expressed during perithecium development (Lehr et al., 2014; Wang et al., 2014; Liu et al., 2017). No information is available about whether the perithecium contains chitosan or how the loss of the two chitin deacetylase genes affects female development.

β-1,3-GLUCAN

β-1,3-glucan is a long unbranched polysaccharide consisting of repeating β-1,3-glucose residues. It is the most abundant component of the vegetative cell wall, making up approximately 35% of the *N. crassa* cell wall mass (Kar et al., 2019). It is the major component of the cell walls found in almost all fungi. β-1,3-glucan is well suited for its role as a major component of the fungal cell wall. The polymer has been shown to have a helical three-dimensional structure that allows for some limited stretching while retaining its structural integrity and its tensile strength (Bohn and Bemiller, 1995). The β-1,3-glucans are cross-linked together to form the basic three dimensional matrix structure of the wall. As such, β-1,3-glucans are found throughout the middle portion of the cell wall (**Figure 1**). The three dimensional β-1,3-glucan matrix would allow for a limited amount of cell wall stretching in all dimensions in response to the cell wall turgor pressure from within the cell. Direct measurements of the turgor pressure in *N. crassa* hyphae give values in the range of 500 pKa (70 psi) indicating that the hyphal cell wall is exposed to a significant amount of pressure (Lew, 2011). Sugar linkage analyses of the monosaccharides released from the *N. crassa* cell wall has failed to identify significant amounts of glucose with 1,6 linkages, while glucoses with 1,3 and 1,4 linkages are abundant (Maddi et al., 2009, 2012; Maddi and Free, 2010; Ao et al., 2016). This indicates that *N. crassa* does not make a β-1,6- polymer. The situation in *N. crassa* clearly differs from that found in the *S. cerevisiae* and *C. albicans* cell walls, where the β-1,6-glucan are used to cross-link the β-1,3-glucans together (Lu et al., 1995; Kollar et al., 1997; Kapteyn et al., 2000).

The FKS-1 β-1,3-glucan synthase is responsible for the synthesis of β-1,3-glucan, and the enzyme has been identified as being critical for cell wall formation in a number of fungi (Beauvais et al., 2001; Dichtl et al., 2015). An *N. crassa* mutant having a single amino acid change in the β-1,3-glucan synthase was isolated and the gene named *do* (*doily*) (McCluskey et al., 2011). The doily mutant has a tight colonial morphology. The *N. crassa* glucan synthase, FKS-1, is encoded by *ncu06871* and the glucan synthase has fourteen putative multiple transmembrane domains and a glucan synthesis domain that attaches a single glucose residue to the non-reducing end of a β-1,3-glucan polymer (Sanchez-Leon and Riquelme, 2015). UDP-glucose serves as the glucose donor, and the glucan is extruded through the plasma membrane into the cell wall space via a pore formed by the transmembrane domains. A β-1,3-glucan synthase regulatory subunit, COT-2 or GS-1, is also highly conserved. The *N. crassa gs-1* gene (*ncu04189*) was initially defined by mutants which lacked glucan synthase activity (Enderlin and Selitrennikoff, 1994; Tentler et al., 1997) and the *cot-2* mutation was isolated as a temperature sensitive colonial mutant (Garnjobst and Tatum, 1967). The RHO-1 GTPase (NCU01484) associates with FKS-1 and functions to regulate its activity (Richthammer et al., 2012). FKS-1 and GS-1 have been localized to the macrovesicle ring of the Spitzenkorper and to the plasma membrane at the hyphal tip (Verdin et al., 2009; Sanchez-Leon and Riquelme, 2015).

MIXED β-1,3/β-1,4 GLUCANS (LICHENIN)

The linkage analysis of the *N. crassa* vegetative cell wall shows that between 15 and 20% of the glucoses in the wall have a 1,4 linkage and lichenin has been shown to be present as defined by a monoclonal antibody directed against lichenin (Ao and Free, 2017; Kar et al., 2019). Lichenin is defined as a polysaccharide with a repeating β-1,4-glucose-β-1,4-glucose-β-1,3-glucose trisaccharide (Perlin and Suzuki, 1962). Lichenin was initially identified in the lichen-forming ascomycete *Cetraria islandica* (Icelandic moss) as a long linear polysaccharide. Lichenin has been shown to be located in the fungal cell wall and in the extracellular matrix formed by the ascomycete cells in the lichen (Honegger and Haisch, 2001). Based on this structure and assuming that all of the 1,4-linked glucose in the cell wall linkage analysis come from lichenin, lichenin would represent approximately 25% of the *N. crassa* vegetative cell wall mass (Kar et al., 2019). It has been shown that lichenin functions as the polysaccharide through which cell wall glycoproteins are cross-linked into the cell wall (Kar et al., 2019). Lichenin may also function to cross-link the β-1,3-glucan together into a matrix structure, but this has not been experimentally verified. In *S. cerevisiae* and *C. albicans*, β-1,6-glucan has been implicated in cross-linking both the β-1,3-glucans and the cell wall proteins into a cell wall matrix (Lu et al., 1995; Kollar et al., 1997; Kapteyn et al., 2000). It is interesting to note that *S. cerevisiae* and *C. albicans* lack lichenin and use β-1,6-glucan to cross-link glycoproteins and β-1,3-glucan into the cell wall while *N. crassa* lacks β-1,6-glucan and uses lichenin to cross-link glycoproteins into the cell wall. As a cross-linking polymer, lichenin is present throughout the middle portion of the cell wall (**Figure 1**).

Mixed β-1,3-/β-1,4- glucans have been found in several filamentous fungi but the proteins involved in their synthesis have not been defined. There are two plausible ways that mixed polymers could be produced. One possibility would be to have a plasma membrane localized glucan synthase, similar to the chitin and β-1,3-glucan synthases that synthesizes their polymers and extrude them through the plasma membrane. A second possibility would be to have two or three glycosyltransferases produce the polymer by the reiterative addition of glucose residues. In this scenario, the mixed β-1,3-/β-1,4- glucan could be produced in the Golgi apparatus and be secreted through the canonical secretory pathway.

Glycosyltransferase type 2 enzymes function to make polymers having β-1,4-glucose bonds (cellulose synthase type enzymes) and would therefore be considered as likely candidates for lichenin synthases. The *N. crassa* genome contains 7 genes (*cps-1/ncu00911*, *ncu09875*, *ncu08226*, *ncu04223*, *ncu03240*, *ncu09906*, and *ncu04167*) that might be considered as plausible

glycosyltransferase type 2 enzymes. The information available on the expression of these genes shows that *cps-1*/*ncu00911* and *ncu03240* are highly expressed in the vegetative hyphae, and the other genes are highly upregulated during perithecium development, suggesting that they might play roles in cell wall formation during female development (Liu et al., 2017). Based on their expression in vegetative hyphae, where lichenin has been shown to be present in the cell wall, CPS-1 and NCU03240 would be considered as the most likely candidates for being lichenin synthases.

CPS-1 contains 510 amino acids and has a signal peptide, a glycosyltransferase domain and two transmembrane domains near its carboxyl terminus. Deletion of *cps-1* (*ncu00911*) gives rise to a cell wall defect that affects all aspects of the *N. crassa* life cycle (Fu et al., 2014a). The rate of vegetative growth is dramatically reduced in the mutant and the mutant is unable to produce aerial hyphae and conidia. The mutant is also unable to form perithecia. When grown in liquid medium the Δ*cps-1* mutant grows in a tight colonial form and releases large amounts of cell wall proteins into the medium (Fu et al., 2014a). Since lichenin is needed for the cross-linking of cell wall proteins into the cell wall (Ao and Free, 2017), the release of cell wall proteins into the medium suggests that *cps-1* might encode a lichenin synthase. However, sugar linkage analysis of the glucan remaining in the mutant cell wall shows the presence of 1-4 linked glucose residues, indicating that some mixed β-1,3/β-1,4-glucan is still present in the Δ*cps-1* mutant (Fu et al., 2014a).

The second likely potential lichenin synthase, NCU03240, is a 651 amino acid protein with five transmembrane domains and a centrally located glycosyltransferase domain. The *ncu03240* deletion mutant is found in the Neurospora deletion library as a heterokaryon (a cell with a mixture of wild type and mutant nuclei) and efforts to isolate the homokaryon mutant (cell containing only mutant nuclei) have not been successful. This suggests that the deletion mutant is inviable, a phenotype that would be consistent with the loss of a major cell wall component.

The current available information leaves open several possibilities, including: (1) that *cps-1*/*ncu00911* and *ncu03240* encode two lichenin synthases and they have overlapping, partially redundant activities, (2) that CPS-1/NCU00911 and NCU03240 synthesize two different glucans, one of which might be lichenin, and (3) that neither *cps-1* nor *ncu03240* encode a lichenin synthase, but encode other cell wall polysaccharide synthases. Although the data doesn't definitely identify either CPS-1 or NCU03240 as being a lichenin synthase, it clearly demonstrates that both of these glycosyltransferases plays critical roles in the synthesis of the *N. crassa* vegetative hyphal cell wall. Clearly, there is still much to be learned about the synthesis of mixed β-1,3-/β-1,4-glucans and the roles they play in *N. crassa* cell wall formation.

α-1,3-GLUCANS

α-1,3-glucans have been identified in a variety of fungal cell walls, including *S. pombe*, *C. neoformans*, *A. fumigatus*, and *N. crassa* (Hochstenbach et al., 1998; Beauvais et al., 2005; Grun et al., 2005; Maubon et al., 2006; Reese et al., 2007; Fontaine et al., 2010; Fu et al., 2014b). The α-1,3-glucan has been shown to be localized in the outer layers of the *Histoplasma capsulatum* yeast cell wall, where it functions to shield the underlying β-1,3-glucan from the host immune system (Rappleye et al., 2007). In the *Aspergillus nidulans* cell wall the α-1,3-glucan is in the outer layer of the cell wall, where it facilitates hyphal cell aggregation (Miyazawa et al., 2018). In addition to being produced in these fungi, α-1,3-glucan synthase genes are found in a number of additional fungal genomes suggesting that the glucan is made by a wide variety of fungi. In some cases, multiple α-1,3-glucan synthase paralogs are encoded in the genome. The α-1,3-glucan synthases have multiple transmembrane domains and a synthase domain located on the cytosolic face of the plasma membrane. Like the β-1,3-glucan synthases, the synthase domain is thought to utilize UDP-glucose as a substrate and attaches a glucose residue to the non-reducing end of an elongating α-1,3-glucan polymer. The elongating α-1,3-glucan is thought to be extruded though a pore formed by the transmembrane domains. No information is available about the three-dimensional structure of the α-1,3-glucan.

The *N. crassa* genome contains two α-1,3-glucan synthase genes, *ags-1* (*ncu08132*) and *ags-2* (*ncu02478*). The *ags-1* gene is responsible for the production of the α-1,3-glucan and is expressed in the aerial hyphae and conidia. AGS-1 is a large protein containing 2374 amino acids. In addition to a glucan synthase domain located on the cytosolic side of the plasma membrane, AGS-1 contains multiple transmembrane domains and an N-terminal putative glucanosyltransferase domain that might attach the α-glucan to the cell wall matrix. Mutants lacking AGS-1 have been extensively characterized (Fu et al., 2014b). The *ags-1* promoter has been used to drive expression of RFP and shown to be direct gene expression in developing aerial hyphae and conidia (Fu et al., 2014b). Antibodies directed against α-1,3-glucan demonstrate that the polymer is located in the cell wall and accessible to the antibody. The production of conidia in the *ags-1* deletion mutants was shown to be reduced by 95% and the conidia that were produced were shown to have a reduced level of viability and to be sensitive to a heat and freezing (Fu et al., 2014b). Clearly the synthesis of the cell type-specific α-1,3-glucan is important for the development and viability of the conidia. The results further demonstrate that the glucan portion of the cell wall can vary dramatically during the *N. crassa* life cycle. No role has been defined for the *ags-2* gene, which is more highly expressed during perithecium development (Liu et al., 2017).

MELANIN

Many fungi produce melanin as one of their cell wall components. Melanin is a large amorphous polymer of phenolic compounds and is generated by a free-radical reaction in which the phenolics are randomly cross-linked together. Cell wall melanin plays a number of very important roles. It provides protection from UV light, desiccation, freezing, and digestion from cell wall digestive enzymes produced by other microbes (Rehnstrom and Free, 1996; Eisenman and Casadevall, 2012; Nosanchuk et al., 2015).

Melanized fungal cells have been shown to be capable of survival in the soil for decades (Davis and DeSerres, 1970). Most pathogenic fungi have melanized cell walls, and the melanin has been shown to be an important virulence factor (Chumley and Valent, 1990; Langfelder et al., 2003; Talbot, 2003; Pihet et al., 2009; Eisenman and Casadevall, 2012).

There are two pathways that can function for the synthesis of fungal melanins, the dihydroxynaphthalene (DHN) pathway and the dihydroxyphenylalanine (DOPA) pathway, and *N. crassa* encodes the proteins for both pathways. The DOPA pathway seems to function for the melanization of the vegetative cell wall under stress conditions. The DOPA pathway requires a single copper-containing enzyme, tyrosinase, which converts tyrosine to dihydroxyphenylalanine (DOPA), which is unstable and spontaneously forms melanin granules. *N. crassa* tyrosinase has been purified, and its activity as a copper-containing enzyme characterized (Lerch, 1982; Kupper et al., 1989). The enzyme requires a proteolytic activation step to become enzymatically active. *N. crassa* vegetative hyphae that are exposed to stress agents produce tyrosinase and become melanized. *N. crassa* tyrosinase mutants have been isolated and characterized (Fuentes et al., 1994). Interestingly, these mutants are unable to form perithecia, the female mating structures. When used as a male parent in a mating, the tyrosinaseless mutant progeny have melanized cell walls, which demonstrates that the DOPA pathway is not used for ascospore melanization. Currently we have no explanation for why tyrosinase would be required for perithecium formation.

In *N. crassa*, the DHN pathway functions in the formation of melanin for the ascospore and for the peridium cell walls. The DHN melanin pathway has been well-characterized in *A. fumigatus* (Langfelder et al., 1998, 2003; Eisenman and Casadevall, 2012). The pathway for DHN synthesis was worked out and includes a polyketide synthase that uses acetyl-CoA and malonyl-CoA as substrates and makes a large heptameric polyketide (Langfelder et al., 1998; Tsai et al., 2001). The heptameric polyketide is then acted on by a hydrolase to generate pentameric tetrahydroxylnapthalene (THN) (Tsai et al., 2001). A THN reductase and a scytalone hydratase act on the THN to remove two of the hydroxyl groups and produce dihydroxynapthalene (DHN). A laccase then acts on the DHN to generate a free-radical form of DHN, which spontaneously reacts with other DHN molecules in a chain reaction manner to create large, amorphous melanin granules (Sugareva et al., 2006). In *A. fumigatus*, Upadhyay et al. (2016a,b) showed that all of the enzymes involved in the synthesis of the DHN are found associated with intracellular vesicles.

All of the enzymes involved in the synthesis of DHN are found encoded in the *N. crassa* genome. Mutants affected in the ability to produce DHN are unable to melanize their ascospores and perithecia, demonstrating that the pathway is responsible for melanizing these structures (Howe and Benson, 1974; Howe, 1976; Johnson, 1977; McCluskey et al., 2011; Ao et al., 2019). The genome has two paralogs for the heptaketide hydrolase and the THN reductase steps in the pathway, and a single gene for the other steps. The expression of the heptaketide hydrolases and the THN reductases occur in a tissue-type specific manner such that a single hydrolase and reductase are expressed in the ascospores, while both paralogs are expressed in the peridium (Ao et al., 2019). Experiments using enzymes tagged with GFP and RFP markers demonstrated that all of the DHN biosynthetic enzymes are found associated with intracellular vesicles (Ao et al., 2019). The laccase needed for the final step in the process was also identified. Experiments tagging the laccase with GFP and RFP markers demonstrated that the laccase has been secreted and localized to the cell wall space at the point in time when the peridium becomes melanized (Ao et al., 2019). It was concluded that melanin formation in *N. crassa* occurs "*in situ*" within the cell wall space and that the forming melanin granules encase the other cell wall components within the forming melanin.

GLYCOPROTEINS

Glycoproteins are found as a major component in all fungal cell walls. Some of these glycoproteins are covalently attached to the cell wall matrix and are considered as integral cell wall components, while other cell wall proteins are incorporated into the wall via non-covalent bonds and can be released from the wall by SDS treatment. Glycoproteins that are released by SDS treatment are considered as cell wall-associated glycoproteins.

Cell wall-associated glycoproteins as well as integral cell wall glycoproteins can function in a wide variety of functions (De Groot et al., 2005; Latge, 2007; Chaffin, 2008; Klis et al., 2010; Free, 2013). Some of the integral cell wall proteins function in the cross-linking reactions described below to generate a three dimensional chitin/glucan/glycoprotein matrix. Other cell wall glycoproteins have been shown to function as adherins and help anchor the fungal cell to the substratum. Cell wall glycoproteins function as receptors for signal transduction pathways that allow the fungus to assess environmental conditions. Many cell wall glycoproteins have hydrolase activities. Some of these hydrolases may function in the remodeling of the cell wall structure to allow for modification of the cell wall and for the formation of new hyphal branches. Other cell wall hydrolases may function in nutrient acquisition by releasing sugars, amino acids, or lipids from their substrates. Cell wall glycoproteins may also play roles in protecting the fungus from other microbes. In the case of plant and animal pathogenic fungi, cell wall glycoproteins can play important roles in the infection of the host and be considered as virulence factors. Major cell wall proteins lacking enzymatic or other known functions have been ascribed a structural role, but some of these "structural proteins" may have functions that remain to be elucidated. Conversely, all of the integral cell wall proteins might be considered to have a "structural role" in that they become part of the cell wall matrix.

Proteins identified in proteomic analyses of purified cell walls have been divided into two groups, referred to as "classical" and "non-classical" cell wall proteins. Classical cell wall glycoproteins have a typical N-terminal signal sequence and are translated by ribosomes associated with the endoplasmic reticulum (ER). These proteins travel through the canonical secretory pathway, and typically have both N-linked and O-linked oligosaccharides attached to them. Proteins identified in cell wall preparations

which lack a signal peptide are referred to as "non-classical" cell wall proteins. Most of these "non-classical" cell wall proteins have well-defined cytosolic functions. For example, chaperone proteins and some proteins that function in glycolysis are often found among the "non-classical" cell wall proteins that are identified in cell wall proteomic analyses. The question of whether these proteins are normal components of the cell wall or are contaminants in purified cell wall preparations remains controversial. The questions of how such proteins might be released into the cell wall space, what functions they might perform in the cell wall space, and how they might be incorporated into the cell wall haven't been elucidated. For the purposes of this review, these "non-classical" cell wall proteins will not be further considered.

In *N. crassa* cell walls, 41 "classical cell wall proteins" have been identified by proteomic analyses. The glycoproteins present in other fungal cell walls were identified by proteomic analyses after the cell wall proteins are released from the wall by alkaline treatment, released into the medium by regenerating spheroplasts, or by having peptides released from purified cell walls by trypsin digestion. In *N. crassa*, the cell wall proteins were identified by treating purified cell wall samples with trifluoromethanesulfonic acid, which hydrolyses the glycosidic linkages in the cell wall glucans and chitin and releases free deglycosylated cell wall proteins (Bowman et al., 2006; Maddi et al., 2009). One advantage of this approach are that because of the removal of the N-linked and O-linked glycosylation, tryptic fragments that would otherwise not be able to be identified because they are glycosylated become available for identification. For highly glycosylated cell wall glycoproteins, a large fraction of the tryptic peptides are glycosylated. A second advantage of the approach is that the *N*-acetylglucosamine that is attached to the asparagine in N-linked oligosaccharides is retained, and by including asparagine-*N*-acetylglucosamine as a possible "amino acid" in the proteomic analysis, the sites of N-linked oligosaccharide addition are easily identified (Maddi et al., 2009). The identified *N. crassa* cell wall proteins are typical of those found in other fungi. They include a number of "cell wall cross-linking" enzymes, a variety of glycosylhydrolases that could be involved in cell wall remodeling or in nutrient acquisition, and a number of cell wall "structural" proteins.

Classical cell wall proteins contain a signal peptide at their N-terminus and are translocated into the ER lumen during their synthesis. As the growing polypeptides are translocated into the lumen of the ER, N-linked oligosaccharides are added. As in other eukaryotic organisms, the N-linked oligosaccharides play an important role in the assessment of protein folding and quality control. The N-linked oligosaccharide is synthesized as a 2 *N*-acetylglucosame:9 Mannose:3 Glucose structure that is attached to a dolichol phosphate moiety. The entire oligosaccharide is transferred "*en bloc*" to asparagine residues in the context of asparagine–*X*-serine or asparagine-*X*-threonine, where X can be any amino acid except proline. The glucoses on the transferred N-linked oligosaccharide function in the assessment of protein folding status and in mediating the unfolded protein response. These glucoses are trimmed in correctly folded glycoproteins.

The major elements of the glycoprotein synthesis in *N. crassa* follow those outlined above. All of the enzymes involved in the synthesis of the N-linked oligosaccharide are encoded in the *N. crassa* genome (Galagan et al., 2003; Colot et al., 2006; Deshpande et al., 2008). Deletion mutants for the several of the steps in N-linked oligosaccharide formation and transfer to nascent polypeptides are available in the knockout library as heterokaryons (isolates having wild type nuclei as well as knock out mutant nuclei in a common cytoplasm) which suggests the knockout mutations are lethal under normal growth conditions in homokaryons (cells having only knockout mutant nuclei). Classical mutations in two of the subunits of the oligosaccharide transferase have been isolated as "tiny" mutants with slow-growing, tight colonial phenotypes (McCluskey et al., 2011). This demonstrates the important roles that N-linked oligosaccharides play in the process of protein folding, protein stability, and in the incorporation of glycoproteins into the cell wall. Glycan profiling and glycan linkage analysis of the N-linked glycans present on cell wall glycoproteins in the Δ*och-1* mutant (which lacks the N-linked oligosaccharide-associated galactomannan described below) demonstrates that *N. crassa* glycoproteins have a typical 2 *N*-acetylglucosamine:9 mannose N-linked oligosaccharide (Deshpande et al., 2008; Kar et al., 2019). Trimming of some of the terminal mannoses occurs on most of the N-linked oligosaccharides and contributes to the heterogeneity seen in N-linked oligosaccharides (Kar et al., 2019).

Approximately half of the integral cell wall proteins have an attached glycosylphosphatidylinositol (GPI) anchor attached to their carboxyl terminus. GPI anchored proteins contain a typical signal peptide at their N-terminus and also contain a well-defined amino acid signal sequence at their carboxyl terminus that acts as a signal for the addition of the GPI anchor. The signal for GPI-anchor addition (the "GPI signal") consists of a carboxyl-terminal hydrophobic domain separated by a short stretch of hydrophilic amino acids from an attachment site termed the omega site, where the protein is cleaved and the GPI anchor is added (Ferguson, 1999; Eisenhaber et al., 2003). The GPI anchor is added in the ER immediately after protein synthesis is completed. The GPI anchor plays an important role in trafficking these proteins to the cell wall. The GPI anchor contains two or three attached lipids and functions to tether or anchor the protein in the lumen leaflet of the secretory pathway organelles and to the outer leaflet of the plasma membrane. In the fungi, virtually all GPI anchored proteins are integral cell wall glycoproteins.

The pathway for the synthesis of the GPI anchor was originally elucidated using *S. cerevisiae* temperature-sensitive mutants, Trypanosomes, and mutant cultured vertebrate cells (Ferguson, 1999; Eisenhaber et al., 2003). The *N. crassa* pathway has also been examined (Bowman et al., 2006, 2009). Mutations affecting most of the steps in the *N. crassa* GPI anchor biosynthetic pathway have been characterized and the major GPI-anchored cell wall proteins have been identified and characterized (Bowman et al., 2006). Deletions for the steps in GPI anchor biosynthesis are lethal in *S. cerevisiae*, and the pathway was characterized using temperature-sensitive mutants, but the equivalent *N. crassa* deletion mutants are viable and grow with an extremely tight colonial morphology.

As the protein passes through the secretory pathway, further post-translational modifications occur. O-linked oligosaccharides are added to multiple serine and threonine sites in the glycoproteins. In fungi, these O-linked oligosaccharides usually have a mannose attached to the serine or threonine and contain additional mannose and/or galactose residues. O-linked glycosylation is important for the stability and folding of fungal glycoproteins (Shental-Bechor and Levy, 2008; Prates et al., 2018). *S. cerevisiae* contains a number of well-characterized protein:mannosyl transferases (PMT enzymes) that add the initial mannose residue to serine and threonine sites. These various PMT enzymes have differing specificities for their glycoprotein substrates (Girrbach and Strahl, 2003). Additional mannose and/or galactose residues are added by mannosyltransferases and/or galactosyltransferases in the ER and Golgi apparatus. In *S. cerevisiae*, the Mnt-1p mannosyltransferase adds the second mannose to the O-linked oligosaccharides (Hausler et al., 1992). These same steps in generating O-linked oligosaccharides occur in *N. crassa*. The *N. crassa* genome contains 3 genes encoding PMT enzymes (*ncu01912*, *ncu01648*, and *ncu09332*). Knockout mutations for *ncu01912* and *ncu09332*, are found in the deletion library as heterokaryons and there is no deletion mutant available for *ncu01648*. This strongly suggests that the addition of O-linked oligosaccharides is important for glycoprotein function and stability. *N. crassa mnt-1* mutants have been isolated and characterized (Bowman et al., 2005). The mutants grow with a tight colonial morphology and are unable produce conidia and perithecia, demonstrating the importance of O-linked glycosylation (Bowman et al., 2005). The severe growth phenotype of the *mnt-1* mutants is best understood from the viewpoint that the formation of the O-linked oligosaccharide is affected on all of the cell wall and secreted proteins. As a result, many of the cell wall proteins are being degraded. The *mnt-1* mutant cell wall is therefore deficient in several cell wall glycoproteins and is severely compromised.

Yet another important post-translational modification found on fungal cell wall glycoproteins is the generation of a galactomannan structure (in filamentous fungi) or an outer chain mannan structure (in *S. cerevisiae* and *C. albicans*) associated with the N-linked oligosaccharide. The synthesis of these oligosaccharide structures begins with the addition of a mannose to a particular site on the N-linked oligosaccharide by the OCH-1 mannosyltransferase (Nakayama et al., 1992) (**Figure 2**). Additional mannoses are then added by a complex of enzymes to create an α-1,6-mannose chain (Hall and Gow, 2013). In the creation of the yeast outer chain mannan, the α-1,6-mannose chain can be well over 100 residues in length, while the a-1,6-mannose chain is much shorter for the *N. crassa* galactomannan (Ao and Free, 2017; Kar et al., 2019). Side chains are then added to the α-1,6-mannose backbone to create the

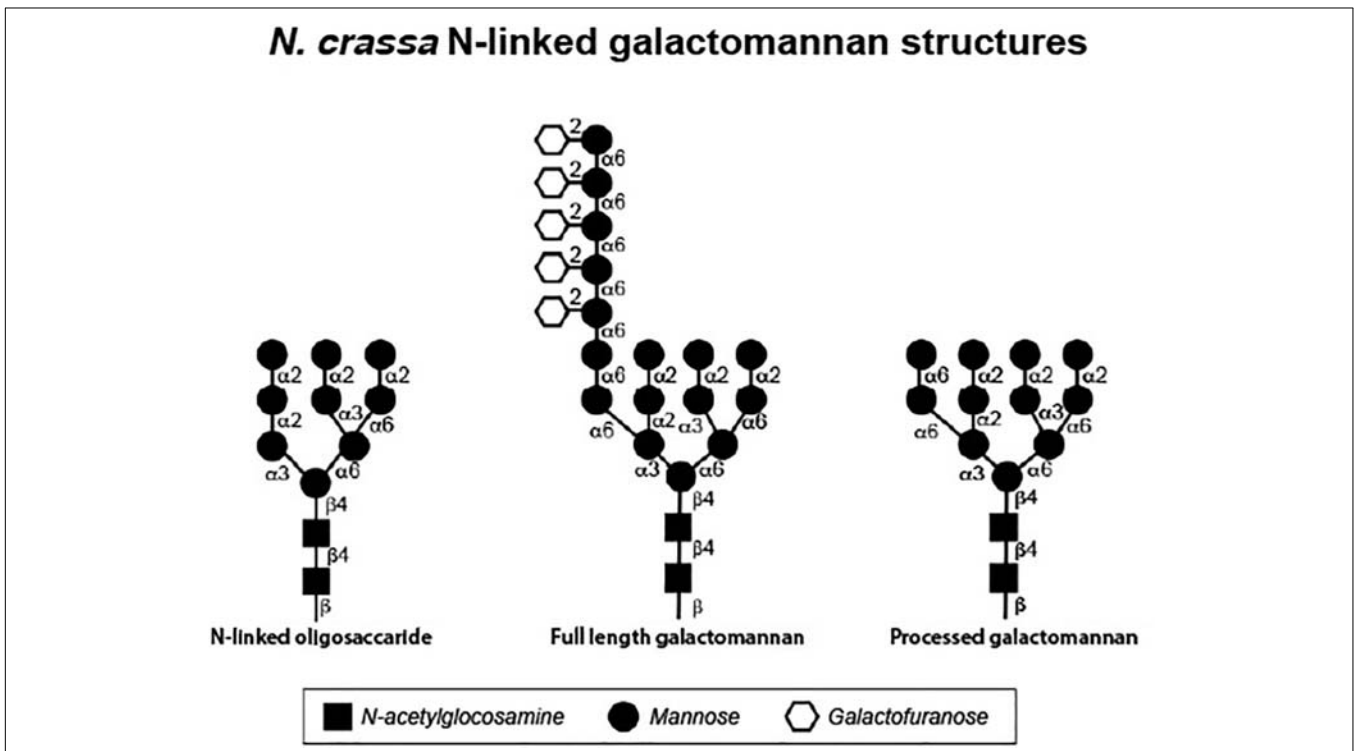

FIGURE 2 | Structures of *N. crassa* N-linked oligosaccharides as determined by glycan profiling experiments. The N-linked oligosaccharide **(left)** was isolated from cell wall glycoproteins synthesized by the Δ*och-1* mutant, which is unable to elaborate the galactomannan. The full length galacatomannan **(middle)** was isolated from cell wall glycoproteins synthesized by the Δ*dfg-5,* Δ*dcw-1* mutant, which lacks the α-1,6-mannanases needed to process the galactomannan. The processed galactomannan **(right)** was isolated from cell wall glycoproteins synthesized by the Δ*gel-1,* Δ*gel-2,* Δ*gel-5* mutant, which is unable to incorporate the processed galactomannan into the cell wall.

outer chain mannans or galactomannans. Multiple variations of the side chains have been seen in outer chain mannans. In *S. cerevisiae* and *C. albicans*, many of the side chains have an α-1,2-mannose-α-1,3-mannose structure but other side chains have been identified (Hall and Gow, 2013). In the filamentous fungi, galactofuranose residues are found in the side chains of the galactomannan. The *N. crassa* galactomannan structure has been characterized for galactomannans released from the cell wall and for galactomannans released from cell wall glycoproteins in glycan profiling experiments (Leal et al., 1996; Kar et al., 2019). The structure of the *N. crassa* full length galactomannan is shown in **Figure 2**. It consists of a short chain of 1,6-linked mannose residues with a single galactofuranose side chain that is attached to the mannose residues at their C2 position The galactofuranosyltransferase responsible for the addition of the galactofuranose side chain to the mannose backbone has not been identified.

In *N. crassa*, mutants affected in the formation of the galactomannan have been identified. The Δ*och-1* mutant (*ncu00609*) has a severe tight colonial morphology and has been carefully characterized (Maddi and Free, 2010). The mutant is unable to produce conidia and perithecia. During growth in a liquid medium, the Δ*och-1* mutant releases large amounts of cell wall proteins into the growth medium and analysis of the cell wall shows that the wall is deficient in cell wall proteins (Maddi and Free, 2010). This demonstrates that the galactomannan is required for the incorporation of cell wall proteins into the wall and suggests that the cell wall proteins are attached to the wall through the galactomannan. Glucan profiling of the N-linked oligosaccharides present on glycoproteins from the Δ*och-1* mutant, shows that the largest N-linked oligosaccharide present on the glycoproteins has a 2 *N*-acetylglucosamine: mannose 9 structure (**Figure 2**). Most of the N-linked oligosaccharides present on N-linked oligosaccharides from the Δ*och-1* mutant contain between 4 and 6 mannose residues, which indicates that mannoses are being removed from the N-linked oligosaccharides after they are transferred onto target glycoproteins.

BIOGENESIS OF THE CELL WALL AS A THREE-DIMENSIONAL MATRIX

Glucanosyltransferases carry out the key reactions needed to cross-link the cell wall glucans and chitins together. The genes encoding these enzymes are found as multigene families and are restricted to fungal genomes. Multiple members of these multigene families are expressed in a single cell type, which creates a situation of redundancy in their cross-linking activities. This redundancy is thought to help insure that a well-formed cell wall is generated across the spectrum of environmental conditions in which the fungus can grow, with different family members being optimally active in different environments (Fonzi, 1999; Calderon et al., 2010). Different combinations of these genes are also expressed in the various cell types generated during the fungal life cycle. The glucanosyltransferases carry out two closely related reactions. They first function as a glucan hydrolase to cleave a cell wall glucan near the reducing end of the glucan. These enzymes contain a characteristic arrangement of glutamate or aspartate residues that participate in the cleavage reaction. During the reaction, the newly generated reducing end of the cleaved glucan becomes covalently attached to a glutamate or aspartate in the active site. The reaction releases a small oligosaccharide from the reducing end of the glucan (Mouyna et al., 1998). In a second reaction, the enzymes function as glucanosyltransferases. The enzymes bind a second glucan and transfer the cleaved glucan from their active site to the second glucan. These transferase reactions can occur in such a way as to transfer the cleaved glucan onto the middle of a second polymer to create a cross-linked matrix with the branch points in the matrix having been created by transferase reactions. These glucanosyltransferases have specificity for both the donor glucan and the acceptor glucan. For example, members of the GH16 family of glycosylhydrolases/glycosyltransferases have been shown to function in cross-linking β-1,3-glucan and β-1,6-glucan (donors) to chitin (receptor) polymers (Pardini et al., 2006; Cabib et al., 2007; Hartl et al., 2011). In *S. cerevisiae*, members of the GH17 family of glucosylhydrolases/glycosyltransferases have been shown to have specificity for cross-linking β-1,3-glucan to β-1,3-glucans (Goldman et al., 1995; Gastebois et al., 2010b). In *S. cerevisiae*, *C. albicans*, and *A. fumigatus*, members of the GH72 family of glucanosyltransferases have also been demonstrated to be able to cross-link β-1,3-glucans together (Hartland et al., 1996; Hurtado-Guerrero et al., 2009; Mazan et al., 2011). A three-dimensional cell wall matrix of chitin and glucan is generated as these different glucanosyltransferases cross-link the cell wall chitin and glucan molecules together. The GH16, GH17, and GH72 families of glycosylhydrolases are common to virtually all fungal cells walls, and have been shown to be important for cross-linking cell wall components. Members of the GH76 family of α-1,6-mannanases are also found in all fungal cell walls. We will discuss each of these families of enzymes and how each of them is thought to function in the formation of *N. crassa* cell walls. Our research focus has been on how the cell wall glycoproteins are incorporated into the cell wall and the information available about the *N. crassa* cross-linking enzymes reflects this bias.

THE GH16 FAMILY OF GLUCANOSYLHYDROLASES/ GLUCANOYSLTRANSFERASES

In *S. cerevisiae* and *C. albicans*, mutational analysis shows that GH16 enzymes function in cross-linking β-1,6-glucan to the cell wall chitin (Pardini et al., 2006; Cabib et al., 2007). In *S. cerevisiae*, there are three GH16 enzymes, Crh1p, Crh2p, and Crr1p. Deletion of Crh1p and Crh2p is needed to create a cell wall defect, indicating that the two enzymes function in a redundant manner to attach β-1,6-glucan to the cell wall chitin. Similarly, *C. albicans* contains three GH16 enzymes, Crh11p, Crh12p, and Utr2p. The proteins function in a redundant manner and deletion of all three genes generates a cell wall defect (Pardini et al., 2006). A GH16 enzyme, Eng2p, has been characterized in *A. fumigatus* and shown to have β-1,3-glucanase and β-1,3-glucanosyltransferase activities (Hartl et al., 2011). These results

demonstrate the importance of the GH16 family of enzymes for the formation of a functional cell wall in yeast, and that the yeast GH16 enzymes function in a redundant manner to cross-link β-1,6-glucans to the cell wall chitin polymers. The results also suggest that there are substrate specificity differences between the *A. fumigatus* enzyme and the yeast enzymes.

The *N. crassa* genome encodes 15 GH16 family glucanosyltransferases (NCU01353, NCU04168, NCU04431, NCU4959, NCU5686, NCU05789, NCU05974, NCU06504, NCU07134, NCU08072, NCU09117, NCU09904, NCU00061, NCU00233, and NCU09672). Different combinations of these GH16 glucanosyltransferases are expressed in the different cell types found in the *N. crassa* life cycle (Lehr et al., 2014; Wang et al., 2014; Liu et al., 2017). Deletion mutants for the GH16 genes are available in the deletion library and all of these deletion mutants have a wild type growth morphology.

THE GH17 FAMILY OF GLUCANOSYLHYDROLASES/ GLUCANOSYLTRANSFERASES

The GH17 family of enzymes have been extensively studied in *S. cerevisiae*, *C. albicans*, and *A. fumigatus*. The enzymatic activity of purified Bgl2p, a GH17 enzyme from *S. cerevisiae*, has been characterized (Klebl and Tanner, 1989; Goldman et al., 1995; Gastebois et al., 2010b). In *in vitro* reactions, the enzyme was shown to be able to cleave a disaccharide from the reducing end of a β-1,3-glucan and to transfer the glucan to the 6 position at the non-reducing end of a second β-1,3-glucan to generate a "kinked" polymer. Two GH17 enzymes, AfBgt1p and AfBgt2p, have been characterized from *A. fumigatus* (Gastebois et al., 2009, 2010a,b). AfBgt1p, like the *S. cerevisiae* Bgl2p, was able to generate a "kinked" glucan by transferring a β-1,3-glucan to the 6 position at the non-reducing terminus of a second β-1,3-glucan in an *in vitro* reaction. AfBgt2p had a slightly different activity. In the *in vitro* assay, the enzyme was able to transfer a β-1,3-glucan to the 6 position on a glucose residue in the middle of an acceptor β-1,3-glucan to generate a branched glucan molecule (Gastebois et al., 2010a,b). The *A. fumigatus* Af*BGT1*, Af*BGT2* double mutant does not have an obvious cell wall defect, which suggests there are other enzymes that also act in cross-linking the β-1,3-glucans together and that the wall has a redundancy of β-1,3-glucan cross-linking enzymes (Gastebois et al., 2009). In *A. fumigatus*, the GH72 family is an obvious possibility for additional β-1,3-glucan cross-linking activity.

The *N. crassa* genome encodes 3 members of the GH17 family of β-1,3-glucan cross-linking enzymes, BGT-1 (NCU06381), BGT-2 (NCU09175), and BGT-3 (NCU09326). Deletion mutants for all three genes are available in the deletion library and these mutants have a wild type growth morphology. BGT-1 and BGT-2 are GPI-anchored proteins and their location on the cell wall and in secretory vesicles in vegetative hyphae and in conidia has been characterized by Martinez-Nunez and Riquelme (2015). Liu et al. (2017) found that BGT-1 and BGT-2 are expressed at high levels in the developing ascospores, while BGT-3, which does not have a GPI anchor, is expressed at high levels during vegetative growth. Martinez-Nunez and Riquelme (2015) demonstrated that the Δ*bgt-1*, Δ*bgt-2* double mutant had a normal morphology, but showed an increased resistance to calcofluor white and congo red, suggesting that the cell wall was affected in the double mutant. The data leaves open the possibility that the three *N. crassa* GH17 glucanosyltransferases are redundant and a triple mutant is needed to demonstrate the role the enzymes play in cell wall formation. Another possibility is that the *N. crassa* GH17 enzymes, like the *A. fumigatus* GH17 enzymes, are not vital for the formation of the cell wall. Further experiments are needed to define the role of the GH17 family enzymes for the formation of the *N. crassa* cell wall.

THE GH76 FAMILY OF α-1,6-MANNANASES

The GH76 α-1,6-mannanases are found in virtually all fungal cell walls. Two GH76 enzymes, Dfg5p and Dcw1p were shown to be important for the formation of the *S. cerevisiae* cell wall and the double mutant is inviable (Mosch and Fink, 1997; Kitagaki et al., 2002; Kitagaki et al., 2004). A similar situation exists in the diploid fungus, *C. albicans*, where the homozygous loss of both CaDfg5p and CaDcw1p alleles is a lethal event (Spreghini et al., 2003). Clearly the GH76 family of α-1,6-mannanases play a vital role in the formation of the cell wall.

The *N. crassa* genome encodes 9 GH-76 α-1,6-mannanase family members. As with the other families of cell wall cross-linking enzymes, different combinations of the GH76 family genes are expressed in the various cell types that define the *N. crassa* life cycle. Two of the GH76 α-1,6-mannanases, DFG-5 (NCU03770) and DCW-1 (NCU08127), are needed for the formation of the cell wall of the vegetative hyphae (Maddi et al., 2012).

The *N. crassa* GH76 enzymes, DFG-5 and DCW-1 have been characterized (Maddi et al., 2012). Unlike the other enzymes discussed in the section, the data strongly suggests that the GH76 enzymes do not function as mannan transferases, but rather function solely as α-1,6-mannan hydrolases. The Δ*dfg-5* mutant has a restricted, semi-colonial pattern of vegetative growth and the Δ*dcw-1* mutant has a subtle defect in vegetative hyphal morphology. The Δ*dfg-5*Δ*dcw-1* double mutant has a tight colonial morphology, demonstrating that the two enzymes have redundant, partially overlapping activities. The double mutant has been shown to release large amounts of cell wall proteins into the growth medium and to have a cell wall that is deficient in glycoproteins (Maddi et al., 2012). This strongly suggests that DFG-5 and DCW-1 function in the incorporation of cell wall proteins into the cell wall. Glycan profiling and sugar linkage analyses of the N-linked glycan found on the glycoproteins of mutant isolates provides evidence that DFG-5 and DCW-1 function as α-1,6-mannanases to cleave the α-1,6-mannose backbone of the N-linked oligosaccharide-associated galactomannans (Kar et al., 2019). The deduced N-linked oligosaccharide-galactomannan structure from the glycoproteins from the Δ*dfg-5*Δ*dcw-1* mutant is shown in **Figure 2**. It represents a "full length" galactomannan and

has an α-1,6-mannan backbone containing approximately 7 mannose residues. The deduced structure for the N-linked glycans that have been processed by DFG-5 and DCW-1 is also shown in **Figure 2**. It is much smaller than the "full length" galactomannan, and is only 2 sugars larger than the N-linked oligosaccharide lacking the galactomannan. The results indicated that DFG-5 and DCW-1 function in processing the galactomannan and are needed for the incorporation of cell wall proteins into the cell wall.

THE GH72 FAMILY OF GLUCANOSYLTRANSFERASES

Members of the GH72 family of glucanosyltransferases have been extensively studied in *S. cerevisiae*, *C. albicans*, *A. fumigatus*, *S. pombe*, and *N. crassa* (Hartland et al., 1996; Ram et al., 1998; Fonzi, 1999; Mouyna et al., 2000b, 2005; Caracuel et al., 2005; Ragni et al., 2007a,b; Gastebois et al., 2009, 2010a,b; Hurtado-Guerrero et al., 2009; de Medina-Redondo et al., 2010; Mazan et al., 2011; Sillo et al., 2013; Popolo et al., 2017; Samalova et al., 2017). The fungal GH72 glucanosyltransferases can be subdivided into two groups, those with a carboxyl terminal carbohydrate-binding domain and those that lack such a domain (Ragni et al., 2007b). GH72 enzymes from *S. cerevisiae* (Gas1p, Gas2p, Gas4p, and Gas5p), *C. albicans* (Phr1p and Phr2p), *A. fumigatus* (Gel1p, Gel2p, and Gel4p), and *S. pombe* (Gas1p, Gas2p, Gas4p, and Gas5p) have all been produced by recombinant DNA technology, purified, and characterized (Mouyna et al., 2000a,b; Carotti et al., 2004; Ragni et al., 2007b; Hurtado-Guerrero et al., 2009; de Medina-Redondo et al., 2010; Mazan et al., 2011; Kovacova et al., 2015; Raich et al., 2016). These recombinant glucanosyltransferases have been shown to be able to cleave a β-1,3-glucan and to transferase the β-1,3-glucan to the non-reducing end of a second β-1,3-glucan. The reaction can lengthen and shorten β-1,3-glucans and has been proposed to function in generating glucans of the proper lengths for incorporation into the cell wall. The enzyme-β-1,3-glucan intermediate has been observed for Gas2p (Hurtado-Guerrero et al., 2009; Raich et al., 2016). Recent evidence suggests that the *S. cerevisiae* Gas1p and *A. fumigatus* Gel4p enzymes are capable of transferring β-1,3-glucan to the 6 position of a glucose residue in the middle of a second β-1,3-glucan to create a branched structure appropriate for an interconnected β-1,3-glucan matrix (Aimanianda et al., 2017).

The x-ray crystal structure of the purified recombinant *S. cerevisiae* Gas2p glucanosyltransferase with an associated β-1,3-glucan has been elucidated and is helpful in evaluating how the enzyme might work (Hurtado-Guerrero et al., 2009; Raich et al., 2016). The crystal structure contains a long cleft into which the β-1,3-glucan fits and makes contacts with several amino acids. The active site is defined by a pair of glutamate residues (E176 and E275), which function in cleaving the glucan and producing an enzyme:glucan covalent intermediate. The glutamate residue participates in the formation of the covalent bond. Based on the data from the *S. cerevisiae*, *C. albicans*, and *A. fumigatus* systems, it is clear that the GH72 glucanosyltransferases can cleave β-1,3-glucan and participate in its transferase to a second polysaccharide. The data has been interpreted as indicating that the GH72 glucanosyltransferases function to cross-link β-1,3-glucans together.

The studies on the *N. crassa* GH72 family of glucanosyltransferases suggests that these glucanosyltransferases may have a second, related enzymatic function – that of cross-linking cell wall proteins into the cell wall. The *N. crassa* genome encodes a family of five GH72 glucanosyltransferases (GEL-1/NCU08909, GEL-2/NCU07253, GEL-3/NCU01162, GEL-4/NCU06850, and GEL-5/NCU06781). Four of these were found to be expressed in proteomic analyses, GEL-1, GEL-2, GEL-3, and GEL-5 (Maddi et al., 2009, 2012; Maddi and Free, 2010; Ao et al., 2016). Deletion mutants for all of these are in the Neurospora deletion library, and all of the single deletion mutants have a wild type morphology. The deletion mutants were shown to be less sensitive to Trichoderma cell wall lysing suggested they had alterations in their cell wall structure (Kamei et al., 2013). All possible combinations of single, double, triple and quadruple deletion mutants have been generated and characterized (Ao and Free, 2017). Triple mutants lacking GEL-1, GEL-2 and GEL-3 grow poorly, are unable to form conidia, and have a tight colonial morphology when grown in liquid medium. The Δ*gel-1*Δ*gel-2*Δ*gel-5* triple mutant and the quadruple mutant have an even more severe phenotype and grow with a tight colonial morphology under all conditions. The Δ*gel-1*Δ*gel-2*Δ*gel-5* mutant phenotype is indistinguishable from that of the Δ*och-1* mutant and the Δ*dfg-5*Δ*dcw-1* double mutant. The Δ*gel-1*Δ*gel-2*Δ*gel-3* and Δ*gel-1*Δ*gel-2*Δ*gel-5* mutants release large amounts of cell wall proteins into the growth medium and their cell walls are deficient in cell wall proteins (Ao and Free, 2017). In a series of experiments to elucidate the function(s) of the GEL1, GEL-2 and GEL-5 glucanosyltransferases, the cell wall proteins from the Δ*och-1* mutant, the Δ*dfg-5*Δ*dcw-1* mutant, and the Δ*gel-1*Δ*gel-2*Δ*gel-5* mutant were assayed for *in vitro* glucanosyltransferase activity. Using experiments in which combinations of cell wall proteins were mixed with β-1,3-glucan or lichenin, it was determined that lichenin (but not β-1,3-glucan) was transferred to cell wall proteins when the assays contained a source of glucanosyltransferase (from the Δ*och-1* mutant or from the Δ*dfg-5*Δ*dcw-1* mutant) and source of cell wall proteins containing the "processed" galactomannan (from the Δ*gel-1*Δ*gel-2*Δ*gel-5* mutant). All three components were needed for the transfer of lichenin to the cell wall proteins (Kar et al., 2019). Cell wall proteins without a galactomannan (from the Δ*och-1* mutant) and cell wall proteins with a full-length unprocessed galactomannan (from the Δ*dfg-5*Δ*dcw-1* mutant) are not able to act as lichenin acceptors in the assay. It was concluded that GEL-1, GEL-2, and GEL-5 can function as lichenin transferases to cross-link cell wall glycoproteins and lichenin. The activity identified for the *N. crassa* GH72 family glucanosyltransferases is similar to that ascribed for the enzymes in *S. cerevisiae*, *C. albicans*, and *A. fumigatus* in that a β-glucan is cleaved and transferred to as second polysaccharide, but the specificities of both the donor and acceptor are different. The family of GH72 glucanosyltransferases may have a much broader range of substrate specificities than previously appreciated. It is

interesting to note that the GH72 glucanosyltransferase genes from *Magnaporthe oryzae*, *Fusarium oxysporum*, and *Tuber melanosporum*, three filamentous fungi related to *N. crassa*, do not complement the *S. cerevisiae gas1* mutant (Caracuel et al., 2005; Sillo et al., 2013; Samalova et al., 2017). This suggests that the GH72 enzymes of these fungi may function in cross-linking glycoproteins into their cell walls.

SUMMARY OF HOW *N. crassa* GENERATES A THREE-DIMENSIONAL CELL WALL MATRIX

In generating the cell wall as a three-dimensional matrix, the three major cell wall components, chitin, glucans and glycoproteins, all need to be joined together. The cross-linking of chitin, glucans, and glycoproteins is vital for the creation of a functional cell wall. Although much remains to be elucidated, it is clear that the cell wall biosynthetic enzymes we have discussed above have the capacity to generate a cross-linked chitin/glucan/glycoprotein matrix. In the *N. crassa* cell wall, the β-1,3-glucans and lichenin are the most abundant glucan component and represent approximately 65% of the total cell wall mass (Maddi and Free, 2010; Maddi et al., 2012; Fu et al., 2014a; Ao and Free, 2017). Chitin and the cell wall glycoproteins are attached to the cell wall glucans in *N. crassa* and other fungi. The GH16 family of glucanosyltransferases from *S. cerevisiae*, *C. albicans*, and *A. fumigatus* have been shown to have the capacity to cross-link glucan to chitin (Pardini et al., 2006; Cabib et al., 2007; Hartl et al., 2011), and it is presumed that they function in this capacity in *N. crassa*. Which of the major glucan polymers, β-1,3-glucan or lichenin, is used in cross-linking the *N. crassa* chitin to the matrix has not been experimentally addressed. Cross-linking of the β-1,3-glucans and lichenin together would be expected to be a critical step in the formation of the cell wall. The *S. cerevisiae* GH17 family of glucanosyltransferase Bgl2p has been shown to be able to cross-link β-1,3-glucans together and the *Neurospora* GH17 enzymes are likely to function in cross-linking the *N. crassa* cell wall together. The question of how the α-1,3-glucan found in the *N. crassa* aerial hyphae and conidia is cross-linked into the cell wall has not been experimentally examined.

The incorporation of cell wall glycoproteins into the wall has been extensively examined in *N. crassa*. As shown in **Figure 2**, the *N. crassa*, cell wall glycoproteins are post-translationally modified by the addition of a galactomannan to their N-linked oligosaccharides (Maddi and Free, 2010). The galactomannan is subsequently cleaved/processed by the α-1,6-mannanases DFG-5 and DCW-1 (Maddi et al., 2012; Kar et al., 2019). The processed galactomannan is then used as the acceptor polysaccharide by the GH72 family of glucanosyltransferases (lichenin transferases) (Kar et al., 2019). These enzymes cleave lichenin and attach it to the processed galactomannan, which effectively cross-links the glycoproteins into the cell wall. The method of cross-linking the glycoproteins into the wall is virtually identical to the process used to cross-link the other cell wall components together. The enzymes needed to cross-link the processed galactomannan into

TABLE 1 | Table of *N. crassa* cell wall proteins.

Protein name	NCU#	GPI anchored	Total # of peptides	Cell type expression
GH17 (β-1,3-endoglucanase)	09175	Yes	20	V and C
GH16 (β-1,3-endoglucanase transferase)	05974	Yes	23	V and C
GEL-1 (GH76 β-glucan transferase)	08909	Yes	16	V and C
GEL-2 (GH76 β-glucan transferase)	07253	Yes	14	V and C
GEL-5 (GH76 β-glucan transferase)	06781	Yes	12	V and C
CHIT-1 (endochitinase)	02184	Yes	16	V and C
ACW-1	08936	Yes	18	V and C
ACW-2	00957	Yes	9	V and C
ACW-3	05667	Yes	17	V and C
ACW-5	07776	Yes	3	V and C
ACW-6	03530	Yes	3	V and C
ACW-7	09133	Yes	7	V and C
ACW-10	03013	Yes	3	V and C
GH17 (β-1,3-endoglucanase)	09326	No	8	V and C
GH3 (β-glucosidase)	08755	No	14	V and C
CAT-3 (catalase)	00355	No	10	V and C
NCW-3	07817	No	1	V and C
GH16 (β1,3-endoglucanase)	01353	Yes	9	V
ACW-8	07277	Yes	2	V
ACW-9	06185	Yes	2	V
ACW-11	02041	Yes	1	V
ACW-12	08171	Yes	12	V
NCW-1	05137	No	18	V
NCW-2	01752	No	7	V
GEL-3 (β-glucan transferase)	01162	Yes	5	C
GH64 (β-1,3-glucanase)	01080	Yes	1	C
ACW-4	09263	Yes	1	C
ACW-13	04493	Yes	1	C
NAG-1 (β-*N*-acetyl hexosaminidase)	10852	No	10	C
CGL-1 (GH55) (β-1,3-glucanase)	07523	No	8	C
GH55 (β-1,3-glucanase)	09791	No	5	C
GH71 (α-1,3-glucanase)	06010	No	1	C
GH31 (α-glucosidase)	09281	No	1	C
NCW-4	02948	No	2	C
NCW-5	00716	No	2	C
NCW-6	00586	No	5	C
NCW-7	08907	No	2	C
NCW-8	04605	No	2	C
NCW-9	03083	No	1	C
HET-C	03125	No	4	C
RDS-1	05143	No	1	C

The various cell wall glycoproteins that have been identified in N. crassa cell wall preparations. The NCU # refers to the gene number assigned in the genome sequence to the protein. The presence or absence of a GPI anchor is noted. The number of unique tryptic peptides identified is also shown. The cell type(s) in which the glycoproteins were found is given with V denoting vegetative hyphae (grown in a liquid medium) and C denoting conidia.

the wall could have easily evolved from glucan cross-linking transferases through small changes in their donor-binding and acceptor-binding clefts to accommodate a new set of donor and acceptor polysaccharides. Although the general principles defined in *N. crassa* for cross-linking glycoproteins into the cell wall may be generally applicable, there will clearly be some differences between different fungal species. For example, the DFG-5 and DCW-1 enzymes are needed for incorporation of cell wall proteins in *C. albicans* (Ao et al., 2015), but *C. albicans* lacks lichenin. A different donor glucan would be needed to attach cell wall proteins in *C. albicans*. The available evidence indicates that β-1,6-glucans are used in attaching glycoproteins into the cell wall in both *C. albicans* and *S. cerevisiae* (Lu et al., 1995; Kollar et al., 1997; Kapteyn et al., 2000). It is also important to recognize that other modes of attaching glycoprotein to the cell wall have been observed. For example, in *S. cerevisiae*, the attachment of a β-1,6-glucan to the GPI anchor present on GPI-anchored cell wall glycoproteins has been observed, which would tether GPI-anchored proteins into the cell wall structure (Kollar et al., 1997; Kapteyn et al., 2000). While some fungi may have multiple ways of attaching glycoproteins to the wall, the incorporation of glycoproteins into the *N. crassa* cell wall seems to be totally dependent upon the processed galactomannan route described above.

The incorporation of melanin into the fungal cell wall is an important process, and is vital to the survival of the melanized cells. For *N. crassa* the question of how melanin is incorporated into the cell wall has been answered by the demonstration that LACM-1, the laccase needed for the final step in the process of melanin formation is located in the cell wall space in developing perithecia at the point in time when melanin is being formed (Ao et al., 2019). At the same point in time, the enzymes involved in the synthesis of DHN, the melanin precursor are located on intracellular vesicles. The results indicate that DHN is synthesized in intracellular vesicles. The DHN is then secreted into the cell wall space, where LACM-1 acts on the DHN to generate melanin granules (Ao et al., 2019). The melanin is made "*in situ*" and as the granules form they encase the other cell wall components.

CHANGING THE CELL WALL THROUGHOUT THE *N. crassa* LIFE CYCLE

One of the interesting aspects of the *N. crassa* cell wall is how the cell wall structure and composition changes during the life cycle of the organism. **Table 1** shows the major cell wall proteins identified via proteomic analyses of the vegetative hyphae and conidia (Bowman et al., 2006; Maddi et al., 2009, 2012; Maddi and Free, 2010; Ao et al., 2016). What is evident is that different combinations of cell wall glycoproteins are expressed in the two cell types. Seventeen of the cell wall glycoproteins in the vegetative cell wall are also present in the conidial cell wall. However, the vegetative hyphal cell wall contains seven major vegetative cell wall glycoproteins which are missing from the conidia cell wall. While sharing seventeen cell wall glycoproteins with the vegetative hyphal cell wall, the conidial cell has seventeen cell wall glycoproteins that are not found in the vegetative cell wall (**Table 1**). Interestingly, most of these additional conidia-specific glycoproteins lack a GPI-anchor. An analysis of the deletion mutants for these conidia-specific cell wall glycoproteins showed that two of them, CGL-1/NCU07523 and NAG-1/NCU10852 play significant roles in conidia development. CGL-1 is a β-glucanase and NAG-1 is an exochitinase, and both activities are needed to remodel the conidia cell wall

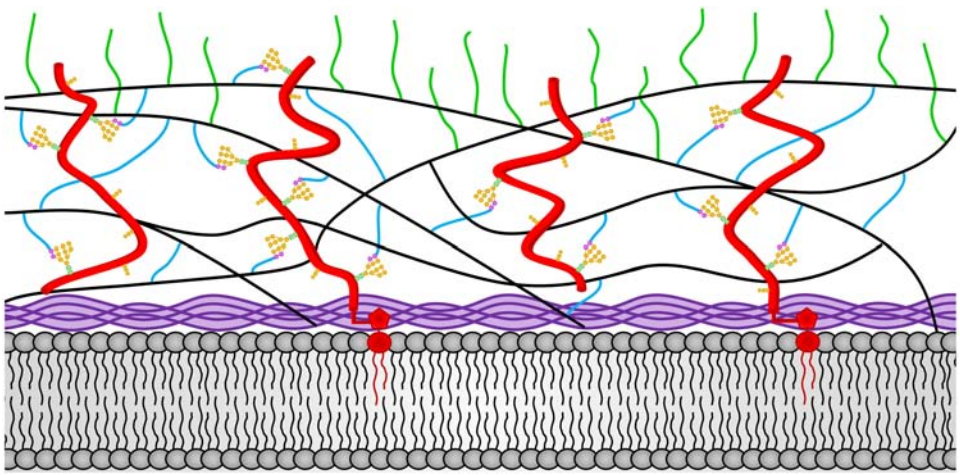

FIGURE 3 | The *N. crassa* conidia cell wall. The locations of the components of the conidial cell wall are depicted. Chitin is shown in purple and is located adjacent to the plasma membrane at the bottom of the diagram. The β-1,3-glucan is shown in black and located in the middle of the cell wall. Cell wall glycoproteins are shown in red. GPI anchors are shown in red and extent into the plasma membrane. N-linked oligosaccharides are shown with *N*-acetylglucosamine residues in green squares, mannoses from the N-linked oligosaccharide shown in orange circles, and processed galactomannans shown in magenta circles. O-linked oligosaccharides are also shown in orange. Lichenin is shown in blue and is attached to the processed galactomannan and to β-1,3-glucans. The α-1,3-glucans are shown in green and are attached to β-1,3-glucan and/or lichenin at the cell wall periphery.

between adjacent conidia to facilitate the separation of the individual conidia in a conidial chain from each other (Ao et al., 2016). The conidia-specific expression of the conidia cell wall associated hydrophobin, EAS (easily wettable)/CCG-2 (NCU08457) is yet another example of an important cell wall difference between vegetative hyphae and conidia (Bell-Pedersen et al., 1992). The EAS/CCG-2 hydrophobin forms a hydrophobic surface rodlet layer around the conidia cell wall and facilitates the dispersal of conidia in an aqueous environment. These conidia-specific cell wall proteins play important roles in the development of the conidia.

A second important difference between the cell wall of the vegetative hyphal cell and the conidia is found in their glucan components. The conidia contains α-1,3-glucan, which is lacking from the vegetative cell wall. Like the expression of the CGL-1 and NAG-1 cell wall remodeling enzymes, synthesis of α-1,3-glucan plays an important role in conidial development (Fu et al., 2014b). Mutants lacking α-1,3-glucan are unable to produce normal conidia. This demonstrates that the formation of conidia requires major changes in the glucan components of the cell wall as well as the expression of conidia-specific glycoproteins. **Figure 3** shows a representation of the conidial cell wall with the α-1,3-glucan being localized at the periphery of the cell wall.

There are no published proteomic analyses of the cell walls produced during the sexual stages of the *N. crassa* life cycle. However, there are three RNAseq analyses of gene expression during sexual development (Lehr et al., 2014; Wang et al., 2014; Liu et al., 2017). In looking through the data from these RNAseq analyses, it is clear that members of the GH16, GH17, GH72, and GH76 gene families which are not expressed in vegetative hyphae are being expressed in the developing ascospores (sexual spores) and in the peridium (a female-derived tissue that surrounds and protects the developing ascospores). In addition to these changes in the cross-linking enzymes, many other genes encoding putative cell wall remodeling enzymes and structural proteins are being differentially expressed during the sexual stages. These changes in gene expression extend to genes encoding putative mixed β-1,3-/β-1,4- glucan synthases. Deletion mutants for the chitin synthases demonstrate that some chitin synthases are critical for the development of perithecia, ascospores, and conidia, further demonstrating that there are important cell wall differences between these different cell types (Fajardo-Somera et al., 2015). Not only are there major changes in the expression of cell wall glycoproteins and glucans, the developing ascospores and peridium cells become heavily melanized. The expression of the DHN pathway enzymes and the LACM-1 laccase are regulated in a cell-type specific manner in the developing ascospores and peridium (Ao et al., 2019). Unfortunately, deletion mutants for the different glycoproteins and glucan synthases expressed uniquely in the ascospores and peridium have not been carefully analyzed. Although the ascospore and peridium cell walls have not been characterized by proteomics, the available data makes it clear that there are major differences between the cell walls produced during sexual development and the cell walls from vegetative hyphae and conidia.

In summary, each of the different cell types in the *N. crassa* life cycle produces a cell wall with a unique combination of glycoproteins, glucans, and melanin. Some of these components, like CGL-1, NAG-1, α-1-3-glucan, and melanin, have been shown to carry out important cell-type specific functions (Fu et al., 2014b; Ao et al., 2016, 2019). There is also a cell-type expression pattern for the members of the GH16, GH17, GH72, and GH76 gene families, with different combinations of these genes being expressed in each cell type (Lehr et al., 2014; Wang et al., 2014; Ao and Free, 2017; Liu et al., 2017). Many other cell wall remodeling enzymes and structural proteins are expressed in cell-type specific fashion (Ao et al., 2016). While the glucan/chitin/glycoprotein matrix remains the basic cell wall structure throughout the entire life cycle of the fungus, this structure is being extensively modified by adding new glycoproteins, changing glucans, and/or the incorporation of melanin to control cell morphology and to facilitate cell development.

AUTHOR CONTRIBUTIONS

PP and SF contributed to the writing and editing of the review.

FUNDING

Funding has been provided by the UB Foundation.

ACKNOWLEDGMENTS

We express our gratitude to Jim Stamos and T. J. Krzystek for their help in preparing the figures.

REFERENCES

Aimanianda, V., Simenel, C., Garnaud, C., Clavaud, C., Tada, R., Barbin, L., et al. (2017). The dual activity responsible for the elongation and branching of beta-(1,3)-glucan in the fungal cell wall. *mBio* 8:e00619-17. doi: 10.1128/mBio.00619-17

Ao, J., Aldabbous, M., Notaro, M. J., Lojacono, M., and Free, S. J. (2016). A proteomic and genetic analysis of the *Neurospora crassa* conidia cell wall proteins identifies two glycosyl hydrolases involved in cell wall remodeling. *Fungal Genet. Biol.* 94, 47–53. doi: 10.1016/j.fgb.2016.07.003

Ao, J., Bandyopadhyay, S., and Free, S. J. (2019). Characterization of the *Neurospora crassa* DHN melanin biosynthetic pathway in developing ascospores and peridium cells. *Fungal Biol.* 123, 1–9. doi: 10.1016/j.funbio.2018.10.005

Ao, J., Chinnici, J. L., Maddi, A., and Free, S. J. (2015). The N-linked outer chain mannans and the Dfg5p and Dcw1p endo-alpha-1,6-mannanases are needed for incorporation of candida albicans glycoproteins into the cell wall. *Eukaryot. Cell* 14, 792–803. doi: 10.1128/EC.00032-15

Ao, J., and Free, S. J. (2017). Genetic and biochemical characterization of the GH72 family of cell wall transglycosylases in *Neurospora crassa*. *Fungal Genet. Biol.* 101, 46–54. doi: 10.1016/j.fgb.2017.03.002

Aranda-Martinez, A., Lopez-Moya, F., and Lopez-Llorca, L. V. (2016). Cell wall composition plays a key role on sensitivity of filamentous fungi to chitosan. *J. Basic Microbiol.* 56, 1059–1070. doi: 10.1002/jobm.201500775

Baker, L. G., Specht, C. A., and Lodge, J. K. (2011). Cell wall chitosan is necessary for virulence in the opportunistic pathogen *Cryptococcus neoformans*. *Eukaryot. Cell* 10, 1264–1268. doi: 10.1128/EC.05138-11

Beauvais, A., Bruneau, J. M., Mol, P. C., Buitrago, M. J., Legrand, R., and Latge, J. P. (2001). Glucan synthase complex of *Aspergillus fumigatus*. *J. Bacteriol.* 183, 2273–2279. doi: 10.1128/jb.183.7.2273-2279.2001

Beauvais, A., Maubon, D., Park, S., Morelle, W., Tanguy, M., Huerre, M., et al. (2005). Two alpha(1-3) glucan synthases with different functions in *Aspergillus fumigatus*. *Appl. Environ. Microbiol.* 71, 1531–1538. doi: 10.1128/aem.71.3.1531-1538.2005

Bell-Pedersen, D., Dunlap, J. C., and Loros, J. J. (1992). The Neurospora circadian clock-controlled gene, ccg-2, is allelic to eas and encodes a fungal hydrophobin required for formation of the conidial rodlet layer. *Genes Dev.* 6, 2382–2394. doi: 10.1101/gad.6.12a.2382

Bohn, J. A., and Bemiller, J. N. (1995). (1→3)-ß-d-Glucans as biological response modifiers: a review of structure-functional activity relationships. *Carbohydr. Polym.* 28, 3–14. doi: 10.1016/0144-8617(95)00076-3

Bowman, S. M., Piwowar, A., Al Dabbous, M., Vierula, J., and Free, S. J. (2006). Mutational analysis of the glycosylphosphatidylinositol (GPI) anchor pathway demonstrates that GPI-anchored proteins are required for cell wall biogenesis and normal hyphal growth in *Neurospora crassa*. *Eukaryot. Cell* 5, 587–600. doi: 10.1128/ec.5.3.587-600.2006

Bowman, S. M., Piwowar, A., Arnone, E. D., Matsumoto, R., Koudelka, G. B., and Free, S. J. (2009). Characterization of GPIT-1 and GPIT-2, two auxiliary components of the *Neurospora crassa* GPI transamidase complex. *Mycologia* 101, 764–772. doi: 10.3852/09-022

Bowman, S. M., Piwowar, A., Ciocca, M., and Free, S. J. (2005). Mannosyltransferase is required for cell wall biosynthesis, morphology and control of asexual development in *Neurospora crassa*. *Mycologia* 97, 872–879. doi: 10.3852/mycologia.97.4.872

Cabib, E., Blanco, N., Grau, C., Rodriguez-Pena, J. M., and Arroyo, J. (2007). Crh1p and Crh2p are required for the cross-linking of chitin to beta(1-6)glucan in the *Saccharomyces cerevisiae* cell wall. *Mol. Microbiol.* 63, 921–935.

Calderon, J., Zavrel, M., Ragni, E., Fonzi, W. A., Rupp, S., and Popolo, L. (2010). PHR1, a pH-regulated gene of candida albicans encoding a glucan-remodelling enzyme, is required for adhesion and invasion. *Microbiology* 156, 2484–2494. doi: 10.1099/mic.0.038000-0

Caracuel, Z., Martinez-Rocha, A. L., Di Pietro, A., Madrid, M. P., and Roncero, M. I. (2005). *Fusarium oxysporum* gas1 encodes a putative beta-1,3-glucanosyltransferase required for virulence on tomato plants. *Mol. Plant Microbe Interact.* 18, 1140–1147. doi: 10.1094/mpmi-18-1140

Carotti, C., Ragni, E., Palomares, O., Fontaine, T., Tedeschi, G., Rodriguez, R., et al. (2004). Characterization of recombinant forms of the yeast gas1 protein and identification of residues essential for glucanosyltransferase activity and folding. *Eur. J. Biochem.* 271, 3635–3645. doi: 10.1111/j.1432-1033.2004.04297.x

Chaffin, W. L. (2008). Candida albicans cell wall proteins. *Microbiol. Mol. Biol. Rev.* 72, 495–544. doi: 10.1128/MMBR.00032-07

Choquer, M., Boccara, M., Goncalves, I. R., Soulie, M. C., and Vidal-Cros, A. (2004). Survey of the botrytis cinerea chitin synthase multigenic family through the analysis of six euascomycetes genomes. *Eur. J. Biochem.* 271, 2153–2164. doi: 10.1111/j.1432-1033.2004.04135.x

Christodoulidou, A., Bouriotis, V., and Thireos, G. (1996). Two sporulation-specific chitin deacetylase-encoding genes are required for the ascospore wall rigidity of *Saccharomyces cerevisiae*. *J. Biol. Chem.* 271, 31420–31425. doi: 10.1074/jbc.271.49.31420

Chumley, F., and Valent, B. (1990). Genetic anlysis of melanin-deficient, nonpathogenic mutants of magnaporthe grisea. *Mol. Plant Microbe Interact.* 3, 135–143.

Colot, H. V., Park, G., Turner, G. E., Ringelberg, C., Crew, C. M., Litvinkova, L., et al. (2006). A high-throughput gene knockout procedure for neurospora reveals functions for multiple transcription factors. *Proc. Natl. Acad. Sci. U.S.A.* 103, 10352–10357. doi: 10.1073/pnas.0601456103

Davis, R. H., and DeSerres, F. J. (1970). Genetic and microbiological research techniques for *Neurospora crassa*. *Meth. Enzymol.* 27, 79–143. doi: 10.1016/0076-6879(71)17168-6

De Groot, P. W., Ram, A. F., and Klis, F. M. (2005). Features and functions of covalently linked proteins in fungal cell walls. *Fungal Genet. Biol.* 42, 657–675. doi: 10.1016/j.fgb.2005.04.002

de Groot, P. W., Yin, Q. Y., Weig, M., Sosinska, G. J., Klis, F. M., and de Koster, C. G. (2007). Mass spectrometric identification of covalently bound cell wall proteins from the fission yeast *Schizosaccharomyces pombe*. *Yeast* 24, 267–278. doi: 10.1002/yea.1443

de Medina-Redondo, M., Arnaiz-Pita, Y., Clavaud, C., Fontaine, T., del Rey, F., Latge, J. P., et al. (2010). beta(1,3)-glucanosyl-transferase activity is essential for cell wall integrity and viability of *Schizosaccharomyces pombe*. *PLoS One* 5:e14046. doi: 10.1371/journal.pone.0014046

Deshpande, N., Wilkins, M. R., Packer, N., and Nevalainen, H. (2008). Protein glycosylation pathways in filamentous fungi. *Glycobiology* 18, 626–637. doi: 10.1093/glycob/cwn044

Dichtl, K., Samantaray, S., Aimanianda, V., Zhu, Z., Prevost, M. C., Latge, J. P., et al. (2015). *Aspergillus fumigatus* devoid of cell wall beta-1,3-glucan is viable, massively sheds galactomannan and is killed by septum formation inhibitors. *Mol. Microbiol.* 95, 458–471. doi: 10.1111/mmi.12877

Din, A. B., Specht, C. A., Robbins, P. W., and Yarden, O. (1996). chs-4, a class IV chitin synthase gene from *Neurospora crassa*. *Mol. Gen. Genet.* 250, 214–222. doi: 10.1007/bf02174181

Din, A. B., and Yarden, O. (1994). The *Neurospora crassa* chs-2 gene encodes a non-essential chitin synthase. *Microbiology* 140(Pt 9), 2189–2197. doi: 10.1099/13500872-140-9-2189

Eisenhaber, B., Maurer-Stroh, S., Novatchkova, M., Schneider, G., and Eisenhaber, F. (2003). Enzymes and auxiliary factors for GPI lipid anchor biosynthesis and post-translational transfer to proteins. *Bioessays* 25, 367–385. doi: 10.1002/bies.10254

Eisenman, H. C., and Casadevall, A. (2012). Synthesis and assembly of fungal melanin. *Appl. Microbiol. Biotechnol.* 93, 931–940. doi: 10.1007/s00253-011-3777-2

Enderlin, C. S., and Selitrennikoff, C. P. (1994). Cloning and characterization of a *Neurospora crassa* gene required for (1, 3) beta-glucan synthase activity and cell wall formation. *Proc. Natl. Acad. Sci. U.S.A.* 91, 9500–9504. doi: 10.1073/pnas.91.20.9500

Fajardo-Somera, R. A., Johnk, B., Bayram, O., Valerius, O., Braus, G. H., and Riquelme, M. (2015). Dissecting the function of the different chitin synthases in vegetative growth and sexual development in *Neurospora crassa*. *Fungal Genet. Biol.* 75, 30–45. doi: 10.1016/j.fgb.2015.01.002

Ferguson, M. A. (1999). The structure, biosynthesis and functions of glycosylphosphatidylinositol anchors, and the contributions of trypanosome research. *J. Cell Sci.* 112(Pt 17), 2799–2809.

Fontaine, T., Beauvais, A., Loussert, C., Thevenard, B., Fulgsang, C. C., Ohno, N., et al. (2010). Cell wall alpha1-3glucans induce the aggregation of germinating conidia of *Aspergillus fumigatus*. *Fungal Genet. Biol.* 47, 707–712. doi: 10.1016/j.fgb.2010.04.006

Fonzi, W. A. (1999). PHR1 and PHR2 of candida albicans encode putative glycosidases required for proper cross-linking of beta-1,3- and beta-1,6-glucans. *J. Bacteriol.* 181, 7070–7079.

Free, S. J. (2013). Fungal cell wall organization and biosynthesis. *Adv. Genet.* 81, 33–82. doi: 10.1016/B978-0-12-407677-8.00002-6

Fu, C., Sokolow, E., Rupert, C. B., and Free, S. J. (2014a). The *Neurospora crassa* CPS-1 polysaccharide synthase functions in cell wall biosynthesis. *Fungal Genet. Biol.* 69, 23–30. doi: 10.1016/j.fgb.2014.05.009

Fu, C., Tanaka, A., and Free, S. J. (2014b). *Neurospora crassa* 1, 3-alpha-glucan synthase, AGS-1, is required for cell wall biosynthesis during macroconidia development. *Microbiology* 160, 1618–1627. doi: 10.1099/mic.0.080002-0

Fuentes, A. M., Connerton, I., and Free, S. J. (1994). Production of tyrosinase defective mutants in *Neurospora crassa*. *Fungal Genet. Newsl.* 41, 38–39. doi: 10.4148/1941-4765.1371

Fukuda, K., Yamada, K., Deoka, K., Yamashita, S., Ohta, A., and Horiuchi, H. (2009). Class III chitin synthase ChsB of *Aspergillus nidulans* localizes at the sites of polarized cell wall synthesis and is required for conidial development. *Eukaryot. Cell* 8, 945–956. doi: 10.1128/EC.00326-08

Galagan, J. E., Calvo, S. E., Borkovich, K. A., Selker, E. U., Read, N. D., Jaffe, D., et al. (2003). The genome sequence of the filamentous fungus *Neurospora crassa*. *Nature* 422, 859–868.

Garnjobst, L., and Tatum, E. L. (1967). A survey of new morphological mutants in *Neurospora crassa*. *Genetics* 57, 579–604.

Gastebois, A., Clavaud, C., Aimanianda, V., and Latge, J. P. (2009). *Aspergillus fumigatus*: cell wall polysaccharides, their biosynthesis and organization. *Future Microbiol.* 4, 583–595. doi: 10.2217/fmb.09.29

Gastebois, A., Fontaine, T., Latge, J. P., and Mouyna, I. (2010a). beta (1-3) glucanosyltransferase Gel4p is essential for *Aspergillus fumigatus*. *Eukaryot. Cell* 9, 1294–1298. doi: 10.1128/EC.00107-10

Gastebois, A., Mouyna, I., Simenel, C., Clavaud, C., Coddeville, B., Delepierre, M., et al. (2010b). Characterization of a new beta (1-3)-glucan branching activity of *Aspergillus fumigatus*. *J. Biol. Chem.* 285, 2386–2396. doi: 10.1074/jbc.M109.077545

Girrbach, V., and Strahl, S. (2003). Members of the evolutionarily conserved PMT family of protein O-mannosyltransferases form distinct protein complexes among themselves. *J. Biol. Chem.* 278, 12554–12562. doi: 10.1074/jbc.m212582200

Goldman, R. C., Sullivan, P. A., Zakula, D., and Capobianco, J. O. (1995). Kinetics of beta-1,3 glucan interaction at the donor and acceptor sites of the fungal glucosyltransferase encoded by the BGL2 gene. *Eur. J. Biochem.* 227, 372–378. doi: 10.1111/j.1432-1033.1995.tb20399.x

Gow, N. A. R., Latge, J. P., and Munro, C. A. (2017). The fungal cell wall: structure, biosynthesis, and function. *Microbiol. Spectr.* 5, 1–25.

Grun, C. H., Hochstenbach, F., Humbel, B. M., Verkleij, A. J., Sietsma, J. H., Klis, F. M., et al. (2005). The structure of cell wall alpha-glucan from fission yeast. *Glycobiology* 15, 245–257. doi: 10.1093/glycob/cwi002

Hall, R. A., and Gow, N. A. (2013). Mannosylation in candida albicans: role in cell wall function and immune recognition. *Mol. Microbiol.* 90, 1147–1161. doi: 10.1111/mmi.12426

Hartl, L., Gastebois, A., Aimanianda, V., and Latge, J. P. (2011). Characterization of the GPI-anchored endo beta-1, 3-glucanase Eng2 of *Aspergillus fumigatus*. *Fungal Genet. Biol.* 48, 185–191. doi: 10.1016/j.fgb.2010.06.011

Hartland, R. P., Fontaine, T., Debeaupuis, J. P., Simenel, C., Delepierre, M., and Latge, J. P. (1996). A novel beta-(1-3)-glucanosyltransferase from the cell wall of *Aspergillus fumigatus*. *J. Biol. Chem.* 271, 26843–26849.

Hausler, A., Ballou, L., Ballou, C. E., and Robbins, P. W. (1992). Yeast glycoprotein biosynthesis: MNT1 encodes an alpha-1, 2-mannosyltransferase involved in O-glycosylation. *Proc. Natl. Acad. Sci. U.S.A.* 89, 6846–6850. doi: 10.1073/pnas.89.15.6846

Hochstenbach, F., Klis, F. M., van den Ende, H., van Donselaar, E., Peters, P. J., and Klausner, R. D. (1998). Identification of a putative alpha-glucan synthase essential for cell wall construction and morphogenesis in fission yeast. *Proc. Natl. Acad. Sci. U.S.A.* 95, 9161–9166. doi: 10.1073/pnas.95.16.9161

Honegger, R., and Haisch, A. (2001). Immunocytochemical location of the (1-3)(1-4)-B-glucan lichenin in the lichen-forming ascomycete *Cetraria islandica* (icelandic moss). *New Phytol.* 150, 739–746. doi: 10.1046/j.1469-8137.2001.00122.x

Howe, H. B. Jr. (1976). Phenotypic diversity among alleles at the per-1 locus of *Neurospora crassa*. *Genetics* 82, 595–603.

Howe, H. B. Jr., and Benson, E. W. (1974). A perithecial color mutant of *Neurospora crassa*. *Mol. Gen. Genet.* 131, 79–83. doi: 10.1007/bf00269389

Hunsley, D., and Gooday, G. W. (1974). The structure and development of septa in *Neurospora crassa*. *Protoplasma* 82, 125–146. doi: 10.1007/bf01276876

Hurtado-Guerrero, R., Schuttelkopf, A. W., Mouyna, I., Ibrahim, A. F., Shepherd, S., Fontaine, T., et al. (2009). Molecular mechanisms of yeast cell wall glucan remodeling. *J. Biol. Chem.* 284, 8461–8469. doi: 10.1074/jbc.M807990200

Johnson, T. E. (1977). Mosaic analysis of autonomy of spore development in neurospora. *Exp. Mycol.* 1, 253–258. doi: 10.1016/s0147-5975(77)80023-6

Kamei, M., Yamashita, K., Takahashi, M., Fukumori, F., Ichiishi, A., and Fujimura, M. (2013). Deletion and expression analysis of beta-(1,3)-glucanosyltransferase genes in *Neurospora crassa*. *Fungal Genet. Biol.* 52, 65–72. doi: 10.1016/j.fgb.2012.12.001

Kapteyn, J. C., Hoyer, L. L., Hecht, J. E., Muller, W. H., Andel, A., Verkleij, A. J., et al. (2000). The cell wall architecture of candida albicans wild-type cells and cell wall-defective mutants. *Mol. Microbiol.* 35, 601–611. doi: 10.1046/j.1365-2958.2000.01729.x

Kar, B., Patel, P., Ao, J., and Free, S. J. (2019). *Neurospora crassa* family GH72 glucanosyltransferases function to crosslink cell wall glycoprotein N-linked galactomannan to cell wall lichenin. *Fungal Genet. Biol.* 123, 60–69. doi: 10.1016/j.fgb.2018.11.007

Kitagaki, H., Ito, K., and Shimoi, H. (2004). A temperature-sensitive dcw1 mutant of *Saccharomyces cerevisiae* is cell cycle arrested with small buds which have aberrant cell walls. *Eukaryot. Cell* 3, 1297–1306. doi: 10.1128/ec.3.5.1297-1306.2004

Kitagaki, H., Wu, H., Shimoi, H., and Ito, K. (2002). Two homologous genes, DCW1 (YKL046c) and DFG5, are essential for cell growth and encode glycosylphosphatidylinositol (GPI)-anchored membrane proteins required for cell wall biogenesis in *Saccharomyces cerevisiae*. *Mol. Microbiol.* 46, 1011–1022. doi: 10.1046/j.1365-2958.2002.03244.x

Klebl, F., and Tanner, W. (1989). Molecular cloning of a cell wall exo-beta-1,3-glucanase from *Saccharomyces cerevisiae*. *J. Bacteriol.* 171, 6259–6264. doi: 10.1128/jb.171.11.6259-6264.1989

Klis, F. M., Boorsma, A., and De Groot, P. W. (2006). Cell wall construction in *Saccharomyces cerevisiae*. *Yeast* 23, 185–202.

Klis, F. M., Brul, S., and De Groot, P. W. (2010). Covalently linked wall proteins in ascomycetous fungi. *Yeast* 27, 489–493. doi: 10.1002/yea.1747

Kollar, R., Reinhold, B. B., Petrakova, E., Yeh, H. J., Ashwell, G., Drgonova, J., et al. (1997). Architecture of the yeast cell wall. beta(1–>6)-glucan interconnects mannoprotein, beta(1–>)3-glucan, and chitin. *J Biol Chem.* 272, 17762–17775. doi: 10.1074/jbc.272.28.17762

Kovacova, K., Degani, G., Stratilova, E., Farkas, V., and Popolo, L. (2015). Catalytic properties of Phr family members of cell wall glucan remodeling enzymes: implications for the adaptation of candida albicans to ambient pH. *FEMS Yeast Res.* 15:fou011. doi: 10.1093/femsyr/fou011

Kupper, U., Niedermann, D. M., Travaglini, G., and Lerch, K. (1989). Isolation and characterization of the tyrosinase gene from *Neurospora crassa*. *J. Biol. Chem.* 264, 17250–17258.

Langfelder, K., Jahn, B., Gehringer, H., Schmidt, A., Wanner, G., and Brakhage, A. A. (1998). Identification of a polyketide synthase gene (pksP) of *Aspergillus fumigatus* involved in conidial pigment biosynthesis and virulence. *Med. Microbiol. Immunol.* 187, 79–89. doi: 10.1007/s004300050077

Langfelder, K., Streibel, M., Jahn, B., Haase, G., and Brakhage, A. A. (2003). Biosynthesis of fungal melanins and their importance for human pathogenic fungi. *Fungal Genet. Biol.* 38, 143–158. doi: 10.1016/s1087-1845(02)00526-1

Latge, J. P. (2007). The cell wall: a carbohydrate armour for the fungal cell. *Mol. Microbiol.* 66, 279–290. doi: 10.1111/j.1365-2958.2007.05872.x

Leal, J. A., Jimenez-Barbero, J., Gomez-Miranda, B., Prieto, A., Domenech, J., and Bernabe, M. (1996). Structural investigation of a cell-wall galactomannan from *Neurospora crassa* and N. *sitophila*. *Carbohydr. Res.* 283, 215–222. doi: 10.1016/0008-6215(95)00400-9

Lee, J. I., Choi, J. H., Park, B. C., Park, Y. H., Lee, M. Y., Park, H. M., et al. (2004). Differential expression of the chitin synthase genes of *Aspergillus nidulans*, chsA, chsB, and chsC, in response to developmental status and environmental factors. *Fungal Genet. Biol.* 41, 635–646. doi: 10.1016/j.fgb.2004.01.009

Lehr, N. A., Wang, Z., Li, N., Hewitt, D. A., Lopez-Giraldez, F., Trail, F., et al. (2014). Gene expression differences among three neurospora species reveal genes required for sexual reproduction in *Neurospora crassa*. *PLoS One* 9:e110398. doi: 10.1371/journal.pone.0110398

Lenardon, M. D., Munro, C. A., and Gow, N. A. (2010). Chitin synthesis and fungal pathogenesis. *Curr. Opin. Microbiol.* 13, 416–423. doi: 10.1016/j.mib.2010.05.002

Lerch, K. (1982). Primary structure of tyrosinase from *Neurospora crassa*. II. complete amino acid sequence and chemical structure of a tripeptide containing an unusual thioether. *J. Biol. Chem.* 257, 6414–6419.

Lew, R. R. (2011). How does a hypha grow? The biophysics of pressurized growth in fungi. *Nat. Rev. Microbiol.* 9, 509–518. doi: 10.1038/nrmicro2591

Liu, H., Li, Y., Chen, D., Qi, Z., Wang, Q., Wang, J., et al. (2017). A-to-I RNA editing is developmentally regulated and generally adaptive for sexual reproduction in *Neurospora crassa*. *Proc. Natl. Acad. Sci. U.S.A.* 114, E7756–E7765. doi: 10.1073/pnas.1702591114

Lu, C. F., Montijn, R. C., Brown, J. L., Klis, F., Kurjan, J., Bussey, H., et al. (1995). Glycosyl phosphatidylinositol-dependent cross-linking of alpha-agglutinin and beta 1,6-glucan in the *Saccharomyces cerevisiae* cell wall. *J. Cell Biol.* 128, 333–340. doi: 10.1083/jcb.128.3.333

Ma, L., Chen, Z., Huang da, W., Kutty, G., Ishihara, M., Wang, H., et al. (2016). Genome analysis of three pneumocystis species reveals adaptation mechanisms to life exclusively in mammalian hosts. *Nat. Commun.* 7:10740. doi: 10.1038/ncomms10740

Maddi, A., Bowman, S. M., and Free, S. J. (2009). Trifluoromethanesulfonic acid-based proteomic analysis of cell wall and secreted proteins of the ascomycetous fungi *Neurospora crassa* and candida albicans. *Fungal Genet. Biol.* 46, 768–781. doi: 10.1016/j.fgb.2009.06.005

Maddi, A., and Free, S. J. (2010). Alpha-1,6-mannosylation of N-linked oligosaccharide present on cell wall proteins is required for their incorporation into the cell wall in the filamentous fungus *Neurospora crassa*. *Eukaryot. Cell* 9, 1766–1775. doi: 10.1128/EC.00134-10

Maddi, A., Fu, C., and Free, S. J. (2012). The *Neurospora crassa* dfg5 and dcw1 genes encode alpha-1,6-mannanases that function in the incorporation of glycoproteins into the cell wall. *PLoS One* 7:e38872. doi: 10.1371/journal.pone.0038872

Magnelli, P. E., Cipollo, J. F., and Robbins, P. W. (2005). A glucanase-driven fractionation allows redefinition of *Schizosaccharomyces pombe* cell wall composition and structure: assignment of diglucan. *Anal. Biochem.* 336, 202–212. doi: 10.1016/j.ab.2004.09.022

Martinez-Nunez, L., and Riquelme, M. (2015). Role of BGT-1 and BGT-2, two predicted GPI-anchored glycoside hydrolases/glycosyltransferases, in cell wall remodeling in *Neurospora crassa*. *Fungal Genet. Biol.* 85, 58–70. doi: 10.1016/j.fgb.2015.11.001

Maubon, D., Park, S., Tanguy, M., Huerre, M., Schmitt, C., Prevost, M. C., et al. (2006). AGS3, an alpha(1-3)glucan synthase gene family member of *Aspergillus fumigatus*, modulates mycelium growth in the lung of experimentally infected mice. *Fungal Genet. Biol.* 43, 366–375. doi: 10.1016/j.fgb.2006.01.006

Mazan, M., Ragni, E., Popolo, L., and Farkas, V. (2011). Catalytic properties of the gas family beta-(1,3)-glucanosyltransferases active in fungal cell-wall biogenesis as determined by a novel fluorescent assay. *Biochem. J.* 438, 275–282. doi: 10.1042/BJ20110405

McCluskey, K., Wiest, A. E., Grigoriev, I. V., Lipzen, A., Martin, J., Schackwitz, W., et al. (2011). Rediscovery by whole genome sequencing: classical mutations and genome polymorphisms in *Neurospora crassa*. *G3* 1, 303–316. doi: 10.1534/g3.111.000307

Miyazawa, K., Yoshimi, A., Kasahara, S., Sugahara, A., Koizumi, A., Yano, S., et al. (2018). Molecular mass and localization of alpha-1,3-glucan in cell wall control the degree of hyphal aggregation in liquid culture of *Aspergillus nidulans*. *Front. Microbiol.* 9:2623. doi: 10.3389/fmicb.2018.02623

Mosch, H. U., and Fink, G. R. (1997). Dissection of filamentous growth by transposon mutagenesis in *Saccharomyces cerevisiae*. *Genetics* 145, 671–684.

Mouyna, I., Fontaine, T., Vai, M., Monod, M., Fonzi, W. A., Diaquin, M., et al. (2000a). Glycosylphosphatidylinositol-anchored glucanosyltransferases play an active role in the biosynthesis of the fungal cell wall. *J. Biol. Chem.* 275, 14882–14889. doi: 10.1074/jbc.275.20.14882

Mouyna, I., Monod, M., Fontaine, T., Henrissat, B., Lechenne, B., and Latge, J. P. (2000b). Identification of the catalytic residues of the first family of beta(1-3)glucanosyltransferases identified in fungi. *Biochem. J.* 347(Pt 3), 741–747. doi: 10.1042/bj3470741

Mouyna, I., Hartland, R. P., Fontaine, T., Diaquin, M., Simenel, C., Delepierre, M., et al. (1998). A 1,3-beta-glucanosyltransferase isolated from the cell wall of *Aspergillus fumigatus* is a homologue of the yeast Bgl2p. *Microbiology* 144(Pt 11), 3171–3180. doi: 10.1099/00221287-144-11-3171

Mouyna, I., Morelle, W., Vai, M., Monod, M., Lechenne, B., Fontaine, T., et al. (2005). Deletion of GEL2 encoding for a beta(1-3)glucanosyltransferase affects morphogenesis and virulence in *Aspergillus fumigatus*. *Mol. Microbiol.* 56, 1675–1688. doi: 10.1111/j.1365-2958.2005.04654.x

Nakayama, K., Nagasu, T., Shimma, Y., Kuromitsu, J., and Jigami, Y. (1992). OCH1 encodes a novel membrane bound mannosyltransferase: outer chain elongation of asparagine-linked oligosaccharides. *EMBO J.* 11, 2511–2519. doi: 10.1002/j.1460-2075.1992.tb05316.x

Nosanchuk, J. D., Stark, R. E., and Casadevall, A. (2015). Fungal melanin: what do we know about structure? *Front. Microbiol.* 6:1463. doi: 10.3389/fmicb.2015.01463

Pardini, G., De Groot, P. W., Coste, A. T., Karababa, M., Klis, F. M., de Koster, C. G., et al. (2006). The CRH family coding for cell wall glycosylphosphatidylinositol proteins with a predicted transglycosidase domain affects cell wall organization and virulence of candida albicans. *J. Biol. Chem.* 281, 40399–40411. doi: 10.1074/jbc.m606361200

Perlin, A. S., and Suzuki, S. (1962). The structure of lichenin: selective enzymolysis studies. *Can. J. Chem.* 40, 50–56. doi: 10.1139/v62-009

Pihet, M., Vandeputte, P., Tronchin, G., Renier, G., Saulnier, P., Georgeault, S., et al. (2009). Melanin is an essential component for the integrity of the cell wall of *Aspergillus fumigatus* conidia. *BMC Microbiol.* 9:177. doi: 10.1186/1471-2180-9-177

Popolo, L., Degani, G., Camilloni, C., and Fonzi, W. A. (2017). The PHR family: the role of extracellular transglycosylases in shaping candida albicans cells. *J. Fungi.* 3:E59. doi: 10.3390/jof3040059

Prates, E. T., Guan, X., Li, Y., Wang, X., Chaffey, P. K., Skaf, M. S., et al. (2018). The impact of O-glycan chemistry on the stability of intrinsically disordered proteins. *Chem. Sci.* 9, 3710–3715. doi: 10.1039/c7sc05016j

Ragni, E., Coluccio, A., Rolli, E., Rodriguez-Pena, J. M., Colasante, G., Arroyo, J., et al. (2007a). GAS2 and GAS4, a pair of developmentally regulated genes required for spore wall assembly in *Saccharomyces cerevisiae*. *Eukaryot. Cell* 6, 302–316. doi: 10.1128/ec.00321-06

Ragni, E., Fontaine, T., Gissi, C., Latge, J. P., and Popolo, L. (2007b). The gas family of proteins of *Saccharomyces cerevisiae*: characterization and evolutionary analysis. *Yeast* 24, 297–308. doi: 10.1002/yea.1473

Raich, L., Borodkin, V., Fang, W., Castro-Lopez, J., van Aalten, D. M., Hurtado-Guerrero, R., et al. (2016). A trapped covalent intermediate of a glycoside hydrolase on the pathway to transglycosylation. insights from experiments and quantum mechanics/molecular mechanics simulations. *J. Am. Chem. Soc.* 138, 3325–3332. doi: 10.1021/jacs.5b10092

Ram, A. F., Kapteyn, J. C., Montijn, R. C., Caro, L. H., Douwes, J. E., Baginsky, W., et al. (1998). Loss of the plasma membrane-bound protein gas1p in *Saccharomyces cerevisiae* results in the release of beta1,3-glucan into the medium and induces a compensation mechanism to ensure cell wall integrity. *J. Bacteriol.* 180, 1418–1424.

Rappleye, C. A., Eissenberg, L. G., and Goldman, W. E. (2007). *Histoplasma capsulatum* alpha-(1,3)-glucan blocks innate immune recognition by the beta-glucan receptor. *Proc. Natl. Acad. Sci. U.S.A.* 104, 1366–1370. doi: 10.1073/pnas.0609848104

Reese, A. J., Yoneda, A., Breger, J. A., Beauvais, A., Liu, H., Griffith, C. L., et al. (2007). Loss of cell wall alpha(1-3) glucan affects *Cryptococcus neoformans* from ultrastructure to virulence. *Mol. Microbiol.* 63, 1385–1398. doi: 10.1111/j.1365-2958.2006.05551.x

Rehnstrom, A. L., and Free, S. J. (1996). The isolation and characterization of melanin-deficient mutants of *Monilinia fructicola*. *Physiol. Mol. Plant Path.* 49, 321–330. doi: 10.1006/pmpp.1996.0057

Richthammer, C., Enseleit, M., Sanchez-Leon, E., Marz, S., Heilig, Y., Riquelme, M., et al. (2012). RHO1 and RHO2 share partially overlapping functions in the regulation of cell wall integrity and hyphal polarity in *Neurospora crassa*. *Mol. Microbiol.* 85, 716–733. doi: 10.1111/j.1365-2958.2012.08133.x

Roncero, C. (2002). The genetic complexity of chitin synthesis in fungi. *Curr. Genet.* 41, 367–378. doi: 10.1007/s00294-002-0318-7

Ruiz-Herrera, J., Elorza, M. V., Valentin, E., and Sentandreu, R. (2006). Molecular organization of the cell wall of candida albicans and its relation to pathogenicity. *FEMS Yeast Res.* 6, 14–29. doi: 10.1111/j.1567-1364.2005.00017.x

Samalova, M., Melida, H., Vilaplana, F., Bulone, V., Soanes, D. M., Talbot, N. J., et al. (2017). The beta-1,3-glucanosyltransferases (Gels) affect the structure of the rice blast fungal cell wall during appressorium-mediated plant infection. *Cell Microbiol.* 19, e12659. doi: 10.1111/cmi.12659

Sanchez-Leon, E., and Riquelme, M. (2015). Live imaging of beta-1,3-glucan synthase FKS-1 in *Neurospora crassa* hyphae. *Fungal Genet. Biol.* 82, 104–107. doi: 10.1016/j.fgb.2015.07.001

Sanchez-Leon, E., Verdin, J., Freitag, M., Roberson, R. W., Bartnicki-Garcia, S., and Riquelme, M. (2011). Traffic of chitin synthase 1 (CHS-1) to the spitzenkorper and developing septa in hyphae of *Neurospora crassa*: actin dependence and evidence of distinct microvesicle populations. *Eukaryot. Cell* 10, 683–695. doi: 10.1128/EC.00280-10

Shental-Bechor, D., and Levy, Y. (2008). Effect of glycosylation on protein folding: a close look at thermodynamic stabilization. *Proc. Natl. Acad. Sci. U.S.A.* 105, 8256–8261. doi: 10.1073/pnas.0801340105

Sillo, F., Gissi, C., Chignoli, D., Ragni, E., Popolo, L., and Balestrini, R. (2013). Expression and phylogenetic analyses of the Gel/Gas proteins of tuber melanosporum provide insights into the function and evolution of glucan remodeling enzymes in fungi. *Fungal Genet. Biol.* 53, 10–21. doi: 10.1016/j.fgb.2013.01.010

Spreghini, E., Davis, D. A., Subaran, R., Kim, M., and Mitchell, A. P. (2003). Roles of candida ALBICANS Dfg5p and Dcw1p cell surface proteins in growth and hypha formation. *Eukaryot. Cell* 2, 746–755. doi: 10.1128/ec.2.4.746-755.2003

Sugareva, V., Hartl, A., Brock, M., Hubner, K., Rohde, M., Heinekamp, T., et al. (2006). Characterisation of the laccase-encoding gene abr2 of the

dihydroxynaphthalene-like melanin gene cluster of *Aspergillus fumigatus*. *Arch. Microbiol.* 186, 345–355. doi: 10.1007/s00203-006-0144-2

Talbot, N. J. (2003). On the trail of a cereal killer: exploring the biology of magnaporthe grisea. *Annu. Rev. Microbiol.* 57, 177–202. doi: 10.1146/annurev.micro.57.030502.090957

Tentler, S., Palas, J., Enderlin, C., Campbell, J., Taft, C., Miller, T. K., et al. (1997). Inhibition of *Neurospora crassa* growth by a glucan synthase-1 antisense construct. *Curr. Microbiol.* 34, 303–308. doi: 10.1007/s002849900186

Tsai, H. F., Fujii, I., Watanabe, A., Wheeler, M. H., Chang, Y. C., Yasuoka, Y., et al. (2001). Pentaketide melanin biosynthesis in *Aspergillus fumigatus* requires chain-length shortening of a heptaketide precursor. *J. Biol. Chem.* 276, 29292–29298. doi: 10.1074/jbc.m101998200

Upadhyay, S., Xu, X., and Lin, X. (2016a). Interactions between melanin enzymes and their atypical recruitment to the secretory pathway by palmitoylation. *mBio.* 7:e001925-16. doi: 10.1128/mBio.01925-16

Upadhyay, S., Xu, X., Lowry, D., Jackson, J. C., Roberson, R. W., and Lin, X. (2016b). Subcellular compartmentalization and trafficking of the biosynthetic machinery for fungal melanin. *Cell Rep.* 14, 2511–2518. doi: 10.1016/j.celrep.2016.02.059

Verdin, J., Bartnicki-Garcia, S., and Riquelme, M. (2009). Functional stratification of the spitzenkorper of *Neurospora crassa*. *Mol. Microbiol.* 74, 1044–1053. doi: 10.1111/j.1365-2958.2009.06917.x

Verdin, J., Sanchez-Leon, E., Rico-Ramirez, A. M., Martinez-Nunez, L., Fajardo-Somera, R. A., and Riquelme, M. (2019). Off the wall: the rhyme and reason of *Neurospora crassa* hyphal morphogenesis. *Cell Surf.* 5:100020. doi: 10.1016/j.tcsw.2019.100020

Wang, Z., Lopez-Giraldez, F., Lehr, N., Farre, M., Common, R., Trail, F., et al. (2014). Global gene expression and focused knockout analysis reveals genes associated with fungal fruiting body development in *Neurospora crassa*. *Eukaryot. Cell* 13, 154–169. doi: 10.1128/EC.00248-13

Yarden, O., and Yanofsky, C. (1991). Chitin synthase 1 plays a major role in cell wall biogenesis in *Neurospora crassa*. *Genes Dev.* 5, 2420–2430. doi: 10.1101/gad.5.12b.2420

Conflict of Interest: The authors declare that the research was conducted in the absence of any commercial or financial relationships that could be construed as a potential conflict of interest.

frontiers in Microbiology

ORIGINAL RESEARCH
published: 30 October 2019
doi: 10.3389/fmicb.2019.02445

New Role of *P. brasiliensis* α-Glucan: Differentiation of Non-conventional Dendritic Cells

Ana Camila Oliveira Souza[1†‡], Cecília Favali[1‡], Naiara Caroline Soares[1], Natalia Machado Tavares[2], Márcio Sousa Jerônimo[1], Paulo Henrique Veloso Junior[1], Clara Luna Marina[1], Claire Santos[2], Cláudia Brodskyn[2] and Anamelia Lorenzetti Bocca[1]*

[1] Departamento de Biologia Celular, Universidade de Brasília, Brasília, Brazil, [2] Centro de Pesquisas Gonçalo Moniz, Fundação Oswaldo Cruz, Salvador, Brazil

OPEN ACCESS

Edited by:
Joshua D. Nosanchuk, Albert Einstein College of Medicine, United States

Reviewed by:
Luis Antonio Pérez-García, Universidad Autónoma de San Luis Potosí, Mexico
Angel Gonzalez, University of Antioquia, Colombia

***Correspondence:**
Anamelia Lorenzetti Bocca
albocca@unb.br

†Present address:
Ana Camila Oliveira Souza, Department of Clinical Pharmacy and Translational Science, The University of Tennessee Health Science Center, Memphis, TN, United States

‡These authors have contributed equally to this work

Specialty section:
This article was submitted to Fungi and Their Interactions, a section of the journal Frontiers in Microbiology

Received: 15 July 2019
Accepted: 11 October 2019
Published: 30 October 2019

Citation:
Souza ACO, Favali C, Soares NC, Tavares NM, Jerônimo MS, Veloso Junior PH, Marina CL, Santos C, Brodskyn C and Bocca AL (2019) New Role of P. brasiliensis α-Glucan: Differentiation of Non-conventional Dendritic Cells. Front. Microbiol. 10:2445. doi: 10.3389/fmicb.2019.02445

The cell wall has a critical role in the host immune response to fungal pathogens. In this study, we investigated the influence of two cell wall fractions of the dimorphic fungi *Paracoccidioides brasiliensis* (Pb) in the *in vitro* generation of monocyte-derived dendritic cells (MoDCs). Monocytes were purified from the peripheral blood of healthy donors and cultivated for 7 days in medium supplemented with IL-4 and GM-CSF in the presence of Pb cell wall fractions: the alkali-insoluble F1, constituted by β-1,3-glucans, chitin and proteins, and the alkali-soluble F2, mainly constituted by α-glucan. MoDCs phenotypes were evaluated regarding cell surface expression of CD1a, DC-SIGN, HLA-DR, CD80, and CD83 and production of cytokines. The α-glucan-rich cell wall fraction downregulated the differentiation of $CD1a^+$ MoDCs, a dendritic cell subset that stimulate Th1 responses. The presence of both cell fractions inhibited DC-SIGN and HLA-DR expression, while the expression of maturation markers was differentially induced in $CD1a^-$ MoDCs. Differentiation upon F1 and F2 stimulation induced mixed profile of inflammatory cytokines. Altogether, these data demonstrate that Pb cell wall fractions differentially induce a dysregulation in DCs differentiation. Moreover, our results suggest that cell wall α-glucan promote the differentiation of $CD1a^-$ DCs, potentially favoring Th2 polarization and contributing to pathogen persistence.

Keywords: Paracoccidiodomycosis, *Paracoccidioides brasiliensis*, dendritic cell differentiation, glucan, cell wall fractions

INTRODUCTION

The cell wall is a complex and dynamic structure that plays essential roles in fungal cell biology. Cell shape, polarized growth, sensing of, response to or protection against surrounding conditions and interaction with the extracellular environment are some of the processes fully dependent on a healthy fungal cell wall. This organelle is a polysaccharide-rich shield that surrounds the outer face of the phospholipidic cell membrane, and its molecular composition and structure varies according to fungal species, morphotype and life cycle. In most fungi, the cell wall is organized as a structural scaffold formed by cross-linked β-1,3-glucan, β-1,6-glucan and chitin, embedded in a more heterogeneous amorphous matrix, often constituted by α-1,3-glucan and mannan. Besides, proteins are often covalently linked to those carbohydrates. Importantly, cell wall components are mostly absent in animals and plants. For this reason, it is an important target for the development of antifungal therapy and its contribution to host immune responses has been vastly investigated. The composition and structure of the fungal cell wall have been described in several other review papers (Bowman and Free, 2006; Latgé, 2010; Free, 2013; Gow et al., 2017).

In the fungal pathogen *Paracoccidioides brasiliensis* (Pb), the development and maintenance of the Pb cell wall is somewhat peculiar due to its thermo-dimorphic nature. Similarly to the other species in the *Paracoccidioides* genus, *P. brasiliensis* grow as a mold in the environment (18–25°C) and at higher temperatures (35–37°C), it switches to a multi-budding yeast cell morphology (Almeida and Lopes, 2001; Shikanai-Yasuda et al., 2006, 2017; Calich et al., 2008; Ferreira, 2009; Fernandes et al., 2015; Turissini et al., 2017). As such, *P. brasiliensis* environmental fungal propagules can be inhaled and transformed into pathogenic yeasts once inside the host tissues. Not surprisingly, differences in the structure and composition of the cell wall during mycelial or yeast growth have been previously reported. The environmental mycelia cell wall presents higher amounts of proteins and β-glucan, while the pathogenic yeast cell wall is thicker and bears higher amounts of chitin (inner layer) and α-1, 3-glucan (95% of total glucan, outer layer) (Kanetsuna et al., 1969; Moreno et al., 1969; Kanetsuna and Carbonell, 1970; San-Blas and San-Blas, 1977; Nóbrega et al., 2010). The protrude presence of peripheral α-glucan in Pb pathogenic yeast is believed to play a role in pathogenicity (Kanetsuna and Carbonell, 1970; San-Blas and San-Blas, 1977; San-Blas et al., 1977), similar to other fungal pathogens, such as *Histoplasma capsulatum* and *Blastomyces dermatitidis* (Klimpel and Goldman, 1988; Hogan and Klein, 1994).

Paracoccidioides brasiliensis is one of the etiologic agents of Paracoccidiodomycosis (PCM), a severe, non-opportunistic granulomatous mycosis endemic in Latin America that, when not quickly diagnosed and adequately treated, can result in a disseminated and life-threatening disease (Bocca et al., 2013). It has been extensively demonstrated that a sustained secretion of Th1 cytokines plays a dominant role in the mechanism of resistance to Pb infection, while an intense humoral response is associated with increased disease dissemination and severity (Almeida and Lopes, 2001; Silvana dos Santos et al., 2011; Camacho and Niño-Vega, 2017). As key players in the development of adaptive immune responses, dendritic cells (DCs) recognize Pb antigens and migrate to lymph nodes, where they activate T helper cells (Silvana dos Santos et al., 2011; Tavares et al., 2012; Pina et al., 2013). However, it has been reported that Pb infection can cause impairment in DCs maturation, leading to a non-adequate cell-mediated response that contributes to the host susceptibility to this pathogen (Ferreira et al., 2004, 2007; Ferreira and Almeida, 2006; Fernandes et al., 2015). Therefore, in this study we analyzed the contribution of two Pb cell wall fractions in the *in vitro* differentiation and maturation of DCs generated from human monocyte cells. Our results demonstrate that both alkali-insoluble β-glucan rich (F1) and alkali-soluble α-glucan rich (F2) cell wall fractions differentially alter *in vitro* differentiation of human monocyte-derived DCs regarding the expression of HLA-DR, DC-SIGN, CD83, and CD80 molecules, and their ability to secrete inflammatory cytokines. Importantly, our findings suggest that Pb cell wall α-glucan stimulates the differentiation of $CD1a^-$ DCs, what can affect polarization of Th1 immune response and play a role in pathogenesis.

MATERIALS AND METHODS

Fungal Strains and Culture

The highly virulent (Pb18) and avirulent (Pb265) strains of *P. brasiliensis* were obtained from the fungal collection of the Applied Immunology Laboratory at the Biology Institute of the University of Brasilia. The fungus was cultured in liquid YPD medium (w/v: 2% peptone, 1% yeast extract, 2% glucose) at 36°C in a rotary shaker (220 rpm). After 5 days of growth, the fungal cells were harvested by centrifugation, washed with PBS and the cell pellet was further used for experiments.

Flow Cytometry Analysis of β-Glucan Exposure

Characterization of β-glucan exposure in Pb18 and Pb265 isolates was performed by flow cytometry. First, 2×10^6 yeast were harvested, resuspended in PBS 1% BSA (Sigma-Aldrich, St. Louis, MO, United States) supplemented with 2% FBS (Gibco, United States) and incubated with polyclonal anti-β-glucan (1:100) for 1 h at 4°C. The polyclonal anti-β-glucan was obtained from mice serum after three consecutive immunizations with depleted zymosan (#tlrl-zyd, InvivoGen, CA, United States) emulsified with Freund's incomplete adjuvant (Sigma-Aldrich, MO, United States) and purified using protein-A column, as described previously (Leenaars and Hendriksen, 2005). Next, the yeasts were washed three times and incubated for 1 h with a polyclonal goat anti-mouse IgG conjugated with fluorescein isothiocyanate (FITC) (1:400 eBioscience), used according the manufacturer's recommendations. *Cryptococcus neoformans* encapsulated strain (H99) was used as a negative control while acapsular strain (Cap65) was used as a positive control (data not shown). Isotypic FITC-conjugated antibody was also used as a control. Cells were acquired in the FACSVerse flow cytometer (BD Biosciences), and the data analyzed in the FlowJo software (version X).

Chemical Fractionation of Pb Cell Wall

Alkali-treatment was utilized to separate the cell wall components of Pb into two fractions: an alkali-insoluble fraction constituted by chitin, β-glucans and amino acids (F1) and an alkali-soluble fraction that is precipitated with acetic acid and constituted mainly by α-glucan (F2). The protocol for Pb cell wall fractionation was followed according to previous reports (Kanetsuna and Carbonell, 1970; San-Blas and San-Blas, 1977; Nóbrega et al., 2010; Puccia et al., 2011). Briefly, after harvesting, yeast cells were inactivated with 5% formaldehyde for 24 h, filtered onto tissue paper, washed three times with distilled water and dried at room temperature. Then, the material was frozen with liquid nitrogen in order to rupture fungal cells, diluted in distilled water and washed five times by centrifugation at 2000 *g*. The raw cell wall material was then subjected to lipid extraction with chloroform:methanol (2:1 v/v). The lipid-free cell wall material was precipitated with alkali solution (1N NaOH) and gently stirred at room temperature for 1 h. After centrifugation at 5000 *g* for 10 min, the supernatant (alkali-soluble) was collected and the procedure was repeated four

times more with the remaining precipitate (alkali-insoluble). The alkali-insoluble precipitate was washed with water until it reached pH 7.0, and then sequentially washed with ethanol, acetone and diethyl ether (v/v/v). The resulting white powder consisted in the alkali-insoluble F1 fraction, constituted mainly by β-glucans, chitin and proteins (Kanetsuna and Carbonell, 1970; Nóbrega et al., 2010; Puccia et al., 2011). The amount of F1 (300 μg/ml) used in these experiments was based on our previous results from migration kinetics experiments (Nóbrega et al., 2010).

To obtain F2, the combined supernatants obtained after alkali extraction of F1 were neutralized by the addition of chloridric acid (1 M HCl). The precipitate was washed three times with distilled water and further diluted in 0.1 M HCl. After successive washes, the insoluble precipitate was collected, resuspended in water and dialyzed against distilled water, resulting in an alkali-soluble F2 fraction, acid precipitable and mostly constituted by α-1,3-glucans (Kanetsuna and Carbonell, 1970; Nóbrega et al., 2010; Puccia et al., 2011). The material was lyophilized and re-suspended to a final concentration of 1 mg/mL. The amount of F2 used in these experiments (450 μg/ml) was defined using our previous results from migration kinetics experiments (data not shown).

Nuclear Magnetic Resonance (NMR) Spectroscopy

The cell wall fractions F1 (1.2 mg) and F2 (1.1 mg) were deuterium-exchanged by lyophilization in D_2O. The dried samples were re-dissolved in 0.5 mL D_2O (99.96% D, Cambridge Isotope Laboratories) and transferred to a 5-mm OD NMR tube. 1-D Proton spectra were acquired on a Varian Inova-500 MHz spectrometer at 25°C. These analyses were performed by the Complex Carbohydrate Research Center (GA, United States).

In vitro Generation of Human Monocyte-Derived Dendritic Cells

Immature monocyte-derived DCs were generated from peripheral blood monocytes (PBMC) obtained from 12 healthy donors (Blood Center of Salvador, HEMOBA, Brumado, Brazil authorization number 100/2006). Briefly, PBMC were obtained from heparinized venous blood by passage over a Ficoll Hypaque gradient (Sigma-Aldrich, St. Louis, MO, United States). PBMC were washed three times, and the $CD14^+$ cell population was enriched by positive selection using magnetic cell sorting (Mini Macs, Miltenyi Biotec, Auburn, CA, United States). Monocytes were resuspended at a concentration of 5×10^5 cells/ml in RPMI-1640 medium (Gibco, Grand Island, NY, United States) supplemented with 2 mM L-glutamine, penicillin (100 U/ml), streptomycin (100 g/ml, Gibco, Grand Island, NY, United States), and 10% heat-inactivated Fetal Bovine Serum (Cripion Biotechnology, Andradina, SP, Brazil), plus IL-4 (100 UI/ml) and GM-CSF (50 ng/ml; PeproTech, Rocky Hill, NJ, United States). Cells were cultured in 24-well tissue plates (Costar, Corning, NY, United States) and incubated at 37°C 5% CO_2 for 7 days. Cell wall fractions F1 (300 μg/ml) or F2 (450 μg/ml) were added on the first day of culture to study the effect of these components on dendritic cell differentiation. At days 3 and 6, fresh medium was replaced with GM-CSF and IL-4 without further addition of antigens. After 7 days, in order to characterize the DCs population, cells were stained and fluorescence was analyzed by FACS (FACSort, Becton Dickinson, San Jose, CA, United States). Supernatants were harvested and maintained at −20°C for cytokine measurement.

Immunophenotyping of MoDCs

After culture, immature DCs were harvested for flow cytometry analyses. Briefly, 10^6 cells were incubated with PBS/1% BSA (Sigma-Aldrich, St. Louis, MO, United States)/0.1% sodium azide (Nuclear) and incubated with 20% FCS to block FcR (Mazurek et al., 2012). Cells were stained with FITC-conjugated anti-CD1a (clone HI149, Ebiosciences, San Diego, CA, United States), PE-CD80 (clone 2D10.4, Ebiosciences, San Diego, CA, United States), PECy5-CD83 (clone HB15e, BD Biosciences, San Jose, CA, United States), PECy-5-HLA-DR (clone LN3, Ebiosciences, San Diego, CA, United States) and PE-anti-DC-specific ICAM-grabbing non-integrin (DC-SIGN, clone DCN46, BD Biosciences, San Jose, CA, United States). All analyses included the appropriate isotype controls. Cells were acquired on FACSort (BD Biosciences, San Jose, CA, United States), and analyzed with FlowJo (10.0.6 Treestar, Ashland, OR, United States). Cells were gated into $CD1a^+$ and $CD1a^-$, and analyzed separately concerning the expression of DC-SIGN, CD80, CD83, and HLA-DR.

Cytokine Bead Array (CBA)

Cytokines on supernatants obtained in the last 24 h of culture were measured by flow cytometry employing BD Cytometric Bead Array (CBA, BD Biosciences, San Jose, CA, United States) Human Inflammatory Cytokine Kit for IL-8, IL-1 beta, IL-6, IL-10, TNFα, and IL-12 p70 detection according to the manufacturer's protocol.

Statistical Analysis

Data were analyzed using GraphPad Prism (5.0, San Diego, CA, United States). Results were expressed as the mean ± SEM, and analyzed by *t*-test with Wilcoxon signed rank test; $^*p < 0.05$, $^{**}p < 0.01$, and $^{***}p < 0.001$ in comparison to control cells. $\#p < 0.05$, $\#\#p < 0.01$, and $\#\#\#p < 0.001$ between samples treated with the cell wall fractions.

RESULTS

Paracoccidioides brasiliensis Strains Show Differences on β-Glucan Exposure

Paracoccidioides brasiliensis yeast cell wall is organized in an inner layer, mostly composed by β-glucan, chitin and proteins, and an outermost layer, which is mainly composed by α-glucan (Moreno et al., 1969; Carbonell et al., 1970; Kanetsuna and Carbonell, 1970; Puccia et al., 2011). As previously described for *H. capsulatum* (Klimpel and Goldman, 1988) and *B. dermatitis* (Hogan and Klein, 1994), the presence of α-glucan in the cell wall often correlates with virulence, possibly because it hinders

immune recognition of β-glucan (Rappleye et al., 2007). In order to confirm the correlation of β-glucan exposure in the cell wall with Pb virulence, we sought to analyze two Pb isolates with well-known disparate virulence profiles: Pb265 (non-virulent) and Pb18 (virulent). The β-glucan staining revealed that the non-virulent Pb265 isolate presented higher levels of β-glucan exposure in the cell surface than the virulent strain Pb18 (**Figure 1**). This result corroborates previous studies that demonstrated that Pb265 stimulated higher cell recruitment to mice peritoneal cavity, as well as that the inoculation of F1 fraction of Pb265 induced a higher subcutaneous nodular formation when compared to Pb18 (Silva et al., 1994).

Next, we analyzed the presence of α-glucan in the alkali-insoluble (F1) and alkali-soluble (F2) fractions of Pb18 yeast cell wall by NMR. While the fraction F2 completely dissolved in the D_2O, sample F1 was mostly insoluble. Therefore, F1 D_2O suspension was centrifuged and only the supernatant was evaluated by NMR. In each NMR spectrum presented at **Figures 1B,C**, there are peaks between 5.36 and 3.81 ppm, which represent the α-glucose anomeric protons present in the α-glucan (H-1: 5.36; H-2: 3.64; H-3: 3.95; H-4: 3.64; H-5: 3.84; H-6: 3.81). Thus, F2 sample (**Figure 1B**) shows well-resolved α-glucose peak, and since this fraction was completely dissolved in D_2O, the presence of β-glucose polymers was ruled out (**Figure 1B**). The F1 fraction showed a less-resolved α-glucose peak with much lower intensity (**Figure 1C**). Considering these results, we confirm previous reports that demonstrated that F2 fraction is mainly composed by α-glucan.

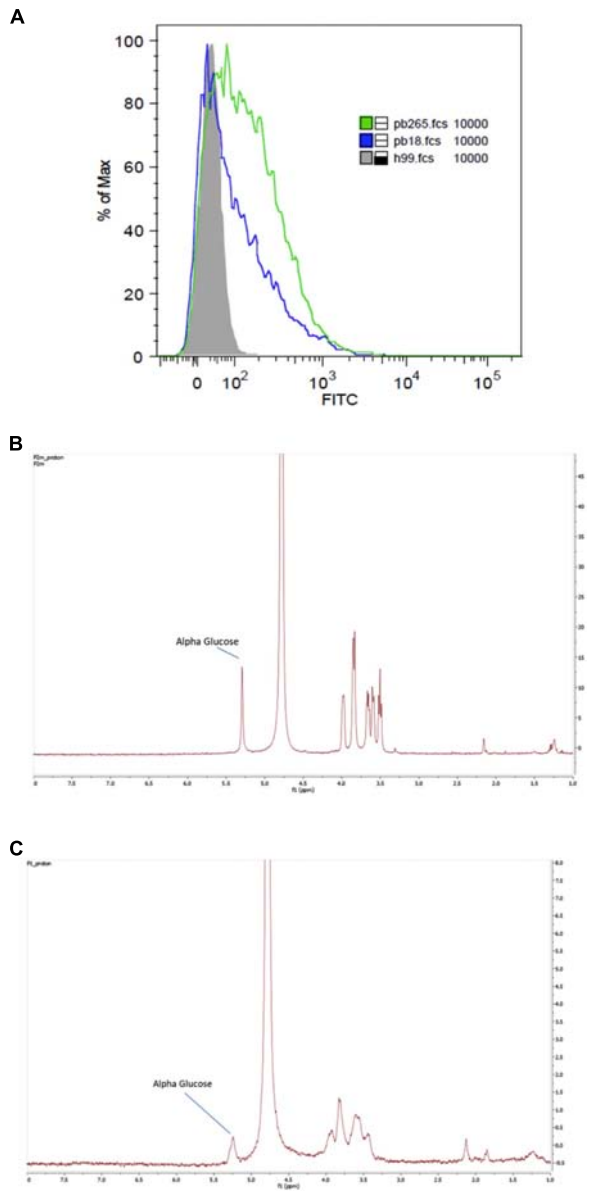

FIGURE 1 | Cell wall α-glucan correlates to decrease in β-glucan exposure in *Paracoccidioides brasiliensis*. Exposure of β-glucan in the cell wall of *P. brasiliensis* virulent (Pb18) and avirulent (Pb265) isolates and *Cryptococcus neoformans* (H99) **(A)**. NMR spectroscopy of F2 **(B)** and F1 **(C)** cell wall fractions.

Paracoccidioides brasiliensis α-Glucan-Rich Cell Wall Fraction Alter Differentiation of CD1a$^+$ MoDCs

In order to elucidate if *P. brasiliensis* cell wall fractions could alter human DCs generation, monocytes were differentiated in the presence of F1 or F2 cell wall fractions. Monocytes not stimulated with cell wall fractions were used as a control (M). After 7 days of culture, we evaluated the expression of differentiation and maturation markers of DCs. First, we evaluated the differentiation of MoDCs regarding the expression of CD1a. This marker discern two DC subsets: CD1a$^+$ DCs favor Th1 polarization, whereas CD1a$^-$ DCs induce Th2 immunity (Chang et al., 2000; Cernadas et al., 2009). The F2 fraction downregulated the differentiation of CD1a$^+$ MoDCs (9.2% ± 6.6%) in comparison with the non-treated samples (31.3 ± 15.3%) (**Figure 2**). On the other hand, the F1 fraction presence did not influence the levels of CD1a$^+$ cells (**Figure 2**).

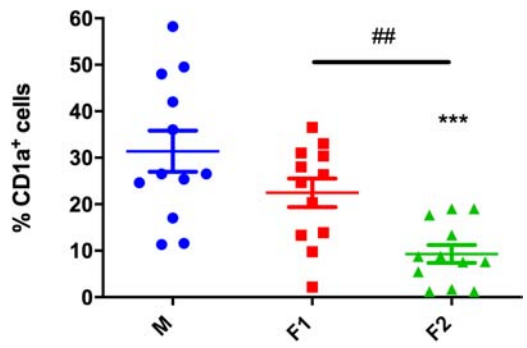

FIGURE 2 | *Paracoccidioides brasiliensis* α-glucan-rich cell wall fraction modulates differentiation of CD1a$^+$ dendritic cells. Cell frequency of CD1a+ cells after differentiation upon F1 or F2 stimulation. Non-stimulated cells were used as a control (M). Each data point represents one donor. Wilcoxon matched pairs *T* test. $^{***}p < 0.01$ in comparison to control group. $^{\#\#}p < 0.01$ between groups treated with cell wall fractions.

Paracoccidioides brasiliensis Cell Wall Fractions Alter MoDCs CD1a Subset Maturation Phenotype

Since we observed that F2 downregulated the development of $CD1a^+$ cells, we decided to evaluate both $CD1a^+$ and $CD1a^-$ subsets separately regarding the expression of specific surface molecules. F2 inhibited the DC-SIGN expression in $CD1a^+$ cells, when compared with the control group (**Figure 3A**), whereas F1 decreased DC-SIGN expression in $CD1a^+$ MoDCs (**Figure 3A**). Besides, both fractions induced significant decrease in HLA-DR expression in both DCs populations (**Figure 3B**). Inhibition of DC-SIGN and HLA-DR indicate negative modulation of antigen presentation (Chudnovskiy et al., 2019). CD80 expression in $CD1a^+$ cells was inhibited by both cell wall fractions (**Figure 3C**). However, in $CD1a^-$ cells, increased expression of CD80 (by F2 fraction, **Figure 3C**) and CD83 (both cell wall fraction, **Figure 3D**) was observed. Altogether, these data demonstrate that Pb cell wall fractions alter CD1a subsets phenotype, downregulating maturation of $CD1a^+$ population. On the other hand, as cell wall fractions downregulate antigen presentation, they enhance expression of co-stimulatory molecules in the $CD1a^-$ subset.

Paracoccidioides brasiliensis Cell Wall Fractions Alter Human MoDCs Inflammatory Cytokines Secretion

At last, we analyzed the profile of inflammatory cytokines produced in the last 24 h of DCs differentiation under stimulation with Pb cell wall fractions. We observed that differentiation upon F1 stimulation induced an increase in IL-6 and IL-10 levels, while decreasing production of IL-12 and TNFα (**Figure 4**). Meanwhile, F2 stimulation induced a decrease in TNFα and IL-8, but significantly induced IL-1β expression. These data indicate that Pb cell wall fractions differentially modulate the ability of inflammatory cytokine production by MoDCs.

DISCUSSION

Dendritic cells are the most specialized antigen-presenting cells and have a crucial role in directing appropriate immune responses to favor PCM resolution. The protection against PCM is related to a prevalent cell-mediated immune response, with production of Th1 cytokines and activation of macrophages and lymphocytes that induce fungal killing

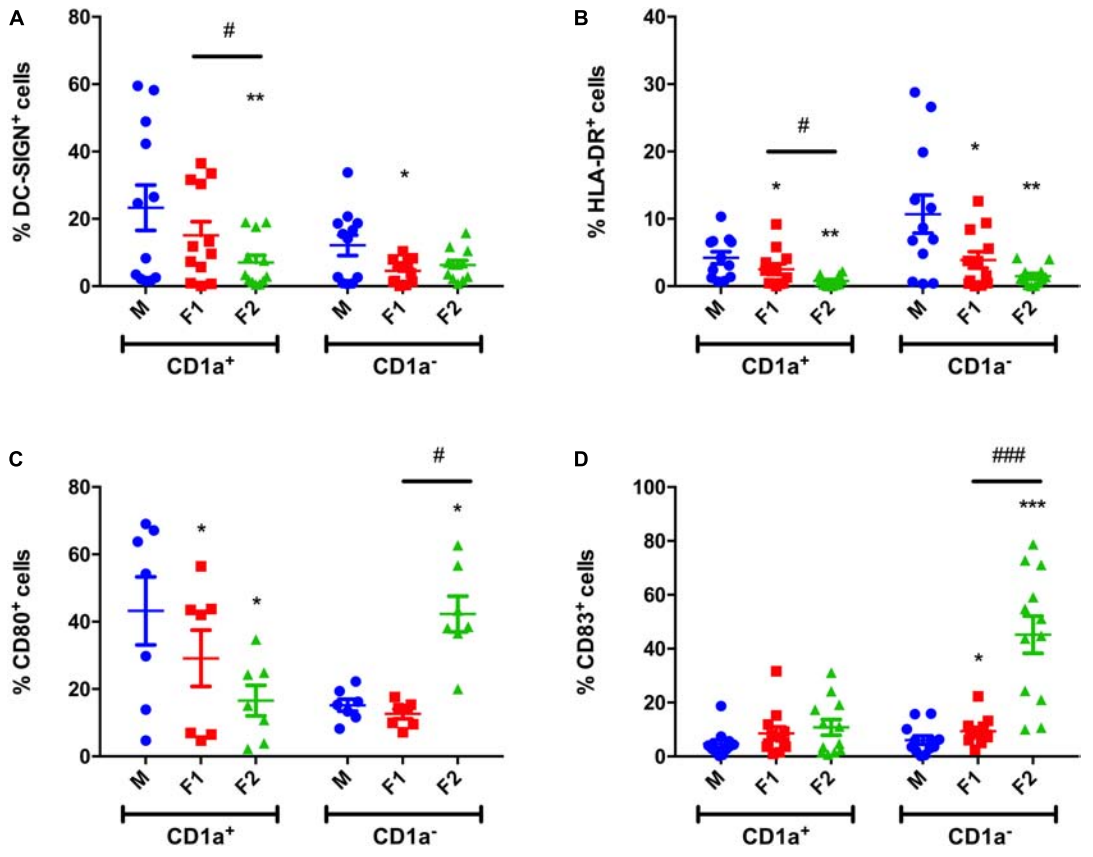

FIGURE 3 | *Paracoccidioides brasiliensis* cell wall fractions modulate CD1a subsets phenotype. Frequency of $DC\text{-}SIGN^+$ **(A)**, $HLA\text{-}DR^+$ **(B)**, $CD80^+$ **(C)**, and $CD83^+$ **(D)** cell populations after differentiation upon F1 or F2 stimulation. Non-stimulated cells were used as a control (M). Each data point represents one donor. Wilcoxon matched pairs *T* test. $^*p < 0.05$, $^{**}p < 0.01$, and $^{***}p < 0.001$ in comparison to control group. $^{\#}p < 0.05$ and $^{\#\#\#}p < 0.001$ between groups treated with cell wall fractions.

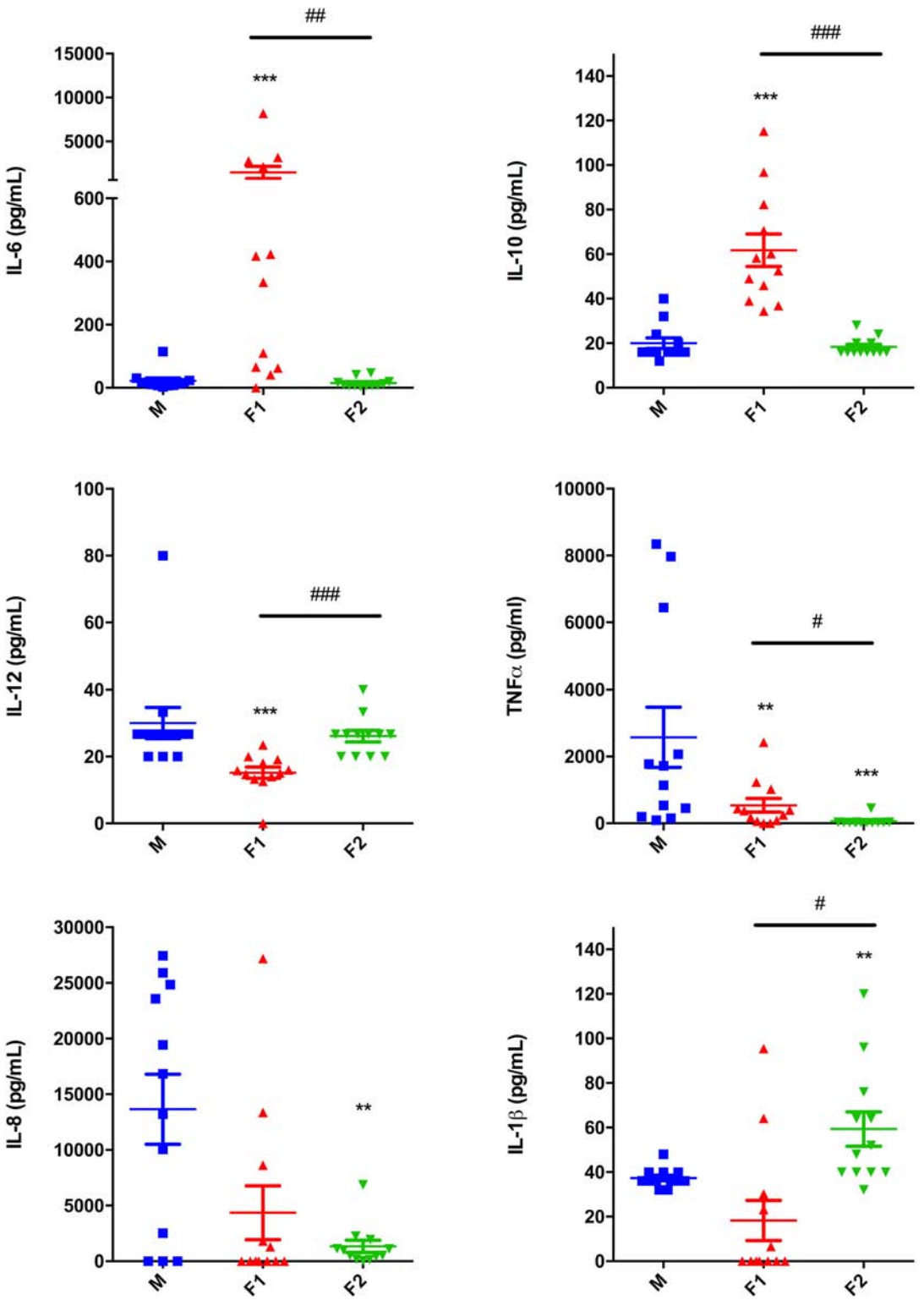

FIGURE 4 | *Paracoccidioides brasiliensis* cell wall fractions modulate cytokine production by dendritic cells. IL-6, IL-10, IL-12, TNF, IL-8, and IL-1β levels were measured in the cell culture supernatants after differentiation upon F1 or F2 stimulation. Non-stimulated cells were used as a control (M). Each data point represents one donor. Wilcoxon matched pairs *T* test. $^{**}p < 0.01$ and $^{***}p < 0.001$ in comparison to control group. $^{\#}p < 0.05$, $^{\#\#}p < 0.01$, and $^{\#\#\#}p < 0.001$ between groups treated with cell wall fractions.

and isolation in well-defined granulomas (Borges-Walmsley et al., 2002; Ferreira, 2009; Bocca et al., 2013). On the other hand, polarization toward a Th2 immune response enhances the disease (Bocca et al., 2013; Camacho and Niño-Vega, 2017; Shikanai-Yasuda et al., 2017). Given the importance of DCs in directing T-cell responses and immune response polarization, we analyzed the impact of Pb cell wall fractions in the differentiation and maturation of human monocyte-derived DCs.

Early studies show that in the *P. brasiliensis* pathogenic yeast the majority of cell wall glucans are α-linked, while only 4% are β-linked (Kanetsuna et al., 1969, 1972). β-glucans form a fibrillary scaffold that stabilizes the cell wall and are likely found closer to the cell membrane (Puccia et al., 2011; Latgé, 2017). On the other hand, α-glucan is embedded in the cell wall as an amorphous substance, forming a prominent outlayer (Puccia et al., 2011; Latgé, 2017). Reduction of cell wall α-glucan severely attenuates virulence in murine models of *H. capsulatum* (Klimpel and Goldman, 1988), *B. dermatitis* (Hogan and Klein, 1994), and *P. brasiliensis* infection (San-Blas et al., 1977). Likewise, abundance of α-glucan in *P. brasiliensis* pathogenic yeasts and its absence in non-pathogenic mycelial forms also corroborates the correlation of this polysaccharide to fungal virulence (San-Blas and San-Blas, 1977). Our results demonstrated that a non-virulent isolate of *P. brasiliensis* presented higher exposure of β-glucan in comparison to a virulent-isolate, possibly because α-glucan masks the inner layer of the cell wall, preventing immune recognition of β-glucan (Sukhithasri et al., 2013). Similarly, the presence of α-glucan on the *H. capsulatum* cell wall blocked the host recognition of β-glucan by dectin-1, reducing TNFα production and avoiding proper activation of the immune system (Rappleye et al., 2007).

Our data demonstrates, however, that besides hindering exposure of β-glucans, α-glucans can also negatively modulate differentiation of $CD1a^+$ DCs. We analyzed CD1a expression after DC differentiation in the presence of cell wall fractions. CD1a is a well described DCs subset marker involved in the presentation of lipid or lipid-based molecules (Cernadas et al., 2009). $CD1a^+$ DCs produce high levels of IL-12 and can polarize Th1 cells, whereas $CD1a^-$ DCs lack IL-12 production and secrete high levels of IL-10, favoring development of Th2 immunity (Chang et al., 2000; Cernadas et al., 2009). DCs differentiation upon F2 led to a significant decrease in $CD1a^+$ cells, suggesting that α-glucan may play a role in Th2 polarization during PCM. The same is true for α-glucan extracted from the cell wall of *Mycobacterium tuberculosis* (Gagliardi et al., 2007), where this polysaccharide is closely related to the impairment of CD1a lipid antigen presentation, limiting the activation of CD1-restricted lipid-specific T lymphocytes. As a matter of fact, CD1a participation in Pb antigenic lipids presentation to T-cells has not yet been assessed. However, it is possible that the α-glucan present in Pb cell wall may subvert the development of $CD1a^+$ population, impairing lipid presentation.

We also observed that both cell wall fractions induced down-regulation of DC-SIGN expression in $CD1a^-$ cells (F1) and $CD1a^+$ cells (F2). DC-SIGN is a C-type lectin receptor restricted to DCs. Likewise antigen recognition, DC-SIGN participates in DCs migration and T-cell priming (Švajger et al., 2010). Other pathogens make use of DC-SIGN to subvert DCs functions in order to escape immune surveillance, such as HIV-1 and *M. tuberculosis* (van Kooyk et al., 2003; Gagliardi et al., 2007). HLA-DR expression was also inhibited by both F1 and F2, suggesting an impairment of antigen presentation capacity. While CD80 expression was inhibited by both cell wall fractions in $CD1a^+$ cells, F2 fraction upregulated its expression in $CD1a^-$ cells. Similarly to CD80 upon F2 treatment, CD83 expression was increased in $CD1a^-$ cells from both F1 and F2 treatments, although levels remained unaltered in $CD1a^+$ cells. Corroborating these data, infection of monocytes with *M. tuberculosis* and Bacillus Calmette-Guérin (BCG), but not with *Mycobacterium avium,* induced lack of CD1a, CD1b and CD1c, presence of maturation markers CD86 and CD83 and down-regulation of CD80 and MHC class II (Gagliardi et al., 2002; Mariotti et al., 2002), and this effect was correlated with α-glucan present in the cell wall (Gagliardi et al., 2007).

In this study, Pb cell wall fractions were able to modulate inflammatory cytokine production by DCs. Both F1 and F2 inhibited production of TNF. In PCM, TNF is required for the persistence of well-formed granulomas and NO production (Figueiredo et al., 1993) and contrarily, it is highly induced in mice after *in vivo* challenge with F1 (Silva et al., 1994). F1 also induced a decrease in IL-12 and an increase in IL-10 and IL-6 by DCs. The same pattern of cytokine production was seen after monocyte differentiation into DCs upon *Candida albicans* β-glucan stimulation (Nisini et al., 2007). Increased IL-10 and low levels of IL-12 downregulate Th1 cell activity, which have a negative outcome for host protection during PCM. F2 stimulation induced decreased IL-8 and increased IL1β levels. These results demonstrate a mixed pattern of cytokine production upon DCs differentiation in the presence of Pb cell wall fractions, with both up- and downregulation of inflammatory mediators.

Our data corroborates previous studies that demonstrated that Pb infection alters DCs maturation, leading to a T cell-mediated response that could influence the susceptibility to this pathogen (Ferreira et al., 2004, 2007; Ferreira and Almeida, 2006; Fernandes et al., 2015). We speculate that, when monocytes migrate to the infection site, they interact with components of the fungal cell wall, especially α-glucans, and undergo an inadequate differentiation into $CD1a^-$ DCs. Further studies are required in order to better understand how Pb cell wall α-glucan influences the host immune response during PCM. To the best of our knowledge, this is the first report that demonstrates the influence of Pb cell wall α-glucan in the differentiation and maturation of human DCs.

DATA AVAILABILITY STATEMENT

The raw data supporting the conclusions of this manuscript will be made available by the authors, without undue reservation, to any qualified researcher.

ETHICS STATEMENT

The studies involving human participants were reviewed and approved by the Blood Center of Salvador, HEMOBA, Brumado, Brazil, authorization number 100/2006. The patients/participants provided their written informed consent to participate in this study.

AUTHOR CONTRIBUTIONS

AS performed the research, analyzed and interpreted the data, and wrote the manuscript. CF designed and performed the research and analyzed the data. NS, NT, CS, MJ, PV, and CM performed the research. CB and AB designed the research, analyzed and interpreted the data, and wrote the manuscript.

FUNDING

This work was supported by the Chemical Sciences, Geosciences and Biosciences Division, Office of Basic Energy Sciences, U.S. Department of Energy grant (DE-SC0015662) to Parastoo Azadi at the Complex Carbohydrate Research Center.

ACKNOWLEDGMENTS

The authors would like to thank the Fundação de Apoio à Pesquisa do Distrito Federal (FAPDF), Conselho Nacional de Pesquisa (CNPq), and Decanato de Pesquisa e Pós-Graduação da Universidade de Brasília (DPP/UnB) for financial support, and CAPES for graduate students' grants.

REFERENCES

Almeida, S. R., and Lopes, J. D. (2001). The low efficiency of dendritic cells and macrophages from mice susceptible to *Paracoccidioides brasiliensis* in inducing a Th1 response. *Brazilian J. Med. Biol. Res.* 34, 529–537. doi: 10.1590/s0100-879x2001000400014

Bocca, A. L., Amaral, A. C., Teixeira, M. M., Sato, P. K., Shikanai-Yasuda, M. A., Soares Felipe, M. S., et al. (2013). Paracoccidioidomycosis: eco-epidemiology, taxonomy and clinical and therapeutic issues. *Future Microbiol.* 8, 1177–1191. doi: 10.2217/fmb.13.68

Borges-Walmsley, M. I., Chen, D., Shu, X., and Walmsley, A. R. (2002). The pathobiology of *Paracoccidioides brasiliensis*. *Trends Microbiol.* 10, 80–87. doi: 10.1016/S0966-842X(01)02292-2

Bowman, S. M., and Free, S. J. (2006). The structure and synthesis of the fungal cell wall. *Bio Essays* 28, 799–808.

Calich, V. L. G., da Costa, T. A., Felonato, M., Arruda, C., Bernardino, S., Loures, F. V., et al. (2008). Innate immunity to *Paracoccidioides brasiliensis* infection. *Mycopathologia* 165, 223–236. doi: 10.1007/s11046-007-9048-1

Camacho, E., and Niño-Vega, G. A. (2017). *Paracoccidioides* Spp.: virulence factors and immune-evasion strategies. *Mediators Inflamm.* 2017:5313691. doi: 10.1155/2017/5313691

Carbonell, L. M., Kanetsuna, F., and Gil, F. (1970). Chemical morphology of glucan and chitin in the cell wall of the yeast phase of *Paracoccidioides brasiliensis*. *J. Bacteriol.* 101, 636–642.

Cernadas, M., Lu, J., Watts, G., and Brenner, M. B. (2009). CD1a expression defines an interleukin-12 producing population of human dendritic cells. *Clin. Exp. Immunol.* 155, 523–533. doi: 10.1111/j.1365-2249.2008.03853.x

Chang, C. C., Wright, A., and Punnonen, J. (2000). Monocyte-derived CD1a+ and CD1a- dendritic cell subsets differ in their cytokine production profiles, susceptibilities to transfection, and capacities to direct Th cell differentiation. *J. Immunol.* 165, 3584–3591. doi: 10.4049/jimmunol.165.7.3584

Chudnovskiy, A., Pasqual, G., and Victora, G. D. (2019). Studying interactions between dendritic cells and T cells in vivo. *Curr. Opin. Immunol.* 58, 24–30. doi: 10.1016/j.coi.2019.02.002

Fernandes, R. K., Bachiega, T. F., Rodrigues, D. R., Golim Mde, A., Dias-Melicio, L. A., Balderramas Hde, A., et al. (2015). *Paracoccidioides brasiliensis* interferes on dendritic cells maturation by inhibiting PGE2 production. *PLoS One* 10:e0120948. doi: 10.1371/journal.pone.0120948

Ferreira, K. S., and Almeida, S. R. (2006). Immunization of susceptible mice with gp43-pulsed dendritic cells induce an increase of pulmonary Paracoccidioidomycosis. *Immunol. Lett.* 103, 121–126. doi: 10.1016/j.imlet.2005.10.014

Ferreira, K. S., Bastos, K. R., Russo, M., and Almeida, S. R. (2007). Interaction between *Paracoccidioides brasiliensis* and pulmonary dendritic cells induces interleukin−10 production and toll−like receptor−2 expression: possible mechanisms of susceptibility. *J. Infect. Dis.* 196, 1108–1115. doi: 10.1086/521369

Ferreira, K. S., Lopes, J. D., and Almeida, S. R. (2004). Down-regulation of dendritic cell activation induced by *Paracoccidioides brasiliensis*. *Immunol. Lett.* 94, 107–114. doi: 10.1016/j.imlet.2004.04.005

Ferreira, M. S. (2009). Paracoccidioidomycosis. *Paediatr. Respir. Rev.* 10, 161–165. doi: 10.1016/j.prrv.2009.08.001

Figueiredo, F., Alves, L. M., and Silva, C. L. (1993). Tumour necrosis factor production in vivo and in vitro in response to *Paracoccidioides brasiliensis* and the cell wall fractions thereof. *Clin. Exp. Immunol.* 93, 189–194. doi: 10.1111/j.1365-2249.1993.tb07964.x

Free, S. J. (2013). Fungal cell wall organization and biosynthesis. *Adv. Genet.* 81, 33–82. doi: 10.1016/B978-0-12-407677-8.00002-6

Gagliardi, M. C., Lemassu, A., Teloni, R., Mariotti, S., Sargentini, V., Pardini, M., et al. (2007). Cell wall-associated alpha-glucan is instrumental for *Mycobacterium tuberculosis* to block CD1 molecule expression and disable the function of dendritic cell derived from infected monocyte. *Cell Microbiol.* 9, 2081–2092. doi: 10.1111/j.1462-5822.2007.00940.x

Gagliardi, M. C., Teloni, R., Mariotti, S., Iona, E., Pardini, M., Fattorini, L., et al. (2002). Bacillus calmette-guérin shares with virulent *Mycobacterium tuberculosis* the capacity to subvert monocyte differentiation into dendritic cell: implication for its efficacy as a vaccine preventing tuberculosis. *Vaccine* 22, 3848–3857. doi: 10.1016/j.vaccine.2004.07.009

Gow, N. A. R., Latge, J.-P., and Munro, C. A. (2017). The fungal cell wall: structure. Biosynthesis, and funcntio. *Microbiol. Spectr.* 5, 3341–3354.

Hogan, L. H., and Klein, B. S. (1994). Altered expression of surface alpha-1,3-glucan in genetically related strains of *Blastomyces dermatitidis* that differ in virulence. *Infect. Immun.* 62, 3543–3546.

Kanetsuna, F., and Carbonell, L. M. (1970). Cell wall glucans of the yeast and mycelial forms of *Paracoccidioides brasiliensis*. *J. Bacteriol.* 101, 675–680.

Kanetsuna, F., Carbonell, L. M., Azuma, I., and Yamamura, Y. (1972). Biochemical studies on the thermal dimorphism of *Paracoccidioides brasiliensis*. *J. Bacteriol.* 110, 208–218.

Kanetsuna, F., Carbonell, L. M., Moreno, R. E., and Rodriguez, J. (1969). Cell wall composition of the yeast and mycelial forms of *Paracoccidioides brasiliensis*. *J Bacteriol.* 97, 1036–1041.

Klimpel, K. R., and Goldman, W. E. (1988). Cell walls from avirulent variants of Histoplasma capsulatum lack alpha-(1,3)-glucan. *Infect. Immun.* 56, 2997–3000.

Latgé, J.-P. (2010). Tasting the fungal cell wall. *Cell. Microbiol.* 12, 863–872. doi: 10.1111/j.1462-5822.2010.01474.x

Latgé, J. P. (2017). 30 years of battling the cell wall. *Med. Mycol.* 55, 4–9. doi: 10.1093/mmy/myw076

Leenaars, M., and Hendriksen, C. F. M. (2005). Critical steps in the production of polyclonal and monoclonal antibodies: evaluation and recommendations. *ILAR J.* 46, 269–279. doi: 10.1093/ilar.46.3.269

Mariotti, S., Teloni, R., Iona, E., Fattorini, L., Giannoni, F., Romagnoli, G., et al. (2002). *Mycobacterium tuberculosis* subverts the differentiation of human

monocytes into dendritic cells. *Eur. J. Immunol.* 32, 3050–3058. doi: 10.1002/1521-4141(200211)32:11<3050::aid-immu3050>3.0.co;2-k

Mazurek, J., Ignatowicz, L., Kallenius, G., Svenson, S. B., Pawlowski, A., Hamasur, B., et al. (2012). Divergent effects of mycobacterial cell wall glycolipids on maturation and function of human monocyte-derived dendritic cells. *PLoS One* 7:e42515. doi: 10.1371/journal.pone.0042515

Moreno, R. E., Kanetsuna, F., and Carbonell, L. M. (1969). Isolation of chitin and glucan from the cell wall of the yeast form of *Paracoccidioides brasiliensis*. *Arch. Biochem. Biophys.* 130, 212–217. doi: 10.1016/0003-9861(69)90026-5

Nisini, R., Torosantucci, A., Romagnoli, G., Chiani, P., Donati, S., Gagliardi, M. C., et al. (2007). Beta-glucan of Candida albicans cell wall causes the subversion of human monocyte differentiation into dendritic cells. *J. Leukoc. Biol.* 82, 1136–1142. doi: 10.1189/jlb.0307160

Nóbrega, Y. K., Lozano, V. F., de Araújo, T. S., de Carvalho, D. D., and Bocca, A. L. (2010). The cell wall fraction from fonsecaea pedrosoi stimulates production of different profiles of cytokines and nitric oxide by murine peritoneal cells in vitro. *Mycopathologia* 170, 89–98. doi: 10.1007/s11046-010-9303-8

Pina, A., de Araujo, E. F., Felonato, M., Loures, F. V., Feriotti, C., Bernardino, S., et al. (2013). Myeloid dendritic cells (DCs) of mice susceptible to paracoccidioidomycosis suppress T cell responses whereas myeloid and plasmacytoid DCs from resistant mice induce effector and regulatory T cells. *Infect. Immun.* 81, 1064–1077. doi: 10.1128/IAI.00736-12

Puccia, R., Vallejo, M. C., Matsuo, A. L., and Longo, L. V. G. (2011). The *Paracoccidioides* cell wall: past and present layers toward understanding interaction with the host. *Front. Microbiol.* 2:257. doi: 10.3389/fmicb.2011.00257

Rappleye, C. A., Eissenberg, L. G., and Goldman, W. E. (2007). Histoplasma capsulatum alpha-(1,3)-glucan blocks innate immune recognition by the beta-glucan receptor. *Proc. Natl. Acad. Sci. U.S.A.* 104, 1366–1370. doi: 10.1073/pnas.0609848104

San-Blas, G., and San-Blas, F. (1977). *Paracoccidioides brasiliensis*: cell wall structure and virulence. *Rev. Mycopathol.* 62, 77–86. doi: 10.1007/bf01259396

San-Blas, G., San-Blas, F., and Serrano, L. E. (1977). Host-parasite relationships in the yeastlike form of *Paracoccidioides brasiliensis* strain IVIC Pb9. *Infect. Immun.* 15, 343–346.

Shikanai-Yasuda, M. A., de Queiroz Telles Filho, F., Mendes, R. P., Colombo, A. L., and Moretti, M. L. (2006). Consenso em paracoccidioidomicose. *Rev. Soc. Bras. Med. Trop.* 39, 297–310. doi: 10.1590/s0037-86822006000300017

Shikanai-Yasuda, M. A., Mendes, R. P., Colombo, A. L., Queiroz-Telles, F., Kono, A. S. G., Paniago, A. M. M., et al. (2017). Brazilian guidelines for the clinical management of paracoccidioidomycosis. *Rev. Soc. Bras. Med. Trop.* 50, 715–740. doi: 10.1590/0037-8682-0230-2017

Silva, C. L., Alves, L. M. C., and Figueiredo, F. (1994). Involvement of cell wall glucans in the genesis and persistence of the inflammatory reaction caused by the fungus *Paracoccidioides brasiliensis*. *Microbiology* 140, 1189–1194. doi: 10.1099/13500872-140-5-1189

Silvana dos Santos, S., Ferreira, K. S., and Almeida, S. R. (2011). *Paracoccidioides brasilinsis*-induced migration of dendritic cells and subsequent t-cell activation in the lung-draining lymph nodes. *PLoS One* 6:e19690. doi: 10.1371/journal.pone.0019690

Sukhithasri, V., Nisha, N., Biswas, L., Anil Kumar, V., and Biswas, R. (2013). Innate immune recognition of microbial cell wall components and microbial strategies to evade such recognitions. *Microbiol. Res.* 168, 396–406. doi: 10.1016/j.micres.2013.02.005

Švajger, U., Anderluh, M., Jeras, M., and Obermajer, N. (2010). C-type lectin DC-SIGN: An adhesion, signalling and antigen-uptake molecule that guides dendritic cells in immunity. *Cell. Signal.* 22, 1397–1405. doi: 10.1016/j.cellsig.2010.03.018

Tavares, A. H., Derengowski, L. S., Ferreira, K. S., Silva, S. S., Macedo, C., Bocca, A. L., et al. (2012). Murine dendritic cells transcriptional modulation upon *Paracoccidioides brasiliensis* infection. *PLoS Negl. Trop. Dis.* 6:e1459. doi: 10.1371/journal.pntd.0001459

Turissini, D. A., Gomez, O. M., Teixeira, M. M., McEwen, J. G., and Matute, D. R. (2017). Species boundaries in the human pathogen *Paracoccidioides*. *Fungal Genet. Biol.* 106, 9–25. doi: 10.1016/j.fgb.2017.05.007

van Kooyk, Y., Appelmelk, B., and Geijtenbeek, T. B. (2003). A fatal attraction: *Mycobacterium tuberculosis* and HIV-1 target DC-SIGN to escape immune surveillance. *Trends Mol. Med.* 9, 153–159. doi: 10.1016/s1471-4914(03)00027-3

Conflict of Interest: The authors declare that the research was conducted in the absence of any commercial or financial relationships that could be construed as a potential conflict of interest.

frontiers in Microbiology

ORIGINAL RESEARCH
published: 07 November 2019
doi: 10.3389/fmicb.2019.02513

Cell Wall-Associated Virulence Factors Contribute to Increased Resilience of Old *Cryptococcus neoformans* Cells

Erika P. Orner[1†], Somanon Bhattacharya[2†], Klea Kalenja[1], Danielle Hayden[1], Maurizio Del Poeta[1,2,3] and Bettina C. Fries[1,2,3]*

[1] Department of Microbiology and Immunology, Stony Brook University, Stony Brook, NY, United States, [2] Department of Medicine, Division of Infectious Disease, Stony Brook University, Stony Brook, NY, United States, [3] Northport Veterans Affairs Medical Center, Northport, NY, United States

As *Cryptococcus neoformans* mother cells generationally age, their cell walls become thicker and cell-wall associated virulence factors are upregulated. Antiphagocytic protein 1 (App1), and laccase enzymes (Lac1 and Lac2) are virulence factors known to contribute to virulence of *C. neoformans* during infection through inhibition of phagocytic uptake and melanization. Here we show that these cell-wall-associated proteins are not only significantly upregulated in old *C. neoformans* cells, but also that their upregulation likely contributes to the increased resistance to antifungal and host-mediated killing during infection and to the subsequent accumulation of old cells. We found that old cells melanize to a greater extent than younger cells and as a consequence, old melanized cells are more resistant to killing by amphotericin B compared to young melanized cells. A decrease in melanization of old *lac*Δ mutants lead to a decrease in old-cell resilience, indicating that age-related melanization is contributing to the overall resilience of older cells and is being mediated by laccase genes. Additionally, we found that older cells are more resistant to macrophage phagocytosis, but this resistance is lost when *APP1* is knocked out, indicating that upregulation of *APP1* in older cells is in part responsible for their increased resistance to phagocytosis by macrophages. Finally, infections with old cells in the *Galleria mellonella* model support our conclusions, as loss of the *APP1, LAC1,* and *LAC2* gene ablates the enhanced virulence of old cells, indicating their importance in age-dependent resilience.

Keywords: *Cryptococcus neoformans*, aging, virulence, antiphagocytic protein, cell wall, melanin

OPEN ACCESS

Edited by:
Joshua D. Nosanchuk, Albert Einstein College of Medicine, United States

Reviewed by:
Livia Kmetzsch, Federal University of Rio Grande do Sul, Brazil
Marilene Henning Vainstein, Federal University of Rio Grande do Sul, Brazil

***Correspondence:**
Bettina C. Fries
Bettina.Fries@stonybrookmedicine.edu

†Co-first authors

Specialty section:
This article was submitted to Fungi and Their Interactions, a section of the journal Frontiers in Microbiology

Received: *29 August 2019*
Accepted: *18 October 2019*
Published: *07 November 2019*

Citation:
Orner EP, Bhattacharya S, Kalenja K, Hayden D, Del Poeta M and Fries BC (2019) Cell Wall-Associated Virulence Factors Contribute to Increased Resilience of Old Cryptococcus neoformans Cells. Front. Microbiol. 10:2513. doi: 10.3389/fmicb.2019.02513

INTRODUCTION

For a pathogen to survive in a host during infection, it must be able to sense its environment and respond accordingly. In the human host, fungal pathogens can withstand high body temperatures, changes in pH and nutrient composition, and the host response by modifying their cell wall. *Cryptococcus neoformans* is a ubiquitous environmental fungus that causes disease in humans who are immune compromised. *C. neoformans* is responsible for upward of 15% of AIDS-related deaths worldwide (Rajasingham et al., 2017). During infection, alveolar macrophages are the

first line of defense against *Cryptococcus* (Alvarez and Casadevall, 2006). In order to establish an infection, *C. neoformans* must find a way to inhibit macrophage phagocytosis and phagocytic killing. *C. neoformans* employs a number of virulence mechanisms to combat macrophage attack including age-dependent cell wall modification (Bouklas et al., 2013), melanization, and secretion of the antiphagocytic protein 1, App1 (Del Poeta, 2004).

Previously, our lab has shown that generational aging of fungi contributes to enhanced resilience in the host (Bouklas et al., 2013, 2017a,b; Bhattacharya and Fries, 2018; Bhattacharya et al., 2019; Orner et al., 2019). *C. neoformans,* like other yeasts, undergoes asymmetric division when replicating, resulting in a mother cell's phenotype that continuously evolves with each division (Bouklas et al., 2013). Generationally aged cells (i.e., 10-generation-old cells) show an increased resistance to phagocytic ingestion, phagocytic killing, and even antifungal killing (Bouklas et al., 2013, 2017a; Orner et al., 2019). What mediates this age-dependent resilience is not known, but experimental data demonstrates the selection and accumulation of generationally older cells during infection in rats and in humans (Bouklas et al., 2013, 2017a).

Antiphagocytic protein 1 (App1) is a virulence factor that is unique to *C. neoformans* (Luberto et al., 2003) and located in the cell wall of *C. neoformans* (Qureshi et al., 2012). This protein is also secreted into the supernatant of cultures and detectable in bronchoalveolar lavage fluid, serum, and cerebral spinal fluid of patients (Luberto et al., 2003; Stano et al., 2009; Williams and Del Poeta, 2011). App1 inhibits phagocytosis by macrophages through a complement-mediated mechanism where the App1 protein competes with iC3b for binding to complement receptor (CR) 3 on macrophages (Stano et al., 2009). During infection, iC3b opsonizes microbes and binds to complement receptor 3 on professional phagocytes like monocytes, macrophages, and dendritic cells to aid in phagocytosis (Stuart, 2002). When App1 binds to CR3, it reduces attachment and ingestion of *C. neoformans* into macrophages both *ex vivo* and *in vitro* in a dose-dependent manor (Luberto et al., 2003). Knockout mutants lacking *APP1* are less virulent in mice, indicating this virulence factor plays an important role in establishing infection. Interestingly, Qureshi et al. (2012) found App1 to have amyloid properties and argue it may also play additional roles in pathogenesis. For example, amyloids have been shown to help evade the immune system by producing a protective coating around the cell wall in various other microbes (Gebbink et al., 2005; Qureshi et al., 2012). Furthermore, different amyloids have been shown to be important for melanin biosynthesis (Qureshi et al., 2012).

Melanin production is a key virulence factor for a wide variety of microbes and multicellular organisms including fungi, bacteria, plants, and animals (Howard and Valent, 1996; van Duin et al., 2002; Nosanchuk and Casadevall, 2003). Melanin synthesis occurs in the cell wall through the oxidation of phenolic substances like dopamine, epinephrine, and norepinephrine into quinones which then polymerize into pigmented melanin products (Williamson, 1994). These substances are found in high concentrations in the central nervous system and may contribute to *C. neoformans*' tropism for the central nervous system (Polacheck et al., 1982). Melanization contributes to resistance against antibody-mediated phagocytosis and phagocytic killing by macrophages (Wang et al., 1995; Casadevall and Perfect, 1998; Zhu and Williamson, 2004) and resistance against free-radical killing by reactive oxygen and nitrogen species (Wang et al., 1995; Missall et al., 2004). Furthermore, melanization provides protection against antifungals like amphotericin B, the first line therapeutic against *C. neoformans* (van Duin et al., 2002).

The laccase gene, *LAC1* encodes the rate-limiting enzyme that catalyzes polymerization of quinones and has been the focus of most *C. neoformans* melanization studies (Torres-Guererro and Edman, 1994; Williamson, 1994). *LAC2* is another cryptococcal laccase gene that exhibits 72% amino acid homology to *LAC1* (Missall et al., 2004). *LAC1* has a unique C-terminal motif that localizes the protein to the cell wall of *C. neoformans* at physiological pH (7.4; Waterman et al., 2007). *LAC2* is truncated in the C-terminal region and is located in the cytosol under normal conditions but can locate to the cell wall in the absence of *LAC1* (Missall et al., 2004). Both *LAC1* and *LAC2* genes contribute to melanization.

Here, we found that *APP1, LAC1,* and *LAC2* genes are all upregulated old *C. neoformans* cells (10 generations old) compared to young cells (0–2 generations old). Interestingly, all three mutants exhibited shorter median lifespans. Furthermore, our data demonstrates that when knockout mutant strains were aged to 10 generations, they no longer exhibited enhanced age-dependent resistance to killing by antifungals, macrophages, or *Galleria mellonella* worms. Furthermore, we also found that *LAC2* is not just a redundant gene to compensate for *LAC1*, but rather, it contributes to age-dependent resilience distinct from *LAC1*.

MATERIALS AND METHODS

Strains and Media

Strains and sources of strains used in this study are shown in **Table 1**. All strains were stored in 30% glycerol at −80°C. When needed, strains were struck on Yeast-Peptone-Dextrose (YPD) agar plates (BD), grown at 37°C and stored at 4°C. Media used in this study is listed in **Table 2**. All liquid cultures were grown at 37°C, shaking at 150 rpm.

Replicative Lifespan and Cell Size Measurement

The replicative lifespan (RLS) of all strains was determined by traditional microdissection methodology (Bouklas et al., 2013).

TABLE 1 | Strains used in this study.

Strain	Source
H99	Dr. John Perfect (Duke University)
Kn99α	Dr. Maurizio Del Poeta (Stony Brook University)
H99Δ*app1*	Dr. Maurizio Del Poeta (Stony Brook University)
H99Δ*lac1*	Dr. Peter Williamson (National Institutes of Health)
Kn99αΔ*lac2*	Dr. Maurizio Del Poeta (Stony Brook University)

TABLE 2 | Media used in this study.

Media	Components per 1 Liter or source
Yeast-Peptone-Dextrose (YPD)	BD – Unmodified
Sabaroud Dextrose (SAB)	BD – Unmodified
Melanization Media (MM)	4 g KH_2PO_4, 2.5 g $MgSO_4 \cdot 7H_2O$, 0.975 g Glycine, 3 g Dextrose, 1 mg Thiamine, 1 mM L-DOPA
Synthetic Media (SM)	1.7 g yeast nitrogen base without amino acids, 1 g drop out mix, 0.4% ethanol, 5 g $(NH_4)_2SO_4$, 3.3 g NaCl, 20 g glucose
RPMI 1640	Gibco – unmodified
DMEM	Gibco – modified with 10% heat inactivated Fetal Bovine Serum, 10% NCTC (Gibco), 1% non-essential amino-acids, and 1% Penicillin-Streptomycin

Briefly, 25–30 cells were lined up on a YPD agar plate using a 25 μm fiber-optic needle (Cora Styles) on a tetrad dissection Axioscope A1 microscope (Zeiss) and grown at 37°C. After 1 division, naïve cells were separated from their mothers and designated as starting mother cells. These cells were then tracked and after every division (every 60–120 min), naïve daughter cells were counted and removed to allow the mothers to continue to divide. In between divisions, cells were incubated at either 37°C or 4°C overnight to slow growth and prevent excessive replication. As cells reached desired generational age, images were taken of the cells on top of an EVOS FL Auto microscope (Thermo Fisher Scientific) and cell sizes were measured using FIJI opensource software.

Isolation of Old Cells

Previously described methods for isolation of old and young cells were slightly modified (Bouklas et al., 2013). Briefly, exponential cells were washed and labeled with 8 mg/mL Sulfo-NHS-LC-LC-Biotin (Thermo Scientific) for 1 h at room temperature. After 1 h, cells were washed with PBS and labeled with 20 μL anti-biotin (Miltenyi Biotec) per 10^7 cells for 1 h at 4°C. After labeling, cells were grown in either sabaroud dextrose (SAB) (Difco) media, melanization media (MM), or synthetic media (SM) as outlined to a specific generation. Recovery of generationally aged mother cells was done using LS magnetic columns (Miltenyi Biotec). The negative fraction that washed off the column was used as the young control group as they were exposed to the same manipulation as old cells retained in the magnetic column.

Quantitative Reverse Transcriptase Polymerase Chain Reaction (qPCR)

RNA was isolated from both young (0–3 generation) and old (10 generation) cells grown in SAB using Qiagen RNAeasy Kit following manufacturer's guidelines. Nanodrop (Biospectrophotometer, Eppendorf) was used to quantify the isolated RNA. An absorption ratio (A260/A280) of 2.0 was considered pure and good quality RNA. 250 ng of RNA was converted to cDNA using Verso cDNA Kit (Thermoscientific) following manufacturer's guidelines. Oligo-dT was used as the primer for the preparation of cDNA. After this, cDNA was diluted 1:5 with nuclease free water (Hyclone) and subjected to qPCR (Roche) utilizing Power SYBR Green Master Mix (Applied Biosystems) following manufacturer's guidelines. The oligonucleotides used for this assay are listed below. Housekeeping gene *ACT1* was used as an internal control. Data was normalized to the gene expression in the young (0–3 generation) cells of both wildtype strains. Data was analyzed using ΔΔCt method as previously described (Livak and Schmittgen, 2001). The following primers were used:

ACT1: F5′-CCCACACTGTCCCCATTTAC-3′, R5′-AACCAC GCTCCATGAGAATC-3′; *APP1:* F5′-CCAAACTGCGTTACTC AGCA-3′, R5′-TAATGCTGCTTTCCCCATTC-3′; *LAC1*: F5′-TT TGGGTCCGCCCCTTAATTATC-3′, R5′-GGATAGGTGCATG AGGAGGA-3′; *LAC2*: F5′-TATCCTCCTCCCGAGAT-3′, R5′-GCATCCCCTTCTTTTCCTTC-3′.

Macrophage Phagocytosis and Killing

J774.16 macrophages were cultured in DMEM (Gibco) media containing 10% heat inactivated Fetal Bovine Serum (FBS), 10% NCTC (Gibco), 1% non-essential amino-acids and 1% Penicillin-Streptomycin. 5×10^5 macrophages/well were plated in 96-well flat-bottomed plate (Costar) and incubated for 24 h at 37°C with 10% CO_2. After 24 h, macrophages were activated with LPS and IFNγ as described previously (Jain et al., 2009). After activation, the macrophages were washed three times and fresh DMEM media was added. In separate tubes, 10^5 young (0–3 generations) or old (10 generation) cells from each *Cryptococcus* strain grown in SAB were incubated with either 10% normal human serum (NHS) or 18B7 antibody for 5 min for opsonization. Opsonized cells were added directly onto the macrophages at a MOI of 1:1 and incubated for 1 h at 37°C with 10% CO_2. After 1 h of phagocytosis, all wells were washed three times with PBS. After 1 h of phagocytosis and washing, half the wells of macrophages were lysed with sterile water and *C. neoformans* cells were plated on YPD agar plates to determine the number of colony-forming units (CFUs) engulfed at time 0. In the second half of wells, fresh DMEM was added and cells were allowed to kill any engulfed cells for 1 h at 37°C with 10% CO_2. After 1 h of killing, macrophages were lysed with sterile water, and surviving *C. neoformans* cells were plated on YPD agar plates to determine the number of CFUs after phagocytic killing. All YPD plates were incubated for 48 h at 37°C. CFUs were counted and percent killing was calculated as $\frac{\#\text{ CFU post phagocytosis time 0} - \#\text{ CFU time 1 h}}{\#\text{ CFU post phsgocytosis time 0}} \times 100\%$.

For phagocytic index, Giemsa staining was used to identify the number of *C. neoformans* cells in each macrophage. Images of cells were taken with EVOS FL Auto microscope (Thermo Fisher Scientific). Phagocytic index was calculated as $\frac{\#\text{ Cn engulfed}}{\text{Total number of Macrophages}} \times 100$ the number of *C. neoformans* cells engulfed by the macrophages divided by the total number *of macrophages engulfing the C. neoformans* cells multiplied by 100 (Zaragoza et al., 2003).

Galleria mellonella Infection

Galleria mellonella infection was carried out as previously described (Bouklas et al., 2015). *C. neoformans* cells grown in SAB were washed and diluted in PBS to 10^6 cells/mL. 10 μL of

the cell suspension was injected into each *G. mellonella* worm (Vanderhorst Wholesale Inc., St. Mary's, OH, United States) and 20 worms were used for each strain. One set of 20 worms were injected with PBS as negative control and another set of twenty larvae were neither injected with PBS nor with *Cryptococcal* cells. This group was used as a quality control for the worms. Survival was noted for a week.

Melanization

To assess melanization, cells were grown in melanization media (MM) for the specified amount of time. Pigmentation was measured by spinning cells down into a PCR tube and capturing an image of the pellets. Pellet pigmentation was analyzed by histogram analysis on a scale of 0-255 (0 = true black, 255 = true white) using FIJI opensource software (Schindelin et al., 2012). Melanization between strains was normalized by ensuring the starting culture concentrations and time in MM was the same across all strains.

Antifungal Killing

Antifungal Killing assays were done as previously described (Jain et al., 2009). Briefly, cells were either melanized and grown in MM or grown in SM. Cells were grown to 10 generations and isolated as described above. The unlabeled fraction served as the young control (0–3 generation) against the 10 generation old cells. Young and old, and melanized and unmelanized cells of all strains were subjected plated in 96 well plates at 10^4 cells/mL and were subjected to 0.5 μg/mL of amphotericin B for 3 h. After 3 h, cells were diluted and plated on YPD plates. After plates were incubated for 48 h at 37°C, the number of colony forming units (CFUs) were counted and compared to CFUs of plates incubated with no antifungals (% killing $= \frac{\#\text{ CFU with drug}}{\#\text{ CFU without drug}}$).

Statistics

Statistical analysis was performed using Graph Pad Prism 6.0 and 8.0. The names of the statistical tests performed for each experiment are listed in the figure legends.

RESULTS

Upregulation of Genes With Age

First, we used qPCR to analyze the expression of genes *APP1*, *LAC1*, and *LAC2* in the young (0–3 generations) and old (10 generation) cells from both wildtype strains H99 and KN99α. All three genes were significantly (>two-fold) upregulated in old wildtype cells when compared to young cells (**Figure 1**).

Macrophage Phagocytosis

Macrophage-mediated phagocytosis assays were performed by opsonizing the fungal cells with either 10% normal human serum (NHS; **Figures 2A,B**) or by opsonizing the fungal cells with 18B7 antibody (Ab; **Figures 2C,D**; Casadevall et al., 1998). As expected, under NHS-mediated opsonization conditions, old wildtype cells were phagocytosed significantly less than young wildtype cells (H99: 185 vs. 292%, respectively; KN99α: 242 vs. 392%, respectively). This age-related resistance to phagocytosis is not observed with old cells isolated from the mutants *app1*Δ, *lac1*Δ, and *lac2*Δ. As expected, young *app1*Δ cells exhibited significantly higher phagocytosis compared to wildtype (375 vs. 292%, respectively). In contrast, neither young *lac1*Δ (331%) nor young *lac2*Δ (373%) cells exhibited altered phagocytosis compared to wildtype (H99: 292%; KN99α: 392%). In contrast, old cells of all three mutants were phagocytized significantly more compared to the old cells of the respective wild type (*app1*Δ: 386 vs. 185%; *lac1*Δ: 373 vs. 185%; *lac2*Δ: 362 vs. 242%).

Next, antibody-mediated opsonization was compared. These experiments indicated a significant decrease in phagocytosis of old KN99α cells when compared to young cells (217 vs. 318%) and the same trend of impaired phagocytosis of old H99 cells was indicated (202 vs. 289%). Again, analogous to the NHS-mediated opsonization, we did not observe significant differences in phagocytosis between the young and old *app1*Δ, *lac1*Δ, and *lac2*Δ mutant cells. Unlike NHS-mediated opsonization, no significant differences were observed in phagocytosis of old wildtype and old mutant cells when opsonized with mAb 18B7.

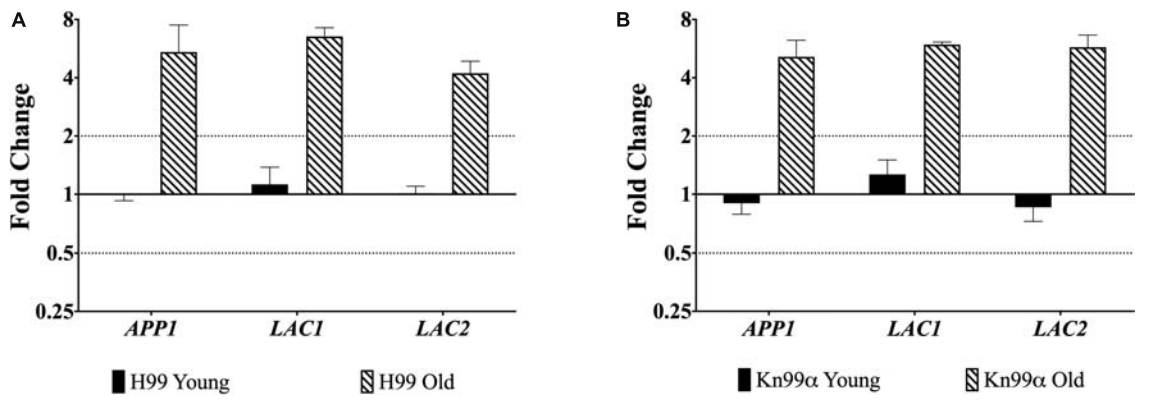

FIGURE 1 | Increased expression of virulence genes in old cells. Expression of genes *APP1*, *LAC1*, and *LAC2* in young (0–3 generations) and old (10 generations) cells from both wildtype H99 **(A)** and KN99α **(B)** was analyzed using qPCR. Data was normalized to the gene expression in young cells. Housekeeping gene *ACT1* was used as an internal control. Twofold up or twofold downregulation, marked by the dotted lines, was considered a significant fold change difference. Error bars signify standard deviation of technical replicates.

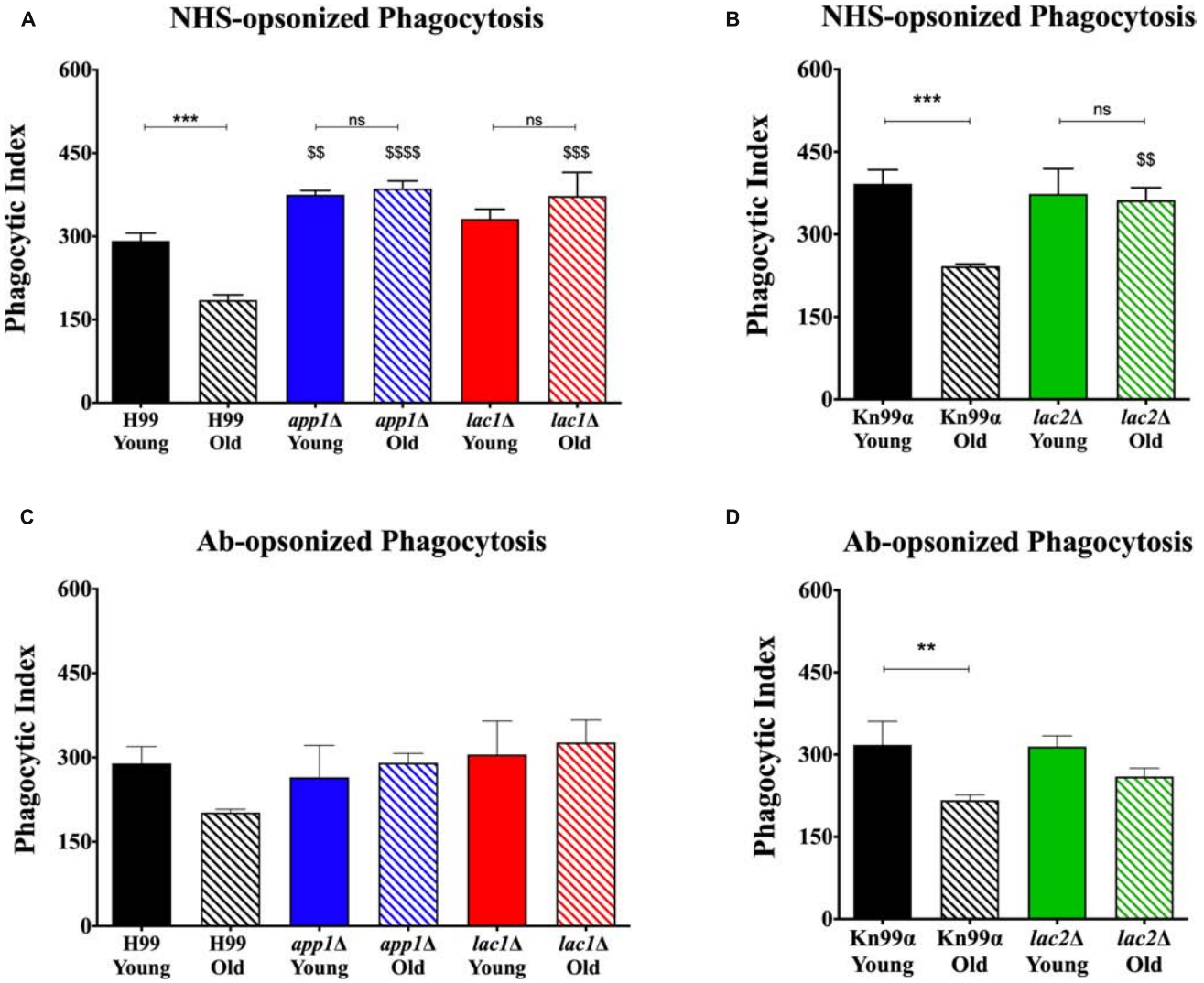

FIGURE 2 | Decreased complement- and antibody-mediated macrophage phagocytosis of old wildtype cells compared to young and mutant cells. Phagocytic index was measured as the number of *C. neoformans* cells engulfed by macrophages divided by the total number of macrophages multiplied by 100. The assays were performed by opsonization of the fungal cells with 10% normal human serum **(A,B)** or by 18B7 antibody **(C,D)**. The assays were done in biological triplicate and error bars signify standard deviation between replicates. $^{**}p < 0.01$, $^{***}p < 0.001$ by one-way ANOVA. Bars without any * are non-significant. $^{\$\$}p < 0.01$, $^{\$\$\$}p < 0.001$, $^{\$\$\$\$}p < 0.0001$ by one-way ANOVA when compared to wildtype counterpart.

Macrophage-Mediated Killing

Since altered phagocytosis can but does not necessarily affect macrophage-mediated killing, both young and old cells isolated from wildtype and mutant strains were subjected to 1-h killing by macrophages and quantification was corrected for the altered phagocytosis index. As expected, a decrease in macrophage-mediated killing was observed for NHS-opsonized old cells compared to young cells of both H99 (35 vs. 65%, **Figure 3A**) and KN99α (40 vs. 65%, **Figure 3B**). Similar to wildtype, NHS-opsonized, old *lac1*Δ and *lac2*Δ mutant cells also showed a significant decrease in macrophage-mediated killing (*lac1*Δ: 36 vs. 61%; *lac2*Δ: 40 vs. 82%). However, no significant change in macrophage-mediated killing was observed between old and young *app1*Δ cells (51 vs. 68%).

In contrast, antibody opsonization did not result in a significant difference in killing between young and old cells for any strain (**Figures 3C,D**) suggesting that serum mediated uptake may play a more important role in the observed age-related loss of resistance in mutants.

Virulence in *Galleria mellonella*

Next, we studied the effects of aging in these mutants in the *Galleria* infection model. Each larva was infected with 10^4 cells as outlined in the materials and methods. Larvae infected with old wildtype cells survived less days than the larvae infected with young wildtype cells (5 vs. 6 days, **Figure 4**, and **Table 3**). No significant change in survival was observed in the larvae infected with young vs. old mutant cells. Similarly, no significant

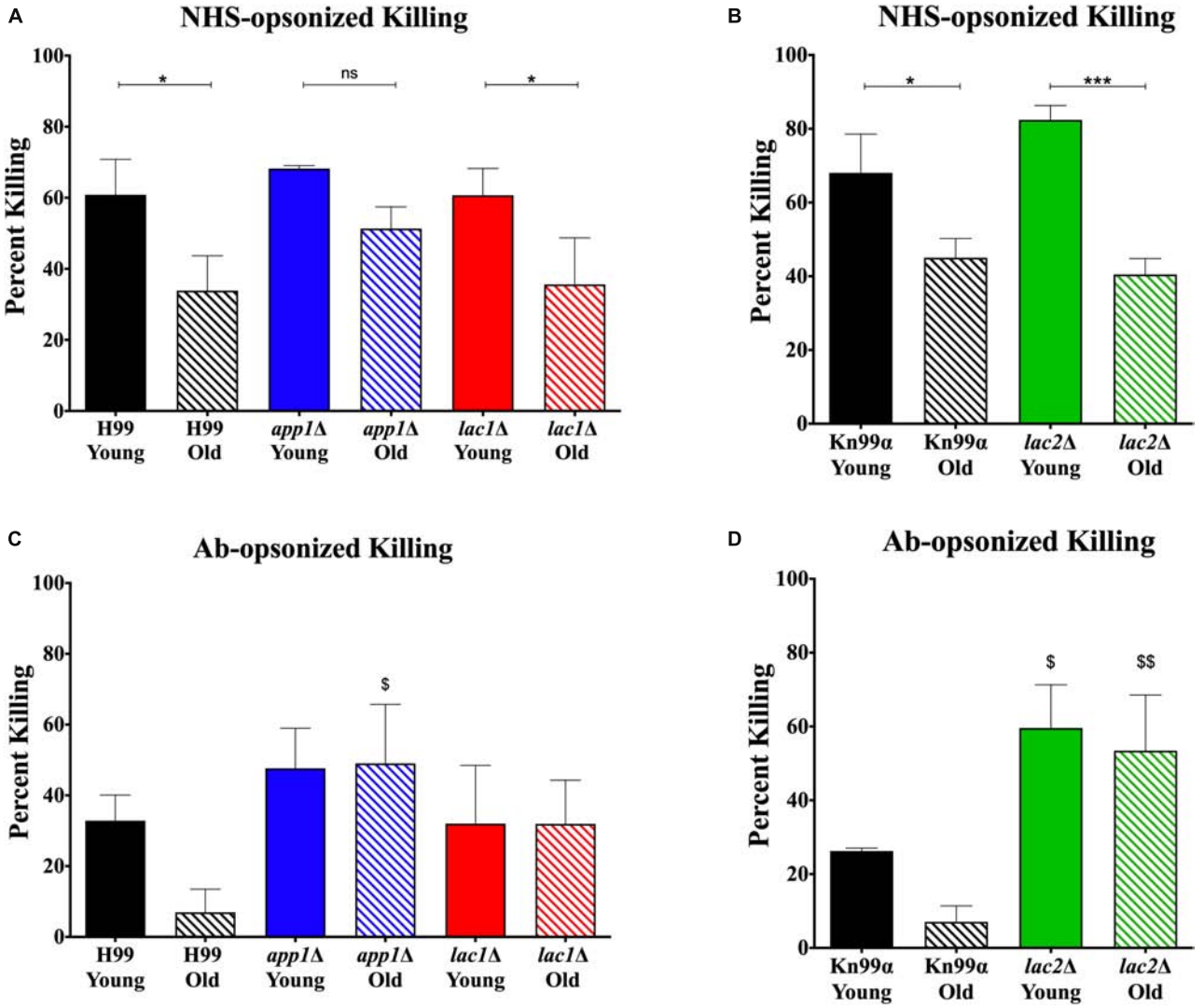

FIGURE 3 | Altered complement-mediated macrophage killing of old cells and mutant cells. Phagocytized cells were incubated for 1 h in macrophages to allow for phagocytic killing. Surviving *C. neoformans* cells were plated on YPD agar plates and CFUs were counted after 48 h incubation at 37°C and normalized to CFUs at time 0 before 1 h of killing. *C. neoformans* cells were opsonized with 10% normal human serum **(A,B)** or by 18B7 antibody **(C,D)**. Assays were done in biological triplicate and error bars signify standard deviation between replicates. One-way ANOVA was performed to analyze the statistical significance. $^{*}p < 0.05$, $^{***}p < 0.001$ by one-way ANOVA. $^{\$}p < 0.05$, $^{\$\$}p < 0.01$ by one-way ANOVA compared to wildtype counterpart.

differences were observed in the survival of the larvae infected with young wildtype cells vs. young mutant cells. Consistent with the loss of impaired phagocytic uptake and killing of mutants, we observed decreased virulence of old mutant cells compared to their respective wildtype aged cells. Specifically, significant differences were observed in survival of the larvae infected with old H99 vs. old *app1*Δ cells (5 vs. 6 days) and old H99 vs. old *lac1*Δ cells (5 vs. 6 days). Similarly, a significant difference was observed in survival of larvae infected with the old KN99α cells vs. old *lac2*Δ cells (5 vs. 7 days).

Melanization

In order to quantify melanization, cell pellets were assessed using histogram analysis to determine intensity values on a black to white scale. On such a black to white intensity scale, true black has an intensity value (IV) of 0 and true white has an IV of 255. When strains were aged in melanization media, old cells melanized to a higher degree than the young, negative fraction (**Figures 5A–D**). Young *app1*Δ (IV = 152) and *lac2*Δ (IV = 150) cells melanized to the same degree as young wildtype cells (IV = 147 for both H99 and Kn99α) whereas young *lac1*Δ cells (IV = 208) were closer to unmelanized cells (IV = 231). H99 old (62) and young (147) cells showed a shift of 85 in magnitude and Kn99α old (103) and young (147) cells showed a shift of 44 in magnitude. None of the mutant strains had as large of a difference in IV as their respective wildtype strains. Compared to H99, *app1*Δ young (152) and old (106) cells only showed a shift of 46 in magnitude and *lac1*Δ young (208) and old (150) cells showed a shift of 58 in magnitude.

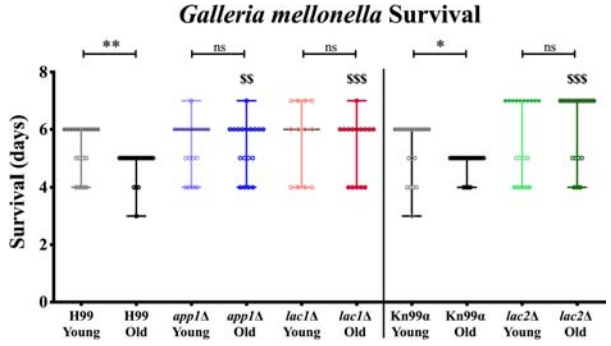

FIGURE 4 | Young cells and mutant strains are less virulent in *Galleria mellonella*. 10^6/ml cells were injected each in 20 *Galleria* larvae and survival was noted for 7 days. $^*p < 0.05$, $^{**}p < 0.01$ by log-rank test. $^{\$\$}p < 0.01$, $^{\$\$\$}p < 0.001$ by log-rank test compared to wildtype counterpart.

*lac2*Δ young (150) and old (125) cells showed the smallest shift of all strains with only a shift of 25 in magnitude.

Antifungal Killing

Since melanization increases resistance to amphotericin B (AMB), we assessed if melanization in old cells further enhances this resistance. Yeast cells were subjected to 3 h of killing by 0.5 μg/mL of AMB, a concentration 4-fold higher than minimum inhibitory concentration (MIC) for all strains (MIC = 0.0625 μg/mL, data not shown). These data confirm findings of previous studies (van Duin et al., 2002) that melanization augments resistance to AMB in wildtype young cells (H99 unmelanized = 36.64%, melanized = 71.01% survival; Kn99α unmelanized = 28.69%, melanized = 65.44% survival). Importantly, melanization markedly increases the enhanced resistance of older cells relative to young melanized cells (H99 Y = 71.01%, O = 97.65% survival; Kn99α Y = 65.44%, O = 77.39% survival) (**Figure 5E**).

Old *app1*Δ cells, exhibited significantly less resistance to AMB than old wildtype cells (26.96 vs. 57.04% survival, respectively). Melanization, however, significantly enhanced antifungal resistance of young and old *app1*Δ mutant cells. Interestingly there was no significant difference between young and old melanized *app1*Δ cells (74.65 vs. 87.36%, respectively).

As expected *lac1*Δ mutant cells exhibited minimal melanization. Hence, no difference between unmelanized young and melanized young *lac1*Δ cells was noted. The minimally melanized old *lac1*Δ cells were therefore significantly more susceptible than melanized old wildtype cells (42.01 vs. 97.65% survival, respectively).

Similar to *lac1*Δ cells, there was no significant difference between young and old unmelanized *lac2*Δ cells or between young and old melanized *lac2*Δ cells. Melanization of *lac2*Δ cells did, however, increase the resistance of young cells (65.82 vs. 37.92% survival, respectively) and old cells (65.46 vs. 42.50% survival, respectively). Lastly, also similar to *lac1*Δ cells, old melanized *lac2*Δ cells were more susceptible than old melanized wildtype cells (65.46 vs. 77.39% survival, respectively).

Replicative Lifespan and Cell Size

In order to determine whether the changes in susceptibility seen with age were associated with changes in lifespans or cell size, we determined the replicative lifespan (RLS) (**Figure 6A**) and assessed the size of mutants and wildtype cells (**Figure 6B**). All mutant strains exhibited shortened median RLS compared to wildtype (**Figure 6C**). This was most pronounced for *app1*Δ cells, which had a median RLS of 21.5 generations (33.9% loss). Both *lac1*Δ cells and *lac2*Δ cells also exhibited shorter lifespans (16.1% loss, and 17.6% loss, respectively).

In all strains a significant increase in cell size was observed with advanced generational age (H99 Y = 4.736 μm, O = 6.824 μm; *app1*Δ Y = 4.952 μm, O = 6.424 μm; *lac1*Δ Y = 5.732 μm, O = 7.399 μm; Kn99α Y = 5.444 μm, O = 7.162 μm; *lac2*Δ Y = 4.894 μm, O = 8.259 μm) (**Figure 6D**). Furthermore, *lac1*Δ cells were larger at young and old age compared to wild-type and *lac2*Δ cells were also significantly larger at old age compared to wildtype. Interestingly, no significant difference between young wildtype and *app1*Δ cells, or old wildtype and *app1*Δ cells was noted despite the significantly shortened lifespan of *app1*Δ cells. Similarly, young *lac2*Δ cells were significantly smaller than wildtype despite the significantly shortened lifespan.

Gene Regulation With Age in Mutants

qPCR was used to evaluate potential compensation between laccase genes in the respective mutant. Though old *lac1*Δ mutant cells showed increased expression of *LAC2* compared to young *lac1*Δ cells (4.51-fold vs. 1.09-fold, **Figure 7A**), the expression of *LAC2* in old *lac1*Δ mutant cells was much lower than the expression of *LAC2* in old wildtype cells (4.51-old vs. 15.75-fold, **Figure 7A**). Similarly, old *lac2*Δ cells showed increased expression of *LAC1* when compared to young cells (2.13-fold vs. 0.83-fold, **Figure 7B**) and the expression of *LAC1* in old *lac2*Δ cells was much lower than *LAC1* expression in old wildtype cells (2.13-fold vs. 4.23-fold, **Figure 7B**). Importantly, these results suggest that *LAC2* expression in old *lac1*Δ cells is higher than *LAC1* expression in *lac2*Δ cells.

DISCUSSION

Previous studies have demonstrated that generationally older *C. neoformans* accumulate during infection, and are more virulent, and more resistant to antifungals (Bouklas et al., 2013, 2017b). This may result from a thickened cell wall, increased cell size, or upregulation of drug exporters in generationally old cells. In this study, we analyzed the roles of three cell-wall-associated proteins, App1, Lac1, and Lac2, in age-dependent virulence and antifungal tolerance in *C. neoformans*. Their transcription was significantly upregulated in 10-generation old cells, suggesting the importance of these proteins in generationally old cells.

APP1 encodes for an antiphagocytic protein and provides protection to the fungal cells against macrophage phagocytosis. As expected, the phagocytic index of young *app1*Δ cells was significantly lower compared to the phagocytic index of young wildtype cells. This confirms previous results which

TABLE 3 | Young cells and mutant strains are less virulent in *Galleria mellonella*.

Strain name	Age	Galleria survival (Median) days	*P*-value	Significance	Remarks
H99	Y	6	0.0015	S	Aging significantly increased virulence
	O	5			
*lac1*Δ	Y	6	0.55	NS	Age-associated increased virulence disappeared
	O	6			
*app1*Δ	Y	6	0.55	NS	App1 important in age-dependent resilience
	O	6			
H99	Y	6	0.0943	NS	Lac2 compensates for Lac1 in young cells
*lac1*Δ	Y	6			
H99	Y	6	0.5238	NS	App1 works via complement and *Galleria* lacks full complement system
*app1*Δ	Y	6			
H99	O	5	0.0002	S	Lac2 failed to compensate for loss of Lac1 in old age
*lac1*Δ	O	6			
H99	O	5	0.0022	S	App1 needed for age-dependent virulence
*app1*Δ	O	6			
KN99α	Y	6	0.004	NS	Aging significantly increased virulence
	O	5			
*lac2*Δ	Y	7	0.47	NS	Lac2 important in age-dependent resilience
	O	7			
KN99α	Y	6	0.02	NS	Lac1 compensates for Lac2 in young cells
*lac2*Δ	Y	7			
KN99α	O	5	0.0004	S	Lac1 failed to compensate for loss of lac2 in old age
*lac2*Δ	O	7			

identify *APP1* as an important player in preventing phagocytosis (Luberto et al., 2003). The phagocytic index for 10-generation-old, NHS-opsonized wildtype cells was significantly lower compared to young wild type cells. However, old *app1*Δ cells exhibited no significant difference in the phagocytic index when compared to that of young *app1*Δ cells. The phagocytic index for 10-generation-old, Ab-opsonized wildtype cells was also lower compared to young wild type cells. However, there was no significant difference in the phagocytic index between *app1*Δ and wildtype cells. This difference between complement- and antibody-mediated phagocytosis is likely due to the fact that App1 inhibits phagocytosis by a complement-mediated and not an Ab-mediated mechanism.

App1 is similarly important in preventing macrophage-mediated killing of generationally older cells. Old wildtype cells are killed significantly less than young cells, however, we found no significant difference in macrophage-mediated killing of young and old *app1*Δ cells. This is true for both Ab-opsonized and NHS-opsonized cells. Thus up-regulation of *APP1* in generationally older *C. neoformans* cells contributes to both the decreased phagocytosis and decreased macrophage-mediated killing in generationally older cells *in vitro*.

We found further support for these findings *in vivo* in the *G. mellonella* insect model. Although, *Galleria* do not have a true complement system they utilize complement-like proteins (Tsai et al., 2016). Survival of *Galleria* worms infected with *app1*Δ cells was not altered by aging whereas older wildtype cells killed the worms faster. This finding is consistent with the *in vitro* killing assays and further indicates that App1 is an important virulence factor that contributes to enhanced resilience of older generation of cells.

In addition to the role of App1 in inhibiting phagocytosis and macrophage-mediated killing, Qureshi et al. (2012) hypothesized that App1 may also play a role in melanization as it has amyloid properties and amyloids have been shown to play a role in melanin biosynthesis in other species. Interestingly, we found that young *app1*Δ cells melanized to the same extent as wildtype cells, whereas old *app1*Δ cells exhibited lower levels of melanization compared to old wildtype cells. Regardless, melanization of both young and old *app1*Δ cells increased their resistance to AMB killing.

Of interest, App1 seems to play a role in age-dependent resistance to AMB as old unmelanized *app1*Δ cells do not survive significantly more than young unmelanized cells and in fact, the old *app1*Δ cells survive significantly less than old wildtype cells. Furthermore, though melanization enhances *app1*Δ cells resistance against AMB killing, there is still no significant difference between young and old melanized *app1*Δ cells. Future studies are required to determine whether loss of App1 alters cell wall structure as App1 is located in the cell wall (Qureshi et al., 2012). If true, it would be interesting to further explore if such changes in the cell wall's composition may also have an effect on the cell membrane, which is below the cell wall. Others have described that changes in cell membrane affect the cell wall and alter its sensitivity to caspofungin and congo red, which target the cell wall (Mesa-Arango et al., 2016; Bhattacharya et al., 2018).

In addition to *APP1*, we studied the effects of the laccase enzyme encoding genes *LAC1* and *LAC2* on age-dependent resilience. Lac1 typically localizes in the cell wall but it is highly pH dependent. In *C. neoformans* cells located in the brain (physiological pH around 7.2-7.4), Lac1 is almost exclusively found in the cell wall. At lower pHs, however, such as pH

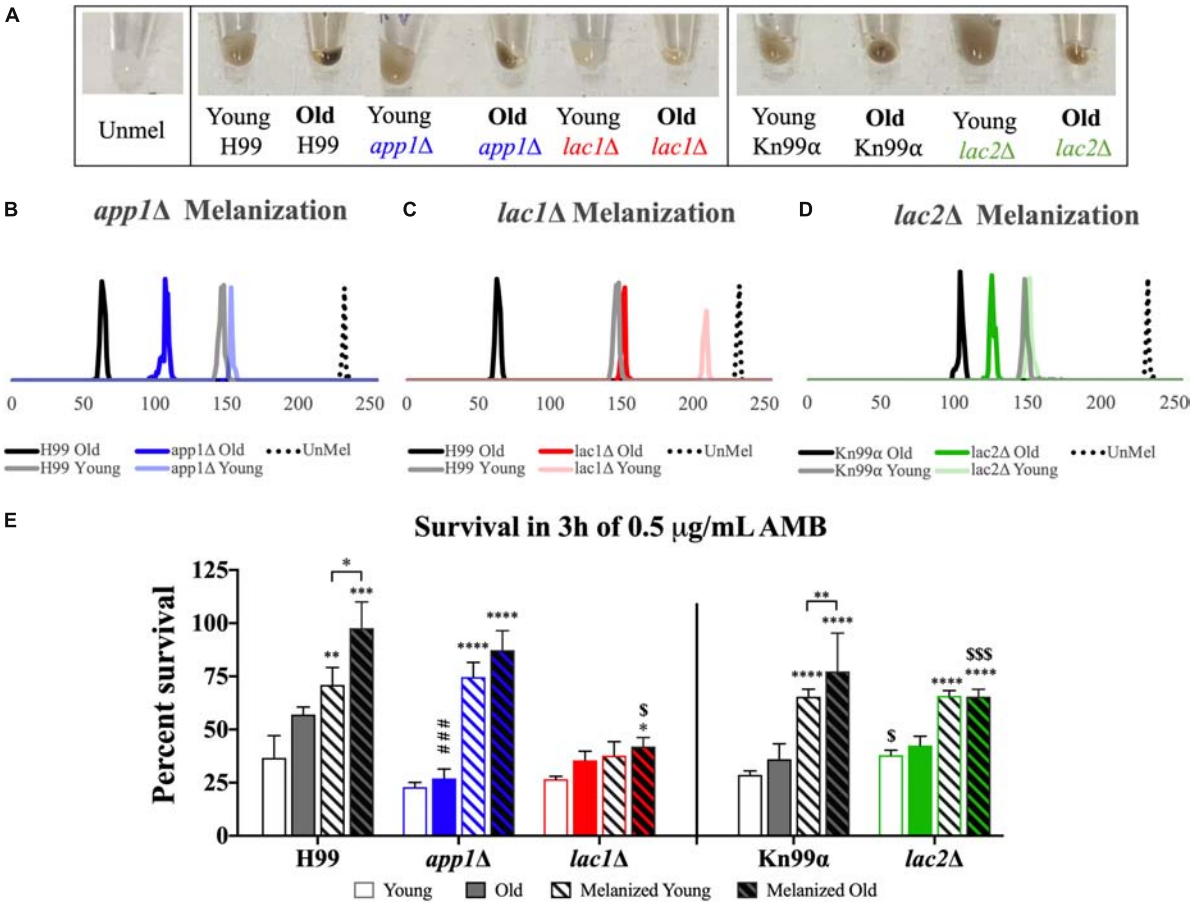

FIGURE 5 | Melanization increases with age which enhances antifungal resistance. Wildtype and mutant cells were aged to 10 generations in melanization media. Old cells were separated from the young, negative fraction and melanization was compared by imaging cell pellets **(A)** and quantifying darkness using black to white histogram analysis (on a scale from 0 to 255. 0, true black, 255, true white). Melanization of young and old fractions of *app1*Δ **(B)**, *lac1*Δ **(C)**, and *lac2*Δ **(D)** were compared to melanization of young and old fractions of their respective wildtype strains. Fractions of young and old cells from each strain grown in control and melanization media were subjected to 3 h of killing by 0.5 μg/mL AMB **(E)**. Percent survival was calculated for each population which was then normalized to the young wildtype strain grown in control media. $^{*}p < 0.05$, $^{**}p < 0.01$, $^{***}p < 0.001$, $^{****}p < 0.0001$ by one-way ANOVA compared to young cells of the same strain grown in control media. $^{\$}p < 0.05$, $^{\$\$\$}p < 0.001$ by one-way ANOVA compared to wildtype counterpart.

of 5 as seen in macrophages, Lac1 tends to get trapped in cytoplasmic vesicles (Waterman et al., 2007). Interestingly, it has been shown that Lac1 plays an important role in extrapulmonary dissemination to the brain but it does not contribute to pulmonary survival or persistence (Noverr et al., 2004). Lac2 is a protein similar to Lac1 and both of them play an important role during melanization. For this study, we obtained the mutant strains lacking *LAC1* and *LAC2*.

First, we assessed whether *LAC1* or *LAC2* are important in macrophage phagocytosis. No significant difference in phagocytosis between young wildtype and mutant cells was documented. Old *lac1*Δ and *lac2*Δ cells, however, were phagocytized significantly more than old wildtype cells indicating both *LAC1* and *LAC2* are important in the age-dependent resilience to macrophage phagocytosis. This was observed for NHS-opsonized cells but not Ab-opsonized cells, suggesting that age-dependent resilience to phagocytosis mediated by *LAC1* and *LAC2* may be through a complement-mediated mechanism.

Because *LAC1* and *LAC2* play a role in phagocytosis, we then assessed whether *LAC1* and *LAC2* were important for macrophage-mediated killing. Both wildtype and mutant populations were more resistant to macrophage killing when aged compared to respective young populations. When cells were opsonized with antibody, however, old *lac1*Δ lost their age-dependent resilience as they were killed at the same rate as young *lac1*Δ cells. Furthermore, both young and old *lac2*Δ were killed at higher rates compared to their respective wildtype populations and old *lac2*Δ cells lost their age-dependent resilience to killing compared to their young counterparts. Taken together, both *LAC1* and *LAC2* seem to play a role in age-dependent resilience to phagocytic killing but only when opsonized by antibody and not complement. Furthermore, *LAC2* may play an important role in resistance against antibody-mediated phagocytic killing.

To further analyze the virulence of the *lac1*Δ and *lac2*Δ mutants *in vivo*, young and old mutant cells were injected into

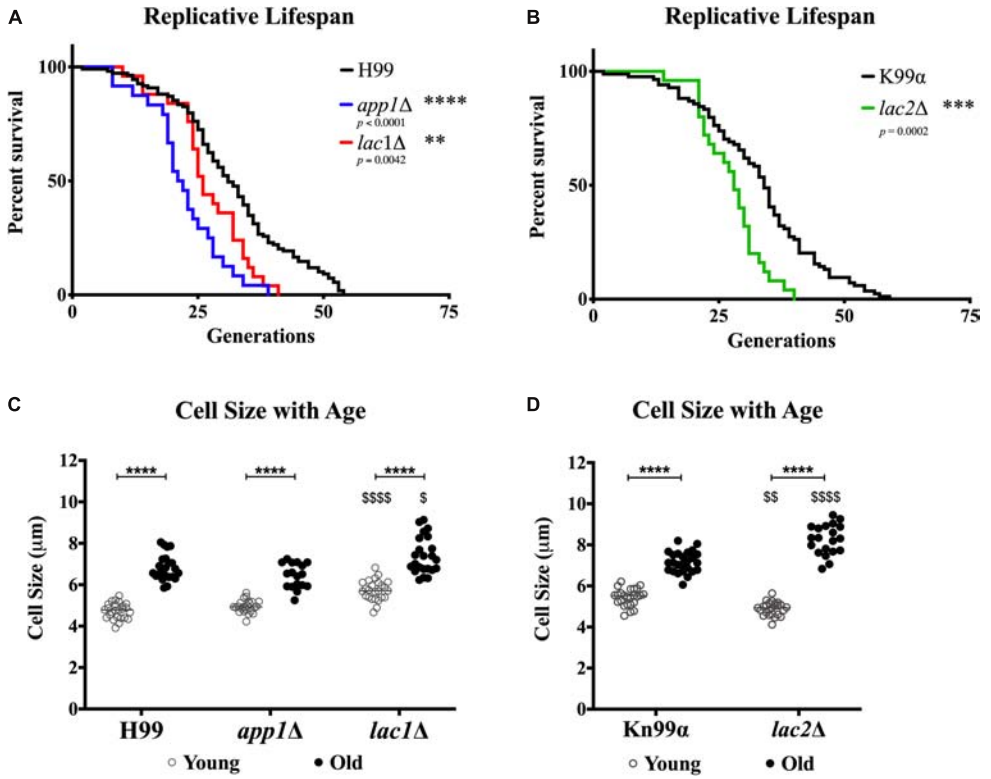

FIGURE 6 | Decreased lifespan of mutants and increased cell size with age. Replicative lifespans were determined for each mutant strain and compared to its respective wildtype **(A,B)**. Cell sizes were measured in the young (0–3 generations) and old (10 generations) fractions of cells after separation to assess the cell size of each population **(C,D)**. $^{**}p < 0.01$, $^{***}p < 0.001$, $^{****}p < 0.0001$ by one-way ANOVA. $^{\$}p < 0.05$, $^{\$\$}p < 0.01$, $^{\$\$\$\$}p < 0.0001$ by one-way ANOVA compared to wildtype counterpart.

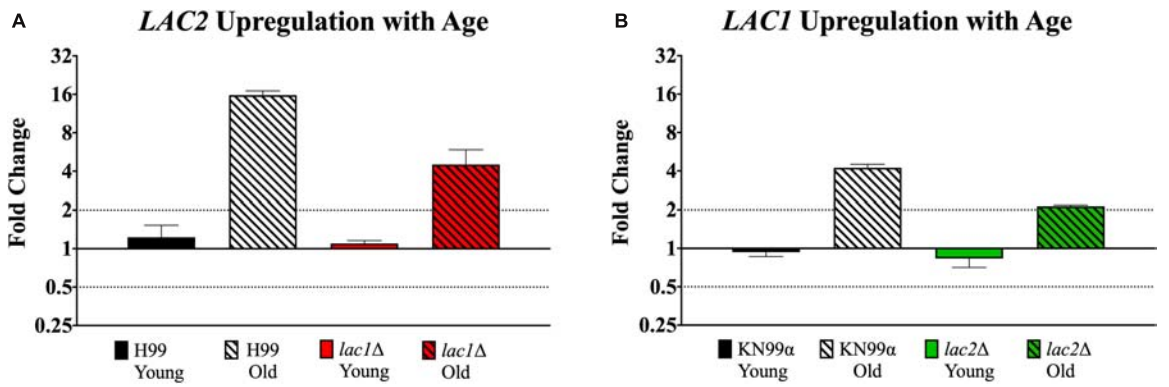

FIGURE 7 | Increased expression of *LAC1* and *LAC2* genes in old cells. Expression of *LAC2* in young (0–3 generations) and old (10 generations) wildtype H99 and *lac1*Δ cells **(A)**. Expression of *LAC1* in young (0–3 generations) and old (10 generations) wildtype KN99α and *lac2*Δ cells **(B)**. Data was normalized to the gene expression in young cells. Housekeeping gene *ACT1* was used as an internal control. Twofold up or twofold downregulation, marked by the dotted lines, was considered a significant fold change difference. Error bars signify standard deviation of technical replicates.

Galleria and survival was assessed. Overall, we observed no significant changes in virulence between young mutants and young wildtype cells. This suggests, in conjunction with our phagocytosis results, that in young cells, Lac1 and Lac2 may be compensating for each other when one gene is absent. However, significant changes in age-dependent virulence were observed. Both *lac1*Δ and *lac2*Δ mutant populations showed a loss of age-dependent virulence as both young and old populations of either mutant strain killed *Galleria* at the same rate. Furthermore, old *lac1*Δ and *lac2*Δ cells were significantly less virulent than wildtype old cells, further indicating Lac1 and Lac2 are important in mediating age-dependent resilience.

Since the most important role of Lac1 and Lac2 is melanization, we analyzed melanization in young and old *lac1*Δ and *lac2*Δ cells and compared them with their respective wildtypes. As expected, loss of either *LAC1* or *LAC2* reduced the ability of cells to melanize. Previously it was thought that *LAC1* was the main contributor and *LAC2* served a less important, redundant role (Missall et al., 2004). This is likely because previous studies only focused on young cultures. Looking at generationally older cells, we see *LAC2* plays an important role in melanization at older ages. *lac1*Δ mutant cells do not melanize well overall, but old cells are able to melanize to a greater extent (shift of 58 IV units between young and old) compared to *lac2*Δ mutant cells (shift of 25 IV units between young and old). Furthermore, when young and old melanized cells were subjected to AMB for 3 h, old *lac1*Δ mutant cells were 11.4% more resistant to killing compared to young. There was no difference, however, in resistance of old and young *lac2*Δ mutant cells (65.5 vs. 65.58%, respectively). Taken together, *LAC2* may partially compensate for loss of *LAC1* in old age. The loss of resistance to AMB in old laccase mutant cells may again be explained by altered composition to the cell wall as seen in the *app1*Δ mutant cells. However, Lac2 is not typically found in the cell wall unless Lac1 is missing so altered cell wall composition in the mutants cannot be the only factor contributing to this loss of AMB resistance in old age.

Since we observed that each of these genes play a significant role in age-dependent resistance, we asked the question whether App1, Lac1, or Lac2 play any role in altering the replicative life span of *C. neoformans*. In *C. neoformans*, strains can only undergo a finite number of divisions before senescence, the cumulative total of which is termed the replicative lifespan (RLS) (Bouklas et al., 2013). When the RLS of a strain is shifted in either direction, the relative age of a 10-generation old cell shifts and the respective age-dependent resilience is altered (Bouklas et al., 2017b). When a wildtype strain lives to be on average 30 generations, 10 generations is one third it's lifespan. If that strain is mutated and its average RLS shifts to only 20 generations, a 10-generation old cell is now through half of its lifespan making it relative older. We have shown previously that this decrease in RLS also alters the strains age-dependent resilience as 10 generation cells from the mutant with a shortened RLS are more resistant to macrophage killing than 10-generation wildtype cells (Bouklas et al., 2017b). To ensure the loss in age-dependent resistance of our mutant strains was not solely due to a shift in RLS, we determined RLS of each mutant. All three mutants exhibited decreased median RLSs compared to their respective wildtypes. Since 10-generation cells of all mutants are relatively older than their wildtype counterparts, their age-dependent resilience should be higher than the wildtype. Similarly, 10-generation old mutant cells are as large or significantly larger than 10-generation wildtype cells. Taken together, we conclude the decrease and loss in age-dependent resilience of mutant strains is likely not due to the change in RLS or their cell size.

Though it is difficult to hypothesize why these virulence factors affect RLS, it has been found that *APP1* transcription is controlled by diacylglycerol (DAG) through the transcription factor *ATF2* (Mare et al., 2005). In *C. neoformans*, DAG also activates Pkc1 (Heung et al., 2004), and Pkc1 regulates Laccase (Heung et al., 2005) and Sir2 silencing (Lee et al., 2013) (an age-regulating gene). Thus, increased DAG would increase activation of App1 through Atf2, as well as Laccase activity and Sir2 silencing through Pkc1, which could result in more App1 being secreted, increased melanization, and longer replicative lifespan. Future studies to investigate these potential mechanisms are planned to discern the common pathway(s) that regulate these genes and their transcription factors to better understand how they contribute to age-dependent resilience.

In conclusion, App1, Lac1, and Lac2 each play a significant role in age-dependent resilience and regulation of replicative life span. App1 is more important for age-dependent resistance against NHS-mediated phagocytosis and killing and AMB killing. Lac1 and Lac2 are more important for age-dependent resistance against Ab-mediated killing, AMB killing, and age-dependent melanization. Furthermore, our data suggest that both Lac1 and Lac2 are needed in generationally old cells. This study thus identifies some of the key-players that contribute to age-dependent resilience of *C. neoformans*.

DATA AVAILABILITY STATEMENT

The raw data generated and analyzed in this study will be made available by the authors to any qualified researcher by request.

AUTHOR CONTRIBUTIONS

EO, SB, and BF contributed to the design of the study, and drafting and editing of the manuscript. MD also contributed to the reading and editing of the manuscript. EO, SB, KK, and DH contributed to acquisition and analysis of the data.

FUNDING

This work was supported in part by Dr. Fries' Stony Brook University start-up fund, in part by NIH awards R01-AI059681 and T32AI007539, in part by NIH R01 AI125770, and in part by Merit Review grant I01BX002624 from the Veterans Affairs Program.

ACKNOWLEDGMENTS

We would like to thank the MD and the Williamson laboratories for their gracious gifting of strains used in this study. We also would like to thank Michael Motley for helping us edit the final manuscript and the Stony Brook Medical Scholars Program for their support.

REFERENCES

Alvarez, M., and Casadevall, A. (2006). Phagosome extrusion and host-cell survival after *Cryptococcus neoformans* phagocytosis by macrophages. *Curr. Biol.* 16, 2161–2165. doi: 10.1016/j.cub.2006.09.061

Bhattacharya, S., Esquivel, B. D., and White, T. C. (2018). Overexpression or deletion of ergosterol biosynthesis genes alters doubling time, response to stress agents, and drug susceptibility in *Saccharomyces cerevisiae*. *mBio* 9:e1291-18. doi: 10.1128/mBio.01291-1218

Bhattacharya, S., and Fries, B. C. (2018). Enhanced efflux pump activity in old *Candida glabrata* cells. *Antimicrob. Agents Chemother.* 62:e2227-17. doi: 10.1128/aac.02227-2217

Bhattacharya, S., Holowka, T., Orner, E. P., and Fries, B. C. (2019). Gene duplication associated with increased fluconazole tolerance in *Candida auris* cells of advanced generational age. *Sci. Rep.* 9:5052. doi: 10.1038/s41598-019-41513-41516

Bouklas, T., Alonso-Crisóstomo, L., Székely, T. Jr., Diago-Navarro, E., Orner, E. P., Smith, K., et al. (2017a). generational distribution of a *Candida glabrata* population: resilient old cells prevail, while younger cells dominate in the vulnerable host. *PLoS Pathog.* 13:e1006355. doi: 10.1371/journal.ppat.1006355

Bouklas, T., Jain, N., and Fries, B. C. (2017b). Modulation of replicative lifespan in *Cryptococcus neoformans*: implications for virulence. *Front. Microbiol.* 8:98. doi: 10.3389/fmicb.2017.00098

Bouklas, T., Diago-Navarro, E., Wang, X., Fenster, M., and Fries, B. C. (2015). Characterization of the virulence of *Cryptococcus neoformans* strains in an insect model. *Virulence* 6, 809–813. doi: 10.1080/21505594.2015.1086868

Bouklas, T., Pechuan, X., Goldman, D. L., Edelman, B., Bergman, A., and Fries, B. C. (2013). Old *Cryptococcus neoformans* cells contribute to virulence in chronic cryptococcosis. *mBio* 4:e455-13. doi: 10.1128/mBio.00455-413

Casadevall, A., Cleare, W., Feldmesser, M., Glatman-Freedman, A., Goldman, D. L., Kozel, T. R., et al. (1998). Characterization of a murine monoclonal antibody to *Cryptococcus neoformans* polysaccharide that is a candidate for human therapeutic studies. *Antimicrob. Agents Chemother.* 42, 1437–1446. doi: 10.1128/aac.42.6.1437

Casadevall, A., and Perfect, J. R. (1998). *Cryptococcus neoformans*. Washington, DC: ASM Press.

Del Poeta, M. (2004). Role of phagocytosis in the virulence of *Cryptococcus neoformans*. *Eukaryot. Cell* 3, 1067–1075. doi: 10.1128/EC.3.5.1067-1075.2004

Gebbink, M. F., Claessen, D., Bouma, B., Dijkhuizen, L., and Wosten, H. A. (2005). Amyloids–a functional coat for microorganisms. *Nat. Rev. Microbiol.* 3, 333–341. doi: 10.1038/nrmicro1127

Heung, L. J., Kaiser, A. E., Luberto, C., and Del Poeta, M. (2005). The role and mechanism of diacylglycerol-protein kinase C1 signaling in melanogenesis by *Cryptococcus neoformans*. *J. Biol. Chem.* 280, 28547–28555. doi: 10.1074/jbc.M503404200

Heung, L. J., Luberto, C., Plowden, A., Hannun, Y. A., and Del Poeta, M. (2004). The sphingolipid pathway regulates Pkc1 through the formation of diacylglycerol in *Cryptococcus neoformans*. *J. Biol. Chem.* 279, 21144–21153. doi: 10.1074/jbc.M312995200

Howard, R. J., and Valent, B. (1996). Breaking and entering: host penetration by the fungal rice blast pathogen *Magnaporthe grisea*. *Ann. Rev. Microbiol.* 50, 491–512. doi: 10.1146/annurev.micro.50.1.491

Jain, N., Cook, E., Xess, I., Hasan, F., Fries, D., and Fries, B. C. (2009). Isolation and characterization of senescent *Cryptococcus neoformans* and implications for phenotypic switching and pathogenesis in chronic cryptococcosis. *Eukaryot. Cell* 8, 858–866. doi: 10.1128/ec.00017-19

Lee, S., Gaspar, M. L., Aregullin, M. A., Jesch, S. A., and Henry, S. A. (2013). Activation of protein kinase C-mitogen-activated protein kinase signaling in response to inositol starvation triggers Sir2p-dependent telomeric silencing in yeast. *J. Biol. Chem.* 288, 27861–27871. doi: 10.1074/jbc.M113.493072

Livak, K. J., and Schmittgen, T. D. (2001). Analysis of relative gene expression data using real-time quantitative PCR and the 2(-delta delta C(T)) method. *Methods* 25, 402–408. doi: 10.1006/meth.2001.1262

Luberto, C., Martinez-Mariño, B., Taraskiewicz, D., Bolaños, B., Chitano, P., Toffaletti, D. L., et al. (2003). Identification of App1 as a regulator of phagocytosis and virulence of *Cryptococcus neoformans*. *J. Clin. Invest.* 112, 1080–1094. doi: 10.1172/JCI18309

Mare, L., Iatta, R., Montagna, M. T., Luberto, C., and Del Poeta, M. (2005). APP1 transcription is regulated by inositol-phosphorylceramide synthase 1-diacylglycerol pathway and is controlled by ATF2 transcription factor in *Cryptococcus neoformans*. *J. Biol. Chem.* 280, 36055–36064. doi: 10.1074/jbc.M507285200

Mesa-Arango, A. C., Rueda, C., Roman, E., Quintin, J., Terron, M. C., Luque, D., et al. (2016). Cell wall changes in amphotericin b-resistant strains from *Candida tropicalis* and relationship with the immune responses elicited by the host. *Antimicrob. Agents Chemother.* 60, 2326–2335. doi: 10.1128/aac.02681-2615

Missall, T. A., Lodge, J. K., and McEwen, J. E. (2004). Mechanisms of resistance to oxidative and nitrosative stress: implications for fungal survival in mammalian hosts. *Eukaryot. Cell* 3, 835–846. doi: 10.1128/ec.3.4.835-846.2004

Nosanchuk, J. D., and Casadevall, A. (2003). The contribution of melanin to microbial pathogenesis. *Cell. Microbiol.* 5, 203–223. doi: 10.1046/j.1462-5814.2003.00268.x

Noverr, M. C., Williamson, P. R., Fajardo, R. S., and Huffnagle, G. B. (2004). CNLAC1 is required for extrapulmonary dissemination of *Cryptococcus neoformans* but not pulmonary persistence. *Infect. Immun.* 72, 1693–1699. doi: 10.1128/iai.72.3.1693-1699.2004

Orner, E. P., Zhang, P., Jo, M. C., Bhattacharya, S., Qin, L., and Fries, B. C. (2019). High-throughput yeast aging analysis for cryptococcus (HYAAC) microfluidic device streamlines aging studies in *Cryptococcus neoformans*. *Commun. Biol.* 2:256. doi: 10.1038/s42003-019-0504-505

Polacheck, I., Hearing, V. J., and Kwon-Chung, K. J. (1982). Biochemical studies of phenoloxidase and utilization of catecholamines in *Cryptococcus neoformans*. *J. Bacteriol.* 150, 1212–1220.

Qureshi, A., Williams, V., and Del Poeta, M. (2012). Expression and characterization of *Cryptococcus neoformans* recombinan. *App1. Mycopathol.* 173, 395–405. doi: 10.1007/s11046-011-9486-9487

Rajasingham, R., Smith, R. M., Park, B. J., Jarvis, J. N., Govender, N. P., Chiller, T. M., et al. (2017). Global burden of disease of HIV-associated cryptococcal meningitis: an updated analysis. *Lancet Infect. Dis.* 17, 873–881. doi: 10.1016/s1473-3099(17)30243-30248

Schindelin, J., Arganda-Carreras, I., Frise, E., Kaynig, V., Longair, M., Pietzsch, T., et al. (2012). Fiji: an open-source platform for biological-image analysis. *Nat. Methods* 9, 676–682. doi: 10.1038/nmeth.2019

Stano, P., Williams, V., Villani, M., Cymbalyuk, E. S., Qureshi, A., Huang, Y., et al. (2009). App1: an antiphagocytic protein that binds to complement receptors 3 and 2. *J. Immunol.* 182, 84–91. doi: 10.4049/jimmunol.182.1.84

Stuart, M. L. (2002). Receptor-mediated recognition of *Cryptococcus neoformans*. *Nippon Ishinkin Gakkai Zasshi* 43, 133–136. doi: 10.3314/jjmm.43.133

Torres-Guererro, H., and Edman, J. C. (1994). Melanin-deficient mutants of *Cryptococcus neoformans*. *J. Med. Vet. Mycol.* 32, 303–313. doi: 10.1080/02681219480000381

Tsai, C. J.-Y., Loh, J. M. S., and Proft, T. (2016). *Galleria mellonella* infection models for the study of bacterial diseases and for antimicrobial drug testing. *Virulence* 7, 214–229. doi: 10.1080/21505594.2015.1135289

van Duin, D., Casadevall, A., and Nosanchuk, J. D. (2002). Melanization of *Cryptococcus neoformans* and *Histoplasma capsulatum* reduces their susceptibilities to amphotericin B and caspofungin. *Antimicrob. Agents Chemother.* 46, 3394–3400. doi: 10.1128/aac.46.11.3394-3400.2002

Wang, Y., Aisen, P., and Casadevall, A. (1995). *Cryptococcus neoformans* melanin and virulence: mechanism of action. *Infect. Immun.* 63, 3131–3136.

Waterman, S. R., Hacham, M., Panepinto, J., Hu, G., Shin, S., and Williamson, P. R. (2007). Cell wall targeting of laccase of *Cryptococcus neoformans* during infection of mice. *Infect. Immun.* 75, 714–722. doi: 10.1128/iai.01351-1356

Williams, V., and Del Poeta, M. (2011). Role of glucose in the expression of *Cryptococcus neoformans* antiphagocytic protein 1. *App1. Eukaryot. Cell* 10, 293–301. doi: 10.1128/EC.00252-210

Williamson, P. R. (1994). Biochemical and molecular characterization of the diphenol oxidase of *Cryptococcus neoformans*: identification as a laccase. *J. Bacteriol.* 176, 656–664. doi: 10.1128/jb.176.3.656-664.1994

Zaragoza, O., Taborda, C. P., and Casadevall, A. (2003). The efficacy of complement-mediated phagocytosis of *Cryptococcus neoformans* is dependent on the location of C3 in the polysaccharide capsule and involves both direct and indirect C3-mediated interactions. *Eur. J. Immunol.* 33, 1957–1967. doi: 10.1002/eji.200323848

Zhu, X., and Williamson, P. R. (2004). Role of laccase in the biology and virulence of *Cryptococcus neoformans*. *FEMS Yeast Res.* 5, 1–10. doi: 10.1016/j.femsyr.2004.04.004

Conflict of Interest: MD is the co-founder and Chief Scientific Officer (CSO) of MicroRid Technologies, Inc.

The remaining authors declare that the research was conducted in the absence of any commercial or financial relationships that could be construed as a potential conflict of interest.

frontiers in Microbiology

ORIGINAL RESEARCH
published: 21 November 2019
doi: 10.3389/fmicb.2019.02589

Trichophyton rubrum Elicits Phagocytic and Pro-inflammatory Responses in Human Monocytes Through Toll-Like Receptor 2

Giovanna Azevedo Celestrino[1], Ana Paula Carvalho Reis[1], Paulo Ricardo Criado[2], Gil Benard[1†] and Maria Gloria Teixeira Sousa[1†]*

[1]Laboratory of Medical Mycology-LIM-53, Clinical Dermatology Division, Hospital das Clínicas FMUSP, Instituto de Medicina Tropical de São Paulo, Universidade de São Paulo, São Paulo, Brazil, [2]Centro Universitário Saúde ABC, Santo André, Brazil

Dermatophytosis is a superficial fungal infection mostly restricted to keratinized tissues such as skin, hair, and nails but with potential to cause invasive or even systemic disease in immunocompromised patients. *Trichophyton rubrum* is the main etiologic agent, accounting for approximately 80% of the cases. Mononuclear phagocytes respond to pathogens through phagocytosis followed by production of several antimicrobial molecules, such as reactive oxygen and nitrogen species, and failure in doing so may contribute to development of chronic fungal infections. Toll-like receptors (TLRs) located on the surface of phagocytic cells bind either directly to target particles or through opsonizing ligands and trigger an actin-mediated ingestion. Even though the mechanisms involved in TLR-mediated cytokine responses are well established, the contribution of TLR in the recognition of *T. rubrum* by adherent monocytes remains unclear. Here, we report that phagocytosis of *T. rubrum* conidia by adherent monocytes is mediated by TLR2. Blockade of TLR2 by neutralizing antibodies impaired the fungicidal activity of monocytes as well their secretion of tumor necrosis factor (TNF)-α, but neither nitric oxide (NO) production nor interleukin (IL)-10 secretion was disturbed. So far, our data suggest that TLR2 is required for efficient conidial phagocytosis, and the absence of TLR2 signaling in human monocytes may impair the subsequent inflammatory response. These findings expand our understanding of phagocyte modulation by this important fungal pathogen and may represent a potential target for interventions aiming at enhancing antifungal immune responses.

Keywords: dermatophytosis, toll-like receptor 2, innate immune, *Trichophyton rubrum*, monocytes, fungal cell wall

OPEN ACCESS

Edited by:
Joshua D. Nosanchuk, Albert Einstein College of Medicine, United States

Reviewed by:
Roberta Gaziano, University of Rome Tor Vergata, Italy
Laura C. Bonifaz, Mexican Social Security Institute (IMSS), Mexico

***Correspondence:**
Maria Gloria Teixeira Sousa
sousa.gloria@gmail.com

†These authors have contributed equally to this work

Specialty section:
This article was submitted to Fungi and Their Interactions, a section of the journal Frontiers in Microbiology

Received: *19 August 2019*
Accepted: *25 October 2019*
Published: *21 November 2019*

Citation:
Celestrino GA, Reis APC, Criado PR, Benard G and Sousa MGT (2019) Trichophyton rubrum Elicits Phagocytic and Pro-inflammatory Responses in Human Monocytes Through Toll-Like Receptor 2. Front. Microbiol. 10:2589. doi: 10.3389/fmicb.2019.02589

INTRODUCTION

Dermatophytosis is a superficial fungal infection that is usually limited to the keratinized layer of the epidermis, hair, and nails, and whose main etiologic agent is *Trichophyton rubrum*, accounting for approximately 80% of the cases (Svejgaard and Nilsson, 2004; Romano et al., 2005; Godoy-Martinez et al., 2009; Lee et al., 2015). In immunocompromised patients, however, dermatophytes proliferate beyond the superficial layers, potentially leading to severe systemic

infection with deep organ involvement (Jones et al., 1973; Teklebirhan and Bitew, 2015).

Cells of the innate immunity, such as dendritic cells, macrophages, and monocytes, recognize fungi by identifying components of the fungal cell wall using pattern recognition receptors (PRRs) on their surface. Toll-like receptors (TLRs), C-type lectins (CLRs), complement, and immunoglobulin Fc receptors are important PRRs in anti-fungal immunity (Hardison and Brown, 2012; Dambuza and Brown, 2015). Yoshikawa et al. (2016), for example, using a murine model of deep dermatophytosis, demonstrated that the absence of the CLRs Dectin-1 and Dectin-2 promoted an inefficient proinflammatory response against *T. rubrum* infection characterized by lower production of TNF-α and IL-1β by spleen cells, impairing disease resolution (Yoshikawa et al., 2016).

TLR2 is expressed in monocytes, neutrophils, and macrophages and recognizes various ligands in the fungal cell wall, e.g., mannan and phospholipomannan. In some fungal infections such as aspergillosis, TLR2 activation promotes increased phagocytosis and cytokine production (Chai et al., 2009). However, because TLR2 can form heterodimers with other receptors, triggering different signaling pathways (Oliveira-Nascimento et al., 2012), its contribution to a specific infection cannot be accurately predicted or can be only marginal, as observed for *Cryptococcus neoformans* infection (Nakamura et al., 2006).

In situ models showed that TLR2 expression was preserved in the epidermis of patients with localized or disseminated dermatophytosis, while TLR4 was poorly expressed in those patients (de Oliveira et al., 2015). Other *in vitro* systems, however, demonstrated that whole *T. rubrum* conidia could diminish TLR2 expression in a keratinocyte cell line (Huang et al., 2015). Thus, it is still unknown if and how TLR2 participates in the immunity to *T. rubrum*, particularly in the human context. Here, we investigated the role of TLR2 in the interaction of human monocytes with *T. rubrum* by examining the capacity of TLR2 to recognize *T. rubrum* conidia and to develop an inflammatory response following the fungal challenge.

MATERIALS AND METHODS

T. rubrum Conidia Production

A clinical isolate of *T. rubrum* (IMT-20) was used in this study. Twelve-day-old cultures grown in potato dextrose agar medium at 25°C were prepared for conidia production. Conidia were collected, suspended in 0.9% NaCl solution, and filtered in 40 μm cell strainers (BD Biosciences) to remove hyphae fragments.

Ethical Statement

Blood samples were collected from 11 healthy adult volunteers (5 males, 6 females, mean age 35 years) who were free of infectious or inflammatory diseases at the moment of sample acquisition. All donors provided written informed consent to participate in this study. This work was approved by the ethical committee of Clinics Hospital, University of São Paulo (approval number 065235/2018).

Monocyte Isolation and Cultures

A total of 70 ml of peripheral blood was collected from each donor in heparin tubes. Peripheral blood mononuclear cells (PBMCs) were obtained by density gradient centrifugation using the commercial reagent Ficoll-Paque™ PLUS (GE Healthcare) as previously described by de Sousa et al. (2015). Monocytes were purified from PBMCs by adherence. Cells were plated on glass coverslips and incubated for 90 min to allow monocyte adherence, followed by washing with phosphate buffer saline (PBS) for removal of non-adherent cells.

Cells were cultured in culture medium [RPMI-1640 with Glutamax™ supplemented with pyruvate (0.02 mM), 100 U/ml penicillin, 100 mg/ml streptomycin (all from Sigma-Aldrich), and 10% human pooled serum] at 37°C, 95% humidity, and 5% CO_2 in 24-well round-bottom plates. Monocytes were preincubated for 50 min with 10 μg/ml of TLR2-blocking antibody (anti-hTLR2-IgA, catalog code: maba2-htlr2) or its isotype control IgA1 (catalog code: maba2-ctrl, both from InvivoGen) before stimulation with *T. rubrum* conidia. The antibody's blocking concentration was based on previous studies (van de Veerdonk et al., 2009).

Phagocytosis Assay

After TLR2 blockade, monocytes (2×10^5 cells) were incubated with *T. rubrum* conidia (10×10^5) at 37°C and 5% CO_2 in 24-well round-bottom plates (with coverslips) for 3 h. Coverslips were removed, washed with PBS at 37°C to remove non-adherent cells, fixed with methanol, stained with 20% Giemsa solution, and analyzed under an optical microscope. For transmission electron microscopy, the protocol from Campos et al. (2006) was used. The phagocytosis index (PI) was calculated by multiplying the percentage of monocytes in the field that phagocytosed at least one conidium by the mean number of phagocytosed particles. For colony-forming unit (CFU) assay, the above phagocytosis assay was performed without coverlips. After 6 h, wells were washed (three times) with PBS 1× to remove free fungi, and monocytes were lysed with 0.1% Triton X-100 solution. A 10-fold dilution of the samples was plated on Sabouraud Agar (Difco) and kept at 30°C up to 7 days. Recovered colonies were counted and multiplied by dilution factor.

NO Measurements

The determination of NO production by monocytes was estimated by the measuring nitrite (NO_2^-) levels in the culture supernatants. Monocytes were incubated with *T. rubrum* conidia at 37°C and 5% CO_2 for 3 h, and supernatants were collected. The accumulation of NO_2^- was quantified by the Griess method. Briefly, 50 μl of supernatant was incubated with an equal volume of the Griess reagent for 10 min at room temperature, and the absorbance was measured using a plate reader with a filter between 520 and 550 nm. NO_2^- concentration was

determined by running in parallel a standard curve with concentrations ranging from 0 to 100 μM.

Cytokine Measurements

The production of the cytokines TNF-α, IL-1β, IL-6, and IL-10 in the supernatants of monocytes cultured for 18 h was evaluated and quantified by ELISA, following the manufacturer's instructions (BD Biosciences). *Escherichia coli* lipopolysaccharides (LPS; 100 ng/ml) and Zymosan (8 μg/ml) were used as the positive control for cytokine release, both from Sigma-Aldrich. The results were expressed in pg/ml and determined from standard curves established for each assay.

Statistical Analysis

Data were expressed as mean ± SEM and analyzed in the software GraphPad Prism (version 6.00 for Windows, GraphPad Software, San Diego, CA, USA; www.graphpad.com) by two-way ANOVA and Bonferroni *post hoc* test. All experiments were performed at least three times, and data were presented as the mean ± SEM of all experiments performed, unless otherwise indicated.

RESULTS

Phagocytosis of *T. rubrum* Is Less Efficient in the Absence of Toll-Like Receptor 2 Activation

TLR2 recognizes various microbial ligands (e.g., phospholipomannan, zymosan, and glucuronoxylomannan) and makes use of different mechanisms to provide specificity to each of them (Oliveira-Nascimento et al., 2012). We first investigated whether TLR2 can be involved in the phagocytosis of *T. rubrum* conidia by human monocytes by determining the PI after 3 h of interaction between phagocytes and fungal particles. Thus, our results showed that while monocytes efficiently ingested *T. rubrum* conidia (117.6 ± 8.6), functional blockade of TLR2 significantly inhibited fungal engulfment (55.5 ± 5.9; **Figure 1**). Consistent with this, the fungicidal activity of monocytes (852.8 ± 97.6) was also impaired when this receptor was blocked (405.5 ± 68.9; **Figure 2A**).

Taken together, these results indicate that TLR2 may be involved in the uptake and killing of *T. rubrum* by monocytes.

Outcome of *T. rubrum* Infection in Monocytes

To determine the fate of *T. rubrum* after its uptake by monocytes, we analyzed the interaction of monocytes and *T. rubrum* conidia in different times (3, 6, 12, and 24 h) by using light and transmission electron microscopy. The results showed that *T. rubrum* conidia developed into hyphae after 24 h of incubation with monocytes (**Figures 2B,C**), reinforcing the notion that monocytes present poor fungicidal activity.

Toll-Like Receptor 2 Does Not Participate in NO Production but Promotes Production of Pro-inflammatory Cytokines After *T. rubrum* Infection

Next, we determined whether NO secretion by monocytes 3 h after fungal addition could also be TLR2 dependent. Albeit *T. rubrum* did not promote an oxidative burst as strong as zymosan or phorbol myristate acetate (PMA), we did observe

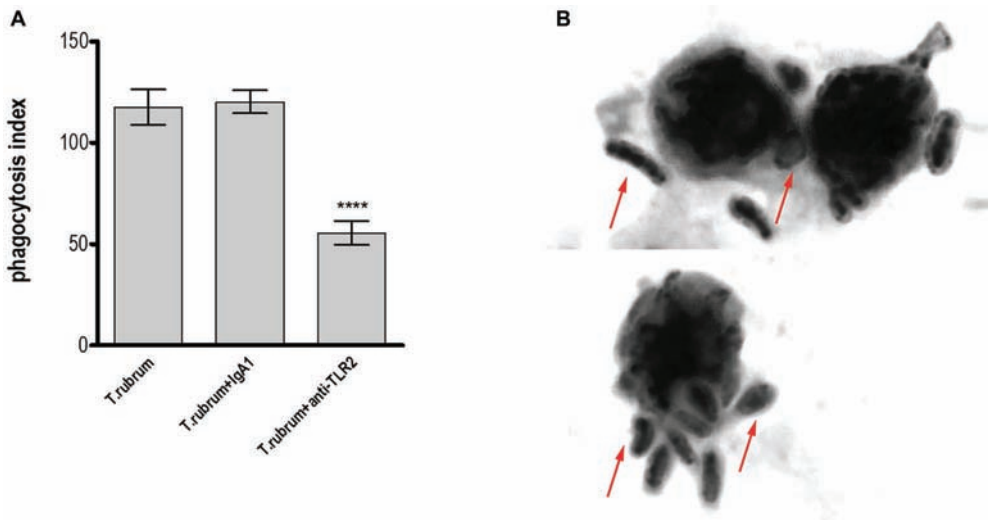

FIGURE 1 | TLR2 blockade leads to impaired phagocytosis by human monocytes. Monocytes treated with TLR2 neutralizing antibody (or isotype control) were co-cultured with *T. rubrum* conidia at a ratio of 1:5 for 3 h, fixed and stained with Giemsa solution. Conidia internalization was counted by optical microscopy, and the phagocytosis index (PI) was calculated. **(A)** PI of *T. rubrum* conidia by monocytes. **(B)** Images of *T. rubrum* conidia phagocytosis by monocytes (without TLR2 blockade) were analyzed by optical microscopy (1,000×), and arrows indicate fungal structures. Two-way ANOVA and Bonferroni *post hoc* test: ****$p < 0.0001$. Microscopy photos taken from one representative of 11 independent experiments, each performed in triplicate, are shown.

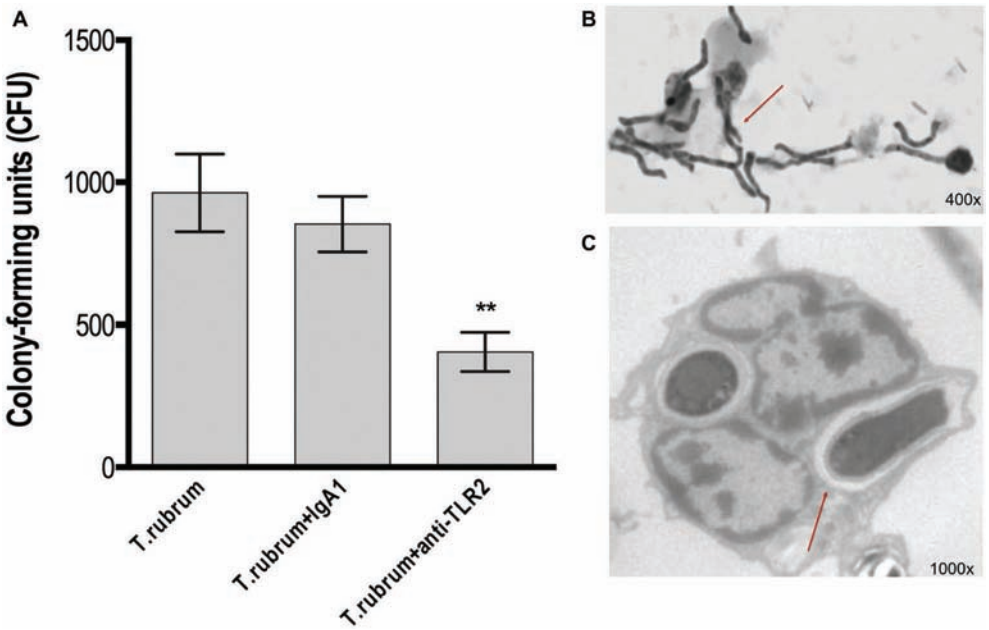

FIGURE 2 | TLR2 blockade decreases fungicidal activity by monocytes. Monocytes treated with TLR2 neutralizing antibody (or isotype control) were incubated with *T. rubrum* conidia at a ratio of 1:5 for 3 h. **(A)** Fungal loads in monocytes were determined by CFU assay. Images of the interaction between monocytes (without TLR2 blockade) and *T. rubrum* conidia analyzed by optical (400×) **(B)** and transmission electron microscopy (1,000×) **(C)** after 24 hours. Arrows indicate fungal structures. Data are expressed as mean ± SEM. Two-way ANOVA and Bonferroni *post hoc* test: $^{**}p < 0.01$. Microscopy photos taken from one representative of four independent experiments, each performed in triplicate, are shown.

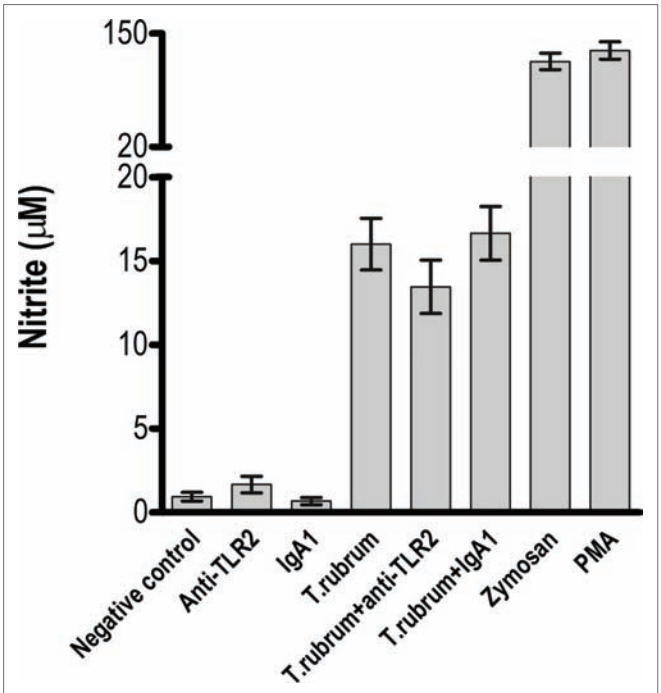

FIGURE 3 | NO release by monocytes is not impaired by TLR2 blockade. Monocytes treated with TLR2 neutralizing antibody (or isotype control) were incubated with *T. rubrum* conidia at a ratio of 1:5. Supernatants were collected after 3 h, and NO_2^- was measured by the Griess method. The results are expressed as mean ± SEM (n = 11), each performed in triplicate. Two-way ANOVA and Bonferroni *post hoc* test.

NO production in our cultures (16 ± 1.5; **Figure 3**). However, TLR2 blocking did not alter the response (13.5 ± 1.6). Curiously, Campos et al. (2006) showed that murine macrophages did not secret NO (Campos et al., 2006), suggesting important differences between human and mice models of dermatophytosis. Finally, we analyzed the cytokine response upon TLR2 blockade. Thus, as shown in **Figures 4A–C**, infected monocytes produced significantly higher levels of TNF-α (398.0 ± 72.2 pg/mL), IL-6 (925.4 ± 51.0 pg/mL) and IL-1β (523,1 ± 36,5 pg/mL) as compared to TLR2 blocked counterparts (respectively, 114,5 ± 21.0 pg/mL, 201,3 ± 31,31 pg/mL, 118,4 ± 16,3 pg/mL). IL-10 secretion (52,2 ± 5,3 pg/mL), however, was not significantly affected by antibody addition (42,6 ± 5,1 pg/mL) (**Figure 4D**). Similar results were obtained in experiments with heat killed (HK) *T. rubrum* conidia as shown in **Figures 5A–C**, TNF-α (447,5 ± 48,7 pg/mL), IL-6 (829,2 ± 48,2 pg/mL) and IL-1β (563,8 ± 59.0 pg/mL) secretion were significantly higher compared to TLR2 blocked group, (respectively, 101.0 ± 21,1 pg/mL, 237,8 ± 26,3 pg/mL, 119,4 ± 13,7 pg/mL). However, IL10 (58,6 ± 4,9 pg/mL) release was not significantly altered with TLR2 blockade in presence of HK *T. rubrum* conidia (59.0 ± 9.0 pg/mL) (**Figure 5D**). Previous studies indicate that *T. rubrum*-infected murine macrophages secreted significant levels of IL-10 and TNF-α (Campos et al., 2006), but here we showed that these responses may require the concomitant signaling of other uncoupled receptors. Zymosan and LPS were used as positive controls. The amounts elicited in the positive control wells (LPS or Zymosan) were significantly higher than in the non-stimulated wells (medium only) for every cytokine.

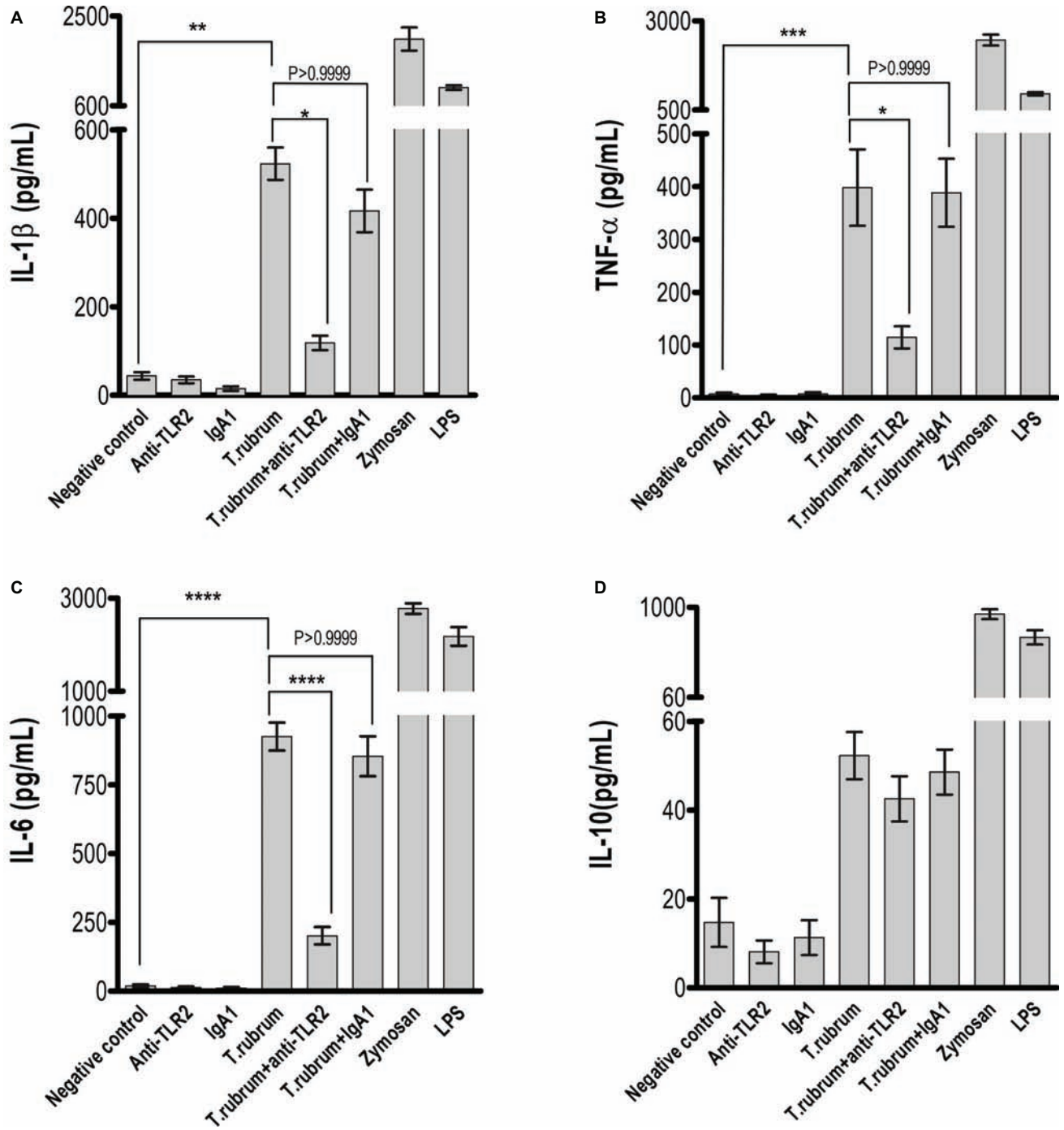

FIGURE 4 | TLR2 blockade impaired pro-inflammatory but not regulatory IL-10 cytokine production by monocytes. **(A)** IL-1β, **(B)** TNF-α, **(C)** IL-6, and **(D)** IL-10 levels were quantified in the culture supernatants by ELISA after 18 h of *T. rubrum* addition. The results are expressed as mean ± SEM ($n = 11$), each performed in triplicate. Two-way ANOVA and Bonferroni *post hoc* test: $^{*}p < 0.05$; $^{**}p < 0.01$; $^{***}p < 0.001$; $^{****}p < 0.0001$.

DISCUSSION

Dermatophytosis is a chronic fungal disease, usually benign but difficult to treat. Few studies, however, have addressed the role of monocytes during the initial phase of this infection. Human and experimental studies have shown that TLRs have an essential function during infectious diseases, particularly fungal infections (Maisonneuve et al., 2014), while preclinical and clinical studies have explored the use of TLR agonists as adjuvants to reinforce the adaptative immune response during vaccination or treatment of infectious diseases (de Sousa et al., 2014; Ashour, 2015).

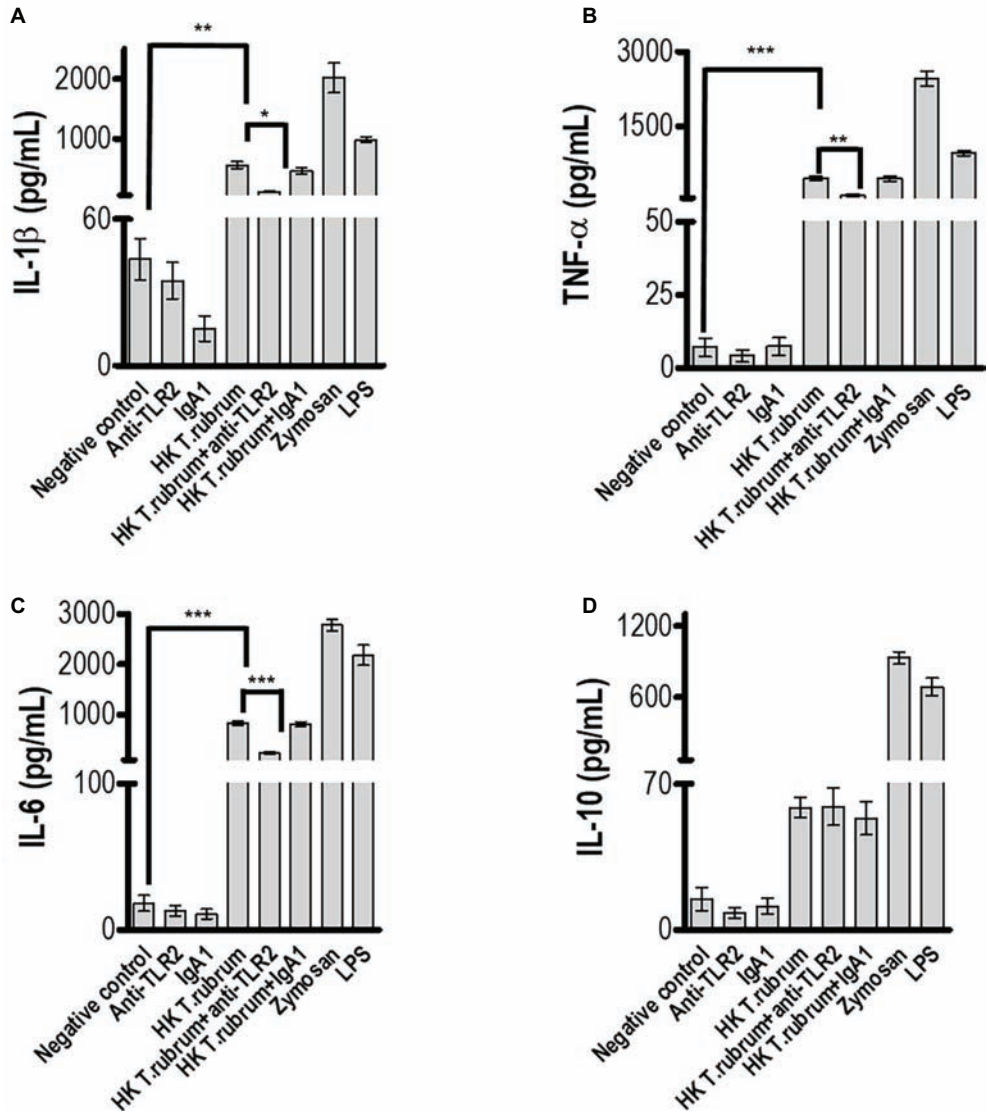

FIGURE 5 | TLR2 blockade impaired pro-inflammatory but not regulatory IL-10 cytokine production by monocytes after infection with HK *T. rubrum* conidia. **(A)** IL-1β, **(B)** TNF-α, **(C)** IL-6, and **(D)** IL-10 levels were quantified in the culture supernatants by ELISA after 18 h of *T. rubrum* addition. The results are expressed as mean ± SEM (n = 11), each performed in triplicate. Two-way ANOVA and Bonferroni *post hoc* test: $^{*}p < 0.05$; $^{**}p < 0.01$; $^{***}p < 0.001$.

In a previous report, we provided evidence that TLR2 participates in the host's epidermis response to dermatophytosis (de Oliveira et al., 2015). These studies suggested that the preserved expression of TLR2 *in situ* acted to limit the inflammatory process and to preserve the epidermal integrity. Alternatively, TLR2 sustained expression could also contribute to the limited inflammation and persistent infection that are characteristic of some dermatophytic infections (de Oliveira et al., 2015).

Previously regarded as superficial fungal infections limited to the keratinized layers of the epidermis, dermatophytic infections in immunocompromised patients may evolve to deep-seated or disseminated infections, implying the involvement of other compartments of the immune system (Lanternier et al., 2013). We thus aimed to investigate the role of TLR2 during the interaction of *T. rubrum* conidia with human monocytes.

TLR2-dependent uptake involves the recognition of fungal carbohydrates, but several studies exploring its role in different models of fungal infections showed conflicting results, suggesting both protective and non-protective effects, which could be explained by differences in the virulence of pathogens, the antigens, and the genetic background of the animals used (Oliveira-Nascimento et al., 2012), and also in differences between animal vs. human studies. In our system, blockade of TLR2 leads to impaired phagocytosis and fungicidal activity. But since TLR2 is not a phagocytic receptor by itself, the inefficient phagocytosis could be explained by

impaired secretion of opsonizing factors by the phagocytes or by a coadjutant role of TLR2 in the function of others *bona fide* internalizing receptors, for example, Dectin-1 (Gantner et al., 2003).

Moreover, whether TLR2 is blocked or not, the ingested conidia differentiated into hyphae, growing and killing the monocytes after 12 h of culture, recapitulating results found in murine macrophage models (Campos et al., 2006). These results indicate that fungal cells are able to inhibit monocyte functions or induce suppressive cytokines that could favor fungal evasion from host response.

Indeed, we showed that TLR2 contributes to *T. rubrum*-induced production of proinflammatory cytokines, but it does not participate in the secretion of the anti-inflammatory cytokine IL-10. The modulatory effects were observed in adherent monocytes and could be induced with both heat-killed and live conidia. Our data support the hypothesis that the absence of TLR2 signals may influence the function of monocytes and could increase the susceptibility to dermatophytosis. It is known that TLR2 influences macrophages and neutrophil anti-fungal activity, mainly through an effect on TNF-α production (Blasi et al., 2005; Gil et al., 2005; Gil and Gozalbo, 2006).

It is well known that IL-10 plays an inhibitory role in monocytes and neutrophil activity against fungal pathogens. Interestingly, normal human monocytes challenged with *T. rubrum* conidia released only small amounts of IL-10. This is in agreement with data from other fungi where conidia were also poor inducer of IL-10 compared, e.g., with the levels of pro-inflammatory cytokines secreted concomitantly, or compared with the IL-10 levels induced with hyphae (Netea et al., 2003). In fact, we speculate that induction of TLR-2-mediated production of IL-10 by *T. rubrum* conidia in normal human monocytes could be counterbalanced by signaling through other receptors, such as TLR4. Several studies showed in both mice and human monocytes that TLR4, which recognizes fungal mannan residues, signaled to increase pro-inflammatory cytokine production while decreasing IL-10 production (Netea et al., 2003; Chai et al., 2011; Kawasaki and Kawai, 2014). This regulation would not take place in monocytes from recurrent dermatophytosis patients, which secrete significantly more IL-10 than normal controls or tinea pedis patients (de Sousa et al., 2015). This may also explain why TLR2 blockade alone did not result in an increase in IL-10 levels.

We are now planning studies aiming to investigate the contribution of other phagocytic receptors (such as Dectin-1, mannose, or other TLRs such as TLR4) and their crosstalk with TLR2 signaling in the response to *T. rubrum*.

Intriguingly, while previous works suggest that TLR2 regulates the release of antimicrobial reactive oxygen and nitrogen species by innate immune cells (Tessarolli et al., 2010; Pinke et al., 2016), we could not recapitulate those findings in our experimental system, observing no TLR2 contribution in *T. rubrum*-induced NO secretion. However, since *T. rubrum* did not induce a high peak of oxidative species (compared to zymosan particles), we can hypothesize that this fungus does not promote a strong oxidative burst in monocytes and TLR2 can be important in regulating intense oxidative stress events.

All together, these data suggest that TLRs play different roles depending on cell type expression during infectious diseases, reinforcing the relevance of studies regarding TLR function in different cells in dermatophytosis.

CONCLUSION

In conclusion, our results demonstrate that TLR2 is important for the ingestion of *T. rubrum* conidia and the production of pro-inflammatory cytokines by human monocytes, uncovering an important branch of the innate immune response in the first step of dermatophyte pathogenesis.

DATA AVAILABILITY STATEMENT

The datasets generated for this study are available on request to the corresponding author.

ETHICS STATEMENT

The studies involving human participants were reviewed and approved by Comissão de Ética para Análise de Projetos – CAAPesq, Hospital das Clínicas, Faculdade de Medicina, Universidade de São Paulo. The participants provided their written informed consent to participate in this study.

AUTHOR CONTRIBUTIONS

GC carried out the experiment with support from AR. PC contributed to the interpretation of the results. GB and MS contributed equally to this work with analyzing the results and writing the manuscript. All authors discussed the results and contributed to the final manuscript.

FUNDING

GB is a senior researcher from Conselho Nacional de Desenvolvimento Científico e Tecnológico do Brasil (CNPq), Brazil. Financial support: Fapesp grants: 2018/16146-8 (GC), 2018/24175-8 (AR), 2017/26208-8, and 2016/16369-1 (MS).

ACKNOWLEDGMENTS

We would like to thank the volunteers for their invaluable cooperation.

REFERENCES

Ashour, D. S. (2015). Toll-like receptor signaling in parasitic infections. *Expert Rev. Clin. Immunol.* 11, 771–780. doi: 10.1586/1744666X.2015.1037286

Blasi, E., Mucci, A., Neglia, R., Pezzini, F., Colombari, B., Radzioch, D., et al. (2005). Biological importance of the two Toll-like receptors, TLR2 and TLR4, in macrophage response to infection with *Candida albicans*. *FEMS Immunol. Med. Microbiol.* 44, 69–79. doi: 10.1016/j.femsim.2004.12.005

Campos, M. R. M., Russo, M., Gomes, E., and Almeida, S. R. (2006). Stimulation, inhibition and death of macrophages infected with *Trichophyton rubrum*. *Microbes Infect.* 8, 372–379. doi: 10.1016/j.micinf.2005.07.028

Chai, L. Y., Kullberg, B. J., Vonk, A. G., Warris, A., Cambi, A., Latgé, J. P., et al. (2009). Modulation of Toll-like receptor 2 (TLR2) and TLR4 responses by *Aspergillus fumigatus*. *Infect. Immun.* 77, 2184–2192. doi: 10.1128/IAI.01455-08

Chai, L. Y., Vonk, A. G., Kullberg, B. J., Verweij, P. E., Verschueren, I., van der Meer, J. W., et al. (2011). *Aspergillus fumigatus* cell wall components differentially modulate host TLR2 and TLR4 responses. *Microbes Infect.* 13, 151–159. doi: 10.1016/j.micinf.2010.10.005

Dambuza, I. M., and Brown, G. D. (2015). C-type lectins in immunity: recent developments. *Curr. Opin. Immunol.* 32, 21–27. doi: 10.1016/j.coi.2014.12.002

de Oliveira, C. B., Vasconcellos, C., Sakai-Valente, N. Y., Sotto, M. N., Luiz, F. G., Belda Junior, W., et al. (2015). Toll-like receptors (TLR) 2 and 4 expression of keratinocytes from patients with localized and disseminated dermatophytosis. *Rev. Inst. Med. Trop. Sao Paulo* 57, 57–61. doi: 10.1590/S0036-46652015000100008

de Sousa, M. D. G., Belda, W., Spina, R., Lota, P. R., Valente, N. S., Brown, G. D., et al. (2014). Topical application of imiquimod as a treatment for chromoblastomycosis. *Clin. Infect. Dis.* 58, 1734–1737. doi: 10.1093/cid/ciu168

de Sousa, M. D. G., Santana, G. B., Criado, P. R., and Benard, G. (2015). Chronic widespread dermatophytosis due to *Trichophyton rubrum*: a syndrome associated with a *Trichophyton*-specific functional defect of phagocytes. *Front. Microbiol.* 6:801. doi: 10.3389/fmicb.2015.00801

Gantner, B. N., Simmons, R. M., Canavera, S. J., Akira, S., and Underhill, D. M. (2003). Collaborative induction of inflammatory responses by Dectin-1 and Toll-like receptor 2. *J. Exp. Med.* 197, 1107–1117. doi: 10.1084/jem.20021787

Gil, M. L., Fradelizi, D., and Gozalbo, D. (2005). TLR2: for or against *Candida albicans*? *Trends Microbiol.* 13, 298–299; discussion 9-301. doi: 10.1016/j.tim.2005.05.003

Gil, M. L., and Gozalbo, D. (2006). TLR2, but not TLR4, triggers cytokine production by murine cells in response to *Candida albicans* yeasts and hyphae. *Microbes Infect.* 8, 2299–2304. doi: 10.1016/j.micinf.2006.03.014

Godoy-Martinez, P., Nunes, F. G., Tomimori-Yamashita, J., Urrutia, M., Zaror, L., Silva, V., et al. (2009). Onychomycosis in São Paulo, Brazil. *Mycopathologia* 168, 111–116. doi: 10.1007/s11046-009-9209-5

Hardison, S. E., and Brown, G. D. (2012). C-type lectin receptors orchestrate antifungal immunity. *Nat. Immunol.* 13, 817–822. doi: 10.1038/ni.2369

Huang, X., Yi, J., Yin, S., Li, M., Ye, C., Lai, W., et al. (2015). *Trichophyton rubrum* conidia modulate the expression and transport of Toll-like receptor 2 in HaCaT cell. *Microb. Pathog.* 83–84, 1–5. doi: 10.1016/j.micpath.2015.04.002

Jones, H. E., Reinhardt, J. H., and Rinaldi, M. G. (1973). A clinical, mycological, and immunological survey for dermatophytosis. *Arch. Dermatol.* 108, 61–65. doi: 10.1001/archderm.1973.01620220033008

Kawasaki, T., and Kawai, T. (2014). Toll-like receptor signaling pathways. *Front. Immunol.* 5:461. doi: 10.3389/fimmu.2014.00461

Lanternier, F., Pathan, S., Vincent, Q. B., Liu, L., Cypowyj, S., Prando, C., et al. (2013). Deep dermatophytosis and inherited CARD9 deficiency. *N. Engl. J. Med.* 369, 1704–1714. doi: 10.1056/NEJMoa1208487

Lee, W. J., Kim, S. L., Jang, Y. H., Lee, S. J., Kim, D. W., Bang, Y. J., et al. (2015). Increasing prevalence of *Trichophyton rubrum* identified through an analysis of 115,846 cases over the last 37 years. *J. Korean Med. Sci.* 30, 639–643. doi: 10.3346/jkms.2015.30.5.639

Maisonneuve, C., Bertholet, S., Philpott, D. J., and De Gregorio, E. (2014). Unleashing the potential of NOD- and Toll-like agonists as vaccine adjuvants. *Proc. Natl. Acad. Sci. USA* 111, 12294–12299. doi: 10.1073/pnas.1400478111

Nakamura, K., Miyagi, K., Koguchi, Y., Kinjo, Y., Uezu, K., Kinjo, T., et al. (2006). Limited contribution of Toll-like receptor 2 and 4 to the host response to a fungal infectious pathogen, *Cryptococcus neoformans*. *FEMS Immunol. Med. Microbiol.* 47, 148–154. doi: 10.1111/j.1574-695X.2006.00078.x

Netea, M. G., Warris, A., Van der Meer, J. W., Fenton, M. J., Verver-Janssen, T. J., Jacobs, L. E., et al. (2003). *Aspergillus fumigatus* evades immune recognition during germination through loss of Toll-like receptor-4-mediated signal transduction. *J. Infect. Dis.* 188, 320–326. doi: 10.1086/376456

Oliveira-Nascimento, L., Massari, P., and Wetzler, L. M. (2012). The role of TLR2 in infection and immunity. *Front. Immunol.* 3:79. doi: 10.3389/fimmu.2012.00079

Pinke, K. H., Lima, H. G., Cunha, F. Q., and Lara, V. S. (2016). Mast cells phagocyte *Candida albicans* and produce nitric oxide by mechanisms involving TLR2 and Dectin-1. *Immunobiology* 221, 220–227. doi: 10.1016/j.imbio.2015.09.004

Romano, C., Gianni, C., and Difonzo, E. M. (2005). Retrospective study of onychomycosis in Italy: 1985–2000. *Mycoses* 48, 42–44. doi: 10.1111/j.1439-0507.2004.01066.x

Svejgaard, E. L., and Nilsson, J. (2004). Onychomycosis in Denmark: prevalence of fungal nail infection in general practice. *Mycoses* 47, 131–135. doi: 10.1111/j.1439-0507.2004.00968.x

Teklebirhan, G., and Bitew, A. (2015). Prevalence of dermatophytic infection and the spectrum of dermatophytes in patients attending a tertiary hospital in Addis Ababa, Ethiopia. *Int. J. Microbiol.* 2015:653419. doi: 10.1155/2015/653419

Tessarolli, V., Gasparoto, T. H., Lima, H. R., Figueira, E. A., Garlet, T. P., Torres, S. A., et al. (2010). Absence of TLR2 influences survival of neutrophils after infection with *Candida albicans*. *Med. Mycol.* 48, 129–140. doi: 10.3109/13693780902964339

van de Veerdonk, F. L., Marijnissen, R. J., Kullberg, B. J., Koenen, H. J. P. M., Cheng, S.-C., Joosten, I., et al. (2009). The macrophage mannose receptor induces IL-17 in response to *Candida albicans*. *Cell Host Microbe* 5, 329–340. doi: 10.1016/j.chom.2009.02.006

Yoshikawa, F. S., Yabe, R., Iwakura, Y., de Almeida, S. R., and Saijo, S. (2016). Dectin-1 and Dectin-2 promote control of the fungal pathogen *Trichophyton rubrum* independently of IL-17 and adaptive immunity in experimental deep dermatophytosis. *Innate Immun.* 22, 316–324. doi: 10.1177/1753425916645392

Conflict of Interest: The authors declare that the research was conducted in the absence of any commercial or financial relationships that could be construed as a potential conflict of interest.

frontiers in Microbiology

MINI REVIEW
published: 21 November 2019
doi: 10.3389/fmicb.2019.02573

Fungal Cell Wall: Emerging Antifungals and Drug Resistance

*Soraia L. Lima[1], Arnaldo L. Colombo[1] and João N. de Almeida Junior[2]**

[1]*Laboratório Especial de Micologia, Disciplina de Infectologia, Universidade Federal de São Paulo, São Paulo, Brazil,*
[2]*Central Laboratory Division, Hospital das Clínicas da Faculdade de Medicina da Universidade de São Paulo, São Paulo, Brazil*

The cell wall is an essential component in fungal homeostasis. The lack of a covering wall in human cells makes this component an attractive target for antifungal development. The host environment and antifungal stress can lead to cell wall modifications related to drug resistance. Antifungals targeting the cell wall including the new β-D-glucan synthase inhibitor ibrexafungerp and glycosyl-phosphatidyl Inositol (GPI) anchor pathway inhibitor fosmanogepix are promising weapons against antifungal resistance. The fosmanogepix shows strong *in vitro* activity against the multidrug-resistant species *Candida auris*, *Fusarium solani*, and *Lomentospora prolificans.* The alternative carbon sources in the infection site change the cell wall β-D-glucan and chitin composition, leading to echinocandin and amphotericin resistance. *Candida* populations that survive echinocandin exposure develop tolerance and show high chitin content in the cell wall, while fungal species such as *Aspergillus flavus* with a higher β-D-glucan content may show amphotericin resistance. Therefore understanding fungal cell dynamics has become important not only for host-fungal interactions, but also treatment of fungal infections. This review summarizes recent findings regarding antifungal therapy and development of resistance related to the fungal cell wall of the most relevant human pathogenic species.

Keywords: fungal cell wall, antifungals, therapy, resistance, 1,3-β-D-Glucan Synthase Inhibitors, ibrexafungerp, manogepix

OPEN ACCESS

Edited by:
Joshua D. Nosanchuk, Albert Einstein College of Medicine, United States

Reviewed by:
Jeniel E. Nett, University of Wisconsin-Madison, United States
Emma Camacho, Johns Hopkins University, United States

****Correspondence:***
João N. de Almeida Junior
jnaj99@gmail.com

Specialty section:
This article was submitted to Fungi and their Interactions, a section of the journal Frontiers in Microbiology

Received: *19 August 2019*
Accepted: *23 October 2019*
Published: *21 November 2019*

Citation:
Lima SL, Colombo AL and de Almeida Junior JN (2019) Fungal Cell Wall: Emerging Antifungals and Drug Resistance. Front. Microbiol. 10:2573. doi: 10.3389/fmicb.2019.02573

INTRODUCTION

The cell wall is an essential component in homeostasis of fungal cells (Latgé, 2007; Gow et al., 2017). It also has a dual interaction process with the surrounding environment, which either negatively or positively impacts fungal cell survival. Cell wall antigens induce immune recognition by the infected host and facilitate phagocytosis (Roy and Klein, 2012). Some antigens, named pathogen-associated molecular patterns (PAMPs), are recognized by a wide range of pattern-recognition receptors (PRRs) on host cell surfaces (Roy and Klein, 2012). Conversely, environmental stresses lead to cell wall modifications that impede immune recognition (Gow et al., 2017).

Representing approximately 40% of the total fungal cell volume, the fungal cell wall forms a tensile and robust core scaffold to which a variety of proteins and superficial components with fibrous and gel-like carbohydrates form polymers, making a strong but flexible structure (Munro, 2013; Gow et al., 2017). Most cell walls have two layers: (1) the inner layer comprising a relatively conserved structural skeleton and (2) the outer layer which is more heterogeneous and has species-specific peculiarities (Gow et al., 2017). The inner cell wall represents the loadbearing, structural component of the wall that resists the substantial internal hydrostatic

pressure exerted on the wall by the cytoplasm and membrane (Latgé, 2007). This layer includes chitin and glucan, in which 50–60% of the dry weight of the cell wall is made up of β-(1-3)-glucan. The outer-layer structure consists of heavily mannosylated glycoproteins with modified N- and O- linked oligosaccharides. The structure of these oligosaccharide side chains differs among fungal species (Shibata et al., 1995; Hobson et al., 2004).

Since human cells do not have a covering wall, antifungals that target the production of cell wall components are more selective and less toxic when compared to azole derivatives and amphotericin B (Patil and Majumdar, 2017). Echinocandins were the first systemic antifungals that targeted the cell wall by disrupting the production of glucans (Patil and Majumdar, 2017). For invasive candidiasis, echinocandins were a great development that lowered the mortality associated with these infections, with low toxicity and few interactions with other medication (Mora-Duarte et al., 2002; Pappas et al., 2016). However, intrinsic and acquired resistance to echinocandins limits its usefulness, leading to research into other targets in the fungal cell wall for antifungal therapy (Hasim and Coleman, 2019).

Cell wall dynamics may play an important role for the development of antifungal resistance and interesting concepts regarding this subject are emerging. Structural and cell wall composition modifications have been investigated in *Candida* and *Aspergillus* isolates presenting antifungal resistance (Seo et al., 1999; Mesa-Arango et al., 2016). In echinocandin-tolerant *Candida* isolates, β-1,3- and β-1,6-glucans crosslinks modifications and higher chitin content have been described (Perlin, 2015), while higher β-D-glucan composition has been found in amphotericin-B-resistant *Aspergillus flavus* isolates (Seo et al., 1999).

In this manuscript, we review the fungal cell wall as a target for antifungal therapy and, in conjunction, visit cell wall modifications that may be related to antimicrobial resistance.

FUNGAL CELL WALL TARGETING ANTIFUNGALS

Antifungals targeting the cell wall have been developed in the last years (Walker et al., 2011; Chaudhary et al., 2013; Mutz and Roemer, 2016; Hasim and Coleman, 2019). Most of these drugs act by inhibiting β-D-glucan synthase, but chitin synthase and glycosylphosphatidylinositol (GPI) anchor pathway inhibitors are also under development (**Figure 1A**).

1,3-β-D-Glucan Synthase Inhibitors

Echinocandins

Echinocandins were first described in the 1970's as antibiotic polypeptides obtained from *Aspergillus nidulans* (Nyfeler and Keller-Schierlein, 1974). These molecules are basically hexapeptide antibiotics with N-linked acyl fatty acid chains that intercalates with the phospholipid layer of the cell membrane (Denning, 2003). This antifungal class inhibits the β-D-glucan synthase, which leads to a decrease of the β-D-glucans in the cell wall after noncompetitively binding to the Fksp subunit of the enzyme (Hector, 1993; Denning, 2003; Aguilar-Zapata et al., 2015; Perlin, 2015; Patil and Majumdar, 2017).

The fungal cell wall β-D-glucan synthase complex has two main subunits: Fks1p and Rho1p (Mazur and Baginsky, 1996; Aguilar-Zapata et al., 2015). Fks1p is the catalytic subunit responsible for the production of glycosidic bonds (Schimoler-O'Rourke et al., 2003), while Rho1p is a Ras-like GTP-binding protein that regulates the β-D-glucan synthase activity (Qadota et al., 1996).

Inhibition of β-D-glucan synthase results in the cell death of the *Candida* species, while echinocandins modify the hyphae morphogenesis and exert a fungistatic effect against *Aspergillus* species (Bowman et al., 2002). Conversely, species belonging to the order Mucorales and the basidiomycetes are intrinsically resistant to this antifungal class (Espinel-Ingroff, 2003; Aguilar-Zapata et al., 2015).

Currently, there are three echinocandins approved by the FDA for the treatment of invasive fungal infections: caspofungin, anidulafungin, and micafungin (Johnson and Perfect, 2003; Rüping et al., 2008; Pappas et al., 2016). Compared to other antifungal classes, the echinocandins show lower kidney or liver toxicity, fewer drug–drug interactions, and have predominant liver elimination, not requiring dose adjustments during renal failure or dialysis (Aguilar-Zapata et al., 2015). However, echinocandins have pharmacokinetic limitations, such as poor bioavailability upon oral administration, high protein binding, and low central nervous system (CNS) penetration (Wiederhold and Lewis, 2003). New glucan synthase inhibitors with better pharmacokinetics profiles, including oral formulations with high bioavailability, are under investigation (Davis et al., 2019).

Rezafungin (CD101, formerly SP3025, Cidara Therapeutics, San Diego, CA, USA), a next-generation echinocandin, is currently in Phase 3 of clinical trials for the treatment of candidemia and invasive candidiasis[1]. This antifungal is a structural analog of anidulafungin, but with a choline moiety replacing the hemiaminal group at the C5 ornithine position, resulting in a stable compound with prolonged half-life (Sandison et al., 2017). It is highly soluble in aqueous systems and has a half-life of over 130 h in humans, compared to 24, 9–11, 10–17 h half-lives of anidulafungin, caspofungin, and micafungin, respectively (Kofla and Ruhnke, 2011; Sandison et al., 2017). The long half-life of rezafungin allows an advantageous weekly dosing regimen (Sandison et al., 2017; Sofjan et al., 2018).

Rezafungin has potent *in vitro* activity against common *Candida* and *Aspergillus* species (Wiederhold et al., 2018; Arendrup et al., 2018a,b). Furthermore, this antifungal has strong *in vitro* antifungal activity against the potential multidrug-resistant species *C. auris* (Berkow and Lockhart, 2018). Moreover, the *in vivo* efficacy of rezafungin in neutropenic murine disseminated candidiasis models was demonstrated against *C. albicans, C. glabrata, C. parapsilosis* (Lepak et al., 2018), and *C. auris* (Hager et al., 2018a).

[1]https://clinicaltrials.gov/ct2/show/NCT03667690

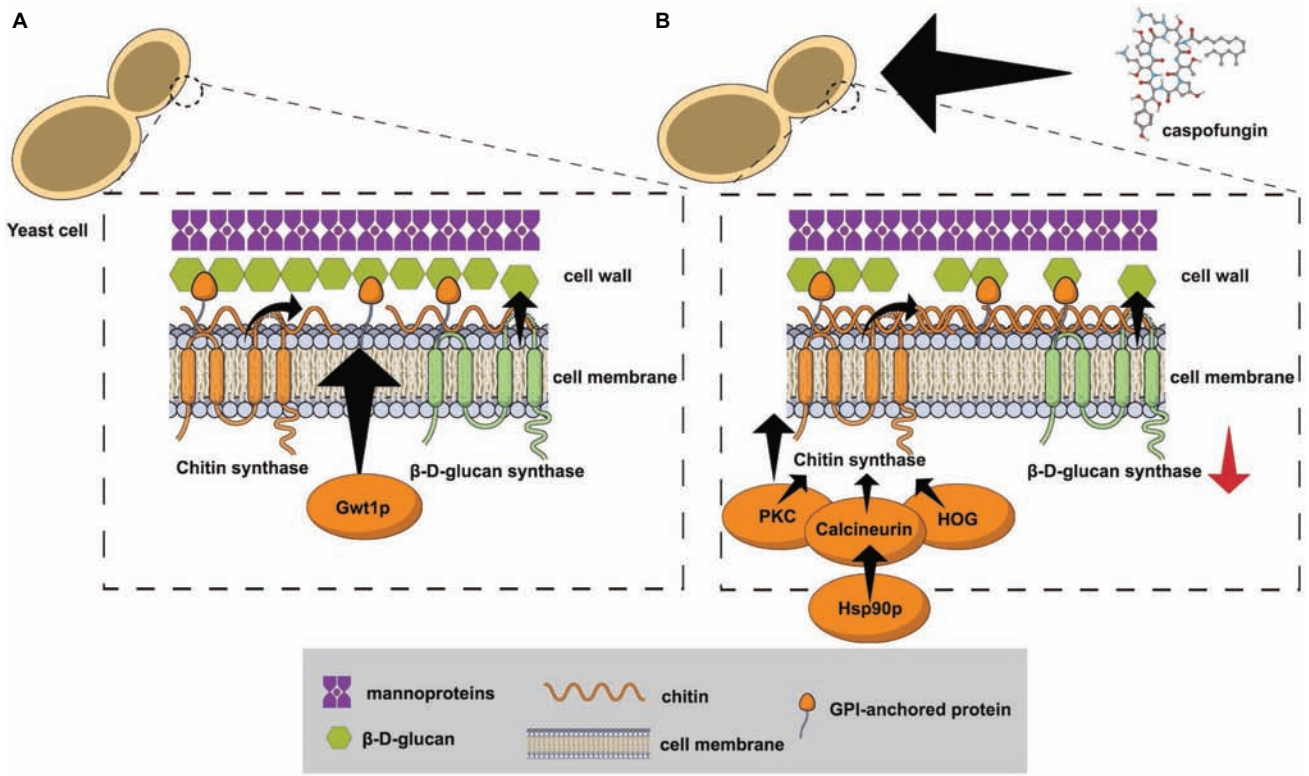

FIGURE 1 | (A) The fungal cell wall and the targets that have been explored for antifungal development: β-D-glucan synthase, chitin synthase, and the enzyme Gwt1 from the GPI anchor pathway; **(B)** Echinocandin exposure causes cell wall stress by inhibition of the β-D-glucan synthase. The protein kinase C (PKC), high osmolarity glycerol response (HOG), and Ca^{+2}-calcineurin pathways have been implicated in the response to cell wall damage and chitin synthase hyper stimulation. Calcineurin is a client protein for the Hsp90 chaperone and genetic compromise of the gene *HSP90* reduces the tolerance mechanism.

Triterpenoids

The triterpenoid class is represented by ibrexafungerp (SCY-078, formerly MK-3118), a new semisynthetic derivate of hemiacetal triterpene glycoside enfumafungin (Synexis Inc., Jersey City, NJ, USA) (Pfaller et al., 2017; Wring et al., 2017; Davis et al., 2019). It is a β-D-glucan synthase inhibitor with similar but not identical biding sites to echinocandins in the catalytic regions Fks1p and Fks2p of the enzyme (Walker et al., 2011; Jiménez-Ortigosa et al., 2017). It has high protein binding and good tissue penetration, although like echinocandins, it has poor CNS penetration (Davis et al., 2019). The pharmacokinetic gain of this new antifungal is its good oral bioavailability (Walker et al., 2011).

Ibrexafungerp has demonstrated good *in vitro* activity against relevant fungal pathogens such as *Candida* spp., including multidrug-resistant *C. glabrata* (Pfaller et al., 2013, 2017; Jiménez-Ortigosa et al., 2017), biofilm producer strains (Marcos-Zambrano et al., 2017b), and *C. auris* (Larkin et al., 2017). Notably, echinocandin-resistant *Candida* strains harboring hot spot mutations at the Fksp may retain susceptibility to ibrexafungerp (Pfaller et al., 2017). A more in-depth study analyzing *C. glabrata* strains with echinocandin resistance and ibrexafungerp susceptibility showed that ibrexafungerp has only partial overlapping at the echinocandins Fksp biding sites in the β-D-glucan synthase enzyme (Jiménez-Ortigosa et al., 2017). Against *Aspergillus* clinically relevant species, ibrexafungerp has also demonstrated potent *in vitro* activity (Davis et al., 2019). Moreover, the combination of ibrexafungerp with either voriconazole or amphotericin B has demonstrated synergy against wild-type *A. fumigatus* strains (Ghannoum et al., 2018). Noteworthy, ibrexafungerp showed some antifungal activity against the multidrug-resistant mold *Lomentospora prolificans* (Lamoth and Alexander, 2015), and it is highly active against *Paecilomyces variotii* (Lamoth and Alexander, 2015). However, ibrexafungerp has little activity against Mucorales spp., *Fusarium* spp., and *Purpureocillium lilacinum* (Lamoth and Alexander, 2015). The *in vitro* activity of ibrexafungerp is summarized in **Table 1**.

In time-to-kill experiments, ibrexafungerp showed mainly fungicidal activity against *Candida albicans* and *non-albicans* isolates (Scorneaux et al., 2017). For *in vivo* murine models of invasive candidiasis caused by *C. albicans*, *C. glabrata*, and *C. parapsilosis*, this drug showed similar concentration-dependent killing of the three Candida species (Lepak et al., 2015).

This antifungal is currently in clinical trials for the treatment of vulvovaginal candidiasis (Phase 3; https://clinicaltrials.gov/ct2/show/NCT03987620), for invasive aspergillosis in combination with voriconazole (Phase 2; https://clinicaltrials.

TABLE 1 | *In vitro* activity of the main cell wall antagonists.

Species	Antifungal class			
	β-D-Glucan synthase inhibitors		Chitin synthase inhibitors	GPI anchor pathway inhibitors
	Echinocandins	Enfumafungin derivatives (Ibrexafungerp)	Nikkomycin Z	Fosmanogepix
Candida species	Strong	Strong	Poor but strong synergism with echinocandins	Strong
Candida auris	Strong	Strong	Not evaluated	Strong
Aspergillus fumigatus	Strong	Strong with synergism with azoles and amphotericin B	Poor	Strong
Fusarium species	Poor	Poor	Poor	Strong
Lomentospora prolificans	Poor	Moderate	Poor	Strong
Coccidioides species	Moderate[1]	Not evaluated	Moderate and with synergism with echinocandins	Strong
Blastomyces dermatitidis	Poor	Not evaluated	Moderate	Not evaluated
Histoplasma capsulatum	Poor	Not evaluated	Moderate	Not evaluated
Cryptococcus species	Poor	Poor	Poor but with strong synergism with azoles	Strong

Strong in vitro activity was considered for the antifungals presenting minimal inhibitory concentrations, usually ≤0.5 mcg/μL for a certain genus or species; moderate in vitro activity was considered for the antifungals presenting minimal inhibitory concentrations usually between 0.5 and 4 mcg/μl for a certain genus or species; poor in vitro activity was considered for the antifungals presenting minimal inhibitory concentrations usually >4 mcg/μl for a certain genus or species.[1]Some studies described poor in vitro activity of echinocandins against Coccidioides spp. (Stevens, 2000; Cordeiro et al., 2006), while a recent study described strong in vitro activity of echinocandins against Coccidioides immitis (Thompson et al., 2017). The data presented in this table are based on the references: Aguilar-Zapata et al. (2015); Arendrup et al. (2018a); Shaw et al. (2018); Castanheira et al. (2012); Goldberg et al. (2000); Hage et al. (2011); Hector et al. (1990); Lamoth and Alexander (2015); Li and Rinaldi (1999); Nakai et al. (2003); Pfaller et al. (2019); Thompson et al. (2017); Viriyakosol et al. (2019); Zhao et al. (2018).

gov/ct2/show/NCT03672292), invasive and mucosal candidiasis (Phase 3; https://clinicaltrials.gov/ct2/show/NCT03059992), and for invasive candidiasis due to *C. auris* (Phase 3; https://clinicaltrials.gov/ct2/show/NCT03363841).

Chitin Synthase Inhibitors

Chitin is an essential component of the fungal cell wall and compounds that affect its synthesis have been investigated as antifungals, such as nikkomycins, polyoxins, and plagiochin (Chaudhary et al., 2013).

Nikkomycins are peptidyl nucleoside agents that competitively inhibit chitin synthase (*CHS*). Nikkomycin Z has some *in vitro* activity against *C. parapsilosis, Coccidioides immitis, and Blastomyces dermatitidis* (Hector et al., 1990), but its usefulness relies on the synergism with echinocandins for *C. albicans, A. fumigatus,* and *C. immitis* (Chiou et al., 2001; Cheung and Hui, 2017). One study using a murine model of invasive candidiasis showed that Nikkomycin Z plus echinocandins were effective for the treatment of infections by echinocandin-resistant *C. albicans* (Cheung and Hui, 2017).

Glycosylphosphatidyl Inositol Anchor Pathway Inhibitors

Glycosylphosphatidyl inositol (GPI) is a component of the eukaryotes cell wall and is synthesized in the endoplasmic reticulum by a conserved pathway (Ikezawa, 2002). GPI glycolipids anchor different proteins to the cell wall and are essential for its integrity (Yadav and Khan, 2018).

Antifungals targeting GPI anchor synthesis pathway have been developed in the last 15 years (Tsukahara et al., 2003; Mutz and Roemer, 2016). One of the targets of the GPI anchor synthesis pathway is the protein Gwt1 (GPI-anchored wall protein transfer 1), an inositol acyltransferase that catalyzes inositol acylation (Tsukahara et al., 2003; Hata et al., 2011). Inhibition of Gwt1 compromises cell wall integrity, biofilm production, germ tube formation, and produces severe fungal growth defects (Yadav and Khan, 2018). In *C. albicans* and *Saccharomyces cerevisiae,* Gwt1 inhibition has been shown to jeopardize the maturation and stabilization of GPI-anchored mannoproteins (McLellan et al., 2012). The first compound used to inhibit the Gwt1 enzyme was the molecule 1-(4-butylbenzyl) isoquinoline (BIQ), described by Tsukahara et al. (2003).

From the BIQ molecule, a new compound with higher antifungal potency was created by the Tsukuba Research Laboratories of Eisai Co., Ltd. (Ibaraki, Japan), the APX001A or manogepix (formerly E1210) (Hata et al., 2011). Later, Amplix Pharmaceuticals Inc. (San Diego, CA, USA) developed the N-phosphonooxymethyl prodrug fosmanogepix (APX001, formerly E1211) with oral and IV formulations. The prodrug is metabolized by phosphatases and converted to manogepix (APX001A, formerly E1210) which inhibits the Gwt1 but not the human homolog Pig-W (Watanabe et al., 2012; Wiederhold et al., 2019). The oral formulation of fosmanogepix presented good bioavailability in murine experiments (Zhao et al., 2018).

The *in vitro* activity of manogepix has been investigated against yeasts and molds (Miyazaki et al., 2011; Castanheira et al., 2012). Low minimal inhibitory concentrations (MICs) of this new antifungal were found against *C. albicans, C. tropicalis, C. glabrata, C. parapsilosis, C. lusitaniae, C. kefyr,* (Miyazaki et al., 2011; Pfaller et al., 2019), and also against multidrug-resistant *C. auris* (Hager et al., 2018a), and echinocandin-resistant *C. glabrata* (Pfaller et al., 2019). However,

in vitro results against *C. krusei* and *C. norvegensis* have been described as poor (Arendrup et al., 2018a). Potent *in vitro* activity of manogepix was also noticed against *Cryptococcus neoformans* and *Cryptococcus gattii* strains (Shaw et al., 2018; Pfaller et al., 2019). Regarding *in vitro* activity against molds, low MICs against *Aspergillus* species from the Section Fumigati, Flavi, Terrei, and Nigri (Miyazaki et al., 2011; Pfaller et al., 2019), *Purpureocillium lilacinum, Cladosporium* species, *Phialophora* species, *Rhinocladiella aquaspersa, Fonsecaea pedrosoi* (Miyazaki et al., 2011), *Scedosporium apiospermum*, and *Scedosporium aurantiacum* (Castanheira et al., 2012), and against the multidrug-resistant species *Fusarium solani* and *L. prolificans* (Castanheira et al., 2012). The *in vitro* activity of manogepix is summarized in **Table 1**.

The *in vivo* activity of manogepix/fosmanogepix has been also investigated in murine models of disseminated candidiasis, aspergillosis, fusariosis (Hata et al., 2011; Hager et al., 2018b), and *Coccidioides immitis* pneumonia (Viriyakosol et al., 2019). In a murine model of disseminated *C. albicans* infection, it showed similar efficacy to caspofungin, fluconazole, and liposomal amphotericin B (Hata et al., 2011). Another study compared the efficacy of manogepix/fosmanogepix and anidulafungin for the treatment of mouse with disseminated *C. auris* infection and found higher survival rates in the group treated with the Gwt1 inhibitor (Hager et al., 2018b). In a murine model of invasive *Aspergillus flavus* infection, mice treated with this new antifungal had similar survival rates when compared to the groups treated with either voriconazole or caspofungin (Hata et al., 2011). In the same study, mice infected by *F. solani* showed a higher survival rate when treated with fosmanogepix 20 mg/kg compared to the control group without antifungal therapy (Hata et al., 2011).

There is currently a Phase 2, single-arm, and open-label trial of fosmanogepix for the first-line treatment of candidemia[2].

FUNGAL CELL WALL MODIFICATIONS AND ANTIFUNGAL RESISTANCE

Modifications in fungal cell wall architecture appear after stresses produced by the host microenvironment and antifungal exposure (Ene et al., 2012; Perlin, 2015; Mesa-Arango et al., 2016).

In vitro studies have shown in conditions that mimic the host microenvironment at the infection site that yeast cells may develop wall modifications and antifungal resistance (Ene et al., 2012; Brown et al., 2014). *C. albicans* cells grown in serum (<0.1% glucose) show major changes in the cell wall architecture, with a decrease in the length of mannan chains, and in the chitin and β-glucan content (Ene et al., 2012). Moreover, growth-challenging conditions with alternative carbon sources, such as lactate, alter cell wall biosynthesis, leading to the production of a leaner but stiffer inner cell wall (Ene et al., 2012). These cell wall-remodeled *C. albicans* cells become resistant to amphotericin B (AMB) and caspofungin (Ene et al., 2012). Similar results were demonstrated for *C. glabrata* strains that grown under an alternative carbon microenvironment showed altered cell wall architecture with a lower content of chitin and β-glucan, and with an increased outer mannan layer (Chew et al., 2019). These *C. glabrata* cells were also resistant to AMB when grown in lactate or oleate (Chew et al., 2019).

An intermediary step to antifungal resistance is the development of tolerance (Perlin, 2015). Cells surviving drug exposure can respond to selection and evolve resistance (Perlin, 2015). Echinocandin exposure causes cell wall stress by inhibition of the β-D-glucan synthesis, which triggers adaptive cellular factors that stimulate chitin production (Walker et al., 2008, 2010). Protein kinase C (PKC), high osmolarity glycerol response (HOG), and Ca^{+2}-calcineurin pathways have been implicated in the response to cell wall damage and chitin synthesis (**Figure 1B**; Lagorce et al., 2003; Bermejo et al., 2008; Walker et al., 2008; Fortwendel et al., 2009). The chaperone Hsp90 is another crucial component for echinocandins tolerance after cell wall stress (Singh et al., 2009; O'Meara et al., 2017). Calcineurin is a client protein for the Hsp90 chaperone and genetic compromise of the gene *HSP90* reduced the tolerance mechanism in *C. albicans* (Singh et al., 2009), *C. glabrata* (Singh-Babak et al., 2012), and *Aspergillus fumigatus* (Lamoth et al., 2014). Another expression of fungal adaptive mechanisms caused by antifungal stress is called the parodoxal effect, which is the recuperation of fungal growth after exposure to antifungals at increasing concentrations above a certain threshold (Aruanno et al., 2019). This phenomenon has been reported in *Candida* spp. and *Aspergillus* spp. after exposure to echinocandins, mainly caspofungin (Rueda et al., 2014; Marcos-Zambrano et al., 2017a; Aruanno et al., 2019). Similar to the tolerance mechanism, the paradoxical effect is related to intracellular signaling pathways that lead to cell wall remodeling with increase of the chitin and loss of β-D-glucan content (Aruanno et al., 2019). In *A. fumigatus*, caspofungin exposure may also lead to an increase in reactive oxygen species (ROS) production and to modifications of the lipid microenvironment surrounding the β-D-glucan synthase, leading to echinocandins resistance (Satish et al., 2019).

In *C. albicans*, other relevant components for echinocandin tolerance may be located at chromosome 5 (Ch5), since some tolerant mutants showed either monosomy of the Ch5, or combined monosomy of the left arm and trisomy of the right arm of Ch5 (Yang et al., 2017). Eventually, persistent echinocandin exposure leads to *FKS* mutations and organisms with marked and stable resistance emerge with a high chitin content in the cell wall (Walker et al., 2013; Perlin, 2015). *FKS* mutations in *Candida* species and echinocandin resistance have been extensively reviewed elsewhere (Walker et al., 2010; Perlin, 2015).

AMB resistance may be explained by multiple mechanisms, among them modifications in the cell wall architecture (Seo et al., 1999; Mesa-Arango et al., 2016). *Aspergillus flavus* isolates with AMB resistance have been related to invasive fungal infections with poor prognosis in neutropenic patients (Koss et al., 2002; Hadrich et al., 2012). Seo, Akiyoshi, and Ohnishi demonstrated that *in vitro* AMB-resistant mutant strains of *A. flavus* have similar sterol content in the cell membrane when compared to susceptible strains (Seo et al., 1999). Conversely,

[2]https://clinicaltrials.gov/ct2/show/NCT03604705

the cell wall from the resistant mutants contained more 1,3-β-D-glucan when compared to susceptible strains (Seo et al., 1999). The authors suggest that the higher content of glucans found in the resistant mutants helps to adsorb AMB, making it more difficult for the antifungal to reach the cell membrane (Seo et al., 1999). Comparisons between biofilm (AMB-resistant) and planktonic (AMB-susceptible) *C. albicans* cells revealed that the cell wall from the biofilm-grown isolates are thicker and have more β-1,3-glucans (Nett et al., 2007). In *C. tropicalis*, AMB resistance has been linked to several potential mechanisms, such as increase in catalase activity, changes in mitochondrial potential, low accumulation of reactive oxygen species, and deficiency in ergosterol at the cell membrane (Forastiero et al., 2013; Mesa-Arango et al., 2014). More recently, cell wall modifications have also been found in AMB-resistant *C. tropicalis* isolates (Mesa-Arango et al., 2016). The AMB-resistant isolates showed thicker cell walls with higher volume when compared to susceptible isolates (Mesa-Arango et al., 2016). Besides, these AMB-resistant organisms had a 2- to 3-fold increase of β-1,3-glucans in the cell wall (Mesa-Arango et al., 2016).

CONCLUSIONS AND PERSPECTIVES

Recent advances in the science of the fungal cell wall have opened the doors to new therapeutic modalities for fungal infections, and have helped to better understand the mechanisms of antifungal resistance. New antifungals targeting the cell wall show better safety and PK/PD profiles than the available toxic polyenes and azole derivative molecules. The new β-D-glucan synthase inhibitor ibrexafungerp has potent *in vitro* activity against multidrug-resistant pathogens such as echinocandin-resistant *C. glabrata*, *C. auris,* and *Aspergillus* species.

Glucan synthase inhibitors such as Nikkomycin Z have strong synergism with echinocandins and may be useful for the treatment of echinocandins-resistant *Candida* infections and refractory aspergillosis.

The GPI anchor pathway inhibitors APX001/APX001A have good pharmacokinetic profiles and strong *in vitro* activity against several fungal pathogenic species, including multiresistant *C. auris, F. solani,* and *L. prolificans*. This makes these drugs the most promising antifungals to be launched in the future.

The microenvironment at the infection site leads to modification in the fungal cell wall, which may lead to antifungal resistance. Cell wall stress induced by echinocandin exposure leads to the emergence of tolerant cells with high chitin content. The PKC, HOG, and Ca^{+2}-calcineurin pathways, as well as the chaperone Hsp90, are crucial components for the phenomenon of antifungal tolerance and should be explored as future targets for antifungal therapy. A few AMB-resistant *A. flavus* and *C. tropicalis* showed higher content of glucans in the cell wall, but further studies analyzing the cell wall modifications and AMB resistance are necessary to increase the strength of this correlation.

AUTHOR CONTRIBUTIONS

SL, AC, and JA conceived of the manuscript. SL and JA conducted the literature review. SL, AC, and JA wrote the manuscript. AC revised the manuscript.

FUNDING

The work of SL is supported by CAPES (Grant 88882.430766/2019-01). The work of JA is supported by FAPESP (Grant 2018/18347-4). AC received grants from CNPq (Grant 307510/2015-8) and FAPESP (Grant 2017/02203-7).

REFERENCES

Aguilar-Zapata, D., Petraitiene, R., and Petraitis, V. (2015). Echinocandins: the expanding antifungal armamentarium. *Clin. Infect. Dis.* 61(Suppl. 6), S604–S611. doi: 10.1093/cid/civ814

Arendrup, M. C., Chowdhary, A., Astvad, K. M. T., and Jørgensen, K. M. (2018a). APX001A in vitro activity against contemporary blood isolates and Candida auris determined by the EUCAST reference method. *Antimicrob. Agents Chemother.* 62, pii: e01225-18. doi: 10.1128/AAC.01225-18

Arendrup, M. C., Meletiadis, J., Zaragoza, O., Jørgensen, K. M., Marcos-Zambrano, L. J., Kanioura, L., et al. (2018b). Multicentre determination of rezafungin (CD101) susceptibility of Candida species by the EUCAST method. *Clin. Microbiol. Infect.* 24, 1200–1204. doi: 10.1016/j.cmi.2018.02.021

Aruanno, M., Glampedakis, E., and Lamoth, F. (2019). Echinocandins for the treatment of invasive aspergillosis: from laboratory to bedside. *Antimicrob. Agents Chemother.* 63, pii: e00399-19. doi: 10.1128/AAC.00399-19

Berkow, E. L., and Lockhart, S. R. (2018). Activity of CD101, a long-acting echinocandin, against clinical isolates of Candida auris. *Diagn. Microbiol. Infect. Dis.* 90, 196–197. doi: 10.1016/j.diagmicrobio.2017.10.021

Bermejo, C., Rodríguez, E., García, R., Rodríguez-Peña, J. M., Rodríguez de la Concepción, M. L., Rivas, C., et al. (2008). The sequential activation of the yeast HOG and SLT2 pathways is required for cell survival to cell wall stress. *Mol. Biol. Cell* 19, 1113–1124. doi: 10.1091/mbc.e07-08-0742

Bowman, J. C., Hicks, P. S., Kurtz, M. B., Rosen, H., Schmatz, D. M., Liberator, P. A., et al. (2002). The antifungal echinocandin caspofungin acetate kills growing cells of *Aspergillus fumigatus* in vitro. *Antimicrob. Agents Chemother.* 46, 3001–3012. doi: 10.1128/AAC.46.9.3001-3012.2002

Brown, A. J. P., Budge, S., Kaloriti, D., Tillmann, A., Jacobsen, M. D., Yin, Z., et al. (2014). Stress adaptation in a pathogenic fungus. *J. Exp. Biol.* 217, 144–155. doi: 10.1242/jeb.088930

Castanheira, M., Duncanson, F. P., Diekema, D. J., Guarro, J., Jones, R. N., and Pfaller, M. A. (2012). Activities of E1210 and comparator agents tested by CLSI and EUCAST broth microdilution methods against *Fusarium* and *Scedosporium* species identified using molecular methods. *Antimicrob. Agents Chemother.* 56, 352–357. doi: 10.1128/AAC.05414-11

Chaudhary, P. M., Tupe, S. G., and Deshpande, M. V. (2013). Chitin synthase inhibitors as antifungal agents. *Mini Rev. Med. Chem.* 13, 222–236. doi: 10.2174/138955713804805256

Cheung, Y.-Y., and Hui, M. (2017). Effects of echinocandins in combination with Nikkomycin Z against invasive *Candida albicans* bloodstream isolates and the fks mutants. *Antimicrob. Agents Chemother.* 61, pii: e00619-17. doi: 10.1128/AAC.00619-17

Chew, S. Y., Ho, K. L., Cheah, Y. K., Sandai, D., Brown, A. J. P., and Than, L. T. L. (2019). Physiologically relevant alternative carbon sources modulate biofilm formation, Cell Wall architecture, and the stress and antifungal resistance of *Candida glabrata*. *Int. J. Mol. Sci.* 20, pii: E3172. doi: 10.3390/ijms20133172

Chiou, C. C., Mavrogiorgos, N., Tillem, E., Hector, R., and Walsh, T. J. (2001). Synergy, pharmacodynamics, and time-sequenced ultrastructural changes of the interaction between nikkomycin Z and the echinocandin FK463 against *Aspergillus fumigatus*. *Antimicrob. Agents Chemother.* 45, 3310–3321. doi: 10.1128/AAC.45.12.3310-3321.2001

Cordeiro, R. A., Brilhante, R. S. N., Rocha, M. F. G., Fechine, M. A. B., Costa, A. K. F., Camargo, Z. P., et al. (2006). In vitro activities of caspofungin, amphotericin B and azoles against *Coccidioides posadasii* strains from northeast, Brazil. *Mycopathologia* 161, 21–26. doi: 10.1007/s11046-005-0177-0

Davis, M. R., Donnelley, M. A., and Thompson, G. R. (2019). Ibrexafungerp: a novel oral glucan synthase inhibitor. *Med. Mycol.* pii: myz083. doi: 10.1093/mmy/myz083

Denning, D. W. (2003). Echinocandin antifungal drugs. *Lancet* 362, 1142–1151. doi: 10.1016/S0140-6736(03)14472-8

Ene, I. V., Adya, A. K., Wehmeier, S., Brand, A. C., MacCallum, D. M., Gow, N. A. R., et al. (2012). Host carbon sources modulate cell wall architecture, drug resistance and virulence in a fungal pathogen. *Cell. Microbiol.* 14, 1319–1335. doi: 10.1111/j.1462-5822.2012.01813.x

Espinel-Ingroff, A. (2003). In vitro antifungal activities of anidulafungin and micafungin, licensed agents and the investigational triazole posaconazole as determined by NCCLS methods for 12,052 fungal isolates: review of the literature. *Rev. Iberoam. Micol.* 20, 121–136.

Forastiero, A., Mesa-Arango, A. C., Alastruey-Izquierdo, A., Alcazar-Fuoli, L., Bernal-Martinez, L., Pelaez, T., et al. (2013). *Candida tropicalis* antifungal cross-resistance is related to different azole target (Erg11p) modifications. *Antimicrob. Agents Chemother.* 57, 4769–4781. doi: 10.1128/AAC.00477-13

Fortwendel, J. R., Juvvadi, P. R., Pinchai, N., Perfect, B. Z., Alspaugh, J. A., Perfect, J. R., et al. (2009). Differential effects of inhibiting chitin and 1,3-{beta}-D-glucan synthesis in ras and calcineurin mutants of *Aspergillus fumigatus*. *Antimicrob. Agents Chemother.* 53, 476–482. doi: 10.1128/AAC.01154-08

Ghannoum, M., Long, L., Larkin, E. L., Isham, N., Sherif, R., Borroto-Esoda, K., et al. (2018). Evaluation of the antifungal activity of the novel Oral Glucan synthase inhibitor SCY-078, singly and in combination, for the treatment of invasive aspergillosis. *Antimicrob. Agents Chemother.* 62, e00244–e00218. doi: 10.1128/AAC.00244-18.

Goldberg, J., Connolly, P., Schnizlein-Bick, C., Durkin, M., Kohler, S., Smedema, M., et al. (2000). Comparison of Nikkomycin Z with amphotericin B and itraconazole for treatment of histoplasmosis in a murine model. *Antimicrob. Agents Chemother.* 44, 1624–1629. doi: 10.1128/AAC.44.6.1624-1629.2000

Gow, N. A. R., Latge, J.-P., and Munro, C. A. (2017). The fungal cell wall: structure, biosynthesis, and function. *Microbiol. Spectrum* 5. doi: 10.1128/microbiolspec.FUNK-0035-2016

Hadrich, I., Makni, F., Neji, S., Cheikhrouhou, F., Bellaaj, H., Elloumi, M., et al. (2012). Amphotericin B in vitro resistance is associated with fatal *Aspergillus flavus* infection. *Med. Mycol.* 50, 829–834. doi: 10.3109/13693786.2012.684154

Hage, C. A., Connolly, P., Horan, D., Durkin, M., Smedema, M., Zarnowski, R., et al. (2011). Investigation of the efficacy of micafungin in the treatment of histoplasmosis using two north American strains of *Histoplasma capsulatum*. *Antimicrob. Agents Chemother.* 55, 4447–4450. doi: 10.1128/AAC.01681-10

Hager, C. L., Larkin, E. L., Long, L. A., and Ghannoum, M. A. (2018a). Evaluation of the efficacy of rezafungin, a novel echinocandin, in the treatment of disseminated Candida auris infection using an immunocompromised mouse model. *J. Antimicrob. Chemother.* 73, 2085–2088. doi: 10.1093/jac/dky153

Hager, C. L., Larkin, E. L., Long, L., Zohra Abidi, F., Shaw, K. J., and Ghannoum, M. A. (2018b). In vitro and in vivo evaluation of the antifungal activity of APX001A/APX001 against Candida auris. *Antimicrob. Agents Chemother.* 62, pii: e02319-17. doi: 10.1128/AAC.02319-17

Hasim, S., and Coleman, J. J. (2019). Targeting the fungal cell wall: current therapies and implications for development of alternative antifungal agents. *Future Med. Chem.* 11, 869–883. doi: 10.4155/fmc-2018-0465

Hata, K., Horii, T., Miyazaki, M., Watanabe, N.-A., Okubo, M., Sonoda, J., et al. (2011). Efficacy of oral E1210, a new broad-spectrum antifungal with a novel mechanism of action, in murine models of candidiasis, aspergillosis, and fusariosis. *Antimicrob. Agents Chemother.* 55, 4543–4551. doi: 10.1128/AAC.00366-11

Hector, R. F. (1993). Compounds active against cell walls of medically important fungi. *Clin. Microbiol. Rev.* 6, 1–21. doi: 10.1128/CMR.6.1.1

Hector, R. F., Zimmer, B. L., and Pappagianis, D. (1990). Evaluation of nikkomycins X and Z in murine models of coccidioidomycosis, histoplasmosis, and blastomycosis. *Antimicrob. Agents Chemother.* 34, 587–593. doi: 10.1128/AAC.34.4.587

Hobson, R. P., Munro, C. A., Bates, S., MacCallum, D. M., Cutler, J. E., Heinsbroek, S. E. M., et al. (2004). Loss of cell wall mannosylphosphate in *Candida albicans* does not influence macrophage recognition. *J. Biol. Chem.* 279, 39628–39635. doi: 10.1074/jbc.M405003200

Ikezawa, H. (2002). Glycosylphosphatidylinositol (GPI)-anchored proteins. *Biol. Pharm. Bull.* 25, 409–417. doi: 10.1248/bpb.25.409

Jiménez-Ortigosa, C., Perez, W. B., Angulo, D., Borroto-Esoda, K., and Perlin, D. S. (2017). De novo Acquisition of Resistance to SCY-078 in *Candida glabrata* involves FKS mutations that both overlap and are distinct from those conferring echinocandin resistance. *Antimicrob. Agents Chemother.* 61, e00833–e00817. doi: 10.1128/AAC.00833-17

Johnson, M. D., and Perfect, J. R. (2003). Caspofungin: first approved agent in a new class of antifungals. *Expert. Opin. Pharmacother.* 4, 807–823. doi: 10.1517/14656566.4.5.807

Kofla, G., and Ruhnke, M. (2011). Pharmacology and metabolism of anidulafungin, caspofungin and micafungin in the treatment of invasive candidosis - review of the literature. *Eur. J. Med. Res.* 16, 159–166. doi: 10.1186/2047-783X-16-4-159

Koss, T., Bagheri, B., Zeana, C., Romagnoli, M. F., and Grossman, M. E. (2002). Amphotericin B-resistant *Aspergillus flavus* infection successfully treated with caspofungin, a novel antifungal agent. *J. Am. Acad. Dermatol.* 46, 945–947. doi: 10.1067/mjd.2002.120627

Lagorce, A., Hauser, N. C., Labourdette, D., Rodriguez, C., Martin-Yken, H., Arroyo, J., et al. (2003). Genome-wide analysis of the response to cell wall mutations in the yeast *Saccharomyces cerevisiae*. *J. Biol. Chem.* 278, 20345–20357. doi: 10.1074/jbc.M211604200

Lamoth, F., and Alexander, B. D. (2015). Antifungal activities of SCY-078 (MK-3118) and standard antifungal agents against clinical non-Aspergillus mold isolates. *Antimicrob. Agents Chemother.* 59, 4308–4311. doi: 10.1128/AAC.00234-15

Lamoth, F., Juvvadi, P. R., Gehrke, C., Asfaw, Y. G., and Steinbach, W. J. (2014). Transcriptional activation of heat shock protein 90 mediated via a proximal promoter region as trigger of caspofungin resistance in *Aspergillus fumigatus*. *J. Infect. Dis.* 209, 473–481. doi: 10.1093/infdis/jit530

Larkin, E., Hager, C., Chandra, J., Mukherjee, P. K., Retuerto, M., Salem, I., et al. (2017). The emerging pathogen Candida auris: growth phenotype, virulence factors, activity of antifungals, and effect of SCY-078, a novel glucan synthesis inhibitor, on growth morphology and biofilm formation. *Antimicrob. Agents Chemother.* 61, pii: e02396-16. doi: 10.1128/AAC.02396-16

Latgé, J.-P. (2007). The cell wall: a carbohydrate Armour for the fungal cell. *Mol. Microbiol.* 66, 279–290. doi: 10.1111/j.1365-2958.2007.05872.x

Lepak, A. J., Marchillo, K., and Andes, D. R. (2015). Pharmacodynamic target evaluation of a novel oral glucan synthase inhibitor, SCY-078 (MK-3118), using an in vivo murine invasive candidiasis model. *Antimicrob. Agents Chemother.* 59, 1265–1272. doi: 10.1128/AAC.04445-14

Lepak, A. J., Zhao, M., VanScoy, B., Ambrose, P. G., and Andes, D. R. (2018). Pharmacodynamics of a long-acting echinocandin, CD101, in a Neutropenic invasive-candidiasis murine model using an extended-interval dosing design. *Antimicrob. Agents Chemother.* 62, pii: e01572-18. doi: 10.1128/AAC.01572-18

Li, R. K., and Rinaldi, M. G. (1999). In vitro antifungal activity of nikkomycin Z in combination with fluconazole or itraconazole. *Antimicrob. Agents Chemother.* 43, 1401–1405. doi: 10.1128/AAC.43.6.1401

Marcos-Zambrano, L. J., Escribano, P., Sánchez-Carrillo, C., Bouza, E., and Guinea, J. (2017a). Frequency of the paradoxical effect measured using the EUCAST procedure with Micafungin, Anidulafungin, and Caspofungin against Candida species isolates causing Candidemia. *Antimicrob. Agents Chemother.* 61, pii: e01584-16. doi: 10.1128/AAC.01584-16

Marcos-Zambrano, L. J., Gómez-Perosanz, M., Escribano, P., Bouza, E., and Guinea, J. (2017b). The novel oral glucan synthase inhibitor SCY-078 shows in vitro activity against sessile and planktonic Candida spp. *J. Antimicrob. Chemother.* 72, 1969–1976. doi: 10.1093/jac/dkx010

Mazur, P., and Baginsky, W. (1996). In vitro activity of 1,3-β-D-Glucan synthase requires the GTP-binding protein Rho1. *J. Biol. Chem.* 271, 14604–14609. doi: 10.1074/jbc.271.24.14604

McLellan, C. A., Whitesell, L., King, O. D., Lancaster, A. K., Mazitschek, R., and Lindquist, S. (2012). Inhibiting GPI anchor biosynthesis in fungi stresses the endoplasmic reticulum and enhances immunogenicity. *ACS Chem. Biol.* 7, 1520–1528. doi: 10.1021/cb300235m

Mesa-Arango, A. C., Rueda, C., Román, E., Quintin, J., Terrón, M. C., Luque, D., et al. (2016). Cell Wall changes in amphotericin B-resistant strains from Candida tropicalis and relationship with the immune responses elicited by the host. *Antimicrob. Agents Chemother.* 60, 2326–2335. doi: 10.1128/AAC.02681-15

Mesa-Arango, A. C., Trevijano-Contador, N., Román, E., Sánchez-Fresneda, R., Casas, C., Herrero, E., et al. (2014). The production of reactive oxygen species is a universal action mechanism of amphotericin B against pathogenic yeasts and contributes to the fungicidal effect of this drug. *Antimicrob. Agents Chemother.* 58, 6627–6638. doi: 10.1128/AAC.03570-14

Miyazaki, M., Horii, T., Hata, K., Watanabe, N.-A., Nakamoto, K., Tanaka, K., et al. (2011). In vitro activity of E1210, a novel antifungal, against clinically important yeasts and molds. *Antimicrob. Agents Chemother.* 55, 4652–4658. doi: 10.1128/AAC.00291-11

Mora-Duarte, J., Betts, R., Rotstein, C., Colombo, A. L., Thompson-Moya, L., Smietana, J., et al. (2002). Comparison of caspofungin and amphotericin B for invasive candidiasis. *N. Engl. J. Med.* 347, 2020–2029. doi: 10.1056/NEJMoa021585

Munro, C. A. (2013). Chitin and glucan, the yin and yang of the fungal cell wall, implications for antifungal drug discovery and therapy. *Adv. Appl. Microbiol.* 83, 145–172. doi: 10.1016/B978-0-12-407678-5.00004-0

Mutz, M., and Roemer, T. (2016). The GPI anchor pathway: a promising antifungal target? *Future Med. Chem.* 8, 1387–1391. doi: 10.4155/fmc-2016-0110

Nakai, T., Uno, J., Ikeda, F., Tawara, S., Nishimura, K., and Miyaji, M. (2003). In vitro antifungal activity of Micafungin (FK463) against dimorphic fungi: comparison of yeast-like and mycelial forms. *Antimicrob. Agents Chemother.* 47, 1376–1381. doi: 10.1128/AAC.47.4.1376-1381.2003

Nett, J., Lincoln, L., Marchillo, K., Massey, R., Holoyda, K., Hoff, B., et al. (2007). Putative role of beta-1,3 glucans in *Candida albicans* biofilm resistance. *Antimicrob. Agents Chemother.* 51, 510–520. doi: 10.1128/AAC.01056-06

Nyfeler, R., and Keller-Schierlein, W. (1974). Metabolites of microorganisms. 143. Echinocandin B, a novel polypeptide-antibiotic from *Aspergillus nidulans* var. echinulatus: isolation and structural components. *Helv. Chim. Acta* 57, 2459–2477. doi: 10.1002/hlca.19740570818

O'Meara, T. R., Robbins, N., and Cowen, L. E. (2017). The Hsp90 chaperone network modulates Candida virulence traits. *Trends Microbiol.* 25, 809–819. doi: 10.1016/j.tim.2017.05.003

Pappas, P. G., Kauffman, C. A., Andes, D. R., Clancy, C. J., Marr, K. A., Ostrosky-Zeichner, L., et al. (2016). Clinical practice guideline for the management of Candidiasis: 2016 update by the infectious diseases society of America. *Clin. Infect. Dis.* 62, e1–e50. doi: 10.1093/cid/civ933

Patil, A., and Majumdar, S. (2017). Echinocandins in antifungal pharmacotherapy. *J. Pharm. Pharmacol.* 69, 1635–1660. doi: 10.1111/jphp.12780

Perlin, D. S. (2015). Echinocandin resistance in Candida. *Clin. Infect. Dis.* 61(Suppl 6), S612–S617. doi: 10.1093/cid/civ791

Pfaller, M. A., Huband, M. D., Flamm, R. K., Bien, P. A., and Castanheira, M. (2019). *In vitro* activity of APX001A (Manogepix) and comparator agents against 1,706 fungal isolates collected during an international surveillance program (2017). *Antimicrob. Agents Chemother.* 63, pii: e00840-19. doi: 10.1128/AAC.00840-19

Pfaller, M. A., Messer, S. A., Motyl, M. R., Jones, R. N., and Castanheira, M. (2013). In vitro activity of a new oral glucan synthase inhibitor (MK-3118) tested against *Aspergillus* spp. by CLSI and EUCAST broth microdilution methods. *Antimicrob. Agents Chemother.* 57, 1065–1068. doi: 10.1128/AAC.01588-12

Pfaller, M. A., Messer, S. A., Rhomberg, P. R., Borroto-Esoda, K., and Castanheira, M. (2017). Differential activity of the oral glucan synthase inhibitor SCY-078 against wild-type and echinocandin-resistant strains of Candida species. *Antimicrob. Agents Chemother.* 61, e00161–e00117. doi: 10.1128/AAC.00161-17

Qadota, H., Python, C. P., Inoue, S. B., Arisawa, M., Anraku, Y., Zheng, Y., et al. (1996). Identification of yeast Rho1p GTPase as a regulatory subunit of 1,3-β-Glucan synthase. *Science* 272, 279–281. doi: 10.1126/science.272.5259.279

Roy, R. M., and Klein, B. S. (2012). Dendritic cells in anti-fungal immunity and vaccine design. *Cell Host Microbe* 11, 436–446. doi: 10.1016/j.chom.2012.04.005

Rueda, C., Cuenca-Estrella, M., and Zaragoza, O. (2014). Paradoxical growth of *Candida albicans* in the presence of caspofungin is associated with multiple cell wall rearrangements and decreased virulence. *Antimicrob. Agents Chemother.* 58, 1071–1083. doi: 10.1128/AAC.00946-13

Rüping, M. J., Vehreschild, J. J., Farowski, F., and Cornely, O. A. (2008). Anidulafungin: advantage for the newcomer? *Expert. Rev. Clin. Pharmacol.* 1, 207–216. doi: 10.1586/17512433.1.2.207

Sandison, T., Ong, V., Lee, J., and Thye, D. (2017). Safety and pharmacokinetics of CD101 IV, a novel echinocandin, in healthy adults. *Antimicrob. Agents Chemother.* 61, e01627–e01616. doi: 10.1128/AAC.01627-16

Satish, S., Jiménez-Ortigosa, C., Zhao, Y., Lee, M. H., Dolgov, E., Krüger, T., et al. (2019). Stress-induced changes in the lipid microenvironment of β-(1,3)-D-glucan synthase cause clinically important echinocandin resistance in *Aspergillus fumigatus*. *mBio* 10:e00779-19. doi: 10.1128/mBio.00779-19

Schimoler-O'Rourke, R., Renault, S., Mo, W., and Selitrennikoff, C. P. (2003). Neurospora crassa FKS protein binds to the (1,3)beta-glucan synthase substrate, UDP-glucose. *Curr. Microbiol.* 46, 408–412. doi: 10.1007/s00284-002-3884-5

Scorneaux, B., Angulo, D., Borroto-Esoda, K., Ghannoum, M., Peel, M., and Wring, S. (2017). SCY-078 is fungicidal against Candida species in time-kill studies. *Antimicrob. Agents Chemother.* 61, pii: e01961-16. doi: 10.1128/AAC.01961-16

Seo, K., Akiyoshi, H., and Ohnishi, Y. (1999). Alteration of cell wall composition leads to amphotericin B resistance in *Aspergillus flavus*. *Microbiol. Immunol.* 43, 1017–1025. doi: 10.1111/j.1348-0421.1999.tb01231.x

Shaw, K. J., Schell, W. A., Covel, J., Duboc, G., Giamberardino, C., Kapoor, M., et al. (2018). In vitroandin vivoevaluation of APX001A/APX001 and otherGwt1 inhibitors against Cryptococcus. *Antimicrob. Agents Chemother.* 62:e00523-18. doi: 10.1128/AAC.00523-18

Shibata, N., Ikuta, K., Imai, T., Satoh, Y., Satoh, R., Suzuki, A., et al. (1995). Existence of branched side chains in the cell wall mannan of pathogenic yeast, *Candida albicans*. Structure-antigenicity relationship between the cell wall mannans of Candida albicans and *Candida parapsilosis*. *J. Biol. Chem.* 270, 1113–1122. doi: 10.1074/jbc.270.3.1113

Singh, S. D., Robbins, N., Zaas, A. K., Schell, W. A., Perfect, J. R., and Cowen, L. E. (2009). Hsp90 governs echinocandin resistance in the pathogenic yeast *Candida albicans* via Calcineurin. *PLoS Pathog.* 5:e1000532. doi: 10.1371/journal.ppat.1000532

Singh-Babak, S. D., Babak, T., Diezmann, S., Hill, J. A., Xie, J. L., Chen, Y.-L., et al. (2012). Global analysis of the evolution and mechanism of echinocandin resistance in *Candida glabrata*. *PLoS Pathog.* 8:e1002718. doi: 10.1371/journal.ppat.1002718

Sofjan, A. K., Mitchell, A., Shah, D. N., Nguyen, T., Sim, M., Trojcak, A., et al. (2018). Rezafungin (CD101), a next-generation echinocandin: a systematic literature review and assessment of possible place in therapy. *J. Glob. Antimicrob. Resist.* 14, 58–64. doi: 10.1016/j.jgar.2018.02.013

Stevens, D. A. (2000). Drug interaction studies of a Glucan synthase inhibitor (LY 303366) and a chitin synthase inhibitor (Nikkomycin Z) for inhibition and killing of fungal pathogens. *Antimicrob. Agents Chemother.* 44, 2547–2548. doi: 10.1128/AAC.44.9.2547-2548.2000

Thompson, G. R., Barker, B. M., and Wiederhold, N. P. (2017). Large-scale evaluation of in vitro amphotericin B, Triazole, and echinocandin activity against Coccidioides species from US. Institutions. *Antimicrob. Agents Chemother.* 61, e02634–e02616. doi: 10.1128/AAC.02634-16

Tsukahara, K., Hata, K., Nakamoto, K., Sagane, K., Watanabe, N.-A., Kuromitsu, J., et al. (2003). Medicinal genetics approach towards identifying the molecular target of a novel inhibitor of fungal cell wall assembly. *Mol. Microbiol.* 48, 1029–1042. doi: 10.1046/j.1365-2958.2003.03481.x

Viriyakosol, S., Kapoor, M., Okamoto, S., Covel, J., Soltow, Q. A., Trzoss, M., et al. (2019). APX001 and other Gwt1 inhibitor Prodrugs are effective in

experimental *Coccidioides immitis* pneumonia. *Antimicrob. Agents Chemother.* 63, pii: e01715-18. doi: 10.1128/AAC.01715-18

Walker, L. A., Gow, N. A. R., and Munro, C. A. (2010). Fungal echinocandin resistance. *Fungal Genet. Biol.* 47, 117–126. doi: 10.1016/j.fgb.2009.09.003

Walker, L. A., Gow, N. A. R., and Munro, C. A. (2013). Elevated chitin content reduces the susceptibility of Candida species to caspofungin. *Antimicrob. Agents Chemother.* 57, 146–154. doi: 10.1128/AAC.01486-12

Walker, L. A., Munro, C. A., de Bruijn, I., Lenardon, M. D., McKinnon, A., and Gow, N. A. R. (2008). Stimulation of chitin synthesis rescues *Candida albicans* from echinocandins. *PLoS Pathog.* 4:e1000040. doi: 10.1371/journal.ppat.1000040

Walker, S. S., Xu, Y., Triantafyllou, I., Waldman, M. F., Mendrick, C., Brown, N., et al. (2011). Discovery of a novel class of orally active antifungal β-1,3-d-Glucan synthase inhibitors. *Antimicrob. Agents Chemother.* 55, 5099–5106. doi: 10.1128/AAC.00432-11

Watanabe, N.-A., Miyazaki, M., Horii, T., Sagane, K., Tsukahara, K., and Hata, K. (2012). E1210, a new broad-spectrum antifungal, suppresses *Candida albicans* hyphal growth through inhibition of glycosylphosphatidylinositol biosynthesis. *Antimicrob. Agents Chemother.* 56, 960–971. doi: 10.1128/AAC.00731-11

Wiederhold, N. P., and Lewis, R. E. (2003). The echinocandin antifungals: an overview of the pharmacology, spectrum and clinical efficacy. *Expert Opin. Investig. Drugs* 12, 1313–1333. doi: 10.1517/13543784.12.8.1313

Wiederhold, N. P., Locke, J. B., Daruwala, P., and Bartizal, K. (2018). Rezafungin (CD101) demonstrates potent in vitro activity against *Aspergillus*, including azole-resistant *Aspergillus fumigatus* isolates and cryptic species. *J. Antimicrob. Chemother.* 73, 3063–3067. doi: 10.1093/jac/dky280

Wiederhold, N. P., Najvar, L. K., Shaw, K. J., Jaramillo, R., Patterson, H., Olivo, M., et al. (2019). Efficacy of delayed therapy with Fosmanogepix (APX001) in a murine model of Candida auris invasive candidiasis. *Antimicrob. Agents Chemother.* 63:e01120-19. doi: 10.1128/AAC.01120-19

Wring, S. A., Randolph, R., Park, S., Abruzzo, G., Chen, Q., Flattery, A., et al. (2017). Preclinical pharmacokinetics and Pharmacodynamic target of SCY-078, a first-in-class orally active antifungal Glucan synthesis inhibitor, in murine models of disseminated candidiasis. *Antimicrob. Agents Chemother.* 61:e02068-16. doi: 10.1128/AAC.02068-16

Yadav, U., and Khan, M. A. (2018). Targeting the GPI biosynthetic pathway. *Pathog. Global Health* 112, 115–122. doi: 10.1080/20477724.2018.1442764

Yang, F., Zhang, L., Wakabayashi, H., Myers, J., Jiang, Y., Cao, Y., et al. (2017). Tolerance to Caspofungin in *Candida albicans* is associated with at least three distinctive mechanisms that govern expression of FKS genes and Cell Wall remodeling. *Antimicrob. Agents Chemother.* 61, e00071–e00017. doi: 10.1128/AAC.00071-17

Zhao, Y., Lee, M. H., Paderu, P., Lee, A., Jimenez-Ortigosa, C., Park, S., et al. (2018). Significantly improved pharmacokinetics enhances in vivo efficacy of APX001 against echinocandin- and multidrug-resistant Candida isolates in a mouse model of invasive candidiasis. *Antimicrob. Agents Chemother.* 62, pii: e00425-18. doi: 10.1128/AAC.00425-18

Conflict of Interest: The authors declare that the research was conducted in the absence of any commercial or financial relationships that could be construed as a potential conflict of interest.

frontiers in Microbiology

REVIEW
published: 09 January 2020
doi: 10.3389/fmicb.2019.02993

The Fungal Cell Wall: *Candida*, *Cryptococcus*, and *Aspergillus* Species

Rocio Garcia-Rubio[1†], Haroldo C. de Oliveira[2†], Johanna Rivera[3] and Nuria Trevijano-Contador[3]*

[1] Center for Discovery and Innovation, Hackensack Meridian Health, Nutley, NJ, United States, [2] Instituto Carlos Chagas, Fundação Oswaldo Cruz (Fiocruz), Curitiba, Brazil, [3] Division of Infectious Diseases, Department of Medicine, Albert Einstein College of Medicine, New York, NY, United States

The fungal cell wall is located outside the plasma membrane and is the cell compartment that mediates all the relationships of the cell with the environment. It protects the contents of the cell, gives rigidity and defines the cellular structure. The cell wall is a skeleton with high plasticity that protects the cell from different stresses, among which osmotic changes stand out. The cell wall allows interaction with the external environment since some of its proteins are adhesins and receptors. Since, some components have a high immunogenic capacity, certain wall components can drive the host's immune response to promote fungus growth and dissemination. The cell wall is a characteristic structure of fungi and is composed mainly of glucans, chitin and glycoproteins. As the components of the fungal cell wall are not present in humans, this structure is an excellent target for antifungal therapy. In this article, we review recent data on the composition and synthesis, influence of the components of the cell wall in fungi-host interaction and the role as a target for the next generation of antifungal drugs in yeasts (*Candida* and *Cryptococcus*) and filamentous fungi (*Aspergillus*).

Keywords: cell wall, *Candida*, *Cryptococcus*, *Aspergillus*, synthesis, composition

OPEN ACCESS

Edited by:
Gustavo Alexis Niño-Vega, University of Guanajuato, Mexico

Reviewed by:
Teresa Gonçalves, University of Coimbra, Portugal
Rebecca Anne Hall, University of Birmingham, United Kingdom

***Correspondence:**
Nuria Trevijano-Contador
ntrevijanocontador@gmail.com

† These authors have contributed equally to this work

Specialty section:
This article was submitted to Fungi and Their Interactions, a section of the journal Frontiers in Microbiology

Received: *16 August 2019*
Accepted: *10 December 2019*
Published: *09 January 2020*

Citation:
Garcia-Rubio R, de Oliveira HC, Rivera J and Trevijano-Contador N (2020) The Fungal Cell Wall: Candida, Cryptococcus, and Aspergillus Species. Front. Microbiol. 10:2993. doi: 10.3389/fmicb.2019.02993

INTRODUCTION

The fungal cell wall is an essential structure with great plasticity that is vital to maintaining cellular integrity and viability. The cell wall plays an important role in different biological functions such as controlling cellular permeability and protecting the cell from osmotic and mechanical stress (Ponton, 2008; Gow et al., 2017; Agustinho et al., 2018). In addition to these important functions, the cell wall mediates interactions with the external environment through adhesins and a large number of receptors that, after their activation, will trigger a complex cascade of signals inside the cell (Ponton, 2008). The cell wall is uniquely composed of polysaccharides and proteins as well as lipids and pigments (Gow et al., 2017). Furthermore, some wall components are very immunogenic and stimulate cellular and humoral responses during infection (Erwig and Gow, 2016). β-glucans and mannans, as well as antibodies directed against them, are very useful diagnostic tools since they can be detected in patients with invasive fungal infection (Pazos et al., 2006). As mentioned above, the cell wall represents an indispensable structure, that its disruption can have serious effects on cell growth and morphology resulting in cell death. Hence, it is considered a good antifungal target (Heitman, 2005; Cortes et al., 2019).

The cell wall is a specific and complex cellular organelle composed of glucans, chitin, chitosan, and glycosylated proteins. Proteins are generally associated with polysaccharides resulting in glycoproteins. Together, these components contribute to the cell wall rigidity. The synthesis and maintenance of cell wall involves a large number of biosynthetic and signaling pathways (Casadevall and Perfect, 1998).

In the following sections, the different components of the fungal cell wall will be reviewed generally and then, specifically focused on three fungi species, *Candida albicans*, *Cryptococcus neoformans*, and *Aspergillus fumigatus*. The characteristics of their components, their relationship with virulence, pathogenicity, and the interaction with the host's immune system are reviewed. We also mention different works in which different components of the cell wall are possible targets for antifungal therapies. Recently, it has been proposed that the cell wall is particularly important in biotechnology to develop new antifungal drugs as well as inhibitors of certain cell wall components that are being tested in clinical trials. For a review on this topic, see reference (Cortes et al., 2019). The fungal cell wall is an extensive and complex topic and we highlight critical literature, but it is not possible to cite every study.

CELL WALL STRUCTURE

The cell wall is structured in different layers where the innermost layer is a more conserved structure on which the remaining layers are deposited and can vary between different species of fungi. The composition and organization of fungal cell walls are compared and contrasted in the text below.

Glucans

Glucan is the most important structural polysaccharide of the fungal cell wall and represents 50–60% of the dry weight of this structure. Most polymers of glucan are composed of 1,3 linkage glucose units (65–90%), although there are also glucans with β-1,6 (in *Candida* but not in *Aspergillus*), β-1,4, α-1,3 and α-1,4 links. The β-1,3-D-glucan is the most important structural component of the wall, to which other components of this structure are covalently linked. The β-1,3-D-glucan is synthesized by a complex of enzymes located in the plasma membrane called glucan synthases. The genes encoding β-1,3-D-glucans, *FKS1* and *FKS2*, were initially identified in *Saccharomyces cerevisiae* (Douglas et al., 1994; Qadota et al., 1996; Ponton, 2008). Analogs of these genes are currently known in several species of *Candida*, *Aspergillus*, *Cryptococcus*, and *Pneumocystis* among other fungi. Disruption of one of these genes affects cell growth (Douglas et al., 1994; Mazur et al., 1995) but elimination of both causes cell death (Mazur et al., 1995; Bowman and Free, 2006). The α-1,3-glucan is also a fundamental component of the fungal cell wall and is synthetized by α-glucan synthase (*AGS1*).

Chitin

The chitin content of the fungal wall varies according to the morphological phase of the fungus. It represents 1–2% of the dry weight of yeast cell wall while in filamentous fungi, it can reach up to 10–20%. Chitin is synthesized from n-acetylglucosamine by the enzyme chitin synthase, which deposits chitin polymers in the extracellular space next to the cytoplasmic membrane. The of chitin content in the *C. albicans* hyphae wall is three times higher than that of yeasts (Chattaway et al., 1968) while the chitin content of the mycelial phases of *Paracoccidioides brasiliensis* and *Blastomyces dermatitidis* is 25–30% of that yeast phase (Kanetsuna et al., 1969).

Glycoproteins

Proteins compose 30–50% of the dry weight of fungal wall in yeast and 20–30% of the dry weight of the wall of the filamentous fungi. Most proteins are associated to carbohydrates by O or N linkages resulting in glycoproteins. Cell wall proteins have different functions including participation in the maintenance of the cellular shape, adhesion processes, cellular protection against different substances, absorption of molecules, signal transmission, and synthesis and reorganization of wall components (Bowman and Free, 2006; Ponton, 2008).

Melanin

Melanin is a pigment of high molecular weight that is negatively charged, hydrophobic and insoluble in aqueous solutions and protects fungi against stressors facilitating survival in the host (Liu et al., 1999; Casadevall et al., 2000; Nosanchuk and Casadevall, 2006; Nosanchuk et al., 2015). The fungi produce melanin by two routes, from 1, 8-dihydroxynaphthalene (DHN) intermediate and from L-3, 4-dihydroxyphenylalanine (L-dopa) (Eisenman and Casadevall, 2012). Melanin production contributes to fungal virulence (Salas et al., 1996; Noverr et al., 2004; Silva et al., 2009), improves resistance to environmental damage such as extreme temperature, UV light and toxins (Rosa et al., 2010; Zalar et al., 2011; Eisenman and Casadevall, 2012), and is important for invasion and dissemination. For example, *C. neoformans* melanin has been linked with dissemination of yeast cells from the lungs to other organs (Noverr et al., 2004), is known to influence the immune response of the host (Eisenman and Casadevall, 2012) and inhibit phagocytosis (Wang et al., 1995). In *Aspergillus*, melanin inhibits macrophage apoptosis that have phagocytosed melanized conidia (Volling et al., 2011).

Candida albicans

Candida species are part of the mucous flora and can cause a broad spectrum of human infections. This genus includes at least 30 species of clinical importance (Pfuller et al., 2011; Silva et al., 2012). During the last decades, the incidence of infections caused by *Candida* genus has increased significantly (Sobel, 2007; Pfuller et al., 2011). *C. albicans* is the species that is most frequently isolated in cases of candidiasis (45–50%) (Del Palacio et al., 2009).

Composition and Biosynthesis

Candida albicans is the most common opportunistic pathogen and cause of invasive fungal infection in hospitalized patients (Sobel, 2007; Pfuller et al., 2011). It is a highly adaptable fungal

species with a large repertoire of virulence factors that allows its transition from commensal organism to pathogen. Thus, one of the key virulence characteristics is its ability to switch morphologies between yeast cells, pseudohyphae, and hyphae (Tsui et al., 2016). The main difference between the yeast and the hyphal form is that the hyphal wall has a slightly higher chitin content than the yeast form (Braun and Calderone, 1978). In addition, the structure of cell wall mannans differs between morphotypes, with a significant decrease in phosphodiesterified acid-labile β-1,2-linked manno-oligosaccharides in the hyphal form, whereas the amount of acid-stable β-1,2 linkage-containing side chains remains the same (Shibata et al., 2007).

Candida albicans cell wall is a two-layered structure. The main core of the cell wall is composed of a β-glucan-chitin skeleton, which is responsible for the strength and shape of the cell wall (see **Figure 1**). Chitin is located in the inner layer of the cell wall (Gow and Hube, 2012) and its chains can form tight antiparallel hydrogen-bonded structures associated with high insolubility (Chaffin, 2008). In *C. albicans*, there is one *CHS* family composed of four genes. It has been described that *CHS1* from class II is an essential chitin synthase and is involved in septum formation, viability, cell shape and integrity (Munro et al., 2001).

As in other fungi, the most abundant molecules in *C. albicans* are β-1,3-glucans. They are in the inner cell wall linked to β-1,6-glucans, which connect the inner and outer cell wall (Brown and Gordon, 2005). β-1,3-glucan synthases are responsible for the synthesis of β-1,3-glucans and consist of an enzyme complex with at least two subunits, Fksp and Rho1p. In *C. albicans*, Fksp is encoded by three ortholog genes, *FKS1*, *FKS2*, and *FKS3*, which catalyzes the transfer of sugar moieties from activated donor molecules to specific acceptor molecules forming glycosidic bonds (Sawistowska-Schroder et al., 1984).

β-1,6-glucans are side chains of variable lengths and distributions that can form complex structures stabilized by interchain hydrogen bonds. They act as a linker molecules binding different cell wall proteins to the β-1,3-glucan-chitin core through glycosylphospatidyl inositol (GPI) proteins (Klis et al., 2001). β-1,6-glucan synthase has not been identified in any fungal species, however, several genes that affect the synthesis of this compound have been described in *S. cerevisiae* (Lesage and Bussey, 2006). Interestingly, *C. albicans* cell wall contains considerably more β-1,6-glucan compared to *S. cerevisiae* due to either an increase in the number of molecules or an increase in glucose residues, or both (Brown and Gordon, 2005). Unlike *Aspergillus* or *Cryptococcus* spp., α-(Ponton, 2008; Gow et al., 2017)-glucan is absent from *Candida* spp. cell wall (Yoshimi et al., 2017).

The outer layer of *C. albicans* cell wall is packed with mannoproteins that are glycosylphosphatidylinositol (GPI)-modified and cross-linked to β-1,6-glucans (Shibata et al., 2007). N-linked mannans are composed of α-1,6-mannose backbone with α-1,2-oligomannose sidechains capped with β-1,2- mono-, di-, tri-, or tetra mannans (Shibata et al., 2007). O-linked mannans are found associated with cell wall glycoproteins. Some protein mannosyltransferases are responsible for the first steps in the O-linked mannans biosynthesis, adding a mannose residue to a serine or threonine residue. Additional mannoses are added by α-1,2-mannosyltransferases which results in a short α-1,2-mannose chain. The last step consists of the addition of an α-1,3-mannoses by α-1,3-mannosyltransferases (Free, 2013).

Mannans are less rigid compared to β-glucans and chitin, so they do not influence the cell shape. However, they have low permeability and porosity which affect the resistance of the cell wall to antifungal drugs and host defense mechanisms (Gow and Hube, 2012). Furthermore, since the outer mannan layer covers the inner layers of the cell wall, it has been described to be important in immune evasion concealing β-glucans from host immune detection (Hernandez-Chavez et al., 2017). Mannans are considered pathogen associated molecular pattern (PAMP) ligands and many host receptors are known to participate in its recognition (Brown et al., 2002; Rubin-Bejerano et al., 2007). *Candida glabrata* contain mannans with a structure closely resembling *S. cerevisiae* mannans since it is genetically more closely related to this species (Kobayashi et al., 1998). In addition, *C. glabrata* cell wall has 50% more protein and a higher mannose/glucose ratio than *S. cerevisiae* walls (de Groot et al., 2008; Lima-Neto et al., 2011).

Influence of *Candida* Cell Wall Components on Fungi-Host Interaction

Fungi cell wall plays an essential role in the interaction with host cells and tissues. The components of the cell wall are of great importance in protecting the fungi, shifting the host immune response in favor of fungal growth allowing dissemination in the host (Poulain and Jouault, 2004; Galan-Diéz et al., 2010; Sem et al., 2016). β-glucan is easily recognized by the host immune system producing an effective response against the infection and thereby, protecting the host. Hence, masking of β-glucan is one of the most important mechanisms of *Candida* species and any disturbance of the synthesis and organization of the cell wall components results in the unmasking of the glucan layer increasing the capacity of the host immune system to recognize and attack the fungi pathogen (Granger, 2018).

Mannoproteins form a fibrillar layer containing O-glycosylated oligosaccharide and N-glycosylated polysaccharide moieties of the most external *Candida* cell wall layer. Mannoproteins are essential in *Candida* interaction with the host allowing the activation and modulation of the immune response against the fungi (Gow and Hube, 2012; Shibata et al., 2012; Paulovicova et al., 2015). They mask the β-glucan layer decreasing the recognition of fungi by the host immune system a process that is mediated by dectin-1, impacting directly the capacity of the host phagocytic cells to uptake and kill *Candida* cells (Galan-Diéz et al., 2010; Bain et al., 2014). In addition, masking the β-glucan layer confers *C. albicans* resistance to complement activation, via classical and alternative pathway, leading to an ineffective activation of the host immune system (Zhang et al., 1997; Boxx et al., 2009, 2010). Ywp1 is an abundant mannoprotein in *C. albicans* cell wall. Mutant strains with disrupted *YWP1* gene resulted in increased exposure of β-glucan in the cell wall. The expression of this protein in germ tubes and hyphae leads to a decrease in the exposure of glucan molecules resulting in decreased glucan accessibility of

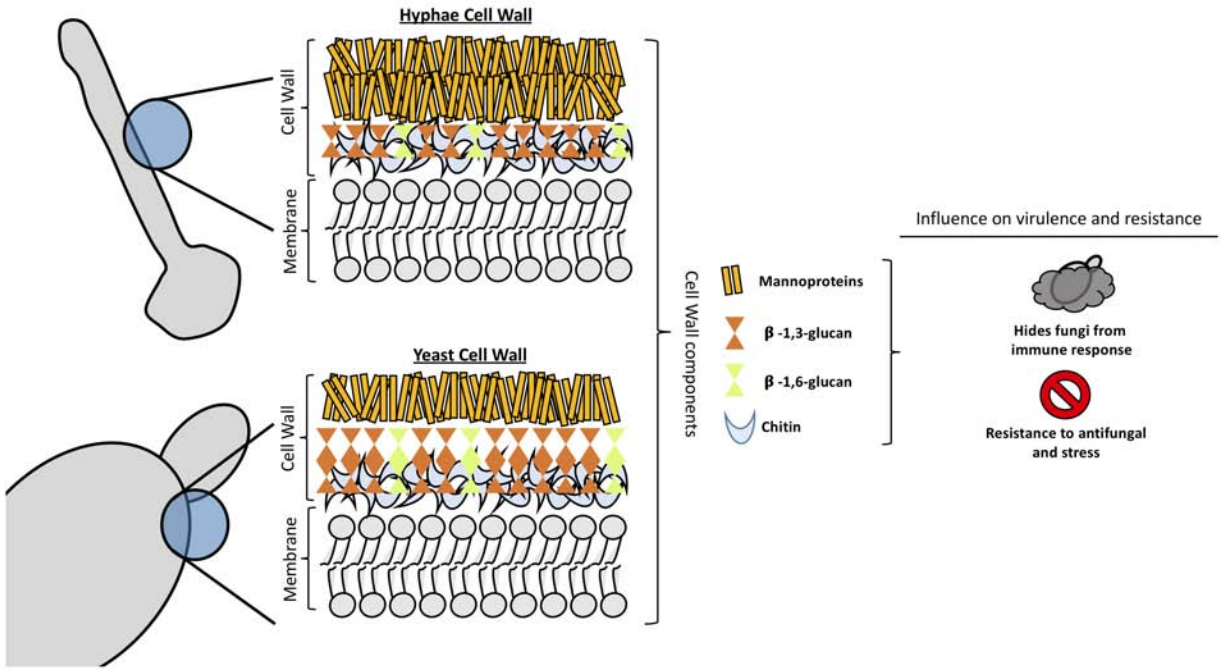

FIGURE 1 | Structural organization and composition of *Candida albicans* cell wall.

those structures (Granger, 2018). MAPK signaling pathway was demonstrated by Galan-Diéz et al. (2010) to be involved in the process of β-glucan masking. They observed that the disruption of the *CEK1*-mediated MAPK pathway generates mutant strains with more exposure of the β-glucan layer in the cell wall, leading to an increase of the Dectin-1-mediated immune responses (Galan-Diéz et al., 2010).

Chitin plays an important role in the interaction of *Candida* species with the host. Chitin-deficient mutant strains display attenuated virulence in immunocompetent and immunosuppressed hosts even though these mutants are able to colonize distinct organs, revealing that the attenuated virulence profile is not due to accelerated clearing (Bulawa et al., 1995). Chitin can block the recognition of *C. albicans* by peripheral blood mononuclear cells (PBMCs) and murine macrophages leading to a significant decrease in cytokine production (Mora-Montes et al., 2011). In addition, an important feature of *C. albicans* cell wall chitin is its important role on arginase-1 induction in host macrophages generating alterations on macrophage nitric oxide production leading to a decrease on macrophage antimicrobial function (Wagener et al., 2017).

Cell Wall as an Antifungal Target

The fungi cell wall is mostly composed of molecules that are not present in the human body and, therefore, constitute an ideal target for the development of clinical antifungal compounds and the design of immunotherapies.

Echinocandins drugs are antifungal compounds that target the β-1,3-glucan synthesis of the cell wall in a non-competitive way (Aguilar-Zapata et al., 2015). There are three commercially available drugs -caspofungin, micafungin, and anidulafungin- and a novel molecule with prolonged half-life -rezafungin (CD101)-, which is currently in phase 3 evaluation (Krishnan et al., 2017; Wiederhold et al., 2018).

Chitin is important for caspofungin resistance in some *Candida* species, such as of *C. albicans*, *C. tropicalis*, *C. parapsilosis*, and *C.guilliermondii*. It has been described that an increase in chitin content in some isolates of *C. krusei* as a consequence of caspofungin exposure (Walker et al., 2013). Strains with elevated levels of chitin in its cell wall also show an echinocandin resistant profile as revealed in a systematic *in vivo* infection model of candidiasis (Lee et al., 2012).

In addition, there is a novel drug called ibrexafungerp (SCY-078) that is a glucan synthase inhibitor belonging to the triterpenoid antifungal class and shows a broad *in vitro* and *in vivo* activity against a broad spectrum of *Candida* (Larkin et al., 2019). *In vitro* studies have demonstrated that this new drug has fungicidal activity against azole-resistant *Candida* spp. isolates similar to the echinocandins, but also against the majority of echinocandin resistant clinical isolates due to *FKS* gene mutations (Scorneaux et al., 2017).

Cryptococcus neoformans

Cryptococcus neoformans is the etiological agent of the cryptococcosis, a systemic mycosis with dissemination to central nervous system causing meningoencephalitis and

primarily affecting immunocompromised patients such as HIV-positive patients (Maziarz and Perfect, 2016; Rajasingham et al., 2017; Beardsley et al., 2019).

Composition, Biosynthesis, and Interaction With the Host

Cryptococcus neoformans cell wall is a dynamic structure that undergoes constant remodeling to modulate the distribution and crosslinking of its components necessary for cellular growth and division (Doering, 2009; Agustinho et al., 2018; Wang et al., 2018). *Cryptococcus* cell wall is a two-layered structure composed by α-1,3-glucan, β-1,3 and β-1,6-glucan, chitin, chitosan, mannoproteins and other GPI-anchored proteins (Baker et al., 2007; Doering, 2009; O'Meara and Alspaugh, 2012; Wang et al., 2018). The inner layer is mainly composed of β-glucans and chitin arranged as fibers parallel to the plasma membrane and the outer layer contains α-glucan and β-glucan (Sakaguchi et al., 1993; Doering, 2009; O'Meara and Alspaugh, 2012; see **Figure 2**). Collectively, these components are essential to maintain the cell shape and for the infection.

The exopolysaccharide capsule is anchored to the outer layer of the cell wall (O'Meara and Alspaugh, 2012; Wang et al., 2018) and this union needs to happen correctly since it is the main virulence factor of this yeast (Vecchiarelli, 2000; McFadden and Casadevall, 2001; Zaragoza et al., 2009). β-1,6-glucan is the most abundant component in *Cryptococcus* cell wall, while β-1,3-glucan is less abundant, contrary to other yeasts (Gilbert et al., 2010; Wang et al., 2018). The main functions of β-1,6-glucan are to maintain and organize the cell wall through interactions with other cell wall components contributing to the integrity of *Cryptococcus* cell wall. Genes such as *KRE5*, *KRE6*, and *SKN1* are involved in β-1,6-glucan synthesis and play an important role in maintaining proper growth, morphology and integrity of the cells (Zaragoza et al., 2009; Gilbert et al., 2010). Mutants for these genes are more sensitive to stress and displayed important alterations in the cell wall composition leading to the loss of virulence in mammalian host (Gilbert et al., 2010).

β-1,3-glucan is structural component of *Cryptococcus* cell wall. In other ascomycetes, β-1,3-glucan is the most abundant component but in *C. neoformans*, the percentage of β-1,3-glucan is lower (Casadevall and Perfect, 1998). β-1,3-glucan synthase gene (*FKS1*) is essential, indicating the importance of this conserved cell wall component (Thompson et al., 1999; O'Meara and Alspaugh, 2012). By activating FKS1, *Cryptococcus* is able to respond to stress by producing β-1,3-glucan (Wang et al., 2018). The inhibition of β-1,3-glucan synthesis induces cell death and changes in cellular morphology (Toh et al., 2017).

α-1,3-glucan is a fundamental component of cryptococcal cell wall and is synthetized by *AGS1*. If the *AGS1* gene is disrupted (*ags1*Δ strain), yeast cells remain alive but there is no capsule on the surface despite production of capsule components (Reese and Doering, 2003; Reese et al., 2007). This showed that α-1,3-glucan is important for the correct capsule-cell wall attachment in *C. neoformans*. In addition, α-1,3-glucan may be involved in protection against the immune system, acting as a shield, hiding the immunogenic β-glucans and chitin molecules, as shown in other pathogenic fungi such as *Histoplasma capsulatum*, *B. dermatitidis*, and *P. brasiliensis* (San-Blas and San-Blas, 1977; Rappleye et al., 2007; Koneti et al., 2008; O'Meara and Alspaugh, 2012).

Chitin is present in minor quantities in *C. neoformans* cell wall, nevertheless it contributes to the strength of the cell wall (Doering, 2009). In *Cryptococcus*, eight chitin synthases and three potential regulatory proteins coordinate and regulate chitin deposition in the cell wall (Banks et al., 2005; Doering, 2009). *CHS3P* is essential to cell integrity and its disruption leads to stress-sensitive cells which show morphological alterations and the inability to retain melanin (Banks et al., 2005; Wang et al., 2018). Chitin plays a crucial role in capsule architecture as revealed in chitin-like structures found in capsular material (Zaragoza et al., 2010). It has been shown that chitin of *C. neoformans* cell wall induces Th2-type immune response increasing the mortality of mice, demonstrating that chitin can modulate host immune system (Wiesner et al., 2015).

Chitosan, the deacetylated form of chitin, is also present in *C. neoformans* cell wall. Chitosan is a more soluble and flexible polymer (Doering, 2009) and the amount in the cell wall is three to five times higher than chitin. This ratio changes with cell wall density (Banks et al., 2005). *C. neoformans* encodes three chitin deacetylases genes, *CDA1*, *CDA2*, and *CDA3*. When these genes are disrupted, the mutants present with decreased chitosan levels which correlates with increased levels of chitin, defects in cell integrity, and increased capsule size (Baker et al., 2007; Doering, 2009). Fonseca et al. (2009) observed *in vitro* that chito-oligomers interfered in the *C. neoformans* capsule assembly. The addition of chito-oligomers to cultures of *C. neoformans*, resulted in aberrant capsules and interference with the connection of the capsule with the cell. Moreover, *in vitro* experiments in which *C. neoformans* chitin synthesis is inhibited by the addition of a glucosamine 6-phosphate synthase inhibitor resulted in capsules loosely connected to the cell wall and polysaccharide fibers with decreased diameter (Fonseca et al., 2009). Chitosan deficient strains displayed slow growth *in vivo* and attenuated virulence in mice model (Baker et al., 2011).

Chitosan mutants promote a protective Th1 host response (Upadhya et al., 2016) showing that chitosan is necessary for full virulence of *Cryptococcus*. An important structure of chitin is the amino sugar N-acetylglucosamine (GlcNAc). Recently, Camacho et al. (2017) showed that *C. neoformans* is able to metabolize exogenous GlcNAc as source of carbon and nitrogen. The supplementation of culture medium with GlcNAc lead to an increase in the chitin-to-chitosan levels. Collectively, the data suggests that *Cryptococcus* can use this exogenous GlcNAc to build its cell-walls and that GlcNAc influence on capsule structure and melanin deposition in the cell-wall.

Melanin is an important virulence factor of *C. neoformans* associated with the cell wall. This pigment is produced by laccase, confers resistance to stress factors, is immunogenic, modulates the host immune response and is known to play essential role in the dissemination of *Cryptococcus* to hosts brains (Liu et al., 1999; Mednick et al., 2005; Nosanchuk and Casadevall, 2006). Melanized *Cryptococcus* cells are less susceptible to amphotericin B and this phenotype may be due to modifications in the cell wall

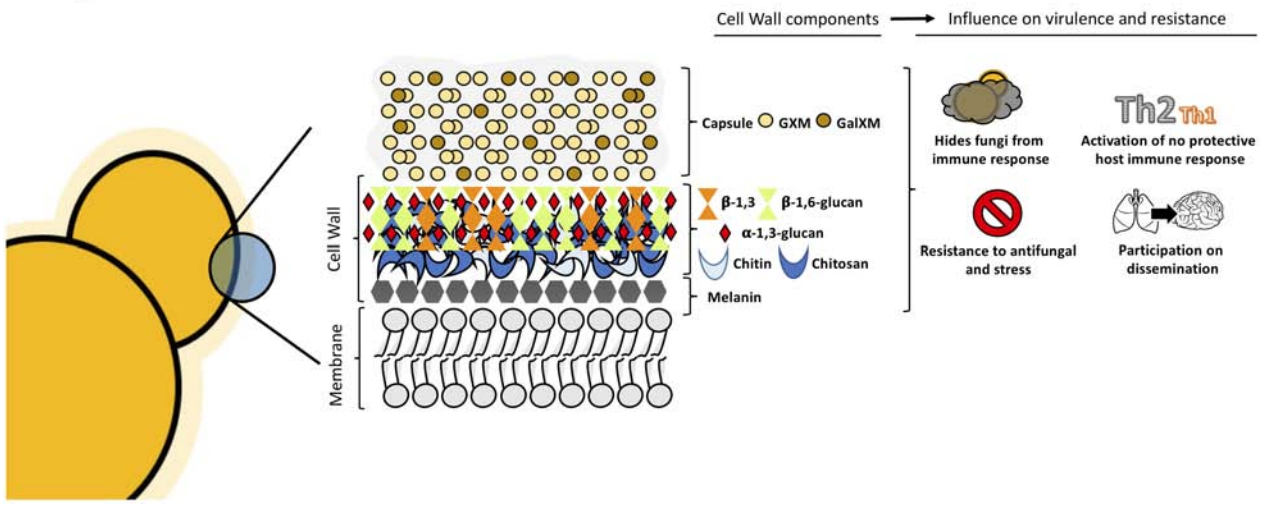

FIGURE 2 | Structural organization and composition of *Cryptococcus neoformans* cell wall.

such as reduction of cell wall pores sizes resulting in melanized cells being considerably less porous than non-melanized yeast cells (Jacobson and Ikeda, 2005).

Finally, the components that complete the structure of *C. neoformans* cell wall are proteins that are embedded in the cell wall carbohydrates. Cryptococcal cell wall contains 29 GPI-anchored proteins, including proteases, carbohydrate-active enzymes and phospholipase B1 (Eigenheer et al., 2007). Phospholipase B1 (Plb1), which is covalently bound to β-1,6-glucan, is involved in membrane homeostasis, remodeling and maintenance of integrity of cell wall contributing to fungal survival in host environment and facilitating tissue invasion (Siafakas et al., 2007; O'Meara and Alspaugh, 2012). Plb1 mutants produced capsules of lower density, which may indicate its importance on capsule attachment to cell wall. In addition, these mutants demonstrated increased sensitivity to cell wall disturbing agents. Furthermore, the amount of Plb1 increases in the cell wall when in higher temperatures, suggesting the role of this protein in the defense of cryptococcal cells from temperature stress (Siafakas et al., 2007). Disruption of Plb1 in *Cryptococcus* results in attenuating its virulence as demonstrated by reduced fungal burden in murine infection models and decreased dissemination with a possible role in translocation through the blood-brain barrier (Santangelo et al., 2004; Chayakulkeeree et al., 2011; Maruvada et al., 2012; Evans et al., 2015).

Cryptococcal cell wall components are unique and are closely related with the capacity of this fungus to cause disease playing essential roles in response to different host and environmental stress (Wang et al., 2018). The capsule is the main virulence factor of *C. neoformans* (Vecchiarelli, 2000; McFadden and Casadevall, 2001; Zaragoza et al., 2009). As previously mentioned, cell wall components are key to proper capsule anchoring (O'Meara and Alspaugh, 2012). *C. neoformans* can increase its size two ways: increasing the size of the capsule which is widely studied (Zaragoza et al., 2008, 2009; Ding et al., 2016; Casadevall et al., 2018; Fonseca et al., 2018; Wang et al., 2018; Zaragoza, 2019) or increasing the size of capsule and cell body resulting in Titan cells, phenomenon less studied, resulting in cells which can reach 100 μM (Okagaki et al., 2010; Zaragoza et al., 2010; Garcia-Rodas et al., 2018). These studies suggesting cell wall re-modelation contribute to occurs during this morphological change. Titan cell formation results in thicker cell wall compared to normal cells (Zaragoza et al., 2010) composed with more glucosamine and less glucose, displaying less β-glucan, possessing in their outer cell wall layer α-glucans and structural mannans. Titan cells cell wall have increased chitin levels compared to normal size cells resulting in detrimental host immune response characterized by increased Th-2 type cytokines contributing to the disease progression in mice (Wiesner et al., 2015; Mukaremera et al., 2018). In addition, *in vitro* studies of Titan cells form thicker cell walls compared with "normal" cells with regular size suggesting cell wall re-modelation during this morphological change (Dambuza et al., 2018; Hommel et al., 2018; Trevijano-Contador et al., 2018).

Cell Wall as an Antifungal Target

β-1,3-glucan synthase is a target for echinocandins compounds. However, while *FKS1* gene is essential in *Cryptococcus* and β-1,3-glucan synthase is sensitive to echinocandins *in vitro*, this antifungal is ineffective against *C. neoformans* infections (Maligie and Selitrennikoff, 2005; O'Meara and Alspaugh, 2012; Toh et al., 2017; Wang et al., 2018). Since internalization of echinocandins by *Cryptococcus* cells is necessary to inhibit β-1,3-glucan synthase, it has been hypothesized that *Cryptococcus* have an unknown mechanism that decreased the influx of the drug. However, this is still unclear and other mechanisms such as the inactivation of echinocandins by this yeast or other resistance mechanism are currently under investigation (Toh et al., 2017; Wang et al., 2018).

Cryptococcus cell wall is a dynamic structure that confers essentials tools necessary for the fungus to adapt to host environment. Yeast cells harbor an extensive molecular arsenal that act by protecting fungi from hosts and environmental stressors. *Cryptococcus* virulence factors such as capsule, formation of Titan cells and melanin are closely related to cell wall dynamics and composition highlighting the importance of the cell wall for *Cryptococcus* pathogenicity.

Aspergillus fumigatus

Aspergillus spp. comprises a variety of environmental filamentous fungus found in diverse ecological niches worldwide and can cause life-threatening diseases in immunocompromised individuals with a wide range of clinical manifestations (Latge, 1999).

Composition and Biosynthesis

Among this genus, *A. fumigatus* is the most prevalent species and is largely responsible for the increased incidence of invasive aspergillosis with high mortality rates in immunocompromised patients (Garcia-Rubio et al., 2017). Due to its clinical importance, this mold has become a model for studying filamentous fungus cell wall and understanding its role in growth and pathogenesis.

Like *Cryptococcus*, the cell wall of *Aspergillus* is a two-layered structure. In *Aspergillus*, the predominant cell wall components are polysaccharides synthesized by transmembrane synthases, transglycosidases and glycosyl hydrolases. The main core of *A. fumigatus* cell wall consists of a polymer of β-1,3-glucan and chitin which is responsible for the rigidity of this structure. β-1,3-glucan is cross-linked to α-1,3-glucan, galactomannan, galactosaminogalactan and a unique mixed molecule of β-1,3-1,4-glucans which has never previously described in fungi, all of them covalently bound one to the other (Fontaine et al., 2000). The composition of the outer cell wall varies between morphotypes, hyphae, and conidium which has a rodlet layer composed of hydrophobins followed by dihydroxynaphtalene melanin (Aimanianda et al., 2009; Bayry et al., 2014). Interestingly, there is no β-1,3-glucan nor chitin in the outer cell wall layer in contrast to other species (see **Figure 3**).

Chitin constitutes a much bigger fraction of the cell wall in filamentous fungi than in yeast, around 10–20% of the dry weight of cell walls. The external side of the membrane, the nascent chitin chain folds back on itself to form anti-parallel chains with intra-chain hydrogen bonds (Chantal et al., 2016). Multiple families of chitin synthases (CHS) are responsible for the synthesis of this compound and many isoforms have been identified bioinformatically. However, the specific function of each of them remains to be established. *A. fumigatus* is predicted to have eight CHS genes (Muszkieta et al., 2014). This multiplicity is conserved among many species and highlights the importance of chitin in fungi.

The other major cell wall component in *A. fumigatus* is β-1,3-glucan which is synthesized by a glucan synthase complex which contains two subunits, using UDP-glucose as a substrate. The catalytic subunit is encoded by *FKS1* gene, the target of echinocandins drugs. This gene is unique but non-essential in *A. fumigatus*. The Δ*fks1* deletion mutant showed a compensatory increase of chitin and galactosaminogalactan with a decrease in cell wall galactomannan (Dichtl et al., 2015). The *FKS1* protein is formed by 16 transmembrane helices and two external loops (Beauvais et al., 2001). The regulatory unit is a Rho1-GTPase encoded by *RHO1* gene, and it has been proposed to have a regulatory interaction between this subunit and the cell wall integrity pathway of *A. fumigatus* (Dichtl et al., 2012). The synthesis of other polysaccharides remains poorly understood. For example, α-1,3-glucan is an important cell wall component of *A. fumigatus* synthesized by three α-1,3-glucan synthases encoded by *AGS1*, *AGS2* and *AGS3* genes but the substrate of these enzymes is still unknown (Beauvais Anne and Latgé, 2006). Deletion of all the three *AGS* genes resulted in the lack of α-(Ponton, 2008; Gow et al., 2017)-glucan in the cell wall, and a decreased virulence in a murine model. However, its growth and germination was not affected (Beauvais et al., 2013).

Another integral component of the fungal cell wall in *A. fumigatus* is long linear chains of repeating mannan units formed of four α-1,6-linked and α-1,2-linked mannoses with side chains of galactofuran covalently bound to the chitin-glucan polysaccharide core. However, major differences have been found in the structural organization of the long mannans in yeasts, such as *S. cerevisiae* and *C. albicans*, compared to *A. fumigatus*. The highly branched mannans of these yeasts are linked to proteins but not covalently bound to the glucan-chitin core as has been found in *A. fumigatus* (Fontaine et al., 2000). Eleven putative mannosyltransferases have been detected in *A. fumigatus* as orthologous genes in yeast responsible for establishing α-1,6- and α-1,2-mannose linkages. However, the complete deletion of these genes did not lead to a reduction in the mycelial cell wall mannan content but caused a decrease in the mannan content of the conidial cell wall (Henry et al., 2016). Other orthologous genes of yeast mannosyltransferases, with a function not associated with mannan polymerization, were investigated and two members of the KTR family (also named Kre2/Mnt1) were found to be responsible for the polymerization of the structural cell wall galactomannan in this mold. Deletion of this gene led to a severe growth phenotype, a strong defect in conidiation, and a reduction of virulence in mouse models (Henry et al., 2019).

Various galactose-containing polymers are located in the *A. fumigatus* cell wall. The galactomannan is composed of mannan and galactofuranose and it is likely to involve a GPI anchor precursor (Costachel et al., 2005), while the galactosaminogalactan is composed of α-1-4 linked galactose and α-1-4 linked N-acetylgalactosamine residues (Fontaine et al., 2011). The presence of β-1,3-1,4-glucan in the *A. fumigatus* cell wall is a unique feature; it was the first description of this molecule in fungi (Fontaine et al., 2000). While this polysaccharide is a well-studied molecule in plants (Doblin et al., 2009), the role of this molecule in *A. fumigatus* is unknown, although, a study suggests one glycosyltransferase encoded by the *TFT1* gene (Three Four Transferase 1) is involved in the cell wall mixed linkage glucan synthesis (Samar et al., 2015).

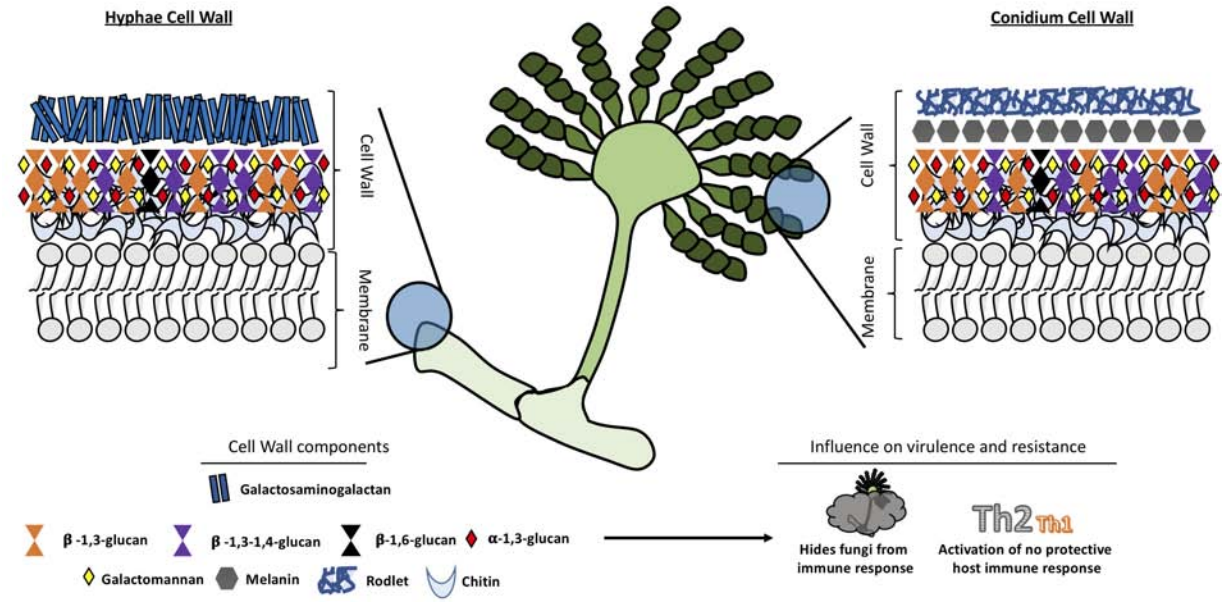

FIGURE 3 | Structural organization and composition of *Aspergillus fumigatus* cell wall.

Once these linear, resynthesized polysaccharides are extruded into the cell wall, they have to be modified and cross-linked to one another resulting in the cell wall structural organization. In this context, some GPI-anchored transglycosidases have an important role in remodeling newly synthesized polysaccharides (Mouyna et al., 2013). For example, enzymes of the Gel family (GH72 family) are responsible for the elongation but also branching of the newly synthesize β-1,3-glucan (Gastebois et al., 2010; Aimanianda et al., 2017), while the DFG family takes part in the covalent binding of the galactomannan to the glucan-chitin core (Muszkieta et al., 2019).

Host Immune Response to *Aspergillus fumigatus* Cell Wall Components

Aspergillus fumigatus releases abundant airborne conidia which are inhaled by humans. The first barrier involved in the *A. fumigatus* conidia clearance is formed by the airway mucociliary cells followed by the alveolar macrophages in the alveolar lumen before they undergo germination (Latge, 1999).

The composition of the cell wall varies depending on the stage of fungal growth, so the host's immune response also varies (Lee and Sheppard, 2016). Dormant conidia have an outer layer formed of rodlets of RodA hydrophobins and dihydroxynaphthalene-melanin which are immunologically inert and mask the inner components of the fungi cell wall. Melanin is an important virulence factor for *Aspergillis* since it protects conidia from macrophages and epithelial cell phagocytic activity inhibiting acidification of phagolysosomes and phagocyte apoptosis (Amin et al., 2014; Bayry et al., 2014). After phagocytosis of conidia by alveolar macrophages and germination, the rodlets are degraded and the cell wall polysaccharides that were concealed become exposed, triggering a potent immune response.

The β-1,3-glucan is specifically recognized by a pattern-recognition-receptor (PRR), Dectin-1 (Herre et al., 2004) which is stimulated only by fibrillary or particulate forms of β-1,3-glucan but not by soluble forms. Dectin-1 is required for IL-23 production by dendritic cells and stimulating IL-17 production by neutrophils (Werner et al., 2009). It is also required for IL-22 responses as well asIL-1α, IL-12, CCL3, CCL4, and TNFα release (Gessner et al., 2012). Dectin-1 plays a role in the adaptive immune response to *A. fumigatus* whose deficiency results in altered specific-T cell maturation (Rivera et al., 2011) leading to an increased production of Dectin-1-dependent CXCL1, CXCL2, and TNFα by bone marrow-derived macrophages (Carrion Sde et al., 2013). These Dectin-1-dependent responses are more relevant in germinating conidia and young hyphae as higher levels of β-1,3-glucans are exposed than in mature hyphae where it is covered by exopolysaccharides (Gravelat et al., 2013). In relation to α-1,3-glucan, no host receptor has been identified. The triple deletion mutant of genes regulating biosynthesis resulted in an increased exposure of surface PAMPs, therefore it could play a role in masking those motifs from immune recognition (Beauvais et al., 2013).

One important exopolysaccharide is galactosaminogalactan, an adhesin that facilitates binding of hyphae to macrophages, neutrophils, and platelets (Fontaine et al., 2011; Rambach et al., 2015). It has been associated with an immunosuppressive activity masking cell wall β-glucans from recognition by Dectin-1, decreased polymorphonuclear neutrophil apoptosis via an NK cell-dependent mechanism and ROS production

(Gravelat et al., 2013; Robinet et al., 2014). In addition, this polysaccharide promotes fungal development in immunocompetent mice due to its immunosuppressive activity associated with diminished neutrophil infiltrates (Fontaine et al., 2011). In humans, the polysaccharide inhibits Th1 and Th17 protective response toward Th2, promoting IL-1Ra secretion by human peripheral blood mononuclear cells (Gresnigt et al., 2014). Galactomannan has also a detrimental effect in the immune system favoring fungal infection. DC-SIGN is an adhesion receptor that specifically interacts with *A. fumigatus* cell wall galactomannans (Serrano-Gomez et al., 2004). Dectin-2 is another receptor that recognizes α-mannans and has an important role in conidia and hyphae binding by THP-1 macrophages, leading to TNF-α and IFN-α release as well as enhanced antifungal activity by plasmacytoid dendritic cells (Loures et al., 2015).

Finally, no host receptor has yet demonstrated for chitin, the inner component of the *Aspergillus* cell wall. The immune response to chitin is discordant and the exact mechanisms determining its inflammatory signature are poorly understood. It was shown to have pro-inflammatory as well as anti-inflammatory properties depending on the presence of costimulatory pathogen-associated molecular patterns and immunoglobulins (Becker et al., 2016). Its role is context specific since its recognition and ability to engage with receptors depends on cell-type, concentration and particle size (Da Silva et al., 2009). However, it seems most of the studies associate chitin with a predominantly type-2 response (Snarr et al., 2017).

Cell Wall as an Antifungal Target

As it has been described before, echinocandins drugs are antifungal compounds that target the β-1,3-glucan synthesis of the cell wall (Aguilar-Zapata et al., 2015). However, due to the limited antifungal activity of these drugs against *Aspergillus* spp., echinocandins compounds are used only as an alternative or a salvage therapy for the treatment of invasive aspergillosis when the first line therapy with azole drugs fails (Aruanno et al., 2019). It is noteworthy that a new antifungal drug called ibrexafungerp (SCY-078) has a broad *in vitro* and *in vivo* activity against a broad spectrum of *Aspergillus* species (Ghannoum et al., 2018).

Currently, there are no *Aspergillus* licensed vaccines to protect humans from aspergillosis (Levitz, 2017). Recently, the Cassone group developed a conjugate of β-1,3-D-glucan in the form of laminarin and the diphtheria toxoid CRM197. Carbohydrate antigens are poorly immunogenic so conjugation with a protein carrier greatly boosts specific antibody responses, protecting in this case against *A. fumigatus* and *C. albicans* (Torosantucci et al., 2005). Additionally, purified cell wall glycans have been used as immunogens through intranasal vaccination with α- and β-1,3-D-glucans but not with galactomannan (Bozza et al., 2009). Given the high morbidity and mortality associated with aspergillosis, much work still needs to be done if vaccines against this pathogen are to become a real option.

CONCLUSION

The fungal cell wall represents an organelle whose composition plays a crucial role in cell viability, morphology and protection against different stressors. Within the fungal kingdom, there is heterogeneity in the composition of the cell wall with species that have unique characteristics that differentiate them from other fungi. The synthesis of the main components of the cell wall is carried out by different genes, among which the *FKS1*, *AGS1*, and *CHS* genes stand out, although there are thousands of genes involved in synthesis, signaling and cell wall assembly. Throughout this review, we have discussed how the different components of the cell wall play an important role in the virulence of these pathogens and how the cell wall interacts with the host's immune system. Mutants of genes involved in the synthesis of different wall components have shown loss of virulence in animal models in *Candida* species. The fungal cell wall remains the most attractive target for the next generation of antifungal drugs. Although it is true that in the last decade, the biology of the fungal cell wall has been studied in depth, many questions remain unanswered requiring additional studies.

AUTHOR CONTRIBUTIONS

NT-C, RG-R, HO, and JR wrote the original draft of the manuscript. HO designed the scheme. JR reviewed the English language of the manuscript. NT-C supervised the study.

REFERENCES

Aguilar-Zapata, D., Petraitiene, R., and Petraitis, V. (2015). Echinocandins: the expanding antifungal armamentarium. *Clin. Infect. Dis.* 61(Suppl. 6), S604–S611. doi: 10.1093/cid/civ814

Agustinho, D. P., Miller, L. C., Li, L. X., and Doering, T. L. (2018). Peeling the onion: the outer layers of *Cryptococcus neoformans*. *Mem. Inst. Oswaldo. Cruz.* 113:e180040. doi: 10.1590/0074-02760180040

Aimanianda, V., Bayry, J., Bozza, S., Kniemeyer, O., Perruccio, K., Elluru, S. R., et al. (2009). Surface hydrophobin prevents immune recognition of airborne fungal spores. *Nature* 460, 1117–1121. doi: 10.1038/nature08264

Aimanianda, V., Simenel, C., Garnaud, C., Clavaud, C., Tada, R., Barbin, L., et al. (2017). The dual activity responsible for the elongation and branching of beta-(1,3)-glucan in the fungal cell wall. *mBio* 8:00619-17. doi: 10.1128/mBio.00619-17

Amin, S., Thywissen, A., Heinekamp, T., Saluz, H. P., and Brakhage, A. A. (2014). Melanin dependent survival of *Apergillus fumigatus* conidia in lung epithelial cells. *Int. J. Med. Microbiol.* 304, 626–636. doi: 10.1016/j.ijmm.2014.04.009

Aruanno, M., Glampedakis, E., and Lamoth, F. (2019). Echinocandins for the treatment of invasive aspergillosis: from laboratory to bedside. *Antimicrob. Agents Chemother.* 63:AAC.00399-19. doi: 10.1128/AAC.00399-19

Bain, J. M., Louw, J., Lewis, L. E., Okai, B., Walls, C. A., Ballou, E. R., et al. (2014). *Candida albicans* hypha formation and mannan masking of beta-glucan inhibit macrophage phagosome maturation. *mBio* 5:e01874. doi: 10.1128/mBio.01874-14

Baker, L. G., Specht, C. A., Donlin, M. J., and Lodge, J. K. (2007). Chitosan, the deacetylated form of chitin, is necessary for cell wall integrity in *Cryptococcus neoformans*. *Eukaryot. Cell* 6, 855–867. doi: 10.1128/ec.00399-06

Baker, L. G., Specht, C. A., and Lodge, J. K. (2011). Cell wall chitosan is necessary for virulence in the opportunistic pathogen *Cryptococcus neoformans*. *Eukaryot. Cell* 10, 1264–1268. doi: 10.1128/EC.05138-11

Banks, I. R., Specht, C. A., Donlin, M. J., Gerik, K. J., Levitz, S. M., and Lodge, J. K. (2005). A chitin synthase and its regulator protein are critical for chitosan production and growth of the fungal pathogen *Cryptococcus neoformans*. *Eukaryot. Cell* 4, 1902–1912. doi: 10.1128/ec.4.11.1902-1912.2005

Bayry, J., Beaussart, A., Dufrene, Y. F., Sharma, M., Bansal, K., Kniemeyer, O., et al. (2014). Surface structure characterization of *Aspergillus fumigatus* conidia mutated in the melanin synthesis pathway and their human cellular immune response. *Infect. Immun.* 82, 3141–3153. doi: 10.1128/IAI.01726-14

Beardsley, J., Sorrell, T. C., and Chen, S. C. (2019). Central nervous system cryptococcal infections in Non-HIV infected patients. *J Fungi* 5:E71.

Beauvais, A., Bozza, S., Kniemeyer, O., Formosa, C., Balloy, V., Henry, C., et al. (2013). Deletion of the alpha-(1,3)-glucan synthase genes induces a restructuring of the conidial cell wall responsible for the avirulence of *Aspergillus fumigatus*. *PLoS Pathog.* 9:e1003716. doi: 10.1371/journal.ppat.1003716

Beauvais, A., Bruneau, J. M., Mol, P. C., Buitrago, M. J., Legrand, R., and Latge, J. P. (2001). Glucan synthase complex of *Aspergillus fumigatus*. *J. Bacteriol.* 183, 2273–2279. doi: 10.1128/jb.183.7.2273-2279.2001

Beauvais Anne, P. D. S., and Latgé, J. P. (2006). Role of α(1-3) glucan in aspergillus fumigatus and other human fungal pathogens. *Fungi Environ.* 269–288. doi: 10.1017/CBO9780511541797.014

Becker, K. L., Aimanianda, V., Wang, X., Gresnigt, M. S., Ammerdorffer, A., Jacobs, C. W., et al. (2016). *Aspergillus* cell wall chitin induces anti- and proinflammatory cytokines in Human PBMCs via the Fc-gamma receptor/Syk/PI3K Pathway. *mBio* 7:01823-15. doi: 10.1128/mBio.01823-15

Bowman, S. M., and Free, S. J. (2006). The structure and synthesis of the fungal cell wall. *Bioessays* 28, 799–808.

Boxx, G. M., Kozel, T. R., Nishiya, C. T., and Zhang, M. X. (2010). Influence of mannan and glucan on complement activation and C3 binding by *Candida albicans*. *Infect. Immun.* 78, 1250–1259. doi: 10.1128/IAI.00744-09

Boxx, G. M., Nishiya, C. T., Kozel, T. R., and Zhang, M. X. (2009). Characteristics of Fc-independent human antimannan antibody-mediated alternative pathway initiation of C3 deposition to *Candida albicans*. *Mol. Immunol.* 46, 473–480. doi: 10.1016/j.molimm.2008.10.008

Bozza, S., Clavaud, C., Giovannini, G., Fontaine, T., Beauvais, A., Sarfati, J., et al. (2009). Immune sensing of *Aspergillus fumigatus* proteins, glycolipids, and polysaccharides and the impact on Th immunity and vaccination. *J. Immunol.* 183, 2407–2414. doi: 10.4049/jimmunol.0900961

Braun, P. C., and Calderone, R. A. (1978). Chitin synthesis in *Candida albicans*: comparison of yeast and hyphal forms. *J. Bacteriol.* 133, 1472–1477.

Brown, G. D., and Gordon, S. (2005). Immune recognition of fungal beta-glucans. *Cell Microbiol.* 7, 471–479. doi: 10.1111/j.1462-5822.2005.00505.x

Brown, G. D., Taylor, P. R., Reid, D. M., Willment, J. A., Williams, D. L., Martinez-Pomares, L., et al. (2002). Dectin-1 is a major beta-glucan receptor on macrophages. *J. Exp. Med.* 196, 407–412. doi: 10.1084/jem.20020470

Bulawa, C. E., Miller, D. W., Henry, L. K., and Becker, J. M. (1995). Attenuated virulence of chitin-deficient mutants of *Candida albicans*. *Proc. Natl. Acad. Sci. U.S.A.* 92, 10570–10574. doi: 10.1073/pnas.92.23.10570

Camacho, E., Chrissian, C., Cordero, R. J. B., Liporagi-Lopes, L., Stark, R. E., and Casadevall, A. (2017). N-acetylglucosamine affects *Cryptococcus neoformans* cell-wall composition and melanin architecture. *Microbiology* 163, 1540–1556. doi: 10.1099/mic.0.000552

Carrion Sde, J., Leal, S. M. Jr., Ghannoum, M. A., Aimanianda, V., Latge, J. P., and Pearlman, E. (2013). The RodA hydrophobin on *Aspergillus fumigatus* spores masks dectin-1- and dectin-2-dependent responses and enhances fungal survival *in vivo*. *J. Immunol.* 191, 2581–2588. doi: 10.4049/jimmunol.1300748

Casadevall, A., Coelho, C., Cordero, R. J. B., Dragotakes, Q., Jung, E., Vij, R., et al. (2018). The capsule of *Cryptococcus neoformans*. *Virulence* 1431087, 1–10. doi: 10.1080/21505594.2018

Casadevall, A., and Perfect, J. (1998). *Cryptococcus Neoformans*. Washington DC: ASM.

Casadevall, A., Rosas, A. L., and Nosanchuk, J. D. (2000). Melanin and virulence in *Cryptococcus neoformans*. *Curr. Opin. Microbiol.* 3, 354–358. doi: 10.1016/s1369-5274(00)00103-x

Chaffin, W. L. (2008). *Candida albicans* cell wall proteins. *Microbiol. Mol. Biol. Rev.* 72, 495–544. doi: 10.1128/MMBR.00032-07

Chantal, F., Gow, N. A. R., and Goncalves, T. (2016). The importance of subclasses of chitin synthaseenzymes with myosin-like domains for the fitnessof fungi. *Br. Mycol. Soc.* 30, 1–14. doi: 10.1016/j.fbr.2016.03.002

Chattaway, F. W., Holmes, M. R., and Barlow, A. J. (1968). Cell wall composition of the mycelial and blastospore forms of *Candida albicans*. *J. Gen. Microbiol.* 51, 367–376. doi: 10.1099/00221287-51-3-367

Chayakulkeeree, M., Johnston, S. A., Oei, J. B., Lev, S., Williamson, P. R., Wilson, C. F., et al. (2011). SEC14 is a specific requirement for secretion of phospholipase B1 and pathogenicity of *Cryptococcus neoformans*. *Mol. Microbiol.* 80, 1088–1101. doi: 10.1111/j.1365-2958.2011.07632.x

Cortes, J. C. G., Curto, M. A., Carvalho, V. S. D., Perez, P., and Ribas, J. C. (2019). The fungal cell wall as a target for the development of new antifungal therapies. *Biotechnol. Adv.* 37:107352. doi: 10.1016/j.biotechadv.2019.02.008

Costachel, C., Coddeville, B., Latge, J. P., and Fontaine, T. (2005). Glycosylphosphatidylinositol-anchored fungal polysaccharide in *Aspergillus fumigatus*. *J. Biol. Chem.* 280, 39835–39842. doi: 10.1074/jbc.m510163200

Da Silva, C. A., Chalouni, C., Williams, A., Hartl, D., Lee, C. G., and Elias, J. A. (2009). Chitin is a size-dependent regulator of macrophage TNF and IL-10 production. *J. Immunol.* 182, 3573–3582. doi: 10.4049/jimmunol.0802113

Dambuza, I. M., Drake, T., Chapuis, A., Zhou, X., Correia, J., Taylor-Smith, L., et al. (2018). The Cryptococcus neoformans Titan cell is an inducible and regulated morphotype underlying pathogenesis. *PLoS Pathog.* 14:e1006978. doi: 10.1371/journal.ppat.1006978

de Groot, P. W., Kraneveld, E. A., Yin, Q. Y., Dekker, H. L., Gross, U., Crielaard, W., et al. (2008). The cell wall of the human pathogen *Candida glabrata*: differential incorporation of novel adhesin-like wall proteins. *Eukaryot. Cell* 7, 1951–1964. doi: 10.1128/EC.00284-08

Del Palacio, A., Villar, J., and Alhambra, A. (2009). [Epidemiology of invasive candidiasis in pediatric and adult populations]. *Rev. Iberoam. Micol.* 26, 2–7.

Dichtl, K., Helmschrott, C., Dirr, F., and Wagener, J. (2012). Deciphering cell wall integrity signalling in *Aspergillus fumigatus*: identification and functional characterization of cell wall stress sensors and relevant Rho GTPases. *Mol. Microbiol.* 83, 506–519. doi: 10.1111/j.1365-2958.2011.07946.x

Dichtl, K., Samantaray, S., Aimanianda, V., Zhu, Z., Prevost, M. C., Latge, J. P., et al. (2015). *Aspergillus fumigatus* devoid of cell wall beta-1,3-glucan is viable, massively sheds galactomannan and is killed by septum formation inhibitors. *Mol. Microbiol.* 95, 458–471. doi: 10.1111/mmi.12877

Ding, H., Mayer, F. L., Sanchez-Leon, E., de S Araújo, G. R., Frases, S., and Kronstad, J. W. (2016). Networks of fibers and factors: regulation of capsule formation in *Cryptococcus neoformans*. *F1000Res* 5:F1000. doi: 10.12688/f1000research.8854.1

Doblin, M. S., Pettolino, F. A., Wilson, S. M., Campbell, R., Burton, R. A., Fincher, G. B., et al. (2009). A barley cellulose synthase-like CSLH gene mediates (1,3;1,4)-beta-D-glucan synthesis in transgenic *Arabidopsis*. *Proc. Natl. Acad. Sci. U.S.A.* 106, 5996–6001. doi: 10.1073/pnas.0902019106

Doering, T. L. (2009). How sweet it is! Cell wall biogenesis and polysaccharide capsule formation in *Cryptococcus neoformans*. *Annu. Rev. Microbiol.* 63, 223–247. doi: 10.1146/annurev.micro.62.081307.162753

Douglas, C. M., Foor, F., Marrinan, J. A., Morin, N., Nielsen, J. B., Dahl, A. M., et al. (1994). The *Saccharomyces cerevisiae* FKS1 (ETG1) gene encodes an integral membrane protein which is a subunit of 1,3-beta-D-glucan synthase. *Proc. Natl. Acad. Sci. U.S.A.* 91, 12907–12911. doi: 10.1073/pnas.91.26.12907

Eigenheer, R. A., Jin Lee, Y., Blumwald, E., Phinney, B. S., and Gelli, A. (2007). Extracellular glycosylphosphatidylinositol-anchored mannoproteins and proteases of *Cryptococcus neoformans*. *FEMS Yeast Res.* 7, 499–510. doi: 10.1111/j.1567-1364.2006.00198.x

Eisenman, H. C., and Casadevall, A. (2012). Synthesis and assembly of fungal melanin. *Appl. Microbiol. Biotechnol.* 93, 931–940. doi: 10.1007/s00253-011-3777-2

Erwig, L. P., and Gow, N. A. (2016). Interactions of fungal pathogens with phagocytes. *Nat. Rev. Microbiol.* 14, 163–176. doi: 10.1038/nrmicro.2015.21

Evans, R. J., Li, Z., Hughes, W. S., Djordjevic, J. T., Nielsen, K., and May, R. C. (2015). *Cryptococcal phospholipase* B1 is required for intracellular proliferation and control of titan cell morphology during macrophage infection. *Infect. Immun.* 83, 1296–1304. doi: 10.1128/IAI.03104-14

Fonseca, F. L., Nimrichter, L., Cordero, R. J., Frases, S., Rodrigues, J., Goldman, D. L., et al. (2009). Role for chitin and chitooligomers in the capsular architecture of *Cryptococcus neoformans*. *Eukaryot. Cell* 8, 1543–1553. doi: 10.1128/EC.00142-09

Fonseca, F. L., Reis, F. C. G., Sena, B. A. G., Jozefowicz, L. J., Kmetzsch, L., and Rodrigues, M. L. (2018). The overlooked glycan components of the *cryptococcus* capsule. *Curr. Top. Microbiol. Immunol*. 422, 31–43. doi: 10.1007/82_2018_140

Fontaine, T., Delangle, A., Simenel, C., Coddeville, B., van Vliet, S. J., van Kooyk, Y., et al. (2011). Galactosaminogalactan, a new immunosuppressive polysaccharide of *Aspergillus fumigatus*. *PLoS Pathog.* 7:e1002372. doi: 10.1371/journal.ppat.1002372

Fontaine, T., Simenel, C., Dubreucq, G., Adam, O., Delepierre, M., Lemoine, J., et al. (2000). Molecular organization of the alkali-insoluble fraction of *Aspergillus fumigatus* cell wall. *J. Biol. Chem.* 275, 27594–27607.

Free, S. J. (2013). Fungal cell wall organization and biosynthesis. *Adv. Genet.* 81, 33–82. doi: 10.1016/B978-0-12-407677-8.00002-6

Galan-Diéz, M., Arana, D. M., Serrano-Gomez, D., Kremer, L., Casasnovas, J. M., Ortega, M., et al. (2010). *Candida albicans* beta-glucan exposure is controlled by the fungal CEK1-mediated mitogen-activated protein kinase pathway that modulates immune responses triggered through dectin-1. *Infect. Immun.* 78, 1426–1436. doi: 10.1128/IAI.00989-09

Garcia-Rodas, R., de Oliveira, H. C., Trevijano-Contador, N., and Zaragoza, O. (2018). Cryptococcal titan cells: when yeast cells are all grown up. *Curr. Top. Microbiol. Immunol.* 422, 101–120. doi: 10.1007/82_2018_145

Garcia-Rubio, R., Cuenca-Estrella, M., and Mellado, E. (2017). Triazole resistance in *Aspergillus* species: an emerging problem. *Drugs* 77, 599–613. doi: 10.1007/s40265-017-0714-4

Gastebois, A., Fontaine, T., Latge, J. P., and Mouyna, I. (2010). beta(1-3)Glucanosyltransferase Gel4p is essential for *Aspergillus fumigatus*. *Eukaryot. Cell* 9, 1294–1298. doi: 10.1128/EC.00107-10

Gessner, M. A., Werner, J. L., Lilly, L. M., Nelson, M. P., Metz, A. E., Dunaway, C. W., et al. (2012). Dectin-1-dependent interleukin-22 contributes to early innate lung defense against *Aspergillus fumigatus*. *Infect. Immun.* 80, 410–417. doi: 10.1128/IAI.05939-11

Ghannoum, M., Long, L., Larkin, E. L., Isham, N., Sherif, R., Borroto-Esoda, K., et al. (2018). Evaluation of the antifungal activity of the novel oral glucan synthase inhibitor SCY-078, singly and in combination, for the treatment of invasive *Aspergillosis*. *Antimicrob. Agents Chemother.* 62:AAC.00244-18. doi: 10.1128/AAC.00244-18

Gilbert, N. M., Donlin, M. J., Gerik, K. J., Specht, C. A., Djordjevic, J. T., Wilson, C. F., et al. (2010). KRE genes are required for beta-1,6-glucan synthesis, maintenance of capsule architecture and cell wall protein anchoring in *Cryptococcus neoformans*. *Mol. Microbiol.* 76, 517–534. doi: 10.1111/j.1365-2958.2010.07119.x

Gow, N. A., and Hube, B. (2012). Importance of the *Candida albicans* cell wall during commensalism and infection. *Curr. Opin Microbiol.* 15, 406–412. doi: 10.1016/j.mib.2012.04.005

Gow, N. A. R., Latge, J. P., and Munro, C. A. (2017). The fungal cell wall: structure, biosynthesis, and function. *Microbiol. Spectr.* 5:FUNK-0035-2016. doi: 10.1128/microbiolspec.FUNK-0035-2016

Granger, B. L. (2018). Accessibility and contribution to glucan masking of natural and genetically tagged versions of yeast wall protein 1 of *Candida albicans*. *PLoS One* 13:e0191194. doi: 10.1371/journal.pone.0191194

Gravelat, F. N., Beauvais, A., Liu, H., Lee, M. J., Snarr, B. D., Chen, D., et al. (2013). *Aspergillus* galactosaminogalactan mediates adherence to host constituents and conceals hyphal beta-glucan from the immune system. *PLoS Pathog.* 9:e1003575. doi: 10.1371/journal.ppat.1003575

Gresnigt, M. S., Bozza, S., Becker, K. L., Joosten, L. A., Abdollahi-Roodsaz, S., van der Berg, W. B., et al. (2014). A polysaccharide virulence factor from *Aspergillus fumigatus* elicits anti-inflammatory effects through induction of Interleukin-1 receptor antagonist. *PLoS Pathog.* 10:e1003936. doi: 10.1371/journal.ppat.1003936

Heitman, J. (2005). Cell biology. A fungal Achilles' heel. *Science* 309, 2175–2176. doi: 10.1126/science.1119321

Henry, C., Fontaine, T., Heddergott, C., Robinet, P., Aimanianda, V., Beau, R., et al. (2016). Biosynthesis of cell wall mannan in the conidium and the mycelium of *Aspergillus fumigatus*. *Cell Microbiol.* 18, 1881–1891. doi: 10.1111/cmi.12665

Henry, C., Li, J., Danion, F., Alcazar-Fuoli, L., Mellado, E., Beau, R., et al. (2019). Two KTR mannosyltransferases are responsible for the biosynthesis of cell wall mannans and control polarized growth in *Aspergillus fumigatus*. *mBio* 10:02647-18. doi: 10.1128/mBio.02647-18

Hernandez-Chavez, M. J., Perez-Garcia, L. A., Nino-Vega, G. A., and Mora-Montes, H. M. (2017). Fungal strategies to evade the host immune recognition. *J. Fungi* 3:51. doi: 10.3390/jof3040051

Herre, J., Willment, J. A., Gordon, S., and Brown, G. D. (2004). The role of Dectin-1 in antifungal immunity. *Crit. Rev. Immunol.* 24, 193–203.

Hommel, B., Mukaremera, L., Cordero, R. J. B., Coelho, C., Desjardins, C. A., Sturny-Leclere, A., et al. (2018). Titan cells formation in *Cryptococcus neoformans* is finely tuned by environmental conditions and modulated by positive and negative genetic regulators. *PLoS Pathog.* 14:e1006982. doi: 10.1371/journal.ppat.1006982

Jacobson, E. S., and Ikeda, R. (2005). Effect of melanization upon porosity of the cryptococcal cell wall. *Med. Mycol.* 43, 327–333. doi: 10.1080/13693780412331271081

Kanetsuna, F., Carbonell, L. M., Moreno, R. E., and Rodriguez, J. (1969). Cell wall composition of the yeast and mycelial forms of *Paracoccidioides brasiliensis*. *J. Bacteriol.* 97, 1036–1041.

Klis, F. M., de Groot, P., and Hellingwerf, K. (2001). Molecular organization of the cell wall of *Candida albicans*. *Med. Mycol.* 39(Suppl. 1), 1–8. doi: 10.1080/714868561

Kobayashi, H., Oyamada, H., Iwadate, N., Suzuki, H., Mitobe, H., Takahashi, K., et al. (1998). Structural and immunochemical characterization of beta-1,2-linked mannobiosyl phosphate residue in the cell wall mannan of *Candida glabrata*. *Arch. Microbiol.* 169, 188–194. doi: 10.1007/s002030050559

Koneti, A., Linke, M. J., Brummer, E., and Stevens, D. A. (2008). Evasion of innate immune responses: evidence for mannose binding lectin inhibition of tumor necrosis factor alpha production by macrophages in response to *Blastomyces dermatitidis*. *Infect. Immun.* 76, 994–1002. doi: 10.1128/iai.01185-07

Krishnan, B. R., James, K. D., Polowy, K., Bryant, B. J., Vaidya, A., Smith, S., et al. (2017). CD101, a novel echinocandin with exceptional stability properties and enhanced aqueous solubility. *J. Antibiot.* 70, 130–135. doi: 10.1038/ja.2016.89

Larkin, E. L., Long, L., Isham, N., Borroto-Esoda, K., Barat, S., Angulo, D., et al. (2019). A Novel 1,3-Beta-d-Glucan Inhibitor, Ibrexafungerp (Formerly SCY-078), shows potent activity in the lower ph environment of *Vulvovaginitis*. *Antimicrob. Agents Chemother.* 63:AAC.02611-18. doi: 10.1128/AAC.02611-18

Latge, J. P. (1999). *Aspergillus fumigatus* and aspergillosis. *Clin. Microbiol. Rev.* 12, 310–350.

Lee, K. K., Maccallum, D. M., Jacobsen, M. D., Walker, L. A., Odds, F. C., Gow, N. A., et al. (2012). Elevated cell wall chitin in *Candida albicans* confers echinocandin resistance in vivo. *Antimicrob. Agents Chemother.* 56, 208–217. doi: 10.1128/AAC.00683-11

Lee, M. J., and Sheppard, D. C. (2016). Recent advances in the understanding of the *Aspergillus fumigatus* cell wall. *J. Microbiol.* 54, 232–242. doi: 10.1007/s12275-016-6045-4

Lesage, G., and Bussey, H. (2006). Cell wall assembly in *Saccharomyces cerevisiae*. *Microbiol. Mol. Biol. Rev.* 70, 317–343. doi: 10.1128/mmbr.00038-05

Levitz, S. M. (2017). *Aspergillus* vaccines: hardly worth studying or worthy of hard study? *Med. Mycol.* 55, 103–108. doi: 10.1093/mmy/myw081

Lima-Neto, R. G., Beltrao, E. I., Oliveira, P. C., and Neves, R. P. (2011). Adherence of *Candida albicans* and *Candida parapsilosis* to epithelial cells correlates with fungal cell surface carbohydrates. *Mycoses* 54, 23–29. doi: 10.1111/j.1439-0507.2009.01757.x

Liu, L., Tewari, R. P., and Williamson, P. R. (1999). Laccase protects *Cryptococcus neoformans* from antifungal activity of alveolar macrophages. *Infect. Immun.* 67, 6034–6039.

Loures, F. V., Rohm, M., Lee, C. K., Santos, E., Wang, J. P., Specht, C. A., et al. (2015). Recognition of *Aspergillus fumigatus* hyphae by human plasmacytoid dendritic cells is mediated by dectin-2 and results in formation of extracellular traps. *PLoS Pathog.* 11:e1004643. doi: 10.1371/journal.ppat.1004643

Maligie, M. A., and Selitrennikoff, C. P. (2005). *Cryptococcus neoformans* resistance to echinocandins: (1,3)beta-glucan synthase activity is sensitive to echinocandins. *Antimicrob. Agents Chemother.* 49, 2851–2856. doi: 10.1128/aac.49.7.2851-2856.2005

Maruvada, R., Zhu, L., Pearce, D., Zheng, Y., Perfect, J., Kwon-Chung, K. J., et al. (2012). *Cryptococcus neoformans* phospholipase B1 activates host cell Rac1 for

traversal across the blood-brain barrier. *Cell Microbiol.* 14, 1544–1553. doi: 10.1111/j.1462-5822.2012.01819.x

Maziarz, E. K., and Perfect, J. R. (2016). Cryptococcosis. *Infect. Dis. Clin. North Am.* 30, 179–206. doi: 10.1016/j.idc.2015.10.006

Mazur, P., Morin, N., Baginsky, W., el-Sherbeini, M., Clemas, J. A., Nielsen, J. B., et al. (1995). Differential expression and function of two homologous subunits of yeast 1,3-beta-D-glucan synthase. *Mol. Cell Biol.* 15, 5671–5681. doi: 10.1128/mcb.15.10.5671

McFadden, D. C., and Casadevall, A. (2001). Capsule and melanin synthesis in *Cryptococcus neoformans*. *Med. Mycol.* 39(Suppl. 1), 19–30. doi: 10.1080/714031007

Mednick, A. J., Nosanchuk, J. D., and Casadevall, A. (2005). Melanization of *Cryptococcus neoformans* affects lung inflammatory responses during cryptococcal infection. *Infect. Immun.* 73, 2012–2019. doi: 10.1128/iai.73.4.2012-2019.2005

Mora-Montes, H. M., Netea, M. G., Ferwerda, G., Lenardon, M. D., Brown, G. D., Mistry, A. R., et al. (2011). Recognition and blocking of innate immunity cells by *Candida albicans* chitin. *Infect. Immun.* 79, 1961–1970. doi: 10.1128/IAI.01282-10

Mouyna, I., Hartl, L., and Latge, J. P. (2013). beta-1,3-glucan modifying enzymes in *Aspergillus fumigatus*. *Front. Microbiol.* 4:81. doi: 10.3389/fmicb.2013.00081

Mukaremera, L., Lee, K. K., Wagener, J., Wiesner, D. L., Gow, N. A. R., and Nielsen, K. (2018). Titan cell production in *Cryptococcus neoformans* reshapes the cell wall and capsule composition during infection. *Cell Surf.* 1, 15–24. doi: 10.1016/j.tcsw.2017.12.001

Munro, C. A., Winter, K., Buchan, A., Henry, K., Becker, J. M., Brown, A. J., et al. (2001). Chs1 of *Candida albicans* is an essential chitin synthase required for synthesis of the septum and for cell integrity. *Mol. Microbiol.* 39, 1414–1426. doi: 10.1046/j.1365-2958.2001.02347.x

Muszkieta, L., Aimanianda, V., Mellado, E., Gribaldo, S., Alcazar-Fuoli, L., Szewczyk, E., et al. (2014). Deciphering the role of the chitin synthase families 1 and 2 in the *in vivo* and *in vitro* growth of *Aspergillus fumigatus* by multiple gene targeting deletion. *Cell Microbiol.* 16, 1784–1805. doi: 10.1111/cmi.12326

Muszkieta, L., Fontaine, T., Beau, R., Mouyna, I., Vogt, M. S., Trow, J., et al. (2019). The glycosylphosphatidylinositol-anchored DFG family is essential for the insertion of galactomannan into the beta-(1,3)-glucan-chitin core of the cell wall of *Aspergillus fumigatus*. *mSphere* 4:00397-19. doi: 10.1128/mSphere.00397-19

Nosanchuk, J. D., and Casadevall, A. (2006). Impact of melanin on microbial virulence and clinical resistance to antimicrobial compounds. *Antimicrob. Agents Chemother.* 50, 3519–3528. doi: 10.1128/aac.00545-06

Nosanchuk, J. D., Stark, R. E., and Casadevall, A. (2015). Fungal melanin: what do we know about structure? *Front. Microbiol.* 6:1463. doi: 10.3389/fmicb.2015.01463

Noverr, M. C., Williamson, P. R., Fajardo, R. S., and Huffnagle, G. B. (2004). CNLAC1 is required for extrapulmonary dissemination of *Cryptococcus neoformans* but not pulmonary persistence. *Infect. Immun.* 72, 1693–1699. doi: 10.1128/iai.72.3.1693-1699.2004

Okagaki, L. H., Strain, A. K., Nielsen, J. N., Charlier, C., Baltes, N. J., Chretien, F., et al. (2010). Cryptococcal cell morphology affects host cell interactions and pathogenicity. *PLoS Pathog.* 6:e1000953. doi: 10.1371/journal.ppat.1000953

O'Meara, T. R., and Alspaugh, J. A. (2012). The *Cryptococcus neoformans* capsule: a sword and a shield. *Clin. Microbiol. Rev.* 25, 387–408. doi: 10.1128/CMR.00001-12

Paulovicova, L., Paulovicova, E., Karelin, A. A., Tsvetkov, Y. E., Nifantiev, N. E., and Bystricky, S. (2015). Immune cell response to *Candida* cell wall mannan derived branched alpha-oligomannoside conjugates in mice. *J. Microbiol. Immunol. Infect.* 48, 9–19. doi: 10.1016/j.jmii.2013.08.020

Pazos, C., Moragues, M. D., Quindos, G., Ponton, J., and del Palacio, A. (2006). Diagnostic potential of (1,3)-beta-D-glucan and anti-*Candida albicans* germ tube antibodies for the diagnosis and therapeutic monitoring of invasive candidiasis in neutropenic adult patients. *Rev. Iberoam. Micol.* 23, 209–215.

Pfuller, R., Graser, Y., Erhard, M., and Groenewald, M. (2011). A novel flucytosine-resistant yeast species, *Candida pseudoaaseri*, causes disease in a cancer patient. *J. Clin. Microbiol.* 49, 4195–4202. doi: 10.1128/JCM.05090-11

Ponton, J. (2008). [The fungal cell wall and the mechanism of action of anidulafungin]. *Rev. Iberoam. Micol.* 25, 78–82.

Poulain, D., and Jouault, T. (2004). *Candida albicans* cell wall glycans, host receptors and responses: elements for a decisive crosstalk. *Curr. Opin. Microbiol.* 7, 342–349. doi: 10.1016/j.mib.2004.06.011

Qadota, H., Python, C. P., Inoue, S. B., Arisawa, M., Anraku, Y., Zheng, Y., et al. (1996). Identification of yeast Rho1p GTPase as a regulatory subunit of 1,3-beta-glucan synthase. *Science* 272, 279–281. doi: 10.1126/science.272.5259.279

Rajasingham, R., Smith, R. M., Park, B. J., Jarvis, J. N., Govender, N. P., Chiller, T. M., et al. (2017). Global burden of disease of HIV-associated cryptococcal meningitis: an updated analysis. *Lancet Infect. Dis.* 17, 873–881. doi: 10.1016/S1473-3099(17)30243-8

Rambach, G., Blum, G., Latge, J. P., Fontaine, T., Heinekamp, T., Hagleitner, M., et al. (2015). Identification of *Aspergillus fumigatus* surface components that mediate interaction of conidia and hyphae with human platelets. *J. Infect. Dis.* 212, 1140–1149. doi: 10.1093/infdis/jiv191

Rappleye, C. A., Eissenberg, L. G., and Goldman, W. E. (2007). *Histoplasma capsulatum* alpha-(1,3)-glucan blocks innate immune recognition by the beta-glucan receptor. *Proc. Natl. Acad. Sci. U.S.A.* 104, 1366–1370. doi: 10.1073/pnas.0609848104

Reese, A. J., and Doering, T. L. (2003). Cell wall alpha-1,3-glucan is required to anchor the *Cryptococcus neoformans* capsule. *Mol. Microbiol.* 50, 1401–1409. doi: 10.1046/j.1365-2958.2003.03780.x

Reese, A. J., Yoneda, A., Breger, J. A., Beauvais, A., Liu, H., Griffith, C. L., et al. (2007). Loss of cell wall alpha(1-3) glucan affects *Cryptococcus neoformans* from ultrastructure to virulence. *Mol. Microbiol.* 63, 1385–1398. doi: 10.1111/j.1365-2958.2006.05551.x

Rivera, A., Hohl, T. M., Collins, N., Leiner, I., Gallegos, A., Saijo, S., et al. (2011). Dectin-1 diversifies *Aspergillus fumigatus*-specific T cell responses by inhibiting T helper type 1 CD4 T cell differentiation. *J. Exp. Med.* 208, 369–381. doi: 10.1084/jem.20100906

Robinet, P., Baychelier, F., Fontaine, T., Picard, C., Debre, P., Vieillard, V., et al. (2014). A polysaccharide virulence factor of a human fungal pathogen induces neutrophil apoptosis via NK cells. *J. Immunol.* 192, 5332–5342. doi: 10.4049/jimmunol.1303180

Rosa, L. H., Almeida Vieira Mde, L., Santiago, I. F., and Rosa, C. A. (2010). Endophytic fungi community associated with the dicotyledonous plant *Colobanthus quitensis* (Kunth) Bartl. (*Caryophyllaceae*) in Antarctica. *FEMS Microbiol. Ecol.* 73, 178–189. doi: 10.1111/j.1574-6941.2010.00872.x

Rubin-Bejerano, I., Abeijon, C., Magnelli, P., Grisafi, P., and Fink, G. R. (2007). Phagocytosis by human neutrophils is stimulated by a unique fungal cell wall component. *Cell Host Microbe* 2, 55–67. doi: 10.1016/j.chom.2007.06.002

Sakaguchi, N., Baba, T., Fukuzawa, M., and Ohno, S. (1993). Ultrastructural study of *Cryptococcus neoformans* by quick-freezing and deep-etching method. *Mycopathologia* 121, 133–141. doi: 10.1007/bf01104068

Salas, S. D., Bennett, J. E., Kwon-Chung, K. J., Perfect, J. R., and Williamson, P. R. (1996). Effect of the laccase gene *CNLAC1*, on virulence of *Cryptococcus neoformans*. *J. Exp. Med.* 184, 377–386. doi: 10.1084/jem.184.2.377

Samar, D., Kieler, J. B., and Klutts, J. S. (2015). Identification and deletion of Tft1, a predicted glycosyltransferase necessary for cell wall beta-1,3;1,4-glucan synthesis in *Aspergillus fumigatus*. *PLoS One* 10:e0117336. doi: 10.1371/journal.pone.0117336

San-Blas, G., and San-Blas, F. (1977). *Paracoccidioides brasiliensis*: cell wall structure and virulence. A review. *Mycopathologia* 62, 77–86. doi: 10.1007/bf01259396

Santangelo, R., Zoellner, H., Sorrell, T., Wilson, C., Donald, C., Djordjevic, J., et al. (2004). Role of extracellular phospholipases and mononuclear phagocytes in dissemination of cryptococcosis in a murine model. *Infect. Immun.* 72, 2229–2239. doi: 10.1128/iai.72.4.2229-2239.2004

Sawistowska-Schroder, E. T., Kerridge, D., and Perry, H. (1984). Echinocandin inhibition of 1,3-beta-D-glucan synthase from *Candida albicans*. *FEBS Lett.* 173, 134–138. doi: 10.1016/0014-5793(84)81032-7

Scorneaux, B., Angulo, D., Borroto-Esoda, K., Ghannoum, M., Peel, M., and Wring, S. (2017). SCY-078 is fungicidal against *candida* species in time-kill studies. *Antimicrob. Agents Chemother.* 61:AAC.01961-16. doi: 10.1128/AAC.01961-16

Sem, X., Le, G. T., Tan, A. S., Tso, G., Yurieva, M., Liao, W. W., et al. (2016). beta-glucan exposure on the fungal cell wall tightly correlates with competitive fitness of *Candida* species in the mouse gastrointestinal tract. *Front. Cell Infect. Microbiol.* 6:186. doi: 10.3389/fcimb.2016.00186

Serrano-Gomez, D., Dominguez-Soto, A., Ancochea, J., Jimenez-Heffernan, J. A., Leal, J. A., and Corbi, A. L. (2004). Dendritic cell-specific intercellular adhesion molecule 3-grabbing nonintegrin mediates binding and internalization of *Aspergillus fumigatus* conidia by dendritic cells and macrophages. *J. Immunol.* 173, 5635–5643. doi: 10.4049/jimmunol.173.9.5635

Shibata, N., Kobayashi, H., and Suzuki, S. (2012). Immunochemistry of pathogenic yeast, *Candida* species, focusing on mannan. *Proc. Jpn. Acad. Ser. B Phys. Biol. Sci.* 88, 250–265. doi: 10.2183/pjab.88.250

Shibata, N., Suzuki, A., Kobayashi, H., and Okawa, Y. (2007). Chemical structure of the cell-wall mannan of *Candida albicans* serotype A and its difference in yeast and hyphal forms. *Biochem. J.* 404, 365–372. doi: 10.1042/bj20070081

Siafakas, A. R., Sorrell, T. C., Wright, L. C., Wilson, C., Larsen, M., Boadle, R., et al. (2007). Cell wall-linked cryptococcal phospholipase B1 is a source of secreted enzyme and a determinant of cell wall integrity. *J. Biol. Chem.* 282, 37508–37514. doi: 10.1074/jbc.m707913200

Silva, M. B., Thomaz, L., Marques, A. F., Svidzinski, A. E., Nosanchuk, J. D., Casadevall, A., et al. (2009). Resistance of melanized yeast cells of *Paracoccidioides brasiliensis* to antimicrobial oxidants and inhibition of phagocytosis using carbohydrates and monoclonal antibody to CD18. *Mem. Inst. Oswaldo Cruz.* 104, 644–648. doi: 10.1590/s0074-02762009000400019

Silva, S., Negri, M., Henriques, M., Oliveira, R., Williams, D. W., and Azeredo, J. (2012). *Candida glabrata*, *Candida parapsilosis* and *Candida tropicalis*: biology, epidemiology, pathogenicity and antifungal resistance. *FEMS Microbiol. Rev.* 36, 288–305. doi: 10.1111/j.1574-6976.2011.00278.x

Snarr, B. D., Qureshi, S. T., and Sheppard, D. C. (2017). Immune recognition of fungal polysaccharides. *J. Fungi* 3:47 doi: 10.3390/jof3030047

Sobel, J. D. (2007). *Vulvovaginal candidosis*. *Lancet* 369, 1961–1971.

Thompson, J. R., Douglas, C. M., Li, W., Jue, C. K., Pramanik, B., Yuan, X., et al. (1999). A glucan synthase FKS1 homolog in *cryptococcus neoformans* is single copy and encodes an essential function. *J. Bacteriol.* 181, 444–453.

Toh, E. A., Ohkusu, M., Shimizu, K., Yamaguchi, M., Ishiwada, N., Watanabe, A., et al. (2017). Creation, characterization and utilization of *Cryptococcus neoformans* mutants sensitive to micafungin. *Curr. Genet.* 63, 1093–1104. doi: 10.1007/s00294-017-0713-8

Torosantucci, A., Bromuro, C., Chiani, P., De Bernardis, F., Berti, F., Galli, C., et al. (2005). A novel glyco-conjugate vaccine against fungal pathogens. *J. Exp. Med.* 202, 597–606. doi: 10.1084/jem.20050749

Trevijano-Contador, N., de Oliveira, H. C., Garcia-Rodas, R., Rossi, S. A., Llorente, I., Zaballos, A., et al. (2018). Cryptococcus neoformans can form titan-like cells in vitro in response to multiple signals. *PLoS Pathog.* 14:e1007007. doi: 10.1371/journal.ppat.1007007

Tsui, C., Kong, E. F., and Jabra-Rizk, M. A. (2016). Pathogenesis of *Candida albicans* biofilm. *Pathog. Dis.* 74:ftw018.

Upadhya, R., Lam, W. C., Maybruck, B., Specht, C. A., Levitz, S. M., and Lodge, J. K. (2016). Induction of protective immunity to cryptococcal infection in mice by a heat-killed, chitosan-deficient strain of *Cryptococcus neoformans*. *mBio* 7:00547-16. doi: 10.1128/mBio.00547-16

Vecchiarelli, A. (2000). Immunoregulation by capsular components of *Cryptococcus neoformans*. *Med. Mycol.* 38, 407–417. doi: 10.1080/714030973

Volling, K., Thywissen, A., Brakhage, A. A., and Saluz, H. P. (2011). Phagocytosis of melanized *Aspergillus* conidia by macrophages exerts cytoprotective effects by sustained PI3K/Akt signalling. *Cell Microbiol.* 13, 1130–1148. doi: 10.1111/j.1462-5822.2011.01605.x

Wagener, J., MacCallum, D. M., Brown, G. D., and Gow, N. A. (2017). *Candida albicans* chitin increases Arginase-1 activity in human macrophages, with an impact on macrophage antimicrobial functions. *mBio* 8:01820-16. doi: 10.1128/mBio.01820-16

Walker, L. A., Gow, N. A., and Munro, C. A. (2013). Elevated chitin content reduces the susceptibility of *Candida* species to caspofungin. *Antimicrob. Agents Chemother.* 57, 146–154. doi: 10.1128/AAC.01486-12

Wang, Y., Aisen, P., and Casadevall, A. (1995). *Cryptococcus neoformans* melanin and virulence: mechanism of action. *Infect. Immun.* 63, 3131–3136.

Wang, Z. A., Li, L. X., and Doering, T. L. (2018). Unraveling synthesis of the cryptococcal cell wall and capsule. *Glycobiology* 28, 719–730. doi: 10.1093/glycob/cwy030

Werner, J. L., Metz, A. E., Horn, D., Schoeb, T. R., Hewitt, M. M., Schwiebert, L. M., et al. (2009). Requisite role for the dectin-1 beta-glucan receptor in pulmonary defense against *Aspergillus fumigatus*. *J. Immunol.* 182, 4938–4946. doi: 10.4049/jimmunol.0804250

Wiederhold, N. P., Locke, J. B., Daruwala, P., and Bartizal, K. (2018). Rezafungin (CD101) demonstrates potent *in vitro* activity against *Aspergillus*, including azole-resistant *Aspergillus fumigatus* isolates and cryptic species. *J. Antimicrob. Chemother.* 73, 3063–3067. doi: 10.1093/jac/dky280

Wiesner, D. L., Specht, C. A., Lee, C. K., Smith, K. D., Mukaremera, L., Lee, S. T., et al. (2015). Chitin recognition via chitotriosidase promotes pathologic type-2 helper T cell responses to cryptococcal infection. *PLoS Pathog.* 11:e1004701. doi: 10.1371/journal.ppat.1004701

Yoshimi, A., Miyazawa, K., and Abe, K. (2017). Function and biosynthesis of cell Wall alpha-1,3-glucan in fungi. *J. Fungi* 3:E63. doi: 10.3390/jof3040063

Zalar, P., Novak, M., de Hoog, G. S., and Gunde-Cimerman, N. (2011). Dishwashers–a man-made ecological niche accommodating human opportunistic fungal pathogens. *Fungal Biol.* 115, 997–1007. doi: 10.1016/j.funbio.2011.04.007

Zaragoza, O. (2019). Basic principles of the virulence of *Cryptococcus*. *Virulence* 10, 490–501. doi: 10.1080/21505594.2019.1614383

Zaragoza, O., Chrisman, C. J., Castelli, M. V., Frases, S., Cuenca-Estrella, M., Rodriguez-Tudela, J. L., et al. (2008). Capsule enlargement in *Cryptococcus neoformans* confers resistance to oxidative stress suggesting a mechanism for intracellular survival. *Cell Microbiol.* 10, 2043–2057. doi: 10.1111/j.1462-5822.2008.01186.x

Zaragoza, O., Garcia-Rodas, R., Nosanchuk, J. D., Cuenca-Estrella, M., Rodriguez-Tudela, J. L., and Casadevall, A. (2010). Fungal cell gigantism during mammalian infection. *PLoS Pathog.* 6:e1000945. doi: 10.1371/journal.ppat.1000945

Zaragoza, O., Rodrigues, M. L., De Jesus, M., Frases, S., Dadachova, E., and Casadevall, A. (2009). The capsule of the fungal pathogen *Cryptococcus neoformans*. *Adv. Appl. Microbiol.* 68, 133–216. doi: 10.1016/S0065-2164(09)01204-0

Zhang, M. X., Lupan, D. M., and Kozel, T. R. (1997). Mannan-specific immunoglobulin G antibodies in normal human serum mediate classical pathway initiation of C3 binding to *Candida albicans*. *Infect. Immun.* 65, 3822–3827.

Conflict of Interest: The authors declare that the research was conducted in the absence of any commercial or financial relationships that could be construed as a potential conflict of interest.

frontiers in Microbiology

ORIGINAL RESEARCH
published: 09 January 2020
doi: 10.3389/fmicb.2019.02930

Thioredoxin Reductase 1 Is a Highly Immunogenic Cell Surface Antigen in *Paracoccidioides* spp., *Candida albicans*, and *Cryptococcus neoformans*

*Fabiana Freire Mendes de Oliveira[1,2], Verenice Paredes[1,3], Herdson Renney de Sousa[1], Ágata Nogueira D'Áurea Moura[4,5], Juan Riasco-Palacios[1], Arturo Casadevall[2], Maria Sueli Soares Felipe[6] and André Moraes Nicola[1,2,3,6]**

[1] Faculty of Medicine, University of Brasília, Brasília, Brazil, [2] Department of Molecular Microbiology and Immunology, Johns Hopkins Bloomberg School of Public Health, Baltimore, MD, United States, [3] Karan Technologies Research and Development, Brasília, Brazil, [4] Department of Microbiology, Institute of Biomedical Sciences II, University of São Paulo, São Paulo, Brazil, [5] Department of Dermatology, Faculty of Medicine, University of São Paulo, São Paulo, Brazil, [6] Graduate Program in Genomic Sciences and Biotechnology, Catholic University of Brasília, Brasília, Brazil

OPEN ACCESS

Edited by:
Maurizio Sanguinetti, Catholic University of the Sacred Heart, Italy

Reviewed by:
Antonio Cassone, Innovation Pole of Genomics, Genetics and Biology (Polo GGB), Italy
Ashok K. Chaturvedi, The University of Texas at San Antonio, United States

***Correspondence:**
André Moraes Nicola
amnicola@unb.br; andre.nicola@gmail.com

Specialty section:
This article was submitted to Fungi and Their Interactions, a section of the journal Frontiers in Microbiology

Received: *20 August 2019*
Accepted: *05 December 2019*
Published: *09 January 2020*

Citation:
Oliveira FFM, Paredes V, Sousa HR, Moura ÁND, Riasco-Palacios J, Casadevall A, Felipe MSS and Nicola AM (2020) Thioredoxin Reductase 1 Is a Highly Immunogenic Cell Surface Antigen in Paracoccidioides spp., Candida albicans, and Cryptococcus neoformans. Front. Microbiol. 10:2930. doi: 10.3389/fmicb.2019.02930

The increasing number of immunocompromised people has made invasive fungal infections more common. The antifungal armamentarium, in contrast, is limited to a few classes of drugs, with frequent toxicity and low efficacy pointing to the need for new agents. Antibodies are great candidates for novel antifungals, as their specificity can result in lower toxicity. Additionally, the immunomodulatory activity of antibodies could treat the underlying cause of many invasive mycoses, immune disfunction. In a previous comparative genomics study, we identified several potential targets for novel antifungals. Here we validate one of these targets, thioredoxin reductase (TRR1), to produce antibodies that could be useful therapeutic tools. Recombinant TRR1 proteins were produced by heterologous expression in *Escherichia coli* of genes encoding the proteins from *Candida albicans*, *Cryptococcus neoformans*, and *Paracoccidioides lutzii*. These proteins were then used to immunize mice, followed by detection of serum antibodies against them by ELISA and western blot. A first set of experiments in which individual mice were immunized repeatedly with TRR1 from a single species showed that all three were highly immunogenic, inducing mostly IgG1 antibodies, and that antibodies produced against one species cross-reacted with the others. In a second experiment, individual mice were immunized three times, each with the protein from a different species. The high titers of antibodies confirmed the presence of antigenic epitopes that were conserved in fungi but absent in humans. Immunofluorescence with sera from these immunized mice detected the protein in the cytoplasm and on the cell surface of fungi from all three species. These results validate TRR1 as a good target for potentially broad-spectrum antifungal antibodies.

Keywords: *Cryptococcus neoformans*, *Candida albicans*, *Paracoccidioides lutzii*, thioredoxin reductase, cell wall, antibodies

INTRODUCTION

Fungal diseases are estimated to affect around a billion people each year, leading to 1.5 million deaths (Bongomin et al., 2017). The incidence for these diseases is bound to remain high, as they frequently affect people that are rendered immunocompromised by advances in Medicine such as organ transplantation, immunossupression and chemotherapy. In addition to opportunistic infections, systemic mycoses caused by primary pathogens such as *Paracoccidioides lutzii* are also important causes of morbidity and mortality in regions such as Latin America (Fortes et al., 2011; Martinez, 2015) Broad-spectrum treatment options for these diseases is restricted to drugs from a few chemical families acting primarily against membrane and cell wall targets, such as azoles, polyenes, and echinocandins (Nett and Andes, 2016). Other antifungal classes such as the pyrimidine analog flucytosine and ergosterol biosynthesis-inhibiting allylamines have much narrower spectra (Sable et al., 2008; Fuentefria et al., 2018). Price and availability in the developing world are a major concern for several of these drugs, as is the increase in resistance (Sable et al., 2008; Chang et al., 2017).

There is thus a dire need for new and effective antifungal drugs, an area of research and technological development in which some advances have been made (Del Poeta and Casadevall, 2012). In a previous work from our group (Abadio et al., 2011), we identified potential targets for antifungals using comparative genomics. We identified ten genes as high-priority targets using several criteria, such as that the target genes should be (a) present in most or all of the most important pathogenic fungi, (b) absent from (or significantly different in) the human genome, (c) essential or important for the survival of the fungi of interest, and (d) located in a part of the fungal cell that is accessible to antifungal agents. Among these genes is *TRR1*, which encodes a thioredoxin reductase. This enzyme is crucial for cellular redox homeostasis and is essential in *Candida albicans* (Abadio et al., 2011) and *Cryptococcus neoformans* (Missall and Lodge, 2005).

Considering that immune dysfunctions are frequent in cases of invasive mycoses, antibodies might be advantageous because they would add to the inhibition of the target a second therapeutic mechanism: immunomodulation (Kullberg et al., 2014; Rodrigues et al., 2016). The objective of this work, then, was to validate TRR1 as a target for antibody development. We found that this protein is highly immunogenic, has conserved epitopes and can be found in the cell wall, which suggest it might be a successful immunotherapy target.

MATERIALS AND METHODS

Microbial Strains and Culture

Escherichia coli BL21 (DE3) and DH5α strains were grown in LB medium at 37°C and conserved with 50% of LB and 50% of glycerol at −80°C. Fungal strains H99 (*C. neoformans*) and SC5314 (*C. albicans*) were grown in solid YPD for 48 h and conserved in 50% of liquid YPD and glycerol 50% at −80°C. *P. lutzii* strain Pb01 was maintained by passage every 7 days in Fava-Netto medium; cells were collected for experiments at 5 days after passaging.

Mammalian Cell Culture and Protein Extraction

Human embryonic kidney (HEK293) cells (Gibco) were thawed and cultured in Freestyle F17 expression medium (Gibco) at 37°C, 5% CO_2. For total protein extraction, cells were pelleted at 200 × *g*, washed with PBS and resuspended in cold RIPA buffer (20 mM Tris–HCl, 140 mM NaCl, 1% Triton X-100, 0.5% SDS, 1 mM EDTA, and 1 mM phenylmethylsulfonyl fluoride, pH 7.5), then vortexed for 30 s, incubated on ice for 30 min and centrifuged at 14,000 × *g*, 10 min. The supernatant containing soluble proteins was stored at −20°C for further analysis.

Mice

Six-week-old female BALB/c mice were used to perform the immunizations. These experiments were made in the Animal Facility of the Johns Hopkins Bloomberg School of Public Health, Johns Hopkins University, or in the Bioassays Laboratory of the Catholic University of Brasília. The experiments were done according to the approved protocols MO15H134 (Johns Hopkins University) and 018/13 (Catholic University of Brasília).

Recombinant Protein Production, Purification, and Quantification

TRR1 genes were codon-optimized and chemically synthesized by two different companies, Epoch Biolabs and Genscript. In both cases, the genes were cloned into the *Xho*I and *Nde*I sites of the pET-21a vector (Novagen), which was purified with a Qiagen plasmid Midiprep kit following manufacturer's instructions. The vector was transformed in *E. coli* BL21 DE3 to produce the recombinant proteins, which were induced with 0.25 mM IPTG when cultures were at optical densities between 0.4 and 0.6. They were purified by affinity chromatography on HisPur™ Cobalt Chromatography Cartridges (Thermo Fisher), with imidazole elution. Protein preparations were analyzed by polyacrylamide gel electrophoresis (Bio-Rad), concentrated by ultrafiltration (Millipore Centriprep™) and quantified by spectrophotometry. For some experiments we also used as negative control an unrelated, his-tagged recombinant protein that was prepared as part of a different project (Moura et al., manuscript in preparation). This protein (*P. lutzii* HSP90) was produced, purified, concentrated, and quantified with a similar strategy.

Murine Immunization

Five groups of one to three animals each were separated according to the condition of the immunization: (1) Control, injected only with PBS in adjuvant. (2) Animals immunized only with *C. albicans* TRR1. (3) Animals immunized only with *P. lutzii* TRR1. (4) Animals immunized only with *C. neoformans* TRR1. (5) Animals immunized sequentially

with TRR1 from the three different species (*C. albicans* – *P. lutzii* – *C. neoformans*). The animals were immunized with a subcutaneous injection in the back of the neck with an emulsion of 50% Freund's adjuvant in PBS containing 50 μg of protein. Three immunizations were made in each mouse, with a 2-week interval between immunizations. The first immunization was made with complete and the others with incomplete Freund's adjuvant. Sera were obtained before all immunizations (and 2 months after the last one) by retro-orbital bleeding using heparin capillary tubes in mice under isoflurane anesthesia.

Western Blot

Purified recombinant proteins (144 ng per lane), HEK293 protein extracts (80 μg per lane) and a molecular weight marker (PageRuler Prestained Protein Ladder – Thermo Fisher) were separated by electrophoresis on denaturing 10% polyacrylamide gels. The proteins were then transferred to a nitrocellulose membrane (GE Healthcare Life Sciences), which was blocked with 5% skim milk in TBS (20 mM Tris–HCl, 150 mM NaCl, pH 7.4). The membranes were then incubated with a 1:6.000 dilution of the sera from immunized mice and, after washing, with a secondary antibody to mouse light chains conjugated with HRP (Jackson Immuno Research). The membranes were then incubated with SuperSignal™ West Pico PLUS Chemiluminescent Substrate (Thermo Fisher) and imaged on a ChemiDoc system (Bio-Rad).

ELISA

TRR1 proteins diluted to 10 μg/mL were used to coat polystyrene plates. After blocking with 1% BSA in PBS, dilutions of the sera from the immunized mice were incubated for 1 h at 37°C. In some of the experiments, we used as secondary antibody a combination of alkaline phosphatase-conjugated goat anti-mouse IgG, IgA, and IgM (Southern Biotech) in a 1:1000 dilution also for 1 h at 37°C. In other experiments, we used isotype-specific (IgA, IgG1, IgG2a, IgG2b, IgG3, and IgM) AP-conjugated secondary antibodies (Southern Biotech). Bound antibodies were detected using p-nitrophenyl phosphate (Sigma) as a substrate, with absorbance measured in a plate spectrophotometer at 405 nm. In some experiments we also included as negative control wells in which the TRR1 proteins were substituted for an unrelated his-tagged protein, to detect antibodies against the tag used for TRR1 purification.

Immunofluorescence

Fungal cells were fixed with 4% paraformaldehyde and washed with PBS. The serum of mice that had been immunized sequentially with TRR1 from all three fungal species was used as primary antibody in a dilution of 1:100, followed by Alexa Fluor® 488 conjugated anti-mouse IgG antibody (ThermoFisher Scientific) diluted 1:100. After washing and mounting, the cells were imaged in a Zeiss AxioObserver Z1 microscope equipped with a 63× objective. Z-stacks were collected and deconvolved using a constrained iterative algorithm with the Zeiss ZEN software.

RESULTS

Production of TRR1 Proteins From *C. albicans*, *C. neoformans*, and *P. lutzii*

Sequences encoding TRR1 from *P. lutzii*, *C. albicans*, and *C. neoformans* were obtained from FungiDB (Basenko et al., 2018), whereas their human homolog was obtained from UniProt. A Clustal Omega alignment of them (**Figure 1**) shows three regions with reasonable variation among the different fungal species interspersed with highly conserved regions. TRR1 proteins from the three species are between 63 and 76% identical among each other, but have only 21 to 24% identity with the human thioredoxin reductase. Genes encoding each of the TRR1 proteins were chemically synthesized and cloned in pET21 vectors for heterologous expression in *E. coli*. As shown in **Figure 2**, we were able to produce highly purified TRR1 proteins from all three species. This experiment was repeated twice with vectors produced from two different companies, with no discernible difference in the proteins produced.

Immunization With TRR1 Proteins Generate High Titers of Cross-Reactive Antibodies

We used the purified recombinant TRR1 proteins to immunize mice in different strategies. Initially, one group was immunized with only *C. albicans* recombinant TRR1 protein, another with only TRR1 from *C. neoformans* and a third with *P. lutzii* TRR1. Each of these mice were immunized three times, and the titers of antibodies (IgA + IgG + IgM) recognizing the recombinant proteins from all three species measured by ELISA. As shown in **Figure 3A**, TRR1 proteins from all three species induced titers of more than 1:5.904.900 of antibodies that bound to the species used as an immunogen (homospecific antibodies). *C. albicans* was the most immunogenic protein, followed by *P. lutzii* and *C. neoformans*. The sera also contained antibodies that were cross-reactive with TRR1 proteins from other species than those that were used as immunogen (heterospecific antibodies). Heterospecific titers varying from 1:72.900 to 1:656.100, being higher in animals immunized with *C. albicans* TRR1 and lower in those immunized with the *C. neoformans* protein. We next immunized animals with a different strategy. They were immunized three times as the other ones were, but with TRR1 from a different species each time. As shown in **Figure 3A**, anti-TRR1 titers in these mice varied from 1:72.900 to 1: 5.904.900. The same sera from mice immunized with all three TRR1 proteins was used in western blot experiments with the recombinant proteins and a protein extract from a human cell line, HEK293 (**Figure 3B**). TRR1 proteins from all three species were recognized by the antibodies, but not the human homolog.

To determine which immunoglobulin isotypes were induced by immunization with TRR1 proteins, we repeated these experiments with isotype specific secondary antibodies. As shown in **Supplementary Figure S1**, the isotype with highest titers in all animals was IgG1, with variable titers for other IgG isotypes and IgM and little IgA. As all TRR1 proteins had a 6x-His tag, we also included as negative control an unrelated his-tagged

FIGURE 1 | Alignment of TRR1 sequences. TRR1 sequences were obtained from online databases and aligned using Clustal Omega (Madeira et al., 2019). *Hs, Homo sapiens; Ca, C. albicans*; *Cn, C. neoformans*; *Pl, P. lutzii*. The symbols indicate full conservation (*), strong similarity (:), and weak similarity (.) in each position.

protein to measure the amount of antibodies that recognized the purification tags instead of the TRR1 protein. The geometric mean of the titers of IgG1 antibodies to this protein in mice immunized with TRR1 proteins was 3.5×10^4, approximately 200 times lower than the geometric mean titer of IgG1 to the immunogens (7.0×10^6).

Given the very high titers and cross-reactivity of antibodies to TRR1, we analyzed the protein sequences using T cell and B cell epitope prediction tools. The NetMHCIIpan tool (Jensen et al., 2018) predicted four different regions that contained peptides that probably bind strongly to mouse MHC class II (**Supplementary Figure S2**). Two of these regions are highly conserved and predicted to occur in all three species. BepiPred-2.0, a linear B cell epitope prediction tool, suggested the existence of 10–12 epitopes in each of the three sequences. Nine of these are predicted to occur in all three species, of which one is identical in all of them, six have 50–90% identity among the species and two have less than 50% identity. Of the nine regions with linear epitopes in all three species, six were also predicted as part of conformational epitopes in the *C. neoformans* TRR1 crystal structure using ElliPro (Ponomarenko et al., 2008). **Supplementary Figure S3** shows the location of some of the epitopes on the TRR1 sequence.

Antibodies to TRR1 Bind to the Fungal Cell Surface

We used the sera from mice that were sequentially immunized with TRR1 proteins from all three species in immunofluorescence experiments with *C. albicans*, *C. neoformans*, and *P. lutzii* yeast cells. As shown in **Figure 4**, we observed significant binding of antibodies in the antiserum to the cell surface in all three types of yeast cells, in a punctate pattern.

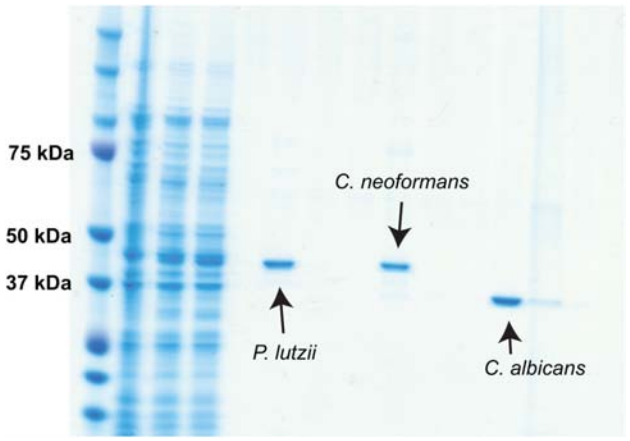

FIGURE 2 | Production of his-tagged TRR1 proteins. Genes encoding *TRR1* from *C. albicans*, *C. neoformans,* and *P. lutzii* were chemically synthesized and cloned into bacterial expression vectors. After transformation in *E. coli* and induction, the recombinant TRR1 proteins were purified by affinity chromatography and analyzed by SDS-PAGE.

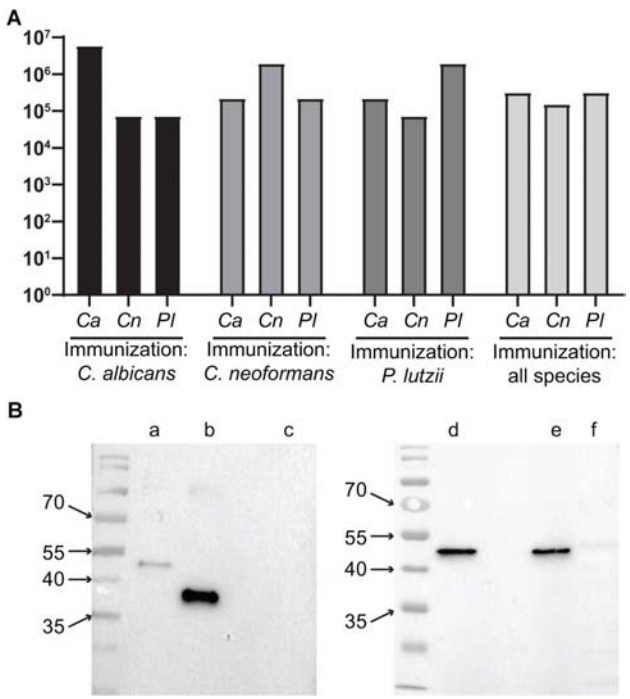

FIGURE 3 | Heterospecific and homospecific antibodies to TRR1. **(A)** Titers of homospecific and heterospecific antibodies in animals immunized with TRR1. Each animal was immunized three times with TRR1 from a single species or with the protein from all three species, one at a time. Two months after the last injection their sera were collected and used in ELISA experiments in which the plates were coated with TRR1 from each of the three fungal species. Bars represent the titers of antibodies (IgA + IgG + IgM) against each one of those species. **(B)** Sera from mice that were immunized with all three fungal species in sequence were used in western blot experiments to detect binding to recombinant *C. albicans* (lane **b**), *C. neoformans* (lanes **a**,**d**), and *P. lutzii* (lane **e**) TRR1 proteins, as well as the protein extract of the human cell line HEK293 (lanes **c**,**f**).

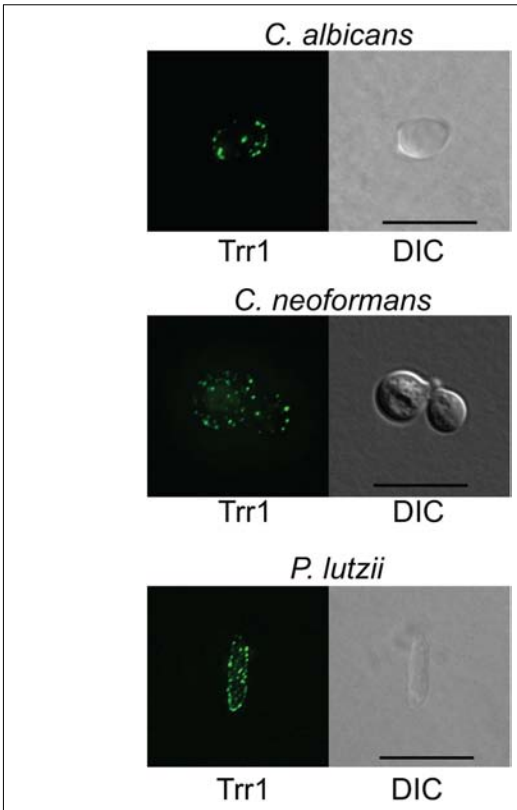

FIGURE 4 | Immunofluorescence with anti-TRR1 sera. *C. albicans, C. neoformans*, and *P. lutzii* yeast cells were fixed, permeabilized and incubated with sera from mice that had been immunized with the TRR1 proteins from all three species. Bound antibodies were detected with a fluorescently labeled secondary antibody. Positive spots can be observed on the surfaces of all three cell types.

DISCUSSION

The increase in the life expectancy of immunocompromised patients afforded by modern medicine has come with a higher incidence of opportunistic fungal infections like invasive aspergillosis and candidiasis. In addition to that, the number of cases of severe mycoses associated with AIDS and infections by primary fungal pathogens such as *Paracoccidioides* spp. and *Histoplasma capsulatum* still remain high (Travassos and Taborda, 2017). Considering the dire need for new antifungal drugs, almost a decade ago we seized the opportunities brought by genomics studies to discover new drug targets (Abadio et al., 2011). Our focus in one of these targets, TRR1, has already resulted in the discovery of new small molecule antifungal candidates (Abadio et al., 2015). TRR1 might also be a target for auranofin, an antirheumatic drug that displayed interesting properties in studies that aimed to repurpose it as an antifungal (Siles et al., 2013; Fuchs et al., 2016; Thangamani et al., 2017; Wiederhold et al., 2017). In this work we made the first steps in validating this target for antibody-based therapies as well.

Antibodies play important roles in the immune response to fungi (Casadevall and Pirofski, 2012), and also have great

potential for immunotherapy of fungal diseases (Zhou and Murphy, 2006; Taborda and Nosanchuk, 2017). The fact that antibodies are naturally found in mammals and the exquisite specificity of the humoral immune response can result in drugs with lower toxicity and lead to less adverse events in comparison with existing therapies. In addition to inhibiting their targets, the immunomodulatory effects of antibodies can also contribute to curing mycoses that frequently happen in immunodepressed individuals (Ravikumar et al., 2015). Two antibody therapies for fungal diseases made it to clinical development: efungumab, an antibody fragment targeting *C. albicans* HSP90 with positive results in phase III clinical trials (Pachl et al., 2006) that was discontinued and 18B7, a murine antibody to the *C. neoformans* capsule that gave promising results in a phase I clinical trial (Larsen et al., 2005).

In addition to these two antibodies that made it to clinical development, several other antibodies have been proposed as candidates for immunotherapy of fungal diseases (Nicola et al., 2018). An anti-β-glucan monoclonal antibody (mAb 2G8) was protective in animal models of invasive mycoses (Rachini et al., 2007), consistent with the protection afforded by a β-glucan vaccine (Torosantucci et al., 2005). Interestingly, other antibodies had as targets proteins that are not traditionally associated with the cell wall like TRR1, such as the cytosolic molecular chaperones HSP90 (Matthews et al., 1991) and HSP60 (Guimarães et al., 2009) and a histone-like protein (Nosanchuk et al., 2003). In *C. neoformans* (Missall and Lodge, 2005) and *Fusarium graminearum* (Fan et al., 2019), GFP-tagged TRR1 was localized in the cytoplasm and mitochondria, the sites in which its enzymatic function is carried out. Our immunofluorescence experiments, however, showed the protein is distributed in a punctate pattern on the surface of the three fungi studied. This pattern has been associated before with increased antifungal activity for an antibody to the *C. albicans* cell wall (Casanova et al., 1990), which is promising for antifungal therapy. Consistent with this extracellular presence of TRR1, it was found in *C. neoformans* extracellular vesicles (Rodrigues et al., 2008) and on the extracellular matrix of mature *C. albicans* biofilms (Martínez et al., 2016). This suggests that cell wall TRR1 would indeed be a good target for therapeutic antibodies, which cannot penetrate intact fungal cells. It also poses an interesting question of whether it is "moonlighting" (Jeffery, 2018) in the cell wall by playing a specific physiologic role there.

Our animal tests showed that TRR1 was highly immunogenic, corroborating a previous study made with *C. albicans* TRR1 (Godoy et al., 2016). Moreover, the immunization led to the production of mostly IgG1 and other IgG isotypes, the expected response to protein antigens (Vidarsson et al., 2014). These are also the isotypes most commonly used to generate therapeutic antibodies, given that the vast majority of therapeutic antibodies are IgG. More importantly, the protein from different species seemed to share B (and probably T) cell epitopes that led to high titers of broadly cross-reactive antibodies, considering the significant phylogenetic distance between the basidiomycete *C. neoformans* and the ascomycetes *C. albicans* and *P. lutzii*. In line with this high immunogenicity and cross-reactivity, a study in which sera from mice infected with *Coccidioides posadasii*, *C. albicans*, and *P. brasiliensis* were incubated with an array containing recombinant *Saccharomyces cerevisiae* proteins detected antibodies that were induced by fungal infection and cross-reacted with baker's yeast TRR1 (Coelho et al., 2015). Strikingly, TRR1 was one of only 16 out of 4,800 different *S. cerevisiae* proteins present on the array that were recognized by antibodies in sera from animals infected with all three fungi, which together with our data indicate that TRR1 is an immunodominant antigen. This has interesting applications for TRR1 as a therapeutic antibody target, suggesting a higher possibility of a broad-spectrum drug. Given that mice immunized with *C. albicans* TRR1 were more resistant in an animal model of invasive candidiasis (Godoy et al., 2016), these findings also raise the question of the role immune responses against cell wall TRR1 play in antifungal immunity.

DATA AVAILABILITY STATEMENT

All datasets generated for this study are included in the article/**Supplementary Material**.

ETHICS STATEMENT

Experiments with animals were reviewed and approved by the Catholic University of Brasília Commision for Ethics on the Use of Animals and the Johns Hopkins University Animal Care and Use Committee.

AUTHOR CONTRIBUTIONS

FO, AN, MF, and AC conceptualized and designed the experiments. FO, HS, ÁM, JR-P, and VP acquired, analyzed, and interpreted data from experiments, which were supervised by AC, AN, and MF. FO and AN drafted the manuscript, which was revised by all authors.

FUNDING

This work was supported by grants and scholarships from the Brazilian funding agencies CNPq, CAPES, and FAP-DF. AC was supported by the National Institutes of Health grants 5R01A1033774, 5R37AI033142, and 5T32A107506, and CTSA grants 1 ULI TR001073-01, 1 TLI 1 TR001072-01, and 1 KL2 TR001071 from the National Center for Advancing Translational Sciences.

SUPPLEMENTARY MATERIAL

The Supplementary Material for this article can be found online at: https://www.frontiersin.org/articles/10.3389/fmicb.2019.02930/full#supplementary-material

REFERENCES

Abadio, A. K., Kioshima, E. S., Leroux, V., Martins, N. F., Maigret, B., and Felipe, M. S. (2015). Identification of new antifungal compounds targeting *Thioredoxin Reductase* of *Paracoccidioides Genus*. *PLoS One* 10:e0142926. doi: 10.1371/journal.pone.0142926 doi: 10.1371/journal.pone.0142926

Abadio, A. K., Kioshima, E. S., Teixeira, M. M., Martins, N. F., Maigret, B., and Felipe, M. S. (2011). Comparative genomics allowed the identification of drug targets against human fungal pathogens. *BMC Genom.* 12:75. doi: 10.1186/1471-2164-12-75

Basenko, E. Y., Pulman, J. A., Shanmugasundram, A., Harb, O. S., Crouch, K., Starns, D., et al. (2018). FungiDB: an integrated bioinformatic resource for fungi and Oomycetes. *J. Fungi* 4:E39. doi: 10.3390/jof4010039

Bongomin, F., Gago, S., Oladele, R. O., and Denning, D. W. (2017). Global and multi-national prevalence of fungal diseases-estimate precision. *J. Fungi* 3:E57. doi: 10.3390/jof3040057

Casadevall, A., and Pirofski, L. A. (2012). Immunoglobulins in defense, pathogenesis, and therapy of fungal diseases. *Cell Host Microb.* 11, 447–456. doi: 10.1016/j.chom.2012.04.004 doi: 10.1016/j.chom.2012.04.004

Casanova, M., Martínez, J. P., and Chaffin, W. L. (1990). Fab fragments from a monoclonal antibody against a germ tube mannoprotein block the yeast-to-mycelium transition in *Candida albicans*. *Infect. Immun.* 58, 3810–3812.

Chang, Y. L., Yu, S. J., Heitman, J., Wellington, M., and Chen, Y. L. (2017). New facets of antifungal therapy. *Virulence* 8, 222–236. doi: 10.1080/21505594.2016.1257457 doi: 10.1080/21505594.2016.1257457

Coelho, P. S., Im, H., Clemons, K. V., Snyder, M. P., and Stevens, D. A. (2015). Evaluating common humoral responses against fungal infections with yeast protein Microarrays. *J. Proteome Res.* 14, 3924–3931. doi: 10.1021/acs.jproteome.5b00365 doi: 10.1021/acs.jproteome.5b00365

Del Poeta, M., and Casadevall, A. (2012). Ten challenges on *Cryptococcus* and cryptococcosis. *Mycopathologia* 173, 303–310. doi: 10.1007/s11046-011-9473-z doi: 10.1007/s11046-011-9473-z

Fan, X., He, F., Ding, M., Geng, C., Chen, L., Zou, S., et al. (2019). Thioredoxin Reductase is involved in development and pathogenicity. *Front. Microbiol.* 10:393. doi: 10.3389/fmicb.2019.00393

Fortes, M. R., Miot, H. A., Kurokawa, C. S., Marques, M. E., and Marques, S. A. (2011). Immunology of paracoccidioidomycosis. *An. Bras. Dermatol.* 86, 516–524.

Fuchs, B. B., RajaMuthiah, R., Souza, A. C., Eatemadpour, S., Rossoni, R. D., Santos, D. A., et al. (2016). Inhibition of bacterial and fungal pathogens by the orphaned drug auranofin. *Future Med. Chem.* 8, 117–132. doi: 10.4155/fmc.15.182 doi: 10.4155/fmc.15.182

Fuentefria, A. M., Pippi, B., Dalla Lana, D. F., Donato, K. K., and de Andrade, S. F. (2018). Antifungals discovery: an insight into new strategies to combat antifungal resistance. *Lett. Appl. Microbiol.* 66, 2–13. doi: 10.1111/lam.12820 doi: 10.1111/lam.12820

Godoy, J. S., Kioshima, É, Abadio, A. K., Felipe, M. S., de Freitas, S. M., and Svidzinski, T. I. (2016). Structural and functional characterization of the recombinant thioredoxin reductase from *Candida albicans* as a potential target for vaccine and drug design. *Appl. Microbiol. Biotechnol.* 100, 4015–4025. doi: 10.1007/s00253-015-7223-8 doi: 10.1007/s00253-015-7223-8

Guimarães, A. J., Frases, S., Gomez, F. J., Zancopé-Oliveira, R. M., and Nosanchuk, J. D. (2009). Monoclonal antibodies to heat shock protein 60 alter the pathogenesis of *Histoplasma capsulatum*. *Infect. Immun.* 77, 1357–1367. doi: 10.1128/IAI.01443-08 doi: 10.1128/iai.01443-08

Jeffery, C. J. (2018). Protein moonlighting: what is it, and why is it important? *Philos. Trans. R. Soc. Lond. B Biol. Sci.* 373:20160523. doi: 10.1098/rstb.2016.0523 doi: 10.1098/rstb.2016.0523

Jensen, K. K., Andreatta, M., Marcatili, P., Buus, S., Greenbaum, J. A., Yan, Z., et al. (2018). Improved methods for predicting peptide binding affinity to MHC class II molecules. *Immunology* 154, 394–406. doi: 10.1111/imm.12889 doi: 10.1111/imm.12889

Kullberg, B. J., van de Veerdonk, F., and Netea, M. G. (2014). Immunotherapy: a potential adjunctive treatment for fungal infection. *Curr. Opin. Infect. Dis.* 27, 511–516. doi: 10.1097/QCO.0000000000000105 doi: 10.1097/qco.0000000000000105

Larsen, R. A., Pappas, P. G., Perfect, J., Aberg, J. A., Casadevall, A., Cloud, G. A., et al. (2005). Phase I evaluation of the safety and pharmacokinetics of murine-derived anticryptococcal antibody 18B7 in subjects with treated cryptococcal meningitis. *Antimicrob. Agents Chemother.* 49, 952–958. doi: 10.1128/aac.49.3.952-958.2005

Madeira, F., Park, Y. M., Lee, J., Buso, N., Gur, T., Madhusoodanan, N., et al. (2019). The EMBL-EBI search and sequence analysis tools APIs in 2019. *Nucleic Acids Res.* 47, W636–W641. doi: 10.1093/nar/gkz268

Martínez, J. P., Blanes, R., Casanova, M., Valentín, E., Murgui, A., and Domínguez, Á (2016). Null mutants of *Candida albicans* for cell-wall-related genes form fragile biofilms that display an almost identical extracellular matrix proteome. *FEMS Yeast Res.* 16, fow075. doi: 10.1093/femsyr/fow075

Martinez, R. (2015). Epidemiology of Paracoccidioidomycosis. *Rev. Inst. Med. Trop. Sao. Paulo.* 57(Suppl. 19), 11–20. doi: 10.1590/S0036-46652015000700004

Matthews, R. C., Burnie, J. P., Howat, D., Rowland, T., and Walton, F. (1991). Autoantibody to heat-shock protein 90 can mediate protection against systemic candidosis. *Immunology* 74, 20–24.

Missall, T. A., and Lodge, J. K. (2005). Thioredoxin reductase is essential for viability in the fungal pathogen *Cryptococcus neoformans*. *Eukaryot. Cell* 4, 487–489. doi: 10.1128/ec.4.2.487-489.2005

Nett, J. E., and Andes, D. R. (2016). Antifungal agents: spectrum of activity, pharmacology, and clinical indications. *Infect. Dis. Clin. North Am.* 30, 51–83. doi: 10.1016/j.idc.2015.10.012

Nicola, A. M., Albuquerque, P., Paes, H. C., Fernandes, L., Costa, F. F., Kioshima, E. S., et al. (2018). Antifungal drugs: new insights in research & development. *Pharmacol. Ther.* 195, 21–38.

Nosanchuk, J. D., Steenbergen, J. N., Shi, L., Deepe, G. S., and Casadevall, A. (2003). Antibodies to a cell surface histone-like protein protect against *Histoplasma capsulatum*. *J. Clin. Invest.* 112, 1164–1175. doi: 10.1172/jci19361

Pachl, J., Svoboda, P., Jacobs, F., Vandewoude, K., van der Hoven, B., Spronk, P., et al. (2006). A randomized, blinded, multicenter trial of lipid-associated amphotericin B alone versus in combination with an antibody-based inhibitor of heat shock protein 90 in patients with invasive candidiasis. *Clin. Infect. Dis.* 42, 1404–1413. doi: 10.1086/503428

Ponomarenko, J., Bui, H. H., Li, W., Fusseder, N., Bourne, P. E., Sette, A., et al. (2008). ElliPro: a new structure-based tool for the prediction of antibody epitopes. *BMC Bioinform.* 9:514. doi: 10.1186/1471-2105-9-514

Rachini, A., Pietrella, D., Lupo, P., Torosantucci, A., Chiani, P., Bromuro, C., et al. (2007). An anti-β-glucan monoclonal antibody inhibits growth and capsule formation of *Cryptococcus neoformans* in vitro and exerts therapeutic, anticryptococcal activity in vivo. *Infect. Immun.* 75, 5085–5094. doi: 10.1128/iai.00278-07

Ravikumar, S., Win, M. S., and Chai, L. Y. (2015). Optimizing outcomes in Immunocompromised hosts: understanding the role of immunotherapy in invasive fungal diseases. *Front. Microbiol.* 6:1322. doi: 10.3389/fmicb.2015.01322

Rodrigues, M. E., Silva, S., Azeredo, J., and Henriques, M. (2016). Novel strategies to fight *Candida* species infection. *Crit. Rev. Microbiol* 42, 594–606. doi: 10.3109/1040841X.2014.974500

Rodrigues, M. L., Nakayasu, E. S., Oliveira, D. L., Nimrichter, L., Nosanchuk, J. D., Almeida, I. C., et al. (2008). Extracellular vesicles produced by *Cryptococcus neoformans* contain protein components associated with virulence. *Eukaryot. Cell* 7, 58–67.

Sable, C. A., Strohmaier, K. M., and Chodakewitz, J. A. (2008). Advances in antifungal therapy. *Annu. Rev. Med.* 59, 361–379.

Siles, S. A., Srinivasan, A., Pierce, C. G., Lopez-Ribot, J. L., and Ramasubramanian, A. K. (2013). High-throughput screening of a collection of known pharmacologically active small compounds for identification of *Candida albicans* biofilm inhibitors. *Antimicrob. Agents Chemother.* 57, 3681–3687. doi: 10.1128/AAC.00680-13 doi: 10.1128/aac.00680-13

Taborda, C. P., and Nosanchuk, J. D. (2017). Editorial: vaccines, immunotherapy and new antifungal therapy against fungi: updates in the new frontier. *Front. Microbiol.* 8:1743.

Thangamani, S., Maland, M., Mohammad, H., Pascuzzi, P. E., Avramova, L., Koehler, C. M., et al. (2017). Repurposing approach identifies Auranofin with broad spectrum antifungal activity that targets Mia40-Erv1 pathway. *Front. Cell Infect. Microbiol.* 7:4. doi: 10.3389/fcimb.2017.00004

Torosantucci, A., Bromuro, C., Chiani, P., De Bernardis, F., Berti, F., Galli, C., et al. (2005). A novel glyco-conjugate vaccine against fungal pathogens. *J. Exp. Med.* 202, 597–606. doi: 10.1084/jem.20050749

Travassos, L. R., and Taborda, C. P. (2017). Linear Epitopes of *Paracoccidioides brasiliensis* and other fungal agents of human systemic mycoses as vaccine candidates. *Front. Immunol.* 8:224. doi: 10.3389/fimmu.2017.00224

Vidarsson, G., Dekkers, G., and Rispens, T. (2014). IgG subclasses and allotypes: from structure to effector functions. *Front. Immunol.* 5:520. doi: 10.3389/fimmu.2014.00520

Wiederhold, N. P., Patterson, T. F., Srinivasan, A., Chaturvedi, A. K., Fothergill, A. W., Wormley, F. L., et al. (2017). Repurposing auranofin as an antifungal: in vitro activity against a variety of medically important fungi. *Virulence* 8, 138–142. doi: 10.1080/21505594.2016.1196301 doi: 10.1080/21505594.2016.1196301

Zhou, Q., and Murphy, W. J. (2006). Immune response and immunotherapy to *Cryptococcus infections*. *Immunol. Res.* 35, 191–208. doi: 10.1385/ir:35:3:191

Conflict of Interest: The authors declare that the research was conducted in the absence of any commercial or financial relationships that could be construed as a potential conflict of interest.

frontiers in Microbiology

ORIGINAL RESEARCH
published: 21 January 2020
doi: 10.3389/fmicb.2019.03094

Calcineurin A Is Essential in the Regulation of Asexual Development, Stress Responses and Pathogenesis in *Talaromyces marneffei*

Yan-Qing Zheng[1†], Kai-Su Pan[1†], Jean-Paul Latgé[2], Alex Andrianopoulos[3], Hong Luo[1], Ru-Fan Yan[1], Jin-Ying Wei[1], Chun-Yang Huang[1] and Cun-Wei Cao[1]*

[1] Department of Dermatology and Venereology, The First Affiliated Hospital of Guangxi Medical University, Nanning, China, [2] School of Medicine, University of Crete, Heraklion, Greece, [3] School of Biosciences, The University of Melbourne, Parkville, VIC, Australia

OPEN ACCESS

Edited by:
Joshua D. Nosanchuk,
Albert Einstein College of Medicine,
United States

Reviewed by:
Praveen Rao Juvvadi,
Duke University, United States
Ence Yang,
Peking University, China
Shizhu Zhang,
Nanjing Normal University, China

***Correspondence:**
Cun-Wei Cao
caocunwei@yeah.net

[†] These authors have contributed equally to this work

Specialty section:
This article was submitted to Fungi and Their Interactions, a section of the journal Frontiers in Microbiology

Received: 06 July 2019
Accepted: 20 December 2019
Published: 21 January 2020

Citation:
Zheng YQ, Pan KS, Latgé JP, Andrianopoulos A, Luo H, Yan RF, Wei JY, Huang CY and Cao CW (2020) Calcineurin A Is Essential in the Regulation of Asexual Development, Stress Responses and Pathogenesis in Talaromyces marneffei. Front. Microbiol. 10:3094. doi: 10.3389/fmicb.2019.03094

Talaromyces marneffei is a common cause of infection in immunocompromised patients in Southeast Asia and Southern China. The pathogenicity of *T. marneffei* depends on the ability of the fungus to survive the cytotoxic processes of the host immune system and grow inside host macrophages. These mechanisms that allow *T. marneffei* to survive macrophage-induced death are poorly understood. In this study, we examined the role of a calcineurin homolog (*cnaA*) from *T. marneffei* during growth, morphogenesis and infection. Deletion of the *cnaA* gene in *T. marneffei* resulted in a strain with significant defects in conidiation, germination, morphogenesis, cell wall integrity, and resistance to various stressors. The Δ*cnaA* mutant showed a lower minimal inhibitory concentration (MIC) against caspofungin (16 μg/ml to 2 μg/ml) and micafungin (from 32 μg/ml to 4 μg/ml) compared with the wild-type. These results suggest that targeting calcineurin in combination with echinocandin treatment may be effective for life-threatening systemic *T. marneffei* infection. Importantly, the *cnaA* mutant was incapable of adapting to the macrophage environment *in vitro* and displayed virulence defects in a mouse model of invasive talaromycosis. For the first time, a role has been shown for *cnaA* in the morphology and pathogenicity of a dimorphic pathogenic filamentous fungus.

Keywords: *Talaromyces* (*Penicillium*) *marneffei*, calcineurin, morphogenesis, cell wall integrity, immune escape, virulence

INTRODUCTION

Calcineurin is a Ca^{2+}/calmodulin (CaM)-dependent protein phosphatase that is ubiquitous and conserved among eukaryotes. The heterodimeric calcineurin protein consists of a catalytic subunit (A) that binds to the calcium sensor CaM and a regulatory subunit (B) that contains four Ca^{2+}-binding domains. The functions of calcineurin have been studied in a variety of fungal species, and it plays important roles in the regulation of cation homeostasis, morphogenesis, cell wall integrity, and pathogenesis (Rusnak and Mertz, 2000; Fox et al., 2001; Fox and Heitman, 2002). In filamentous fungi, calcineurin regulates conidial architecture, polarized growth extension and branching, sclerotial and appresorial development, cell wall integrity and stress adaptation (Fortwendel et al., 2009; Juvvadi et al., 2014; Juvvadi and Steinbach, 2015). Calcineurin activation

leads to the dephosphorylation and activation of the transcription factor Crz1p/Tcn1p, which is involved in cell survival and calcium homeostasis in *Saccharomyces cerevisiae* (Cyert, 2003; Roque et al., 2016). It is involved in antifungal tolerance, cell morphogenesis (Sanglard et al., 2003; Bader et al., 2006; Cordeiro Rde et al., 2014), growth in an alkaline pH or high-temperature environment, membrane stress, mating, and virulence in *Candida albicans* (Cruz et al., 2002; Reedy et al., 2010; Liu et al., 2014). Previous reports on the dimorphic fungus *Paracoccidioides brasiliensis* have implicated calcineurin in morphogenesis, environmental stress responses and mycelium-to-yeast dimorphism (Fernandes et al., 2005; Campos et al., 2008; Matos et al., 2013).

Talaromyces marneffei is an emerging opportunistic fungal pathogen that is endemic in southern China, Taiwan, Hong Kong, Thailand, Laos, Vietnam, and northeastern India (Supparatpinyo et al., 1994; Antinori et al., 2006; Vanittanakom et al., 2006). *T. marneffei* can cause a life-threatening systemic infection in immunocompromised individuals, especially HIV-positive patients (Woo et al., 2012). In recent years, *T. marneffei* has become a leading AIDS-defining diagnosis in Southern Asia, trailing only tuberculosis and cryptococcosis in incidence (Wu et al., 2008; Le et al., 2011; Hien et al., 2016; Lee et al., 2019). Furthermore, *T. marneffei* infection has recently been increasingly observed in HIV-negative adults with no reported immunosuppressive condition, but immunodeficiency is suspected to be the cause of these infections (Ramos-e-Silva et al., 2012; Kauffman et al., 2014). The mortality rate of *T. marneffei* infection exceeds 50% despite antifungal therapy (Le et al., 2011; Hu et al., 2013). Understanding the pathogenic mechanism is fundamental to combating *T. marneffei* infection.

Talaromyces marneffei is an intracellular pathogen; conidia are inhaled into a patient's lungs and subsequently engulfed by alveolar macrophages, where the conidia transform into yeast cells and cause infection (Supparatpinyo et al., 1994). During this process, *T. marneffei* conidia will face a variety of stresses, such as heat, salt stress, oxidative substances, high osmolarity, nutrient deprivation and cytokine-mediated killing (Cao et al., 2009a; Wang et al., 2009; Kummasook et al., 2011). There are several important mechanisms in *T. marneffei* infection, including the conversion of conidia to the yeast phase, resistance to phagocytic killing and oxidative, and heat stress responses (Pongpom et al., 2017), that result in *T. marneffei* survival in macrophages. These strategies are the key processes of immune escape.

In our previous study, we found that the minimal inhibitory concentrations (MICs) of echinocandins were quite low for the *T. marneffei* hyphal form, but *T. marneffei* manifested resistance in its yeast forms (Cao et al., 2009b; Mo et al., 2014). The mechanism by which the *T. marneffei* yeast form is resistant to echinocandins is still unclear, but the cell wall composition is suspected to play a role. Echinocandins are antifungals that inhibit cell wall β-(1,3)-D-glucan synthesis (Douglas et al., 1997). It has been reported that β-(1,3)-D-glucan and chitin are two major components of the fungal cell wall (the other main components are 1,6-β-glucans and mannoproteins) (Klis et al., 2002). Reduced synthesis of β-(1,3)-D-glucan can result in reduced susceptibility to caspofungin, and elevated chitin content can reduce echinocandin efficacy in many fungi (Fortwendel et al., 2009; Cordeiro Rde et al., 2014). In a preliminary study, we found that *T. marneffei* yeast forms were more sensitive to calcium than the hyphal form (Cao et al., 2007). As calcium activates the calcineurin pathway, it is postulated that it may also affect the resistance of *T. marneffei* to echinocandins by regulating cell wall composition and could represent a potential drug target for augmenting echinocandin use in *T. marneffei* infection. Thus, in this study, we aimed to investigate calcineurin function by characterizing the *cnaA* gene and exploring the mechanism of immune escape in *T. marneffei*.

MATERIALS AND METHODS

Strains, Media, and Growth Conditions

Strains used in this study are listed in **Table 1**. *T. marneffei* FRR2161 is the type strain and was used as the wild-type for all experiments. *T. marneffei* G816 (Δ*ligD niaD*$^{-}$ *pyrG*$^{-}$) is a uracil/uridine auxotroph (*pyrG*) mutant of FRR2161 (Bugeja et al., 2012). Transformation was performed using the protoplast method (Borneman et al., 2000). The Δ*cnaA* mutant was generated by transforming strain G816 with a linearized Δ*cnaA* deletion construct and selecting for uracil/uridine (*pyrG*$^{+}$) prototrophic transformants. The complemented strain Δ*cnaA cnaA*$^{+}$ was generated by transforming the Δ*cnaA* mutant with the *cnaA-ble*-pKB plasmid and selecting for bleomycin (*ble*$^{+}$)-resistant transformants. *T. marneffei* strains were grown at 25°C in *A. nidulans* minimal medium (ANM) with 10 mM $(NH_4)_2SO_4$ and supplemented appropriately as previously described (Borneman et al., 2000). *T. marneffei* strains were grown at 37°C in BHI medium. *Escherichia coli* DH5α (Invitrogen, United States) was used to clone and propagate the various constructs and was grown in Luria-Bertani broth at 37°C.

To test the radial growth and the spore-producing ability of the mutants, strains were grown in ANM for 14 days at 25°C, and conidia were harvested into sterile Stroke physiological saline solution. A suspension of 1×10^5 conidia per milliliter was prepared. The wild-type, Δ*cnaA* mutant and complemented Δ*cnaA cnaA*$^{+}$ strains were inoculated with a 5-μl drop of the 1×10^5 conidia per milliliter suspension onto ANM with

TABLE 1 | Strains and plasmids used in this study.

Strain or plasmid	Genotype or characteristic
T. marneffei FRR2161	Wild-type of *T. marneffei*
T. marneffei G816	*ligD*$^{-}$ *niaD*$^{-}$ *pyrG*$^{-}$
T. marneffei Δ*cnaA*	*cnaA*$^{-}$ *pyrG*$^{+}$ of *T. marneffei*
T. marneffei Δ*cnaA cnaA*$^{+}$	*cnaA*$^{+}$*pyrG*$^{-}$ *ble*$^{+}$ of *T. marneffei*
pBluescript II pSK	Ampicillin-resistant plasmid
cnaA-pSK	pBluescript II containing the *cnaA gene*
pyrG blaster pSK	Plasmid containing the *A. nidulans pyrG* gene
Δ*cnaA* deletion	Plasmid with *A. nidulans pyrG* gene replacing the *cnaA* coding region
cnaA-ble- pKB	Plasmid containing the *cnaA* gene and *ble* resistance gene

10 mM $(NH_4)_2SO_4$ with or without uracil, BHI medium or SD medium supplemented with 10 mM $(NH_4)_2SO_4$. The conidia were incubated at either 25°C or 37°C, and radial growth was measured every day over a period of 14 days. For conidial counts, the number of spores per square millimeter were counted after 14 days at 25°C. The results were analyzed by the *T*-test analysis of variance.

To test for stress responses of the strains, a 5-μl drop of the 1×10^5 conidia per milliliter suspension of each strain was inoculated onto agar-solidified ANM with 10 mM $(NH_4)_2SO_4$ and 5 mM uracil and supplemented as follows: 0.2, 0.4, 0.6, and 1 M KCl (salt stress); 2, 5 and 8 mM H_2O_2(oxidative stress); 0.5, 1, and 1.5 M sorbitol (for osmotic stress); 2.5 and 5 μM Congo red; or 0.1, 5, and 10 μg/ml calcofluor white (cell wall stress). All cultures were incubated for 14 days at 25°C.

Microscopy

To examine hyphal and yeast cell morphogenesis, conidial germination and cell wall architecture were examined by light microscopy using differential interference contrast (DIC) or epifluorescence optics after staining with calcofluor (CAL). For hyphal growth, conidia were inoculated onto slides covered with a thin layer of agar-solidified ANM with 10 mM $(NH4)_2SO_4$, with or without 5 mM uracil, and incubated at 25°C for 10 days (Borneman et al., 2000). For yeast growth, conidia were inoculated onto slides covered with a thin layer of agar-solidified BHI or SD medium supplemented with $(NH_4)_2SO_4$ and incubated at 37°C for 10 days.

Ultrastructure analysis was performed using scanning electron microscopy (SEM) and transmission electron microscopy (TEM). For SEM, strains were fixed with 2.5% glutaraldehyde for 2 h at 4°C, washed in 0.1 mol/L phosphate-buffered saline (PBS) three times for 10 min each time and fixed with 1% osmium tetroxide for 1 h. Then, they were washed in 0.1 mol/L PBS three times for 10 min each time and ethanol-dehydrated by sequential washing in 50%, 70%, 80%, 90%, and 100% ethanol. The samples were soaked in hexamethyldisilane three times and dried under vacuum. Thin sections were examined with a Vega 3 LMU-apollo X Scanning Electron Microscope (Tescan, Czechia). For TEM, strains were fixed, washed and dehydrated as described for SEM. The samples were embedded in white resin, and thin sections were examined with a Hitachi H-7650 Transmission Electron Microscope (Hitachi, Japan).

For germination experiments, 10^6 spores of each strain were inoculated into 30 ml of SD medium supplemented with 10 mM $(NH_4)_2SO_4$ and incubated for 4, 8, 16 or 24 h at 25°C and 37°C. The rates of germination were determined microscopically by counting the number of germinating conidia in a population of approximately 100 randomly selected spores. Three independent experiments were performed.

Antifungal Susceptibility Testing

Antifungal susceptibility testing was performed according to the standardized M27-A method approved by the National Committee for Clinical Laboratory Standards (NCCLS) and previously reported methods (Nakai et al., 2003). Caspofungin (CAS), micafungin (MCFG), amphotericin B (AMB), fluconazole (FLC), itraconazole (ITC), and vorconazole (VOC) were purchased from Med Chem Express (New Jersey, NJ, United States). Stock solutions were made with sterile distilled water (MCFG and AMB) or 100% dimethyl sulfoxide (CAS, FLC, ITC and VOC). The stock solutions were diluted in RPMI 1640 medium prepared according to the Clinical and Laboratory Standards Institute (CLSI) standards and then further serially diluted twofold. The final concentration ranges of the antifungals were 0.0625 to 32 μg/ml (CAS and MCFG), 0.0156 to 8 μg/ml (AMB), 0.125 to 64 μg/ml (FLC), and 0.0013 to 1 μg/ml (ITC and VOC). Wild-type and Δ*cnaA* mutant strains were incubated in the presence or absence of drug for 48 h at 25°C and 37°C, and all experiments were performed in triplicate. *Candida parapsilosis* ATCC22019 served as a control.

Macrophage Assay

RAW264.7 macrophages (1×10^5) (InvivoGen, Hong Kong) were co-incubated with 1×10^6 conidia in DMEM containing 10% fetal bovine serum (Gibco, United States) and 8 mM penicillin-streptomycin at 37°C for 2 h. The cells were then washed with PBS to remove unengulfed conidia and incubated for an additional 24 h at 37°C. Infected macrophages were harvested for microscopy or to determine fungal load. For microscopy, cells were either fixed and prepared for TEM or stained with 5 μM Dil (Invitrogen, United States) for 10 min, washed twice in PBS, fixed in 4% paraformaldehyde, stained with 1 mg/ml calcofluor and examined by light microscopy to observe yeast morphogenesis. For fungal load determination, the number of surviving conidia in macrophages were determined by lysing infected macrophages in cold PBS, diluting 1:100, and plating on YPD medium. After incubating for 72 h at 25°C, the CFU was determined. The test was performed three times in triplicate, and the results were analyzed by *T*-test analysis of variance.

Murine Model of *Talaromyces marneffei* Infection

Eight-week-old BALB/c mice (male and female) were immunosuppressed with intraperitoneal injections of cyclophosphamide (Sigma-Aldrich) at a dose of 200 mg/kg of body weight on days −4 and −1 and the day of infection, as well as triamcinolone acetonide (Sigma-Aldrich) at a dose of 40 mg/kg of body weight on the day of infection. To evaluate the histopathological progression of disease, four groups of 36 mice were infected with a sublethal dose (10^6 conidia in 100 μl of physiological saline) of the wild-type, Δ*cnaA*, or Δ*cnaA cnaA*$^+$ strains or a diluent control (0.9% physiological saline). The mice were sacrificed on days 3, 6, and 9 after inoculation, and their tissue was harvested under sterile conditions. The lung, hepatic and splenic tissues were removed to determine the number of *T. marneffei* by measuring CFU in YPD medium. The test was performed three times in triplicate, and the results were analyzed by *T*-test analysis of variance. To evaluate the mortality rates, four groups of 36 immunosuppressed mice were challenged with 100 μl of suspensions containing 10^8 conidia/ml of each strain. The morbidity and mortality of the mice were observed every day for 14 days. Survival was plotted on a Kaplan-Meier

curve, and a log-rank test was used for pairwise comparisons among the strains.

RESULTS

Calcineurin Genes in *Talaromyces marneffei*

The sequence of the *T. marneffei cnaA* gene was obtained from GenBank (GenBank accession no. XM_002147834.1, ATCC 18224). The gene encompasses 2261 bp and encodes a putative gene product of 557 amino acids. In searches against the GenBank database, the *T. marneffei cnaA* gene showed strong homology to the sequences in *Talaromyces stipitatus* (XM_002482031.1, 88% identity), *Aspergillus aculeatus* (XM_020205250.1, 79% identity), and *Aspergillus nomius* (XM_015546462.1, 78% identity).

Loss of *cnaA* Affects Colonial Morphology and Radial Growth

Wild-type *T. marneffei* growing at 25°C produces colonies comprised of vegetative hyphae that appear fluffy around the periphery and green in the center due to asexual development (conidiation) and the production of pigmented conidia. The colony edge is relatively uniform and compact. In contrast, colonies of the Δ*cnaA* mutant exhibited a significant reduction in radial growth rate with sparse growth and low aerial hyphae production. The colony surface was wrinkled, and the periphery was irregular. The colony also produced more of the red pigment that is characteristic of *T. marneffei* (**Figure 1A**). The Δ*cnaA* mutant colonies also readily detached from the medium, indicating a lack of invasive growth. The complemented strain (Δ*cnaA cnaA*$^+$) displayed colony phenotypes that were very similar to that of the wild-type.

The radial growth rate of the wild-type, Δ*cnaA* and Δ*cnaA cnaA*$^+$ strains was quantified during growth on solid medium at both 25°C and 37°C. At 25°C, the wild-type and Δ*cnaA cnaA*$^+$ strains showed similar growth rates, while that of the Δ*cnaA* mutant was substantially reduced. Similarly, at 37°C, the wild-type and Δ*cnaA cnaA*$^+$ strains showed similar growth rates, while that of the Δ*cnaA* mutant was reduced (**Figure 1B**).

Loss of *cnaA* Affects Conidiophore Development and Conidial Germination

To examine the cellular basis of the poor conidiation observed for the Δ*cnaA* mutant, the various strains were examined by SEM. After 14 days of incubation at 25°C, the wild-type showed conidiophores composed of a stalk cell bearing four to seven phialides, and each phialide had many conidia arranged in a chain. The wild-type conidial chains were very long and resulted in the production of abundant conidia. In contrast, conidiophore integrity was aberrant and conidiation was reduced in the Δ*cnaA* mutant. Phialides of the Δ*cnaA* mutant were abnormal in morphology, and their number was highly reduced compared with that of the wild-type strain (**Figure 2A**). Compared with the wild-type strain, the Δ*cnaA* mutant showed a statistically significant decrease in conidial density ($P < 0.01$), which directly correlates with the reduced phialide numbers. The Δ*cnaA cnaA*$^+$ complemented strain was identical to the wild-type (**Figure 2B**).

The kinetics of germination were measured by counting the number of germinating conidia in a population of approximately 100 conidia after incubation for 4, 8, 16, and 24 h in Sabouraud's (SD) liquid medium at either 25°C and 37°C. In contrast to the wild-type and Δ*cnaA cnaA*$^+$ strains, the Δ*cnaA* strain show a visible delayed germination at 25°C and 37°C. In the first 4 h, a steady rate of germination was evident for both the wild-type and complemented strains, which was comparable to that of the Δ*cnaA* mutant, although the Δ*cnaA* mutant at 37°C started to show a decrease in germination compared with that at 25°C. This difference was accentuated at the longer time points and became evident by 8 h. By 24 h, the Δ*cnaA* mutant exhibited a germination percentage that was half that of the wild-type and complemented strains, which may be one reason why the mutant exhibited a delay in growth at longer incubation time points (**Figure 2C**).

Δ*cnaA* Mutant Displays Defects in Hyphal and Yeast Morphogenesis

To examine the cellular basis for the observed macroscopic growth defects observed in the Δ*cnaA* strain, all strains were grown on ANM or BHI medium for 10 days at 25°C and 37°C and either stained with calcofluor white (CAL) to visualize the cell walls by fluorescence microscopy or processed for SEM. The wild-type hyphal cells showed a smooth and uniform hyphal diameter with regular septation and uniform staining with CAL. In contrast, the Δ*cnaA* mutant exhibited irregularly shaped hyphal cells that were enlarged in diameter, particularly at septation sites, and showed abnormal CAL-stained chitin deposits along the hyphae. This result suggests that calcineurin is important for proper hyphal extension (**Figure 3A**). Compared with the wild-type, the poles of the yeast cell of the Δ*cnaA* mutant showed abnormal swelling and exhibited abnormal chitin deposits. Therefore, the *cnaA* mutant displayed defects in yeast morphogenesis (**Figure 3B**).

cnaA Is Required for Correct Cell Wall Biosynthesis in *Talaromyces marneffei*

The hyphal and yeast morphogenesis defects noted for the Δ*cnaA* strain were examined further by TEM. The strains were grown on agar-solidified ANM and BHI medium for 10 days at 25°C and 37°C and processed for TEM. For the wild-type strain, transverse sectioning of the hyphal cells showed a cell wall composed of three layers, namely, a thin inner membrane-proximal layer that was electron-dense, a thick middle layer that was electron-transparent and an irregular outer layer with protrusions. The wild-type yeast cells showed a similar cell wall architecture but with a smoother outer wall layer. In both cell types, the organelles could also be clearly seen. In contrast, the Δ*cnaA* mutant displayed cell wall perturbations in all of the layers for both hyphal and yeast cells, and the organelles appeared less distinct (**Figure 4A**).

The observed changes in the cell wall architecture were further examined by testing the sensitivity of the various strains to

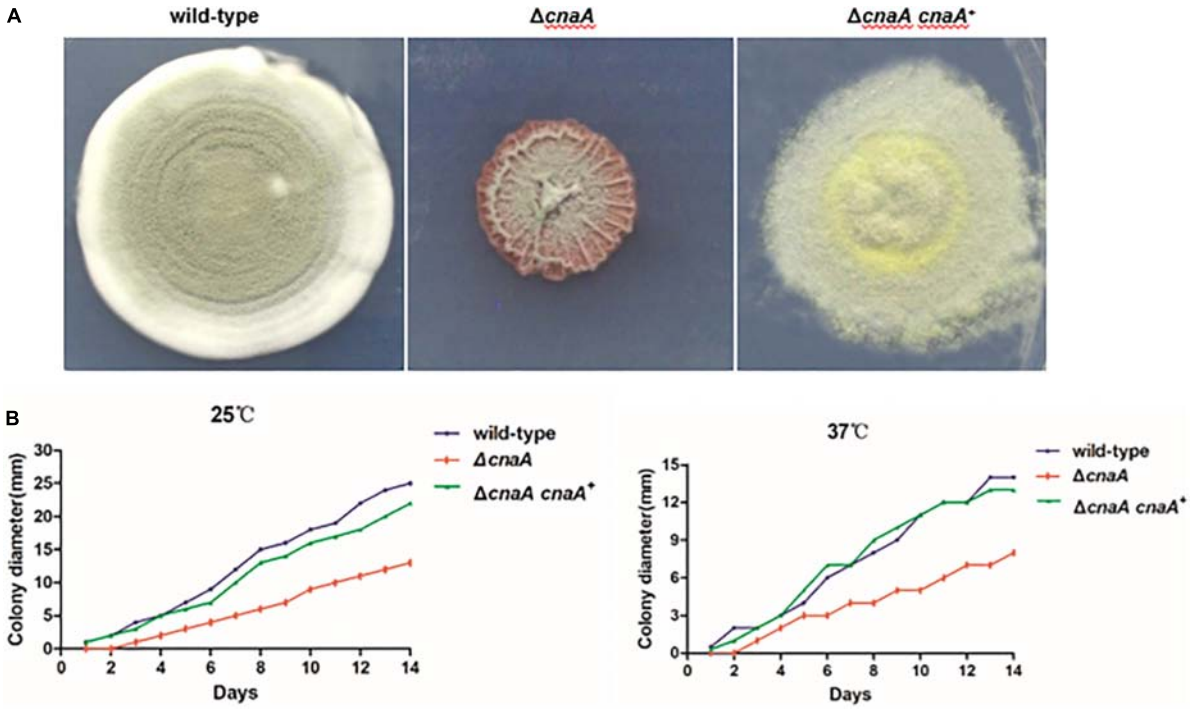

FIGURE 1 | Loss of *cnaA* affects colonial morphology and radial growth. **(A)** *T. marneffei* wild-type and Δ*cnaA cnaA*$^{+}$ strains exhibited highly vegetative hyphae that appeared fluffy and green and developed many conidiophores at 25°C when grown on ANM. The colony edge was relatively uniform and compact. Colonies of the Δ*cnaA* mutant showed thin growth and exhibited decreased aerial hyphae production, resulting in a film-like surface morphology that was wrinkled. **(B)** Conidia from each strain were inoculated on ANM or BHI medium and incubated for 1–14 days at 25°C and 37°C. The Δ*cnaA* mutant grew less than the wild-type and Δ*cnaA cnaA*$^{+}$ complemented strain.

cell wall-perturbing agents and a variety of antifungal drugs. Compared with the wild-type strain, the Δ*cnaA* mutant was more sensitive to Congo red at 5 mM and 25°C but equally sensitive to different CAL white concentrations (**Figure 4B**). When tested for sensitivity to various anti-fungal agents, the MICs for caspofungin (CAS) and micafungin (MCFG) for the mycelial form were much lower than those for the yeast form in the parental strain of *T. marneffei*. In contrast to the parental strain, potent activity against the yeast form of the Δ*cnaA* mutant was observed. The MIC of CAS was reduced from 16 μg/ml (wild-type) to 2 μg/ml (mutant), and the MIC of MCFG was similarly reduced from 32 μg/ml to 4 μg/ml at 37°C. When testing azole-based antifungals, the MICs of fluconazole (FLC), itraconazole (ITC), and voriconazole (VOC) for the mutant were a gradient lower than the corresponding MICs for the wild-type strain (**Table 2**). All of the above evidence suggests that the *cnaA* gene participates in cell wall integrity in a direct manner.

cnaA Is Required for *Talaromyces marneffei* Adaptation to High Osmolarity *in vitro*

To investigate whether the Δ*cnaA* mutant of *T. marneffei* exhibits sensitivity to salt stress, oxidative stress and high osmolarity conditions, the Δ*cnaA* mutant and parental strain were incubated on ANM containing different concentrations of potassium chloride (KCl), H_2O_2, or sorbitol. The results revealed that the Δ*cnaA* mutant was highly sensitive to oxidative stress. Compared with the parental strain, the Δ*cnaA* mutant exhibited gradually reduced growth in increasing KCl concentrations, and the growth inhibition was more obvious at high concentrations (0.6 M, 1 M KCl) than at low concentrations (**Figure 5A**). The growth of the Δ*cnaA* mutant was similar to that of the parental strain at low concentrations of sorbitol, but mutant growth inhibition was obvious in 1M and 1.5 M sorbitol. In contrast to the parental strain, the Δ*cnaA* mutant was highly sensitive to oxidative stress; the growth of the mutant was inhibited in 5 and 8 mM H_2O_2 (**Figure 5B**).

cnaA Is Essential for Immune Escape in Macrophages

To assess whether the observed changes in the cell wall architecture and sensitivity to a broad range of stressors in the Δ*cnaA* strains affected its ability to interact with host macrophages, the various strains were co-incubated with RAW264.7 macrophages and examined after 12, 24, and 48 h of incubation. The wild-type conidia co-incubated with RAW264.7 macrophages were rapidly phagocytosed and germinated into ellipsoid-shaped yeast cells. By 24 h, these yeast cells had grown in size and were dividing by fission. This continued to 48 h, where macrophages were filled with dividing yeast cells. Conidia from

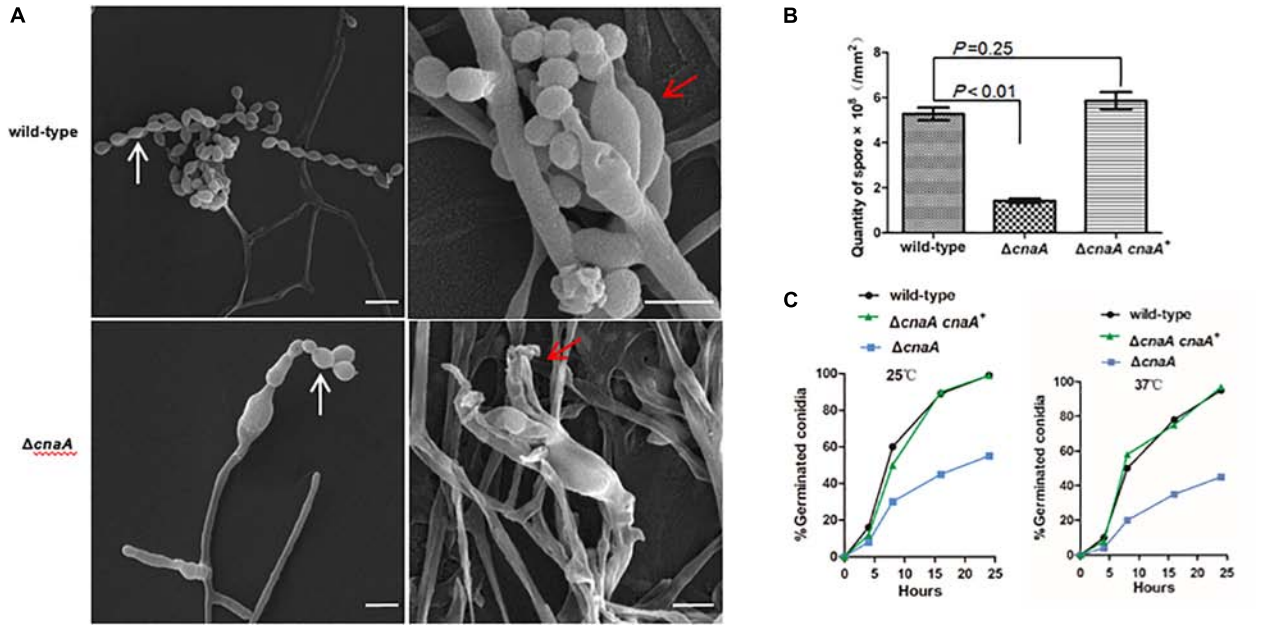

FIGURE 2 | Loss of *cnaA* affects conidiophore development and conidial germination. **(A)** Wild-type and Δ*cnaA* strains were grown on ANM + $(NH_4)_2SO_4$ for 14 days at 25°C and examined by SEM. The wild-type strain showed a conidiophore that was composed of four to seven phialides (red arrow) and long chains of conidia (white arrow), resulting in the production of abundant conidia. In the Δ*cnaA* mutant, the conidiophore displayed abnormal phialide and spore chains with decreased numbers of conidia. Scale bars, 10 μm. **(B)** Compared with the wild-type and Δ*cnaA cnaA*$^+$ complemented strain, the Δ*cnaA* mutant showed a statistically significant decrease in conidial density ($P < 0.01$). **(C)** The kinetics of germination were measured at both 25°C and 37°C by counting the number of germinating conidia in a population of approximately 100 spores after incubation for 4, 8, 16, and 24 h in SD liquid medium. In contrast to the wild-type, the percentage of germination decreased in the Δ*cnaA* mutant.

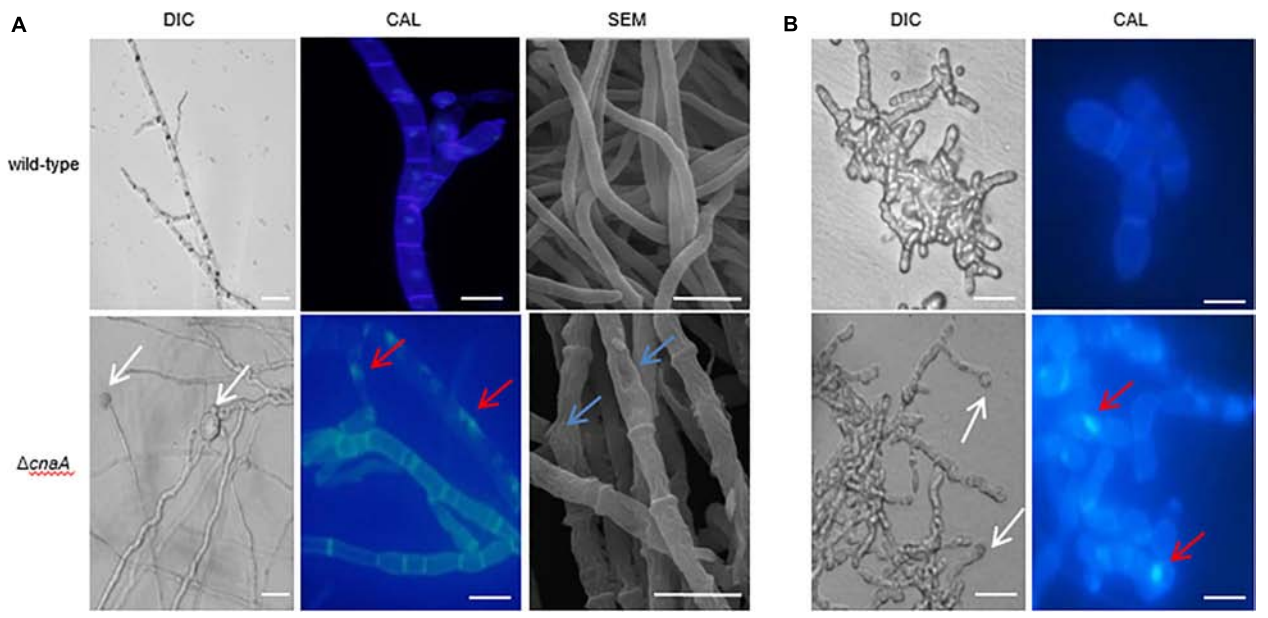

FIGURE 3 | The *cnaA* mutant displays defects in hyphal and yeast morphogenesis. **(A)** Wild-type and Δ*cnaA* strains were inoculated onto ANM medium and grown at 25°C for 10 days, followed by either staining with calcofluor to visualize cell walls by light microscopy or SEM. The wild-type hyphal cells showed a smooth and uniform hyphal diameter with regular septation and uniform staining with calcofluor white. In contrast, the Δ*cnaA* mutant showed irregular hyphal growth with enlarged cells (white arrow) and exhibited abnormal chitin deposits along the hyphae (red arrow). SEM images show that the mutant hyphal cells appear shrunken and irregularly shaped with very prominent septa. **(B)** The terminal ends of yeast cells of the Δ*cnaA* mutant were swollen (white arrow) and exhibited abnormal chitin deposits (red arrow). Scale bars, 10 μm.

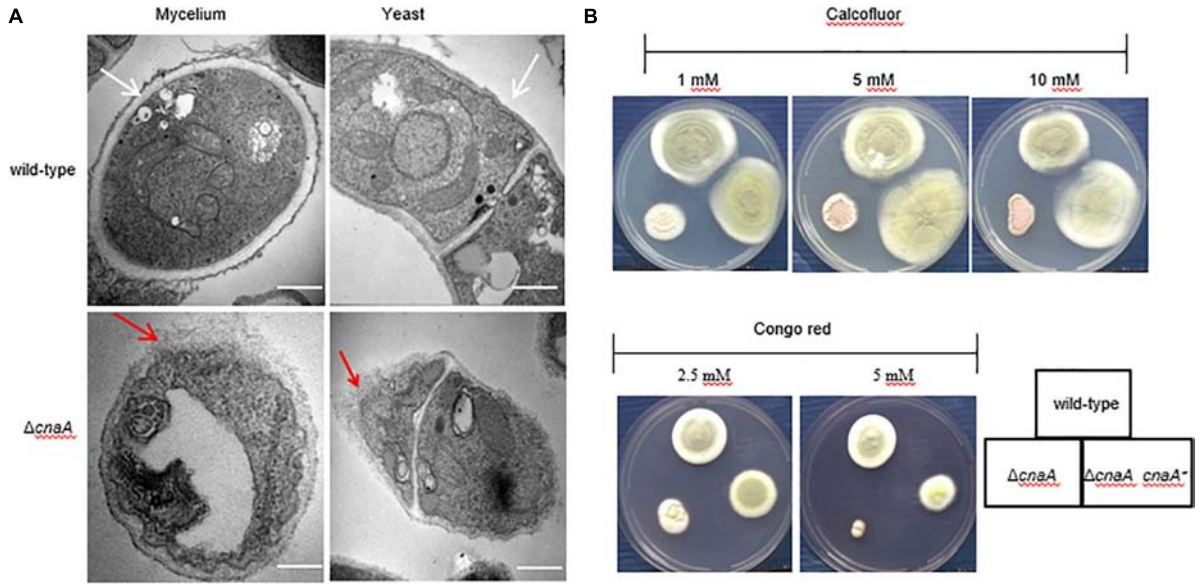

FIGURE 4 | The *cnaA* gene is required for correct cell wall biosynthesis. **(A)** The morphology of the strains was observed by TEM after 10 days of growth in ANM medium at 25°C and 37°C. The cell wall of the wild-type strain was smooth and intact in the hyphal and yeast forms *in vitro*, and the organelles were clearly visible (white arrow). In contrast, the Δ*cnaA* mutant showed cell wall deformation with less distinct layering, and the organelles of the mutant appeared disordered (red arrow). Scale bars, 0.2 μm. **(B)** Strains were grown on ANM medium at 25°C after the addition of various concentrations of calcofluor white or Congo red. Compared with the wild-type, the Δ*cnaA* mutant showed greater sensitivity to Congo red at concentrations of 5 mM, but there was no difference in calcofluor white staining.

the Δ*cnaA* strain were also readily phagocytosed by RAW264.7 macrophages, and by 12 h, the conidia showed clear signs of germination into ellipsoid-shaped yeast cells, similar to the wild-type. However, by 24 h, the Δ*cnaA* yeast cells showed much slower growth than the wild-type cells, with only minimal signs of division. At 48 h, there were very few yeast cells remaining in macrophages, showing that most of the yeast cells had been killed and degraded (**Figure 6A**). TEM observations clearly showed that wild-type cells maintained normal cellular morphology and developed into yeast cells in macrophages. The septum was visible, the cell wall of yeast cells was complete and uniform, organelles were clear and the cytoplasm was uniform. However, most of the Δ*cnaA* conidia were atrophic and destroyed by the phagosome (**Figure 7**).

Conidia survival was measured by lysing a fixed number of macrophages infected with either the wild-type or Δ*cnaA* strain after co-incubation for 24 h and counting viable *T. marneffei* cells (colony forming units, CFU) on YPD medium after 72 h of incubation at 25°C. The number of surviving Δ*cnaA* mutant cells was drastically lower than the number of surviving wild-type cells, and over 60% of the Δ*cnaA* cells were killed at this time point ($P < 0.01$) (**Figure 6B**). Therefore, *cnaA* plays an important role in resisting macrophage killing.

Loss of *cnaA* Abrogates Virulence in a Murine Model of Invasive *Talaromyces marneffei* Infection

To examine the role of *cnaA* in virulence, a murine model of *T. marneffei* infection was utilized to mimic human disease. Four groups of 36 mice were infected by intraperitoneal injection with a sublethal dose (10^6 conidia in 100 μl of physiological saline) of the wild-type, Δ*cnaA*, Δ*cnaA* and *cnaA*$^+$ strains and a diluent control (0.9% physiological saline). The mice were sacrificed on days 3, 6, and 9 postinfection, and their tissues (lung, liver, and spleen) were harvested under sterile conditions. These tissues were macerated, plated on YPD medium and incubated at 25°C for 72 h for CFU assessment. Compared with the control group, the Δ*cnaA* mutant group exhibited sharply decreased CFU in the lung, hepatic, and splenic tissues ($P < 0.001$) (**Figure 8**). Infected mice displayed severe signs of invasive disease, including hunched posture, shivering, ruffled fur and emaciation. To evaluate the mortality rates, four groups of 36 immunosuppressed mice were challenged with 100 μl of suspensions containing 10^8 conidia/ml of each strain. The mortality rates of the mice infected with either the wild-type or Δ*cnaA cnaA*$^+$ strains were similar, and these mice all died by 14 days postinfection. In contrast, the mortality rate of the Δ*cnaA* mutant-infected mice was 45% at 14 days (**Figure 8**). These data

TABLE 2 | *In vitro* assay of antifungal susceptibility.

Antifungal drugs	Hyphal MIC (μg/ml)		Yeast MIC (μg/ml)	
	wild-type	Δ*cnaA*	wild-type	Δ*cnaA*
Amphotericin B	0.5	0.5	0.5	0.5
Itraconazole	8	8	8	4
Fluconazole	0.03	0.03	0.03	0.01
Voriconazole	0.06	0.03	0.06	0.03
Caspofungin	2	0.5	16	2
Micafungin	4	2	32	4

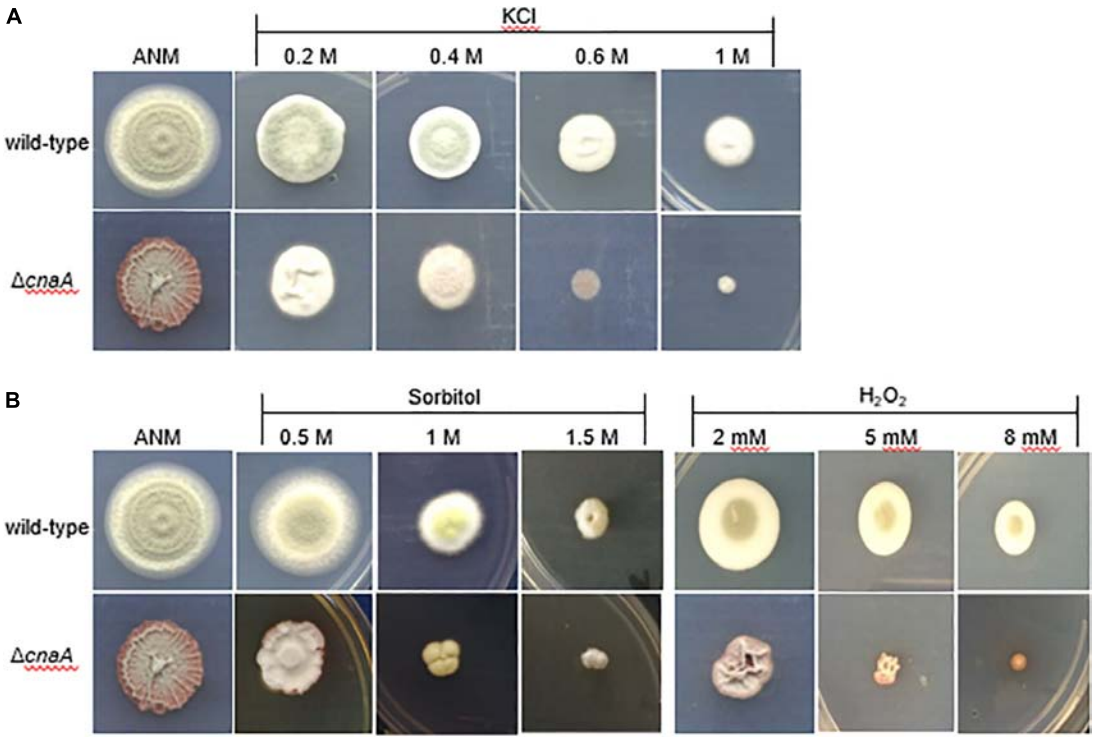

FIGURE 5 | The *cnaA* gene is required for adaptation to osmotic stress *in vitro.* To test the stress resistance of mutants, wild-type, and Δ*cnaA* strains were inoculated with a 5-μl drop of a 1×10^5 conidia/ml suspension onto ANM supplemented as follows: **(A)** for salt stress using 0.2, 0.4, 0.6, and 1M KCl; **(B)** for oxidative stress adding 2, 5 and 8 mM H_2O_2; and for osmotic stress adding 0.5, 1, and 1.5 M sorbitol, followed by incubation for 14 days at 25°C. The Δ*cnaA* mutant showed a gradual reduction in growth with increasing concentrations of the stress agent, especially for oxidative stress.

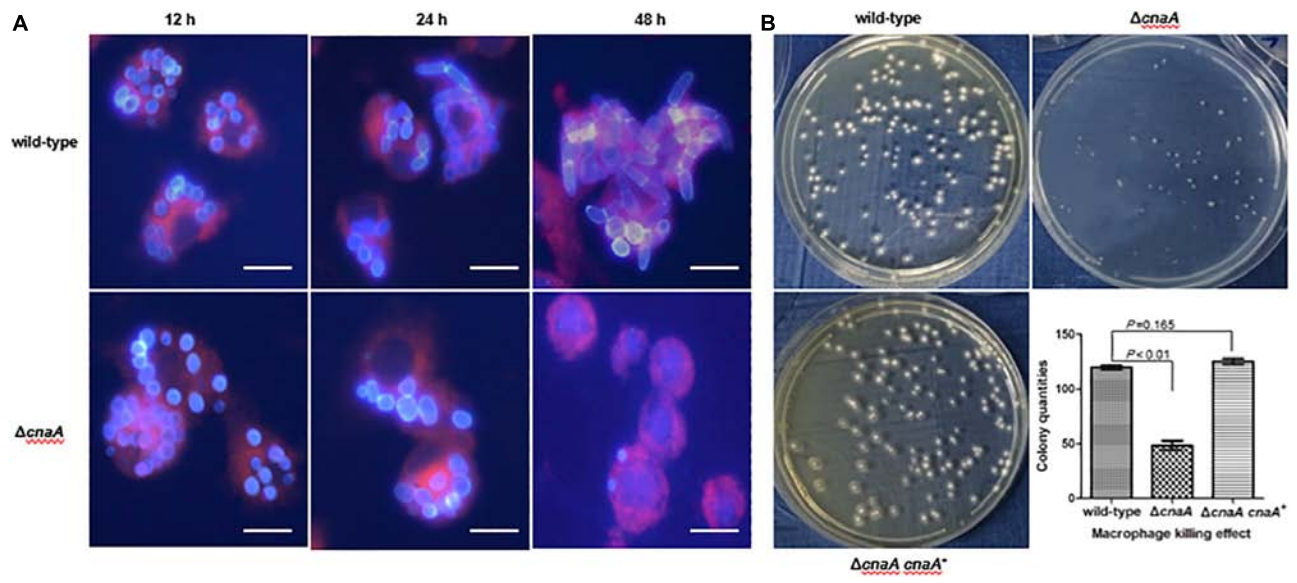

FIGURE 6 | The *cnaA* gene is essential for immune escape in macrophages. **(A)** Wild-type and Δ*cnaA* strains were co-cultured with RAW264.7 macrophages and observed by confocal microscopy. After 12, 24, and 48 h following phagocytosis, the Δ*cnaA* mutant conidia showed increased sensitivity to the cytotoxic activity of the macrophages and were killed and eliminated, compared with the wild-type, which germinated into yeast cells and replicated profusely intracellularly. Scale bars, 20 μm. **(B)** Conidial survival was measured by counting CFU on SD medium after lysis of *T. marneffei*-infected macrophages. The number of surviving Δ*cnaA* mutant cells was drastically lower than the number of surviving wild-type cells ($P < 0.01$).

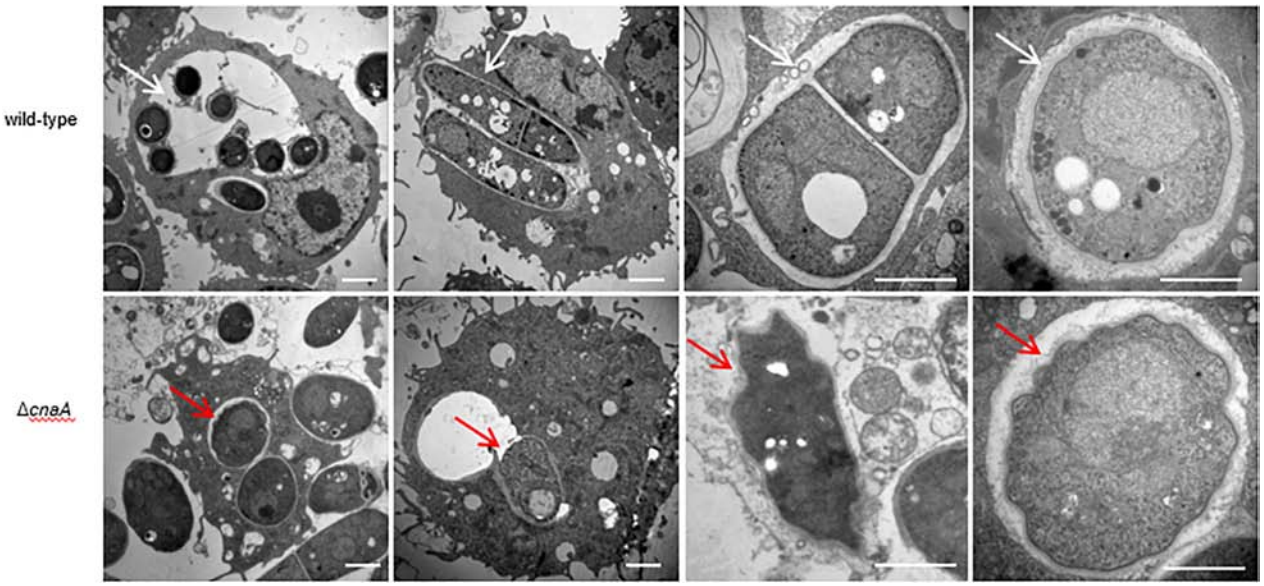

FIGURE 7 | The *cnaA* gene is essential for survival in macrophages. Wild-type and Δ*cnaA* strains were co-cultured with RAW264.7 macrophages and observed by TEM. Wild-type conidia germinated into yeast cells and maintained cellular integrity and morphology after 24 h. The septum of dividing cells is clearly visible, the cell wall is complete and uniform, and organelles are distinct (white arrow). In contrast, most of the Δ*cnaA* mutant conidia failed to germinate or were clearly atrophic with little to no organellar integrity (red arrow). Scale bars, 2 μm.

clearly demonstrate that *cnaA* affects virulence in a murine model of invasive *T. marneffei* infection.

DISCUSSION

This study investigated the roles of a calcineurin homolog (*cnaA*) in the dimorphism and pathogenicity of the opportunistic human fungal pathogen *T. marneffei*. We have shown that *cnaA* (i) is necessary for conidiation, germination, hyphal and yeast cell morphogenesis and growth; (ii) plays an essential role in cell wall integrity of both hyphal and yeast cell types; (iii) is required for stress adaptation for hyphal and yeast cell types; (iv) plays a unique role during immune escape; and (v) is required for full virulence in a murine model of invasive *T. marneffei* infection.

Conidia are an important cell type for almost all fungi and are often the infectious propagules of pathogenic fungi. Their production is tightly regulated, as is their capacity to sense the environment and germinate to initiate vegetative growth. Thus, conidiation and germination are central aspects of fungal cell survival and propagation and important pathogenicity determinants (Boyce and Andrianopoulos, 2007). Infection by *T. marneffei* is believed to occur by inhalation of conidia into the lungs, where they subsequently germinate and transform into yeast cells that cause disseminated infection. Deletion of the *cnaA* gene severely affected asexual reproduction, with the mutant showing defects in the development of the conidiophore, and this resulted in a sharp decrease in the number of conidia produced. It has been reported that calcineurin controls conidiation in *Aspergillus fumigatus* (Shwab et al., 2019), *Aspergillus nidulans* (Wang et al., 2012), and *Penicillium digitatum* (Zhang et al., 2013). In addition, a Δ*cnaA* mutant in *Beauveria bassiana* has been shown to have differential defects in conidial germination, vegetative growth and conidiation capacity (Huang et al., 2015; Wang et al., 2017). These findings show that *cnaA* plays important roles in both production of conidia and their ability to convert to vegetatively growing cells, both of which are likely to affect invasive infection in *T. marneffei*.

The cell wall is a physically rigid, yet plastic, structure that is responsible for the shape of the cell, protects the fungal cell from its environment, prevents killing by predators and mediates cell-cell interaction (Fontaine et al., 2000). Fungal cell walls are unique, and cell wall carbohydrates and proteins play important roles in cell physiology and disease pathogenesis (Mancuso et al., 2018). In *Candida tropicalis,* it has been shown that calcineurin is essential for tolerance of azoles, caspofungin, anidulafungin, and cell wall-perturbing agents (Chen et al., 2014). Similarly, in *Cryptococcus neoformans,* caspofungin tolerance is mediated by multiple pathways downstream of calcineurin function (Pianalto et al., 2019). This study showed that the *T. marneffei*Δ*cnaA* mutant displays defects in the hyphal and the yeast cell wall and that the *cnaA* gene is important for cell wall integrity. This was supported by the observation that yeast cells of the Δ*cnaA* mutant showed a lower MIC against caspofungin (CAS; eightfold) and micafungin (MCFG; eightfold) than wild-type cells (**Table 2**). CAS and MCFG are members of the echinocandin class of antifungal agents that inhibit fungal cell wall biosynthesis by inhibiting cell wall β-(1,3)-D glucan synthesis (Douglas et al., 1997). These results suggest that targeting calcineurin in combination with echinocandin treatment may be effective in *T. marneffei* infection, whereas echinocandins on their own are not.

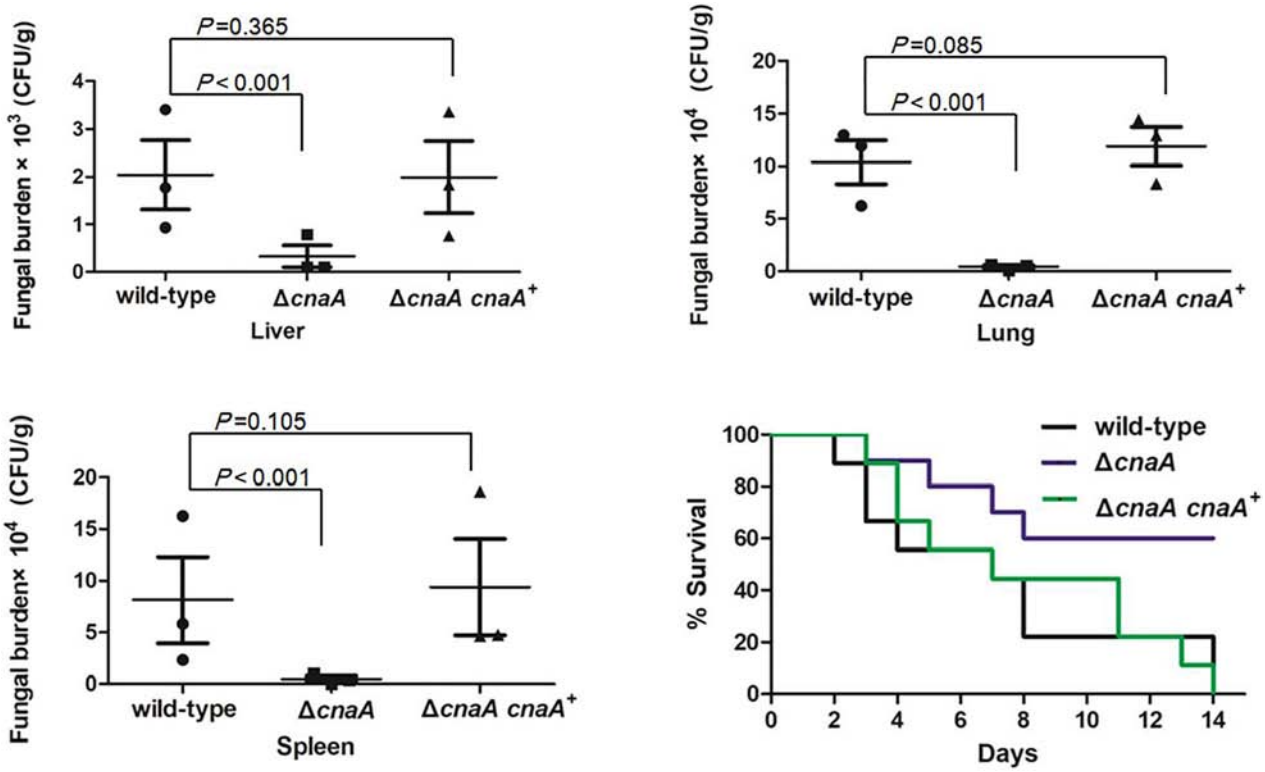

FIGURE 8 | Loss of *cnaA* abrogates virulence in a murine model of invasive *T. marneffei* infection. Mice were infected with 10^6 conidia from the wild-type, Δ*cnaA* or Δ*cnaA cnaA*$^+$ strains by intraperitoneal injection. Organs were harvested 3, 6, or 9 days after infection, and 3 mice were sacrificed every day. Tissue was then assayed for viable *T. marenffei*. Compared with that for the wild-type and Δ*cnaA cnaA*$^+$ strains, the number of CFU for the Δ*cnaA* mutant was significantly reduced in lung, hepatic and splenic tissue. The results were statistically significant based on *T*-test analysis of variance ($P < 0.001$) for all comparisons. The morbidity and mortality of infected mice were assessed every day for 14 days. Survival was plotted on a Kaplan-Meier curve and showed that mice infected with the Δ*cnaA* mutant had a reduced fatality rate (45%) at 14 days compared with the wild-type and Δ*cnaA cnaA*$^+$ strains.

The first line of defense in the human body against *T. marneffei* infection is the innate immune system (Romani, 2011). For *T. marneffei*, initial interactions are characterized by phagocytosis of the conidia by leukocytes in the lungs, followed by leukocyte-facilitated hematogenous dissemination (Vanittanakom et al., 2006). *T. marneffei* conidia face a variety of stresses, such as heat, salt, oxidative stress, osmolarity, nutrient deprivation and cytokine-mediated killing (Pongpom et al., 2017; Ellett et al., 2018). *T. marneffei* shows strong stress tolerance and the ability to resist the cytotoxicity of macrophages in the innate immune system (Pongpom et al., 2005; Vanittanakom et al., 2009). The Δ*cnaA* mutant showed increased sensitivity to salt, H_2O_2 and osmotic stress *in vitro* during hyphal growth. It has been reported that calcineurin is essential in stress resistance in *C. albicans* (Reedy et al., 2010; Liu et al., 2014). This stress adaptation not only helps *T. marneffei* survive in extreme environments but also plays important roles in resisting killing and replication inside macrophages. In fact, morphogenesis and survival of the Δ*cnaA* yeast was compromised inside host cells, but the mutant cells were still able to germinate and develop *in vitro*. During macrophage infection, the Δ*cnaA* mutant conidia hardly germinated or underwent yeast morphogenesis after being phagocytosed, and at longer incubation times, these conidia were killed and eliminated by the macrophages. Thus, the Δ*cnaA* mutant is defective in resisting killing by macrophages.

The phenotypes of the Δ*cnaA* mutant suggested that it would likely be compromised in virulence, and we showed that the deletion of *cnaA* resulted in a drastic increase in the mean survival time of systemically infected mice, with a substantially reduced fungal burden in the lung, hepatic and splenic tissues compared with the wild-type-infected mice. These results indicated that *T. marneffei cnaA* affects virulence in the murine model of invasive *T. marneffei* infection and that it is important for full virulence but does not block infection and dissemination. The capacity for the *T. marneffei*Δ*cnaA* mutant to disseminate despite showing severely compromised survival in an *in vitro* macrophage assay may suggest that there are additional routes of dissemination in an animal host. The importance of calcineurin in virulence has also been shown in *A. fumigatus*, *C. neoformans*, and *C. tropicalis* (Fox et al., 2001; Chen et al., 2014; Juvvadi et al., 2014).

In summary, our findings show that *cnaA*, and therefore calcineurin, plays a key role in controlling fungal morphogenesis and the response of *T. marneffei* to external stresses, including antifungal drugs as well as the host immune response and subsequent fungal pathogenicity. It is required for full virulence

in a murine model of invasive *T. marneffei* infection. Moreover, *cnaA* could be a potential target for combinatorial antifungal therapy during life-threatening *T. marneffei* systemic infections.

DATA AVAILABILITY STATEMENT

All datasets generated for this study are included in the article/supplementary material.

ETHICS STATEMENT

This study protocol was approved by the Ethics Committee of the First Affiliated Hospital of Guangxi Medical University (ethics amendment dated 4/3/2012, approval number KY-074). All experiments in this study were conducted according to internationally accepted standards and regulations on the administration of experimental animals in China (8/1/2011 C-WISC).

AUTHOR CONTRIBUTIONS

C-WC designed this study and drafted the manuscript. Y-QZ and K-SP performed the experiment and data analysis. Y-QZ calculated the statistics and edited the manuscript. J-PL and AA provided the valuable advice, supported the experiment protocol, and critically revised the manuscript. AA critically revised the manuscript. HL, R-FY, J-YW, and C-YH assisted in completing the experiment. All authors have read and approved the final manuscript.

FUNDING

This study was supported by grants from the National Natural Science Foundation of China (Nos. 81571971 and 81271804) and the Natural Science Foundation of Guangxi Province of China (AB18221017 and 2018GXNSFAA294090). The funders had no role in the study design, data collection and analysis, decision to publish or preparation of the manuscript.

REFERENCES

Antinori, S., Gianelli, E., Bonaccorso, C., Ridolfo, A. L., Croce, F., Sollima, S., et al. (2006). Disseminated *Penicillium marneffei* infection in an HIV-positive Italian patient and a review of cases reported outside endemic regions. *J. Travel Med.* 13, 181–188. doi: 10.1111/j.1708-8305.2006.00039.x

Bader, T., Schroppel, K., Bentink, S., Agabian, N., Kohler, G., and Morschhauser, J. (2006). Role of calcineurin in stress resistance, morphogenesis, and virulence of a *Candida albicans* wild-type strain. *Infect. Immun.* 74, 4366–4369. doi: 10.1128/IAI.00142-06

Borneman, A. R., Hynes, M. J., and Andrianopoulos, A. (2000). The abaA homologue of *Penicillium marneffei* participates in two developmental programmes: conidiation and dimorphic growth. *Mol. Microbiol.* 38, 1034–1047. doi: 10.1046/j.1365-2958.2000.02202.x

Boyce, K. J., and Andrianopoulos, A. (2007). A p21-activated kinase is required for conidial germination in *Penicillium marneffei*. *PLoS Pathog.* 3:e162. doi: 10.1371/journal.ppat.0030162

Bugeja, H. E., Boyce, K. J., Weerasinghe, H., Beard, S., Jeziorowski, A., Pasricha, S., et al. (2012). Tools for high efficiency genetic manipulation of the human pathogen *Penicillium marneffei*. *Fungal Genet. Biol.* 4 9, 772–778. doi: 10.1016/j.fgb.2012.08.003

Campos, C. B., Di Benedette, J. P., Morais, F. V., Ovalle, R., and Nobrega, M. P. (2008). Evidence for the role of calcineurin in morphogenesis and calcium homeostasis during mycelium-to-yeast dimorphism of *Paracoccidioides brasiliensis*. *Eukaryot. Cell* 7, 1856–1864. doi: 10.1128/EC.00110-08

Cao, C., Li, R., Wan, Z., Liu, W., Wang, X., Qiao, J., et al. (2007). The effects of temperature, pH, and salinity on the growth and dimorphism of *Penicillium marneffei*. *Med. Mycol.* 45, 401–407. doi: 10.1080/13693780701358600

Cao, C., Liu, W., and Li, R. (2009a). *Penicillium marneffei* SKN7, a novel gene, could complement the hypersensitivity of *S. cerevisiae* skn7 Disruptant strain to oxidative stress. *Mycopathologia* 168, 23–30. doi: 10.1007/s11046-009-9192-x

Cao, C., Liu, W., Li, R., Wan, Z., and Qiao, J. (2009b). In vitro interactions of micafungin with amphotericin B, itraconazole or fluconazole against the pathogenic phase of *Penicillium marneffei*. *J. Antimicrob. Chemother.* 63, 340–342. doi: 10.1093/jac/dkn494

Chen, Y. L., Yu, S. J., Huang, H. Y., Chang, Y. L., Lehman, V. N., Silao, F. G., et al. (2014). Calcineurin controls hyphal growth, virulence, and drug tolerance of *Candida tropicalis*. *Eukaryot. Cell* 13, 844–854. doi: 10.1128/EC.00302-13

Cordeiro Rde, A., Macedo Rde, B., Teixeira, C. E., Marques, F. J., Bandeira Tde, J., Moreira, J. L., et al. (2014). The calcineurin inhibitor cyclosporin A exhibits synergism with antifungals against *Candida parapsilosis* species complex. *J. Med. Microbiol.* 63(Pt 7), 936–944. doi: 10.1099/jmm.0.073478-0

Cruz, M. C., Goldstein, A. L., Blankenship, J. R., Del Poeta, M., Davis, D., Cardenas, M. E., et al. (2002). Calcineurin is essential for survival during membrane stress in *Candida albicans*. *EMBO J.* 21, 546–559. doi: 10.1093/emboj/21.4.546

Cyert, M. S. (2003). Calcineurin signaling in *Saccharomyces cerevisiae*: how yeast go crazy in response to stress. *Biochem. Biophys. Res. Commun.* 311, 1143–1150. doi: 10.1016/s0006-291x(03)01552-3

Douglas, C. M., D'Ippolito, J. A., Shei, G. J., Meinz, M., Onishi, J., Marrinan, J. A., et al. (1997). Identification of the FKS1 gene of *Candida albicans* as the essential target of 1,3-beta-D-glucan synthase inhibitors. *Antimicrob. Agents Chemother.* 41, 2471–2479. doi: 10.1128/aac.41.11.2471

Ellett, F., Pazhakh, V., Pase, L., Benard, E. L., Weerasinghe, H., Azabdaftari, D., et al. (2018). Macrophages protect *Talaromyces marneffei* conidia from myeloperoxidase-dependent neutrophil fungicidal activity during infection establishment in vivo. *PLoS Pathog.* 14:e1007063. doi: 10.1371/journal.ppat.1007063

Fernandes, L., Araujo, M. A., Amaral, A., Reis, V. C., Martins, N. F., and Felipe, M. S. (2005). Cell signaling pathways in *Paracoccidioides brasiliensis*–inferred from comparisons with other fungi. *Genet. Mol. Res.* 4, 216–231.

Fontaine, T., Simenel, C., Dubreucq, G., Adam, O., Delepierre, M., Lemoine, J., et al. (2000). Molecular organization of the alkali-insoluble fraction of *Aspergillus fumigatus* cell wall. *J. Biol. Chem.* 275, 27594–27607. doi: 10.1074/jbc.M9 09975199

Fortwendel, J. R., Juvvadi, P. R., Pinchai, N., Perfect, B. Z., Alspaugh, J. A., Perfect, J. R., et al. (2009). Differential effects of inhibiting chitin and 1,3-{beta}-D-glucan synthesis in ras and calcineurin mutants of *Aspergillus fumigatus*. *Antimicrob. Agents Chemother.* 53, 476–482. doi: 10.1128/AAC.01154-08

Fox, D. S., Cruz, M. C., Sia, R. A. L., Ke, H. M., Cox, G. M., Cardenas, M. E., et al. (2001). Calcineurin regulatory subunit is essential for virulence and mediates interactions with FKBP12-FK506 in *Cryptococcus neoformans*. *Mol. Microbiol.* 39, 835–849. doi: 10.1046/j.1365-2958.2001.02295.x

Fox, D. S., and Heitman, J. (2002). Good fungi gone bad: the corruption of calcineurin. *Bioessays* 24, 894–903. doi: 10.1002/bies.10157

Hien, H. T. A., Thanh, T. T., Thu, N. T. M., Nguyen, A., Thanh, N. T., Lan, N. P. H., et al. (2016). Development and evaluation of a real-time polymerase chain reaction assay for the rapid detection of *Talaromyces marneffei* MP1 gene in human plasma. *Mycoses* 59, 773–780. doi: 10.1111/myc.12530

Hu, Y., Zhang, J., Li, X., Yang, Y., Zhang, Y., Ma, J., et al. (2013). *Penicillium marneffei* infection: an emerging disease in mainland China. *Mycopathologia* 175, 57–67. doi: 10.1007/s11046-012-9577-0

Huang, S., He, Z., Zhang, S., Keyhani, N. O., Song, Y., Yang, Z., et al. (2015). Interplay between calcineurin and the Slt2 MAP-kinase in mediating cell wall

integrity, conidiation and virulence in the insect fungal pathogen *Beauveria bassiana*. *Fungal Genet. Biol.* 83, 78–91. doi: 10.1016/j.fgb.2015.08.009

Juvvadi, P. R., Lamoth, F., and Steinbach, W. J. (2014). Calcineurin-mediated regulation of hyphal growth, septation, and virulence in *Aspergillus fumigatus*. *Mycopathologia* 178, 341–348. doi: 10.1007/s11046-014-9794-9

Juvvadi, P. R., and Steinbach, W. J. (2015). Calcineurin orchestrates hyphal growth, septation, drug resistance and pathogenesis of *Aspergillus fumigatus*: where do we go from here? *Pathogens* 4, 883–893. doi: 10.3390/pathogens4040883

Kauffman, C. A., Freifeld, A. G., Andes, D. R., Baddley, J. W., Herwaldt, L., Walker, R. C., et al. (2014). Endemic fungal infections in solid organ and hematopoietic cell transplant recipients enrolled in the transplant-associated infection surveillance network (TRANSNET). *Transpl. Infect. Dis.* 16, 213–224. doi: 10.1111/tid.12186

Klis, F. M., Mol, P., Hellingwerf, K., and Brul, S. (2002). Dynamics of cell wall structure in *Saccharomyces cerevisiae*. *FEMS Microbiol. Rev.* 26, 239–256. doi: 10.1111/j.1574-6976.2002.tb00613.x

Kummasook, A., Tzarphmaag, A., Thirach, S., Pongpom, M., Cooper, C. R. Jr., and Vanittanakom, N. (2011). *Penicillium marneffei* actin expression during phase transition, oxidative stress, and macrophage infection. *Mol. Biol. Rep.* 38, 2813–2819. doi: 10.1007/s11033-010-0427-1

Le, T., Wolbers, M., Chi, N. H., Quang, V. M., Chinh, N. T., Lan, N. P., et al. (2011). Epidemiology, seasonality, and predictors of outcome of AIDS-associated *Penicillium marneffei* infection in Ho Chi Minh City, Viet Nam. *Clin. Infect. Dis.* 52, 945–952. doi: 10.1093/cid/cir028

Lee, P. P., Lao-Araya, M., Yang, J., Chan, K. W., Ma, H., Pei, L. C., et al. (2019). Application of flow cytometry in the diagnostics pipeline of primary immunodeficiencies underlying disseminated *Talaromyces marneffei* Infec- tion in HIV-negative children. *Front. Immunol.* 10:2189. doi: 10.3389/fimmu.2019.02189

Liu, Y., Solis, N. V., Heilmann, C. J., Phan, Q. T., Mitchell, A. P., Klis, F. M., et al. (2014). Role of retrograde trafficking in stress response, host cell interactions, and virulence of *Candida albicans*. *Eukaryot. Cell* 13, 279–287. doi: 10.1128/EC.00295-13

Mancuso, R., Chinnici, J., Tsou, C., Busarajan, S., Munnangi, R., and Maddi, A. (2018). Functions of *Candida albicans* cell wall glycosidases Dfg5p and Dcw1p in biofilm formation and HOG MAPK pathway. *PeerJ* 6:e5685. doi: 10.7717/peerj.5685

Matos, T. G., Morais, F. V., and Campos, C. B. (2013). Hsp90 regulates *Paracoccidioides brasiliensis* proliferation and ROS levels under thermal stress and cooperates with calcineurin to control yeast to mycelium dimorphism. *Med. Mycol.* 51, 413–421. doi: 10.3109/13693786.2012.725481

Mo, D., Li, X., Wei, L., Sun, C., Liang, H., and Cao, C. (2014). In vitro interactions of calcineurin inhibitors with conventional antifungal agents against the yeast form of *Penicillium marneffei*. *Mycopathologia* 178, 217–220. doi: 10.1007/s11046-014-9787-8

Nakai, T., Uno, J., Ikeda, F., Tawara, S., Nishimura, K., and Miyaji, M. (2003). In vitro antifungal activity of Micafungin (FK463) against dimorphic fungi: comparison of yeast-like and mycelial forms. *Antimicrob. Agents Chemother.* 47, 1376–1381. doi: 10.1128/aac.47.4.1376-1381.2003

Pianalto, K. M., Billmyre, R. B., Telzrow, C. L., and Alspaugh, J. A. (2019). Roles for stress response and cell wall biosynthesis pathways in caspofungin tolerance in *Cryptococcus neoformans*. *Genetics* 213, 213–227. doi: 10.1534/genetics.119.302290

Pongpom, M., Vanittanakom, P., Nimmanee, P., Cooper, C. R. Jr., and Vanittanakom, N. (2017). Adaptation to macrophage killing by *Talaromyces marneffei*. *Future Sci. OA* 3:FSO215. doi: 10.4155/fsoa-2017-0032

Pongpom, P., Cooper, C. R. Jr., and Vanittanakom, N. (2005). Isolation and characterization of a catalase-peroxidase gene from the pathogenic fungus, *Penicillium marneffei*. *Med. Mycol.* 43, 403–411. doi: 10.1080/13693780400007144

Ramos-e-Silva, M., Lima, C. M., Schechtman, R. C., Trope, B. M., and Carneiro, S. (2012). Systemic mycoses in immunodepressed patients (AIDS). *Clin. Dermatol.* 30, 616–627. doi: 10.1016/j.clindermatol.2012.01.008

Reedy, J. L., Filler, S. G., and Heitman, J. (2010). Elucidating the *Candida albicans* calcineurin signaling cascade controlling stress response and virulence. *Fungal Genet. Biol.* 47, 107–116. doi: 10.1016/j.fgb.2009.09.002

Romani, L. (2011). Immunity to fungal infections. *Nat. Rev. Immunol.* 11, 275–288. doi: 10.1038/nri2939

Roque, A., Petrezselyova, S., Serra-Cardona, A., and Arino, J. (2016). Genome-wide recruitment profiling of transcription factor Crz1 in response to high pH stress. *BMC Genomics* 17:662. doi: 10.1186/s12864-016-3006-6

Rusnak, F., and Mertz, P. (2000). Calcineurin: form and function. *Physiol. Rev.* 80, 1483–1521. doi: 10.1152/physrev.2000.80.4.1483

Sanglard, D., Ischer, F., Marchetti, O., Entenza, J., and Bille, J. (2003). Calcineurin A of *Candida albicans*: involvement in antifungal tolerance, cell morphogenesis and virulence. *Mol. Microbiol.* 48, 959–976. doi: 10.1046/j.1365-2958.2003.03495.x

Shwab, E. K., Juvvadi, P. R., Waitt, G., Soderblom, E. J., Barrington, B. C., Asfaw, Y. G., et al. (2019). Calcineurin-dependent dephosphorylation of the transcription factor CrzA at specific sites controls conidiation, stress tolerance, and virulence of *Aspergillus fumigatus*. *Mol. Microbiol.* 112, 62–80. doi: 10.1111/mmi.14254

Supparatpinyo, K., Khamwan, C., Baosoung, V., Nelson, K. E., and Sirisanthana, T. (1994). Disseminated *Penicillium marneffei* infection in southeast Asia. *Lancet* 344, 110–113. doi: 10.1016/s0140-6736(94)91287-4

Vanittanakom, N., Cooper, C. R. Jr., Fisher, M. C., and Sirisanthana, T. (2006). *Penicillium marneffei* infection and recent advances in the epidemiology and molecular biology aspects. *Clin. Microbiol. Rev.* 19, 95–110. doi: 10.1128/CMR.19.1.95-110.2006

Vanittanakom, N., Pongpom, M., Praparattanapan, J., Cooper, C. R., and Sirisanthana, T. (2009). Isolation and expression of heat shock protein 30 gene from *Penicillium marneffei*. *Med Mycol* 47, 521–526. doi: 10.1080/13693780802566358

Wang, F., Tao, J., Qian, Z., You, S., Dong, H., Shen, H., et al. (2009). A histidine kinase PmHHK1 regulates polar growth, sporulation and cell wall composition in the dimorphic fungus *Penicillium marneffei*. *Mycol. Res.* 113(Pt 9), 915–923. doi: 10.1016/j.mycres.2009.03.006

Wang, J., Zhu, X. G., Ying, S. H., and Feng, M. G. (2017). Differential roles for six p-type calcium ATPases in sustaining intracellular Ca(2+) homeostasis, asexual cycle and environmental fitness of *Beauveria bassiana*. *Sci. Rep.* 7:1420. doi: 10.1038/s41598-017-01570-1

Wang, S., Cao, J., Liu, X., Hu, H., Shi, J., Zhang, S., et al. (2012). Putative calcium channels CchA and MidA play the important roles in conidiation, hyphal polarity and cell wall components in *Aspergillus nidulans*. *PLoS One* 7:e46564. doi: 10.1371/journal.pone.0046564

Woo, P. C., Lam, C. W., Tam, E. W., Leung, C. K., Wong, S. S., Lau, S. K., et al. (2012). First discovery of two polyketide synthase genes for mitorubrinic acid and mitorubrinol yellow pigment biosynthesis and implications in virulence of *Penicillium marneffei*. *PLoS Negl. Trop. Dis.* 6:e1871. doi: 10.1371/journal.pntd.0001871

Wu, T. C., Chan, J. W., Ng, C. K., Tsang, D. N., Lee, M. P., and Li, P. C. (2008). Clinical presentations and outcomes of *Penicillium marneffei* infections: a series from 1994 to 2004. *Hong Kong Med. J.* 14, 103–109.

Zhang, T., Xu, Q., Sun, X., and Li, H. (2013). The calcineurin-responsive transcription factor Crz1 is required for conidation, full virulence and DMI resistance in *Penicillium digitatum*. *Microbiol. Res.* 168, 211–222. doi: 10.1016/j.micres.2012.11.006

Conflict of Interest: The authors declare that the research was conducted in the absence of any commercial or financial relationships that could be construed as a potential conflict of interest.

frontiers in Microbiology

ORIGINAL RESEARCH
published: 07 February 2020
doi: 10.3389/fmicb.2020.00147

Radioimmunotherapy of Blastomycosis in a Mouse Model With a (1→3)-β-Glucans Targeting Antibody

*Muath Helal[1], Kevin J. H. Allen[1], Bruce van Dijk[2], Joshua D. Nosanchuk[3], Elisabeth Snead[4] and Ekaterina Dadachova[1]**

[1] College of Pharmacy and Nutrition, University of Saskatchewan, Saskatoon, SK, Canada, [2] Department of Orthopedics, University Medical Center Utrecht, Utrecht, Netherlands, [3] Department of Medicine, Albert Einstein College of Medicine, The Bronx, NY, United States, [4] Western College of Veterinary Medicine, University of Saskatchewan, Saskatoon, SK, Canada

OPEN ACCESS

Edited by:
Carlos Pelleschi Taborda, University of São Paulo, Brazil

Reviewed by:
Bruce Klein, University of Wisconsin-Madison, United States
Todd B. Reynolds, The University of Tennessee, Knoxville, United States
Bettina Fries, Stony Brook Medicine, United States

***Correspondence:**
Ekaterina Dadachova
ekaterina.dadachova@usask.ca

Specialty section:
This article was submitted to Fungi and Their Interactions, a section of the journal Frontiers in Microbiology

Received: *30 July 2019*
Accepted: *21 January 2020*
Published: *07 February 2020*

Citation:
Helal M, Allen KJH, van Dijk B, Nosanchuk JD, Snead E and Dadachova E (2020) Radioimmunotherapy of Blastomycosis in a Mouse Model With a (1→3)-β-Glucans Targeting Antibody. Front. Microbiol. 11:147. doi: 10.3389/fmicb.2020.00147

Invasive fungal infections (IFI) cause devastating morbidity and mortality, with the number of IFIs more than tripling since 1979. Our laboratories were the first to demonstrate that radiolabeled microorganism-specific monoclonal antibodies are highly effective for treatment of experimental fungal, bacterial and viral infections. Later we proposed to utilize surface expressed pan-antigens shared by major IFI-causing pathogens such as beta-glucans as RIT targets. Here we evaluated *in vivo* RIT targeting beta-glucan in *Blastomyces dermatitidis* which causes serious infections in immunocompromised and immunocompetent individuals and in companion dogs. *B. dermatitidis* cells were treated with the 400-2 antibody to (1→3)-β-glucans radiolabeled with the beta-emitter 177Lutetium (^{177}Lu) and alpha-emitter 213Bismuth (^{213}Bi) and the efficacy of cell kill was determined by colony forming units (CFUs). To determine the antigen-specific localization of the 400-2 antibody *in vivo*, C57BL6 mice were infected intratracheally with 2×10^5 *B. dermatitidis* cells and given ^{111}In-400-2 antibody 24 h later. To evaluate the killing of *B. dermatitidis* cells with RIT, intratracheally infected mice were treated with 150 μCi ^{213}Bi-400-2 and their lungs analyzed for CFUs 96 h post-infection. ^{213}Bi-400-2 proved to be more effective in killing *B. dermatitidis* cells *in vitro* than ^{177}Lu-400-2. Three times more ^{111}In-400-2 accumulated in the lungs of infected mice, than in the non-infected ones. ^{213}Bi-400-2 lowered the fungal burden in the lungs of infected mice more than 2 logs in comparison with non-treated infected controls. In conclusion, our results demonstrate the ability of an anti-(1-3)-beta-D-glucan antibody armed with an alpha-emitter ^{213}Bi to selectively kill *B. dermatitidis* cells *in vitro* and *in vivo*. These first *in vivo* results of the effectiveness of RIT targeting pan-antigens on fungal pathogens warrant further investigation.

Keywords: radioimmunotherapy, *Blastomyces dermatitidis*, (1→3)-β-glucan, mouse model, 213Bismuth

INTRODUCTION

Invasive fungal infections (IFI) cause devastating morbidity and mortality, especially in organ transplant patients, cancer patients and patients in intensive care units, with the number of IFIs more than tripling since 1979 (Enoch et al., 2017). There are three main categories of medications used for the treatment of IFI: polyenes (primarily amphotericin B), azoles (fluconazole, itraconazole, voriconazole, posaconazole), and echinocandins (caspofungin, micafungin, anidulafungin). Additionally, flucytosine is primarily utilized in combination with amphotericin B for the treatment of cryptococcosis. Hence, the number of medications available to combat mycostic infections is significantly less than what is available for treating bacterial diseases and the number of targets of these antifungal medications are far fewer (polyenes and azoles: cell membrane sterols; echinocandins: cell wall beta-1,3-glucans; flucytosine: RNA, DNA). Furthermore, the echinocandins, the last new class approved by the Food and Drug Administration (FDA), have been available for ∼10 years with no appearance of new drug classes for the severe fungal diseases.

Radioimmunotherapy (RIT) utilizes antigen-antibody interaction to deliver lethal doses of ionizing radiation to cells and has demonstrated efficacy in several types of cancer (Tomblyn, 2012; Larson et al., 2015). The distinct advantages of RIT over other drugs are: (1) its cytocidal nature, meaning that RIT does not merely abrogate a single cellular pathway but physically destroys targeted cells or cellular machinery; (2) it is less subject to drug resistance mechanisms; (3) its efficacy is independent of the immune status of a host; and (4) it has low toxicity in comparison to chemotherapy due to the specific tumor targeting.

Our laboratories were the first to demonstrate that microorganism-specific monoclonal antibodies (mAbs) are highly effective for the treatment of experimental fungal, bacterial and viral infections (Dadachova et al., 2003; reviewed in Helal and Dadachova, 2018) as well as virally induced cancers (Wang et al., 2007; Phaeton et al., 2016). Using *Cryptococcus neoformans* as a model organism and the antibodies to its polysaccharide capsule as targeting molecules for the radionuclides we investigated various aspects of RIT of fungal disease such as long term efficacy of the treatment with infected mice being observed for up to 75 days post RIT, high inoculum, acute versus established infection (Dadachova et al., 2003; Bryan et al., 2009; Jiang et al., 2012). We also investigated the radiobiological and immunological mechanisms of actions of infections RIT (Dadachova et al., 2006a,b; Bryan et al., 2008). Several years ago, we proposed that we can utilize surface-expressed antigens shared by major IFI-causing pathogens as targets for radiolabeled mAbs (Nosanchuk and Dadachova, 2012). This approach is different than that utilized to date in cancer RIT, where the selected mAbs target a specific cell type. Fortunately, IFI-causing fungi do share common cell wall associated antigens that also constitute major virulence factors for these fungi, which we called "pan-antigens," such as melanin, heat shock protein 60 (HSP60) (Guimarães et al., 2009) and beta-glucans. These antigens are exposed on the surface of fungal cells and thus are accessible to the radiolabeled mAbs for binding and delivering cytocidal payloads to those cells. Using *C. neoformans* and *Candida albicans* as model organisms, our *in vitro* experiments showed that antibodies to the above pan-antigens killed 80–100% of fungal cells when radiolabeled with alpha-particles emitting radionuclide 213Bismuth (Bryan et al., 2012).

In this work, we provide first experimental *in vivo* evidence that pan-antigens on IFI causing pathogens can be targeted with RIT. *Blastomycosis dermatitidis* was chosen as a model for this project. It is an example of an invasive fungal pathogen that causes serious infections in immunocompromised patients (Pappas et al., 1993), immunocompetent individuals (Gray and Baddour, 2002) and in companion dogs (Davies et al., 2013). It has relatively high prevalence in different areas in Canada and the United States (Davies et al., 2013) and the endemic regions may be increasing, as evidenced by reports in New York, Vermont, Texas, Nebraska, and Kansas (McDonald et al., 2018). We have chosen (1→3)-β-glucan as an RIT target because of the encouraging results in our *in vitro* work (Bryan et al., 2012) and because the antibodies to this antigen are commercially available. We have demonstrated that those antibodies in the radiolabeled form bind specifically to *B. dermatitidis* cells *in vitro* and *in vivo* and that their administration to infected mice results in several logs reduction of the infectious burden.

MATERIALS AND METHODS

Fungal Cultures and Antibodies

Acapsular *C. neoformans* (ATCC 208821) cells were cultured in Emmons' modification of Sabouraud's agar overnight (37°C) until sufficient cell numbers were reached. Wild type strain of *B. dermatitidis* Gilchrist et Stokes (ATCC 26199) was used in all experiments. As 26199 strain is a Biological Safety Level (BSL) 3 pathogen in Canada, all manipulations with the cells were conducted using standard operating procedures which enhanced BSL2 (BSL2 +) facilities with the approval by the Public Health Agency of Canada and by the Biosafety Office at University of Saskatchewan. To prevent the formation of the potentially infectious spores, the cells were kept at 37°C at all times except when frozen for storage. *B. dermatitidis* cells were cultured in *Histoplasma* macrophage medium (HMM) (Worsham and Goldman, 1988), at 37°C for 5–7 days until sufficient numbers of cells were reached. The media was prepared by dissolving glucose (18.2 g), glutamic acid (1.0 g), cysteine (1.0 g) and HEPES (6.0 g) in 1 L of water. The solution was filter sterilized followed by the addition of 10.6 g of F-12 Nutrient mixture (cat. number: N6760, Sigma). Passage 2–4 were used throughout the work. Agar was prepared by suspending 19.47 g of MiddleBrook 7H10 Agar Base (cat. number: M0303, Sigma) in 900 ml distilled water followed by the addition of 5 ml glycerol. The mixture was then autoclaved and left at room temperature to cool down. Dubos Oleic Albumin Complex (cat. number: 215333, BD Difco) was added as a media additive to enhance the growth of *B. dermatitidis*. The agar was poured in Petri dishes and left to solidify. The dishes were left at 4°C until needed. Murine IgG2b mAb 2G8 to (1→3)-β-glucan (Torosantucci et al., 2005) was

produced by Diatheva Srl, Cartoceto, Italy, and was a kind gift from Dr. A. Torosantucci (Istituto Superiore di Sanità, Rome, Italy). Its Kd is 1.34×10^{-9} M according to the manufacturer's data. 400-2 murine IgG1 mAb to (1→3)-β-glucan was procured from Biosupplies Australia Pty. Ltd. (Parkville, Australia). The murine isotype control IgG1 antibody MOPC-21 was procured from Invitrogen (Waltham, United States).

Radionuclides and Radiolabeling of Antibodies

400-2, 2G8 and MOPC21 antibodies were first conjugated to a chelating agent *C*-functionalized *trans*-cyclohexyldiethylene-triamine pentaacetic acid derivative (CHXA″) (Macrocyclics, San Antonio, TX, United States) with a 10 molar excess to enable its subsequent radiolabeling with ^{111}In, ^{177}Lu or ^{213}Bi. Conjugation and labeling was carried out according to a previously published method (Allen et al., 2018, 2019). In short, the conjugation reaction was carried out for 1.5 h at 37°C in sodium carbonate buffer at pH 8.5. The reaction was followed by exchanging the buffer into 0.15 M ammonium acetate buffer, pH 6.5. ^{225}Ac for construction of the ^{213}Bi/^{225}Ac radionuclide generator was purchased from Oak Ridge National Laboratory, TN, United States. ^{177}Lu in form of ^{177}Lu chloride was acquired from RadioMedix (TX, United States), and ^{111}In chloride – from BWXT Canada. The CHXA″- conjugated antibodies were radiolabeled with ^{111}In, ^{177}Lu and ^{213}Bi. The radiolabeling of CHXA″ conjugates with ^{111}In and ^{177}Lu was performed to achieve the specific activity of 5 μCi/μg of the antibody. 800 μCi of ^{111}In or ^{177}Lu chloride was added to 10 μL 0.15 M ammonium acetate buffer and added to a microcentrifuge tube containing 160 μ*g* of the desired CHXA″ conjugated antibody in 0.15 M ammonium acetate buffer. The reaction mixture was incubated for 60 min at 37°C, and then the reaction was quenched by the addition of 3 μL of 0.05 M EDTA solution. For radiolabeling with ^{213}Bi, it was eluted from a ^{213}Bi/^{225}Ac radionuclide generator with a 300 μL 0.1 M hydroiodic acid (HI) solution followed by 300 μL milliQ H_2O. The pH of the solution was adjusted to 6.5 with 80 μL of 5 M ammonium acetate buffer prior to addition to the desired CHXA″ conjugated antibody and the reaction mixture was incubated for 5 min at 37°C. The ^{213}Bi-labeled mAbs were purified from HI on a 0.5 mL Amicon disposable size exclusion filter (30 K MW cut off, Fisher). The percentage of radiolabeling was measured by QQsilica gel-instant thin layer chromatography (SG-iTLC) using 0.15 M ammonium acetate buffer as the eluent (top containing unlabeled ^{111}In/^{213}Bi/^{177}L, bottom containing radiolabeled antibody). SG-iTLCs were read on a PerkinElmer 2470 Automatic Gamma Counter. Greater than 98% labeling was routinely achieved and ^{111}In- and ^{177}Lu-labeled mAbs were used immediately with no need for further purification.

Determination of the Binding Ability of Radiolabeled Antibodies to Fungal Cell Surfaces

We radiolabeled fungal beta-glucan-specific (400-2 or 2G8) mAbs with ^{177}Lu. Five million acapsular *C. neoformans* cells were incubated for 3 h (37°C) with a radiolabeled mAb in albumin-pre-coated Eppendorf tubes. A radiolabeled isotype antibody (^{177}Lu-MOPC-21) was also used as a control. In addition, samples with radiolabeled mAb without cells were used to rule out non-specific binding to the plastic tubes. Radiolabeled antibody at a specific activity of 5:1 (25 μCi or 50 μCi radioactivity) were used in this experiment. Following incubation, the tube with the cells and the radiolabeled antibody was measured using PerkinElmer© Gamma Counter. The cells were then centrifuged, the supernatant was removed and its radioactivity measured in a gamma counter. The cellular pellet was washed twice with phosphate buffered saline (PBS), and the radioactivity of the pellet was measured in a gamma counter. The percentages of the radiolabeled antibody bound to the cells and of the unbound antibody were calculated using the following formulae:

$$\text{Radiolabeled antibody bound to the pellet, \%} = (\text{Counts in the pellet}/\text{Counts in the tube}) \times 100$$

$$\text{Unbound radiolabeled antibody, \%} = 100 - (\text{Counts in the pellet}/\text{Counts in the tube}) \times 100$$

Determination of RIT Cytotoxicity Against *B. dermatitidis*

10^4 *B. dermatitidis* cells were incubated with ^{213}B-400-2 mAb (1 or 5 μCi at a specific activity of 5 μCi/μg) or ^{177}Lu 400-2 (20 μCi at a the same specific activity) for 1 h. MOPC-21 was used as an isotype control. After 1 h incubation, the cells were centrifuged and washed to remove any radioactivity. Cells were then cultured on MiddleBrook agar at 37°C for 3 days 37°C after which the colony forming units (CFUs) were counted in each group and the percentages of cell survival were calculated.

Biodistribution of the Radiolabeled 400-2 Antibody in *B. dermatitidis* Infected and Healthy Mice

All animal studies were approved by the Animal Research Ethics Board of the University of Saskatchewan. The objective of this experiment was to determine if the ^{111}In-400-2 mAb accumulated in the *B. dermatitidis* infected lungs in mice to a higher extent than in non-infected animals. Twenty female black C57B16 mice (4–6 weeks old) were randomized into 4 groups (each with 5 mice). Only groups one and two were infected intratracheally with 2×10^5 *B. dermatitidis* cells while groups three and four received PBS alone Mice received isoflurane with oxygen for anesthesia purposes to enable the intratracheal infection. After 24 h, all mice received intraperitoneal injection of ^{111}In-400-2 antibody (30 μCi). Groups one and three were euthanized at 48 h post-infection while groups two and four were euthanized at 96 h post-infection. Lungs were then isolated. Radioactivity was then measured for each lung tissue using PerkinElmer© Gamma Counter in reference to the radiolabeled antibody standard as described (Allen et al., 2018). Radioactivity was then determined per unit weight of each isolated lung.

Radioimmunotherapy of *B. dermatitidis*-Infected Mice

This experiment was conducted to measure the *in vivo* effectiveness of RIT in treating mice infected with *B. dermatitidis*. For this, 27 female black C57B16 mice were infected intratracheally with 10^6 *B. dermatitidis* cells. Twenty four hours after the infection, mice were randomized into 4 groups. The first (9 mice) and second (5 mice) groups received 150 μCi ^{213}Bi-400-2 and 150 μCi ^{213}Bi-MOPC-21, respectively. The third group (8 mice) received no treatment, while the fourth group (5 mice) received only cold 400-2 antibody (30 μg). All treatments were given intraperitoneally. A fifth group consisted of two healthy mice which received neither infection or treatment. Mice were observed for 72 h post treatment and then euthanized. Lungs were isolated and passed through cell strainers. Aseptic conditions were maintained through all the procedures. The cells were centrifuged, concentrated in 700 μL PBS and plated on MiddleBrook agar for 24 h at 37°C. ImageJ software was then used to calculate the area on the colonies formed on the Petri dish in each sample. For the same dish, the average areas of 10 random colonies was also determined. Total area was divided by the average colony area to estimate the number of colonies formed for each plate. In addition, the aliquots of homogenized lungs were obtained from four mice in untreated infected control and ^{213}Bi-400-2 groups. DNA was then isolated from the samples using GenomicPrep Mini Spin kit (Cat. Number 28-9042-58) according to the manufacturer protocol. The levels of *BAD1* and *C57BL/6L* genes were quantified in each sample using real-time PCR system (Bio-Rad CFX96 Real Time System) and SYBR Master Mix. Levels of *BAD1* and C57BL/6L correlate to those of *B. dermatitidis* and mouse cells, respectively. Primers for *BAD1* were forward (5′-AAGTGGCTGGGTAGTTATACGCTAC-3′) and reverse (5′-TAGGTTGCTGATTCCATAAGTCAGG-3′ primers) (Sidamonidze et al., 2012) while a genomic marker found in C57BL/6J mice was detected using the forward (5′-AACTCTCAGGGGTCCTGTGT-3′ and reverse (5′-CCTGGGC CTCACTTATTGGG-3′) primers. The quantity of *BAD1* was then referenced to that of C57BL/6L genomic marker in both control and ^{213}Bi-400-2 groups.

Statistical Analysis

The data are presented as mean ± standard deviation (SD). One-way ANOVA followed by Tukey's *post hoc* test was employed to determine the significant difference between the different groups using GraphPad Prism 5 software (San Diego, CA, United States). A p-value less than 0.05 was considered significant.

RESULTS

The Antibodies to (1→3)-β-Glucan Preserved Their Immunoreactivity After Radiolabeling

Initially, the immunoreactivity toward (1→3)-β-glucan antigen of 400-2 and 2G8 mAbs radiolabeled with ^{111}In was determined by binding to acapsular *C. neoformans* cells. Results show that both 400-2 and 2G8 antibodies were able to bind significantly higher than the MOPC-21 irrelevant control mAb (**Figure 1A**) while there was no binding of 400-2 and 2G8 antibodies to the plates alone without the cells. Conversely, there was significantly more non-bound antibody in case of MOPC-21 than 400-2 or 2G8 (**Figure 1B**). There were approximately 4×10^{13} antibody molecules in 10 μg of the antibody added to 5×10^6 cryptococcal cells. If to assume that every cell expresses around 10^4 antigen binding sites, it means that around 16 and 50 antibody molecules were bound to every cryptococcal cell for 400-2 and 2G8 mAbs, respectively. As Kd for 2G8 is 1.34×10^{-9} M according to the manufacturer, Kd for 400-2 was estimated from the binding data to be 4×10^{-9} M. As commercial availability of 2G8 antibody for further work was limited, 400-2 mAb was utilized in all subsequent experiments.

Radiolabeled mAb 400-2 Specifically Killed *B. dermatitidis* Cells *in vitro*

In vitro results show a significantly higher reduction in cell survival when treated with an alpha-emitter labeled ^{213}Bi-400-2 (1 μCi) antibody compared to ^{213}Bi-MOPC-21 (1 μCi), cold 400-2 and PBS controls (**Figure 2A**). No significant difference was observed between ^{213}Bi-400-2 and ^{213}Bi-MOPC-21 treated cells when the radioactivity was 5 μCi, which can be explained by non-specific killing due to the high radioactivity concentration in a small volume. When a beta-emitter ^{177}Lu was used for radiolabeling, ^{177}Lu-400-2 mAb also demonstrated significant cell killing in comparison to ^{177}Lu-MOPC-21, cold 400-2 and PBS controls (**Figure 2B**).

Biodistribution of Radiolabeled mAb 400-2 in Infected and Healthy Mice Showed Preferential Uptake in the Infected Lungs

The biodistribution of ^{111}In-400-2 in *B. dermatitidis*-infected and healthy mice was performed to evaluate the ability of 400-2 mAb to bind to *B. dermatitidis* in the lungs of infected mice. Our results showed significantly higher accumulation of ^{111}In-400-2 in the lungs of infected mice compared to non-infected ones at 24 h post-injection of the antibody (**Figure 3**) with the uptake equalizing between infected and non-infected lungs at 72 h after antibody administration. There was no significant difference between injected dose per gram in the blood of infected and non-infected mice at both the 24 and 72 h time points (**Figure 3**).

RIT of *B. dermatitidis*-Infected Mice Reduced the Fungal Burden in the Lungs by Several Logs

This experiment was conducted to determine the ability of ^{213}Bi-labeled 400-2 mAb to reduce the burden of infection in *B. dermatitidis*-infected mice. Results demonstrated that single administration of ^{213}Bi-400-2 mAb resulted in more than 2 logs reduction in CFUs in comparison with untreated controls and in more than 1 log reduction – in comparison with the unlabeled ("cold") and ^{213}Bi-MOPC-21 groups (**Figures 4A–F**). The cold

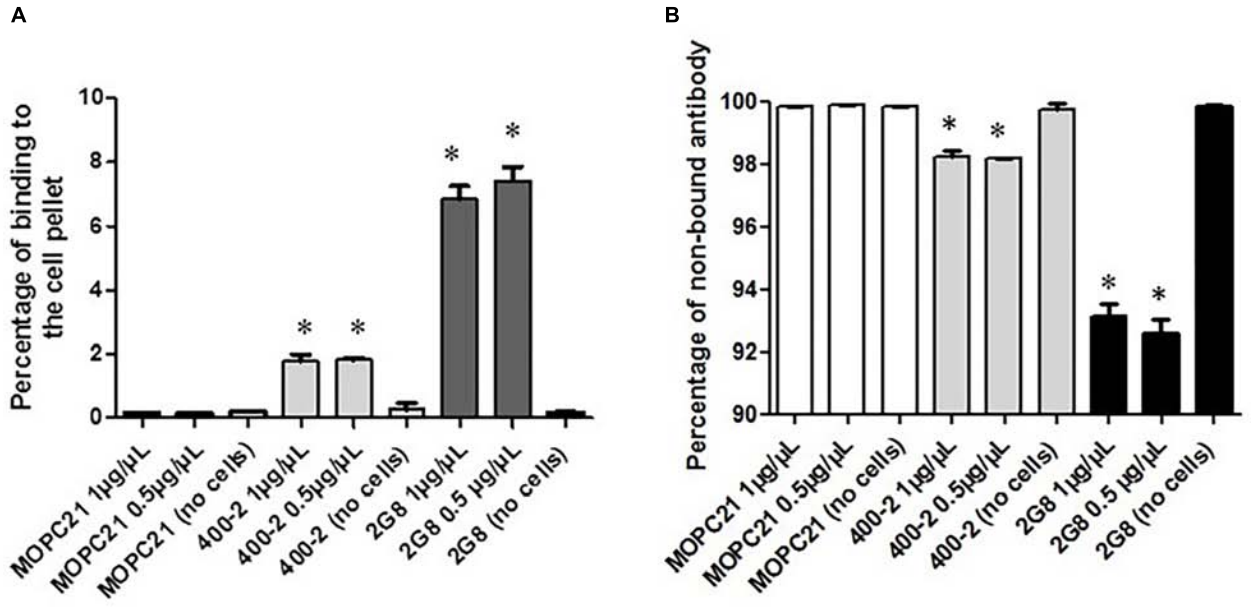

FIGURE 1 | Evaluation of the binding of ^{177}Lu-400-2 and ^{177}Lu-2G8 antibodies to (1→3)-β-glucans antigen after their incubation with acapsular *C. neoformans* cells for 3 h. ^{177}Lu-MOPC 21 was used as an IgG irrelevant control. **(A)** percentage of radiolabeled antibody in a sample bound to the cell pellet: **(B)** percentage of non-bound antibody. *Indicates a significant difference between the groups (*P* value < 0.05).

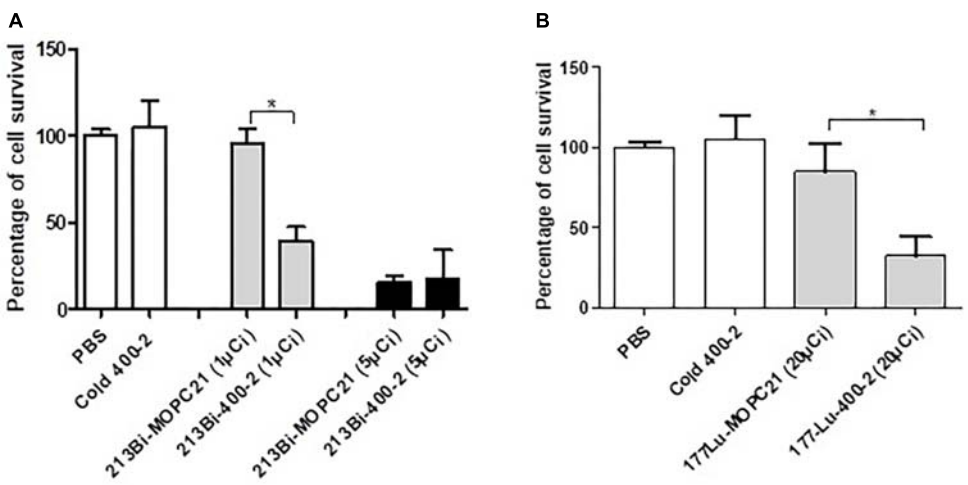

FIGURE 2 | Cytotoxicity of radioimmunotherapy (RIT) toward *B. dermatitidis*. **(A)** ^{213}Bi-400-2 mAb; **(B)** ^{177}Lu-400-2 mAb. Cells were incubated with the radiolabeled antibodies for 1 h at 37°C followed by plating for determination of CFUs. Samples treated with PBS, cold 400-2 mAb and ^{213}Bi- or ^{177}Lu–labeled MOPC-21 mAb were used as controls. *Indicates a significant difference between the groups (*P* value < 0.05).

and ^{213}Bi-MOPC-21 antibodies treatments reduced the CFUs by 1 log, this is probably attributable to opsonisation and non-specific radiation killing of fungal cells, respectively. However, the decrease in fungal burden in control groups was significantly ($p < 0.05$) less than what was observed in the ^{213}Bi-400-2 group. The PCR results show that *B. dermatitidis BAD1* gene levels were significantly ($p = 0.001$) lowered in the lungs of mice that received ^{213}Bi-400-2 treatment in comparison with the untreated infected controls (**Figure 4G**).

DISCUSSION

Our laboratories are developing RIT targeting pan-antigens found in all major human pathogenic fungi as a novel approach for the treatment of IFI (Bryan et al., 2012; Nosanchuk and Dadachova, 2012). This approach is a potential alternative to treat invasive infections that are difficult to cure with currently available drugs. In this study, we employed a radiolabeled antibody (^{213}Bi-400-2) that targets fungal (1-3)-beta-D-glucan

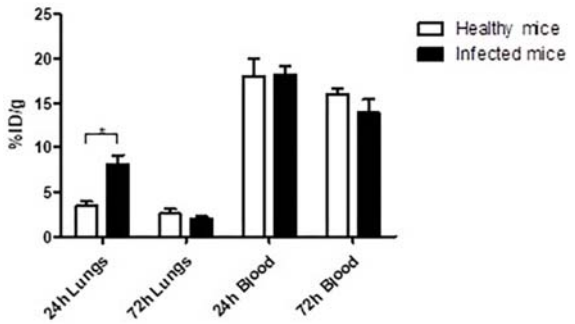

FIGURE 3 | Biodistribution of ^{111}In-400-2 mAb in *B. dermatitidis*-infected and in healthy mice. C57Bl6 mice were infected intratracheally with *B. dermatitidis* 2×10^5 cells, injected IP with ^{111}In-400-2 mAb 24 h after infection, and euthanized at 24 or 72 h post antibody administration. Five animals per group were used. %ID/g represents the percentage of injected dose of the radiolabeled antibody per gram tissue (blood and lungs). *Indicates a significant difference between the groups (*P* value < 0.05).

antigen for delivery of a potent radionuclide as a novel and potent treatment option to treat experimental blastomycosis in mice. Additionally, as (1-3)-beta-D-glucan is expressed in a wide range of fungal cells (Odabasi et al., 2006), we anticipate that radiolabeled antibodies to this antigen could be effective in treating a wide range of fungal diseases.

Before proceeding with *in vivo* experiments, we evaluated the specificity of 400-2 antibody binding to *B. dermatitidis* cells *in vitro* which was done in the absence of mammalian cells (**Figure 1**). 400-2 antibody to beta-glucan demonstrated binding to *B. dermatitidis* cells while the control antibody MOPC-21 – did not. These results provided reassurance that 400-2 is binding specifically to *B. dermatitidis*. We also compared the *in vitro* killing ability toward *B. dermatitidis* cells of 400-2 mAb when conjugated to two different radionuclides, an alpha emitter ^{213}Bi and a beta emitter ^{177}Lu. Although both radioisotopes were able to kill significant percentage of *B. dermatitidis* cells, ^{213}Bi showed a higher potency than ^{177}Lu. That is, 20 μCi ^{177}Lu-400-2 was required to cause cell death equivalent to the damage caused by 1 μCi ^{213}Bi-400-2. Interestingly, fungal cytotoxicity of radiolabeled 400-2 was observed despite the relatively low expression levels of (1-3)-beta-D-glucan in these cells (Girouard et al., 2007). These results are concordant with our previous results on *in vitro* killing with ^{213}Bi-2G8 antibody of *C. neoformans* cells which also has low levels of (1-3)-beta-D-glucans and provide further evidence of the effectiveness of RIT in killing the targeted cells.

Our *in vivo* biodistribution results showed a significantly higher accumulation of ^{111}In-400-2 antibody in the lungs

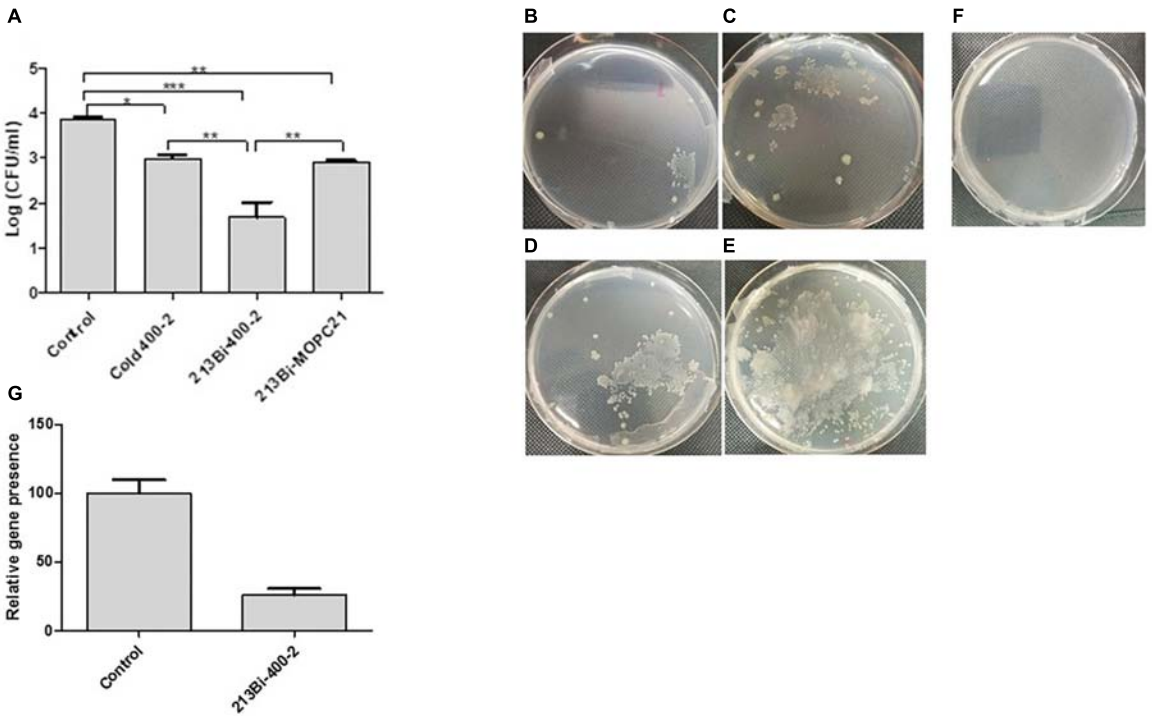

FIGURE 4 | Radioimmunotherapy (RIT) of *B. dermatitidis* infected mice. **(A)** CFUs in the lungs of the mice infected with 10^6 *B. dermatitidis* cells for 24 h and then either left untreated (control) or treated intraperitoneally with 30 μg 400-2 cold antibody, 150 μCi ^{213}Bi-400-2, or 150 μCi ^{213}Bi-MOPC-21 and were euthanized at 96 h post-infection. * Indicates *P* value < 0.05; ** < 0.01; *** < 0.001. **(B–F)** images of representative plates seeded with the homogenates from lungs isolated from various treatment groups: **(B)** ^{213}Bi-400-2; **(C)** ^{213}Bi-MOPC-21; 1 **(D)** 400-2 cold antibody; **(E)** no treatment; **(F)** uninfected, untreated mice; **(G)** real time PCR results, showing *B. dermatitidis BAD1* gene levels significantly ($p = 0.001$) lowered in the lungs of mice that received ^{213}Bi-400-2 treatment in comparison with untreated infected controls.

of the infected mice compared to its accumulation in non-infected ones. This provides a strong evidence of the co-localization of the 400-2 antibody with *B. dermatitidis* cells. There was almost 3 times more ^{111}In-400-2 mAb in the lungs of infected mice than non-infected once at 24 h post administration of the antibody (**Figure 3**). Similar results were observed during the biodistribution of capsular polysaccharide-targeting mAb 18B7 in mice infected intratracheally with *C. neoformans* (Dadachova et al., 2003). The decrease in lung uptake to the background levels in infected mice at 72 h post antibody administration was, most likely, due to the 400-2 mAb coming off (1-3)-beta-D-glucan. However, since the lungs will only experience high radiation doses in the first 4 h after administration of ^{213}Bi-400-2 due to ^{213}Bi short physical half-life of 46 min, the increased accumulation of the antibody in the lungs early after administration will be sufficient to deliver the cytocidal doses of radiation to *B. dermatitidis* cells.

The biodistribution results provided impetus to pursue RIT experiments. Treatment of infected mice with ^{213}Bi-400-2 antibody was able to decrease the lungs CFUs more than 2 logs compared to non-treated infected mice (**Figure 4**). To the best of our knowledge, this is the first *in vivo* demonstration of the efficacy of RIT targeting fungal pan antigens. This 2 logs (1,000 fold) reduction in infection burden compared favorably with cancer RIT, which typically causes 5–100 fold decrease in the tumor size in comparison with untreated controls in experimental cancer models (Jiao et al., 2019; Quelven et al., 2019). In regard to the *in vivo* specificity of RIT, before performing therapy experiments, we demonstrated that 400-2 antibody was specific for beta-glucan both *in vitro* (cell binding and cell killing results), and *in vivo*, when it concentrated 3 times more in the lungs of the infected mice than non-infected mice during the biodistribution study. If it would be binding non-specifically to Fc receptors on resident macrophages and on other cells in the lungs, there would be no difference in the lungs uptake between infected and healthy mice, and the uptake in the infected lungs would be growing with time, as more inflammatory cells are moving in. ^{213}Bi is a powerful alpha-emitter which can cause significant off target effects, including stimulation of immune system. Nevertheless, the effect of ^{213}Bi-labeled control antibody on the infection burden was 10 times lower than that of ^{213}Bi-400-2. This, in our opinion, is the most direct proof of the specificity of RIT treatment. The effect of the unlabeled 400-2 antibody on the fungal burden should be considered separately. In this regard, FDA approved radiolabeled antibody Zevalin for treatment of non-Hodgkin lymphoma is capable of inducing some ADCC which contributes to the antibody overall efficacy.

In the past we have performed extensive evaluation of RIT toxicity in mouse models of fungal infection using the same radioactive doses of ^{213}Bi-labeled antibodies used in the current study. In this regard, the toxicity evaluation in RIT-treated mice infected intratracheally with *C. neoformans* showed the absence of acute hematologic and long-term pulmonary toxicity (Dadachova et al., 2004a,b,c). RIT proved to be much better tolerated by the infected mice than current standard of care Amphotericin B (Bryan et al., 2010). Finally, RIT spared bystander mammalian cells such as macrophages which were able to perform their functions such as nitric oxide production post-RIT exposure (Bryan et al., 2013). The technology of attaching radionuclides to mAbs is mature and can be easily translated from the cancer field into infectious diseases. Importantly, nuclear medicine departments in hospitals world-wide are now routinely treating cancer patients with RIT and are fully equipped for deployment of infectious diseases RIT. Portable imaging equipment is available for imaging patients receiving RIT to ascertain the targeting of radiolabeled mAbs and to monitor the progression of the disease.

In conclusion, our results demonstrate the ability of an anti-(1-3)-beta-D-glucan antibody armed with an alpha-emitter ^{213}Bi to selectively kill *B. dermatitidis* cells *in vitro* and *in vivo*. These results provide encouraging first *in vivo* results of the effectiveness of RIT targeting pan-antigens on fungal pathogens. The goal of our group is to pursue a clinical trial of RIT in companion dogs with spontaneous blastomycosis; this research is in progress.

DATA AVAILABILITY STATEMENT

The datasets generated for this study are available on request to the corresponding author.

ETHICS STATEMENT

The animal study was reviewed and approved by the Animal Research Ethics Board of the University of Saskatchewan.

AUTHOR CONTRIBUTIONS

MH, KA, and BD performed the experiment. ED and ES came up with the concept of the study. JN participated in the discussion of the concept and results. MH and ED wrote the manuscript. All authors edited the manuscript.

FUNDING

This research was funded by the Saskatchewan Health Research Foundation and partially supported by the Sylvia Fedoruk Canadian Centre for Nuclear Innovation.

ACKNOWLEDGMENTS

The authors would like to thank Dr. Marcel Wüthrich from the Department of Pediatrics, University of Wisconsin School of Medicine and Public Health, for the encouraging discussions at the beginning of the project.

REFERENCES

Allen, K. J. H., Jiao, R., Malo, M. E., Frank, C., and Dadachova, E. (2018). Biodistribution of a radiolabeled antibody in mice as an approach to evaluating antibody pharmacokinetics. *Pharmaceutics* 10:E262. doi: 10.3390/pharmaceutics10040262

Allen, K. J. H., Jiao, R., Malo, M. E., Frank, C., Fisher, D. R., Rickles, D., et al. (2019). Comparative radioimmunotherapy of experimental melanoma with novel humanized antibody to melanin labeled with 213Bismuth and 177Lutetium. *Pharmaceutics* 11, 348–360.

Bryan, R. A., Guimaraes, A. J., Hopcraft, S., Jiang, Z., Bonilla, K., Morgenstern, A., et al. (2012). Toward developing a universal treatment for fungal disease using radioimmunotherapy targeting common fungal antigens. *Mycopathologia* 173, 463–471. doi: 10.1007/s11046-011-9476-9

Bryan, R. A., Huang, X., Morgenstern, A., Bruchertseifer, F., Casadevall, A., and Dadachova, E. (2008). Radiofungicidal effects of external gamma radiation and antibody-targeted beta and alpha radiation on *Cryptococcus neoformans*. *Antimicrob. Agents Chemother.* 52, 2232–2235. doi: 10.1128/AAC.01245-07

Bryan, R. A., Jiang, Z., Howell, R. C., Morgenstern, A., Bruchertseifer, F., Casadevall, A., et al. (2010). Radioimmunotherapy is more effective than antifungal treatment in experimental cryptococcal infection. *J. Infect. Dis.* 202, 633–637. doi: 10.1086/654813

Bryan, R. A., Jiang, Z., Huang, X., Morgenstern, A., Bruchertseifer, F., Sellers, R., et al. (2009). Radioimmunotherapy is effective against a high infection burden of *Cryptococcus neoformans* in mice and does not select for radiation-resistant phenotypes in cryptococcal cells. *Antimicrob. Agents Chemother.* 53, 1679–1682. doi: 10.1128/AAC.01334-08

Bryan, R. A., Jiang, Z., Morgenstern, A., Bruchertseifer, F., Casadevall, A., and Dadachova, E. (2013). Radioimmunotherapy of *Cryptococcus neoformans* spares bystander mammalian cells. *Future Microbiol.* 8, 1–9. doi: 10.2217/fmb.13.79

Dadachova, E., Bryan, R. A., Apostolidis, C., Morgenstern, A., Zhang, T., Moadel, T., et al. (2006a). Interaction of radiolabeled antibodies with fungal cells and components of immune system in vitro and during radioimmunotherapy of experimental fungal infection. *J. Infect. Dis.* 193, 1427–1436. doi: 10.1086/503369

Dadachova, E., Bryan, R. A., Frenkel, A., Zhang, T., Apostolidis, C., Nosanchuk, J. S., et al. (2004a). Evaluation of acute hematological and long-term pulmonary toxicity of radioimmunotherapy of *Cryptococcus neoformans* infection in murine models. *Antimicrob. Agents Chemother.* 48, 1004–1006. doi: 10.1128/aac.48.3.1004-1006.2004

Dadachova, E., Burns, T., Bryan, R. A., Apostolidis, C., Brechbiel, M. W., Nosanchuk, J. D., et al. (2004b). Feasibility of radioimmunotherapy of experimental pneumococcal infection. *Antimicrob. Agents Chemother.* 48, 1624–1629. doi: 10.1128/aac.48.5.1624-1629.2004

Dadachova, E., Howell, R. W., Bryan, R. A., Frenkel, A., Nosanchuk, J. D., and Casadevall, A. (2004c). Susceptibility of the human pathogenic fungi *Cryptococcus neoformans* and *Histoplasma capsulatum* to γ-radiation versus radioimmunotherapy with α- and β-emitting radioisotopes. *J. Nucl. Med.* 45, 313–320.

Dadachova, E., Nakouzi, A., Bryan, R. A., and Casadevall, A. (2003). Ionizing radiation delivered by specific antibody is therapeutic against a fungal infection. *Proc. Natl. Acad. Sci. U.S.A.* 100, 10942–109427.

Dadachova, E., Patel, M. C., Toussi, S., Apostolidis, C., Morgenstern, A., Brechbiel, M. W., et al. (2006b). Targeted killing of virally infected cells by radiolabeled antibodies to viral proteins. *PLoS Med.* 3:e427. doi: 10.1371/journal.pmed.0030427

Davies, J. L., Epp, T., and Burgess, H. J. (2013). Prevalence and geographic distribution of canine and feline blastomycosis in the *Canadian prairies*. *Can. Vet. J.* 54, 753–760.

Enoch, D. A., Yang, H., Aliyu, S. H., and Micallef, C. (2017). The changing epidemiology of invasive fungal infections. *Methods Mol. Biol.* 1508, 17–65. doi: 10.1007/978-1-4939-6515-1_2

Girouard, G., Lachance, C., and Pelletier, R. (2007). Observations on (1-3)-beta-D-glucan detection as a diagnostic tool in endemic mycosis caused by *Histoplasma* or *Blastomyces*. *J. Med. Microbiol.* 56, 1001–1002. doi: 10.1099/jmm.0.47162-0

Gray, N. A., and Baddour, L. M. (2002). Cutaneous inoculation blastomycosis. *Clin. Infect. Dis.* 34, E44–E49.

Guimarães, A. J., Frases, S., Gomez, F. J., Zancopé-Oliveira, R. M., and Nosanchuk, J. D. (2009). Monoclonal antibodies to heat shock protein 60 alter the pathogenesis of *Histoplasma capsulatum*. *Infect. Immun.* 77, 1357–1367. doi: 10.1128/IAI.01443-08

Helal, M., and Dadachova, E. (2018). Radioimmunotherapy as a novel approach in HIV, bacterial, and fungal infectious diseases. *Cancer Biother. Radiopharm.* 33, 330–335. doi: 10.1089/cbr.2018.2481

Jiang, Z., Bryan, R. A., Morgenstern, A., Bruchertseifer, F., Casadevall, A., and Dadachova, E. (2012). Treatment of early and established *Cryptococcus neoformans* infection with radiolabeled antibodies in immunocompetent mice. *Antimicrob. Agents Chemother.* 56, 552–554. doi: 10.1128/AAC.00473-11

Jiao, R., Allen, K. J. H., Malo, M. E., Helal, M., Jiang, Z., Smart, K., et al. (2019). Evaluation of novel highly specific antibodies to cancer testis antigen Centrin-1 for radioimmunoimaging and radioimmunotherapy of pancreatic cancer. *Cancer Med.* 8, 5289–5300. doi: 10.1002/cam4.2379

Larson, S. M., Carrasquillo, J. A., Cheung, N. K., and Press, O. W. (2015). Radioimmunotherapy of human tumours. *Nat. Rev. Cancer* 15, 347–360. doi: 10.1038/nrc3925

McDonald, R., Dufort, E., Jackson, B. R., Tobin, E. H., Newman, A., Benedict, K., et al. (2018). Notes from the field: blastomycosis cases occurring outside of regions with known endemicity - New York, 2007-2017. *MMWR Morb. Mortal Wkly. Rep.* 67, 1077–1078. doi: 10.15585/mmwr.mm6738a8

Nosanchuk, J. D., and Dadachova, E. (2012). Radioimmunotherapy of fungal diseases: the therapeutic potential of cytocidal radiation delivered by antibody targeting fungal cell surface antigens. *Front. Microbiol.* 12:283. doi: 10.3389/fmicb.2011.00283

Odabasi, Z., Paetznick, V. L., Rodriguez, J. R., Chen, E., McGinnis, M. R., and Ostrosky-Zeichner, L. (2006). Differences in beta-glucan levels in culture supernatants of a variety of fungi. *Med. Mycol.* 44, 267–272. doi: 10.1080/13693780500474327

Pappas, P. G., Threlkeld, M. G., Bedsole, G. D., Cleveland, K. O., Gelfand, M. S., and Dismukes, W. E. (1993). Blastomycosis in immunocompromised patients. *Medicine* 72, 311–325. doi: 10.1097/00005792-199309000-00003

Phaeton, R., Jiang, Z., Revskaya, E., Fisher, D. R., Goldberg, G. L., and Dadachova, E. (2016). Beta emitters Rhenium-188 and Lutetium-177 are equally effective in radioimmunotherapy of HPV-positive experimental cervical cancer. *Cancer Med.* 5, 9–16. doi: 10.1002/cam4.562

Quelven, I., Monteil, J., Sage, M., Saidi, A., Mounier, J., Bayout, A., et al. (2019). 212Pb Alpha-Radioimmunotherapy targeting CD38 in multiple Myeloma: a preclinical study. *J. Nucl. Med.* doi: 10.2967/jnumed.119.239491 [Epub ahead of print],

Sidamonidze, K., Peck, M. K., Perez, M., Baumgardner, D., Smith, G., Chaturvedi, V., et al. (2012). Real-time PCR assay for identification of *Blastomyces dermatitidis* in culture and in tissue. *J. Clin. Microbiol.* 50, 1783–1786. doi: 10.1128/JCM.00310-12

Tomblyn, M. (2012). Radioimmunotherapy for B-cell non-hodgkin lymphomas. *Cancer Control* 19, 196–203. doi: 10.1177/107327481201900304

Torosantucci, A., Bromuro, C., Chiani, P., Bernardis, F. D., Berti, F., Galli, C., et al. (2005). A novel glyco-conjugate vaccine against fungal pathogens. *J. Exp. Med.* 202, 597–606. doi: 10.1084/jem.20050749

Wang, X. G., Revskaya, E., Bryan, R. A., Strickler, H. D., Burk, R. D., Casadevall, A., et al. (2007). Treating cancer as an infectious disease–viral antigens as novel targets for treatment and potential prevention of tumors of viral etiology. *PLoS One* 2:e1114. doi: 10.1371/journal.pone.0001114

Worsham, P. L., and Goldman, W. E. (1988). Quantitative plating of *Histoplasma capsulatum* without addition of conditioned medium or siderophores. *J. Med. Vet. Mycol.* 26, 137–143. doi: 10.1080/02681218880000211

Conflict of Interest: The authors declare that the research was conducted in the absence of any commercial or financial relationships that could be construed as a potential conflict of interest.

Advantages of publishing in Frontiers

OPEN ACCESS
Articles are free to read for greatest visibility and readership

FAST PUBLICATION
Around 90 days from submission to decision

HIGH QUALITY PEER-REVIEW
Rigorous, collaborative, and constructive peer-review

TRANSPARENT PEER-REVIEW
Editors and reviewers acknowledged by name on published articles

Frontiers
Avenue du Tribunal-Fédéral 34
1005 Lausanne | Switzerland

Visit us: www.frontiersin.org
Contact us: info@frontiersin.org | +41 21 510 17 00

REPRODUCIBILITY OF RESEARCH
Support open data and methods to enhance research reproducibility

DIGITAL PUBLISHING
Articles designed for optimal readership across devices

FOLLOW US
@frontiersin

IMPACT METRICS
Advanced article metrics track visibility across digital media

EXTENSIVE PROMOTION
Marketing and promotion of impactful research

LOOP RESEARCH NETWORK
Our network increases your article's readership